



**BRITISH
COLUMBIA**

Ministry of Energy and Mines
Geological Survey Branch

**GEOLOGICAL
FIELDWORK 2004**
A Summary of Field Activities and
Current Research

Paper 2005-1

Mines and Minerals Division
Geological Survey Branch

Parts of this publication may be quoted or reproduced if source and authorship is acknowledged. The following is the recommended format for referencing individual works contained in this publication:

Alldrick, D.J., Nelson, J.L. and Barresi, T. (2005): Geology and Mineral Deposits of the Upper Iskut River Area: Tracking the Eskay Rift through Northern British Columbia; *in Geological Fieldwork 2004, British Columbia Ministry of Energy and Mines*, Paper 2005-1, p 1-30.

Individual manuscripts in this publication are available, free of charge, as **colour digital files** in Adobe Acrobat PDF format from the BC Ministry of Energy and Mines internet website at:

<http://www.em.gov.bc.ca/Mining/Geolsurv/Publications/catalog/catfldwk.htm>

COVER PHOTO: Mitch Mihalyuk, British Columbia Geological Survey, carrying out regional geological mapping in the area of the Nakina and Sloko rivers in the mountains south of Atlin, northern British Columbia

British Columbia Cataloguing in Publication Data

Main entry under title:

Geological Fieldwork: - 1974 -

Annual.

Issuing body varies

Vols. For 1978-1996 issued in series: Paper / British Columbia. Ministry of Energy, Mines and Petroleum Resources; vols for 1997- 1998, Paper / British Columbia. Ministry of Employment and Investment; vols for 1999- , Paper / British Columbia Ministry of Energy and Mines.

Includes Bibliographical references.

ISSN 0381-243X=Geological Fieldwork

1. Geology - British Columbia - Periodicals. 2. Mines and mineral resources - British Columbia - Periodicals. 3. Geology - Fieldwork - Periodicals. 4. Geology, Economic - British Columbia - Periodicals. 5. British Columbia. Geological Survey Branch - Periodicals. I. British Columbia. Geological Division. II. British Columbia. Geological Survey Branch. III. British Columbia. Geological Survey Branch. IV. British Columbia. Dept. of Mines and Petroleum Resources. V. British Columbia. Ministry of Energy, Mines and Petroleum Resources. VI. British Columbia. Ministry of Employment and Investment. VII. British Columbia Ministry of Energy and Mines. VIII. Series: Paper (British Columbia. Ministry of Energy, Mines and Petroleum Resources). IX. Series: Paper (British Columbia. Ministry of Employment and Investment). X. Series: Paper (British Columbia Ministry of Energy and Mines).

QE187.46 622.1'09711 C76-083084-3 (Rev.)



VICTORIA
BRITISH COLUMBIA
CANADA

JANUARY 2005

FOREWORD

The British Columbia Ministry of Energy and Mines presents the results of provincial geoscience surveys in its thirtieth edition of *Geological Fieldwork: A Summary of Fieldwork and Current Research*. Most articles are contributions from staff of the Geological Survey Branch or are related to field programs being carried out by the Branch. These field surveys have led directly to claim staking and enhanced mineral exploration expenditures, which may ultimately lead to new mines in the province. As in previous years, the volume also publishes studies by university and industry authors.

This past year, the British Columbia Geological Survey regional field surveys and collaborative geoscience studies were delivered largely through partnerships with government, industry and universities. The Geological Survey of Canada was a strong partner in the Iskut and Toodoggone field programs in northern British Columbia through their Targeted Geoscience Initiatives Program. Articles in this volume include reports on continuing programs of regional mapping and geochemical surveys in the area north and east of the Eskay Creek gold mine and in the Toodoggone mining camp north of Kemess mine.

Industry partnerships provided operating funds and access to private sector information for both the porphyry copper-gold program (Galore Creek, Iron Mask and Mt Polley) and the Kalum gold project near Terrace.

Two articles report results of investigations into the province's diamond potential. They provide significant new information on the setting and increased potential for discoveries in the northeast corner of British Columbia.

This volume also includes 16 articles derived from projects funded, at least in part, by the BC and Yukon Chamber of Mines through their *Rocks to Riches* program. These span a wide spectrum from geochemical and geophysical surveys, geological mapping and to new tools for accessing the provincial databases.

During the past year the Geological Survey Branch published *Geological Fieldwork 2003*, 17 Open Files, 4 Geoscience Maps, 13 GeoFiles, 7 Information Circulars and 1 Paper. Geoscience publications are now routinely posted to the Ministry of Energy and Mines website. MapPlace, one of the world's premier geoscience internet-map systems, continues to improve with the addition of new tools and data layers. The site is expected to exceed four million hits in 2004.

This *Fieldwork* volume reflects the hard work and expertise of numerous authors who have earned our thanks for their contributions. The articles have been improved by peer and supervisor review. The quality services of RnD Technical are acknowledged for their help in publication production. Again, for yet another year, Brian Grant earns special commendation for coordinating the organization and publication of the volume.

*D.V. Lefebure
Director – Chief Geologist
Geological Survey Branch*

CONTENTS

Aldrick, D.J., Nelson, J.L. and Barresi, T.: Geology and Mineral Deposits of the Upper Iskut River Area: Tracking the Eskay Rift through Northern BC.	1
Barresi, T., Nelson, J.L., Aldrick, D.J. and Dostal, J.: Pillow Basalt Ridge Facies: Detailed Mapping of Eskay Creek–Equivalent Stratigraphy in Northwestern BC. . .	31
Barresi, T. and Dostal, J.: Geochemistry and Petrography of Upper Hazelton Volcanics: VHMS-Favourable Stratigraphy in the Iskut River and Telegraph Creek Map Areas, Northwestern BC	39
Mortensen, J.K., Wojdak, P., Macdonald, R., Gordee, S.M. and Gabites, J.E.: Regional Studies of VMS Mineralization and Potential within the Early Jurassic Hazelton Group, West-Central BC	49
Lett, R.E., Friske, P.W.B. and Jackaman, W.: National Geochemical Reconnaissance Program in Northwestern BC: Bowser Lake Regional Geochemical Survey.	61
Mihalynuk, M.G. and Friedman, R.M.: Gold and Base Metal Mineralization near Kitsumkalum Lake, North of Terrace, West-Central BC	67
Canil, D., Mihalynuk, M.G. and Charnell, C.: Heavy Mineral Sampling and Provenance Studies for Potentially Diamond-Bearing Source Rocks in the Jurassic Laberge Group, Atlin-Nakina Area, Northwestern BC .	83
Diakow, L., Nixon, G., Lane, B. and Rhodes, R.: Toodoggone Geoscience Partnership: Preliminary Bedrock Mapping Results from the Swannell Range: Finlay River–Toodoggone River Area, North-Central BC	93
Schiarizza, P. and Tan, S.H.: Geology and Mineral Occurrences of Quesnel Terrane between the Mesilinka River and Wrede Creek, North-Central BC.	109
MacIntyre, D.G. and Payie, G.: Geological Setting and Economic Potential of Gold Occurrences in the Kliyul Creek–Solo Lake Area, North-Central BC.	131
Friedman, F., Gabites, J., and Schiarizza, P.: U-Pb and K-Ar Isotopic Dates from the Beece Creek–Tatlayoko Lake Area, Southwestern BC	153
Johnston S.T. and Pyle, L.: Aley Carbonatite: A Paleozoic Iron Oxide Copper Gold (IOCG) Deposit in North-Central BC?.	159
Scheel, E., Nixon, G.T., and Scoates, J.S.: Geology of the Turnagain Alaskan-type Ultramafic Intrusive Suite and Associated Ni-Cu-PGE Mineralization, BC	167
Hora, Z.D., Langrova, A. and Pivec, E.: Contribution to the Mineralogy of the Arthur Point Rhodonite Deposit, Southwestern BC.	177
Lett, R.E. and Ronning, C.: Towards a Rock Geochemical Atlas for BC	187
ROCKS TO RICHES	
Deyell, C.L. and Tosdal, R.M.: Alkaline Cu-Au Deposits of BC: Sulphur Isotope Zonation as a Guide to Mineral Exploration	191
Greene, A.R., Scoates, J.S. and Weis, D.: Wrangellia Terrane on Vancouver Island: Distribution of Flood Basalts with Implications for Potential Ni-Cu-PGE Mineralization in Southwestern BC	209
Jackaman, W.: Spatsizi River Stream Sediment and Water Survey, Northwestern BC	221
Høy T. and Jackaman, W.: Geology of the Grand Forks Map Sheet, Southeastern BC.	225
Kilby, W.E.: MapPlace.ca Image Analysis Toolbox, BC: Phase 2	231
Logan, J.M.: Alkaline Magmatism and Porphyry Cu-Au Deposits at Galore Creek, Northwestern BC.	237
Logan, J.M. and Mihalynuk, M.G.: Regional Geology and Setting of the Cariboo, Bell, Springer and Northeast Porphyry Cu-Au Zones at Mount Polley, South-Central BC.	249
Logan, J.M. and Mihalynuk, M.G.: Porphyry Cu-Au Deposits of the Iron Mask Batholith, Southeastern BC . . .	271
Mahoney, J.B., Hooper, R.L., Gordee, S.M., Haggart, J.W. and Mortensen, J.K.: Initial Evaluation of Bedrock Geology and Economic Mineralization Potential of Southern Whitesail Lake Area, West-Central BC . . .	291
Marshall, D., Close, S., Podstawskyj, N. and Aichmeier, A.: Gold Mineralization and Geology in the Zeballos Area, Nootka Sound, Southwestern BC	301
Gordee, S.M., Mortensen, J.K., Mahoney, J.B. and Hooper, R.L.: Volcanostratigraphy, Lithochemistry and U-Pb Geochronology of the Upper Hazelton Group, West-Central BC: Implications for Eskay Creek–Type VMS Mineralization in Southwest Stikinia.	311
Shives, R.B.K.: Helicopterborne Gamma-Ray Spectrometric and Magnetic Surveys, Central BC: Status Report . . .	323
Simandl, G.J., Ferbey, T., Levson, V.M., Demchuk, T.E., Smith, I.R. and Kjarsgaard, I.: Kimberlite Indicator Minerals in the Fort Nelson Area, Northeastern BC . .	325
Simandl, G.J. and Davis, W.: Cratonic Basement in Northeastern BC: New U-Pb.	337
Simmons, A.T., Tosdal, R.M., Baker, D.E.L., Friedman, R.M. and Ullrich T.D.: Late Cretaceous Volcanoplutonic Arcs in Northwestern BC: Implications for Porphyry and Epithermal Deposits	347
Smyth, C.P.: Workshops on Multielement and Multisite Regional Geochemical Survey (RGS) Anomalies Meriting Follow-Up Work in BC	361

Geology and Mineral Occurrences of the Upper Iskut River Area: Tracking the Eskay Rift through Northern British Columbia (Telegraph Creek NTS 104G/1, 2; Iskut River NTS 104B/9, 10, 15, 16)

By D.J. Alldrick¹, J.L. Nelson¹ and T Barresi²

KEYWORDS: bedrock mapping, Eskay Creek, Eskay Rift, Hazelton Group, Stuhini Group, mineral deposits, VMS, Targeted Geoscience Initiative-II (TGI-II)

INTRODUCTION

The Eskay Creek gold-silver mine, located in northwest British Columbia, is the highest-grade precious-metal volcanogenic massive sulphide deposit in the world. The mining industry continues to spend more than \$2 million each year on exploration for similar deposits in the area. The geologic setting at the minesite is well studied, but large tracts in north-central British Columbia require more detailed surveys to determine if favourable sites exist for formation and preservation of additional deposits. In 2003, the British Columbia Geological Survey and the Geological Survey of Canada launched a two-year mapping program to delineate the ore horizon through the region north of the mine, and to assess potential for additional Eskay Creek type deposits. This horizon lies within Lower to Middle Jurassic, arc-related, rift sequence rocks along the northwest perimeter of the Bowser Basin, a large (48,000 km²) Middle Jurassic to Early Cretaceous sedimentary basin (Fig. 1).

The field portion of the project has now covered 1,300 km², extending 125 km north from the Eskay Creek mine to the Red Chris deposit (Fig. 2). The paved Stewart-Cassiar Highway (Highway 37) runs northward along the eastern edge of the map area. In 2003, the first field season, an eight-person team mapped 70 km along the rift sequence between Kinaskan Lake and More Creek (Fig. 2). In 2004, three geologists mapped 40 km along the rift sequence between More Creek and Palmiere (Volcano) Creek. Ongoing work will include compilation from published sources and completion of two final 1:50,000-scale maps and one 1:100,000-scale map, scheduled for release in 2005.

¹ British Columbia Ministry of Energy and Mines, Email: Dani.Alldrick@gems6.gov.bc.ca

² Department of Earth Science, Dalhousie University

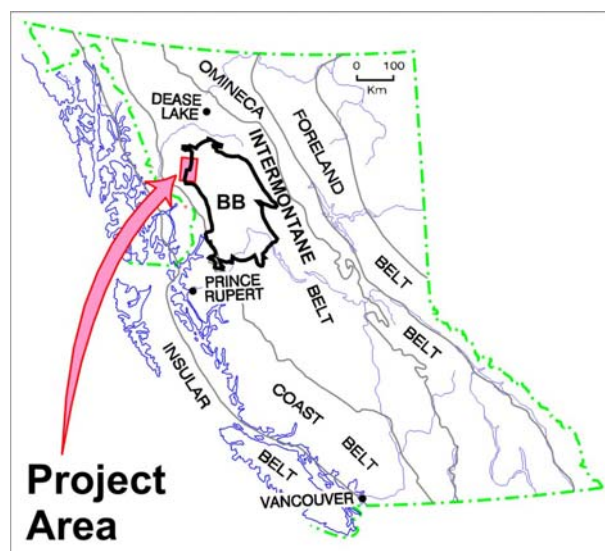


Figure 1. Project location map showing Bowser Basin (BB). Modified from Logan (2000).

The project area straddles the eastern edge of the Coast Mountains and the broad valley of the upper Iskut River. This area lies within the Tahltan First Nation traditional area and they participated directly in this project. Topography varies from rounded glacial valleys along the upper Iskut River, to the extensive Spatsizi Plateau, to high serrated ridges and peaks that are being actively glaciated. Elevations range from 250 m above sea level at the confluence of Iskut River and Forrest Kerr Creek, up to 2,662 m at the summit of Hankin Peak in the west-central region of the field area. Mount Edziza can be seen rising to 2780 m near the northern boundary of the study area. Vegetation comprises boreal spruce-pine-fir forest at low elevations. Timberline is at 1400 m elevation with subalpine fir and meadow areas above.

Regional-scale geology maps and reports for this area include Operation Stikine (1957), Souther (1972), Read *et al.* (1989), Evenchick (1991), Logan *et al.* (1990, 1992, 1993, 1997, 2000), Gunning (1996), Ash *et al.* (1995, 1996, 1997a, 1997b) and Evenchick *et al.* (2002) (Fig. 2). Detailed geological maps are available

in theses by Schmitt (1977) and Kaip (1997) and in many company assessment reports cited in ARIS and MINFILE. The most recent and most comprehensive study of the Eskay Creek orebodies is the PhD thesis by Tina Roth (2002) which offers an extensive bibliography of all previous reports on the deposit, including many progress reports and final reports that were part of the Iskut Metallogeny Project of the Mineral Deposits Research Unit at the University of British Columbia (Macdonald *et al.*, 1996).

Anderson (1993) interpreted the present study area as the northern extension of a large fault-bounded belt or rift. Sections of this rift have been mapped at 1:50,000 scale by Read (1991), Logan *et al.* (1990, 1992, 1993) and Ash *et al.* (1997b). The current project will complete 1:50,000-scale coverage between these earlier mapping projects, with more detailed mapping of the strata of the upper Hazelton Group, and detailed stratigraphic investigations within the Eskay Rift (e.g. Simpson and Nelson, 2004; Barresi *et al.*, this volume). The federal and provincial governments have jointly funded this study as part of the "Bowser Basin Energy and Mineral Resource Potential Targeted Geoscience Initiative".

REGIONAL GEOLOGIC SETTING

The project area lies on the western edge of the Intermontane Tectonic Belt, within Stikine terrane, and is bounded to the east by the Bowser sedimentary basin

(Fig. 1). It straddles the tectonic elements of the Bowser structural basin and the Stikine Arch to the northwest.

Souther (1972) and Logan *et al.* (2000) describe the geological history of the area as a series of five mid-Paleozoic to mid-Mesozoic volcanic arcs developed in sediment-poor and sediment-rich marine settings. Lulls in volcanism at the Triassic-Jurassic boundary and in the uppermost Lower Jurassic were marked by tectonic uplift, deformation and erosion, termed the Inklinian and Nassian orogenies respectively (Souther, 1972).

Strata range in age from Devonian to Holocene (Fig. 3). The major stratigraphic units exposed within the project area are the Paleozoic Stikine Assemblage, Triassic Stuhini Group, Lower to Middle Jurassic Hazelton Group, Jurassic-Cretaceous Bowser Lake Group and Pleistocene Mount Edziza Complex. The Stikine Assemblage was defined by a Geological Survey of Canada team (Operation Stikine, 1957) and has most recently been described by Logan *et al.* (2000). It consists of Early Devonian to mid-Permian volcanic and sedimentary strata, characterized by thick carbonate members. The Upper Triassic Stuhini Group typically consists of pyroxene porphyritic basalt flows and breccias with intercalated clastic sedimentary rocks and minor carbonate units. The Early to Middle Jurassic Hazelton Group is an island arc succession composed of a lower package of intermediate volcanic rocks and derived clastic sedimentary units; a middle interval of thin, but widely distributed felsic volcanic rocks; and an upper unit of fine clastic sedimentary rocks with local bimodal volcanic rocks dominated by basalt.

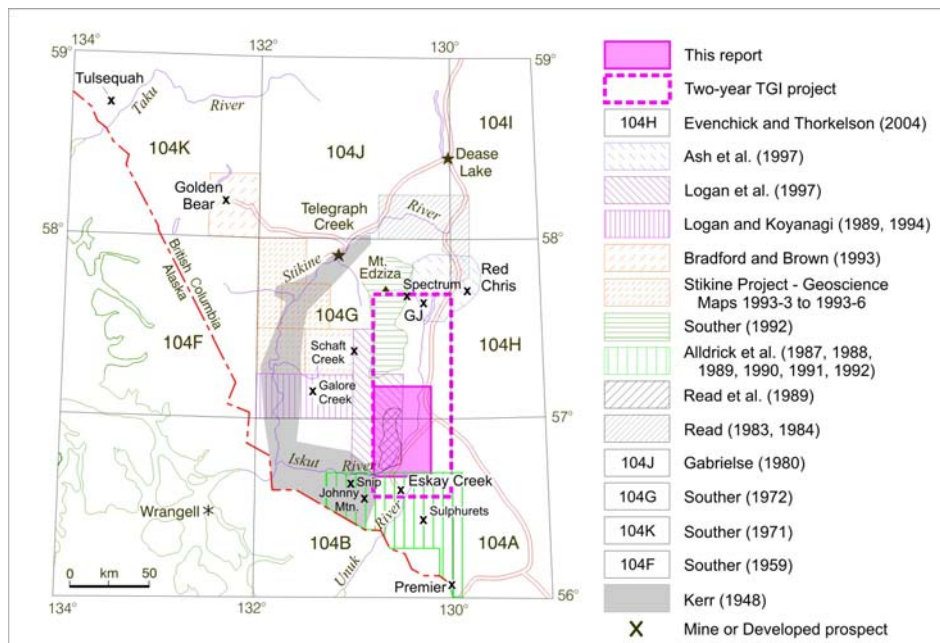


Figure 2. Current project outline and previous geologic mapping. Modified from Logan (2000).

Carbonate units are rare or absent in Hazelton Group strata. The Middle Jurassic to Early Cretaceous Bowser Lake Group is a thick, clastic marine sedimentary succession. Miocene to Recent volcanic strata from the Mount Edziza volcanic complex blanket the northwest part of the project area.

Regional-scale unconformities within the study area include a Late Permian - Early Triassic unconformity, a Late Triassic - Early Jurassic angular unconformity and nonconformity, and a late Early Jurassic angular unconformity.

Logan *et al.* (2000) describe five plutonic episodes in the area (Middle to Late Triassic Stikine; Late Triassic to Early Jurassic Copper Mountain; Early Jurassic Texas Creek; Middle Jurassic Three Sisters; Eocene Hyder). The four youngest plutonic suites generated important mineral deposits.

To the south, mid-Cretaceous regional metamorphism reached a maximum grade of lower greenschist facies (Alldrick, 1993). In the current field area, chlorite is rare to absent and prehnite is present, thus the regional metamorphic grade is interpreted as sub-greenschist, mid-prehnite-pumpellyite facies (Alldrick *et al.*, 2004).

GEOLOGY OF THE MAP AREA

Mapping in the 2004 field season covered Paleozoic to Middle Jurassic strata at the southern end of the two-year project area (Fig. 2). Several

topographic features in this year's map area have been informally named to simplify description of locations (Fig. 4). Simplified geology of the 2004 map area is presented in Figure 5. Age control is provided by fossil collections from Souther (1972), Read *et al.* (1989), Logan *et al.* (2002) and Evenchick *et al.* (2001), and by isotopic age dates tabulated in the new BCAGE database (Breitsprecher and Mortensen, 2004).

Stratified Rocks

STIKINE ASSEMBLAGE (MIDDLE TO UPPER PALEOZOIC)

Volcanic and carbonate upper Paleozoic strata of the Stikine Assemblage were mapped in this year's survey. A large tract of complexly faulted Permian, Triassic and Jurassic strata crops out immediately north of Pillow Basalt Ridge, underlying a well glaciated spine called Sixpack Range (Fig. 4 and 5). The strata are emplaced along a series of south verging thrust faults that stack Paleozoic to Jurassic stratigraphic successions into three repetitions (Fig. 5).

Stikine Assemblage rock types exposed in this area include green chloritic tuff, lapilli tuff, massive andesitic to dacitic feldspar-porphyrific flows, massive and flow-banded dacite and rhyolite, pillow basalt, tuffaceous and siliceous siltstone, ribbon chert and several thin, highly recrystallized white carbonate beds. These rocks are all interpreted to be Permian age.

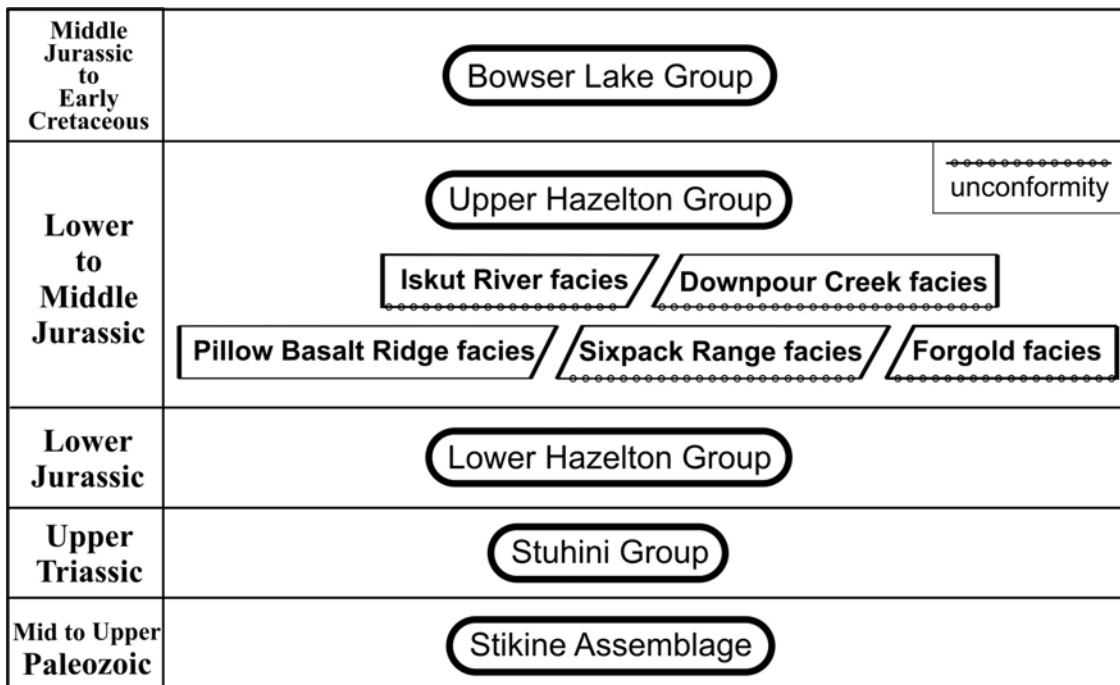


Figure 3. Schematic regional stratigraphy of the 2004 map area.

Permian strata are strongly foliated everywhere and multiple generations of foliation are apparent in most outcrops. Thin-bedded units may also show crenulations. Bedding is parallel or sub-parallel to the foliation. Some weathered outcrop surfaces in the carbonate rocks reveal sparse crinoid ossicles that are not visible on fresh surfaces of the recrystallized limestone.

Basal contacts are thrust faults. Upper contacts are commonly erosional unconformities. In one location close to Forrest Kerr Creek, pillow lavas of Early to Middle Jurassic age (?) lie unconformably upon strongly foliated Paleozoic strata.

STUHINI GROUP (UPPER TRIASSIC)

In the map area, the Stuhini Group consists of mafic to felsic (dacitic) volcanic flows; thin-bedded, interbedded black and olive green waterlain tuffs; derived clastic sediments including orange-weathering carbonate cemented sandstones; siliceous black siltstones; black and white limestone beds; and weakly pyritic black rhyolite and white rhyolite units.

Pyroxene-bearing basalts are common and typically fine-grained to weakly augite +/- feldspar porphyritic. Thick (20-30 m) massive andesitic to dacitic flow units are finely feldspar porphyritic and show faint columnar jointing in cliff-face exposures.

Extensive orange-weathering, well-sorted sandstone forms a thick stratigraphic interval that includes intercalated black siliceous siltstone, massive black and white limestone units and regionally extensive, flow-layered chert that varies from black to pale grey to white, and carries dust-size disseminated pyrite. Individual horizons within the buff- to orange-weathering sandstone host fossil wood debris.

The pyritic rhyolite units have been explored in three separate locations (Bench, Sinter and Southmore prospects) where structurally disrupted, crackled rhyolite beds are highly gossanous. Upper Triassic copper-bearing mafic volcanics exposed between 1800 to 2000 m elevation near the crest of Sixpack Range have not yet been explored (*see* Malachite Peak prospect).

On the southeast side of the Sixpack Range, these strata are cut by two small diorite and gabbro plugs and by a more extensive sill of hornblende and plagioclase porphyritic, potassium feldspar megacrystic granodiorite similar to the intrusions of the Texas Creek Suite exposed elsewhere in this region.

HAZELTON GROUP (LOWER TO MIDDLE JURASSIC)

Lower Jurassic

Strata of the Lower Hazelton Group form two belts in the northern part of the map area (Fig. 5). Northeast

of Downpour Creek, a dominantly volcanic sequence includes andesite and rhyolite flows, hematitic epiclastic siltstones, sandstones and coarse, heterolithic epiclastic conglomerates, and black siltstones. The calcareous sandstone units are favourable hosts for fossil wood debris and fossil-rich bioclastic horizons that contain ammonites and bivalves. A collection from one of these intervals contains Sinemurian ammonites (Logan *et al.*, 2000, p. 45).

A second, north-trending belt of feldspar-phyric extrusive dacites and related plagioclase (\pm Kspar) phyric granodiorite to monzonite intrusions lies along the eastern side of the Forrest Kerr fault from the headwaters of Downpour Creek to north of More Creek. As described below, numerous showings and alteration zones on the RDN claims are related to this unit, including the Marcasite Gossan and the spectacular Gossan Creek Porphyry gossan. Three U-Pb ages of 193.0 ± 1.3 Ma, 193.6 ± 0.3 Ma and 193.6 ± 1.0 Ma on both intrusive and extrusive bodies establish the age of these rocks as Late Sinemurian (Mortensen *et al.*, this volume). It is thus coeval with, but different in character from, the sequence east of Downpour Creek, giving an insight into the degree of local variability of volcanic facies in the lower Hazelton Group.

Lower to Middle Jurassic

Rocks of probable late Early Jurassic (Toarcian) to Middle Jurassic (Aalenian to Bathonian) age occur in several distinct outcrop areas located between Forrest Kerr Creek to the west, More Creek to the north, and the Iskut River to the east (Fig. 5). The different outcrop areas are described here as five different facies packages (Fig. 3 and 5) because of the pronounced variations in stratigraphy and thicknesses between them.

These units are considered to be broadly coeval (Fig. 3), although precise age controls are lacking in most areas. The Downpour Creek facies has been dated as Toarcian through Bathonian, based on macrofossils, conodonts and radiolaria (Read *et al.*, 1989; Logan *et al.*, 2000). The thick pile of pillow basalts that dominates the Pillow Basalt Ridge (PBR) facies has been correlated with the Middle Jurassic hangingwall basalt unit at the Eskay Creek mine. Similar, although much thinner, basalts crop out sporadically northwards from western PBR into the Forgold area. The Sixpack Range facies lies unconformably on Paleozoic and Triassic basement, and interfingers with and underlies the Downpour Creek facies. The Iskut River unit contains fossils dated as Middle to possibly early Late Jurassic (Collection F141, Read *et al.*, 1989). The Iskut River unit continues south and east across the Iskut River, to Iskut-Palmiere Ridge, where it overlies a basalt unit that is correlated with the hangingwall basalt at the Eskay Creek mine.

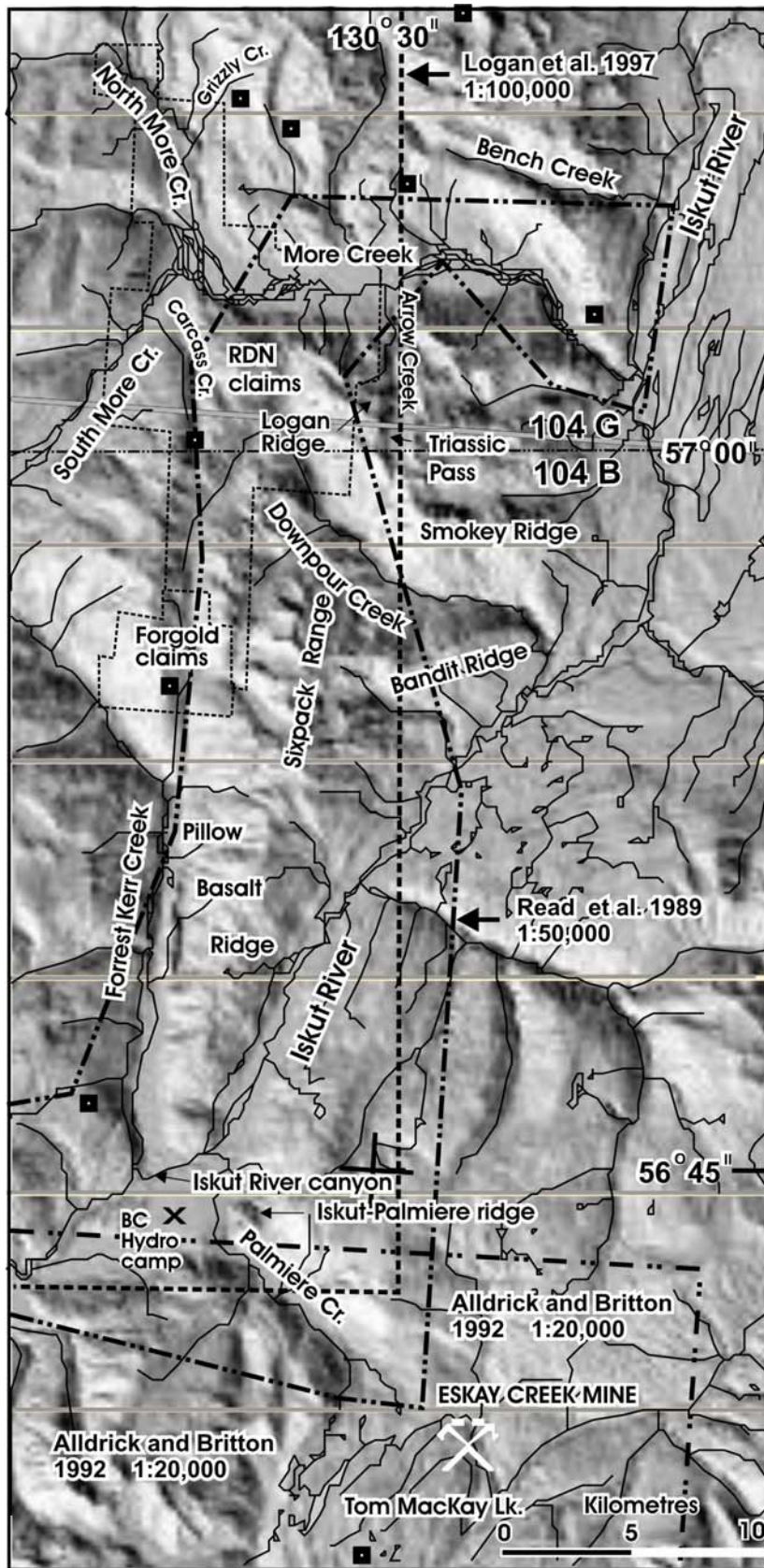


Figure 4. Shaded DEM map showing major topographic features in the 2004 map area and boundaries of previous regional mapping projects.

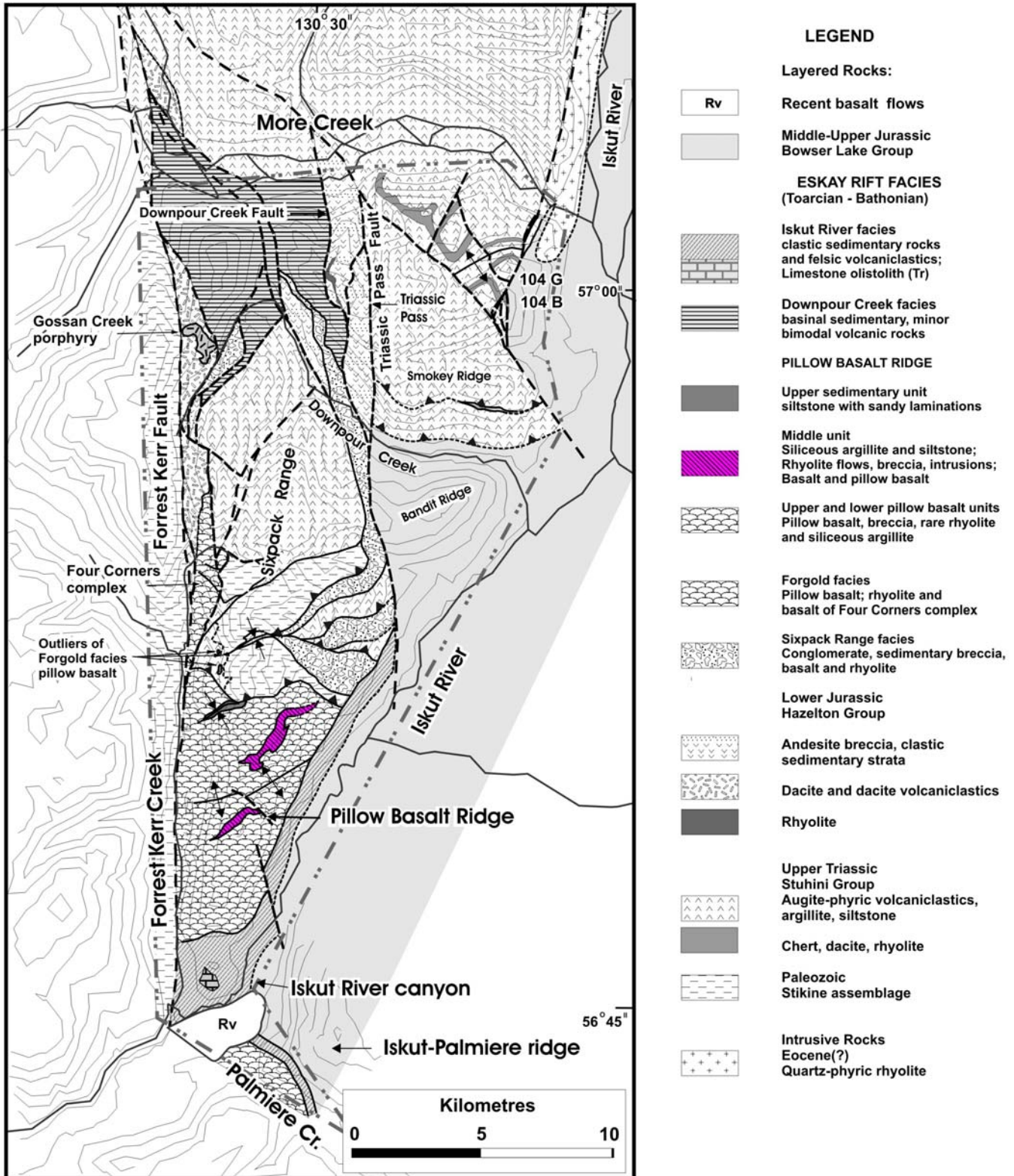


Figure 5. Simplified geologic map of the More Creek - Palmiere Creek area.

Pillow Basalt Ridge (PBR facies)

Pillow Basalt Ridge is 12 km long and 6 km wide. It is the main ridge between the Iskut River and lower Forest Kerr Creek. With the exception of overlying Iskut River unit rocks exposed at lower elevations to the east and south, the entire ridge is composed of PBR facies rocks. To the west, the Forest Kerr fault juxtaposes the PBR facies against Paleozoic rocks. To the north, the Kerr Bend fault thrusts Paleozoic, Triassic and Jurassic strata over PBR.

Features of the PBR facies are summarized here; they are fully described in Barresi *et al.* (this volume). Pillow Basalt Ridge is composed of over 2000 m of mostly pillow basalt and pillow basalt breccia. A "Middle Unit" of variable thickness within the pillow basalt sequence is composed of more than 50% mafic rock (fine- to medium-grained massive basalt and pillow basalt), rhyolite flows, domes, and breccias, and fine-grained siliceous pyritic argillite and tuff. Some individual rhyolite and sedimentary horizons within this bimodal igneous-sedimentary Middle Unit can be traced for at least 3 km along strike.

The voluminous volcanic rock and large regional extent of the Pillow Basalt Ridge facies suggests deposition within a major Middle Jurassic rift segment, similar to that of Table Mountain, located to the north (Alldrick *et al.*, 2004; Simpson and Nelson, 2004). The discovery of the bimodal igneous/sedimentary Middle Unit within the PBR facies indicates that significant intervals with potential to form and preserve Eskay Creek-style mineralization may be present within extensive, less prospective pillow basalt sequences throughout the length of the Eskay rift.

The PBR facies is overlain by two separate units: the Iskut River facies, described in the following section; and a homogeneous, siltstone-dominated unit that occupies the core of a small northeast-trending syncline next to the Kerr Bend fault (Barresi *et al.*, this volume). In the syncline, a transitional contact is observed. Pillow basalts interfinger with sand-laminated siltstone and limy siltstone fills inter-pillow interstices. The sedimentary rock types within this unit, and the nature of its contact with the PBR basalts, are in strong contrast to the Iskut River unit.

Iskut River unit

The Iskut River unit overlies the PBR facies in the lowlands along the west side of the Iskut River (Fig. 5), east and downslope of the crest of Pillow Basalt Ridge, and on the low hill south of Pillow Basalt Ridge and extending into the Iskut River Canyon near the old BC Hydro camp (Fig. 4). Correlative strata occur on the Iskut-Palmiere Ridge, where they lie depositionally between basalt assigned to the Eskay hangingwall unit, and basal strata of the Bowser Lake Group. A fossil age for this unit, from samples collected along the Iskut River canyon, is Middle Jurassic or possibly early Late

Jurassic (Collection F141; H.W. Tipper in Read *et al.*, 1989), making it one of the younger units in the Lower-Middle Jurassic Eskay Rift sequence.

Downhill and east of Pillow Basalt Ridge, the Iskut River unit consists of mixed siliciclastic and felsic volcanic strata, with a preponderance of coarse clastic material. The felsic rocks are mostly light green to pale grey volcanoclastics, rhyolite and dacite breccias, and fine crystal-dust tuffs. One outcrop ridge of massive rhyolite was located in the course of two traverses in the area; it is likely that more could be identified with further detailed work. The siliciclastics comprise interbedded white arkosic sandstone, sedimentary breccia, quartz-feldspar granule conglomerate and dark grey silty argillite. In some areas, thinly interbedded sandstone and argillite resemble the Bowser Lake Group. They are distinguishable, however, based on the presence of felsic detritus and the absence of chert clasts in the sandstones, and on the presence of interbeds of felsic volcanoclastic material. In other exposures, bedding is uneven and soft-sediment deformation features and sedimentary intraclasts are present. A notable feature of this sequence is the common occurrence of large felsic volcanoclastic olistoliths as well as small white, pale green and bright sea-green felsic clasts within sedimentary breccias. They show irregular, wispy outlines indicative of incorporation in the matrix while still unconsolidated. Felsic detritus decreases in abundance northward. North of Pillow Basalt Ridge (north of the Kerr Bend fault), the sequence consists of a thick, cliff-forming unit of white arkosic sandstone overlain by dark grey slate that extends east as far as the Iskut River.

South of Pillow Basalt Ridge, the Iskut River unit is dominated by dacitic volcanoclastic material, with subordinate black argillite and other rock types. The felsic breccias are chaotic and unsorted. Clasts range in size up to olistoliths many metres across. All clasts are angular. Concentrations of coarser clasts show incipient fragmental (crackle breccia) to disaggregated (mosaic breccia) textures. Pulverised, fine-grained, sand-sized material occurs as both the clast component with an aphanitic groundmass, and as the groundmass component to larger clast populations. The source volcanic rock, as seen in clasts, is pale green, aphanitic to porphyritic dacite with small, sparse feldspar crystals. Massive dacite is rare. One outcrop of black, flow-banded rhyolite was noted. Its contact relationships are unknown, it could be either a local flow or a large block within the breccia.

Read *et al.* (1989) show a single outcrop of limestone at the base of the felsic unit on the south slope of Pillow Basalt Ridge from which they extracted Early Permian conodonts (collection F129). This limestone is an olistostromal block surrounded by felsic breccia matrix. Other smaller limestone exposures occur within the felsic breccia. The nearest present exposures of Early Permian limestone are 4 km west of Forrest Kerr

Creek, and 10 km to the north within the uplifted block of Paleozoic rocks north of the Kerr Bend fault.

The hill immediately south of Pillow Basalt Ridge, and immediately northeast of the mouth of Forrest Kerr Creek is underlain by basalt, andesite and dacite flows or tuffs and mixed sedimentary rocks, and is intruded by small diorite and gabbro plugs. This strata is cut by a recent volcanic chimney south of the hill's summit area, where a small circular lake fills the vent. Carbonates on this hill have given Triassic conodont ages (Collection F138, Read *et al.*, 1989); they could be olistostromes like the Paleozoic body described above.

North of Palmiere (Volcano) Creek, a thin unit of felsic volcanoclastics and argillite crops out in the saddle between the main high ridge to the northeast and the small spur that overlooks the lower Iskut River Valley to the west. The lower part of this unit consists of chaotic, unsorted felsic breccia similar to the breccias of the Iskut River unit exposed at the south end of Pillow Basalt Ridge. The source rock is a pale grey-green to white, aphanitic to microporphyrific dacite or rhyolite. Clasts of medium-grained granodiorite are also present in the breccia. Most common are angular-clast breccias and crystal-dust tuffs, all without visible bedding. Rhyolite mosaic breccia with a black, siliceous matrix is present in places. The felsic breccias are overlain transitionally by black, siliceous, pyritic argillite which hosts the Iskut-Palmiere mineral occurrence. Beds of felsic breccia and individual felsic clasts occur within the basal part of the argillite. All these rocks overlie basalt, which is correlated with the Eskay hangingwall unit and the PBR basalts, and these rocks are overlain in turn by sandstones and mudstones of the Bowser Lake Group.

The Iskut River unit overlies the pillow basalts and siliceous siltstones of Pillow Basalt Ridge facies with angular discordance, truncating units in the gently folded underlying sequence. A strong set of northeasterly topographic linears on southeastern PBR, interpreted as flow-layering between separate eruptions of pillow basalt, is deflected northwards towards the base of the Iskut River unit. The Kerr Bend fault does not penetrate the base of the Iskut River unit. North of the fault, Iskut River unit arkose overlies rocks of the hangingwall strata of the Kerr Bend fault. The upper contact of the Iskut River unit with the Bowser Lake Group was not observed during this study.

The Iskut River unit exhibits a marked departure in volcanic and sedimentary regime from the underlying PBR facies. Quiet basalt effusion was succeeded by explosive felsic, mainly dacitic volcanism, while the pelagic, distal sedimentation associated with PBR was succeeded by coarse siliciclastic sedimentation in the Iskut River unit. Steep slopes are indicated by coarse grain sizes, synsedimentary deformation, and olistoliths sourced from both felsic breccias within the sequence, and from Paleozoic and Triassic limestones and possibly other strata from within the basement. Its

unconformable relationships with the PBR rocks and with the Kerr Bend fault suggest that it postdated thrust displacement on the fault. Thus the Iskut River unit marks a profound change in basin geometry, with renewed uplift of rift margins, fault reactivation and the development of new fault patterns.

Forgold facies and the Four Corners complex

The Forgold facies, which hosts the Four Corners volcanic complex, is located east of Forest Kerr Creek, and south of the headwaters of Downpour Creek. It is a north-south elongated, fault-bounded segment of mainly volcanic rock, inferred to be Middle Jurassic rift-related strata (pending U/Pb dates). The main Forest Kerr fault to the west, and a splay of the Forest Kerr fault to the east, juxtapose the Forgold facies units with Paleozoic, Triassic and Lower Jurassic units. To the south, basalts of the Forgold facies lie in unconformable contact on Paleozoic and Triassic strata, exposed in a waterfall as remnant patches of undeformed pillow basalt resting on highly deformed basement. At the northernmost extent of the Forgold facies, on the eastern side of Downpour Creek's headwaters, pillow basalts lie in unconformable contact on Lower Jurassic strata to the west and in faulted contact with Triassic strata to the east.

Overall, the volcanic and sedimentary rocks of the Forgold facies are similar to those of Pillow Basalt Ridge. In contrast to Pillow Basalt Ridge, the Forgold facies is dominated by a local felsic volcanic centre (the Four Corners complex) which is similar to, but larger than, the volcanic complexes found in the Middle Unit of the Pillow Basalt Ridge facies. With the exception of the Four Corners felsic volcanic complex, the Forgold facies is composed of aphanitic, rarely vesicular, pillow basalt, pillow basalt breccia, and rare flow-banded basalt.

The Four Corners complex is a volcanic centre composed of intrusive and extrusive felsites and fine- to medium-grained basalt, with overlapping pillow basalts and fine, siliceous sedimentary rock. The structural orientations of sedimentary and layered volcanic rocks on and around the dome are largely controlled by the paleotopography of the dome. The core of the dome is composed of feldspar-phyric felsic rock (Fig. 6a) that is crosscut by 1 to 3 m thick aphanitic and feldspar phyric, flow-banded rhyolite dikes, and sets of medium-grained diabase (basalt) dikes. Near the core of the dome, the contacts between felsic and mafic dikes, and between the dikes and the surrounding dome, are amoeboid (Fig. 6b), indicating that they are magma-mixing textures developed between coeval intrusions. The flanks of the dome are composed of 1 to 5 m thick, layered rhyolite flows with interbedded layers of siliceous sedimentary rocks, massive basalt flows and pillow basalt flows. All are crosscut by rhyolite dikes. Overlying the felsic dome are a decreasing proportion of coarse-grained, massive basalt and fine-grained rhyolite flows, and an increasing proportion of pillow basalt flows. Felsic

A)



B)



Figure 6. A) Rhyolite intrusion in the centre of the Four Corners complex. B) Detail of irregular contacts between felsic and mafic dikes in the complex, indicating coeval emplacement.

dikes are less common. Basalt that erupted above the felsic dome was likely superheated, as suggested by the presence of fire fountain deposits.

The suite of rocks that comprise the Four Corners complex and immediate surrounding area is similar to that found in the Middle Unit of the Pillow Basalt Ridge facies. Felsic rocks include aphanitic white and cream weathering, flow-banded rhyolite with semi-translucent fresh surfaces; and white to salmon weathering feldspar-phryic rhyolite. These are accompanied by medium-grained basalt that has characteristic radiating feldspar microlites (first described near the Eskay Creek mine by Lewis *et al.* [2001]) and, in places, a distinctive glomeroporphyritic texture of feldspar and/or pyroxene. On the flanks of the dome, these rocks are extrusive, and take the form of breccias and flows. In one location, a breccia of toppled columnar-jointed basalt is preserved. Onlapping sedimentary rocks are rusty weathering, siliceous, pyritic, fine-grained, dark grey to black mudstones and/or tuff and/or chert. They are bedded on a 1 to 15 cm scale and have sharply eroded upper contacts. Some beds have spherical, white weathering crystals up to 1 cm in diameter, similar to prehnite found in the mudstones at Eskay Creek mine and on Pillow Basalt Ridge (Ettliger, 2001; Barresi *et al.*, this volume).

The Forgold facies is fault bounded. Consequently its relationship to other rift fragments is uncertain. The facies bears a strong resemblance to that of Pillow Basalt Ridge, and may represent a narrower northern extension of the rift basin that accommodated the Pillow Basalt Ridge facies. Alternatively it may be an independent rift fragment. The unconformable contact between this facies and underlying Upper Paleozoic, Upper Triassic and Lower Jurassic strata suggests that it was deposited on a block of these strata which had already undergone significant uplift and erosion.

Sixpack Range facies

Strata of the Upper Hazelton Group crop out extensively on the eastern slopes of Sixpack Range, extending from the Kerr Bend fault in the south to Downpour Creek in the north.

The basal units are well exposed immediately north of Kerr Bend fault. The basal talus breccia (Fig. 7a) is overlain by a thick (>500 m) interval of massive crystalline basalt flows cut by rare white rhyolite dikes, sills and flows. Towards the top of this thick mafic volcanic interval, these rocks are progressively interlayered with overlying monolithic to heterolithic volcanic breccias, conglomerates and sandstones. These thick sequences of volcanic sandstones and granule to pebble conglomerates consist predominantly of felsic volcanic clasts. Locally, clast composition varies and can include up to 20% limestone clasts, up to 25% hornblende-plagioclase porphyritic potassium feldspar megacrystic granodiorite clasts, or up to 10%

black siltstone clasts. Local concentrations of scattered clasts of pyritic siltstone produce weakly gossanous weathered surfaces. Sandstones locally display graded bedding and good cross-bedding (Fig. 7b and 7c). Intercalated rock units are grey to black limestone, black siltstone, a single minor rhyolite flow, and minor sills and dikes of rhyolite and hornblende-plagioclase porphyritic potassium feldspar megacrystic granodiorite.

At its southern limit, the base of this stratigraphic unit is a thick talus breccia of predominantly carbonate clasts, that rests unconformably above foliated Permian carbonate rocks. The talus breccia evolves in character moving away from the Permian footwall rocks, changing from monolithic carbonate breccia, to heterolithic, volcanic-dominated breccia to coarse, well-bedded to cross-bedded sandstones and grits. These in turn are overlain by the thick succession of massive basalt flows.

Elsewhere the basal contact of the Jurassic strata is an unconformity, overlying Triassic or Permian footwall rocks (Fig. 7d). Where exposed, the upper contact for this strata is a thrust fault contact, with overlying Permian or Triassic rocks in the hangingwall.

Downpour Creek facies

The Downpour Creek facies is exposed north of Downpour Creek on both sides of the pass that separates Downpour Creek from More Creek. To the west, rocks of this facies are cut off by the Forrest Kerr fault. Their eastern limit is the north-striking Downpour Creek fault that juxtaposes them against Lower Jurassic strata (Fig. 8a).

These rocks were previously mapped by Read *et al.* (1989) and Logan *et al.* (2000). Remapping in 2004 has led to a modified structural interpretation and revised stratigraphic context. The Downpour Creek facies is dominated by fine-grained clastic rocks, with less than 10% basalt, diabase, gabbro, and felsic volcanic and intrusive rocks. Clastic rocks are dark grey to black argillite with minor thin beds of orange-weathering ankeritic siltstone and sandstone, and rare granule to pebble conglomerate (Fig. 8b). Laminated siliceous siltstone beds become more common in the higher parts of the sequence, whereas coarser interbeds become more rare.

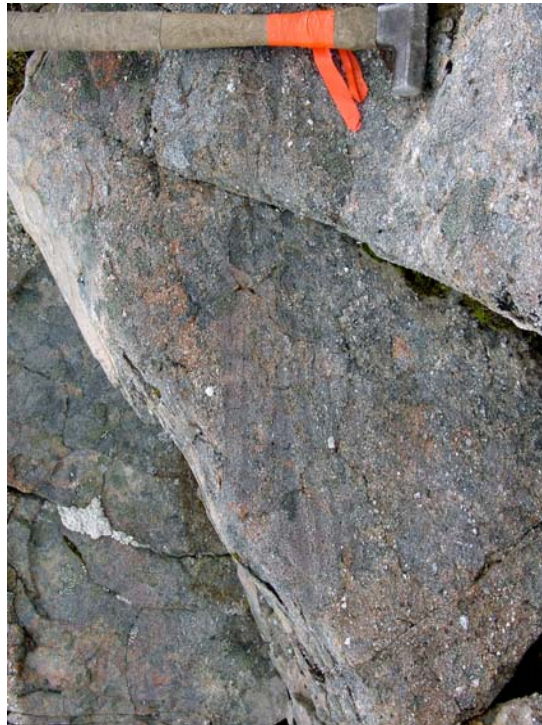
A variety of volcanic rock suites are exposed in this facies. Lenticular pillow basalt flows, black matrix rhyolite breccia, and cobble conglomerate are present within the thick sedimentary sequence. In addition, the ridgetops to the west and northwest of Downpour Creek are capped by volcanic and intrusive rock. The resistant igneous caprock mapped by Logan *et al.* (2000) includes Lower Jurassic and Middle Jurassic volcanic sequences as well as mafic intrusive bodies. The Lower Jurassic volcanic sequences, like those in the Middle



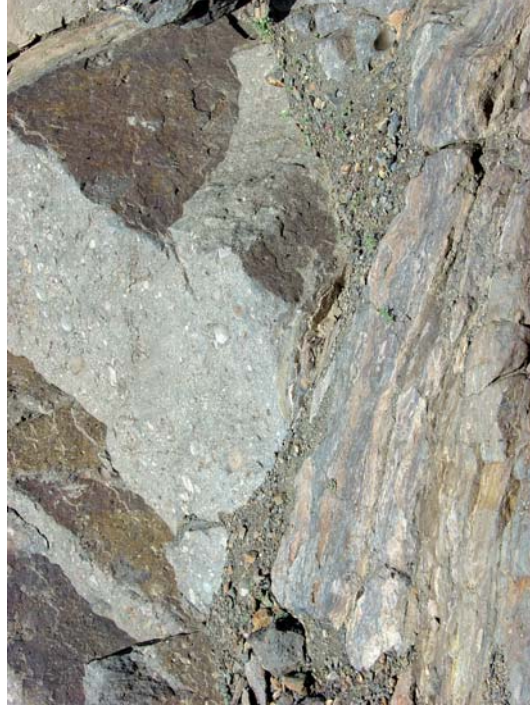
A.



B.



C.



D.

Figure 7. Mid-Jurassic Sixpack Range facies exposures. A. Polymictic talus breccia. B. Graded bedding in granule conglomerate. C. Crossbedding in pebble conglomerate D. Basal unconformity showing polymictic conglomerate overlying well-foliated Paleozoic Stikine Assemblage tuffs.

Jurassic, have pillow basalts and rhyolites, but also contain varied volcanoclastic rocks including volcanic conglomerates and ash and lapilli tuffs. Complicating the volcanic stratigraphy in this area are stocks of diabase and gabbro that have the same radiating microlites and glomeroporphyritic textures as the extrusive Middle Jurassic basalt mapped at Pillow Basalt Ridge, the Four Corners complex, and the Sixpack Range.

The internal stratigraphy of the Downpour Creek facies is not completely understood. Fossil collections are reported from this unit by Souther (1972), Read *et al.* (1989) and Logan *et al.* (2000). Along the ridgecrest west of the pass between Downpour and More creeks, Late Toarcian conodonts occur at two sites (Read *et al.*, 1989); however, Logan *et al.* (2000) report Bathonian macrofossils from the same area. Further north, Logan *et al.* (2000) collected an Aalenian ammonite. Souther (1972) lists Middle Bajocian macrofossil collections east of the pass. Structures in the Downpour Creek area are complex, involving tight folds and multiple fault strands that significantly modify the single syncline inferred in Logan *et al.* (2000).

On the eastern side of Downpour Creek, fine-grained sedimentary beds of the Downpour Creek facies overlie coarse polymictic conglomerates of the Sixpack Range facies in a gradational, interfingering contact. A similar relationship can be inferred several kilometres to the southwest near the headwaters of Downpour Creek, in spite of extensive fault slivering. There, conglomerates are accompanied by monolithologic, chaotic, volcanic-derived debris-flow breccias and minor basalt flows like those seen farther south in the Sixpack Range. East of Downpour Creek, the conglomerates are relatively thin and overlie plagioclase-phyric volcanic rocks correlated with the lower Hazelton Group (Fig. 8b). Based on these observations, the Sixpack Range facies is interpreted as a basal conglomerate to the finer-grained Downpour Creek facies, and as its more southerly, coarse-grained, more proximal equivalent.

Lower – Middle Jurassic facies summary

The units described above illustrate pronounced facies variations in time and space that characterize the late Early to early Middle Jurassic rift environment between the Eskay Creek mine and More Creek.

Pillow Basalt Ridge facies is a 2000 m thick basaltic sequence with a prominent interval in which rhyolites and rhythmically bedded, siliceous, pyritic siltstones are also important. The PBR basalt, which thins dramatically southwards towards the Eskay Creek mine, is overlain by coarse siliciclastic and felsic breccia deposits of the Iskut River unit, which indicates major felsic volcanic eruption and rapid erosion. This unit records a higher energy depositional environment that developed prior to the onset of Bowser Lake Group

sedimentation. By contrast, in the syncline on northwestern Pillow Basalt Ridge, only black argillite interfingers with the uppermost PBR basalts, indicating a more quiescent part of the basin.

The massif north of the Kerr Bend fault contains two distinct facies (Fig. 9). On its eastern side, facing the Iskut River, conglomerates, debris-flow breccias, rhyolites and basalts of the Sixpack Range facies unconformably overlie deformed Paleozoic and Triassic basement. To the west, north of the Kerr Bend fault on the slopes facing west over Forrest Kerr Creek and its northern tributary, thin sediment-free pillow basalt outliers of the Forgold facies unconformably overlie the same basement. These sub-Middle Jurassic unconformities on rocks as old as Paleozoic are unique within the Eskay rift system: everywhere else, the base of the sequence ranges from conformable on slightly older Jurassic strata to an unconformity on Upper Triassic or Lower Jurassic basement.

The relationships between these two facies, north of Kerr Bend fault, to each other and to the Pillow Basalt Ridge facies are not well understood. Clasts in the polymictic conglomerates are correlated with Paleozoic and early Mesozoic rocks in the core of the uplift and with quartz-plagioclase-potassium feldspar porphyry intrusions that are known to occur both in the core of the uplift and to the northwest, along the northern tributary of Forrest Kerr Creek. It seems reasonable to derive these conglomerates from the west. If so, the lack of a basal conglomerate below the pillow basalts on the west side of the Sixpack Range must be explained. A possible scenario is that this area was initially exposed subaerially and eroded, and later became a north-trending rift basin.

Both of these facies are juxtaposed abruptly with the thick, monotonous pillow basalt pile south of the Kerr Bend fault (Fig. 3 and 9). The base of the PBR facies is not exposed. It is not known whether it has a basal conglomerate like the Sixpack Range facies to the northeast, or whether the pillow basalts lie directly on older basement as seen to the northwest.

Facies relationships northwards into the Downpour Creek area are clearer. The coarse, proximal Sixpack Range facies passes northward into basinal sediments and lesser bimodal igneous rocks of the Downpour Creek facies (Fig. 9). The northernmost basalts of the Forgold facies unconformably overlie Lower Jurassic dacites in the headwaters of Downpour Creek, just southwest of the proximal to distal transition in the clastic strata. These basalts are over 200 m thick and have no associated sedimentary strata, like those along strike to the south in the western hangingwall strata above the Kerr Bend fault.

The following scenario integrates the various facies packages (Fig. 3 and 9). The Sixpack Range proximal clastic facies is probably oldest, since it in part underlies the Late Toarcian and younger Downpour Creek basinal



A.



B.

Figure 8. Mid-Jurassic Downpour Creek facies exposures. A. View eastward to the fault contact of black, carbonaceous Downpour Creek facies argillite and siltstone against Lower Jurassic rhyolite on Logan Ridge, east of the Downpour Creek fault. B. Looking northwest towards the pass between Downpour Creek and More Creek. Downpour Creek facies argillites in foreground with thin ankeritic sandstone beds overlie ankeritic lower Hazelton Group volcanics. Topographic linears in background are fault strands related to the main Downpour Creek fault.

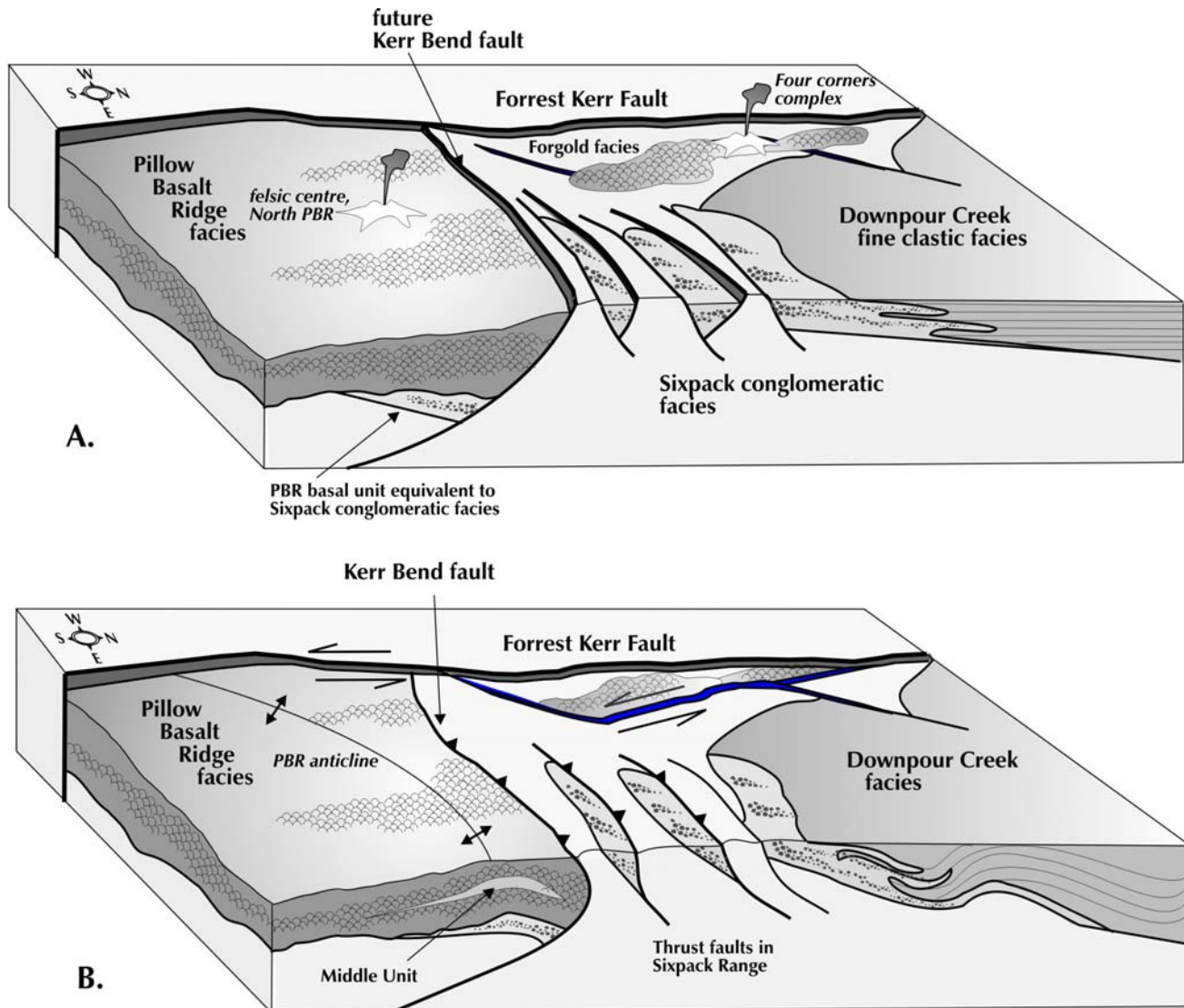


Figure 9. Cartoon block diagrams of map area - view from southeast. Shows the relationships between different mid-Jurassic facies: A. In their inferred syn-rift structural context, and B. during later sinistral shear and basin inversion.

facies. We infer that these two clastic facies were deposited on the eastern and northern flanks of a horst within the Eskay rift system, now preserved as the Paleozoic-Triassic uplift in the core of the Sixpack Range. The horst could have been an elongate, north-tilted block with steepest scarps along its southeastern margin near the present Kerr Bend fault where the coarsest conglomerates and breccias occur. We also infer that the adjacent graben to the immediate south of this scarp filled first with clastic detritus from the north, and later became the site of eruption for the voluminous PBR pillow basalts. The absence of a basal conglomerate in the Forgold facies and Four Corners complex suggests that these volcanic rocks were erupted at a still later stage, as faulting and uplift waned and the exposed highlands were drowned.

The Kerr Bend fault separates two distinctive Middle Jurassic facies - a thick pile of basalts to the south versus a clastic-dominated package to the north

(Fig. 9). Thrust faults that demarcate abrupt facies and thickness changes may be remobilized original growth faults (McClay *et al.*, 1989). As shown in Figure 9, the locus of the present Kerr Bend fault is interpreted as a remobilized graben-bounding fault which separated the Sixpack Range horst from an adjacent graben to the south. The Kerr Bend fault corresponds roughly in position and orientation to the precursor normal fault. Read *et al.* (1989) inferred 2.5 km of post-Middle Jurassic displacement on the Forrest Kerr fault, based on offsets of the northeast- to east-northeast-trending faults and folds such as the PBR anticline. These features, which are only developed near the Forrest Kerr fault, can be related kinematically to sinistral transcurrent motion along it (Fig. 9 and 10).

The change in kinematics to sinistral transpression first steepened the original fault surface, and then overturned it to the south. Continued thrust motion on this fault would have obscured any basal clastic facies

rocks on the southern (PBR) side, by burying them in the footwall.

Since deposition of the Iskut River unit likely post-dates the last movement on the Kerr Bend fault, its Middle to early Late Jurassic fossil age constrains the episode of sinistral motion on the north-trending Forrest Kerr fault and related deformation of the PBR facies to a time immediately after the formation of the Eskay Creek orebodies. Renewed high relief created by offsets on the Forrest Kerr and Kerr Bend faults could account for the high energy sedimentary environment in the unit and gravity transport of olistoliths into the basin. This model is revisited in the discussion of structure in the area.

BOWSER LAKE GROUP

Strata of the Middle to Upper Jurassic Bowser Lake Group overlap the older volcanic sequences along the eastern part of the study area and have been most recently mapped by Evenchick (1991) and Ricketts and Evenchick (1991). To the east, stratigraphy and nomenclature for the Bowser Lake Group in the Spatsizi River map sheet (NTS 104H) have been wholly revised and updated (Evenchick and Thorkelson, 2005).

Regionally, the basal contact of the Bowser Lake Group grades upward from the upper sedimentary strata of the Salmon River Formation (Spatsizi Formation) of the underlying Hazelton Group. The Middle Jurassic boundary between these similar sedimentary packages roughly coincides with the Bajocian-Bathonian transition at 166 Ma.

Anderson (1993) describes the lowest units within the Bowser Lake Group as thin- to thick-bedded, fine- to coarse-grained siliciclastic rocks including turbiditic shale, siltstone, greywacke, fine- to medium-grained sandstone and rare conglomerate. Anderson cautions that these units are indistinguishable in the field from similar rock types at the top of the underlying Salmon River Formation of the Hazelton Group.

Evenchick (1991), mapping in the current study area, correlated black siltstone, fine-grained sandstone and minor to large proportions of chert pebble conglomerate with the Ashman Formation of the Bowser Lake Group. Evenchick and Thorkelson (2005) note that the Hazelton Group - Bowser Lake Group contact is gradational, however, they place the boundary where thin, white-weathering tuffaceous laminae, typical of the upper Spatsizi Formation (Salmon River Formation), are no longer present in black siltstones.

Bowser Lake Group strata are well exposed along Bandit Ridge, an east-trending ridge immediately southwest of the mouth of Downpour Creek. The western contact of this unit is an east-dipping fault against older strata of the Sixpack Range facies. Sedimentary strata of the Bowser Lake Group are highly contorted and disrupted within 500 m of this fault con-

tact. Within this zone, pebble conglomerate units correlated with the Ashman Formation of the Bowser Lake Group display stretched pebbles with length to width ratios of 4:1. For the next 4 km to the east, Bowser Lake Group rock types include a thick, highly folded and faulted succession of siltstone, mudstone, sandstone and rare thin limestone beds.

MOUNT EDZIZA VOLCANIC COMPLEX

The Late Cenozoic Mount Edziza volcanic complex blankets an area of 1,000 km², including part of the northwest corner of the project area. The complex is comprehensively described and illustrated in Geological Survey of Canada Memoir 420 (Souther, 1992). Volcanic rocks range in age from 7.5 Ma to 2 Ka. The complex comprises alkaline basalt and hawaiite with lesser intermediate and felsic volcanic flows, and records five major cycles of magmatic activity.

Intrusive Rocks

STIKINE SUITE

Middle to Late Triassic tholeiitic to calcalkaline granitoid plutons of the Stikine Suite intrude Stuhini Group volcanic and sedimentary strata in this region and are interpreted as comagmatic intrusions (Logan *et al.*, 2000). Examples are the small stocks of diorite and gabbro mapped near the south end of the Sixpack Range.

COPPER MOUNTAIN PLUTONIC SUITE

Small ultramafic stocks of the Late Triassic to Early Jurassic Copper Mountain Suite (Logan *et al.*, 2000) are distributed throughout this region, but have not been noted in the present map area.

TEXAS CREEK PLUTONIC SUITE

A variety of fine- to medium-grained, commonly porphyritic, leucocratic intrusive rocks found in the map area are correlated with the Early Jurassic Texas Creek Suite (Logan *et al.*, 2000). The intrusions appear as simple stocks or as clusters of anastomosing dikes. Intrusions of this suite are important regional loci for porphyry copper-gold, transitional gold, and epithermal gold-silver deposits. In the 2004 map area, a string of small stocks of this age trend northward along both sides of the Forrest Kerr fault (Fig. 5).

THREE SISTERS PLUTONIC SUITE

Fine- to medium-grained equigranular diorite stocks and a small medium-grained gabbro plug cut Lower to Middle Jurassic strata to the northwest of northern Downpour Creek. These plutons are assigned to the Middle Jurassic (179-176 Ma) Three Sisters Suite defined by Anderson (1983).

HYDER PLUTONIC SUITE

The Eocene Hyder Suite forms the eastern margin of the Coast Crystalline Belt to the west of the study area. This continental-scale magmatic event is recorded within the map area by a series of north-trending, fine-grained to aphanitic rhyolite dikes first identified by Souther (1972). One of these north-trending dikes intrudes Triassic strata north and south of the mouth of More Creek (Fig. 5). These intrusions are likely feeders to overlying felsic flows that have been subsequently eroded.

Structure

The large-scale structural framework of the area is dominated by north-striking faults of regional significance (Fig. 5 and 10). The Forrest Kerr fault is the most prominent of these, with a mapped strike length over 50 km, east-side-down throw of more than 2 km and post-mid Jurassic sinistral displacement of more than 2.5 km (Read *et al.*, 1989). It has a number of splays. Some of them bound blocks of mid-Jurassic exposures near the Four Corners complex. Another significant set of fault splays deflects northeastward into

the headwaters of Downpour Creek and includes the north-striking Downpour Creek fault, which appears to be cut off by the Triassic Pass fault. Both the Downpour Creek fault and the Triassic Pass fault have down-to-the-west stratigraphic throws, opposite to that on the Forrest Kerr fault. Their northern extensions are inferred to turn northwestward and merge with the main Forrest Kerr fault somewhere along the north branch of More Creek. To the south, the Downpour Creek fault may extend along the eastern side of Pillow Basalt Ridge roughly along the outcrop belt of the Iskut River unit (Fig. 5 and 10). Overall, the fault pattern is one of anastomosing, braided strands typical of a regional transcurrent fault system.

The main strand of the Forrest Kerr fault crosses the pass at the head of Carcass Creek on the RDN property between the Downpour Creek and More Creek drainages. It is expressed as a zone of finely comminuted, highly altered fault breccia.

Field relationships show that motion on the Forrest Kerr fault system accompanied as well as post-dated mid-Jurassic bimodal igneous activity. Detailed mapping of strands of the Forrest Kerr fault located east of the main fault near the Four Corners complex showed

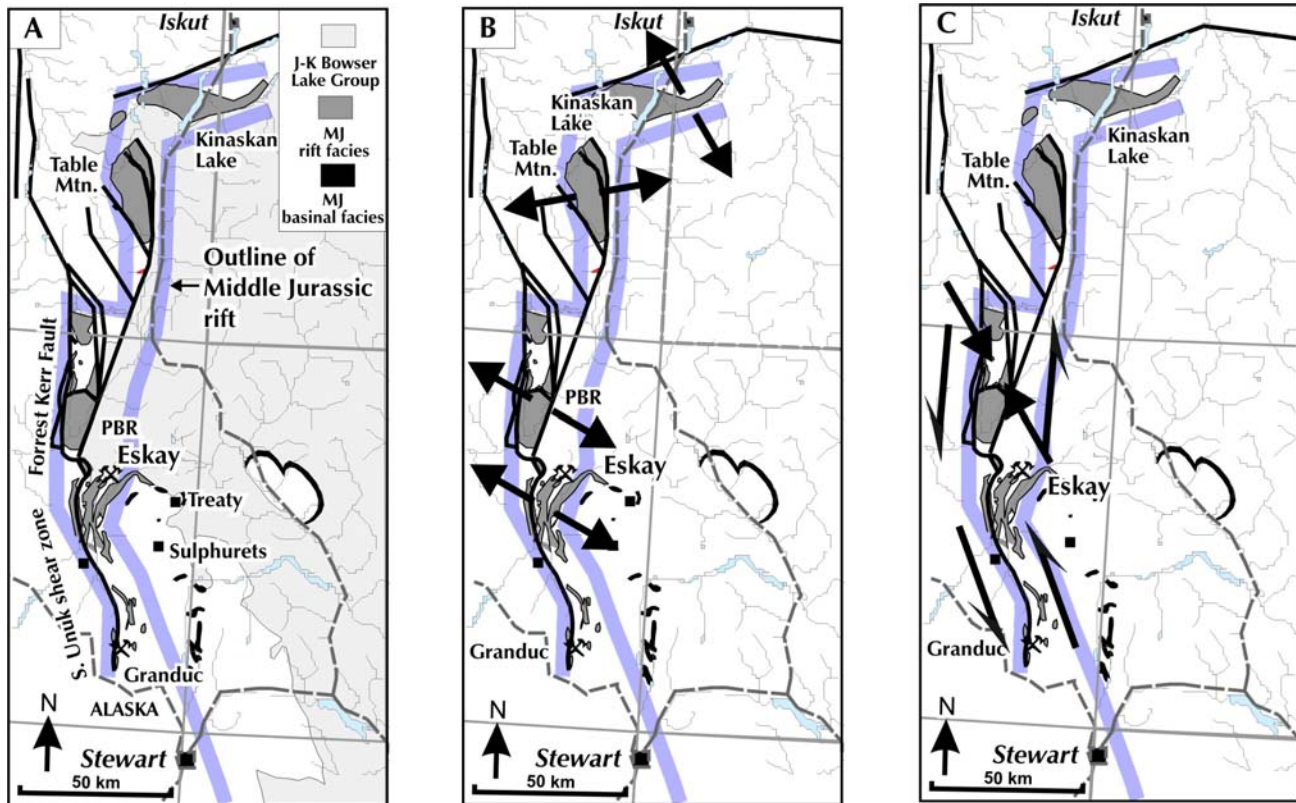


Figure 10. Cartoon regional structural history of west-central Stikinia in mid-Jurassic time. A. Present faults and outcrop areas of mid-Jurassic strata. B. Circa 180 to 174 Ma, the extensional rift regime that gave rise to the bimodal volcanic and related sedimentary sequences. Orientations of tensional features such as dikes and feeder zones suggests straight-on extension in northern part of the belt, and a slight dextral transtensional component in the south, with northeasterly extension. C. Circa 172 to 167 Ma, sinistral strike-slip regime imposed on the pre-existing rift system gives rise to northeasterly compressional features within it.

them to be zones of intense deformation tens of metres wide over a minimum strike length of 2 km. They consist of fault breccia with black argillite matrix probably derived from Triassic strata that crop out nearby. Clasts include disrupted siltstone beds from within the argillite, and exotic fragments such as basalt and plagioclase porphyries. Typically, the clasts are centimetre to decimetre size, but larger basalt blocks are also present. Some of them are strongly altered to carbonate and, less commonly, quartz-carbonate-mariposite assemblages. Mid-Jurassic pillow basalts and the bimodal Four Corners complex lie west of the fault strands and are truncated by minor splays from them. Two outcrops of fault breccia are surrounded by the rocks of the Four Corners complex. One outcrop is in the bottom of a small cirque on the north side of the complex. The cirque walls south of it form a continuous outcrop of basalt and felsite that isolates the northern outcrop of fault breccia from the fault zone farther south. In the other outcrop, fault breccia contains numerous clasts of plagioclase-phyric hypabyssal granodiorite. They are unlike the igneous rocks of the Four Corners complex, but similar to unit Jfp (Jurassic feldspar porphyry) of Read *et al.* (1989). A rhyolite dike cuts off the breccia. Thus construction of the Four Corners igneous complex postdated major motion and brecciation on some splays of the Forrest Kerr fault; however, other splays containing identical breccias outlasted it.

In the main through-going splay that truncates the Four Corners complex to the east, lineations defined by clast elongations generally plunge at less than 25°. Clast asymmetries and shear bands show a consistent sinistral sense of motion both in outcrop and in thin section. Steep lineations, such as slickenlines and clast elongations, are also present but are less common. The pre-Four Corners breccia outcrops contain inconclusive kinematic indicators and poorly developed steep lineations.

A set of east-northeast–striking, south-directed reverse faults and related folds affects the uplifted Paleozoic/Triassic block east of the Forrest Kerr fault (Fig. 5 and 9). The most significant of these, the Kerr Bend fault, first recognized by Read *et al.* (1989), places Paleozoic and younger hangingwall strata on top of the mid-Jurassic basalts of Pillow Basalt Ridge. The layered rocks on Pillow Basalt Ridge are also involved in northeasterly folding. The eastern extents of these faults and folds are truncated by exposures of the Middle to early Late Jurassic Iskut River clastic-felsic unit. Northward deflection of bedding and structures on Pillow Basalt Ridge as they approach the base of the Iskut River unit (Fig. 5) may be related to a north-striking sinistral fault, possibly an extension of the Downpour Creek fault, either along the basal contact or buried beneath the Iskut River unit itself. The coarse, unsorted deposits and olistoliths in this unit are consistent with deposition in a fault-controlled basin.

We infer that its western bounding fault lies at or near the present western contact of the unit.

Read *et al.* (1989) calculated a minimum 2.5 km sinistral displacement along the Forrest Kerr fault based on the offset of folds across it. We are in accord with their structural interpretation, although we have modified it in several respects. First, we interpret the Kerr Bend fault and other northeast to east-northeast compressional features as the consequence of the sinistral motion on the north-striking Forrest Kerr fault. Second, detailed work has shifted and realigned the mapped axis of the PBR anticline on Pillow Basalt Ridge such that it does not intersect, and thus does not fold the Kerr Bend fault. Instead, both the PBR anticline and the small syncline to the northwest of it are folds in the footwall strata cut off by the Kerr Bend thrust fault. Read *et al.* (1989) considered the dark grey shale-siltstone unit in the core of the syncline on northwestern Pillow Basalt Ridge to be Bowser Lake Group strata, and structures affecting it – the syncline itself and the Forrest Kerr fault by association – were thought to be post-Bowser, mid-Cretaceous in age. However, the intimate interbedding of the shale and siltstone with pillow basalts (Barresi *et al.*, this volume) indicates that this is an uppermost unit in the mid-Jurassic Hazelton Group sequence. Structures affecting it are only required to be post-mid-Jurassic.

This set of east-northeast– to northeast-striking– folds and reverse faults can be modeled as a compressional transfer zone between the Forrest Kerr fault to the west and the southern extension of the Downpour Creek fault to the east (Fig. 5 and 10). Northeast-striking faults link the two north-striking fault systems into a single sinistral transcurrent zone.

The Triassic Pass fault is located east of the Downpour Creek fault, and truncates it at a low angle (Fig. 5). Its southern, unmapped extension lies in the Iskut River valley. East of the Triassic Pass fault, the Smokey Ridge thrust fault imbricates Triassic and overlying pebbly sandstone on the mountainside immediately north of Downpour Creek (Fig. 5). The fault crops out in several incised gullies. In its footwall, cross-stratified Bowser Lake Group(?) sandstone with scattered chert pebbles and plant debris unconformably overlies Triassic tuffaceous mudstone above a well-developed regolith (Fig. 11). The fault is a zone of strong shearing that places Upper Triassic black phyllite and tuffaceous mudstone on top of undeformed sandstone of the Bowser Lake Group (Fig. 11). A second thrust fault is inferred lower down this slope, in the valley of Downpour Creek, that places the Triassic exposures below the unconformity on top of the Bowser Lake Group section that is exposed on Bandit Ridge, south of Downpour Creek. Folds in the Upper Triassic sequence and in the Bowser Lake Group trend eastward; these are consistent with the orientation of the Smokey Ridge Thrust fault.

The Triassic Pass fault truncates both of these thrust faults, as well as footwall Bowser Lake Group strata. Thus, motion on it must be younger than the Jurassic-Cretaceous Bowser Lake Group.

In the northeastern part of the area, a north-trending, near-vertical fault is exposed both north and south of More Creek. A large quartz-phyric rhyolite dike and a panel of highly sheared tuffaceous sedimentary beds and coal of probable Eocene age occur within the fault zone (Fig. 5 and 10).

MINERAL DEPOSITS

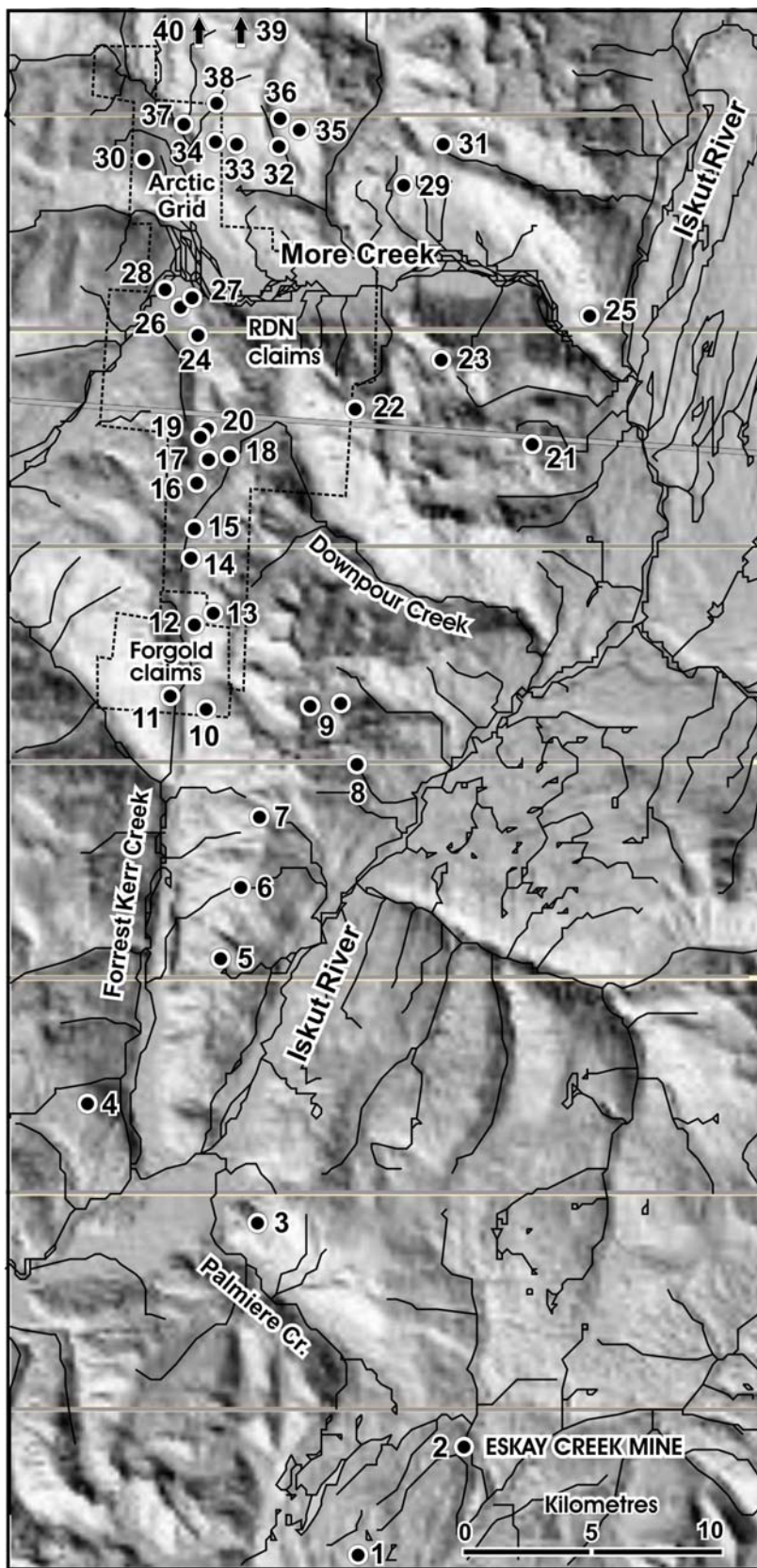
Northwestern BC hosts a variety of mineral deposit types characteristic of magmatic arc environments, including calc-alkaline porphyry copper-gold deposits (Fig. 1 in Schroeter and Pardy, 2004); Eskay Creek-type subaqueous hot spring deposits (Massey, 1999a); Kuroko-type VMS deposits (Massey, 1999b); and low-sulphidation epithermal deposits (Fig. 1 in Schroeter and Pardy, 2004). Near the current study area, intrusion-related Cu-Ni deposits (Lefebvre and Fournier, 2000) and Besshi-type VMS deposits (Massey, 1999b) are hosted in rock units that may be present locally. Sedimentary strata of the Bowser Lake Group host coal deposits and have elevated concentrations of molybdenum and nickel (Alldrick *et al.*, 2004c). Recent study of the Bowser Lake Group has shown potential for the generation and accumulation of petroleum (Evenchick *et al.*, 2002; Ferri *et al.*, 2004).

Figure 12 shows the distribution of mineral deposits and prospects in the study area. Occurrences are concentrated in the volcanic strata that pre-date deposition of the Bowser Lake Group. This distribution is reflected in metal concentrations detected in the Regional Geochemical Surveys (*see* Fig. 5 and 7 in Lett and Jackaman, 2004). The metal-rich region lies west of Highway 37 and corresponds to the eastern edge of the Coast Mountains. Bowser Lake Group sedimentary strata, with its coal, petroleum and sediment-hosted metal potential, generally lie east of Highway 37.

Intrusion-related deposit types in or near the study area include porphyry copper-gold deposits, which are particularly common in this region (Schroeter and Pardy, 2004); intrusion-related low-sulphidation epithermal deposits; and magmatic copper-nickel deposits. Volcanic-hosted deposits include both the Eskay Creek deposits and some low-sulphidation epithermal veins (Massey, 1999a). Stratiform or stratabound deposit types include sediment-hosted molybdenum and nickel, Besshi-type sediment-hosted massive sulphide deposits, as well as volcanic-hosted VMS deposits (Massey, 1999b). Limestone units are favourable host rocks for gold-rich skarn deposits (*e.g.*, McLymont Creek).



Figure 11. Composite photo of the thin Bowser Lake Group clastic sequence on Triassic basement, in the footwall of the Smokey Ridge thrust fault, which is expressed as highly sheared Triassic argillite overriding the undeformed pebbly sandstones of the Bowser Lake Group. Actual thickness of Bowser sediments in this exposure is about 50 m.



MINERAL OCCURRENCES

1. SIB / Lulu
2. Eskay Creek Mine
3. Iskut-Palmiere
4. Forrester
5. Mohole
6. PBR North
7. Malachite Peak
8. Sunkist
9. Twin West / Twin East
10. Four Corners
11. Forgold
12. Boundary
13. RTB
14. South Gossan
15. Marcasite Gossan
16. Steen Vein
17. Gossan Creek Porphyry
18. Jungle Anomaly
19. Wedge
20. Waterfall
21. Southmore
22. Logan Ridge
23. Sinter
24. GEM
25. Iskut River
26. Baseline
27. Main Zone
28. RDN (Camp)
29. Lucifer
30. KC
31. Bench
32. East
33. Arctic Grid (Ochre swamp)
34. Downstream
35. Biskut
36. Bis
37. Arctic 8
38. Little Les / Grizzly Creek
39. Ice
40. North Glacier / Arctic 1



Figure 12. Mineral deposits and prospects in the 2004 map area. Note the concentration of mineral showings along the Forrester Kerr fault.

During the 2004 mapping program, six new mineral showings were located by government geologists working on the Targeted Geoscience Initiative project. As these crews focus on mapping, not prospecting, this is a surprisingly high number of new mineral occurrences, which reflects the high mineral potential of the region. More exploration work is justified based on these discoveries and on the presence of Eskay-equivalent strata in this map area.

The following deposit descriptions are listed from south to north; see Figure 12 for locations.

1. SIB / Lulu (104B 376) (UTM 09 / 0408589E / 6273080N)

This showing crops out near middle of the 9 km long trend of gossans and alteration that extends southwestward from the Eskay Creek mine area. Mudstones interbedded with felsic volcanics host pyrite, stibnite and sphalerite with trace native gold, pyrrargyrite and arsenopyrite. A 2002 drillhole intersected 11.7 m grading 19.5 ppm Au and 1703 ppm Ag.

2. Eskay Creek (104B 008) (UTM 09 / 0412514E / 6279588N)

Roth (2002) classifies Eskay Creek as a polymetallic, precious metal rich, volcanogenic massive sulphide and sulphosalt deposit. Ore is contained in a number of stratiform zones and stockwork vein systems that display varied textures and mineralogy. The deposits formed during two periods of early Middle Jurassic hydrothermal activity, both of which were characterized by evolving fluid chemistry and mineralogy. Past production and reserve and resource estimates total 2.34 million tonnes grading 51.3 g/t Au and 2,326 g/t Ag.

3. Iskut-Palmiere (UTM 09 / 0403565E / 6287490N)

Realgar ± orpiment is hosted in both black siliceous siltstones and in a cross-cutting quartz vein. This small outcrop is exposed in a north-draining creek, and lies stratigraphically above a thick dacite unit on the north side of Palmiere (Volcano) Creek. Assays of two grab samples returned arsenic values greater than 1.0%, with negligible associated precious metals. However, creeks draining this low ridge to the north and south returned anomalously high gold grain counts in the heavy mineral concentrates collected during the recent Regional Geochemical Survey (Lett *et al.*, this volume).

4. Forrest (104B 380) (UTM 09 / 0396988E / 62192649N)

This prospect is located on the west side of Forrest Kerr Creek, opposite the south end of Pillow Basalt Ridge. Gold- and silver-bearing quartz-chalcopyrite veins occur in extensive quartz stockworks and individual veins associated with the Forrest Kerr fault. Grab samples assay up to 17.1 g/t Au. Visible gold occurs with bornite and hematite in quartz veins that assay up to 110.4 g/t Au.

5. Mohole (UTM 09 / 0401956E / 6297577N)

A deep drillhole has been completed in central Pillow Basalt Ridge. Hole PBR01-01 was located near the anticlinal fold axis on Pillow Basalt Ridge, to intersect the Eskay Creek horizon ("Contact Mudstone") at depth (see Baressi *et al.*, this volume). This drillhole was completed in two stages. In 2001, Homestake completed the hole to a depth of 1419 m. In 2003 Roca Mines Inc. deepened the hole to 1770 m.

6. PBR North (new showing) (UTM 09 / 0403150E / 6300650N)

On Pillow Basalt Ridge, locally thickened units of weakly pyritic, massive to flow-banded rhyolite are deposited within a succession of pillow lava, massive crystalline basalt flows and interlayered pyritic siliceous siltstones. The thicker rhyolite zones are interpreted as cryptodomes marking eruptive centres; thinner rhyolite units are interpreted as flows. Assays of grab samples collected from the pyritic siltstones have anomalous Zn, Ag and Ba values.

7. Malachite Peak (new showing) (UTM 09 / 0403620E / 6304260N)

North of the Kerr Bend fault, copper-bearing mafic volcanics crop out between 1800 to 2000 m elevation near the crest of Sixpack Range. Host rocks are fine-grained equigranular to weakly augite-feldspar porphyritic basalts. The massive basalt is cut by a network of fine fractures hosting pyrite and chalcopyrite. Malachite is prominent on weathered surfaces and along near-surface fractures.

8. Sunkist (new showing) (UTM 09 / 0406950E / 6305900N)

Ankerite alteration within an east-trending fault forms prominent bright orange gossans near the toe of Fourth Glacier. Best assays from three chip samples are 239 ppm Zn and 279 ppm As .

9. Twin (new showing) Twin East (UTM 09 / 0405840E / 6308160N) Twin West (UTM 09 / 0405120E / 6308015N)

Two prominent orange-weathering gossan zones are exposed on north-facing cliffs near the northeast end of Sixpack Range. A single elongate gossan is divided into two zones where a north-flowing valley glacier cuts through the host strata. The outcrops have not been examined, but this showing may be similar to Sunkist.

10. Four Corners (new showing) (UTM 09 / 0401000E / 6307715N)

A major volcanic centre is preserved northwest of Pillow Basalt Ridge. Numerous rhyolite dikes and flows are emplaced in a sequence of intercalated basalt and sedimentary rocks. Mineralization consists of minor to sparse disseminated pyrite and rare galena.

11. Forgold (104B 378) (UTM 09 / 0399429E / 6309294N)

This property is located west of Downpour Creek and just south of the RDN claimblock. Epithermal gold- and silver-bearing pyrite and chalcopyrite stringer veins assayed up to 30.5 g/t Au and 15.85% Cu (Assessment Report 20,540). Malensek *et al.* (1990) identified three styles of mineralization which are controlled by the Forrest Kerr fault. Chalcopyrite, galena and sphalerite stringers, and quartz-carbonate-sphalerite-galena-chalcopyrite stockwork veins grade up to 2.09 g/t Au. Disseminated chalcopyrite within silicified zones grade up to 112.46 g/t Au and 17.16% Cu. Proximal stocks of monzonite may be genetically associated with the alteration and mineralization.

12. Boundary (RDN) (UTM 09 / 0400040E / 6310950N)

A narrow silicified zone hosts a thin chalcopyrite veinlet. Assays returned anomalous gold values (Savell, 1990). Noranda Exploration Ltd. drilled five holes on this target area in 1991. The best intersection was 11.6 m grading 23.9 g/t Au (Logan *et al.*, 1992 and Awmack, 1997). The best assays obtained from 1998 surface samples were 56.7 ppm Au, 44 ppm Ag, 44 ppm As, 6.34% Cu, 18.7 ppm Hg, 3.900 ppm Pb, and 9,360 ppm Zn (Awmack and Baknes, 1998).

13. RTB (new showing) (RDN) (UTM 09 / 0400710E / 6311425N)

This prospect consists of disseminated and fine fracture-hosted pyrite, chalcopyrite, tetrahedrite and galena in flow-banded rhyolite and adjacent fine sandstone. Rare tetrahedrite and native silver were noted

in some samples. Nearby pillow lavas of plagioclase-potassium feldspar porphyry display interbeds and selvages of pyrite- and tetrahedrite-bearing jasper. Best assay results from five chip samples are 0.5% Cu, 2.2% Pb, 8.8% Zn, 245 ppm Ag, 1.4 ppm Au, 2690 ppm Sb, 87 ppm Hg and 499 ppm As.

14. South Gossan (RDN) (UTM 09 / 0399935E / 6313870N)

South Gossan is a large resistant knob of massive dacite flow on the east bank of the headwaters of Downpour Creek. Ubiquitous fine hairline fractures host a weakly developed 'stockwork' of pyrite, calcite and quartz. Subsequent weathering has coated the entire surface of this large outcrop area with striking buff-orange ankeritic weathering. No significant metal values have been obtained (Savell, 1990).

15. Marcasite Gossan (UTM 09 / 0400135E / 6314780N)

This prominent gossan crops out on the east bank of upper Downpour Creek, 900 m north of South Gossan. In this area, strata dip moderately westward with tops up to the west. The showing consists of three stacked dacitic flow units separated by locally fossiliferous siltstone, sandstone and limestone. Dacites are weakly to strongly pyritic, the sedimentary units host only trace to minor pyrite. The middle dacite unit is the most intensely mineralized, and hosts a stockwork of marcasite-pyrite-chalcedony-calcite-pyrobitumen-barite veins. Individual veins range up to 10 cm thick. Mineralization ends abruptly along strike at the north side of the outcrop area against a synmineralization fault. The easternmost, topographically higher but stratigraphically lower, Upper Marcasite Gossan consists of a weaker quartz-chalcedony-pyrite-pyrobitumen stockwork. Savell (1990) reports that gold and base metal values are negligible, but assay results from surface samples include 141 g/t Ag, 2,750 ppm As, 122 ppb Sb, 124 ppm Mo and 5,240 ppb Hg. Even higher values have been obtained from mineralized float boulders near the Upper Marcasite Gossan. Four drillholes completed to date did not intersect mineralization.

16. Steen Vein (RDN) (UTM 09 / 0400290E / 6316195N)

This polymetallic vein crops out in the north wall of the lower gorge of Cole Creek, a small creek that drains southeastward into upper Downpour creek, just south of the Gossan Creek Porphyry. Discovered in 1997, this quartz-galena-sphalerite-tetrahedrite vein follows an east-northeast-trending fault. Chip samples across a true vein width of 2.0 m averaged 279 g/t Ag, 1.86% Pb, 0.77% Zn and 350 ppb Au.

17. Gossan Creek Porphyry (RDN) (UTM 09 / 0400910E / 6317240N)

The Gossan Creek porphyry intrusion (Fig. 5), located near the headwaters of Downpour Creek, roughly correlates with a large bleached gossan (Fig. 13a, b). Three geophysical targets were drill-tested by Noranda in 1991 (Savell and Grill, 1991). DDH 18 intersected argillic-altered feldspar porphyry hosting 5 to 15 % fine- to medium-grained pyrite disseminations and veinlets. From 103.4 to 113.3 m, stringers of sphalerite and chalcopyrite assayed 0.18% Cu, 0.14% Pb, 0.43% Zn 1.17 g/t Ag and 0.07 g/t Au. Other drillholes cut pyritic stockwork with up to 25% fine pyrite.

18. Jungle Anomaly (RDN) (UTM 09 / 0401420E / 6317365N)

This exploration target is a 100 by 450 m soil geochemical anomaly located in thick brush on the west bank of upper Downpour Creek, 2.6 km north of the Marcasite Gossan and just north of the Gossan Creek Porphyry. Samples indicate anomalous Au, As, Ag and Pb values in soils overlying bedrock of clastic sedimentary rocks, rhyolite and basalt. A float cobble of pyritic, silicified argillite collected near the centre of the anomaly assayed 25.44 g/t Au. Pyritic chert float also collected from this area does not occur elsewhere on the extensive property. Subsequent geophysical surveys and drilling have not located a bedrock source.

19. Wedge (RDN) (UTM 09 / 0399975E / 6319070N)

The Wedge prospect crops out low on a west-facing, heavily wooded hillside, just northeast of the headwaters of Carcass Creek at the toe of a glacier, and 5 km south of the current exploration camp. Five drillholes completed in 1990-91 cut mineralized veins in eleven intersections with best assays of 137.8 ppm Au, 62.4 ppm Ag, 2.7% Cu, 0.48% Pb and 3.26% Zn (Awmack and Baknes, 1998).

20. Waterfall (RDN) (UTM 09 / 0400115E / 6319230N)

A quartz-sulphide vein is discontinuously exposed for 50 m (Savell, 1990).

21. Southmore (UTM 09 / 0413310E / 6318760N)

The east wall and south wall of a small north-draining cirque reveal six outcrop areas of strongly

gossanous, pyritic, flow-layered white rhyolite. This unit is correlated with the regionally distributed Upper Triassic pyritic rhyolite that also hosts the Bench and Sinter showings. Adjacent units of thin-bedded black siltstone are also pyritic. Associated rock types include buff-weathering sandstone with horizons of wood debris, black limestone, and one rhyolite flow. The strata are cut by a 1.5 m thick sill of flow-banded basalt. Three gossanous outcrops were sampled, the best assays are 28 ppm Mo, 16 ppm Cu, 10 ppm Pb, 25 ppm Zn, 214 ppb Ag, 24 ppm As, 777 ppb Hg and 4 ppm Sb.

22. Logan Ridge (UTM 09 / 0406030E / 6319780N)

A prominent, resistant ridge of intensely gossanous rhyolite spines marks the skyline west of Arrow Creek. Since 1990, this ground has been held as the STOW and PINE claims, and is currently registered as the MOR 8 claims; no exploration results have been reported.

23. Sinter (UTM 09 / 0409560E / 6322175N)

Recent glacier retreat has exposed an extensive area of strong pyritic stockwork, south of More Creek and east of Arrow Creek. During the summer of 1988, the area was explored by Valley Gold Ltd., Noranda Ltd. and Corona Corporation (Bale and Day, 1989). Follow-up work by Noranda Ltd in 1990 (Grill and Savell, 1991) discovered no base or precious metal mineralization, but anomalous mercury (up to 196 ppm Hg), arsenic and antimony were obtained all along the 2 km long trace of the northwest-trending Citadel fault. Barrick Resources sampled the prospect in 2003. An unreported single drillhole was collared at the toe of the west-flowing glacier by Noranda; no results are known. The best assay results from three chip samples collected in 2004 are 122 ppm Cu, 350 ppm Zn, 7 ppm Pb, 24 ppm Ag, 5,750 ppm Ba, 13 ppm Hg and 24 ppm As.

24. GEM (RDN) (UTM 09 / 0399565E / 6322980N)

This prospect crops out 1000 m south of the Main showing on the east side on Carcass Creek, and is hosted in the same massive dacite unit. Discovered by Noranda geologists in 1991 (McArthur *et al.*, 1991), the best assay obtained from grab samples was 5.1 ppm Au. Resampling in 1997 returned a best assay of 2.16 ppm Au and 32 ppm Ag (Awmack, 1997). A soil survey over the area indicates that the dacitic volcanic hostrocks have anomalous Au, Ag, Cu, Pb, Zn, As, Sb and Mn values.



A.



B.

Figure 13. The Gossan Creek Porphyry gossan. A. Looking southwest. The glaciated peak in background lies on the west side of the Forrest Kerr fault. B. The same gossan zone viewed from the south across Downpour Creek

25. Iskut River (104G 104) (UTM 09 / 0415471E / 6324464N)

A major (>100 m thick) fossiliferous limestone unit of Upper Triassic age is exposed on cliffs near the mouth of More Creek.

26. Baseline (RDN) (UTM 09 / 0399180E / 6323665N)

This prospect is a quartz vein breccia exposed 240 m southwest of the Main Zone. A chip sample assayed 6.21 g/t Au.

27. Main Zone (RDN) (UTM 09 / 0399355E / 6323810N)

This prospect crops out on the east side of Carcass Creek, 700 m east of the current exploration camp. This showing was discovered by Noranda geologists in 1991 (McArthur *et al.*, 1991) and has remained a focus of exploration efforts on this large property. Host rock is Early Jurassic dacite that is locally porphyritic, spherulitic or silicified. Mineralization consists of disseminated sulphides in areas where the dacite is bleached and silicified. The best assays reported from a series of chip samples (McArthur *et al.*, 1991) are 5 ppm Au, 32.8 g/t Ag, 0.5% Cu, 0.5% Pb, and 10% Zn. A soil survey over the area indicates that the dacitic volcanic rocks have anomalous Au, Ag, Cu, Pb, Zn, As, Sb and Mn values. Subsequent exploration has shown that the prospect is an intensely silicified fault breccia trending 060 degrees (Awmack, 1996); a chip sample across its 8.3 m width returned 3.1 ppm Au, 0.49% Pb and 1.13% Zn. A separate outcrop area 130 m to the west-southwest is called the Club Zone. This 7m long outcrop of silicified breccia returned maximum assays of 2700 ppm Pb, 1205 ppm Zn and 515 ppb Au from three chip samples.

28. RDN (UTM 09 / 0398770E / 6323970N)

The name RDN refers to a large north-trending claim block containing several prospects. The core claims were staked in 1987, predating the discovery of the Eskay Creek 21 Zone. Additional claim blocks to the north and south have been added over the last 17 years. The UTM coordinates above give the location of the current exploration camp. Noranda Exploration Ltd. explored these claims from 1989 to 1991, including a fifteen-hole drill program in 1990 and a further 15 drillholes in 1991. Pathfinder Resources explored the claim block from 1994 to 1996. Rimfire Minerals acquired all the claims in 1997 and conducted soil sampling, geological mapping, trenching and prospect-

ing in 1997 and 1998. Barrick explored the property under option in 2002 to 2003. Northgate Minerals Corporation and Rimfire Minerals completed a nine-hole drill program in 2004, targeting the Wedge Zone, Jungle Anomaly and Marcasite Gossan prospects.

29. Lucifer (104G 145) (UTM 09 / 0407979E / 6329387N)

An extensive carbonate-pyrite-sericite-silica alteration zone has anomalous Au, As, Ba, Cd, Cu, Mo, Pb and Zn values. Country rock is Upper Triassic sedimentary and volcanic rocks intruded by a set of Early Jurassic potassium feldspar megacrystic dikes. Alteration is most intense along steep northeast-trending faults. Two holes drilled on the property in 1991 intersected 1.36 m grading 15 ppm Au and 5.7 m grading 0.7 ppm Au (Dewonck, 1991).

30. KC (RDN) (UTM 09 / 0397140E / 6329780N)

Chalcopyrite veins and veinlets are hosted in Early Jurassic feldspar porphyritic, potassium feldspar megacrystic granodiorite. Several massive chalcopyrite veins up to 12 cm wide are hosted by a dioritic phase of the leucocratic granodiorite (Bobyne, 1991, p.13, 15). The veins are vertical and exposed in a small creek bed over a width of 4 m. Selected grab samples have anomalous Au, Cu and Ag values.

31. Bench (UTM 09 / 0409490E / 6330105N)

A band of massive to semi-massive, fine-grained, bright pyrite crops out at the base of a high cliff of black, pyritic, flow-layered rhyolite near the head of Bench Creek. The upper part of the cliff is faintly banded, black to charcoal rhyolite with a fine dusting of pyrite evenly disseminated throughout the rock. Within the lower 5 m along the base of the cliff, the rhyolite is transected by many fine hairline cracks filled with pyrite. Along most of the length of the cliff, a talus pile of coarse blocks and boulders is piled up against the basal rhyolite layer with the pyritic fractures. At one location near the upstream end of the cliff, the top of the talus pile is lower and exposes 2 feet of massive, fine-grained granular pyrite and semi-massive granular pyrite disseminated in white, fine-grained quartz. The significance of this small showing is its stratabound character and the high probability that this mineralization extends laterally under the blocky talus cover. In 2004, eight samples were collected from this unit along a 2 km strike length. Best assays were 51 ppm Mo, 70 ppm Cu, 44 ppm Pb, 89 ppm Zn, 15 ppb Au, 1099 ppb Ag, 15 ppm As, 2.7 ppm Sb and 394 ppb Hg.

32. East (RDN) (UTM 09 / 0402900E / 6330095N)

Mineralized float samples collected downstream from the Bis prospect assayed 1.9 ppm Au and 771 ppm As.

33. Arctic Grid (RDN) (UTM 09 / 0401400E / 6330165N)

The Arctic Grid is the northernmost claim block of the RDN claim package. The Arctic claims were staked and extensively explored in 1990 by Skeena Resources (Boby, 1991). Eight mineral prospects lie on the Arctic claim block: Grizzly Creek (Little Les), North Glacier, Arctic 8, KC, Ice, Bis, Downstream and East. The coordinates above give the location of a large ochre-coloured swamp east of the centre of the claim block.

34. Downstream (RDN) (UTM 09 / 0400485E / 6330215N)

This showing is located 2.5 km downstream of the Grizzly showing, on the southeast bank of Grizzly Creek. Narrow chalcedony veins within pyritic felsite/rhyolite host stringers of massive pyrite up to 5 cm wide. Grab samples from two of these pyrite veins assayed 75 ppm Hg, 580 ppm Sb and 4860 ppm As (Boby, 1991; Awmack, 1997).

35. Biskut (104G 146) (UTM 09 / 0403381E / 6331472N)

High on the north slope of More Creek, a 300 by 100 m alteration zone of quartz-sericite-pyrite-clay is developed in Upper Triassic volcanic and sedimentary rocks. Sulphide mineralization locally ranges up to 5% pyrite, with minor galena and arsenopyrite.

36. Bis (RDN) (UTM 09 / 0402915E / 6331215N)

Felsite dike or flow rock hosts 3 to 5% disseminated pyrite and trace arsenopyrite. A grab sample of strongly gossanous felsic rock assayed 5 ppm Au, 570 ppm Cu, 41.9 ppm Ag, 391 ppm As and 124 ppm Mo (Boby, 1991, p. 8 and 12).

37. Arctic 8 (RDN) (UTM 09 / 0399065E / 6331145N)

One creek north of Grizzly Creek, and near the unnamed creek's junction with More Creek, several carbonate lenses up to 0.75 m wide are interbedded with

greywacke and conglomerate. The carbonate rocks host 1 to 2% galena and trace chalcopyrite and sphalerite (Boby, 1991, p. 12 and Map 1). No assays are reported.

38. Little Les / Grizzly Creek (RDN) (104G 079) (UTM 09 / 0400720E / 6331860N)

This is the only prospect on the extensive RDN claim group where pre-1987 exploration is recorded. Initially named Little Les, this prospect has also been named More, Two More and is now referred to as the Grizzly showing on the Arctic Grid, RDN property. To the east of the north branch of More Creek, on the present Arctic Grid, a large gossan is developed where volcanic rocks are intruded by dikes of potassium feldspar megacrystic granodiorite dikes (Folk, 1980). Pyritic alteration hosts trace chalcopyrite, galena, sphalerite, malachite and molybdenite(?). Average grades from 11 chip samples are 0.3% Cu, 1.71 g/t Ag and 0.41 g/t Au. Newmont drilled two short holes on this target in 1970; no results are available (Geology, Exploration and Mining, 1971). Boby (1991, p. 12) described porphyry copper-style mineralization exposed over a 300 by 25 m area along the upper part of the northernmost tributary of Grizzly Creek. The host rock is carbonate-chlorite-sericite altered andesitic flows and tuffs. Mineralization is 2 to 5% disseminated chalcopyrite with 1 to 3% disseminated and fracture-fill pyrite. Throughout the area of the showing, stringers of massive chalcopyrite range up to 5 cm wide, with pods and lenses up to 50 cm wide. Trace galena and sphalerite are also present. Mineralization is fracture controlled and best developed proximal to the many feldspar porphyry and felsite dikes, which cut the volcanics.

39. Ice (RDN) (UTM 09 / 0401535E / 6336200N)

Hornblende diorite hosts up to 25% pyrrhotite near the intrusive contact of this large stock (Boby, 1991, Map 1). A grab sample assayed 31 ppb Au, 3.7 ppm Ag and 3152 ppm Cu. Similar mineralization occurs in a similar setting 3 km south; in the southwest corner of Upper More 1 claim, on the north bank of the stream immediately northwest of the Grizzly Creek prospect, gossanous cliffs host up to 7% disseminated pyrrhotite and pyrite (Boby, 1991, p. 12-13).

40. North Glacier / Arctic 1 (RDN) (UTM 09 / 0400065E / 6337235N)

Mineralized float samples collected from glacial moraines returned assays ranging up to 4.5 ppm Au, 9,034 ppm Cu, 74.6 ppm Ag and 20,147 ppm As.

METALLOGENY

In the map area and in the surrounding region, Upper Triassic mineralization includes large porphyry copper-gold systems (GJ, Galore Creek), Besshi-type VMS deposits (Rock and Roll), pyritic rhyolite/exhalite (Bench, Citadel, Southmore) and vuggy rhyolite dikes and flows with elevated Au, Ag, Hg, Sb and As concentrations (Rainbow). Lower Jurassic mineralization that predates the erosional interval marked by Nassian uplift is represented by large porphyry copper-molybdenum systems (Mary, Red-Chris), stratabound bulk-tonnage epithermal mineralization (Hank), and precious metal-rich skarn deposits (McLymont). Lower to Middle Jurassic mineralization that post-dates the Nassian uplift includes the Griz prospect and many areas of pyritic felsic volcanic units and derived volcanoclastic sedimentary rocks (*e.g.*, Fig. 4 in Simpson and Nelson, 2004), plus the Eskay Creek gold mine and numerous nearby prospects (Lulu, 22 Zone, HSOV).

Exploration Potential

Discovery of a number of small prospects during this season's regional mapping program indicate that the potential of this area has not yet been thoroughly assessed.

Due to the highly dissected terrain, geochemical stream sediment sampling has proven to be a particularly successful and cost-effective tool for assessing the potential of larger areas (Lett and Jackaman, 2004; Lett *et al.*, 2005) and should be equally powerful as a second phase follow-up technique. The middle unit of Pillow Basalt Ridge is favourable for the deposition and preservation of exhalative sulphides and should be selectively prospected. Other areas of quiescent, distal sedimentation will be particularly conducive to the accumulation and preservation of exhalative sulphides (*e.g.*, northern Downpour Creek area).

DISCUSSION AND CONCLUSIONS

This project has provided important new detailed geological surveys of the northern Eskay Rift rocks within the Iskut map area. Tracts of "Eskay equivalent" strata crop out on Pillow Basalt Ridge and north to More Creek. They are correlative in general with sequences mapped in 2003 on Table Mountain, on Willow Ridge and on ridges east and west of Kinaskan Lake (Alldrick *et al.*, 2004a, 2004b).

Fieldwork in 2004 has clarified the nature, stratigraphic and structural context, and mineral potential of the "Eskay equivalent" strata in northern Iskut map area. They can be divided into five separate facies units, Pillow Basalt Ridge, Forgold, Sixpack

Range, Downpour Creek and Iskut River. The Sixpack Range is a coarse, proximal, conglomeratic facies (Fig. 7), similar to conglomerates identified in 2003 on Table Mountain and near Kinaskan Lake (Alldrick *et al.*, 2004a, 2004b). They represent rift-margin deposits related to scarps. By contrast, the Forgold basalts rest directly on older basement without intervening clastic units.

Felsic centres are located in the Four Corners complex and the "middle unit" on Pillow Basalt Ridge. Laminated siliceous argillite and rhyolitic tuffaceous siltstones - the "pajama beds" (Anderson, 1993) - are also present at both of these sites.

The Forrest Kerr fault and related faults form the present structural framework for the rift system that localized the Eskay VMS deposit, its host rocks, and correlative strata (Fig. 10). It forms the western boundary of mid-Jurassic exposures as far north as the headwaters of More Creek. Its northern extension is buried under the Mt. Edziza volcanic centre (Fig. 2). North of More Creek, the zone of mid-Jurassic bimodal/sedimentary exposures steps east to the Table Mountain/Kinaskan Lake area. There, it is bounded to the west by local scarps that Alldrick *et al.* (2004b) interpreted as rift margins. Coarse, unsorted conglomerates related to the scarps underlie sedimentary strata containing Toarcian-Bajocian macrofossils.

The trace of the Forrest Kerr fault coincides with a major magnetic lineament (Alldrick, 2000). South of the Iskut River, the Forrest Kerr fault is connected to the Harrymel fault through a complex step-over zone (Read *et al.*, 1989; Alldrick, 2000). This structure continues south to the Granduc mine area, where it is expressed as a 2 km wide zone of transcurrent ductile deformation, the South Unuk shear zone (Lewis, 1992). Uranium-lead dates on syn- and post-kinematic plutons constrain sinistral motion to between 172 and 167 Ma (Fig. 10c; Lewis, 2001).

Geological observations in the present project area are consistent with the interpretation of Read *et al.* (1989) that an episode of sinistral motion on the Forrest Kerr fault post-dated deposition of the Pillow Basalt Ridge strata. The Middle to early Late Jurassic Iskut River unit is interpreted as a fault-related deposit localized along a north-striking sinistral fault that is a splay of the Forrest Kerr fault zone. This offset is contemporaneous with sinistral motion on the South Unuk shear zone. We infer that a regional sinistral shear couple existed along the north-striking bounding faults of the mid-Jurassic rift system, deforming strata and modifying structures created during earlier stress regimes.

Evidence for the stress regime during deposition of the Eskay Creek host rocks and their correlatives consists mainly of observed orientations of rift-related features. These vary along strike of the rift (Fig. 5 and

10). In the Table Mountain area, lines of rhyolite centres and dike swarms are oriented north-northwesterly (Alldrick *et al.*, 2004a, 2004b). This season, a north-northwesterly horizon of pyritic sinters has been discovered on south-central Table Mountain (A. Birkeland, pers comm, 2004). On northern Pillow Basalt Ridge, a line of small rhyolite intrusive centres trends northeasterly (30 degrees). Finally, in the vicinity of the Eskay mine the alignment of felsite centres, feeder dikes and stockwork-style mineralized zones parallel to the fold axis of the northeast-trending Eskay anticline suggests that this fold could be an inverted rift basin (McClay *et al.*, 1989).

The combined Forrest Kerr and Harrymel faults provide a possible locus for the western margin of the rift zone. A northerly-trending line of altered Early(?) Jurassic porphyry intrusions lies immediately west of the Forrest Kerr fault along Forrest Kerr Creek (Read *et al.*, 1989; Logan *et al.*, 2000). Similarly, mapping by Equity Engineering and this project team has outlined a northerly trend of Early Jurassic dacite intrusive/extrusive centres east of the fault, near the headwaters of Downpour Creek. The alignment of these centres along the Forrest Kerr fault suggests that it was a zone of crustal weakness in Early Jurassic time, prior to development of the Eskay rift. The east-side-down West Slope fault truncates the Early Jurassic plutons, but is older than the main Forrest Kerr strand (Read *et al.*, 1989). It could have been a mid-Jurassic, graben-bounding normal fault. The Forrest Kerr splay that is cut off by the Four Corners complex is another example of a probable syn-rift fault.

In the Table Mountain area, north-northwesterly tensional features parallel the western rift margin, consistent with orthogonal extension (Alldrick *et al.*, 2004). In contrast, the northeasterly orientation of mid-Jurassic dikes on Pillow Basalt Ridge suggests an oblique component to extension across the north-striking bounding faults (Fig. 10b). Because these features are extensional rather than compressional, movement due to this component would have been opposite to that manifested in the latest mid Jurassic event, *i.e.*, dextral rather than sinistral. Similarly, in the vicinity of the Eskay mine, north-northeasterly extensional features require an oblique stress component. Thus, evidence for dextral, syn-rifting offset is seen in the area from More Creek at least as far south as Tom Mackay Lake. It corresponds to the unique Paleozoic horst and deep graben in this area, evidenced by the unusually thick Pillow Basalt Ridge basalts.

Figure 10 summarizes the inferred structural development of the Eskay rift zone. In mid-Jurassic time, rifting took place in en echelon zones between Kinaskan Lake and the Granduc mine. Over most of the area, orthogonal rifting prevailed. A dextral component across the Forrest Kerr fault led to strong horst and

graben development, oblique to the main northerly trend.

In early Bajocian time (172 to 167 Ma), a new stress regime, controlled by a sinistral shear couple across the dominant northerly faults, was superimposed on the rift basins and terminated their development. It caused fault reversal and created local high energy depositional environments in the Iskut River unit.

SUMMARY

Mapping has refined the stratigraphic and structural picture of the More Creek – Palmiere Creek area. Important contributions include the recognition of the near absence of strata representing the lower Hazelton Group, and recognition of regional-scale unconformities that form irregular boundaries between major stratigraphic packages.

Strata deposited within the Eskay rift extend northward through the present map area, displaying a range of different facies which reflect the proximity to volcanic centres and the depositional setting. The Pillow Basalt Ridge facies and the Four Corners complex comprise bimodal volcanic rock types and related sedimentary strata correlative with strata that host the Eskay Creek orebodies to the south.

ACKNOWLEDGMENTS

Magan Havard provided capable field assistance. We thank Dave Mehner, Murray Jones, Dave Caulfield, David Gale, Martin Stewart, Waldo Perez, Arne Birkeland and Richard Mann for valuable discussions in the field. Karl Desjarlais of Interior Helicopters Ltd. provided safe, swift and reliable helicopter support.

REFERENCES

- Alldrick, D.J. (1993): Geology and metallogeny of the Stewart mining camp, northwestern British Columbia; *British Columbia Ministry of Energy and Mines*, Bulletin 85, 105 pages.
- Alldrick, D.J. (2000): Exploration significance of the Iskut River fault; *British Columbia Ministry of Energy and Mines*, Geological Fieldwork 1999, Paper 2000-1, pages 237-248.
- Alldrick, D.J. and Britton J.M. (1992): Unuk River area geology; *British Columbia Ministry of Energy, Mines and Petroleum Resources*, Open File Map 1992-22, scale 1:20 000, 5 sheets.
- Alldrick, D.J., Stewart, M.L., Nelson, J.L. and Simpson, K.A. (2004a): Geology of the More Creek-Kinaskan Lake area, northwestern British Columbia; *British Columbia Ministry of Energy and Mines*, Open File Map 2004-2, scale 1:50 000.
- Alldrick, D.J., Stewart, M.L., Nelson, J.L. and Simpson, K.A. (2004b): Tracking the Eskay rift through northern

- British Columbia - geology and mineral occurrences of the Upper Iskut River area; *British Columbia Ministry of Energy and Mines*, Geological Fieldwork 2003, Paper 2004-1, pages 1-18.
- Alldrick, D.J., Jackaman, W. and Lett, R.E.W. (2004c): Compilation and analysis of regional geochemical surveys around the Bowser Basin; *British Columbia Ministry of Energy and Mines*, Geological Fieldwork 2003, Paper 2004-1, pages 163-166.
- Alldrick, D.J., Nelson, J.L. and Barresi, T. (2005): Geology of the More Creek - Palmiere Creek area, northwestern British Columbia; *British Columbia Ministry of Energy and Mines*, Open File Map 2005-5, scale 1:50 000.
- Anderson, R.G. (1983): The geology of the Hotailuh batholith and surrounding volcanic and sedimentary rocks, north-central British Columbia; unpublished PhD thesis, *Carleton University*.
- Anderson, R.G. (1989): A stratigraphic, plutonic and structural framework for the Iskut Map area, northwestern British Columbia; *Geological Survey of Canada*, Current Research, Part E, Paper 89-1 E, pages 145-154.
- Anderson, R.G. (1993): A Mesozoic stratigraphic and plutonic framework for northwestern Stikinia, northwestern British Columbia, Canada; in *Mesozoic Paleogeography of the western United States-II*, Dunne, G. and McDougall, K., editors, *Pacific Section SEPM*, Volume 71, pages 477-494.
- Anderson, R.G. and Thorkelson, D.J. (1990): Mesozoic stratigraphy and setting for some mineral deposits in Iskut River map area, northwestern British Columbia; in *Current Research, Part E, Geological Survey of Canada*, Paper 90-1 E, pages 131-139.
- Ash, C.H., Fraser, T.M., Branchflower, J.D. and Thurston, B.Q. (1995): Tatogga Lake project, northwestern British Columbia (104H/11, 12); in *Geological Fieldwork 1994*, Grant, B. and Newell, J.M., editors, *British Columbia Ministry of Energy, Mines and Petroleum Resources*, Paper 1995-1, pages 343-358.
- Ash, C.H., Stinson, P.K. and Macdonald, R.W.J. (1996): Geology of the Todagin Plateau and Kinaskan Lake area (104H/12, 104G/9); in *Geological Fieldwork 1995*, Grant, B. and Newell, J.M., editors, *British Columbia Ministry of Energy, Mines and Petroleum Resources*, Paper 1996-1, pages 155-174.
- Ash, C.H., Macdonald, R.W.J. and Friedman, P.M. (1997a): Stratigraphy of the Tatogga Lake Area, Northwestern British Columbia (104G/9,16); in *Geological Fieldwork 1996*, Lefebure, D.V., McMillan, W.J. and McArthur, J.G., Editors, *British Columbia Ministry of Employment and Investment*, Paper 1997-1, pages 283-297.
- Ash, C.H., Macdonald, R.W.J., Stinson, P.K., Fraser, T.M., Read, P.R., Pustka, J.F., Nelson, K.J., Ardan, K.M., Friedman, R.M. and Lefebure, D.V. (1997b): Geology and mineral occurrences of the Tatogga Lake area, northwestern British Columbia (104G/9E & 16SE, 104H/12NW & 13SW); *British Columbia Ministry of Energy and Mines*, Open File Map 1997-3, scale 1:50 000.
- Awmack, H.J. (1996): 1996 geological, geochemical and geophysical report on the RDN 1-10 claims; *British Columbia Ministry of Energy and Mines*, Assessment Report No. 24,719, 32 pages.
- Awmack, H.J. (1997): 1997 geological and geochemical report on the RDN 1-10 claims; *British Columbia Ministry of Energy and Mines*, Assessment Report No. 25,336, 29 pages.
- Awmack, H.J. and Baknes, M.E. (1998): 1998 geological, geochemical and trenching report on the RDN 1-18 claims; *British Columbia Ministry of Energy and Mines*, Assessment Report No. 25,813, 39 pages.
- Bale, W.C. and Day, R.C. (1989): Prospecting assessment report on the Wad, Sinter, and Bill mineral claims; *British Columbia Ministry of Energy and Mines*, Assessment Report No. 19,216, 6 pages.
- Barresi, T., Nelson, J.L., Alldrick, D.J. and Dostal, J. (2005): Pillow Basalt Ridge facies - detailed mapping of Eskay Creek equivalent stratigraphy (Iskut River NTS 104B/9, 10, 15, 16); *British Columbia Ministry of Energy and Mines*, Geological Fieldwork 2004, this volume.
- Barresi, T. and Dostal, J. (2005): Geochemistry and petrography of Upper Hazelton volcanics - VHMS favorable stratigraphy in the Iskut River and Telegraph Creek Map Areas, northwest British Columbia; *British Columbia Ministry of Energy and Mines*, Geological Fieldwork 2004, this volume.
- Bartsch, R.D. (1993): A rhyolite flow dome in the upper Hazelton Group, Eskay Creek area; in *Geological Fieldwork 1992*, *British Columbia Ministry of Energy, Mines and Petroleum Resources*, Paper 1993-1, pages 331-334.
- Boby, M.G. (1991): Summary report on geological mapping, prospecting, and geochemistry of the Arctic/Upper More Claim Group; *British Columbia Ministry of Energy and Mines*, Assessment Report 21,529, 22 pages.
- Breitsprecher, K. and Mortensen, J.K. (2004): BCAGE 2004 - a database of isotopic age determinations for rock units in British Columbia; *British Columbia Ministry of Energy and Mines, Geological Survey*, Open File 2004-3.
- Dewonck, B. (1991): Assessment report on the Rumsen 1-4 claims for Gzolden Pyramid Resources Inc.; *British Columbia Ministry of Energy and Mines*, Assessment Report No. 21,890, 18 pages.
- Ettlinger, A.D. (2001): Eskay Creek 21 Zone; in *Metallogenesis of the Iskut River Area, Northwestern British Columbia*, Lewis, P.D., Toma, A. and Tosdal, R.M., editors, *Mineral Deposit Research Unit*, Special Publication 1.
- Evenchick, C.A. (1991): Jurassic stratigraphy of east Telegraph Creek and west Spatsizi map areas, British Columbia; in *Current Research, Part A, Geological Survey of Canada*, Paper 91-1A, pages 155-162.
- Evenchick, C.A., Poulton, T.P., Tipper, H.W. and Braidek, I. (2001): Fossils and facies of the northern two-thirds of the Bowser Basin, British Columbia; *Geological Survey of Canada*, Open File Report 3956, 103 pages.
- Evenchick, C.A., Hayes, M.C., Buddell, K.A. and Osadetz, K.G. (2002): Vitrinite and bitumen reflectance data and preliminary organic maturity model for the northern two thirds of the Bowser and Sustut basins, north-central British Columbia; *Geological Survey of Canada*, Open File Map 4343, scale 1:250 000.

- Evenchick, C.A. and McNicoll, V.J. (2002): Stratigraphy, structure, and geochronology of the Anyox Pendant, northwest British Columbia, and implications for mineral exploration; *Canadian Journal of Earth Sciences*, Volume 39, pages 1313-1332.
- Evenchick, C.A. and Thorkelson, D.J. (2005): Geology of the Spatsizi River map area, north-central British Columbia; *Geological Survey of Canada*, Bulletin 577.
- Ferri, F., Osadetz, K. and Evenchick, C.E. (2004): Petroleum source rock potential of Lower to Middle Jurassic clastics, Intermontane basins, British Columbia; *British Columbia Ministry of Energy and Mines, Resource Development and Geoscience Branch*, Summary of Activities 2004, pages 87-97.
- Folk, P.G. (1980): Geological and geochemical geophysical report on the More and Two More mineral claims; *British Columbia Ministry of Energy and Mines*, Assessment Report 9041, 19 pages.
- Geology, Exploration and Mining (1971): Little Les; in *Geology, Exploration and Mining in British Columbia 1971*, *British Columbia Ministry of Energy and Mines*, pages 37-38.
- Grill, E. and Savell, M. (1991): Geological, geochemical and geophysical report on the Wad, Sinter and Bill mineral claims; *British Columbia Ministry of Energy and Mines*, Assessment Report 21,311, 16 pages.
- Gunning, M.H. (1996): Definition and interpretation of Paleozoic volcanic domains, northwestern Stikinia, Iskut River area, British Columbia; unpublished PhD thesis, *University of Western Ontario*, 388 pages.
- Kaip, A.W. (1997): Geology, alteration and mineralization on the Hank property, northwestern British Columbia: a near-surface, low-sulfidation epithermal system; unpublished MSc thesis, *University of British Columbia*, 198 pages.
- Lefebvre, D.V. and Fournier, M.A. (2000): Platinum group element mineral occurrences in British Columbia; *British Columbia Ministry of Energy and Mines*, Geofile Map 2000-2, scale 1:2 000 000.
- Lett, R. and Jackaman, W. (2003): Reanalysis of regional stream sediment survey samples from the Iskut River area; *British Columbia Ministry of Energy and Mines*, Geofile 2003-20, 189 pages.
- Lett, R. and Jackaman, W. (2004): Iskut River and Telegraph Creek - new exploration opportunities in the BC regional geochemical survey database; *British Columbia Ministry of Energy and Mines*, Geological Fieldwork 2003, Paper 2004-1, pages 199-207.
- Lett, R.E., Friske, P.W.B. and Jackaman, W. (2005): The National Geochemical Reconnaissance Program in northwest British Columbia - the Bowser Lake (NTS 104A) Regional Geochemical Survey; *British Columbia Ministry of Energy and Mines*, Geological Fieldwork 2004, Paper 2005-1
- Lewis, P. D. (1992): Structural geology of the Prout Plateau region, Iskut River map area, British Columbia; *British Columbia Ministry of Energy, Mines and Petroleum Resources*, Paper 1992-1, pages 521-527.
- Lewis, P.D. (2001): Structural evolution of the Iskut River area - preliminary results; in *Metallogenesis of the Iskut River area, northwestern British Columbia*, Lewis, P.D., Toma, A. and Tosdal, R.M., editors, *Mineral Deposit Research Unit*, Special Publication Number 1, pages 63-76.
- Lewis, P.D., Macdonald, A.J. and Bartsch, R.D. (2001): Hazelton Group/Bowser Lake Group stratigraphy in the Iskut River area - progress and problems; in *Metallogenesis of the Iskut River Area, Northwestern British Columbia*, Lewis, P.D., Toma, A. and Tosdal, R.M., editors, *Mineral Deposit Research Unit*, Special Publication Number 1, pages 9-30.
- Logan, J.M., Koyanagi, V.M. and Drobe, J.R. (1990): Geology and mineral occurrences of the Forrest Kerr - Iskut River area (104B/15); *British Columbia Ministry of Energy, Mines and Petroleum Resources*, Open File Map 1990-2, scale 1:50 000.
- Logan, J.M., Drobe, J.R. and Elsby, D.C. (1992): Geology, geochemistry and mineral occurrences of the More Creek area, northwestern British Columbia (104G/2); *British Columbia Ministry of Energy, Mines and Petroleum Resources*, Open File 1992-5.
- Logan, J.M. and Drobe, J.R. (1993): Geology of the Mess Lake area, northwestern British Columbia (104G/7W); *British Columbia Ministry of Energy, Mines and Petroleum Resources*, Open File 1993-6.
- Logan, J.M., Drobe, J.R., Koyanagi, V.M. and Elsby, D.C. (1997): Geology of the Forest Kerr - Mess Creek area, northwestern British Columbia (104B/10,15 & 104G/2 & 7W); *British Columbia Ministry of Employment and Investment*, Geoscience Map 1997-3, scale 1:100 000.
- Logan, J.M., Drobe, J.R. and McClelland, W.C. (2000): Geology of the Forest Kerr - Mess Creek area, Northwestern British Columbia (104B/10,15 & 104G/2 & 7W); *British Columbia Ministry of Energy and Mines*, Bulletin 104, 164 pages.
- Malensek, G.A., Baker, N. and Cavey, G. (1990): Assessment report on the Forgold project for Santa Marina Gold Ltd.; *British Columbia Ministry of Energy and Mines*, Assessment Report No. 20,722, 30 pages.
- MacDonald, J.A., Lewis, P.D., Thompson, J.F.H., Nadaraju, G., Bartsch, R.D., Bridge, D.J., Rhys, D.A., Roth, T., Kaip, A., Godwin, C.I. and Sinclair, A.J. (1996): Metallogeny of an early to middle Jurassic Arc, Iskut River area, northwestern British Columbia; *Economic Geology*, Volume 91, no 6, pages 1098-1114.
- Massey, N.W.D. (1999a): Potential for subaqueous hot-spring (Eskay Creek) deposits in British Columbia; *British Columbia Ministry of Energy and Mines*, Open File Map 1999-14, scale 1:2 000 000.
- Massey, N.W.D. (1999b): Volcanogenic massive sulphide deposits in British Columbia; *British Columbia Ministry of Energy and Mines*, Open File Map 1999-2, scale 1:2 000 000.
- McArthur, G., Campbell, I. and LeBel, J.L. (1991): More Creek project - geological, geochemical and geophysical report on the more 5 and 6 mineral claims; *British Columbia Ministry of Energy and Mines*, Assessment Report Number 22,238, 22 pages.
- McClay, K.R., Insley, M.W. and Anderton, R. (1989): Inversion of the Kechika Trough, northeastern British Columbia; in *Inversion Tectonics*, Cooper, M.A. and Williams, G.D., editors, *Geological Society of London*, Special Publication 44, pages 235-257.
- Mortensen, J.K., Wojdak, P., MacDonald, R., Gordee, S.M. and Gabites, J.E. (2005): Regional studies of VMS

- mineralization and potential within the Early Jurassic Hazelton Group, British Columbia; *British Columbia Ministry of Energy and Mines*, Geological Fieldwork 2004, this volume.
- Operation Stikine (1957): Stikine River area, British Columbia (104A, B, G, H, I, J); Map 9-1957.
- Read, P.B., Brown, R.L., Psutka, J.F., Moore, J.M., Journeay, M., Lane, L.S. and Orchard, M.J. (1989): Geology, More and Forest Kerr Creeks (parts of 104B/10,15,16 & 104G/1, 2), northwestern British Columbia; *Geological Survey of Canada*, Open File 2094.
- Ricketts, B.D. and Evenchick, C.A. (1991): Analysis of the middle to upper Jurassic Bowser Basin, northern British Columbia; in *Current Research, Part A*, *Geological Survey of Canada*, Paper 91-1A, pages 65-73.
- Roth, T. (2002): Physical and chemical constraints on mineralization in the Eskay Creek deposit, northwestern British Columbia: evidence from petrography, mineral chemistry, and sulfur isotopes; unpublished PhD thesis, *University of British Columbia*, 401 pages.
- Savell, M. (1990): Geological, geochemical and geophysical report on the RDN and GOZ mineral claims; *British Columbia Ministry of Energy and Mines*, Assessment Reptot Number 20,769, 18 pages.
- Schmitt, H.R. (1977): Triassic - Jurassic granodiorite monzodiorite pluton southeast of Telegraph Creek, BC; unpublished BSc thesis, *University of British Columbia*, 79 pages.
- Schroeter, T.G. and Pardy, J.W. (2004): Lode gold production and resources in British Columbia; *British Columbia Ministry of Energy and Mines*, Open File 2004-1.
- Simpson, K.A. and Nelson, J.L. (2004): Preliminary interpretations of mid-Jurassic volcanic and sedimentary facies in the East Telegraph Creek map area; *Geological Survey of Canada*, Current Research 2004-A1, 8 pages.
- Souther, J.G., 1972: Telegraph Creek map-area, British Columbia; *Geological Survey of Canada*, Paper 71-44.

Pillow Basalt Ridge Facies: Detailed Mapping of Eskay Creek–Equivalent Stratigraphy in Northwestern British Columbia

By T. Barresi¹, J.L. Nelson², D.J. Alldrick² and J. Dostal³

KEYWORDS: bedrock mapping, Eskay Creek, Eskay Rift, Hazelton Group, Pillow Basalt Ridge, bimodal volcanism, Targeted Geoscience Initiative-II (TGI-II)

INTRODUCTION

In 2003, the British Columbia Geological Survey and the Geological Survey of Canada initiated a joint project to map lower Middle Jurassic, upper Hazelton Group rocks in the Telegraph Creek and Iskut River map areas of northwestern British Columbia. In this region, the upper Hazelton Group is host to the Eskay Creek volcanic-hosted massive sulphide (VHMS) deposit, as well as numerous showings, prospects and geochemical anomalies, making it one of the most highly prospective regions in British Columbia. The

scope of the project includes regional and detailed mapping of the upper Hazelton Group, as well as geochemical and geochronological studies. Fieldwork between Kinaskan Lake and More Creek in the Telegraph Creek map area in 2003 (Alldrick *et al.*, 2004a; 2004b) extended southwards into the Iskut and Forrest Kerr areas in 2004 (Alldrick *et al.*, this volume), including Pillow Basalt Ridge. Funding is provided by the British Columbia Ministry of Energy and Mines and by the Geological Survey of Canada's Targeted Geoscience Initiative II.

This paper describes the features of the Pillow Basalt Ridge (PBR) facies, as defined in Alldrick *et al.* (this volume) in the Iskut River map area. Pillow Basalt Ridge is the prominent ridge, 12 km long by 6 km wide, between the Iskut River and Forrest Kerr Creek, north of their confluence (Fig. 1).

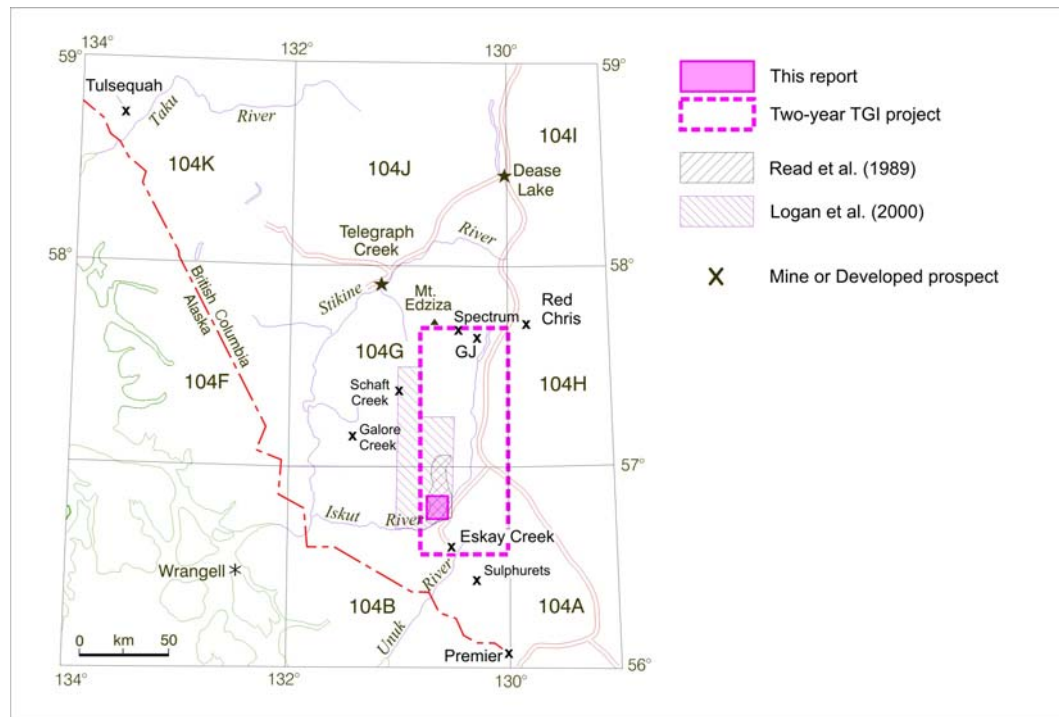


Figure 1. Location map of study area.

¹Department of Earth Science, Dalhousie University, Halifax, NS, B3H 3J5, e-mail: TN42550@dal.ca.

²British Columbia Ministry of Energy and Mines

³Department of Geology, Saint Mary's University, Halifax, NS

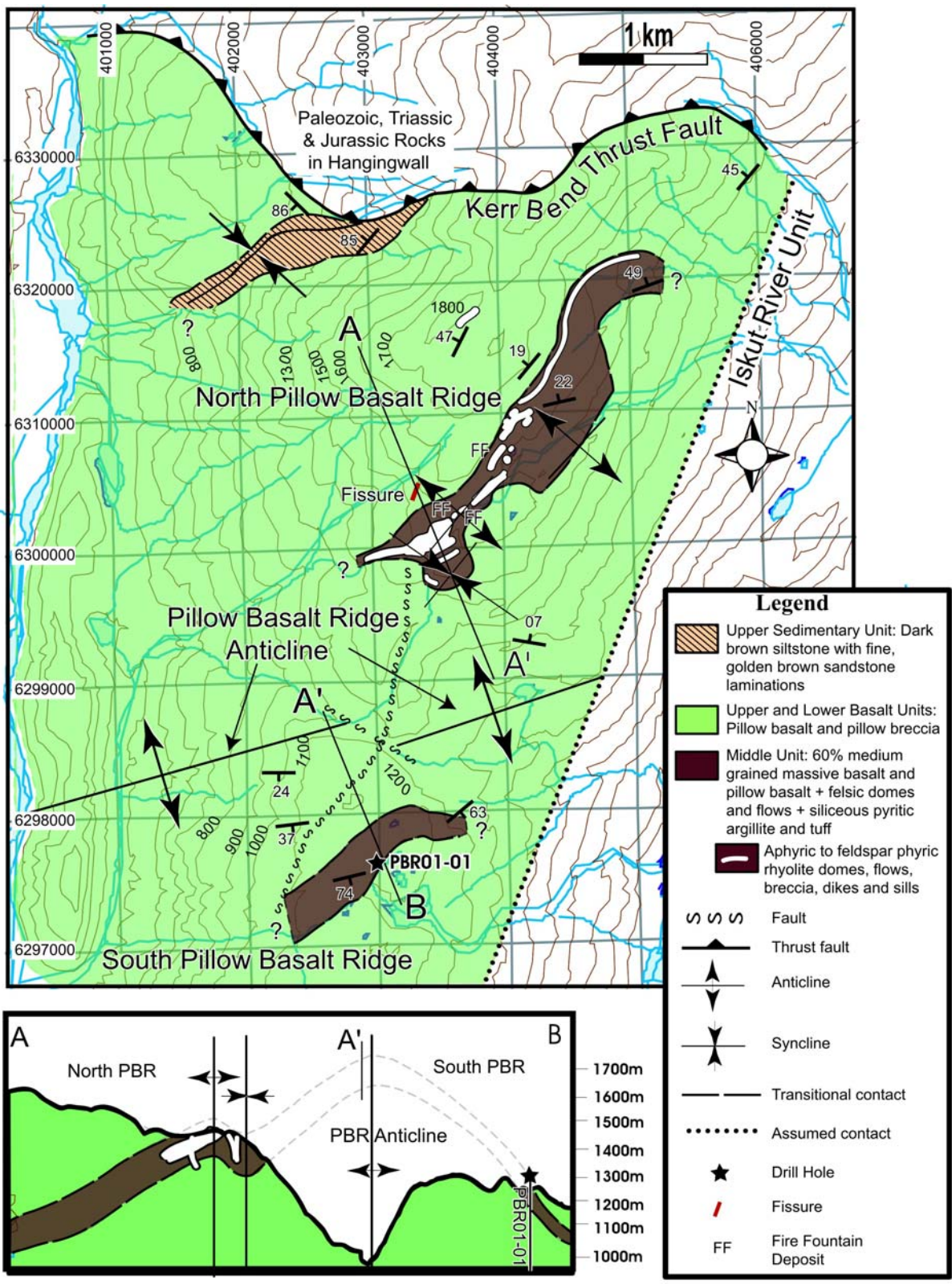


Figure 2. Geologic map and cross-section of Pillow Basalt Ridge.

The overlying Iskut River Unit crops out in the lowlands to the east and south, however the entire northern 9 km of the ridge is composed of PBR facies rocks. To the west, the Forrest Kerr fault juxtaposes the PBR facies against Paleozoic rocks. To the north, the Kerr Bend fault thrusts Paleozoic, Triassic and Jurassic units over PBR facies strata.

GEOLOGICAL SETTING

Pillow Basalt Ridge is located within the Stikine Terrane in northwestern British Columbia. In the Iskut River and Telegraph Creek map areas, the Stikine Terrane is composed of three major pre-accretionary units and two younger, syn- and post-accretionary units (Alldrick *et al.*, 2004a). The main stratigraphic components are 1) metavolcanic and metasedimentary Stikine Assemblage of Devonian to Permian age, 2) island-arc volcanic rocks of the Late Triassic Stuhini Group, 3) Early to Middle Jurassic island-arc volcanic and sedimentary rocks of the Hazelton Group, 4) Middle Jurassic to Cretaceous Bowser Lake Group, which is a sedimentary overlap assemblage that overlies the eastern margin of the Stikine Terrane units, and 5) upper Miocene to Holocene Mount Edziza volcanic complex.

The Pillow Basalt Ridge facies is considered to be of lower Middle Jurassic age and is assigned to the uppermost Hazelton Group (Read *et al.*, 1989; Logan *et al.*, 1994). Previous mapping of PBR identified its major bounding structures and the PBR anticline (Read *et al.*, 1989; Logan *et al.*, 1990). Read *et al.* (1989) depicted PBR as consisting entirely of pillow basalt. Logan *et al.* (1990; 1997) identified five narrow sedimentary intervals within the pillow basalt, which they depicted as discontinuous sedimentary lenses.

In the Telegraph Creek map area to the north, the uppermost Hazelton Group is interpreted to have been deposited in a subaqueous volcano-sedimentary environment, typical of rift settings (Alldrick *et al.*, 2004a). The exact temporal and structural relationship of the Pillow Basalt Ridge facies to rift segments in the Telegraph Creek area is uncertain. The PBR facies is closely affiliated, both spatially and stratigraphically, with the hangingwall sequence of pillow basalts at the Eskay Creek mine. Mapping of the central and southern portion of PBR by Homestake Mining Company (Vaskovic and Huggins, 1998) identified a zone approximately 300 m wide, which contains siliceous argillite beds up to 4 m thick, interbedded with pillow basalt. Homestake collared a diamond-drill hole (PBR01-01) in this zone, at what was then mapped as the crest of the PBR anticline (Fig. 2). The hole penetrated 1419 m of mainly basalt, with minor intervals of mudstone. In 2003, Roca Mines re-entered the hole, drilling to 1770 m without penetrating through the basalt or intersecting

the Eskay equivalent contact mudstones and rhyolites that were hoped to underlie PBR.

STRATIGRAPHY

In 2004, 1:20,000-scale mapping of Pillow Basalt Ridge defined new stratigraphy and refined previously described structures (Fig. 2). The Pillow Basalt Ridge facies is divided into four units: the Lower and Upper Pillow Basalt units are separated by a Middle Unit and overlying the Upper Pillow Basalt Unit are distinctive sedimentary rocks of the Upper Sedimentary Unit. The Middle Unit varies in thickness from 130 to 200 m and contains bimodal volcanics and horizons of siliceous argillites and tuffs (Fig. 3).

Lower and Upper Pillow Basalt Units

The Lower Pillow Basalt Unit is at least 1000 m thick and the Upper Unit is at least 850 m thick. Together they form a volcanic pile which accounts for over 90% of the PBR facies. Both pillow basalt units are composed of two main variants: pillow basalts and pillow basalt breccias with transitional intervals of intact pillows in a breccia matrix. The volcanic pile is made up of many flows that interfinger and onlap one another. Individual flows are 5 to 30 m thick and are defined on a broad scale by different textures and weathering characteristics. There are a great variety of pillow forms, which range in size from 15 cm to 1.5 m in diameter (Fig. 4 and 5). Pillow geometries range from spheres to flattened lobes; most pillows display tail and drape geometry.

Basalt is mainly aphanitic, with medium to dark green fresh surfaces and orange-brown weathered surfaces. Most pillow rims are thin and have textures similar to the pillow centres. However, in some layers, pillow rims are glassy and moderately thick (up to 4 cm). These basalts have a black vitreous appearance and the pillows are often surrounded by a hyaloclastite matrix. Rarely PBR basalts have a porphyritic texture; plagioclase phenocrysts range up to 8 mm long. Variolites (spherical, white weathering, devitrification features typically 1 to 3 mm in diameter) and chlorite-filled vesicles are present in approximately 25% of PBR basalts.

A number of fire fountain deposits were identified in both the lower and upper basalt units (Fig. 2). Fire fountain deposits are characterized by irregular-shaped fluidal clasts in a matrix of blocky and curvilinear fragments (Simpson and McPhie, 2001) and are interpreted to be the result of proximal submarine volcanism, deposited within 10 m of a fissure or vent. Simpson and Nelson (2004) identified these deposits in upper Hazelton Group rift segments to the north.

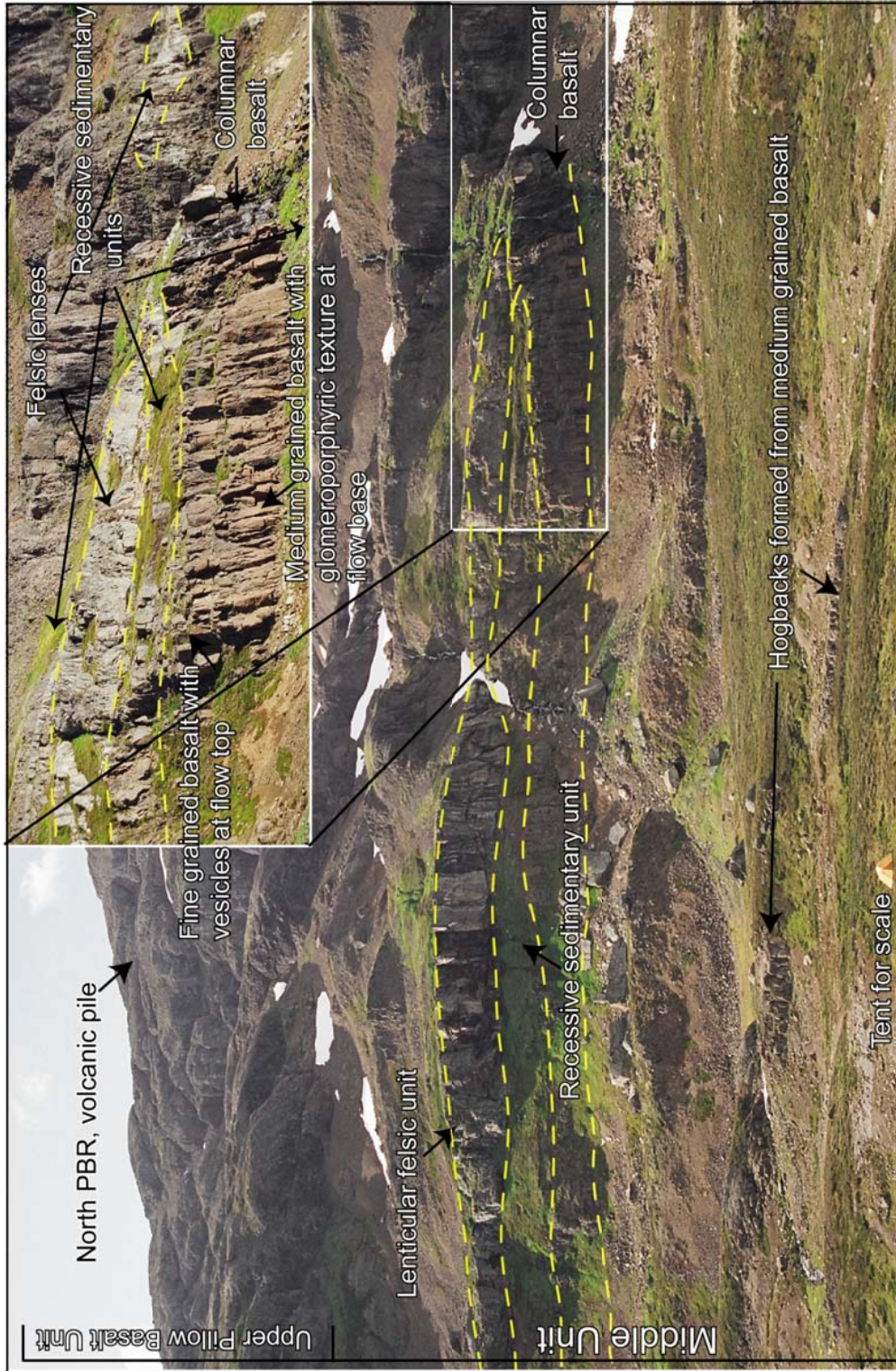


Figure 3. Northern Pillow Basalt Ridge, looking west at the Middle Unit and Upper Pillow Basalt Unit.

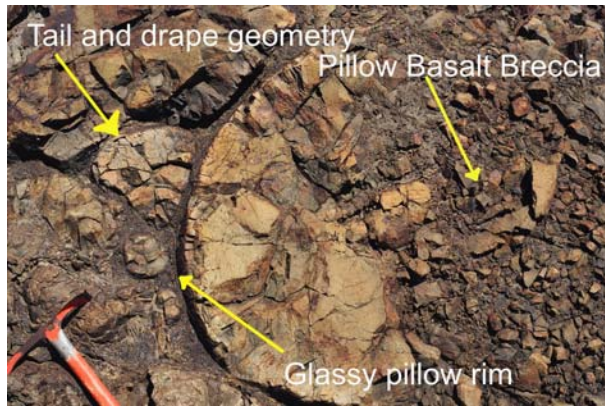


Figure 4. Typical well-developed basalt pillows.



Figure 5. Pillows from the Upper Pillow Basalt Unit directly above the Middle Unit, that range up to 1.5 m in diameter.

In the Upper Pillow Basalt Unit, a crack and fill feature was identified. A 20 m wide fissure cuts 65 m vertically down through a massive pillow basalt layer. This gap is completely infilled with a dense basalt breccia. On the fissure's margins the basalt breccia drapes over intact pillows of the fissure wall.

Although the Upper and Lower Basalt units strongly resemble each other, the following features set them apart: 1) fire fountain deposits, as well as pillows with the largest diameters, are concentrated in the Upper Pillow Basalt Unit immediately above the Middle Unit,

2) in northern PBR, the Upper Pillow Basalt Unit has higher proportions of thick glassy rims and hyaloclastite matrix (Fig. 4); 3) in the northwestern portion of PBR, just below the Upper Sedimentary Unit, a breccia in the Upper Pillow Basalt Unit consists of angular basalt clasts supported in a blue-grey limestone matrix.

Middle Unit - Bimodal Igneous and Sedimentary Zone

The Middle Unit is exposed on both limbs of the PBR anticline (Fig. 2). Pillow basalts in the Middle Unit are interlayered with other lithologies that represent a distinct depositional and volcanic regime different from that seen on the majority of PBR. The thickness of the Middle Unit varies, partly controlled by the paleotopography of the top of the Lower Pillow Basalt Unit.

The Middle Unit is a bimodal igneous and sedimentary zone predominately composed of mafic volcanic rocks interbedded with clastic sedimentary lithologies and felsic volcanic rocks. Overall, 60% of rock exposures in the zone are mafic, but in particular intervals, felsic and sedimentary rocks are the dominant rock types. On cliff exposures, flows of medium-grained, massive basalt form 5 to 25 m thick, orange-brown weathering, vertical faces, with metre-scale columnar joints (Fig. 3). Felsic units form 0.5 to 10 m thick, pale weathering, vertical, resistant cliff faces. Sedimentary intervals are typically 1 to 6 m thick, rusty weathering and recessive. A 30 m thick section of the bimodal igneous and sedimentary rock suite also occurs as a discontinuous band within the Upper Pillow Basalt Unit (Fig. 2).

Mafic Rock of the Middle Unit

Where the Middle Unit crops out on southern PBR, all mafic layers are pillow basalts. On northern PBR, the majority of mafic rock is medium-grained, non-pillowed basalt, which forms massive, columnar-jointed, outcrops. However, pillow basalt is also present. The presence of vesicles and absence of upper chill margins, indicate that the medium-grained massive basalt layers are extrusive flows. They exhibit gradational stratification with the coarsest texture at the bottom of each flow and a vesicular, finer grained texture near the flow tops. The medium-grained basalt commonly contains radiating plagioclase microlites, and locally displays a distinctive glomeroporphyritic texture with feldspars up to 2.5 mm long. Lewis *et al.* (2001) describe a similar texture in the hangingwall basalts of the Eskay Creek mine.

Sedimentary Rock of the Middle Unit

Sedimentary layers are discontinuous and onlap both felsic and mafic flows. Their upper contacts with igneous flows are sometimes peperitic, and in one location several beds are entrained and folded within a felsic flow. Sedimentary rocks of the Middle Unit are medium bedded (5 to 25 cm thick) and can be internally laminated or graded. Some beds have an undulating base, grading and flat upper contacts, which are typical of beds deposited by density currents in a deep basin (Bouma 1962). The most common rock types are interbedded dark brown to black siliceous argillites and light-coloured felsic tuffs (Fig. 6), known as "pyjama beds" (Anderson, 1993). Light-coloured felsic tuff layers are generally more abundant near the tops of sedimentary intervals. Other sedimentary lithologies include light green intermediate to mafic tuff, dark blue-grey massive siltstone, and thin graphite-rich mudstone beds. Beds are typically siliceous; some are highly siliceous with a conchoidal fracture. Most beds contain a distinct felsic volcanic component of potassium feldspar and quartz. Disseminated pyrite crystals, less than 1 mm in size, can constitute up to 10% of the rock volume. Rarely, 1 to 3 mm thick pyrite laminations are preserved. About 20% of the black argillite beds have spherical, white weathering prehnite rosettes up to 1 cm in diameter. These have also been identified in other upper Hazelton Group rocks, including the Contact Mudstones in the Eskay Creek mine area (Ettlinger, 2001) and in the mudstones of the Four Corners complex in the Forgold facies (Alldrick *et al.*, this volume).



Figure 6. Siliceous dark argillites and light felsic tuffs of the Middle Unit.

Felsic Rock of the Middle Unit

Intrusive and extrusive felsic rocks are an important part of the Middle Unit on northern PBR. Intrusive bodies include dikes, sills and cryptodomes; extrusive bodies include flows, domes and breccias. Felsic flows are typically autobrecciated, white to light grey, and locally display flowbanding. Some flows are peperitic,

incorporating up to 30% sedimentary clasts and matrix. The felsic rock is aphanitic, locally spherulitic, has a semi-translucent dove-grey fresh surface, and often contains pyrite. Most felsic rocks have fine (less than 1 mm) potassium feldspar phenocrysts, and rarely quartz and plagioclase microphenocrysts, in a groundmass of potassium feldspar and quartz. Some quartz microphenocrysts are partly resorbed, and they occur in aggregates with potassium feldspar. Flow facies are highly variable and change rapidly between massive flows, autobrecciated flows, and breccias and conglomerates. Some felsic breccias are polymictic with sedimentary clasts and a variety of distinct felsic clasts. At least one flow has a thickness of 10 m or more over a strike length of 3 km; other felsic bodies form lenticular exposures that are less than 10 m across.

Two small felsic volcanic centres were delineated within the Middle Unit on northern PBR. These show rapid thickening into roughly dome-shaped exposures. These two felsic complexes are composed of massive, mainly unbrecciated, felsic rock which is intruded by both felsic and mafic dikes. The contacts between the felsic and mafic dikes, and between the dikes and the surrounding dome, are highly irregular and curvilinear, indicating intrusion into semi-solid bodies. A network of feeder dikes and sills underlies each dome. The domes are surrounded by sedimentary rocks. Large wedges of sedimentary rock up to 4 m thick were incorporated into the magma as giant xenoliths. Bedding attitudes in the sedimentary strata adjacent to the domes depart from the normal PBR structural grain, indicating that they may be controlled locally by the paleoslope of the domes, or deformed by the mafic and felsic dikes.

Upper Sedimentary Unit

The Upper Sedimentary Unit overlies the Upper Pillow Basalt Unit at the northwestern edge of Pillow Basalt Ridge. Here, a syncline developed in the immediate footwall of the Kerr Bend fault exposes the depositional contact between the two units. The Upper Sedimentary Unit is composed of dark grey siltstone with golden brown sandstone laminations. The sedimentary strata interfinger with pillow basalts and in places form the matrix in pillow breccia. This intimate association with the volcanic rocks indicates that the sedimentary rocks are part of the upper Hazelton Group, rather than Bowser Lake Group as suggested in Read *et al.* (1989).

STRUCTURE

Pillow Basalt Ridge is structurally bounded to the north by the Kerr Bend thrust fault, and to the west by the Forrest Kerr fault. As described in the accompanying regional description of Alldrick *et al.*

(this volume), these may be original basin-bounding faults. Although the present Kerr Bend fault places older strata over PBR, and was therefore active following PBR deposition, there is evidence that it was also a controlling structure for a horst of Paleozoic and Triassic rock that was uplifted during PBR deposition.

Alldrick *et al.* (this volume) propose that two stress regimes controlled the major structures on PBR. An early extensional regime is responsible for the northeasterly orientation of the felsic eruptive centres, dikes, fissures, fissure eruptions and fire fountain deposits preserved in Pillow Basalt Ridge. These extensional features are syn-rift.

A later compressional stress regime is responsible for folding which produced the PBR anticline, a broad regional fold that affects all of PBR. The PBR anticline trends 060°, and has been offset by an inferred east-southeast-trending fault that occupies the deep valley separating northern and southern PBR (Fig. 2). Minor folds trending north-northeast to northeast within the Middle Unit are probably related to this folding event. This small-scale buckling of the Middle Unit helped accommodate the space requirements of the fold in the thicker, more rigid, pillow basalt units.

The later compressional regime is related to a sinistral shear couple that straddles PBR (Alldrick *et al.*, this volume). Shearing on the eastern side of PBR is responsible for the northern deflection of PBR strata as it trends towards the Iskut River. This shearing also accommodated deposition of the overlying Iskut River Unit. In contrast to the high energy deposits of the Iskut River Unit, the syncline at the northwestern edge of PBR exposes conformable, fine-grained distal sedimentary rocks that were deposited in a relatively quiescent part of the basin.

FACIES INTERPRETATION

Pillow Basalt Ridge represents a major rift segment where more than 2 km of pillow basalt filled a subsiding subaqueous basin. The total thickness of the PBR facies remains unknown, as does the type of rock that lies beneath it. Alldrick *et al.* (this volume) suggest that basal Middle Jurassic deposits of coarse clastic rock interfingered with medium-grained basalt and felsic rock that are exposed in the hangingwall of the Kerr Bend fault, may also underlie the PBR facies.

The Middle Unit records an interruption in the volcanic and depositional events that characterize the thick Upper and Lower Pillow Basalt units on PBR. The presence of fine-grained felsic turbidites in this interval suggest that there was a period of significant length during which the extrusion of mafic lava was suppressed. If, rather than erupting, mafic magma accumulated at depth, it could have provided sufficient

heat to cause crustal-level partial melting. Hart *et al.* (2004) link the partial ascent of mantle in rift environments to the generation of felsic magmas and the convective hydrothermal systems that are necessary for the formation of VHMS deposits. The reduced amount of mafic eruptions in the Middle Unit may also have allowed time for crystallization to occur in the magma chamber. When this magma next extruded it produced the coarser grained basalt that is characteristic of the Middle Unit on PBR. This sequence of events may also have generated other upper Hazelton bimodal volcanic sequences where massive basalt with a similar coarse texture is observed.

The felsic domes and cryptodomes of the PBR Middle Unit are too small to have produced the adjacent felsic flows and breccias. At least one felsic centre, now either buried or eroded, must have been significantly larger than those currently exposed on PBR.

Sparse paleo-direction indicators, including branching pillows, lava tubes, and the orientation of sedimentary layers entrained into lava flows, show a pattern of southerly flow. This suggests that the main eruptive centre was located on northern PBR or even farther to the north. The relatively thin (150 m thick) interval of PBR equivalent strata in the hangingwall of the Eskay Creek mine probably represents the fringe of this volcanic accumulation.

The differences between the Middle Unit exposures on northern and southern PBR are also consistent with north-south, proximal-to-distal progression. The Middle Unit on northern PBR is thicker than on southern PBR. It contains significant amounts of felsic and medium-grained mafic volcanics. The thinner Middle Unit on southern PBR contains only pillow basalts with sedimentary intervals; it does not contain any of the more viscous volcanic rocks that characterize the northern exposures.

Farther to the north, in the Forgold facies (Alldrick *et al.*, this volume), a larger felsic centre, the Four Corners complex, is present. If the Forgold facies was initially part of the same rift segment as the PBR facies, this may represent further northward thickening of the Middle Unit.

The suite of rock types that comprise the Middle Unit of PBR is not restricted to the Middle Unit. A narrow, discontinuous zone that repeats the Middle Unit's rock suite is also present within the Upper Pillow Basalt Unit. Variations of this rock suite were also observed in the Four Corners complex of the Forgold facies, and in the Sixpack Range (Alldrick *et al.*, this volume). This suggests that the events that led to the suppression of mafic volcanism, the deposition of sediments, generation of felsic volcanism, and the production of coarser grained massive basalt, were repeated several times throughout the history of the rift. Each of these intervals may represent favourable

stratigraphy for the formation and preservation of VHMS mineralization.

CONCLUSIONS

Detailed mapping of Pillow Basalt Ridge in the Iskut River map area has defined four map units: a Lower Pillow Basalt Unit; a Middle Unit which consists of bimodal volcanic rocks and intercalated clastic sedimentary strata; an Upper Pillow Basalt Unit; and the overlying siltstones of the Upper Sedimentary Unit. The PBR facies is interpreted to have been deposited in an extensional submarine setting where basin subsidence kept pace with the accumulation of at least a 2 km thickness of volcanic and sedimentary rocks.

The Middle Unit represents a time interval when there were decreased mafic eruptions, but a sustained presence of a large mafic magma chamber. Heat from the mafic magma chamber generated felsic magmas from partial melting of the crust, and could potentially have driven VHMS mineralizing systems.

The presence of bimodal volcanism, fire fountain deposits, and pyritic sedimentary and felsic horizons are all indications that the Middle Unit of PBR may be favourable strata for the presence of VHMS style mineralization. The presence of bimodal igneous and sedimentary rock suites in the Middle Unit, elsewhere on PBR, and in other rift facies (the Forgold and Sixpack facies; Alldrick *et al.*, this volume), indicates that otherwise less prospective pillow basalt sequences do contain strata that is favourable to VHMS formation and preservation.

Strata underlying PBR at depth also represent an attractive exploration target. The new interpretation of the location and orientation of the PBR anticline presented in this article should facilitate future exploration of this blind strata.

REFERENCES

Alldrick, D.J., Stewart, M.L., Nelson, J.L. and Simpson, K.A. (2004a): Tracking the Eskay Rift through northern British Columbia - geology and mineral occurrences of the Upper Iskut River area; *British Columbia Ministry of Energy and Mines*, Geological Fieldwork 2003, Paper 2004-1, pages 1-18.

- Alldrick, D.J., Stewart, M.L., Nelson, J.L. and Simpson, K.A. (2004b): Geology of the More Creek - Kinaskan Lake area, northwestern British Columbia; *British Columbia Ministry of Energy and Mines*, Open File Map 2004-2, scale 1:50 000.
- Anderson, R.G. (1993): A Mesozoic stratigraphic and plutonic framework for northwestern Stikinia, northwestern British Columbia, Canada; *in* Mesozoic Paleogeography of the Western United States-II, Dunne, G. and McDougall, K., editors, *Pacific Section SEPM*, Volume 71, pages 477-494.
- Bouma, A.H. (1962): Sedimentology of some flysch deposits; *Elsevier*, Amsterdam, 168 pages.
- Ettlinger, A.D. (2001): Eskay Creek 21 Zone; *in* Metallogensis of the Iskut River Area, Northwestern British Columbia, Lewis, P.D., Toma, A. and Tosdal, R.M., editors, *Mineral Deposit Research Unit*, Special Publication Number 1.
- Hart, T.R., Gibson, H.L. and Leshner, C.M. (2004): Trace element geochemistry and petrogenesis of felsic volcanic rocks associated with volcanogenic massive Cu-Zn-Pb sulfide deposits; *Economic Geology*, Volume 99, pages 1003-1013.
- Lewis, P.D., Macdonald, A.J. and Bartsch, R.D. (2001): Hazelton Group/Bowser Lake Group stratigraphy in the Iskut River area: progress and problems; *in* Metallogensis of the Iskut River Area, Northwestern British Columbia, Lewis, P.D., Toma, A. and Tosdal, R.M., editors, *Mineral Deposit Research Unit*, Special Publication Number 1.
- Logan, J.M., Koyanagi, V.M. and Drobe, J.R. (1990): Geology and mineral occurrences of the Forrest Kerr - Iskut River area (104B/15); *British Columbia Ministry of Energy Mines and Petroleum Resources*, Open File Map 1990-2, scale 1:50 000.
- Logan, J.M., Drobe, J.R., Koyanagi, V.M. and Elsby, D.C. (1997): Geology of the Forrest Kerr-Mess Creek area, northwestern British Columbia (105B/10, 15 & 105G/2 and 7W); *Ministry of Employment and Investment*, Geoscience Map 1997-3, scale 1:100 000.
- Read, P.B., Brown, R.L., Psutka, J.F., Moore, J.M., Journeay, M., Lane, L.S. and Orchard, M.J. (1989): Geology, More and Forrest Kerr Creeks (parts of 104B/10, 15, 16 & 104G/1, 2), northwestern British Columbia; *Geological Survey of Canada*, Open File 2094.
- Simpson, K.A. and McPhie, J. (2001): Fluidal-clast breccia generated by submarine fire fountaining, Trooper Creek Formation, Queensland, Australia; *Journal of Volcanology and Geothermal Research*, Volume 109, pages 339-355.
- Simpson, K.A. and Nelson, J.L. (2004): Preliminary interpretations of mid-Jurassic volcanic and sedimentary facies in the East Telegraph Creek map area; *Geological Survey of Canada*, Current Research 2004-A1, 8 pages.
- Vaskovic, M.S. and Huggins, C. (1998): Assessment report on rock and stream geochemical sampling on the PBR Property; *BC Ministry of Energy and Mines*, Assessment Report No. 25,777, 20 pages.

Geochemistry and Petrography of Upper Hazelton Group Volcanics: VHMS-Favourable Stratigraphy in the Iskut River and Telegraph Creek Map Areas, Northwestern British Columbia

By T. Barresi¹ and J. Dostal²

KEYWORDS: Eskay Creek, Eskay Rift, Hazelton Group, geochemistry, petrochemistry, island arc, bimodal volcanism, VMS deposits, Targeted Geoscience Initiative II (TGI-II)

INTRODUCTION

In 2003, the British Columbia Geological Survey and the Geological Survey of Canada initiated a joint project to map lower Middle Jurassic, upper Hazelton Group rocks in the Telegraph Creek and Iskut River map areas of northwestern British Columbia. In this region, the upper Hazelton Group is host to the Eskay Creek volcanic-hosted massive sulphide (VHMS) deposit, as well as numerous showings, prospects and geochemical anomalies, making it one of the most highly prospective regions in British Columbia. The scope of the project includes regional and detailed mapping of the upper Hazelton Group as well as geochemical and geochronological studies. Funding is provided by the British Columbia Ministry of Energy

and Mines, and by the Geological Survey of Canada's Targeted Geoscience Initiative II.

This paper is the first of a series that will present and interpret whole rock and mineral chemistry data from the study area. The purpose of studying these data is to better understand the igneous and tectonic processes that were dominant during the formation of the Eskay Creek VHMS deposit, and to determine the significance of similarities and variations in the geochemistry of Eskay Creek time-equivalent volcanic rocks along the length of the Eskay Rift. This study may lead to a better understanding of how whole rock geochemistry can be used as an exploration tool in finding VHMS style mineralization. The data presented in this article are whole rock geochemical analyses of 17 volcanic and related intrusive rocks that were collected during the 2003 field season from the area between More Creek and Kinaskan Lake, in the Telegraph Creek map area (Fig. 1). The focus of this study is on Lower to Middle Jurassic, upper Hazelton Group rocks, which in the study area are assigned to the Willow Ridge Complex (Alldrick *et al.*, 2004a; Alldrick *et al.*, 2004b).

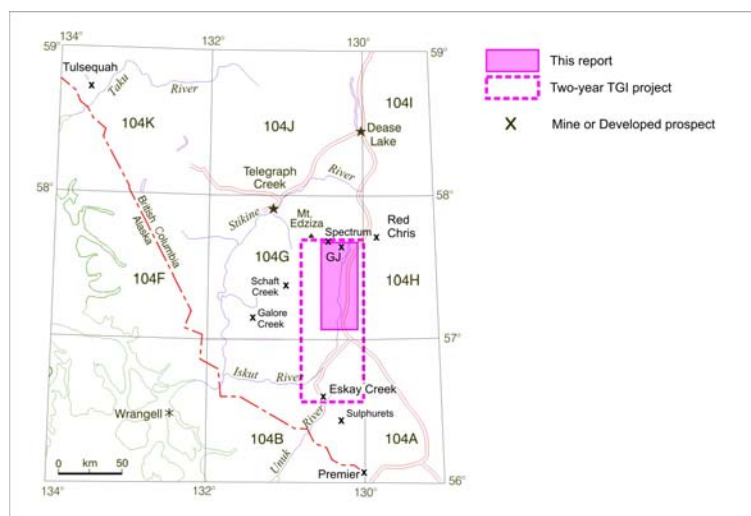


Figure 1. Project location map; modified from Logan *et al.* (2000)

1 – Department of Earth Science, Dalhousie University, Halifax, NS, B3H 3J5 e-mail: TN425520@dal.ca

2 – Department of Geology, Saint Mary's University, Halifax, NS, B3H 3C3

GEOLOGICAL SETTING

The Willow Ridge Complex (WRC) is located within the Stikine Terrane in northwestern British Columbia (Fig. 2). The Stikine Terrane, in the Iskut and Telegraph Creek map areas, is composed of three major pre-accretionary units and two younger, syn- and post-accretionary, units (Alldrick *et al.*, 2004a). The main stratigraphic components are: 1) the metavolcanic and metasedimentary Stikine Assemblage of Devonian to Permian age; 2) island-arc volcanic rocks of the Late Triassic Stuhini Group; 3) Early to Middle Jurassic island-arc volcanic and sedimentary rocks of the Hazelton Group; 4) the Middle Jurassic to Cretaceous Bowser Lake Group, which is a sedimentary overlap assemblage that overlies the eastern margin of the Stikine Terrane units; and 5) the upper Miocene to Holocene Mount Edziza Volcanic Complex.

The Willow Ridge Complex is defined by Alldrick *et al.* (2004a). It is considered to be a part of the Eskay Creek Facies of Anderson and Thorkelson (1990) and is interpreted to have been deposited in a subaqueous volcano-sedimentary environment, typical of rift settings (Alldrick *et al.*, 2004a). Alldrick *et al.* (2004a) describe the WRC as a “thick package of basalt lava flows and feeder dikes, minor interlayered dacite and rhyolite lava flows, breccias, feeder dikes and lava domes, and intercalated volcanoclastic sedimentary rocks”. Alldrick *et al.* (2004a) interpret the volcanic rocks within the complex as a bimodal volcanic suite. The full thickness of the complex is uncertain, but on Table Mountain it is at least 4 km thick. The complex is divided into three units: a Lower Basalt Unit, a Middle Sedimentary Unit, and an Upper Basalt Unit, which unconformably overlie older, Stuhini Group or lower Hazelton Group volcanic breccias. All three WRC units have intercalated felsic flows and feeder dikes and sills. The Middle Sedimentary Unit is predominantly composed of clastic rocks but also contains bimodal volcanics, including a north-northwesterly trending line of felsic domes. The reader is referred to Alldrick *et al.* (2004a), Alldrick *et al.* (2004b), and Simpson and Nelson (2004) for detailed maps and descriptions of the geology in the study area.

PETROGRAPHY

The WRC consists of a bimodal, felsic and mafic igneous rock suite. Mafic rocks consist mainly of basalt and minor andesite; felsic rocks are rhyolite.

Mafic rock in the WRC is aphanitic and dark to olive green. Mafic intrusions include dikes and sills, and, on Willow Ridge, stocks assigned to the Three Sisters Plutonic Suite. Extrusive units include massive flows, pillowed flows and pillow breccia, hyaloclastite,

and breccias of fluidly shaped clasts typical of fire fountain deposits (Simpson and Nelson, 2004). Basalts and andesites are commonly amygdaloidal and have characteristic white weathering variolites, a devitrification feature. Their primary mineralogy includes densely packed plagioclase laths and clinopyroxene phenocrysts in a devitrified glassy matrix. Amygdules are filled with chlorite and minor quartz and calcite. The primary mineralogy of basalts and andesites is well preserved with the exception of secondary calcite in the matrix and clinopyroxene phenocrysts that are in some cases replaced by chlorite and quartz. Secondary alteration accounts for between 5 and 25% of the modal mineralogy in mafic samples.

Felsic rock in the WRC is aphanitic, white to pale green, commonly spherulitic and rarely has small vesicles/amygdules that are elongated parallel to flow. High-level felsic intrusions include dikes, sills and cryptodomes; extrusive bodies occur as flows, breccias and domes. The rhyolites are generally aphyric, and rarely feldspar porphyritic with potassium feldspar and lesser plagioclase phenocrysts. The groundmass has undergone minor devitrification and is mainly composed of quartz and potassium feldspar. Accessory amounts of sphene are common; sample JN01-08 also contains zircon. The proportion of opaque minerals is low in most samples, but sample JN04-11 contains 14% opaque minerals. The samples have undergone varying degrees of alteration and contain secondary epidote, chlorite, calcite, quartz and white mica. Secondary alteration products account for between 5 and 15% of the modal mineralogy in rhyolite samples.

ANALYTICAL METHODOLOGY AND SAMPLING PROCEDURE

Seventeen samples for whole rock and trace element analysis were collected from surface exposures during regional mapping (Fig. 2; Alldrick *et al.* 2004a; Alldrick *et al.* 2004b). They were selected to represent the least altered instances of the full range of volcanic lithologies that occur commonly in the study area. Four samples (A03-14-7, A03-18-6, JN-07-01 and MS-03-07-02) represent the Triassic Stuhini Group and lower Hazelton Group. The remaining samples are upper Hazelton Group rocks of the Willow Ridge Complex. The data for all samples are presented in Table 1. For the analysis discussed in this paper, four samples are discarded. Sample A03-18-6 is discarded because it is a tuff. Samples A03-14-7 and MS-03-06-05 are discarded due to high degrees of alteration. Sample KS04-23B is discarded because it contains a high proportion of mafic xenocrysts. The remaining samples represent three lithologies: rhyolite, basalt and andesite.

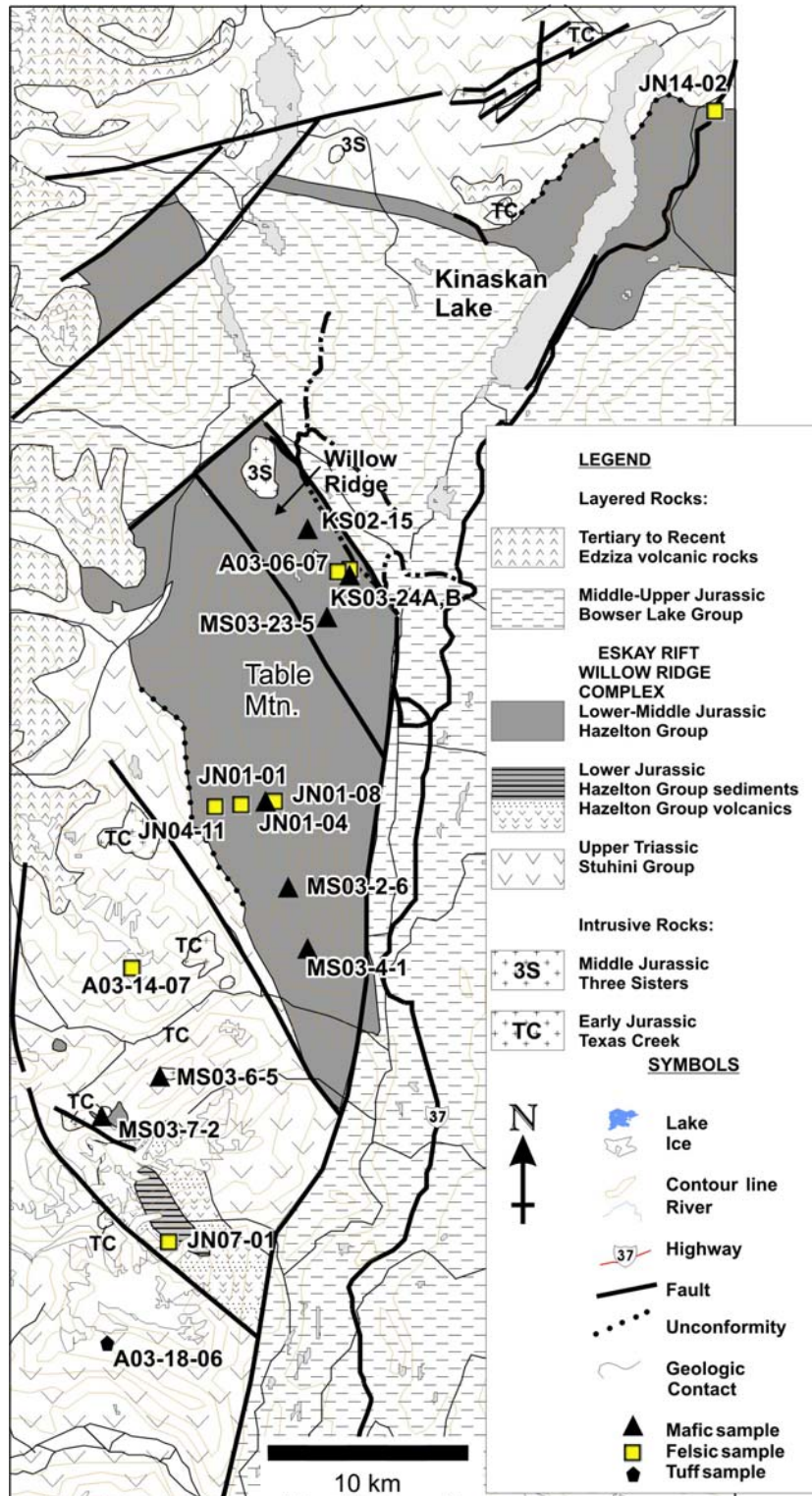


Figure 2. Geology map with sample locations; modified from Alldrick *et al.* (2004a).

TABLE 1. WHOLE ROCK GEOCHEMISTRY OF 17 SAMPLES FROM THE AREA BETWEEN MORE CREEK AND KINASKAN LAKE, IN THE TELEGRAPH CREEK MAP AREA

	WRC Rhyolite						WRC Mafic Rock						Triassic Rock			Discarded Samples		
	A03-06-07	JN01-01	JN01-08	JN04-11	JN14-02	JN01-04	KS02-15	KS03-24A	MS-03-23-05	MS-03-2-6	MS-03-04-01	JN07-01	MS-03-07-02	A03-14-07	A03-18-06	KS03-24B	MS-03-06-05	
Nothing	421260	416387	417267	415228	437134	417070	418813	421488	420457	419124	418694	412100	410866	409615	409310	421488	412705	
Easting	6367558	6357233	6357929	6357218	6390500	6357677	6369407	6367159	6365319	6353741	6351346	6336122	6340927	6349481	6330150	6367159	6342981	
SiO ₂	82.58	76.48	81.94	69.01	69.87	46.11	47.09	51.77	56.7	61.77	53.91	83.9	52.93	96.58	64.9	71.02	55.34	
TiO ₂	0.1	0.15	0.23	0.5	0.18	1.51	0.98	1.94	1.73	1.15	1.36	0.12	0.87	0.05	0.94	0.68	0.68	
Al ₂ O ₃	8.27	11.84	7.73	12.68	14.06	13.02	16.09	13.64	14.89	13.55	15.06	7.46	18.23	0.07	12.93	13.34	16.38	
Fe ₂ O ₃	0.52	1.72	1.37	5.48	3.14	9.75	10.31	13.01	10.85	9.18	10.52	1.62	5.92	0.6	7.51	3.15	6.09	
MnO	0.01	0.01	0.01	0.1	0.09	0.18	0.12	0.25	0.1	0.1	0.1	0.01	0.2	0.01	0.01	0.01	0.12	
MgO	0.02	0.23	0.49	0.72	0.2	3.35	8.6	4.5	3.17	3.08	5.26	0.15	0.79	0.01	2.56	0.94	1.8	
CaO	0.07	0.03	0.31	0.3	0.98	11.47	6.17	2.39	2.25	1.08	3.44	0.21	8.39	0.05	1.19	1	5.15	
Na ₂ O	0.21	4.55	0.23	4.78	3.38	4.4	3.98	0.67	5.67	3.52	4.53	2.18	4.21	0.01	1.89	5.32	3.08	
K ₂ O	6.96	3.07	5.46	1.12	5.19	0.64	0.62	6.03	0.02	2.42	1.13	2.75	1.99	0.18	2.68	2.22	3.83	
P ₂ O ₅	0.03	0.01	0.07	0.1	0.05	0.28	0.15	0.74	0.31	0.34	0.31	0.01	0.34	0.01	0.15	0.28	0.3	
Ba	0.09	0.15	0.27	0.1	0.15	0.06	0.07	0.17	0.02	0.11	0.11	0.21	0.14	0.03	0.02	0.06	0.2	
LOI	0.37	0.98	1.14	4.63	2	8.14	5.32	4.46	3.89	3.31	3.88	0.7	5.48	1.33	4.84	1.35	6.36	
Total	99.23	99.22	99.25	99.52	99.29	98.91	99.5	99.57	99.6	99.61	99.61	99.32	99.49	99.73	99.62	99.37	99.33	
V (ppm)	11	10	8	16	7	280	169	292	132	52	231	7	136	19	160	65	124	
Y	14.55	48.05	31.73	51.76	32.08	35.52	18.47	40.79	39.04	31.04	43.53	42.67	22.63	4.34	19.92	30.98	18.82	
Zr	99.19	365.48	216.59	352.68	308.44	147.48	68.5	157.27	189.8	186.33	222.51	253.57	135.22	17.10	163.88	178.48	140.75	
Nb	5.00	21.03	11.50	21.88	17.94	13.53	6.17	9.01	14.95	15.08	15.1	20.53	12.34	3.72	10.05	9.19	13.8	
La	19.79	26.97	14.15	23.23	32.48	10.96	4.25	15.38	18.35	13.23	15.37	7.68	18.65	6.00	13.81	20.12	16.3	
Ce	37.28	53.69	26.26	46.59	60.97	24.58	10.62	31.83	37.28	31.18	33.33	17.29	35.62	13.36	28.78	42.07	30.42	
Pr	3.50	6.65	3.53	5.92	7.18	3.48	1.69	4.50	5.06	4.50	4.50	2.44	4.53	1.43	4.34	5.37	3.80	
Nd	11.42	27.65	14.46	25.04	27.20	16.36	8.79	20.71	22.54	20.57	20.08	11.22	19.38	5.44	18.90	22.03	16.05	
Sm	1.84	6.41	3.17	6.06	5.30	4.39	2.52	5.39	5.47	5.30	5.15	3.57	4.33	0.70	4.54	4.74	3.58	
Eu	0.14	1.05	0.58	1.63	0.89	1.40	0.90	1.47	1.33	1.23	1.43	0.67	1.43	0.11	1.24	0.96	0.98	
Gd	1.51	6.96	3.87	7.34	5.25	5.66	3.18	6.87	6.63	6.02	6.50	4.93	4.50	0.53	4.63	4.98	3.62	
Tb	0.30	1.30	0.73	1.32	0.89	0.98	0.54	1.16	1.10	1.01	1.13	1.04	0.69	0.10	0.72	0.85	0.56	
Dy	2.28	8.83	5.20	9.01	5.82	6.49	3.54	7.54	7.04	6.38	7.66	7.26	4.30	0.71	4.43	5.55	3.50	
Ho	0.57	1.96	1.19	2.03	1.29	1.41	0.76	1.63	1.50	1.29	1.67	1.63	0.89	0.16	0.87	1.22	0.73	
Er	2.11	6.34	3.81	6.43	4.09	4.28	2.25	4.91	4.43	3.73	5.08	5.08	2.56	0.50	2.48	3.72	2.20	
Tm	0.37	1.01	0.59	1	0.64	0.64	0.33	0.72	0.65	0.55	0.77	0.79	0.38	0.07	0.37	0.55	0.33	
Yb	2.74	7.15	4.12	6.81	4.48	4.24	2.13	4.81	4.35	3.60	5.14	5.52	2.46	0.60	2.51	3.70	2.27	
Lu	0.43	1.08	0.59	0.99	0.64	0.6	0.30	0.70	0.61	0.52	0.75	0.78	0.36	0.09	0.37	0.53	0.32	
Hf	3.58	8.74	4.64	7.35	6.55	3.49	1.59	3.65	4.36	4.43	4.79	5.56	3.12	0.32	3.75	3.98	3.28	
Ta	0.66	1.06	0.54	0.93	0.90	0.39	0.11	0.45	0.70	0.73	0.56	0.78	0.51	0.06	0.40	0.58	0.51	
Th	13.77	6.07	3.93	6.41	11.43	1.60	0.25	2.26	3.23	3.56	3.30	4.51	3.61	0.42	1.75	5.46	5.75	

Processing of samples included the removal of weathered surfaces by selective chip sampling. Samples were pulped in a chrome steel swing mill. The major oxides as well as Ba and V were determined by x-ray fluorescence (XRF) using a fused disc and Siemens spectrometer at Global Discovery Labs in Vancouver, British Columbia. Loss on ignition was determined by fusion at 1100°C. Trace element concentrations, including analyses of Y, Zr, Nb, Hf, Ta, Th and the rare earth elements (REE) were determined by inductively coupled plasma mass spectrometry (ICP-MS) at Memorial University of Newfoundland (rock powders were dissolved with Na₂O₂). The quality of analysis was monitored by simultaneous analysis of standard reference rocks. Major oxides and trace elements have been recalculated to anhydrous for all discussion in this paper. Table 1 contains the results of all original data, which are not recalculated to anhydrous compositions.

WHOLE ROCK GEOCHEMISTRY

WRC Rocks

Analysis of major oxides of metamorphosed and altered rocks, such as those from the WRC, poses difficulties because many major elements have a high degree of mobility. In particular, the hydrothermal alteration of feldspars and glass results in the loss of alkalis (Saeki and Date, 1980), and the formation of chlorite can affect Mg and Fe concentrations (Lentz, 1999). Other major elements, such as Al₂O₃ and TiO₂, are normally considered immobile. For this study an effort was made to collect samples exhibiting the least amount of alteration. However, petrography shows that many samples have been subject to significant alteration. As a result, the emphasis of this study is on trace element geochemistry utilizing mainly the REE and high field strength elements, which are considered to be immobile under low-grade alteration conditions (Whitford *et al.*, 1988; Lentz, 1999).

According to SiO₂ vs Zr/TiO₂ ratios, WRC rocks range, on an anhydrous basis, from basalts and andesites to dacites and rhyolites (Fig. 3). Two samples have very high contents of SiO₂ (83%), indicating that they were affected by secondary SiO₂ enrichment. In addition, petrography shows that secondary quartz is present in some mafic samples, which suggests that the rocks which plot as andesites may be silicified basalt. Because of this apparent SiO₂ mobility, classification of WRC rocks must be done using trace elements. According to Zr/TiO₂ vs Nb/Y ratios, the WRC volcanics are a bimodal rock suite, consisting of mafic rocks that range in composition from basalts to andesite-basalts, and felsic rocks that are all rhyolites (Fig. 4).

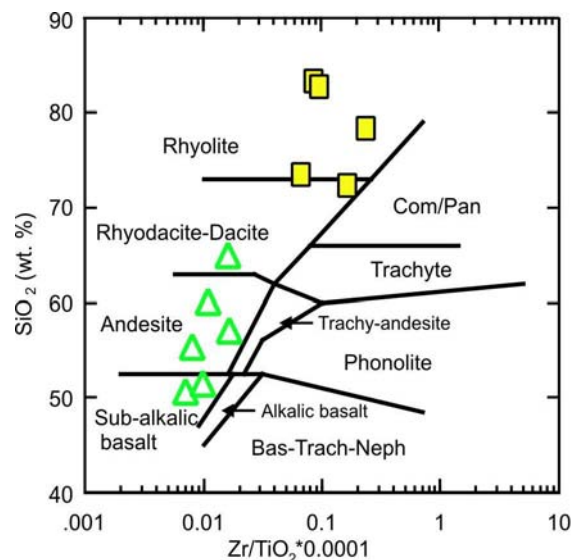


Figure 3. Classification of WRC volcanic rocks; squares = felsic samples, triangles = mafic samples; Com/Pan = comendite and pantellerite; Bas-Trach-Neph = basanite and trachyte and nephelinite; Winchester and Floyd (1977).

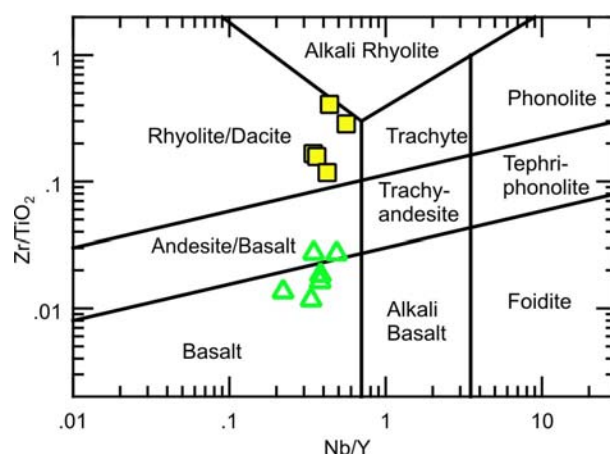


Figure 4. Classification of WRC volcanic rocks according to immobile elements; squares = felsic samples, triangles = mafic samples; Pearce (1996).

Both classification systems agree that the WRC rocks are sub-alkalic. A plot of TiO₂ vs Mg# (Mg# = Mg/(Mg+Fe_{tot})) supports the bimodality of the suite, showing that the felsic and mafic rocks form two distinct populations (Fig. 5).

WRC Mafic Rocks

Mafic rocks of the Willow Ridge Complex are basalts and andesites (Fig. 4). According to their negative trend on a TiO₂ vs Mg# diagram (Fig. 5) and overall high TiO₂ values (1.3 – 2%), they have a

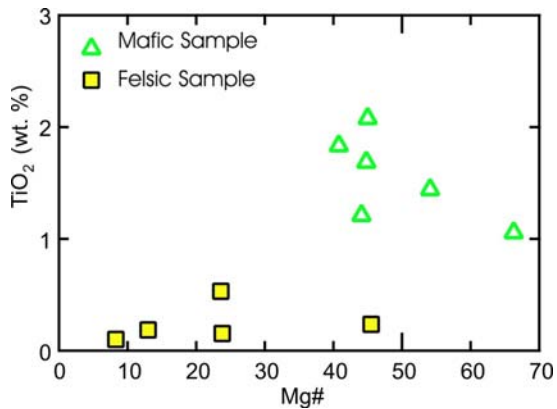


Figure 5. TiO_2 vs Mg\# ($\text{Mg\#} = \text{Mg}/(\text{Mg} + \text{Fe}_{\text{tot}})$) plot of WRC mafic and felsic volcanic rocks; shows two unrelated populations; mafic samples have high TiO_2 concentrations and a negative slope.

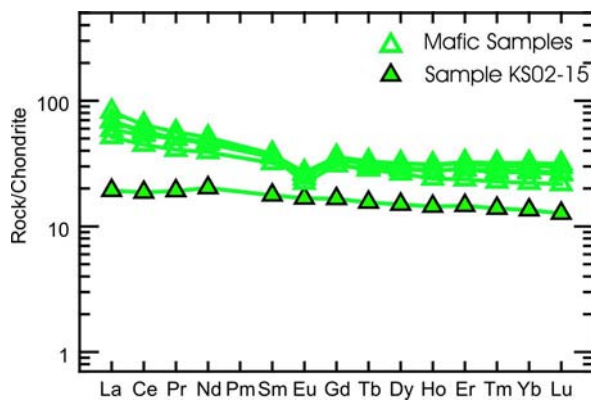


Figure 6. Chondrite normalized REE plot of WRC mafic rocks; Sun and McDonough (1989).

tholeiitic MORB affinity. Rare earth elements (REE) show a slight enrichment in light REE (LREE) ($\text{La}_n/\text{Sm}_n = 1.83$), flat heavy REE (HREE) ($\text{Gd}_n/\text{Yb}_n = 1.19$) and a small negative Eu anomaly (Fig. 6). Sample KS-02-15 has lower absolute abundance of REE and a nearly flat pattern ($\text{La}_n/\text{Yb}_n = 1.43$). Mantle normalized trace element abundance patterns for the mafic rocks show a slight enrichment of strongly incompatible elements, sloping from Th to Sm with a small but distinct negative Nb anomaly (Fig. 7). Sample KS02-15 has lower absolute abundances of incompatible elements than the other mafic samples, and it does not show a negative Nb anomaly. There are no significant systematic differences between the trace element characteristics of basalts and andesites.

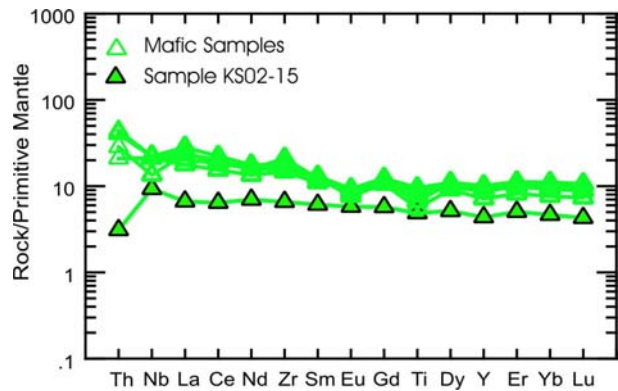


Figure 7. Primitive mantle normalized immobile element plot of WRC mafic rocks; Sun and McDonough (1989).

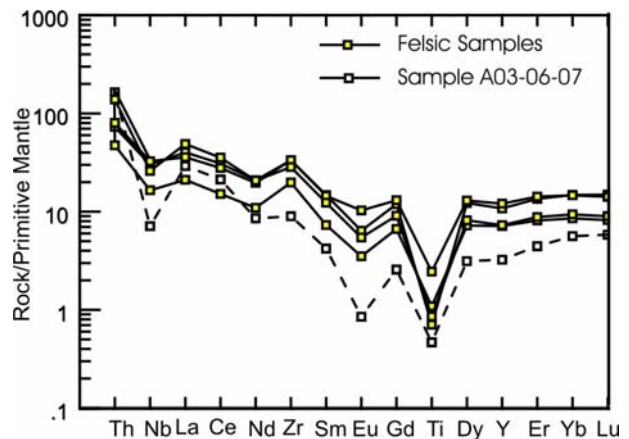


Figure 8. Chondrite normalized REE plot of WRC felsic rocks; Sun and McDonough (1989).

WRC Felsic Rocks

The very high concentrations of SiO_2 (between 72% and 83%) in the rhyolites suggest that at least some samples were affected by secondary silicification. The majority of felsic samples follow the same pattern on REE diagrams and show enrichment in LREE ($\text{La}_n/\text{Sm}_n = 3.01$), flat HREE ($\text{Gd}_n/\text{Yb}_n = 0.86$) and a slight negative Eu anomaly (Fig. 8). One sample (A03-06-07) has a very different, V-shaped, REE pattern. It has a moderately steep downward slope from La to Sm ($\text{La}_n/\text{Sm}_n = 6.93$), a shallow upward slope from Gd to Lu ($\text{Gd}_n/\text{Yb}_n = 0.46$) and a strong negative Eu anomaly. Mantle normalized trace element plots also distinguish sample A03-06-07 from the main felsic population (Fig. 9). The four felsic samples that plot together have a

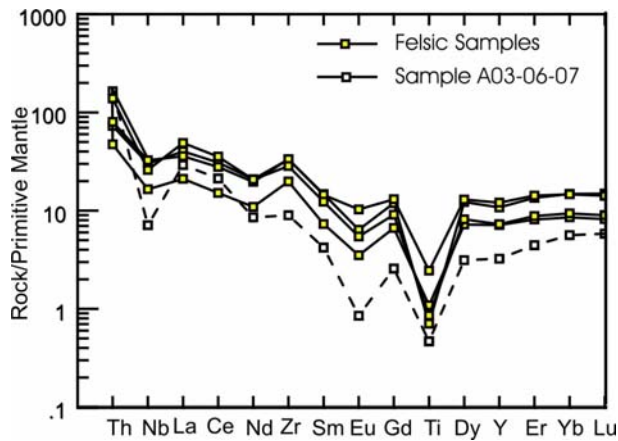


Figure 9. Primitive mantle normalized immobile element plot of WRC felsic rocks; Sun and McDonough (1989).

shallow downward slope up to Sm with mildly negative Nb, strongly negative Ti and weak positive Zr anomalies. Sample A03-06-07 has a lower absolute abundance of most incompatible elements, a steeper negative slope up to Sm and stronger negative Nb and Eu anomalies.

DISCUSSION

The volcanic rocks of the Willow Ridge Complex form a bimodal, sub-alkalic suite that is consistent with a rifting arc environment. Two sources are proposed for the mafic rocks within the complex. Sample KS02-15, which has a flat REE pattern and a positive Nb anomaly on a mantle normalized profile (Fig. 7), is typical of rift-related basalts generated from asthenospheric mantle. The remaining samples, which are relatively enriched in LREE and incompatible elements such as Th, and have a slight negative Nb anomaly, are derived from sub-arc lithospheric mantle.

Rhyolites in the WRC show a distinct grouping according to Zr/TiO_2 and Nb/Y ratios (Fig. 4). No intermediate or alkali rocks are represented. The absolute abundances of trace elements of rhyolites and basalts overlap (Fig. 10). This precludes the possibility that the rhyolites were derived from fractional crystallization of the basalts. Therefore they must have a different source than the WRC mafic rocks. The most obvious source of the rhyolites is melting of crustal rocks. Sample A03-06-07 has a very different trace element signature than most of the WRC rhyolites; this may be a result of the heterogeneous nature of the crust from which it is derived. A variety of explanations for similar V-shaped REE signatures in felsic rocks are described by Dostal and Chatterjee (1995).

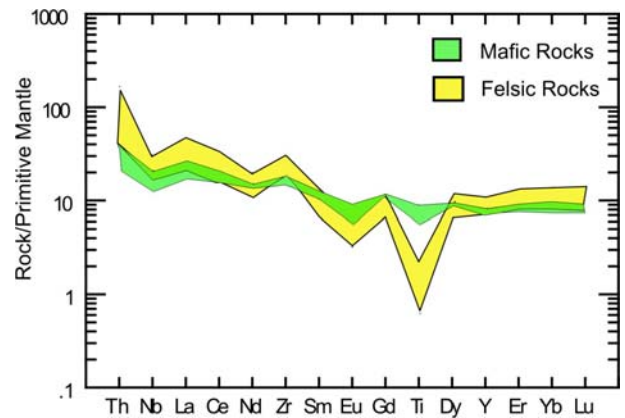


Figure 10. Primitive mantle normalized immobile element plot showing the overlap in element concentrations for WRC felsic and mafic rocks; Sun and McDonough (1989).

Field relations within the WRC and on a regional scale suggest that the upper Hazelton Group in the Telegraph Creek and Iskut River map areas is rift related. The geochemistry of the WRC is consistent with a rifting arc environment. Bimodal volcanism, as expressed in the WRC, is common of rift environments. The following is the most likely scenario that accounts for the range of volcanic rock compositions found within the WRC. Rift-related decompression melting of the asthenosphere produced mafic magmas represented by sample KS-02-15. However, the majority of the magma, which erupted during the period represented by the WRC, was derived from a sub-arc lithospheric mantle source. Heat derived from the mafic magmas caused partial melting within the crust. This generated felsic magmas, which have similar trace element abundances as the sub-arc mantle derived mafic rocks but different relative enrichment patterns, notably Nb and Ti depletions, which reflect their crustal source. Rift-related faulting allowed these magmas to erupt with minimal mixing, which accounts for the bimodality of the WRC volcanic suite.

Comparison of WRC and Eskay Creek Igneous Rocks

Volcanic rocks from the WRC and the Eskay Creek mine have similar chemical characteristics but there are also some subtle differences between them. Rhyolites at Eskay Creek are significantly enriched in the absolute abundances of REE with respect to basalts. This is similar to the relationship between the rhyolites of the WRC and the one asthenospherically derived mafic sample, but contrasts with the relationships seen between WRC rhyolites and the majority of basalts found in the complex. Significantly, Barrett and Sherlock (1996) indicate that the rhyolite and basalt

magmas at Eskay Creek could be derived from different sources. They suggest that the rhyolites are derived from tholeiitic crustal rocks, and the basalts are derived from primitive mantle. This is also the most likely scenario for the genesis of the rhyolites, and the primitive basalt sample from the WRC. Barrett and Sherlock (1996) also agree that the eruption of primitive basalt at Eskay Creek might be due to rift-related deep faulting. Average element concentrations between Eskay Creek rhyolites and basalts are similar to WRC rhyolites and basalts but there are some differences. Barrett and Sherlock (1996) use approximate values of Zr, Y, Nb and $(La/Yb)_n$ to characterize Eskay rhyolites (Table 2). Willow Ridge Complex and Eskay Creek rhyolites have comparable $(La/Yb)_n$ ratios, but the absolute element concentrations are elevated in the WRC rhyolites. Barrett and Sherlock (1996) characterized Eskay Creek basalts by their range of immobile element concentrations. The ranges of element concentrations in WRC basalts have significant overlap with those of Eskay Creek basalts (Table 3).

Rhyolites from both Eskay Creek and from the WRC have incompatible element characteristics that are consistent with FIII type rhyolites of Lescher *et al.* (1986). These types of rhyolites are host to most of the Archean age VHMS deposits in the Superior Province as well as large tonnage VHMS deposits of other ages worldwide (*e.g.*, Kidd Creek, United Verde).

The bimodal volcanic suite of the WRC shows a marked departure from the volcanism in the lower part of the Hazelton Group. Early Jurassic rocks of the Hazelton Group have dominantly intermediate compositions with a calc-alkaline affinity (Marsden and Thorkelson, 1992). Macdonald *et al.* (1996) interpreted the Early Jurassic volcanic environment to be a partly emergent volcanic arc. The geochemical and field characteristics of the WRC both indicate that a shift occurred from an Early Jurassic arc-related environment to a rifting-arc environment during the Middle Jurassic.

CONCLUSIONS

Volcanic rocks from the Willow Ridge Complex are bimodal. Mafic rocks are rift-related tholeiites and all but the most primitive basalts were derived from the sub-arc lithospheric mantle. Rhyolites are derived from partial melting of a heterogeneous crust. The bimodality of the volcanics from the WRC, and the tholeiitic affinity of the mafic rocks, are consistent with field observations which suggest that the WRC represents a rift environment. Volcanic rocks from the WRC represent a shift from Early Jurassic arc formation to Middle Jurassic arc rifting, which has been observed elsewhere in the region, notably at Eskay Creek. Chemically the WRC volcanic rocks are very similar to those at Eskay Creek but there are some subtle differences in their geochemical signatures. Both WRC

and Eskay Creek rhyolites have incompatible element characteristics that are consistent with FIII type rhyolites of Lescher *et al.* (1986). FIII type rhyolites are highly prospective and host most of the Archean VHMS deposits in the Superior province, and many other high tonnage deposits worldwide.

TABLE 2. COMPARISONS OF SELECTED IMMOBILE ELEMENTS IN RHYOLITES FROM ESKAY CREEK AND THE WRC

	Eskay Rhyolite	WRC Rhyolite
Zr	170 ppm	228 ppm
Y	55 ppm	37 ppm
Nb	30 ppm	16 ppm
$(La/Yb)_n$	2-4	2-5

TABLE 3 COMPARISONS OF SELECTED IMMOBILE ELEMENTS IN BASALTS FROM ESKAY CREEK AND THE WRC

	Eskay Basalt	WRC Basalt
TiO ₂	1.3–2%	1.1–1.8%
Zr	60–90 ppm	73–235 ppm
Y	25–40 ppm	19–46 ppm
Nb	2–6 ppm	6–17 ppm

ACKNOWLEDGMENTS

We would like to thank Dani Alldrick, JoAnne Nelson, Martin Stewart and Kirstie Simpson for collecting the geochemical rock samples that are described in this article. We also thank JoAnne Nelson and Dani Alldrick for valuable discussions about upper Hazelton Group geology and for their constructive reviews of this article.

REFERENCES

- Alldrick, D.J., Stewart, M.L., Nelson, J.L. and Simpson, K.A. (2004a): Tracking the Eskay Rift through northern British Columbia - geology and mineral occurrences of the Upper Iskut River area; *British Columbia Ministry of Energy and Mines, Geological Fieldwork 2003, Paper 2004-1*, pages 1-18.
- Alldrick, D.J., Stewart, M.L., Nelson, J.L. and Simpson, K.A. (2004b): Geology of the More Creek - Kinaskan Lake area, northwestern British Columbia; *British Columbia Ministry of Energy and Mines, Open File Map 2004-2, scale 1:50 000*.
- Barrett, T.J. and Sherlock, R.L. (1996): Geology, lithochemistry and volcanic setting of the Eskay Creek Au-Ag-Cu-Zn deposit, northwestern British Columbia; *Exploration and Mining Geology, Volume 5*, pages 339-368.

- Dostal, J. and Chatterjee, A.K. (1995): Origin of topaz-bearing and related peraluminous granites of the Late Devonian Davis Lake pluton, Nova Scotia, Canada: Crystal versus fluid fractionation; *Chemical Geology*, Volume 123, pages 67-88.
- Lentz, D.R. (1999): Petrology, geochemistry, and oxygen isotope interpretation of felsic volcanic and related rocks hosting the Brunswick 6 and 12 massive sulfide deposits (Brunswick belt), Bathurst mining camp, New Brunswick, Canada; *Economic Geology*, Volume 94, pages 57-86.
- Lescher, C.M., Goodwin, A.M., Campbell, I.H. and Gorton, M.P. (1986): Trace-element geochemistry of ore-associated and barren, felsic metavolcanic rocks in the Superior Province, Canada; *Canadian Journal of Earth Science*, Volume 23, pages 222-237.
- Logan, J.M., Drobe, J.R. and McClelland, W.C. (2000): Geology of the Forest Kerr - Mess Creek Area, Northwestern British Columbia (104B/10,15 & 104G/2 & 7W); *British Columbia Ministry of Energy and Mines*, Bulletin 104, 164 pages.
- MacDonald, J.A., Lewis, P.D., Thompson, J.F.H., Nadaraju, G., Bartsch, R.D., Bridge, D.J., Rhys, D.A., Roth, T., Kaip, A., Godwin, C.I. and Sinclair, A.J. (1996): Metallogeny of an Early to Middle Jurassic arc, Iskut River area, northwestern British Columbia; *Economic Geology*, Volume 91, no 6, pages 1098-1114.
- Marsden, H. and Thorkelson, D.J. (1992): Geology of the Hazelton volcanic belt in British Columbia: Implications for the Early to Middle Jurassic evolution of Stikinia; *Tectonics*, Volume 11, no 6, pages 1222-1287.
- Pearce, J.A. (1996): A user's guide to basalt discrimination diagrams; *Geological Association of Canada*, Short Course Notes, Volume 12, pages 79-113.
- Saeki, Y. and Date, J. (1980): Computer application to the alteration data of the footwall dacite lava at the Ezuri Kuroko Deposits, Akito Prefecture; *Mining Geology*, Volume 30, pages 241-250.
- Simpson, K.A. and Nelson, J.L. (2004): Preliminary interpretations of mid-Jurassic volcanic and sedimentary facies in the East Telegraph Creek map area; *Geological Survey of Canada*, Current Research 2004-A1, 8 pages
- Sun, S-S. and McDounough, W.F. (1989): Chemical and isotope systematics of oceanic basalts: Implications for mantle composition and processes; *Geological Society*, Special Publication 42, pages 313-345.
- Whitford, D.J., Korsch, M.J., Porritt, P.M. and Craven, S.J. (1988): Rare-earth element mobility around the volcanogenic massive sulfide deposit at Que River, Tasmania, Australia; *Chemical Geology*, Volume 68, pages 105-199.
- Winchester, J.A. and Floyd, P.A. (1977): Geochemical discrimination of different magma series and their differentiation products using immobile elements; *Chemical Geology*, Volume 20, pages 325-343.

Regional Studies of VMS Mineralization and Potential within the Early Jurassic Hazelton Group, British Columbia

By J.K. Mortensen¹, P. Wojdak², R. Macdonald³, S.M. Gordee¹ and J.E. Gabites¹

KEYWORDS: volcanogenic massive sulphide deposits, Eskay Creek, Hazelton Group, Stikinia, Early Jurassic, Bella Coola area, Whitesail Lake area, southern Babine Range, Stewart area, Forrest Kerr Creek area, Rocks to Riches program

INTRODUCTION

Eskay Creek type (ECT) volcanogenic massive sulphide (VMS) deposits within the Early and early Middle Jurassic Hazelton Group are currently the focus of a considerable amount of mineral exploration effort because of their substantial tonnage potential and high precious metal content. A project was begun in 2003 with the goal of identifying the specific controls that lead to formation of an ECT deposit instead of a more typical polymetallic, “Kuroko-type” VMS deposit. Both of these types of VMS deposits are known to exist within the Hazelton Group in Stikinia (Massey, 1999; Massey et al., 1999); however, deposits in the immediate area of Eskay Creek are the only significant ECT deposits that have been discovered thus far in British Columbia. Funding for the project derives in part from the Rocks to Riches Program, which is administered by the BC & Yukon Chamber of Mines, and by a consortium of mining and exploration companies, with matching funds from the Natural Sciences and Engineering Research Council of Canada (NSERC).

Work during the 2003 and 2004 field seasons included 1) a detailed study of upper Hazelton Group strata in the northern Bella Coola and southern Whitesail Lake area in southern Stikinia known to host VMS occurrences that display some ECT characteristics (Mortensen et al., 2004; Gordee et al., 2005; Mahoney et al., 2005); and 2) a regional investigation of key features, such as crystallization age, geochemistry and eruption temperature of volcanic rocks that host known VMS occurrences within the Hazelton Group, as well as water depth and paleotopography of the immediate area in which the mineralization formed (Mortensen et al., 2004).

Results of the 2004 field work in the Bella Coola and Whitesail Lake areas are summarized by Gordee et al.

(2005). This paper reports the results of field studies, as well as U-Pb dating and Pb isotopic studies of the Hazelton Group and contained mineralization from several parts of Stikinia, including the northern Bella Coola and southern Whitesail Lake areas, the southern Babine Range east and southeast of Smithers, the Homestake Ridge area southeast of Stewart, and the Forrest Kerr Creek area (RDN property) north of the Eskay Creek mine (Figure 1). Mineral occurrences that have previously been interpreted to be syngenetic (VMS) in character are present in each of these areas.

NORTHERN BELLA COOLA AND SOUTHERN WHITESAIL LAKE AREA

The regional setting and local geology of the southern Stikinia Terrane in the northern Bella Coola and southern Whitesail Lake area (Figure 1) are described by Gordee et al. (2005) and Mahoney et al. (2005). Previous workers have provided brief descriptions of VMS mineralization at the Nifty occurrence (Ray et al., 1998; Diakow et al., 2002), which is hosted in felsic volcanic rocks of early Middle Jurassic age and hence roughly age equivalent to the Eskay Creek deposit. Other mineralization presently known within this part of Stikinia includes disseminations and veins of specular hematite (locally associated with minor malachite; Gordee et al., 2005) and several small chalcopyrite-bearing quartz-vein breccia zones in the Mt. Preston area.

Lead isotopic compositions determined for galena from four samples of the Nifty mineralization (Table 1) fall within the general field of Pb isotopic values for mineralization of Early to Middle Jurassic age in northwestern Stikinia (‘Jurassic cluster’ in Figure 2) and closely overlap the field of Pb compositions from the Eskay Creek deposit itself (Childe, 1996). This is consistent with the interpreted syngenetic character of the Nifty mineralization and its coeval relationship with the Eskay Creek deposit. A single Pb analysis of chalcopyrite from a mineralized quartz-vein breccia from southeast of Mt. Preston also falls within the Jurassic cluster, but is distinctly less radiogenic than the Nifty sulphides. Nonetheless, the isotopic composition suggests that the vein breccias formed as part of an Early or Middle Jurassic metallogenic event, possibly analogous to epigenetic mineralization of Early Jurassic age in the Iskut River area in northwestern Stikinia.

¹Mineral Deposit Research Unit, Earth & Ocean Sciences, UBC, Vancouver, BC

²BC Ministry of Energy and Mines, Smithers, BC

³Bravo Venture Group, 1550-1185 West Georgia St., Vancouver, BC

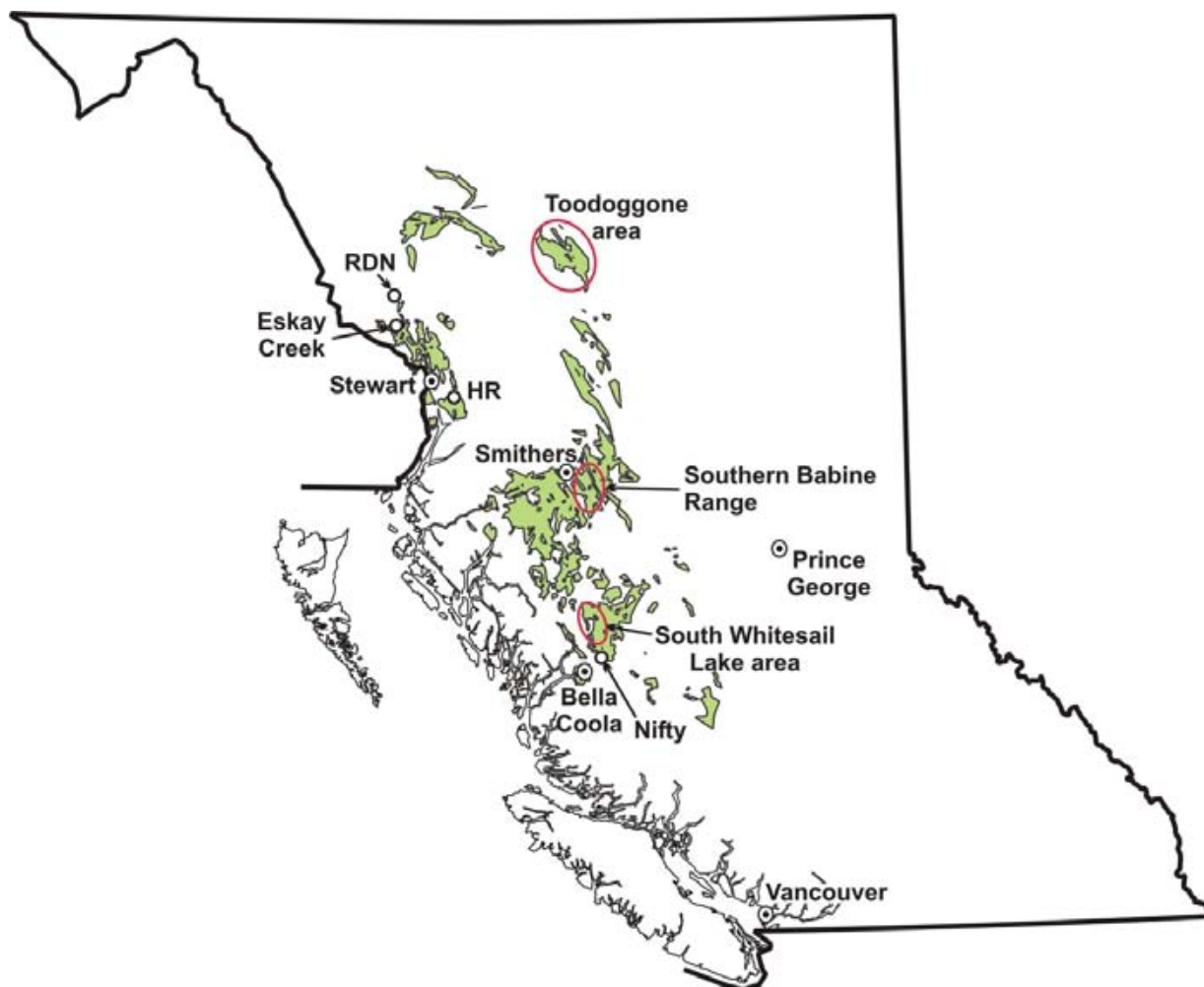


Figure 1. Distribution of Early and Middle Jurassic volcanic and sedimentary strata of the Hazelton Group within the Stikine Terrane of British Columbia.

SOUTHERN BABINE RANGE

Several mineral occurrences hosted by Hazelton Group volcanic strata in the southern Babine Range east of Smithers (Figure 1) were interpreted by Wojdak (1998) to be potentially syngenetic in origin. MacIntyre (1989) assigned volcanic and sedimentary strata in this area to the Telkwa and Nilkitkwa formations based on overall lithology and sparse Late Sinemurian to earliest Toarcian fossil ages. This suggests an age of ~195–180 Ma for the host rocks to mineralization; hence, syngenetic (?) mineralization in the area would appear to be somewhat older than that at Eskay Creek.

One of these prospects (Harry Davis; BC MINFILE 093L 203, 204, 205 and 214) includes several individual occurrences located near the summit of Mt. Harry Davis, north of Houston. It consists mainly of disseminated and fracture-filling sphalerite, chalcopyrite, galena and locally fluorite, although, in one instance (the “Hilltop showing”), sphalerite occurs as disseminations along bands in massive to laminated chert. The upper portion of Mt. Harry Davis is underlain by a thick section of flow-banded, quartz- and

feldspar-phyric rhyolite that is associated with bedded red and maroon lapilli tuffs which locally contain accretionary lapilli. A sample of the rhyolite is calc-alkaline in composition, with a volcanic-arc signature (Mortensen et al., 2004). Four fractions of zircon recovered from a sample of the massive rhyolite give concordant analyses (Table 2; Figure 3a), and the oldest two concordant analyses (C and E, Figure 2a) give overlapping $^{206}\text{Pb}/^{238}\text{U}$ ages of 179.3 ± 0.8 Ma (Late Toarcian), which is taken as the crystallization age of the sample. This age is near the upper age limit for Hazelton Group strata that had been recognized in this area on the basis of fossil age constraints. It is also similar to the age of the Salmon River Formation that hosts the Eskay Creek deposit; however, the rhyolite at Mt. Harry Davis is geochemically distinct from that at Eskay Creek (calcalkaline vs. tholeiitic).

The Lakeview prospect (BC MINFILE 093L 030), located approximately 6 km northeast of the Harry Davis occurrence, was visited briefly during 2004. Mineralization comprises medium- to coarse-grained, massive to crudely banded specular hematite, chalcopyrite, pyrite and sphalerite. It appears to be roughly stratabound, and associ-

ated with a limy horizon within steeply northwest-dipping felsic pyroclastic rocks (Wojdak, 1998). The immediate wallrocks for the sulphides are strongly hematized and epidotized. The overall character of the mineralization, including the mineralogy, relatively coarse grain size of the sulphides, and association with carbonate rocks, is most reminiscent of a skarn, although the possibility that the occurrence comprises Early or Middle Jurassic syngenetic (?) mineralization that has been strongly recrystallized in the contact aureole of a younger intrusion (not presently exposed) cannot be ruled out.

One day was spent examining and sampling the Ascot prospect (BC MINFILE 093L 024), which comprises several individual occurrences near the head of Canyon Creek, approximately 30 km east of Smithers (Figure 1). The property is underlain by a package of mixed sedimentary rocks (mainly thinly bedded limestone, carbonaceous argillite and argillaceous wacke) and intermediate to felsic breccias,

all of which are cut by widely spaced andesite dikes. The rock units in this area have been variably deformed, and weaker lithologies (e.g., limestones and argillites) show a moderate to strong foliation and locally abundant minor folding (e.g., Figure 4a). Two distinct styles of mineralization were observed: 1) disseminations and bedding-parallel stringers of fine-grained sphalerite and galena in impure argillaceous limestones, and 2) galena in fine quartz stringers and disseminations in a felsic breccia unit (Figure 4b). The mineralized stringers in this latter style of mineralization are truncated at the margins of the clasts, indicating that the veining predated brecciation and the mineralization therefore must be broadly syngenetic with respect to the felsic volcanic event.

Lead isotopic compositions have been determined for sulphide samples from all of the potentially syngenetic occurrences in the southern Babine Range and are shown in Figure 2. Although there is some scatter in the data, all anal-

TABLE 1. PB ISOTOPIC COMPOSITIONS OF SULPHIDE MINERALS FROM OCCURRENCES IN THE NORTHERN BELLA COOLA-SOUTHERN WHITESAIL LAKE AREA AND SOUTHERN BABINE RANGE.

Occurrence	Mineral	$^{206}\text{Pb}/^{204}\text{Pb}$			$^{207}\text{Pb}/^{204}\text{Pb}$			$^{208}\text{Pb}/^{204}\text{Pb}$		
			Error (abs.)	Error (%)		Error (abs.)	Error (%)		Error (abs.)	Error (%)
Northern Bella Coola/southern Whitesail Lake area										
Nifty	sl	18.8094	0.0277	0.15	15.6009	0.0238	0.15	38.543	0.0647	0.17
03M-01 Nifty	py	18.8018	0.0082	0.04	15.6131	0.0102	0.07	38.5262	0.0334	0.09
03M-01a Nifty	py	18.8107	0.013	0.07	15.5789	0.0109	0.07	38.3262	0.0435	0.11
03M-01a Nifty	py	18.8089	0.0155	0.08	15.6075	0.0116	0.07	38.4445	0.0486	0.13
03M-05	cp	18.7266	0.0093	0.05	15.5958	0.0108	0.07	38.4479	0.0352	0.09
Southern Babine Range										
Del Santo-1	py	18.6942	0.0106	0.06	15.592	0.0108	0.07	38.3059	0.0373	0.1
Lakeview 2	py	18.8699	0.0184	0.1	15.6703	0.0158	0.1	38.6114	0.0737	0.19
Lakeview-2	py	18.8329	0.0104	0.05	15.5823	0.0105	0.07	38.4059	0.0397	0.1
Lakeview-3	py	18.7949	0.0104	0.06	15.5978	0.011	0.07	38.4427	0.0365	0.09
Su	py	18.7183	0.0226	0.12	15.6213	0.0142	0.09	38.2534	0.0634	0.17
Su	py	18.7529	0.012	0.06	15.6406	0.0122	0.08	38.4829	0.0385	0.1
HD	py	18.7918	0.0141	0.07	15.6642	0.0138	0.09	38.6877	0.0415	0.11
Ascot	sl	18.7192	0.0286	0.15	15.6187	0.0206	0.13	38.3998	0.0743	0.19
Del Santo-2	py	18.6965	0.0185	0.1	15.5905	0.0152	0.1	38.2679	0.0548	0.14
Homestake Ridge										
03M-100 Myborg adit	gl	18.9478	0.0083	0.04	15.6773	0.0102	0.07	38.7255	0.0337	0.09
03M-101 Myborg adit	cp	18.8793	0.0228	0.12	15.6657	0.0104	0.07	38.5461	0.0553	0.14
03M-101 Myborg adit	cp	18.8166	0.0262	0.14	15.5736	0.0227	0.15	38.4641	0.0617	0.16
03M-102 Myborg adit	cct	19.8714	0.0526	0.26	15.6951	0.0418	0.27	39.2944	0.1085	0.28
03M-105 vein in seds adjacent to South Dome rhyolite	cp	18.9611	0.0141	0.07	15.6418	0.0118	0.08	38.647	0.0419	0.11
03M-107a Dilly Zone	py	18.7506	0.0112	0.06	15.625	0.0111	0.07	38.7768	0.0376	0.1
03M-108 Dilly Zone	gl	18.9137	0.0084	0.04	15.6255	0.0102	0.07	38.5199	0.0337	0.09
03M-110 Dilly Zone	gl	18.9072	0.0086	0.05	15.6089	0.0103	0.07	38.5437	0.0342	0.09
03M-111 Dilly Zone	gl	18.9535	0.0082	0.04	15.6692	0.0102	0.06	38.7193	0.0335	0.09
Vanguard Cu	cp	18.9132	0.0261	0.14	15.6552	0.0182	0.12	38.5787	0.0718	0.19
Vanguard Cu	cp	18.9158	0.0094	0.05	15.6362	0.0107	0.07	38.5963	0.0351	0.09
Silver Crown	py	19.1597	0.0115	0.06	15.6415	0.0109	0.07	38.6905	0.0376	0.1
RDN Property										
RDN01-19 94.0	gl	18.826	0.0294	0.16	15.6883	0.0247	0.16	38.506	0.0687	0.18
RDN01-20	gl	18.8837	0.0091	0.05	15.612	0.0104	0.07	38.5669	0.0345	0.09
RDN99-01	py	18.8383	0.0094	0.05	15.6051	0.0102	0.07	38.4062	0.0349	0.09

All errors given at the 2 sigma level.

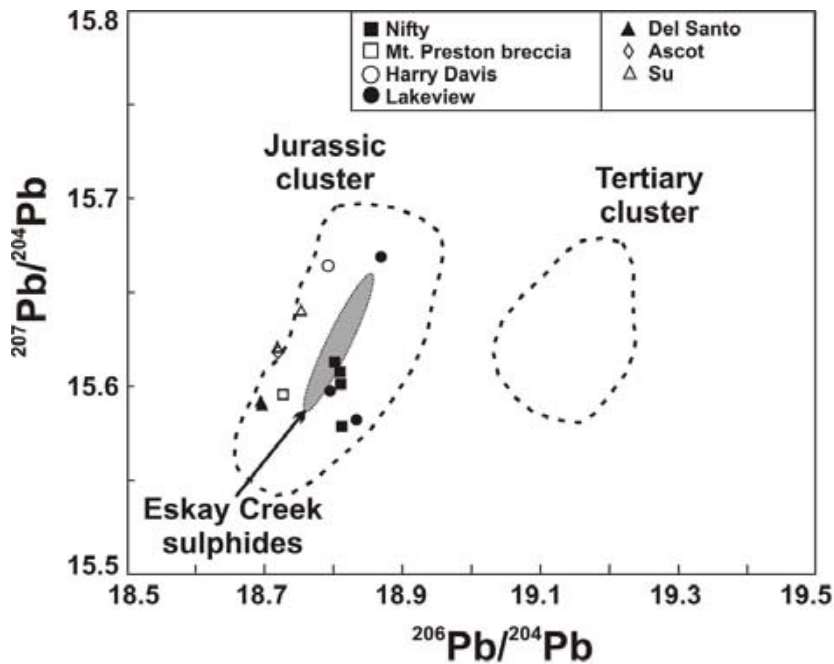


Figure 2. Lead isotopic compositions of sulphide minerals from occurrences in the northern Bella Coola–southern Whitesail Lake area and southern Babine Range. Fields for Jurassic and Tertiary sulphide Pb compositions are from Rhys et al. (1995). Field for Eskay Creek sulphide Pb compositions is from Childe (1996).

yses fall within the ‘Jurassic cluster’, suggesting that mineralization in all cases is of Early or Middle Jurassic age. In particular, three analyses from the Lakeview prospect overlap completely with analyses from the Nifty occurrence. These results are somewhat surprising, especially because the mineralization at the Del Santo prospect (BC MINFILE 093L-025) has been interpreted by most previous workers as a skarn, possibly associated with an Early Tertiary diorite intrusion on the property (M. Marchand, pers. comm., 2004).

HOMESTAKE RIDGE AREA

The Homestake Ridge property, approximately 32 km southeast of Stewart (Figure 1), which is currently being explored by the Bravo Ventures Group Inc., comprises over 80 individual base and precious metal occurrences. The property is underlain by a Late Triassic to Early and Middle (?) Jurassic package of basaltic, andesitic and rhyolitic volcanic and volcanoclastic and clastic sedimentary rocks (Figure 5). The property hosts more than 80 individual mineral occurrences, some of which have been worked since 1914. Previous work on the property by Noranda Exploration Ltd. and TeckCominco Ltd. identified several highly prospective targets, including shear-hosted veins hosting high-grade precious metals, broad areas of gold-enriched, quartz-sericite-pyrite mineralization with bulk tonnage potential, and a volcanic-sedimentary stratigraphy with precious metal-enriched VMS potential.

Hazelton Group rocks on the property consist of basaltic, andesitic and dacitic volcanic and volcanoclastic rocks that are equated to the Early Jurassic Betty Creek For-

mation, as well as fine-grained clastic sedimentary rocks that may correlate with the early Middle Jurassic Salmon River Formation. Mineralization and alteration is focused around subvolcanic hornblende-feldspar porphyry intrusions that resemble and are believed to be equivalent in age to the Goldslide intrusions at Red Mountain, located approximately 25 km northeast of the property (Rhys et al., 1995). These porphyry intrusions occur along structural breaks in the rock package and are associated with broad areas of rocks with locally intense sericite-quartz-pyrite alteration. Two large accumulations of flow-banded rhyolitic volcanics, tuff and coarse fragmental rocks are present on the property and are referred to as the North Dome and South Dome. The felsic units were previously equated with the Mt. Dilworth Formation, which served to highlight the potential of the property for ECT-type VMS mineralization.

The property displays a relatively complex structural history. Northwest- and northeast-trending fault-bound rifts appear to have controlled the deposition of the Early Jurassic sequence and localized the emplacement of porphyry intrusions. Large-scale, southwest-directed, open to isoclinal, disharmonic folds and thrusts likely formed in the Cretaceous, but were strongly controlled by the earlier basin geometry. East-west extension and dextral strike-slip faulting of probable Tertiary age produced block faulting and minor lateral offsets on numerous, highly visible, north-east-trending fault structures.

The Homestake Ridge property hosts a very large number of precious and base mineral occurrences. Mineralization is typically structurally controlled, with some of the occurrences having a close spatial association with variably altered hornblende-feldspar porphyry. Brief descriptions of some of the individual occurrences shown on Figure 5 are given here to highlight the diverse nature of mineralization present.

The Homestake Crown Grant area covers an epithermal vein system hosted by an upper unit of massive to coarse fragmental andesitic volcanics and lower units of heterolithic to monolithic debris flows, dacitic fragmentals and feldspar-hornblende porphyry, and andesitic to dacitic volcanic rocks. High-grade gold-silver shoots are localized near the intersection of the main mineralized shears. Mineralization is hosted within pyritiferous quartz stockworks and breccias with trace to several percent chalcopyrite, sphalerite and galena in a hostrock that is intensely altered to sericite and K-feldspar. Drilling during 2003 intersected broad zones (up to 43 m thick) of highly anomalous gold (0.7 g/t) and silver (10.2 g/t) mineralization with several >1 m wide intervals of 6–13.9 g/t Au and up to 2 oz./t Ag.

TABLE 2. U-PB ZIRCON AGES FOR FELSIC VOLCANIC AND PLUTONIC ROCKS, SOUTHERN BABINE RANGE.

Sample Description ¹	Sample weight (mg)	U (ppm)	Pb ² (ppm)	²⁰⁶ Pb/ ²⁰⁴ Pb (meas.) ³	Total common Pb (pg)	% ²⁰⁸ Pb ²	²⁰⁶ Pb/ ²³⁸ U ⁴ (± % 1)	²⁰⁷ Pb/ ²³⁵ U ⁴ (± % 1)	²⁰⁷ Pb/ ²⁰⁶ Pb ⁴ (± % 1)	²⁰⁶ Pb/ ²³⁸ U age (Ma; ± % 2)	²⁰⁷ Pb/ ²⁰⁶ Pb age (Ma; ± % 2)
Sample 03M-113 (rhyolite on Mt. Harry Davis; UTM zone 9, 641824E, 6035173N)											
A: N5,+74	0.013	193	5.6	1242	3	14.7	0.02710(0.38)	0.1846(1.20)	0.04921(1.10)	173.1(1.3)	159.1(51.3)
C: N5,+74	0.03	146	4.4	2661	3	16.1	0.02825(0.15)	0.1947(0.46)	0.04997(0.42)	179.6(0.5)	193.6(19.7)
D: N5,+74	0.021	128	3.8	1758	3	15.5	0.02781(0.20)	0.1903(0.55)	0.04962(0.52)	176.8(0.7)	177.3(24.3)
E: N5,+74	0.029	240	7.5	3783	3	18	0.02818(0.16)	0.1924(0.33)	0.04952(0.28)	179.1(0.6)	172.7(12.9)
Sample 03M-106 (South Dome rhyolite; UTM zone 9, 463288E, 6177315N)											
A: N2,+104	0.01	219	7.6	1698	3	10.3	0.03452(0.16)	0.2385(0.53)	0.05010(0.48)	218.8(0.7)	199.6(22.2)
C: N2,+104	0.007	344	11.9	2934	2	8.3	0.03489(0.18)	0.2463(0.44)	0.05120(0.38)	221.1(0.8)	249.8(17.6)
D: N2,+104	0.005	104	3.9	511	2	12.3	0.03594(0.44)	0.2830(1.68)	0.05709(1.60)	227.6(2.0)	495.1(71.2)
Sample RDN-01-16-85.34m (RDN property, Boundary Zone, K-feldspar-phyrlic monzonite; UTM zone 9, 399935E, 6311081N)											
A: N2,+134	0.031	407	12.7	4184	6	12	0.03049(0.11)	0.2102(0.20)	0.05000(0.13)	193.6(0.4)	195.0(5.9)
B: N2,+134	0.033	435	13.6	8338	3	11.6	0.03048(0.13)	0.2096(0.20)	0.04986(0.11)	193.6(0.5)	199.6(5.3)
C: N2,+134	0.037	396	12.5	17960	2	12.8	0.03049(0.12)	0.2111(0.35)	0.05021(0.31)	193.6(0.5)	204.7(14.3)
D: N2,+134	0.044	445	14	7982	5	12.4	0.03048(0.10)	0.2108(0.21)	0.05015(0.16)	193.5(0.4)	201.9(7.3)
E: N2,+134	0.41	388	12.1	18600	2	12.1	0.03034(0.24)	0.2103(0.27)	0.05028(0.11)	192.7(0.9)	207.7(5.3)
Sample RDN-01-19-94.0m (RDN property, Wedge Zone, Gossan Creek porphyry; UTM zone 9, 399971E, 6319397N)											
A: N2,+134	0.027	269	8.1	4005	3	7.4	0.03079(0.17)	0.2133(0.28)	0.05027(0.20)	195.5(0.6)	207.3(9.1)
C: N2,+134	0.02	359	11.1	3240	4	10.7	0.03050(0.15)	0.2095(0.30)	0.04987(0.22)	193.7(0.6)	189.0(10.3)
D: N2,+134	0.023	493	15.4	487	44	12.4	0.03034(0.25)	0.2087(2.05)	0.04989(1.94)	192.7(1.0)	189.7(90.2)
E: N2,+134	0.027	352	10.7	5186	3	10.4	0.03016(0.13)	0.2074(0.23)	0.04986(0.16)	191.6(0.5)	188.6(7.2)
Sample RDN-01-20-23.2m (RDN property, Wedge Zone, plagioclase-phyrlic dacite; UTM zone 9, 399997E, 6319193N)											
A: N2,134-149	0.014	303	9.1	2841	3	8.8	0.03049(0.30)	0.2084(0.64)	0.04957(0.57)	193.6(1.1)	175.1(26.5)
B: N2,134-149	0.009	436	13.2	2918	3	11	0.02981(0.16)	0.2075(0.38)	0.05043(0.32)	189.6(0.6)	214.6(14.7)
E: N2,134-149	0.014	152	4.8	2010	2	14.3	0.02974(0.17)	0.2053(0.62)	0.05007(0.57)	188.9(0.6)	198.2(26.4)

¹ N2 = non-magnetic 2 degrees side slope on Frantz isodynamic magnetic separator; grain size given in microns.

² radiogenic Pb; corrected for blank, initial common Pb, and spike

³ corrected for spike and fractionation

⁴ corrected for blank Pb and U, and common Pb

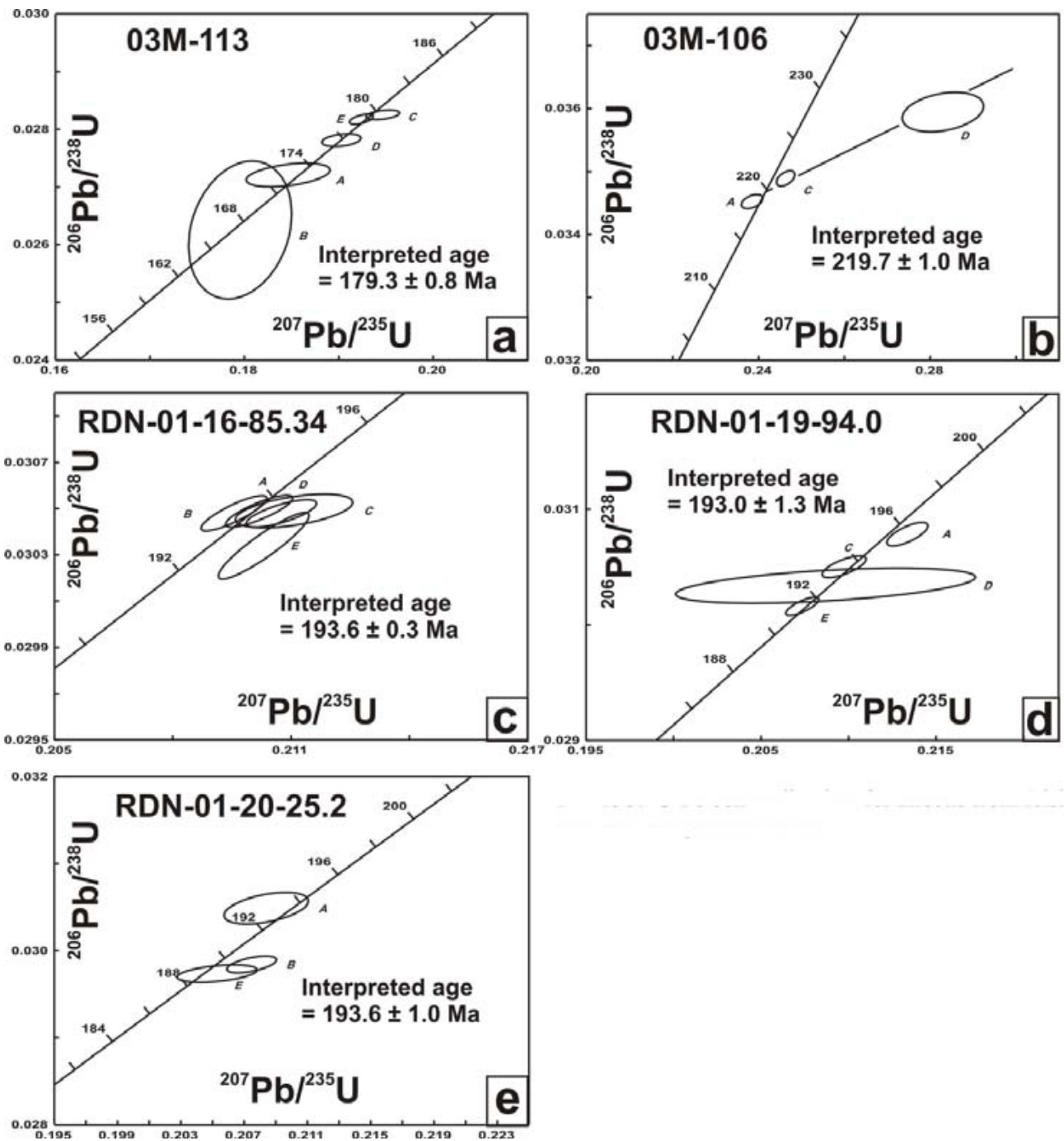


Figure 3. U-Pb concordia plots for zircons from felsic volcanic and plutonic rocks.

Calcite-barite veins exposed in historical trenches at the Vanguard gold showing run up to 9.56 g/t Au and 10.5 g/t Ag over 6.0 m. The zone dips steeply to the north-east and can be traced on surface for about 200 m.

The Dilly and Dilly west zones comprise a series of north-northwest-trending precious and base metal mineral occurrences that form two subparallel linear trends with strike lengths of 1500 m and 600 m, respectively. The occurrences are found at or near the contact between a felsic volcanic package and a bedded, fine-grained clastic succes-

sion. Styles of mineralization include massive sulphide base metal showings, semimassive to massive arsenopyrite showings, massive laminated galena-sphalerite showings and sulphide stockworks within felsic volcanic pyroclastics. Bravo Venture geologists interpreted the western rhyolite-sedimentary contact as predominantly a structural feature with mineralization occurring in north-west- to west-northwest-directed shears along the contact zone.



Figure 4. Mineralized specimens from the Ascot occurrence: A) deformed argillaceous limestone and disseminated galena; B) felsic fragmental rocks with fine, galena-bearing quartz stringers that predate brecciation and deposition.

In the south end of the Dilly zone, galena-rich, banded massive sulphide mineralization was observed in several surface occurrences along a 300 m strike length. This mineralization is hosted in a chlorite-sericite-altered felsic volcanic rock and includes a 6–10 cm wide zone of massive galena and sphalerite.

The Silver Crown occurrence is located within a sediment-sill complex and is marked by a collapsed adit in argillaceous sedimentary rocks. Massive sphalerite-galena (tetrahedrite) sulphide boulders occur in a waste pile near the mouth of the adit. Sampling of the boulders by TeckCominco Ltd. returned values of up to 14.15 g/t Au, 5740 g/t Ag, 11.55% Pb and 3.3% Zn. Mineralization cannot be traced beyond the immediate vicinity of the adit.

Lead isotope analyses were carried out on a number of samples from several of the zones of mineralization on the RDN property. All but one of the analyses fall well within the field of compositions for Early and Middle Jurassic mineralization in northwestern British Columbia (Figure 6). The only exception is galena from the Ag-rich Silver Crown vein, which yields a composition that falls within the Tertiary cluster of isotopic compositions (Figure 6). This indicates that at least some of the Ag-rich veins in the area represent an Early Tertiary metallogenic event that overprints the main Early and Middle Jurassic mineralization.

A sample of the South Dome rhyolite (Figure 5) was sampled for U-Pb zircon dating. This body appears to be intrusive into dacite and basalt, as well as fine-grained sedimentary rocks that were thought to be part of the Hazelton Group. Three fractions of zircon from the South Dome sample were analyzed. Two fall on or near concordia at about 219 Ma and a third analysis falls well to the right of concordia, indicating the presence of a significant inherited zircon component (Figure 3b). A regression through the three analyses yields calculated lower and upper intercept ages of 219.7 ± 1.0 Ma and 2.85 Ga, indicating a Late Triassic (early Norian) crystallization age and Late Archean inheritance. This result is very surprising, since it indicates

that at least some of the stratigraphic units on the Homestake Ridge property actually form part of the Stuhini Group rather than the Hazelton Group. The implications of this age for the structure and stratigraphy on the property are still being assessed.

FORREST KERR CREEK AREA

The RDN property of Rimfire Minerals Corp. (BC MINFILE 104G 144; Figure 1), located in the Forest Kerr Creek area approximately 40 km northeast of the Eskay Creek mine, covers a package of felsic volcanic rocks overlain by mafic volcanic rocks and carbonaceous argillites that are thought to correlate, at least in part, with the early Middle Jurassic Salmon River Formation that hosts the Eskay Creek deposit (Figure 7). Although most of the mineralization located on the property thus far consists of structurally controlled mineralized veins and breccias, strong precious and base metal geochemical anomalies within argillite sections are very reminiscent of that associated with ECT mineralization. Diamond-drilling has intersected a thick section of dacitic to rhyolitic flows, domes and volcanoclastic rocks in the stratigraphically lower part of the section.

Three felsic units from the lower felsic sequence were dated using conventional U-Pb zircon methods. Sample RDN-01-16-85.34m is a weakly foliated, very strongly sericitized and clay-altered K-feldspar-phyric monzonite from the Boundary Zone in the southern part of the RDN property (Figure 7). Five strongly abraded fractions of zircon were analyzed (Table 2; Figure 3c). Four of these fractions give overlapping concordant analyses with a total range in $^{206}\text{Pb}/^{238}\text{U}$ ages of 193.6 ± 0.5 Ma, which is taken as the crystallization age of the sample. The fifth fraction falls slightly below the concordia and appears to have suffered minor Pb loss. A second sample (RDN-01-19-94.0m) consists of massive, plagioclase-phyric porphyry of the 'Gossan Creek porphyry' unit from near the northern end of the Wedge Zone (Figure 7). The porphyry is strongly car-

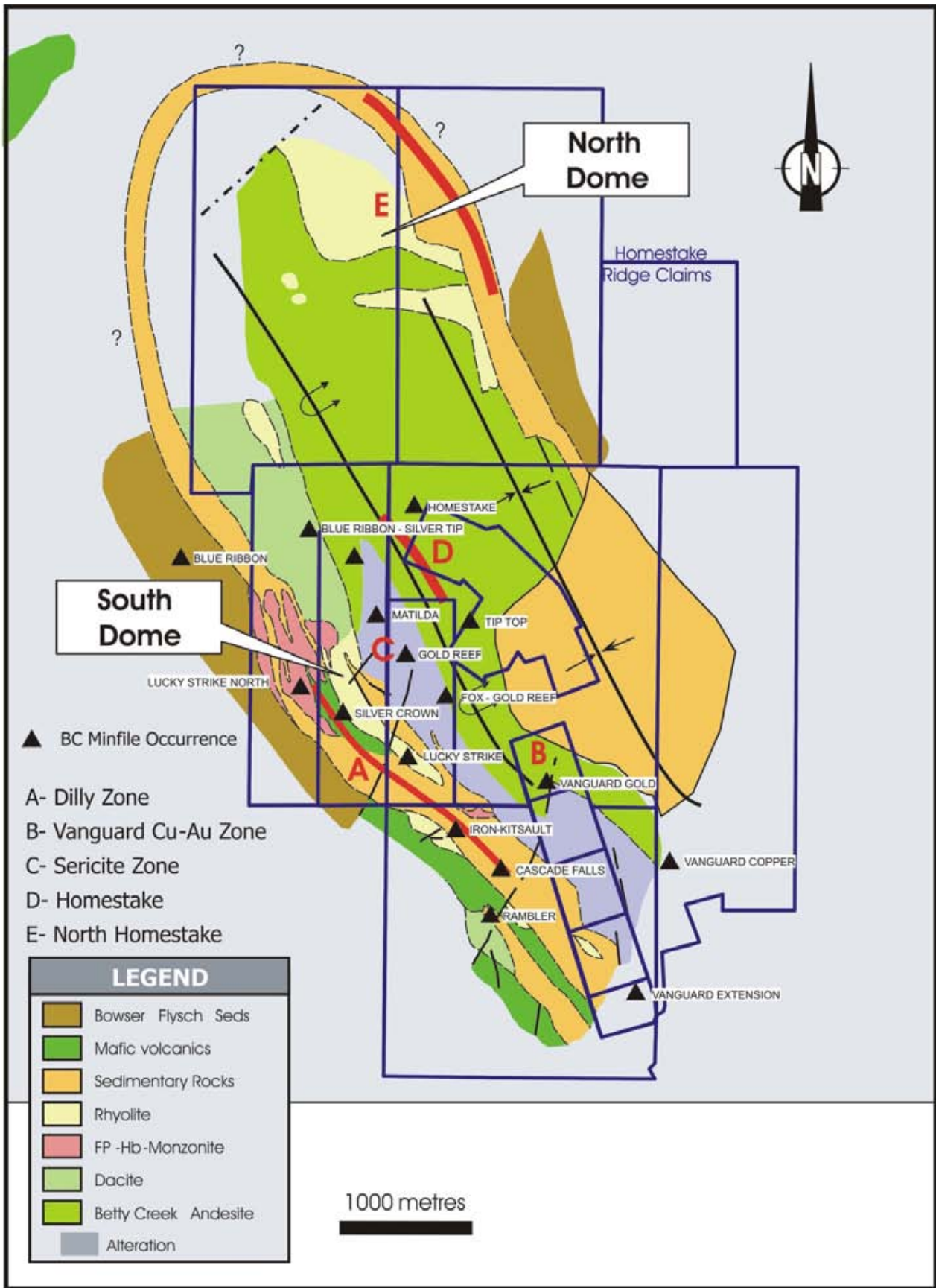


Figure 5. Simplified geology of the Homestake Ridge property (courtesy of TeckCominco Ltd.).

bonate altered and contains abundant fine stringers of carbonate. Three fractions of abraded zircon yield concordant analyses but with some scatter along the concordia (Figure 3d). The best estimate for the crystallization age of this sample is considered to be given by the total range of $^{206}\text{Pb}/^{238}\text{U}$ ages for the oldest two concordant fractions, at 193.0 ± 1.3 Ma. Fraction E has suffered minor Pb loss and fraction A appears to contain a minor component of older, inherited zircon. The third sample (RDN-01-20-23.2m) was from massive feldsparphyric dacite from the central part of the Wedge zone (Figure 7). Three fractions of strongly abraded zircon were analyzed. All three analyses fall on or near concordia (Figure 3e), and the best estimate for the crystallization age of the sample is given by the oldest $^{206}\text{Pb}/^{238}\text{U}$ age of 193.6 ± 1.1 Ma.

These new data indicate that the lower felsic volcanic package on the RDN property is Late Sinemurian in age and thus significantly older than either the Eskay rhyolite or the footwall dacite in the immediate Eskay area. Fossil ages from locally tuffaceous argillite in the overlying argillite-basalt sequence in the vicinity of the RDN range from Toarcian to as young as Bathonian (Logan et al., 2000), indicating that strata that are age equivalent to the Salmon River Formation in the Eskay Creek area are indeed present on the RDN property. These results raise the possibility that a significant unconformity may separate the lower felsic package from the overlying argillite-basalt sequence in the RDN area.

Three samples of galena from crosscutting veinlets in argillite in drillcore on the RDN were analyzed for Pb isotope composition. All three analyses fall well within the field of Jurassic Pb dates (Fig. 6), confirming that the epigenetic mineralization in this area is part of the Early to Middle Jurassic mineralizing event in northwestern British Columbia.

DISCUSSION AND CONCLUSIONS

Results of the study provide new constraints on the nature of base and precious metal mineralization within the Hazelton Group in several parts of Stikinia, and specifically on the potential for some of the known occurrences to represent ECT mineralization. The Nifty occurrence in the Bella Coola map area closely resembles Eskay Creek in terms of age and Pb isotopic composition, although the geochemistry of the hostrocks at Nifty is calcalkaline as opposed to the tholeiitic hosts for the Eskay Creek deposit itself. Although the Nifty shares some of the geochemical traits of ECT mineralization (Ray et al., 1998; Diakow et al., 2002) it does not appear to have the strong gold enrichment that is seen at Eskay Creek. The only other mineraliza-

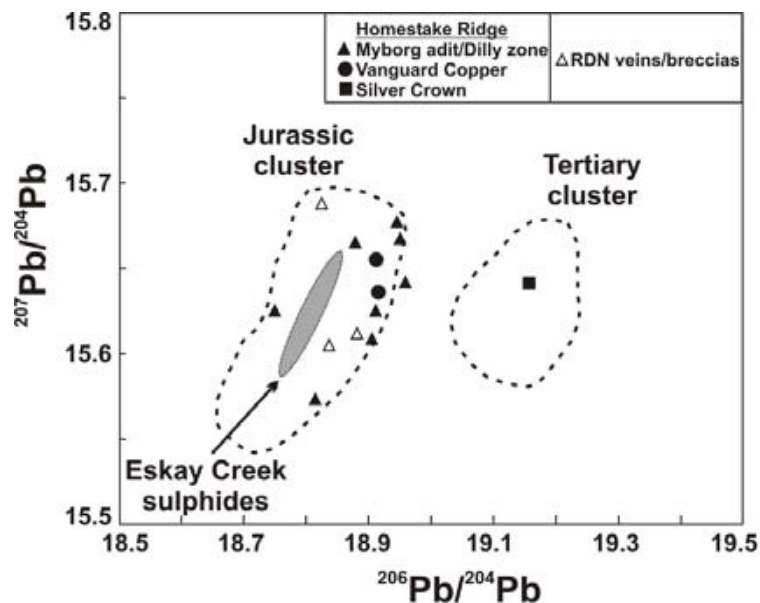


Figure 6. Lead isotope compositions of sulphide minerals from occurrences in the Homestake Ridge area and from the RDN property. Fields for Jurassic and Tertiary sulphide Pb compositions are from Rhys et al. (1995). Field for Eskay Creek sulphide Pb compositions is from Childe (1996)

tion identified thus far within the Hazelton Group section in northern Bella Coola and southern Whitesail Lake map areas consists of small, chalcopyrite-bearing quartz-vein breccias. Lead isotopic compositions of this style of mineralization indicate that it also represents part of an Early or Middle Jurassic metallogenic event, and is not related to Early Cretaceous and younger intrusions in the area. Despite the limited evidence for additional VMS occurrences within the Hazelton Group in this area, widespread semiconformable epidote alteration within the section, association with a coeval subvolcanic (?) felsic intrusion and the presence of significant synvolcanic fault structures (Gordee et al., this volume; Mahoney et al., this volume) suggest that the area has very high potential for hosting additional VMS occurrences.

The nature and age of several mineral occurrences in the southern Babine Range that were identified by Wojdak (1998) as possible VMS targets remains partially unresolved. Lead isotopic compositions from all of the occurrences are consistent with an Early or Middle Jurassic age of mineralization; however, at least two of the occurrences (Del Santo and Lakeview) appear in the field to be either skarns or possibly syngenetic mineralization that has been strongly recrystallized and overprinted in the contact aureole of intrusions. At least some of the mineralization at the Ascot occurrence predates brecciation and subsequent deposition of felsic volcanic units, and must therefore be broadly syngenetic. Although none of the various styles of mineralization at the Harry Davis occurrence is conclusively syngenetic in character, a U-Pb age of 179.3 ± 0.8 Ma for a flow-banded rhyolite unit indicates that volcanic rocks in this area are age equivalent to the Salmon River Formation that hosts the Eskay Creek deposit.

Mineralization in the Homestake Ridge area is mainly structurally controlled and many occurrences have a close spatial association with hornblende-feldspar porphyry dikes and sills of presumed Early Jurassic age. These occurrences yield Pb isotopic compositions that are consistent with an Early or Middle Jurassic age, and this style of mineralization appears to be analogous to that at the Red Mountain and/or Silbak Premier deposits to the north and west. Other Ag-rich vein occurrences such as Silver Crown have Pb isotopic compositions that indicate they are Early Tertiary in age and represent a younger, superimposed metallogenic event.

The Late Triassic U-Pb zircon age reported here for the South Dome rhyolite indicates that not all of the supracrustal units in the Homestake Ridge area belong to the Hazelton Group, but at least some of them are part of the underlying Stuhini Group. This suggests that there may be major, previously unrecognized structural complexities in this region. None of the mineralization in the Homestake Ridge area has been proven to be syngenetic; however, VMS mineralization does occur at the Sault occurrence (BC MINFILE 103P 233), approximately 6 km east of the Homestake Ridge property. The Sault occurrence is hosted within felsic volcanic rocks that have given a U-Pb zircon age of 193.5 ± 0.4 Ma (Late Sinemurian; Mortensen and Kirkham, 1992), and is one of several Ag-rich VMS occurrences that have been identified in the upper Kitsault River valley (e.g., Dolly Varden, Torbrit; Pinsent, 2001). The Sault occurrence is therefore approximately equivalent in age to some of the intermediate-composition maroon and green volcanic breccias that underlie parts of the Homestake Ridge property and are thought to correlate with the Betty Creek formation, as recognized farther to the north (Lewis and Tosdal, 2001). There does appear to be some potential for VMS mineralization on the Homestake Ridge property, although it would likely be at a lower stratigraphic level than that at the Eskay Creek deposit.

Studies of the RDN property in the Forrest Kerr Creek area support the suggestion that geochemical anomalies and scattered base and precious metal occurrences there are potentially close analogues of the Eskay Creek deposit. Felsic volcanic and volcanoclastic rocks that make up the lower part of the stratigraphic sequence on the RDN property are ~193 Ma in age, and therefore equivalent in age to

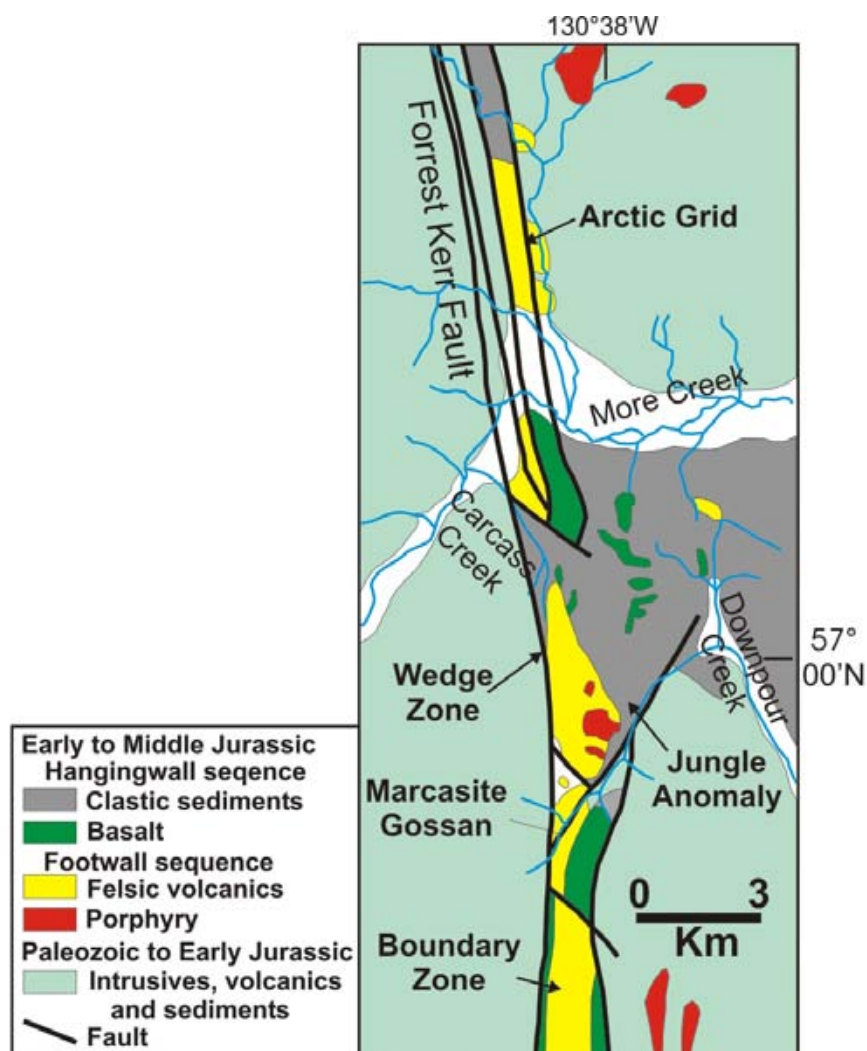


Figure 7. Simplified geology of the RDN property (from Rimfire Minerals Corporation website, <http://www.rimfire.bc.ca/Home.asp>).

host rocks for the Sault VMS occurrence (see discussion above). Laminated pyrite was intersected in one drillhole within this package of felsic rocks on the RDN property (M. Jones, pers. comm., 2004), suggesting that an older VMS horizon may be present on the property. Most of the geochemical anomalies that are thought to be more analogous to the Eskay Creek deposit on the RDN occur within the overlying argillite-basalt package, which contains fossils indicating that the units are correlative with the Salmon River Formation.

ACKNOWLEDGMENTS

We thank Graeme Evans of TeckCominco Ltd. for many insights and discussions regarding the Homestake Ridge property geology. We also thank Richard Friedman at the Pacific Centre for Isotopic and Geochemistry Research for critical assistance in producing the U-Pb data reported here, and for providing a critical review of the manuscript.

REFERENCES

- Childe, F. (1996): U-Pb geochronology and Nd and Pb isotope characteristics of the Au-Ag-rich Eskay Creek volcanogenic massive sulfide deposit, British Columbia; *Economic Geology*, Volume 91, pages 1209–1224.
- Diakow, L.J., Mahoney, J.B., Gleeson, T.G., Hrudey, M.G., Struik, L.C. and Johnson, A.D. (2002): Middle Jurassic stratigraphy hosting volcanogenic massive sulphide mineralization in eastern Bella Coola map area (NTS 093/D), southwest British Columbia; in *Geological Fieldwork 2001, BC Ministry of Energy, Mines and Petroleum Resources*, Paper 2002-1, pages 119-134.
- Lewis, P.D. and Tosdal, R.M. (2000): Metallogenesis of the Iskut River area, northwestern British Columbia; *Mineral Deposit Research Unit*, Special Publication No. 1, 337 pages.
- Logan, J.M., Drobe, J.R. and McClelland, W.C. (2001): Geology of the Forrest Kerr–Mess Creek area, northwestern British Columbia (NTS 104B/10, 15 & 104G/2 & 7W); *BC Ministry of Energy, Mines and Petroleum Resources*, Bulletin 104, 163 pages.
- MacIntyre, D.G., Desjardins, P. and Tercier, P. (1989): Jurassic stratigraphic relationships in the Babine and Telkwa ranges (93L/10, 11, 14, 15); in *Geological Fieldwork 1988, BC Ministry of Energy, Mines and Petroleum Resources*, Paper 1989-1, pages 195–208.
- Massey, N.W.D. (1999): Volcanogenic massive sulphide deposits in British Columbia; *BC Ministry of Energy and Mines*, Open File 1999-2.
- Massey, N.W.D., Alldrick, D.J. and Lefebvre, D.V. (1999): Potential for subaqueous hot-spring (Eskay Creek) deposits in British Columbia; *BC Ministry of Energy and Mines*, Open File 1999-14.
- Mortensen, J.K. and Kirkham, R. (1992): A U-Pb zircon age for host rocks of a syngenetic strontium (-zinc) occurrence in the Kitsault Lake area, west-central British Columbia; *Geological Survey of Canada*, Paper 91-2, pages 118–185.
- Mortensen, J.K., Gordee, S.M., Mahoney, J.B. and Tosdal, R.M. (2004): Regional studies of Eskay Creek–type and other volcanogenic massive sulphide mineralization in the upper Hazelton Group in Stikinia: preliminary results; in *Geological Fieldwork 2003, BC Ministry of Energy, Mines and Petroleum Resources*, Paper 2004-24, pages 249–262.
- Pinsent, R.H. (2001): Mineral deposits of the Upper Kitsault River area, British Columbia (103P/W); in *Geological Fieldwork 2000, BC Ministry of Energy, Mines and Petroleum Resources*, Paper 2001-1, pages 313–326.
- Ray, G.E., Brown, J.A., Friedman, R.M. and Cornelius, S.B. (1998): Geology of the Nifty Zn-Pb-Ba prospect, Bella Coola district, British Columbia; in *Geological Fieldwork 1997, BC Ministry of Energy, Mines and Petroleum Resources*, Paper 1998-1, pages 20-1–20-28.
- Rhys, D.A., Sieb, M., Frostad, S.R., Swanson, C.L., Prefontaine, M.A., Mortensen, J.K. and Smit, H.Q. (1995): Geology and setting of the Red Mountain gold-silver deposit, northwestern British Columbia; in Schroeter, T.G., *Porphyry Deposits of the Northwestern Cordillera of North America, Canadian Institute of Mining and Metallurgy*, Special Volume 46, pages 811–828.
- Wojdak, P. (1998): Volcanogenic massive sulphide deposits in the Hazelton Group, Babine Range, BC; *BC Ministry of Energy, Mines and Petroleum Resources*, Exploration and Mining in British Columbia 1998, pages C1–C13.

National Geochemical Reconnaissance Program in Northwestern British Columbia: Bowser Lake (NTS 104A) Regional Geochemical Survey

By R.E.Lett¹, P.W.B.Friske² and W. Jackaman³

KEYWORDS: National Geochemical Reconnaissance Program, Regional Geochemical Survey, multi-element, stream sediment, stream water, Bowser Lake, heavy minerals

INTRODUCTION

This paper describes a reconnaissance scale regional stream sediment-water survey carried out over the Bowser Lake map sheet (NTS 104A) as part of the National Geochemical Reconnaissance (NGR) program. Since 1974, this program has generated high quality stream and lake sediment and surface water data from geochemical surveys carried out across Canada. In British Columbia the NGR Program, known as the Regional Geochemical Survey (RGS), has covered roughly 70% of the province with stream sediment and stream water sampling at an average sample density of one sample per 13 km². In the process just over 45,000 samples have been collected and analyzed for up to 50 elements including gold copper,

molybdenum and zinc. The existing NGR-RGS survey coverage, including the most recent Bowser Lake survey area, is shown in Figure 1.

Figure 1 also shows a stream sediment survey carried out to NGR specifications over the adjacent Spatsizi Lake map sheet (NTS 104H). This survey is described by Jackaman (this volume).

Mineral exploration in northwest British Columbia will benefit from publication of the Bowser Lake survey results because it completes NGR sampling coverage of the area linking existing regional geochemical surveys of NTS 104B (Iskut River), 103P (Nass River) and 94D (McConnell Creek). Moreover, the stream sediment data produced will extend regional geochemical trends for Ni and Hg that have been recently identified by Alldrick *et al.* (2004) from contoured element maps.

BOWSER LAKE SURVEY

Prominent physiographic features of the Bowser Lake map sheet are the Skeena Mountains in the east and the Coast Range Mountains in the west. Between these two northwest-trending mountain ranges is the Nass Basin, an irregularly shaped area of low relief drained by the Nass River and its tributaries (Holland, 1964). Much of the area is underlain by the Bowser Basin, a Middle Jurassic to Middle Cretaceous sedimentary basin formed on Stikinia terrane after its amalgamation with ancestral North America. Jurassic to Cretaceous deltaic sedimentary rocks forming the basin are represented by the Bowser Lake, Skeena and Sustut Groups (Ferri *et al.*, 2004). In the western part of the map sheet, the Bowser Lake Group rests on fine-grained clastic sedimentary and volcanic rocks of the Early to Middle Jurassic upper Hazelton Group. Geological mapping by Alldrick *et al.* (2004) identified the Salmon River Formation as the gradational contact between Hazelton and Bowser Lake strata. There is also an inlier of Hazelton Group rocks in the Oweeggee Dome surrounding Delta Peak to the north of Bowser Lake.

Stikinia volcanic and sedimentary rocks surrounding the basin are metallogenically well endowed and host the

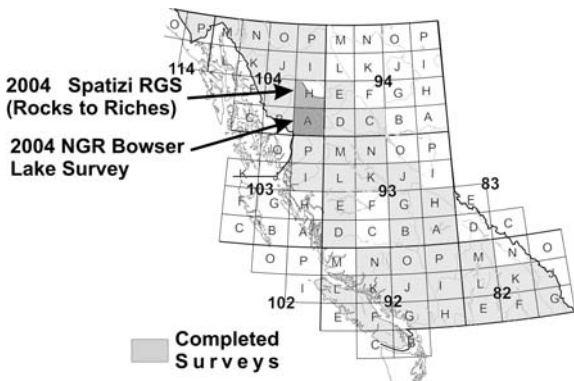


Figure 1. NGR survey coverage in British Columbia and location of 2004 surveys.

¹ British Columbia Ministry of Energy and Mines, PO Box 9333 Stn. Prov. Govt., Victoria, BC, V8W 9N3

² Geological Survey of Canada, 601 Booth Street, Ottawa, Ont., K1A 0E8

³ 3011 Felderhof Road, Sooke, BC, V0S 1N0

world-class Eskay Creek gold mine in addition to several past-producing gold-copper mines and 170 documented MINFILE smaller precious and base metal mineral prospects. Three previously operating copper-gold-silver mines, the Red Cliff, Goat and Roosevelt in the Stewart mining camp are located in the southwestern part of NTS 104A. These subvolcanic vein type deposits, produced over 9000 g of gold, 1.8 million g of silver and 40,000 kg of copper. The area also has potential for alkalic porphyry Cu-Mo-Au-Ag deposits similar to Red Chris in NTS 104H and new epithermal VMS deposits in Stikina rocks similar to those that host the Eskay Creek deposit to the west in NTS 104B.

There is a sequence of Early to Middle Jurassic black carbonaceous sediments (Upper Hazelton Group) at the base of the Bowser Basin. These rocks indicate an anoxic environment favourable for the formation of sedimentary exhalative type base metal deposits (Ferri, pers comm, 2004).

Stream sediment and water samples were collected by helicopter and along roads in July 2004 from 1028 sites at an average density of one sample per 13.2 km² over an area of 13,560 km² in NTS 104A. All water samples were analyzed in the field for pH and conductivity. In addition, 217 of the water samples from the survey were filtered and acidified in the field for later trace metal analysis. The minus 80 mesh (<0.177 mm) fraction of the sediment samples will be analyzed for up to 50 elements by instrumental neutron activation analysis (INAA), aqua regia digestion-inductively coupled plasma mass spectrometry (ICPMS) and loss on ignition by a gravimetric method (GRAV). Elements, detection limits and the methods used for analysis are listed in Table 1. Figure 2 shows location of the stream sediment samples.

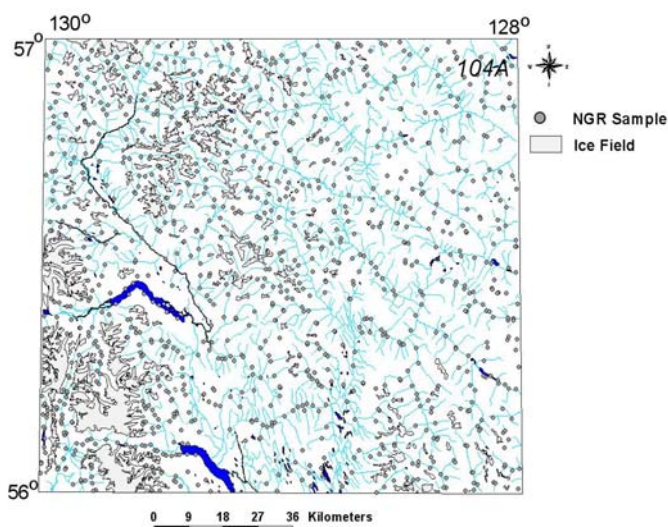


Figure 2. NGR sample sites in NTS 104A.

TABLE 1. ELEMENTS DETERMINED IN STREAM SEDIMENTS

Element	Detection	Units	Method
Aluminum	0.01	%	ICPMS
Antimony	0.02/0.1	ppm	ICPMS / INAA
Arsenic	0.1/0.5	ppm	ICPMS / INAA
Barium	0.5/50	ppm	ICPMS / INAA
Bismuth	0.02	ppm	ICPMS
Bromine	0.5	ppm	INAA
Cadmium	0.01	ppm	ICPMS
Calcium	0.01/1	%	ICPMS / INAA
Cerium	5	ppm	INAA
Cesium	0.5	ppm	INAA
Chromium	0.5/2	ppm	ICPMS / INAA
Cobalt	0.1/5	ppm	ICPMS / INAA
Copper	0.01	ppm	ICPMS
Europium	1	ppm	INAA
Gallium	0.2	ppm	ICPMS
Gold	0.2/2	ppb	ICPMS / INAA
Hafnium	1	ppm	INAA
Iron	0.01/0.2	%	ICPMS / INAA
Lanthanum	0.5/2	ppm	ICPMS / INAA
Lead	0.01	ppm	ICPMS
Lutetium	0.2	ppm	INAA
Magnesium	0.01	%	ICPMS
Manganese	1	ppm	ICPMS
Mercury	5	ppb	ICPMS
Molybdenum	0.01	ppm	ICPMS
Nickel	0.1	ppm	ICPMS
Phosphorus	0.001	%	ICPMS
Potassium	0.01	%	ICPMS
Rubidium	5	ppm	INAA
Samarium	0.1	ppm	INAA
Scandium	0.1/0.2	ppm	ICPMS / INAA
Selenium	0.1	ppm	ICPMS
Silver	2	ppb	ICPMS
Sodium	0.001/0.02	%	ICPMS / INAA
Strontium	0.5	ppm	ICPMS
Sulphur	0.02	%	ICPMS
Tantalum	0.5	ppm	INAA
Tellurium	0.02	ppm	ICPMS
Terbium	0.5	ppm	INAA
Thallium	0.02	ppm	ICPMS
Thorium	0.1/0.2	ppm	ICPMS / INAA
Titanium	0.001	%	ICPMS
Tungsten	0.2/1	ppm	ICPMS / INAA
Uranium	0.1/0.2	ppm	ICPMS / INAA
Vanadium	2	ppm	ICPMS
Ytterbium	2	ppm	INAA
Zinc	0.1/50	ppm	ICPMS / INAA
Fluorine	10	ppm	ION
Loss on Ignition	0.1	%	GRAV

DETAILED GEOCHEMISTRY

A detailed stream geochemical study was carried out jointly with the Geological Survey of Canada. Bulk

stream sediment samples were collected from 34 sites from which heavy mineral concentrates (HMC) were prepared. These focused on the area of the Eskay Creek Mine and regions underlain by Hazelton Group rocks. The objective of the study is to

1. Characterize the HMC dispersal train related to the Eskay mineralization and compare it to the standard silt response. Do the HMC provide an aerially more extensive and/or stronger geochemical signature than the silts?
2. Provide guidelines to the exploration community on the use of HMC.
3. Highlight the type of information that can be garnered from HMC, *e.g.*, kimberlite indicator minerals (KIM) and mineralogy of the HMC, which provides information on source material and can help explain silt anomalies.
4. Re-sampling historical RGS sites in the Telegraph Creek map sheet to determine long-term geochemical variability and the source of unexplained sediment mercury and nickel anomalies.

Sample Collection

Standard stream sediment, bulk sediment samples for the preparation of HMC and stream water samples were collected from 34 sites in NTS sheets 104A, 104B and 104G. The location of the sites where the samples were collected is shown in Figure 3. Ideal sites for the collection of sediments for the heavy mineral concentrate fraction are located at the upstream points of mid-channel bars. Material was collected from a single point where possible, or within close proximity otherwise. A five-gallon plastic pail was lined with a heavy-duty polyethylene plastic bag (18x24 inches, 4 Mil). Material was wet-sieved through a 12-mesh (1.68 mm) stainless steel sieve until a sample weight of 10 to 15 kg was attained (Plate 1). The sample was weighed in the pail before the opening was taped shut with black plastic (electrical) tape and placed into a second bag with a sample number and taped. Samples were shipped directly to a commercial laboratory for preparation and analysis.

Preparation of Heavy Mineral Concentrates

Bulk sediment samples were progressively reduced by different laboratory procedures to concentrate heavy minerals. Initially a 500 g character sample was taken and stored before a low-grade table concentrate was prepared from the remainder. Gold grains were observed at this stage and counted, measured and classified as to degree of wear (*i.e.*, distance of transport). The table reject was re-tabled to scavenge possible unrecovered kimberlite indicator minerals and magmatic massive sulphide indicator minerals. The concentrate from both tabling runs

was separated in methylene iodide diluted with acetone to S.G. 3.20 to recover heavy minerals including Cr-diopside and forsterite olivine. Magnetite was removed after the heavy liquid separation and the remaining concentrate cleaned with oxalic acid to remove limonite stains. The dried concentrate was sieved into several size fractions, (<0.25 mm, 0.25 to <0.5 mm, 0.5 to <1.0 mm, ≥ 1.0 to 2.0 mm). The <0.25 mm fraction was kept for chemical analysis and the 0.25 to 0.50 mm fraction was sorted with a Carpc® drum magnetic separator into strongly, moderately, weakly and non-paramagnetic fractions.



Plate 1. Bulk stream sediment sample collection.

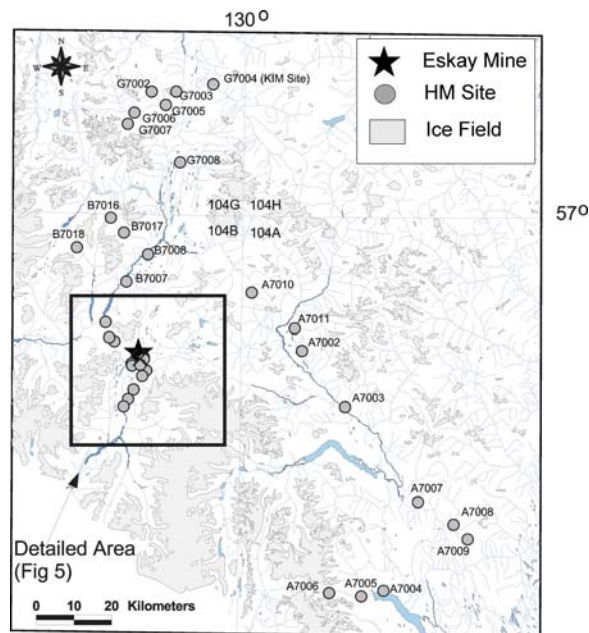


Figure 3. Heavy mineral sites.

Preliminary Results

A preliminary examination of the heavy mineral concentrates has revealed that several of them have a large number of gold grains (Fig. 4).

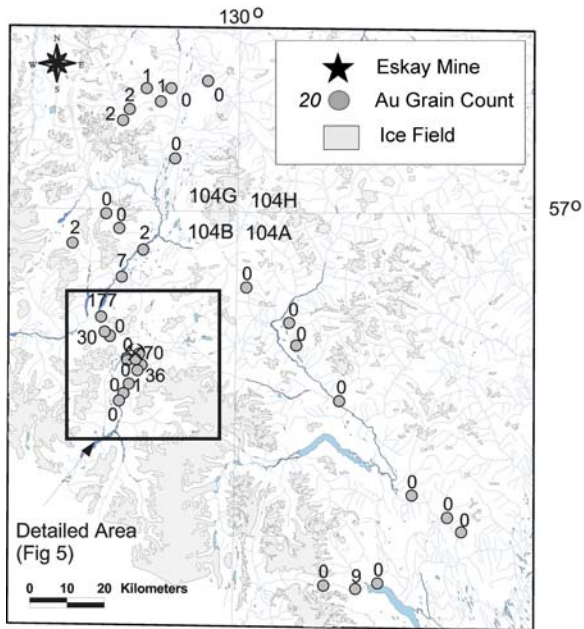


Figure 4. Gold grain counts in bulk stream sediment samples.

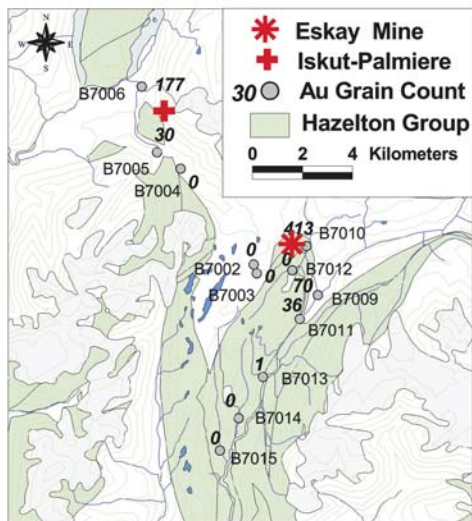


Figure 5. Detailed sampling around the Eskay Creek Mine.

Gold grains counts from the 34 samples ranged from 0 to 413 with a median value of 0. The Eskay Creek mineralized area is clearly outlined by the HMC gold grain counts. The highest value of 413 grains is from a site just east of the mine site (Fig. 5). A second sample (B7009) along this creek (approximately 3 km down drainage) is also highly anomalous containing 70 grains. Another distinct drainage to the southwest is also highlighted by the gold grain counts returning a value of 36 grains (Fig. 5).

Bulk stream sediment samples from two drainages northwest of the Eskay Mine have up to 177 gold grains in the sediment. The streams drain a low ridge on which is located the Iskut-Palmiere prospect. At this prospect Alldrick *et al.* (2005) report that “Realgar +/- orpiment is hosted in both black siliceous siltstones and in a cross-cutting quartz vein. This small outcrop is exposed in a north-draining creek, and lies stratigraphically above a thick dacite unit on the north side of Volcano (Palmiere Creek). Assays of two grab samples returned arsenic values greater than 1.0 percent with negligible associated precious metals”. Less than 10 ppb gold was detected in sediment sampled during a previous regional geochemical survey (Matysek *et al.*, 1988b) from streams adjacent to the bulk sample sites.

Five of the heavy mineral samples were selected for kimberlite indicator mineral (KIM) processing. The samples yielded many KIM (mostly olivine) that are indicative of not only kimberlites, but also other rock types such mafic/ultramafic volcanics or intrusives. The total absence of pyrope garnet in the concentrate indicates that the source of the minerals is most likely not kimberlitic but rather mafic/ultramafic rock.

The KIM counts (Table 2) are preliminary “raw lab counts” and the mineralogy needs to be confirmed by probe work. For example, the three magnesium ilmenites identified in sample A7011 may, in fact, be ilmenite or chromite or some other phase. Site G7004 is closely spatially associated with alkalic and mafic volcanics (olivine basalt necks, breccia and pillow flows similar to the Maitland volcanics in 104H). The presence of these rock types would explain the olivine and would also be the cause of high Ni (>140 ppm) found in regional survey stream sediment samples by Matysek *et al.* (1988a). Similarly site G7006 is in a drainage basin that contains significant mafic volcanics. This illustrates how knowledge of heavy mineral concentrate mineralogy can be valuable for interpreting stream sediment geochemical data.

TABLE 2. KIM COUNTS IN HMC SAMPLES (GARNETS NOT DETECTED)

Site	Diopside	Ilmenite	Chromite	Forserite
A7005	0	0	55	0
A7011	0	3	8	3
B7007	0	0	4	0
G7004	0	6	1	78,019
G7006	2	1,505	10	10,402

CONCLUSIONS

- A regional stream sediment-water survey carried out over the Bowser Lake map sheet in July 2004 will produce new multi-element geochemical data from the analysis of samples from 1028 sites.

- Up to 413 gold grains were counted in heavy mineral concentrates collected from streams close to the Eskay Creek mine. Several streams southwest and northwest of the mine have lesser, but anomalous gold-grain counts.
- Abundant gold grains in the two creeks northwest of the Eskay Creek mine may reflect precious metal mineralization associated with the Iskut-Palmiere prospect. Background gold values were detected in sediment collected from these two creeks during a previous regional stream sediment survey.
- Although absence of pyrope garnet in the heavy mineral concentrates suggests an ultramafic rather than kimerlitic source, the abundant olivine in two of the samples is an explanation for high nickel values in stream sediment samples.
- Heavy minerals are effective for enhancing gold anomaly contrast in stream sediments and provide information for interpreting stream geochemical data.

ACKNOWLEDGMENTS

The authors would like to thank pilots Mick Burbage and Phil O'Driscoll of Lakelse Air, Terrace, British Columbia, for providing skilled helicopter support during the regional survey and the detailed sampling. Dave Bond, Lakelse Air, generously assisted the survey by placing fuel caches. The Bell Two lodge staff willingly tolerated sampling supplies and analytical equipment scattered through their cabins and are thanked for providing shelter to dry samples. Brian Wardrop and Steve Fraser of McElhanney Consulting worked extremely hard to complete the sampling and their efforts are most appreciated. Eric Jackaman is credited with the photograph shown in Plate 1 and his assistance with the detailed sampling is also very much appreciated. Acme

Analytical, Vancouver, prepared the stream sediment samples. Overburden Drilling Management, Nepean, Ontario, processed the heavy mineral concentrates. Brian Grant is thanked for his encouragement in the field and for his editorial advice on the text of this paper.

REFERENCES

- Alldrick, D., Nelson, J.L. and Barresi, T. (2005): Geology and Mineral Occurrences of the upper Iskut River area - Tracking the Eskay Rift through northern British Columbia; *in Geological Fieldwork, 2004, BC Ministry of Energy and Mines*, Open File 2005-1.
- Alldrick, D., Jackaman, W. and Lett, R.E.W. (2004): Compilation and analysis of regional geochemical surveys around the Bowser Basin; *in Geological Fieldwork, 2003, BC Ministry of Energy and Mines*, Open File 2004-1, pages 163-166.
- Ferri, F., Osadetz, K and Evenchick, C. (2004): Petroleum source rock potential of Lower to Middle Jurassic clastic, Intermountain basins, British Columbia; *in Geological Fieldwork, 2004, BC Ministry of Energy and Mines, Resources Development and Geoscience Branch, Summary of Activities 2004*, pages 87 to 96.
- Holland, S.S. (1964): Landforms of British Columbia; *British Columbia Department of Mines and Petroleum Resources*, Bulletin no 48, 138 pages.
- Jackaman, W. (2005) Spatsizi River stream sediment and water survey; *in Geological Fieldwork, 2004, BC Ministry of Energy and Mines*, Open File 2005-1.
- Matysek, P.F., Day, S.J., Gravel, J.L. and Jackaman, W. (1988a): 1987 Regional Geochemical Survey 104F-Sumtum and 104G Telegraph Creek; *BC Ministry of Energy, Mines and Petroleum Resources*, RGS 19; *Geological Survey of Canada*, Open File 1646.
- Matysek, P.F., Day, S.J., Gravel, J.L. and Jackaman, W. (1988b): 1987 Regional Geochemical Survey 104B-Iskut River; *BC Ministry of Energy, Mines and Petroleum Resources*, RGS 18; *Geological Survey of Canada*, Open File 1645.

Gold and Base Metal Mineralization near Kitsumkalum Lake, North of Terrace, West-Central British Columbia

By M.G. Mihalynuk¹ and R.M. Friedman²

Keywords: intrusive-related gold mineralization, gold-silver-lead, carbonate alteration, metamorphism, structural deformation, U-Pb geochronology, crustal extension

INTRODUCTION

Geological and geochemical indications of an environment prospective for gold deposits are found in an area extending approximately 12 km east and west of Kitsumkalum Lake in west-central British Columbia (Fig. 1). More than 20 gold mineral occurrences, some with silver, are located within the area, including two with minor past production and an active placer operation. Most occurrences are gold-arsenic-quartz or base and precious-metal quartz veins that are presumably related to one of the many stocks and plutons in the area (Fig. 1). Carbonate alteration envelopes are ubiquitous around sheeted precious-metal-bearing quartz veins (\pm arsenopyrite-pyrite-sphalerite-galena-chalcopyrite). Regional geochemical stream sediment surveys show elevated gold, mercury and arsenic in the Kitsumkalum area (bismuth and antimony were not analyzed; BC Ministry of Energy and Mines, 2001).

Since 2002, Eagle Plains Resources Ltd. has conducted mineral exploration in the area, primarily west of Kitsumkalum Lake. In 2004, Bootleg Exploration Inc. (a wholly owned subsidiary of Eagle Plains Resources Ltd.) and the British Columbia Ministry of Energy and Mines entered into a partnership agreement aimed at evaluating the regional potential for intrusive-related gold mineralization, both on their Kalum property and around plutons to the east. Geological field investigations were focused on interiors and contacts of intrusive bodies associated with gold mineralization and lode vein occurrences.

In this report, we use the following nomenclature conventions. 'Kitsumkalum area' refers to the areas of the Kitsumkalum valley that lie within an ~12 km radius of Kitsumkalum Lake. 'Kalum area' refers the part of the 'Kitsumkalum area' that lies west of the lake, principally the 'Kalum property', centred west of Mount Allard, as

well as the 'LCR property', on the ridges south of the lower stretches of the Little Cedar River. A possible source of confusion arises over the historical use of 'Kalum' and 'Kalum Lake', which are names of developed prospects on the northeast and southwest shores of Kitsumkalum Lake.

ACCESS

The Kalum area is centred approximately 35 km north-northwest of Terrace in west-central British Columbia. With a population of nearly 14 000, Terrace supports a regional airport, rail yard, and most other amenities. It is located at the confluence of the Skeena, Zymoetz and Kitsumkalum Rivers, and at the junction of Highways 6 and 37. Excellent road access is afforded by logging roads that extend off of the new, paved Nisga'a Highway and the old gravel-surfaced Aiyansh Highway on the east and west sides of the Kitsumkalum valley. Steep alpine topography

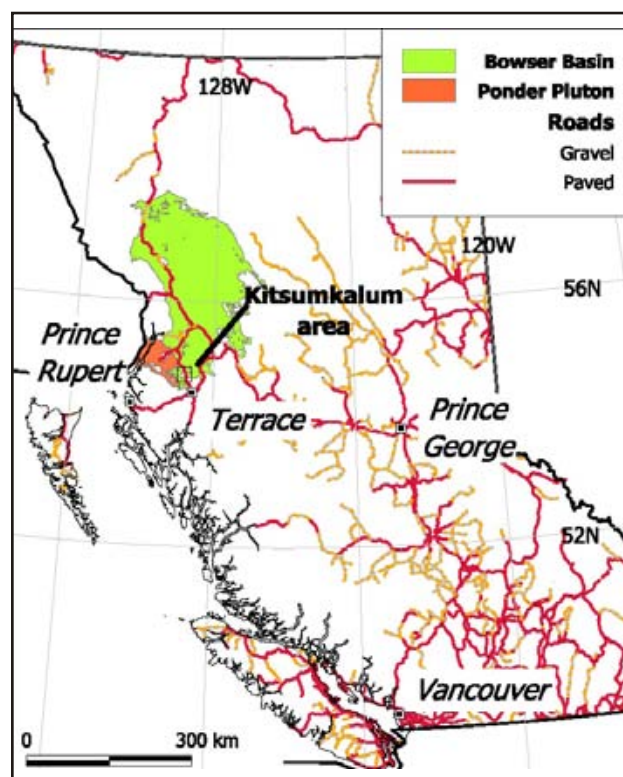


Figure 1. Location of the Kalum project area, 35 km north of Terrace. Geology from Massey (2004).

¹ British Columbia Ministry of Energy and Mines, e-mail: Mitch.Mihalynuk@gems5.gov.bc.ca

² Pacific Centre for Isotopic and Geochemical Research, Department of Earth and Ocean Sciences, University of British Columbia

and dense temperate rainforest, both characteristic of the area, can prove logistically challenging for travelling even short distances from existing access routes.

OBJECTIVES

This report is a summary of field and laboratory data acquired from the Kalum fieldwork completed in 2004. We include the results and interpretations of geological mapping, petrographic and geochemical analysis and geochronological investigations. Objectives are to

- describe and sample the mineralized occurrences;
- determine what intrusive phases, if any, are associated with gold mineralization, and attempt to establish field criteria that link the intrusive phase(s) to mineralization;
- establish a geochronological framework for mineralization and/or mineralizing intrusive phases; and
- investigate petrographic evidence that constrains the mineralizing event(s).

METHODS

Fieldwork was conducted over an 18-day period in mid to late August. About two-thirds of the work was conducted from the road network below treeline, the remainder was by helicopter access, mainly near or above treeline. Approximately half of the geological mapping and sample collection was directed toward tenured lands in which Eagle Plains Resources Ltd. hold an interest. In the course of mapping, magnetic susceptibility of rock units and their altered or metamorphosed equivalents was routinely recorded in order to provide calibration for aeromagnetic data collected during past and future surveys. A total of 39 samples were collected for petrographic analysis (see photomicrographs that follow); 6 samples were collected for U-Pb geochronology (5 pending, data for one presented here), 9 samples were collected for $^{40}\text{Ar}/^{39}\text{Ar}$ geochronology (results pending); 54 samples were collected for assay by inductively coupled plasma – emission spectroscopy (ICP-ES) and instrumental neutron activation analysis (INAA), and 10 samples were collected for major and rare earth element analysis (REE results are pending).

Twenty-seven of fifty-four samples submitted for ICP-ES and INAA are reported, based upon their ICP-ES values, as follows: Au >500 ppb or Ag >1000 ppb or Cu, Zn, Pb >0.2%. Quality-control data are also reported. Note that the variation in Au and Ag ICP-ES values from the accepted standard was 101% and 8%, respectively, as a %RSD (relative standard deviation) measure. Variation in analytical results for duplicates averaged 89% and 36% (Au and Ag, Table 2). These uncertainties need to be considered during the following discussion on mineralization.

REGIONAL GEOLOGY AND PREVIOUS WORK

Duffell, Souther and others from the Geological Survey of Canada (GSC) conducted comprehensive geological

work in the area in the late 1950s (Duffell and Souther, 1964). This remains the most complete written work published, although the GSC conducted several years of revision mapping, mainly in the mid-1980s (Woodsworth *et al.*, 1985), and topical thesis studies were completed. The most germane to exploration in the Kalum area is probably that of Heah (1991), which deals with contractional ductile and superimposed extensional deformation in the Shames River area, west of Terrace. A geological compilation by Evenchick *et al.*, (2004) and Massey *et al.* (2003) provide recent synoptic geological settings for the Kalum area. Geology west of Kalum Lake is detailed by Downie and Stephens (2003) on the Bootleg Exploration property. This latter report also provides an excellent overview of mineral exploration activity in the area west of Kitsumkalum Lake. For mineral occurrences east of the lake, the British Columbia Ministry of Energy and Mines MINFILE is the best source of information.

According to Woodsworth *et al.* (1985), the geology of the Kalum area is dominated by Middle to Late Jurassic marine deltaic and turbiditic strata of the Bowser Lake Group, as well as Lower Cretaceous fluvial-deltaic strata of the Skeena Group. A small window of Early Jurassic volcanic strata is preserved near the north end of Kitsumkalum Lake. All of these strata have been structurally thickened by gently south and north-dipping thrusts prior to extensive intrusion by mainly Cretaceous to Early Eocene magmatic bodies. Largest of these bodies is the huge, composite Ponder pluton (>1500 km² in British Columbia; Harrison *et al.*, 1978; Sisson, 1985; Van der Heyden, 1989), which lies outside the map area to the west. Numerous small intrusive bodies (<10 km²) cut the deformed strata within, and east of, the Kitsumkalum valley.

Timing of thin-skinned fold and thrust deformation is best constrained by the Skeena Group and older rocks of the Skeena fold belt northeast of Terrace. Contractional deformation there is as old as Late Jurassic (Albian to Oxfordian), with final shortening of Latest Cretaceous or Paleocene age (Evenchick, 1991).

Structurally and magmatically thickened and thermally weakened parts of the Coast Belt continental arc were subject to extensional collapse in the Early Tertiary. In the southern Coast Belt, this occurred principally in Paleocene time (Friedman and Armstrong, 1988), whereas the event is dated as Paleocene to Eocene in the central Coast Belt near Terrace, (Andronicos *et al.*, 2003). Extensional collapse facilitated synorogenic emplacement of 60–50 Ma magmatic rocks, which constitute 25% of the crust over thousands of square kilometres in areas west and northwest of Terrace (Andronicos *et al.*, 2003).

STRATIGRAPHY

Four stratigraphic packages underlie the Kalum area: volcanic rocks correlated with the Early Jurassic Hazelton Group (Woodsworth *et al.*, 1985) and three clastic units belonging to the overlying Upper Jurassic Bowser Lake Group. Volcanic rocks include pillow basalt and structurally overlying calcareous tuff, which are exposed east of

northern Kitsumkalum Lake. These rocks have been affected by at least two phases of deformation (*see* 'Structure' section) and few protolith textures are preserved. No age data exist for these rocks within the Kalum area.

Bowser Lake Group strata in the Kalum area are dominated by one of three main lithologies: chert pebble conglomerate, sandy turbidites, or silty and carbonaceous argillite.

In roadcuts immediately west of the low mountain between northern Kitsumkalum Lake and the Mayo Creek

valley (Fig. 2) are found the best exposures of chert pebble conglomerate (Fig. 3). Here, tabular to lenticular conglomerate units are interbedded with medium-grained arkosic sandstone and argillaceous siltstone. Elsewhere, chert pebbles are less abundant, occurring mainly within lags at the erosional bases of turbidite flow units. More commonly, the turbidite sequences are sand-dominated, lacking beds or lenses of chert pebble conglomerate. Turbidite successions are light grey to rusty-weathering. Typical turbidite sequences are composed of 2–6 m thick units with bases com-

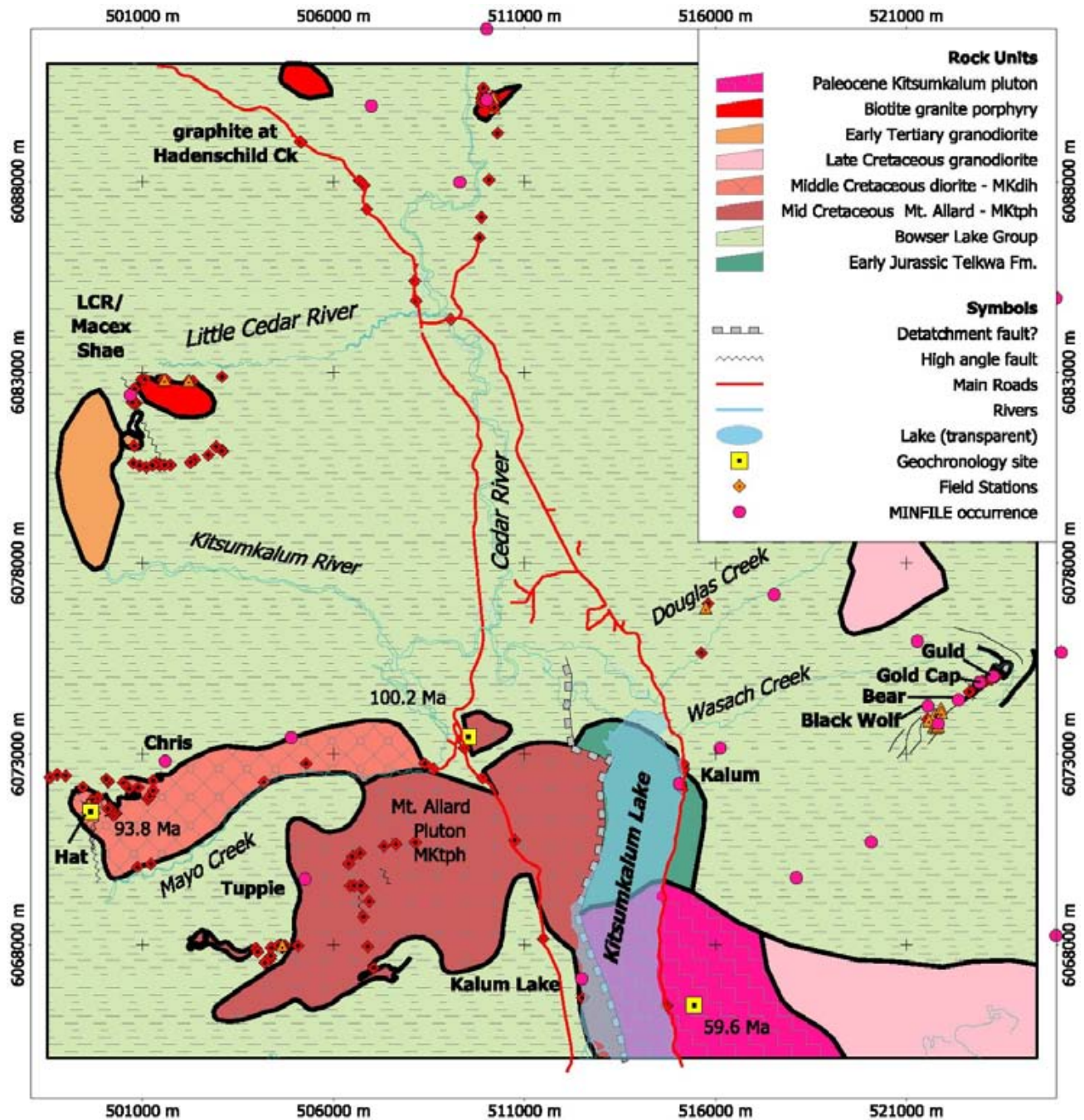


Figure 2. Generalized geology of the Kitsumkalum area. Sources of information: this project, Downie and Stevens (2003), Massey *et al.* (2003), and Woodsworth *et al.* (1985).

posed of rip-up clasts of underlying, dark brown argillite. Conglomerate grades up into medium to coarse-grained, planar-laminated light grey sandstone, parts of which may be interlaminated with millimetre-thick argillite. Laminated sandstone gives way up section to cross-stratified, clean lithic arkose. Cross-stratified sandstone constitutes at least 50% of each fining-upward unit, and they are overlain by silty argillite in which a high content of carbonaceous material is common. This argillaceous siltstone can attain thicknesses of several metres in both packages. It is commonly cut by slaty cleavage at a high angle to bedding. In a few localities, it can be mapped as a separate unit, tens of metres thick, that may include broad areas of pencil shale. Thermally metamorphosed, woody macerals can easily be mistaken for mica in hand samples. Such meta-macerals look like detrital mica that characterizes the Skeena Group. However, marine shelf and slope turbidites of the Bowser Lake Group can be distinguished on the basis of sedimentary facies from fluvial units that are more typical of the Skeena Group (C. Evenchick, personal communication, 2004).

INTRUSIVE PHASES

Semicircular plutons and tabular bodies, mainly of diorite to granodiorite composition, extensively intrude the Bowser Lake and older strata within the Kitsumkalum area. The volume of intrusions increases to the west, toward the Coast Plutonic Complex. Relative ages of the intrusive



Figure 3. Hornfelsed chert pebble conglomerate.

units are based upon crosscutting relationships, sparse geochronological data and degree of deformation. The latter criterion must be applied with caution because strong strain partitioning can impart fabrics to younger or synkinematic plutons while older, cold plutons are unaffected. The following intrusive phases are listed in presumed order of intrusion, from oldest to youngest.

Poikilitic Hornblende Tonalite

Euhedral, poikilitic hornblende phenocrysts characterize this tonalite, which forms the Mount Allard pluton (Downie and Stephens, 2003; Fig. 4, unit MKtph). This pluton is a >35 km², homogeneous body. Poikilocrysts enclosed by hornblende are plagioclase (with strong oscillatory zoning) and opaque minerals (Fig. 4b). Lithologically similar dikes, locally hornblende megacrystic, may display strong foliation and/or carbonate alteration. The Mount Allard pluton cuts unit MKdih. A K/Ar (hornblende) cooling age of 100.2 ± 6.8 Ma reported for this body is (Godwin, unpublished in Breitsprecher and Mortensen, 2004). Alteration or possibly regional low-grade metamorphism of one

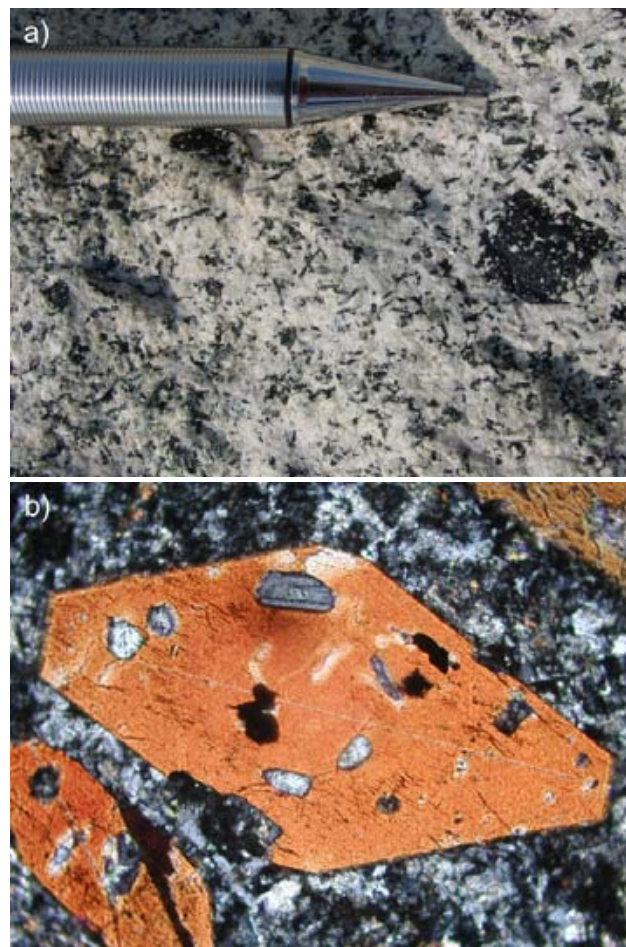


Figure 4. **a)** Typical texture of poikilitic hornblende porphyry of the Mount Allard pluton (unit MKtph). Note the weak magmatic fabric. **b)** Photomicrograph of euhedral hornblende with poikilocrysts of plagioclase and opaque minerals. Width of photo is ~4 mm.

fresh-looking outcrop is carbonate>prehnite~chlorite>epidote>pumpellyite+ ?zoisite.

Hornblende-Pyroxene Quartz Diorite

A weak to strong foliation and local folding are displayed within this quartz diorite body (unit MKdih) in the northwestern part of the study area, just north of Mayo Creek. Quartz is interstitial to subidiomorphic and strained plagioclase that is weakly altered to carbonate, white mica and possibly prehnite. Pyroxene is the dominant mafic mineral; it is glomeroporphyritic and fresh. Hornblende is extensively altered to chlorite and pumpellyite. Folding is accommodated in part by slip along dense networks of discrete microfaults (Fig. 5). This body intrudes and thermally metamorphoses strata correlated with the Bowser Lake Group, a relative age that is confirmed by a U-Pb age of 93.8 Ma (*see* 'U-Pb Geochronology' section).

Quartz-Biotite Granite Porphyry

Quartz-biotite granite porphyry (unit Tpqb) may be the youngest intrusive phase in the Kalum area. It is exposed at low elevations in the Little Cedar River valley, near the LCR occurrence (Fig. 2). Relative age is based upon a lack of biotite hornfels, deformation fabric or regional metamorphic overprint. Locally, it is host to porphyry-style copper-molybdenum mineralization (Fig. 6) and has caused country rocks near its contacts to be locally replaced by sulphides (*see* below).

At higher elevations in the Little Cedar River valley, offshoots of the granite occur as rusty quartz-eye porphyry felsic dikes (unit Tpqhb) that contain 20% 1–3 mm tabular feldspar, 6% 5 mm acicular hornblende and 5% biotite. Quartz is up to 8 mm in diameter, coconstituting up to 5% of the rock. Pyrite is disseminated throughout and also occurs as sparse veinlets and blebs (up to 4% combined). These dikes apparently postdate folding in Bowser strata because they parallel the axial surfaces of the folds.

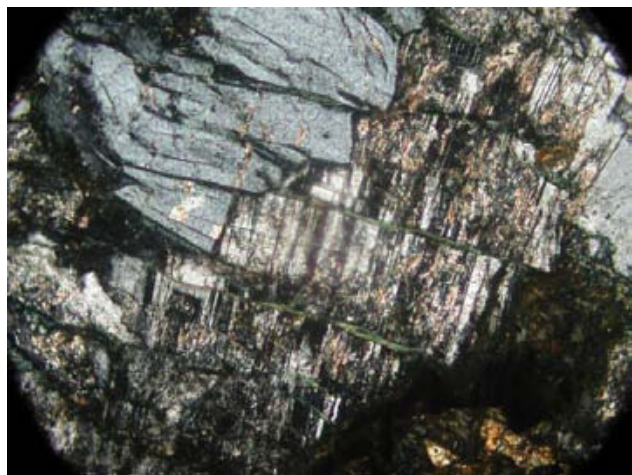


Figure 5. Microfaults in unit MKdih with apparent dextral offset cut a plagioclase-clinopyroxene grain boundary. Note intergranular quartz at the center-right edge of the photo. Width of photo is ~3 mm.

Kitsumkalum Pluton

Above the southeastern shores of Kitsumkalum Lake is a medium to coarse-grained, titaniferous metagranodiorite with enclaves of mafic schist, the Kitsumkalum pluton (Woodsworth *et al.*, 1985). It is of Paleocene age 59.6 +0.2/-0.1 Ma (Gareau *et al.*, 1997) and, notably, is much more strongly deformed than plutons dated more than 40 m.y. younger.

Dikes

Four phases of dikes repeatedly cut the sedimentary rocks and major plutons in the Kalum area. Based upon these crosscutting relationships, relative ages can be established.

Sugary aplite to graphic granite dikes with minor dikelet offshoots, which commonly have dark grey quartz-rich cores, occur in the Tuppie area, where they cut the Mount Allard pluton.

Acicular hornblende-feldspar porphyry dikes are common regionally. At least one variety cuts the Mount Allard pluton and dilatent quartz-carbonate veins (Fig. 7).

Chilled, very fine grained to aphanitic, dark green dikes look fresh and young, but may locally be affected by

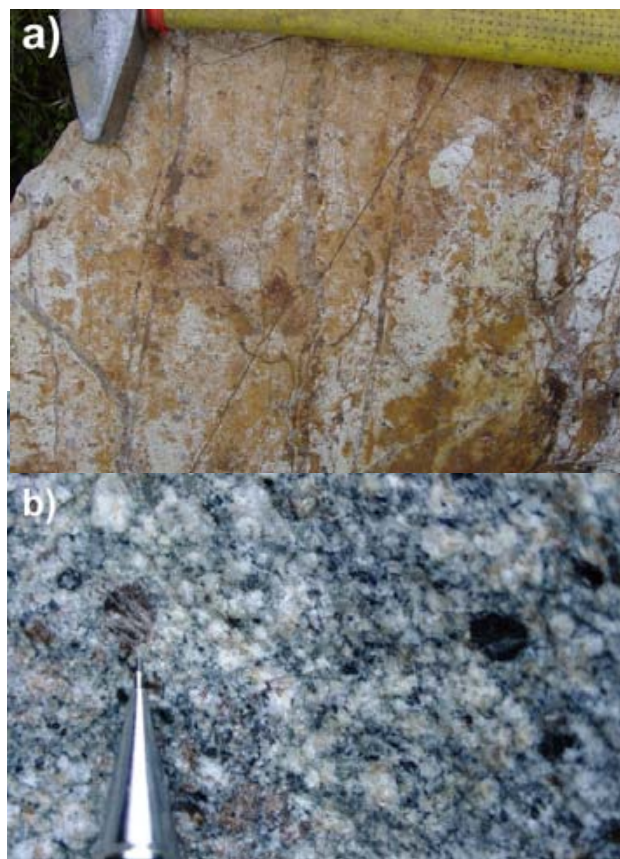


Figure 6. **a)** Sheeted quartz veins in bleached and rusty-weathering biotite-quartz porphyry (unit Tpqb) with disseminated chalcopyrite at the Shae occurrence. **b)** Representative view of unaltered porphyry showing a smoky quartz eye just above the pencil tip.



Figure 7. Acicular hornblende porphyry dike cuts dilant veins and older mafic dike at the Tuppie occurrence.

ductile deformation. Where they cut unit JKqdi, they form a swarm of 1–2 m thick bodies that consistently trend due north. Relative age with respect to other intrusive phases is not known.

Chilled, metre-thick lamprophyre dikes contain amygdules of a salmon pink mineral, tentatively identified petrographically as heulandite (low temperature zeolite). These dikes cut all structures within Bowser Lake strata and may be the youngest intrusive unit mapped in the area.

U-PB GEOCHRONOLOGY

Approximately 30 kg of unweathered pyroxene-hornblende quartz diorite was collected from near the Hat occurrence for determination of its crystallization age using the isotope dilution – thermal ionization mass spectrometry U-Pb method (ID-TIMS). All work was carried out at the Pacific Centre for Isotopic and Geochemical Research at the Department of Earth and Ocean Sciences, University of British Columbia. Mineral separation and U-Pb analytical techniques are given in Friedman *et al.* (2001). Results are plotted on a standard concordia diagram (Fig. 8) and listed in Table 1.

Results for five multigrain zircon fractions intersect the concordia between about 93 and 94 Ma. Slightly younger ages are attributed to very minor Pb loss, given the 1000–1800 ppm uranium concentrations of these zircons. A preferred age estimate of 93.8 ± 0.5 Ma is based on $^{206}\text{Pb}/^{238}\text{U}$ results for the three oldest concordant and overlapping fractions, B, C and D.

STRUCTURE

All layered rocks within the Kalum area have been affected by at least one phase of folding. Folds are open to close, although intrafolial isoclinal folds are developed in the most ductile zones (Fig. 9). Faulting is common and obvious within both the Bowser Lake strata and the intrusive bodies.

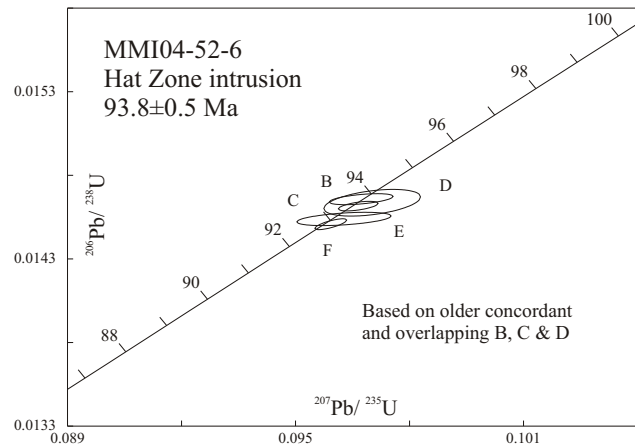


Figure 8. Concordia plot showing results for five zircon fractions from unit MKdih. The preferred interpreted age is 93.8 ± 0.5 Ma.

Both concentric and similar fold styles are recognized within strata correlated with the Bowser Lake. Competent sandstone layers tend to act as beams and form concentric folds, except where they have folded at elevated temperatures. Argillaceous units tend to form similar folds, especially where graphitic. Intrafolial motion is ubiquitous within graphitic argillite, and these units are typically the locus of thrust fault flats.

Thrust faults developed within the Bowser Lake can be identified indirectly in incompletely exposed and isoclinally folded stratigraphy, where apparent fold limbs on either side of a hinge zone both face in the same direction. Thrust faults can be observed directly where they follow sheared bedding planes and then ramp up section. Orientations of dilant veins in the hangingwall of bedding-parallel faults can also be used to confirm thrust motion (Fig. 107). In rare instances, duplex structures with horses on the scale of metres to tens of metres long are well exposed. Slickensides on slip planes are less reliable indicators of thrust motion because they can also be formed by flexural slip, particularly in concentric folds, or during late minor fault motion related to unroofing or deglaciation.



Figure 9. Transposed layering and intrafolial isoclinal folds near the eastern shore of northern Kitsumkalum Lake.

TABLE 1. ID-TIMS U-PB ANALYTICAL DATA FOR THE HAT ZONE PYROXENE-HORNBLENDE QUARTZ DIORITE

Fraction ¹	Wt mg	U ² ppm	Pb ^{*3} ²⁰⁶ Pb ⁴ ppm ²⁰⁴ Pb		Pb ⁵ ²⁰⁸ Pb ⁶ pg	Isotopic ratios (1, %) ⁷			Apparent ages (2, Ma) ⁷			
			²⁰⁶ Pb/ ²³⁸ U	²⁰⁷ Pb/ ²³⁵ U		²⁰⁷ Pb/ ²⁰⁶ Pb	²⁰⁶ Pb/ ²³⁸ U	²⁰⁷ Pb/ ²³⁵ U	²⁰⁷ Pb/ ²⁰⁶ Pb			
Hat Zone intrusion: age estimate of 93.8 ± 0.5 Ma based on ²⁰⁶ Pb/ ²³⁸ U dates for fractions B, C and D.												
B 6	0.014	1087	17	2216	6	17.7	0.01466 (0.11)	0.0967 (0.43)	0.04786 (0.39)	93.8 (0.2)	93.8 (0.8)	93 (18)
C 11	0.017	1232	20	5377	4	17.8	0.01462 (0.10)	0.0967 (0.27)	0.04796 (0.23)	93.5 (0.2)	93.7 (0.5)	97 (11)
D 8	0.012	1016	16	2281	5	17.0	0.01464 (0.27)	0.0970 (0.66)	0.04808 (0.59)	93.7 (0.5)	94.0 (1.2)	103 (28)
E 8	0.010	969	15	1004	9	18.0	0.01454 (0.14)	0.0963 (0.64)	0.04802 (0.60)	93.1 (0.3)	93.3 (1.2)	101 (28)
F 27	0.012	1784	28	5013	4	16.9	0.01451 (0.11)	0.0959 (0.22)	0.04796 (0.15)	92.9 (0.2)	93.0 (0.4)	97.1 (7.2)

¹ Upper case letter is zircon fraction identifier. All fractions were air abraded, with at least 20% volume removed. Selected zircons were greater than 100 micrometers, (dimension of longest axis), and were clear, pale pink, stubby prisms and tabular grains. Selected grains also contained internal c-axis parallel tubes extending much of their length. All grains were selected from the most non-magnetic split (nonmagnetic at 2 degrees sideslope and 2 amperes field strength on Franz™ magnetic separator; front slope 15 degrees). Progressively finer grains were selected for B-E; F comprises pieces of grains broken during abrasion. In the left column of the table each fraction is followed by the number of grains or grain fragments dissolved.

² U blank correction of 1pg ± 20%; U fractionation corrections were measured for each run with a double ²³³U-²³⁵U spike (about 0.004/amu).

³Radiogenic Pb

⁴Measured ratio corrected for spike and Pb fractionation of 0.0037/amu ± 20% (Daly collector) which was determined by repeated analysis of NBS Pb 981 standard throughout the course of this study.

⁵Total common Pb in analysis based on blank isotopic composition.

⁶Radiogenic Pb

⁷Blank Pb was 1-3 pg throughout the course of this study; U < 1 pg; common Pb composition for corrections based on Stacey Kramers (1975) model Pb at the age of the rock or the ²⁰⁷Pb/²⁰⁶Pb age of the rock.

LCR-Shae Area

Bowser Lake strata are intruded by quartz-phyric dikes, sills and stocks on the ridges above the LCR prospect. Good exposures extend for ~3 km eastward along the ridge from its contact with a body of hornblende-biotite granodiorite plus quartz diorite. Here, the Bowser strata are dominated by turbiditic units. Upright, open, north-northeast-trending concentric folds are intruded in their hinge zones by axis-parallel, rusty-weathering pyritic dikes that range in thickness from 1 to 5 m (intrusive unit Tpqhb). Farther west, folds apparently are of higher amplitude, with some fold axes occupied by thrust faults. At treeline to the east, an ~10 m thick sill (oriented 330 /30 is cut by a steeply dipping southeast-trending fault (133 /82 S) with southeast-side-down sense of motion (based on mapped offset in concert with slickensides on the fault surface). A strong lineament, which outlines the creek along which mineralization at the LCR is exposed, extends to a saddle in the ridge near UTM easting 501500 (Fig. 2) that is occupied by rusty-weathering argillaceous siltstone felsenmeer. No obvious change in lithology or in bedding orientation occurs across the saddle; however, it does mark the eastern limit of a zone of abundant dikes (rusty dikes of intrusive unit Tpqhb) with average orientations of ~200 /60 W. This orientation is parallel to fold hinges, suggesting a structural control.

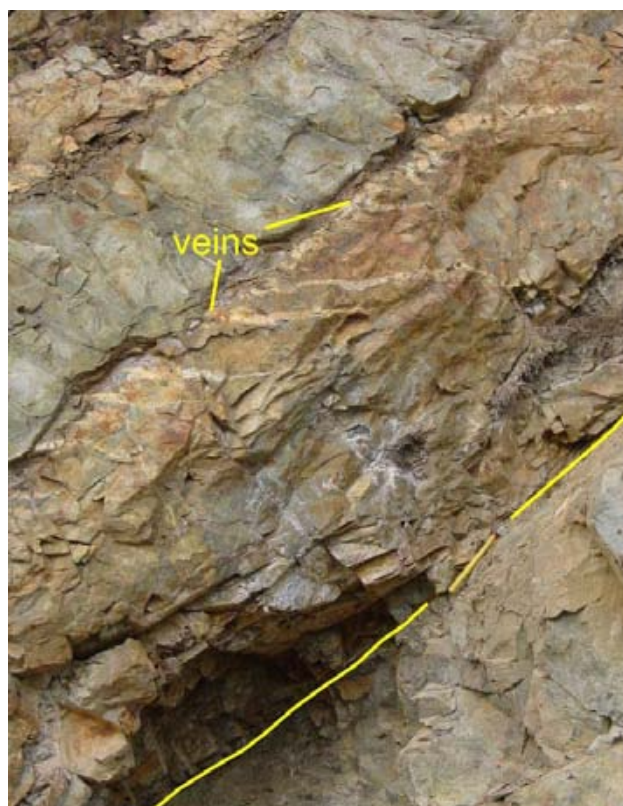


Figure 10. Dilatant quartz gash veins above thrust fault (at yellow hammer) indicate top-up-to-right (south) sense of motion, which is consistent with flat-ramp configuration (outside field of view).



Figure 11. Green, chlorite-altered brittle fault cuts orange carbonate alteration envelope around quartz veins.

Mount Allard – Tuppie area

A weak magmatic foliation is common in the homogeneous Mount Allard pluton, but tectonic fabrics are also developed locally. For example, a scaly brittle fabric occurs in zones of chlorite alteration and magnetite destruction that are metres to tens of metres thick. These zones terminate at discrete brittle faults, measured in one locality at $\sim 345 / 75$. Brittle fault zones, with scaly chlorite, cut belts of extensive carbonate alteration within the pluton (Fig. 14). Carbonate alteration belts range from several metres to ~ 12 m in thickness and are developed around sets of parallel quartz-carbonate veins that are generally less than 5 cm thick and oriented $\sim 120 / 80$ S (Fig. 12).

Hat area

Deformation within the Hat area has resulted in open to close folds within turbiditic sandstone correlated with the Bowser strata. Tight intrafolial isoclinal folds occur in rusty ar-



Figure 12. Carbonate alteration of unit MKtph. Inset shows one of a minority of veins that are composed of euhedral quartz crystals growing into a cavity that was later infilled with calcite.



Figure 13. North-dipping carbonate alteration zones on near horizon and on dark ridge beyond (north is to the right). Such zones host quartz-sulphide veins (arsenopyrite-pyrite-sphalerite-chalcopyrite-galena).

gillaceous strata and suggest that isoclinal folding has affected this fine-grained unit, at least at an outcrop scale. Folded strata are intruded by hornblende-pyroxene quartz diorite of unit MKdih, which has also been folded and is the dominant host to mineralization in the Hat area. Many mineralized veins dip at shallow angles and are clearly developed along brittle shears that dip shallowly to the north ($\sim 300 / 30$ N, $230 / 20$ N; Fig. 11, 13) and south ($110 / 30$ S). At one locality, veins within the carbonate alteration zone appear folded and rodded ($320 / 20$ N; Fig. 14). This type of folding may be restricted to hinge zones of folds that have straight limbs (*cf.* Fig. 13). If this is correct, the dominant limbs are north dipping, suggesting an overall south vergence.

East of Kitsumkalum Lake

Rocks east of Kitsumkalum Lake are affected by ductile fabrics developed during at least two deformational events. These fabrics are well displayed by the border phases of the Kitsumkalum pluton. A pervasive strong foliation of $\sim 200 / 50$ W (variable) contains a persistent mineral lineation $\sim 250 / 45$. Locally developed C^S fabrics indicate top-to-the-west sense of motion. Late brittle faults are oriented $\sim 350 / 60$ E. All fabrics that affect the pluton must be younger than the age of the body, which is reported as $59.6 \pm 0.2 / -0.1$ Ma (Gareau *et al.*, 1997).

East of the north end of Kitsumkalum Lake, retrograded calcareous chlorite schist (*see next section*) is deformed into south-verging, recumbent folds. Minor fold hinges defined by recessive carbonate layers, as well as pygmatically folded quartz veins, display a dominant hinge orientation of $\sim 070 / 25$ S. Subparallel with the long limbs of the enveloping folds are thrust faults (oriented $\sim 240 / 55$ N) that were likely active during the folding event. Gash veins in the hanging walls of the thrusts are consistent with top-to-the-south motion on the thrust faults.



Figure 14. Carbonate alteration zone between the Hat and Chris prospects. This zone is more than 12 m thick and contains several arsenopyrite-pyrite-sphalerite-galena-chalcopyrite-bearing quartz-carbonate veins. Quartz rods in the foreground may have been produced by post-vein folding.

Folds with long limbs and tight hinges are typical of the sedimentary rocks hosting mineralization near the Black Wolf prospect, on the north flank of Maroon Mountain (*see below*). Mineralized veins appear to largely post-date this tight folding and follow the foliation that is at a low angle to bedding on the long limbs. Thus, veins appear in many places to be nearly concordant. These tight folds are, in turn, folded by an open kilometre-scale antiform with an east-northeast-trending axial trace (approximately parallel to Wasach Creek) that is interpreted based upon bedding orientations visible in airphotos and northwest-striking layers north of Wasach Creek.

METAMORPHISM

Biotite hornfels is the most common metamorphic facies within the Kalum area. Outside of the thermal metamorphic aureoles, a change in regional metamorphic grade occurs, with increases both west and east of the Kalum area. For example, sillimanite and granulite grades are attained to the west, within the Coast Belt (Sisson, 1985). East of northern Kitsumkalum Lake, retrograde spotted chlorite schist contains relicts of andalusite porphyroblasts with internal schistosity that is discordant with respect to the enclosing schistosity. In contrast, near Sand Lake to the north or along the Copper River to the southeast (Mihalynuk and

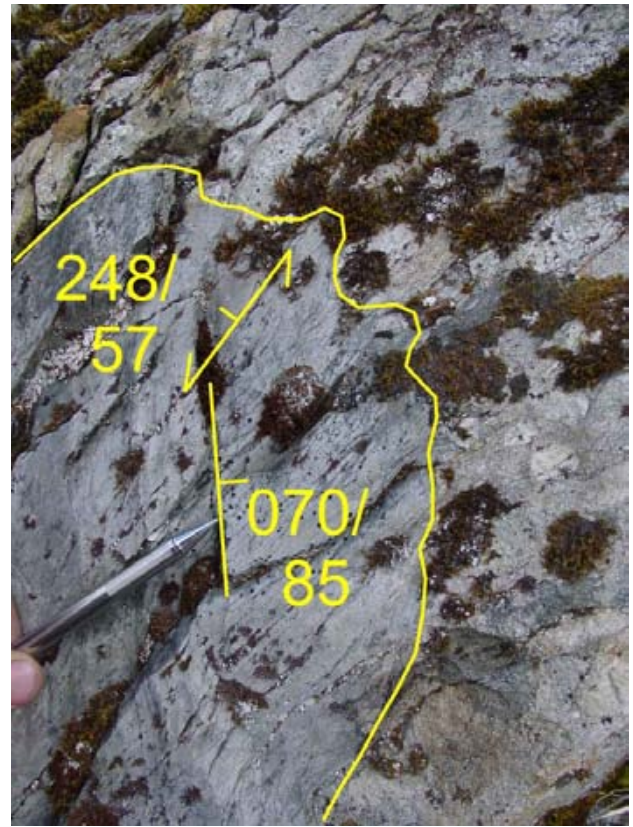


Figure 15. Well-bedded argillite in core of tight fold with straight limbs. Outside of fold is conglomerate. Clast elongation ($050^{\circ}/20^{\circ}$) is approximately parallel to resistant ridges underlain by conglomerate.

Ghent, 1996), strata are metamorphosed only to zeolite facies.

MINERALIZATION

Mineral occurrences near Kitsumkalum Lake were examined during this study. Many are located on the Kalum and LCR properties held by Eagle Plains Resources and others on four crown grants on Maroon Mountain. We also report on newly discovered mineralization at the Shea occurrence, as well as newly discovered veins near the Hat prospect.

We investigated four styles of mineralization in the Kitsumkalum Lake area:

Type 1: porphyry-style copper-molybdenum-zinc vein stockworks in quartz-biotite granite porphyry at the Shea occurrence, and in adjacent country rocks

Type 2: semimassive sulphide replacement copper-zinc-molybdenum mineralization in clastic country rocks at the Shea occurrence

Type 3: quartz-polymetallic sulphide veins (zinc, lead, copper-silver-gold-arsenic), commonly within a carbonate envelope in an intrusive host at the the Hat and Tuppie occurrences

TABLE 2. INAA RESULTS FOR SELECTED ELEMENTS AND SELECTED SAMPLES

Field	Element	Units											
		Au	Ag	As	Ba	Fe	Sb	Sc	W	Zn	La		
		ppb	ppm	ppm	ppm	%	ppm	ppm	ppm	ppm	ppm		
	Detect limit	2	5	0.5	50	0.02	0.1	0.1	1	50	0.1		
Number	Sample Type	Easting	Northing										
MMI04-44-20	LCR at PWLCV3	500784	6082170	27	-5	7.0	-50	2.72	1.5	0.6	-1	117	-0.5
MMI04-44-24	Shae sulphide blocks	501065	6082814	60	-5	5.8	240	13.7	1.7	8.9	-1	-50	15.2
MMI04-45-7	Kalum 65cm vein	512513	6066613	2305	214	427	-280	2.32	3270	0.5	-2	324	-0.5
MMI04-47-10	Tuppie qtz-py-cc (dike)	504653	6067933	8	9	27.4	780	3.61	12.5	9.5	6	183	-0.5
MMI04-47-10b	Tuppie qtz-sulphide vein	504653	6067933	880	44	11000	-310	1.41	2470	2.6	-2	9320	4.4
MMI04-47-8	Tuppie qtz-sulphide vein	504609	6068011	29	-5	296	-50	6.32	12.0	3.5	3	906	3.3
MMI04-48-10	Tojo -block from buttress	499833	6071878	1670	206	157	-50	1.79	676	2.2	7	5580	-0.5
MMI04-48-12b	Tojo -block from buttress	499680	6071795	1610	-24	42400	-650	8.51	-4.1	15.2	-4	-70	8.1
MMI04-48-13	Hat qtz-sulphide (aspy)	499559	6071473	1540	-30	93600	-970	10.3	-6.1	2.9	91	-87	-0.6
MMI04-48-14	Hat qtz-sulphide bx	499610	6071522	615	53	87.0	-50	4.96	61.3	2.8	-1	38200	-0.5
MMI04-48-14b	Hat qtz-sulphide bx block	499610	6071522	349	85	427	-50	2.14	141	1.5	-1	6130	0.9
MMI04-48-2	Hat E - carbonate altered	501186	6071889	6	-5	90.2	200	3.20	73.0	5.2	140	100	2.6
MMI04-48-3	Hat E - qtz-chl-? (black)	501275	6072040	453	-5	96.6	-50	1.52	3.7	0.8	3	63	1.4
MMI04-49-2	" 76cm chip, 62cm vein	500274	6071433	974	-12	26100	-380	9.19	208	3.8	1300	5300	8.9
MMI04-49-4	Hat E - qtz-gn vein	500186	6071472	47	8	71.4	170	1.45	13.3	1.2	7	265	2.1
MMI04-49-5	77cm chip, 42cm vein	500180	6071552	29	9	44.5	315	3.76	9.3	5.6	22	854	4.3
MMI04-49-8	4-22cm bx qtz-sulphide	499602	6071658	2220	56	765	581	3.96	27.3	10.4	16	32700	2.9
MMI04-49-8b	20 cm vein in block	499602	6071658	1450	194	15200	1100	4.50	284	3.4	294	51200	15.3
MMI04-49-9	Hat -sheared aspy-qtz	499620	6071620	1420	-14	23300	-245	6.68	24.6	20.8	49	11700	13.8
MMI04-50-5	grab - Kalum	515131	6072073	2940	-5	9.9	-35	6.08	2.0	27.0	-1	-50	4.2
MMI04-51-10	grab - Shae/LCR	501529	6082792	10	-5	5.5	301	1.00	0.3	1.5	-1	84	3.5
MMI04-51-5	grab - Big Joe	510211	6089930	166	-5	189	595	8.60	4.6	2.2	11	-50	16.5
MMI04-51-8	grab - Shae	502207	6082773	17	-5	6.1	126	8.36	0.3	15.4	6	130	13.1
MMI04-52-15	grab - Bear 10m trench/adit	522686	6074653	56200	129	78.8	-50	2.35	72.8	1.9	-1	297	1.8
MMI04-52-15R	grab - Bear 10m trench/adit	522686	6074653	55300	156	75.7	200	1.75	108	1.8	-1	286	1.7
MMI04-52-4	Hat -grab 1.3m bx vein	499669	6071516	462	104	345	-50	1.35	62.7	0.8	4	310	0.8
RFR04-3-13	grab - small adit	521922	6074080	57500	169	40.5	840	14.6	152	5.2	-1	27700	5.9
RFR04-3-9	grab - Black Wolf adit	521841	6073893	7600	104	225	-50	3.79	123	0.5	-1	5990	-0.5
QC													
	GSB Till 99 Std.			66	-5	55.4	590	6.0	14.1	23.6	-1	418	-0.5
	GSB Till 99 Std.			31	-5	50.1	990	6.2	10.9	23.6	-1	311	25.4
	GSB Till 99 Std.			38	-5	62.7	810	6.2	14.4	23.4	-1	319	-0.5
Mean				45	-5	56.1	797	6.1	13	24	-1	349	8
SD				19	0	6.3	200	0.1	2	0	0	60	15
% RSD				42	0	11.3	25	1.5	15	0	0	17	184
GSB Till 99	Recom. Values			32	-5	61.7	827	8.2	13.4	29.9	-1	390	30.8
	58070 MMI04-52-15			56200	129	78.8	-50	2.4	72.8	1.9	-1	297	1.8
	58076 MMI04-52-15R			55300	156	75.7	200	1.8	108	1.8	-1	286	1.7
% Difference				1.6	18.9	4.0	333.3	29.3	38.9	5.4	0.0	3.8	5.7
	58133 MMI04-35-6			4	-5	13.1	950	3.9	1.7	9.9	-1	110	6.6
	58136 MMI04-35-6R			15	-5	4.9	950	3.6	3.5	9.5	-1	116	6.0
% Difference				114	0	91.1	0	7.7	69.23	4.1	0	5.3	9.5

Table Notes: Coordinates are UTM Zone 9, NAD83

A full list of samples and elements analyzed can be obtained for both INAA (Table 2) and ICP-ES (Table 3) suites from: <http://www.em.gov.bc.ca/Mining/Geosurv/Publications/catalog/catfldwk.htm>

QC = Quality Control

Type 4: lead-silver-gold veins, commonly in an argillite matrix; at the Guld, Gold Cap, Bear and Black Wolf occurrences

Kalum Property

Three main styles of mineralization are seen on the Kalum property, west of Kitsumkalum Lake. One style of mineralization is a stockwork of quartz veins that contain sulphides, mainly chalcocopyrite and pyrite, and appreciable molybdenite (type 1), south of the Little Cedar River (LCR). It is known as the Macex or LCR. A second style of

A variation of type 3 mineralization is seen at the Kalum Lake prospect, with elevated bismuth values, more typical of intrusive-related gold deposits.

TABLE 3. ICP-ES RESULTS FOR SELECTED ELEMENTS AND SELECTED SAMPLES.

Field Number	Element	Detect limit Sample Type / Units	Au	Ag	Cu	Pb	Zn	Mo	As	Mn	Fe	Cd	Sb	Bi	Ba	S	Hg	Se	Ga
			ppb	ppb	ppm	ppm	ppm	ppm	ppm	ppm	ppm	ppm	%	ppm	ppm	ppm	ppm	%	ppb
MMI04-44-20	LCR at PWLCV3	44.2	2490	2722.51	2.61	91.9	>2000	>2000	-0.1	45	3.68	0.0	0.5	0.61	4.4	3.67	25	4.4	2.5
MMI04-44-24	Shae sulphide blocks	56.9	1303	2895.64	7.18	102.4	157.8	157.8	-0.1	441	15.09	1.0	0.1	2.89	31	8.33	-5	10.2	4.7
MMI04-45-7	Kalium 65cm vein	1221.3	>100000	4219.8	2879.61	284.5	1.44	226.7	35	2.29	4.37	3.9	>2000	559.87	34.6	1.16	6019	15.6	0.1
MMI04-47-10	Tuppie qtz-py-cc (dike)	2.3	6800	148.78	92.53	180.8	1.24	18.2	715	7.15	4.37	1.1	7.4	0.24	54.6	0.61	-5	0.3	3
MMI04-47-10b	Tuppie qtz-sulphide vein	636.5	27454	134.07	5344.66	9260.7	1.22	>10000	58	1.56	1.56	98.4	>2000	1.56	16.2	0.93	154	1.2	1.3
MMI04-47-8	Tuppie qtz-sulphide vein	27.9	1063	180.9	33.59	1221.1	17.5	417.7	979	8.27	13.2	13.2	5.9	2.03	11.4	1.48	11	3.1	6
MMI04-48-10	Tojo -block from buttress	1537.1	>100000	854.23	>10000	6706.7	1.65	127.7	78	2.06	59.7	724.5	0.09	18.5	15.5	1.55	425	0.7	0.4
MMI04-48-12b	Tojo -block from buttress	1238.2	690	5.3	9.66	68.4	0.53	>10000	1553	6.75	0.2	24.4	0.4	35.7	1.64	-5	1.6	7.1	1.1
MMI04-48-13	Hat qtz-sulphide (aspy)	1060.3	2342	48.42	39.04	59.1	3.47	>10000	634	9.92	7.26	475.4	72.3	0.04	28.4	4.98	17	4.4	1.2
MMI04-48-14	Hat qtz-sulphide bx	651.2	72090	205.11	5226.28	>10000	1.06	102.3	2525	7.26	7.26	64.3	127.1	0.02	10.3	4.76	735	0.7	2.7
MMI04-48-14b	Hat qtz-sulphide bx block	443.7	88429	173.61	1589.41	6770.9	0.57	465.8	517	2.37	3.77	0.7	69.4	0.03	31.7	1.37	161	0.1	0.8
MMI04-48-2	Hat E - carbonate altered	3.2	5400	93.97	15.71	98.9	0.36	88.8	1474	3.77	3.77	0.3	69.4	0.03	31.7	0.02	69	-0.1	0.9
MMI04-48-3	Hat E - qtz-chl-? (black)	1682.3	919	31.51	7.24	34.1	0.64	78.1	792	1.75	0.01	0.01	0.5	0.02	13.1	0.01	-5	0.1	2.2
MMI04-49-2	" 76cm chip, 62cm vein	1735.8	11400	83.45	1233.36	5600.8	2.11	>10000	5182	7.78	6.41	211.7	31.6	0.33	81	2.45	229	1.1	3.3
MMI04-49-4	Hat E - qtz-gn vein	26.1	8500	7.45	1241.58	198.3	0.76	70.4	548	1.55	1.55	1.1	7.1	-0.02	36.5	0.1	-5	0.1	0.4
MMI04-49-5	77cm chip, 42cm vein	25.5	12100	28.72	2974.55	931.7	3.36	42.9	1919	4.18	4.18	8.3	5.7	1.28	62.9	0.34	37	0.2	2.1
MMI04-49-8	4-22cm bx qtz-sulphide	3452.8	53000	358.4	1528.46	>10000	1.43	978	694	4.05	4.05	466.8	19.0	0.22	78.8	1.66	522	0.5	4.5
MMI04-49-8b	20 cm vein in block	1719.8	>100000	45.08	>10000	>10000	67.97	>10000	831	4.74	4.74	528.7	197.1	0.11	38.5	5.18	1585	2	1.5
MMI04-49-9	Hat -sheared aspy-qtz	1677.1	12100	145.81	1054.14	>10000	1.21	>10000	1528	6.41	6.41	211.7	31.6	0.33	81	2.45	229	1.1	3.3
MMI04-50-5	grab - Kalum	6152.2	8000	3152.18	5.98	60.2	0.59	8.2	561	3.79	3.79	0.4	0.7	4.93	98.2	0.03	7	1.4	3.8
MMI04-51-10	grab - Shael/LCR	3.4	662	740.25	1.79	58.8	6.92	1	163	1.19	1.19	0.6	0.1	0.18	30.4	0.34	-5	0.7	1.7
MMI04-51-5	grab - Big Joe	250.8	5600	267.65	50.05	24.4	1364	230.8	30	10.88	0.0	0.0	1.5	16.36	6.9	9.82	12	3.1	1.2
MMI04-51-8	grab - Shae	25.6	771	2252.41	6.39	142.4	30.8	-0.1	3007	9.09	0.3	0.3	4.55	16.4	16.4	4.08	-5	7	10.8
MMI04-52-15	grab - Bear 10m trench/adit	32456.3	>100000	170.74	>10000	331.2	1.04	61.4	30	2.28	2.28	1.5	60.9	11.54	11.6	0.61	81	9	0.2
MMI04-52-15R	grab - Bear 10m trench/adit	75827.7	>100000	198.12	>10000	340.7	1.06	78.1	27	2.47	2.47	2.0	100.4	17.69	13.3	1.02	149	14.9	0.3
MMI04-52-4	Hat - grab 1.3m bx vein	468.4	>100000	182.45	65.21	392.2	0.37	410	304	1.75	1.75	7.8	64.0	0.02	9.1	0.28	67	-0.1	1
RFR04-3_13	grab - small adit	>100000	>100000	3296.57	>10000	>10000	0.38	38.1	1836	19.07	356.5	154.2	0.39	28.9	28.9	>10	190	4.2	1.3
RFR04-3_9	grab - Black Wolf adit	11364.3	>100000	227.07	>10000	8096.5	0.41	312.1	360	5.31	5.31	85.3	148.3	0.44	5.5	6.25	121	3.8	0.7
QC																			
	GSB Till 99 Sid.	15.9	1315	157.87	185.02	344.1	0.87	48.4	1408	6.29	6.29	0.7	7.9	0.23	262.6	-0.01	297	0.4	8.3
	GSB Till 99 Sid.	124	1422	173.85	255.34	393	0.87	53.6	1583	7.48	7.48	0.7	9.2	0.25	292.3	-0.01	334	0.4	9.2
	GSB Till 99 Sid.	20.6	1266	155.34	204	350.1	0.77	49.7	1306	6.49	6.49	0.6	7.8	0.22	266	-0.01	297	0.4	7.9
Mean		72.3	1344	164.595	229.67	371.55	0.82	51.65	1445	6.985	6.985	0.7	8.5	0.235	279.15	-0.01	315.5	0.4	8.55
SD		73.1	110.3	13.1	36.3	30.3	0.1	2.8	195.9	0.7	0.7	0.0	1.0	0.0	18.6	0.0	26.2	0.0	0.9
% RSD		101.1	8.2	8.0	15.8	8.2	8.6	5.3	13.6	10.0	10.0	6.4	11.2	9.0	6.7	0.0	8.3	0.0	10.8
GSB Till 99	Recom. Values	28.60	1221.00	157.69	183.76	326.95	0.81	50.00	1288.0	6.30	6.30	0.64	7.59	0.22	233.60	-0.01	298.50	0.35	8.40
58070	MMI04-52-15	32456.3	10000	170.74	10000	331.2	1.04	61.4	30	2.28	2.28	1.5	60.9	11.54	11.6	0.61	81	9	0.2
58076	MMI04-52-15R	75827.7	10000	198.12	10000	340.7	1.06	78.1	27	2.47	2.47	2.0	100.4	17.69	13.3	1.02	149	14.9	0.3
% Difference		80.1	0.0	14.8	0.0	2.8	1.9	23.9	10.5	8.0	8.0	29.4	49.0	42.1	13.7	50.3	59.1	49.4	40.0
58133	MMI04-35-6	12	203	39.72	24.4	59	0.68	12.1	708	1.95	1.95	0.2	1.1	0.35	342	-0.01	5	0.4	8
58136	MMI04-35-6R	4.1	434	46.21	98.12	62	0.51	4.9	650	1.9	1.9	0.2	2.6	0.63	284.8	0.02	9	0.4	7.5
% Difference		98.1	72.5	15.1	120.3	5.0	28.6	84.7	8.5	2.6	2.6	28.6	80.5	57.1	18.3	600.0	57.1	0.0	6.5

mineralization was discovered near the LCR property. Called the Shae occurrence, this mineralization is massive sulphide replacement of clastic strata (type 2; Fig. 16, 17). It is attributed to a mineralized quartz-biotite granite porphyry (Fig. 18) that might also be responsible for stockwork veining at the LCR. The most widely developed style of mineralization is base-metal sulphide-quartz (\pm carbonate) veins and networks of veins related to brecciation and shearing within zones of carbonate alteration (type 3; Fig. 19, 20).

Other zones of type 3 mineralization were discovered during mapping, mainly between the Hat and Chris occurrences, in areas recently exposed by the thaw of multiyear snow pack. There, additional arsenopyrite and base-metal sulphide veins within carbonate alteration zones were discovered (Fig. 17, 18).

HAT AREA

Tabular carbonate alteration zones are common between the Hat and Chris prospects. Chlorite-altered and folded hornblende-pyroxene quartz diorite is the main hostrock for mineralized veins in the Hat area. These zones range up to more than 12 m thick and typically contain multiple arsenopyrite-pyrite-sphalerite-galena-chalcopyrite-bearing quartz-carbonate veins (type 3). Mineralized quartz veins are commonly banded and brecciated, and form two sets, mainly oriented at low to moderate angles. Mineralization in low-angle veins occurs as massive coarse-grained sulphide (Fig. 19) or as mats of arsenopyrite needles that may be intergrown with sphalerite, galena and minor chalcopyrite (Fig. 20). One of the most impressive veins discovered during mapping was an ~20 cm thick vein consisting mainly of coarsely crystalline arsenopyrite, lesser sphalerite, galena and chalcopyrite, and broken quartz prisms, originally >10 cm long. Veins have been folded and sheared, and some sulphides appear to have been mobilized during these events, as indicated by the occurrence of chalcopyrite in microfractures oriented perpendicular to shear banding. Late gash veins oriented at a steep angle to the main sheared veins are generally not well mineralized.

LCR AREA – NEW SHAE OCCURRENCE

A logging road crosses an overgrown clearcut at an elevation intermediate between the main LCR mineralized zone and the Little Cedar River. Angular, rusty, sulphide-rich boulders containing up to 30% pyrrhotite and 2% chalcopyrite were found near the western termination of this road. Similar boulders were traced along the roadbed and colluvial banks for approximately 1.3 km to the east, down the valley to a mineralized outcrop (Fig. 14). This mineralization constitutes the Shae occurrence. The presence of mineralized boulders upstream and ‘up-ice’ of the known mineralized outcrops suggests that the boulders have not been transported by either river water or glacial activity. Consequently, a large mineralizing system is indicated.

Approximately midway between the end of the road and the easternmost mineralized outcrop (Fig. 16) is an exposure of biotite-quartz granite porphyry (unit Tqbp; Fig. 2, 18) with pyrite-chalcopyrite disseminated through-

out and concentrated in a hydrothermal breccia zone roughly 20 cm thick. Massive sulphide replacement-style mineralization (Fig. 16) in outcrop and boulders is attributed to this mineralized porphyry body. A representative sample of the massive sulphide returned 2895 ppm Cu, 1303 ppb Ag, 157 ppm Mo (0.28% Cu, 1.3 g/t Ag, 0.015% Mo) and a trace of Au (57 ppb; Table 3, sample MMI04-44-24). The occurrence of mineralization over a distance of more than 1300 m indicates the Shae may be part of a large mineralizing system that warrants further investigation.

Isolated veins and vein stockworks at the LCR lack iron-stained carbonate alteration halos that accompany the base-precious metal veins elsewhere on the property. Instead, a grey clay-rich (?) halo appears to envelop some of the veins (these veins were not analyzed in detail, nor were they sampled for petrographic analysis). Veining at the LCR may be related to the mineralizing intrusion at the Shae occurrence.



Figure 16. Rich Friedman on a low roadcut outcrop of sulphide replacement-style mineralization at the new Shae occurrence.

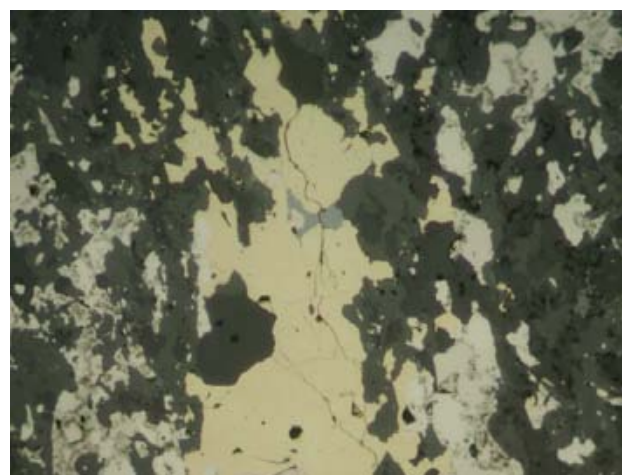


Figure 17. Reflected-light photomicrograph of replacement-style mineralization at the Shae occurrence. Yellow chalcopyrite with light grey inclusion of sphalerite; white mineral is pyrite; dark grey is gangue, mostly quartz. Field of view is ~0.9 mm.

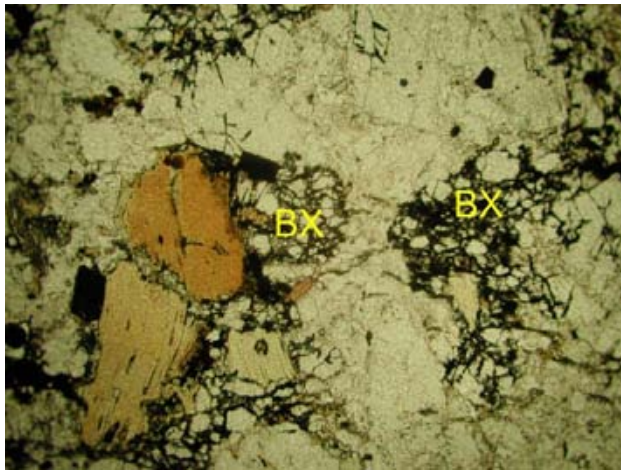


Figure 18. Photomicrograph of Fe-oxide > chalcopyrite cemented breccia zones (BX) within quartz-eye biotite porphyry at the Shae occurrence. Field of view is approximately 4 mm.



Figure 19. Jesse Campbell at a newly discovered ~15 cm thick arsenopyrite vein. This mineralization is exposed because of record-breaking thaws. Note relicts of the rapidly melting glacier in immediate background. A sample of the massive arsenopyrite vein is shown in the inset.

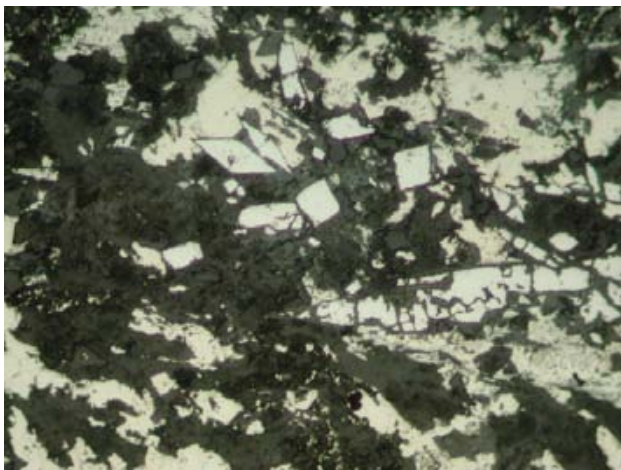


Figure 20. Highly reflective, slightly corroded, blue-white acicular needles of arsenopyrite, with diamond-shaped cross-sections, idiomorphic within white pyrite and yellowish chalcopyrite. Field of view ~0.9 mm.

TUPPIE AREA MINERALIZATION

The Tuppie showing is located at the western contact of the Mount Allard pluton, mainly in hornfelsed country rocks that are extensively crosscut by dikes. Petrographic observations show that pervasive chlorite alteration post-dates carbonate alteration in some parts of the pluton. At the Tuppie showing, however, poikilitic hornblende megacrystic dikes are chlorite altered and then overprinted by carbonate alteration. Intensity of overprinting correlates with intensity of foliation fabric development, which increases near the sheared and strongly lineated eastern contact (150 /20). Silica and sulphides have accumulated at the eastern contact of one dike, probably late during the deformational episode because both are brecciated and annealed by quartz-carbonate and sulphide. A sample of foliated dike returned 6800 ppb Ag, in contrast to the immediately adjacent brecciated quartz vein that returned 27 454 ppb Ag and 636 ppb Au (Table 3, samples MMI04-47-10, 10b).

Zones of cryptic brecciation, up to 5 m across, occur within rusty, hornfelsed argillite. Black and rust, finely crystalline silica has flooded these zones. One grab sample of breccia returned values of 4400 ppb Ag (sample not listed in Table 2 or 3), indicating that such zones warrant further prospecting.

Maroon Mountain

Mineralization on the north flank of Maroon Mountain includes auriferous quartz and base-metal sulphide veins (type 4) that occur along a section a low ridge underlain near treeline by resistant conglomerate layers. Four occurrences listed in MINFILE are found along the northeast-trending ridge: Guld, Gold Cap, Bear and Black Wolf (from northeast to southwest, MINFILE #1031181, 028, 029, 030). Most MINFILE descriptions refer to the veins as concordant below a 35–75 m thick conglomerate layer. However, the conglomerate layer is tightly folded with hinges and clast elongation approximately parallel the northwest-trending (057°) ridge. The veins appear to largely postdate this folding and follow the foliation, which is at a low angle to bedding on the long limb.

Best assays were returned from two galena-rich quartz veins separated by an along-strike distance of 950 m (each about equidistant from the recorded location of the Bear occurrence; MINFILE 1031029). These are in the range 56 200 to >100 000 ppb Au (samples MMI04-52-15, RFR04-3-13; Tables 2 and 3). Orientation of the northern vein is 054 /58 S. It is a drusy, 35 cm thick, multistrand quartz-galena vein within graphitic phyllite. This vein is adjacent to a late, north-northwest-trending, high-angle fault with undetermined sense of motion.

Hadenschild Creek Graphite

Highway exposures of well-layered sedimentary strata immediately west of Hadenschild Creek are extensively cut by bedding-parallel faults. Typically, the faults are local-

ized in carbonaceous strata. Some display 30–50 cm of gouge, and within these fault zones are seams of graphite, commonly 20 cm thick. Impurities are locally scarce and are mainly calcite veinlets or fragmented veinlets. Graphite in the thickest seams is a homogeneous shiny grey and lacks anisotropy. Graphite quality test results are pending.

GEOCHEMICAL ANALYSES OF MINERAL OCCURRENCES

Keeping in mind the degree of analytical uncertainty for the ICP-ES and INAA analyses, some preliminary conclusions can be drawn. First, many of the mineral occurrences contain significant Au values. In fact, more than half of the 54 samples collected contain anomalous concentrations (greater than 40 ppb Au by ICP-ES). This includes mineral occurrences on both sides of Kitsumkalum Lake. For example, mineralized prospects on Maroon Mountain yield consistently high Au values. Surprisingly, these are higher than values reported in MINFILE. Similar lode veins in the area to the north are the likely source of placer gold in Douglas Creek, which has been recovered since the late 1800s.

INTRUSIVE-RELATED GOLD MODEL

Gold deposits that form during intrusion of magma into sedimentary strata rank amongst the largest known reservoirs of gold in the Earth's crust. These deposits fall into two major categories: 1) those hosted within or immediately adjacent to the intrusions (i.e., the intrusion-related/hosted or thermal aureole deposits); and 2) those hosted in sedimentary rocks, some of them many kilometres from the nearest known intrusion (i.e., the sediment hosted/Carlin type deposits; e.g., Lefebvre and Ray, 1995). Contained gold values can be hundreds to thousands of tonnes. Famous sediment-hosted deposits, such as Maruntau in Uzbekistan (>5000 t; Morelli, 2004), Telfer in Australia (>450 t; Rowins *et al.*, 1997), and deposits of the Carlin trend in Nevada (Carlin, 320 t; Betze, ~1000 t; Meikle, >200 t) tend to have grades in the range 3–14 g/t. Intrusion-hosted deposits, such as Kori Kollo in Bolivia (160 t; Long *et al.*, 1992), Fort Knox and Donlin Creek in Alaska (>200 t, Bakke, 1995; 775 t, Goldfarb *et al.*, 2004), or Dublin Gulch in Yukon (46.5 t, Yukon EMR, 2004) typically have gold grades around 0.5–3 g/t.

The role of magmatic fluids in sourcing and carrying gold is disputed, although most workers agree that intrusions provide the thermal gradient required to drive these mineralizing systems. Exploration for such deposits is guided regionally by their association with placer deposits and high-grade lodes (e.g., Dublin Gulch). Geochemical associations are elevated Au, Bi, Te, W ± (Mo, As, Pb) within or adjacent to the intrusion, and Au-As-Sb-Hg±(Ag, Pb, Zn) in distal deposits (Hart *et al.*, 2000, 2002). Currently accepted, broad application of the intrusive-related gold model includes distal, base, and precious metal veins (Au, Pb, Zn, As, Sb, Hg; Lang and Baker, 2001), which may point to a prospective intrusive system, if lacking merit as the base metal veins commonly do, in terms of grade and

tonnage. Mineralizing fluids are reduced, with ore mineral assemblages containing arsenopyrite, pyrite or pyrrhotite, and lacking Fe-oxides. However, sulphide contents tend to be low overall (<5%; Lang and Baker, 2001). Carbon-dioxide-rich fluid exsolution during magma crystallization may be critical in destabilizing other ligands (e.g., bisulphide) that are responsible for Au solubility (Lowenstern, 2001). Evidence of carbonic fluid interaction is theoretically predicted and empirically verified in known deposits (Baker and Lang, 2001). Gold-rich intrusive systems have potential for huge gold resources. Consequently, they are attractive exploration targets. Features of mineralization in the Kalum area, particularly type 3 sulphide veins with carbonate alteration envelopes, are similar to those found within producing intrusion-related deposits.

DISCUSSION

By far the most common type of mineralization in the Kitsumkalum Lake area is polymetallic sulphide veins (type 3). These occur within and adjacent to both the Mount Allard pluton and diorite at the Hat occurrence. The intensity of carbonate alteration (±sulphide mineralization) may be enhanced by strain localization within the alteration zone. Quartz-carbonate veining in the Mount Allard pluton is not folded, but folding has definitely affected at least some of the veins in the Hat diorite. Fold styles may be similar to those seen on northern Kitsumkalum Lake and Maroon Mountain: long, fairly straight limbs and tight, relatively convolute hinges. However, our structural investigation was not extensive enough to permit unequivocal determination of the source of veins in the Hat intrusion. A possible linkage between mineralization and extensional structures needs to be further evaluated.

We originally considered the Hat diorite to be older than the Mount Allard pluton because it is more strongly deformed. However, available isotopic age data, if correct, indicate an inverse relationship between the degree of deformation and age of the intrusive body. Three age determinations are available for intrusive rocks in the Kalum area: a cooling age of 100.2 ± 6.8 Ma for the relatively undeformed Mount Allard pluton (Godwin, in Breitsprecher and Mortensen, 2004); 93.8 ± 0.5 Ma for the Hat diorite (reported here); and $59.6 +0.2/-0.1$ Ma (Gareau *et al.*, 1997) for the strongly deformed North Kitsumkalum pluton. These relationships show that deformation did outlast Early Eocene plutonism. They also indicate that the degree of deformation in these bodies may be determined more by how much the pluton has cooled prior to deformation, or proximity to a ductile fault zone, than by how much/many of the deformational episode(s) the intrusion has experienced.

Polymetallic quartz-carbonate veins and alteration zones cut thermal metamorphic halos and plutons at least as young as the Mount Allard pluton. Mineralization cannot be attributed to the phases of the Mount Allard pluton that are cut by mineralized veins. However, exsolved fluids related to late crystallization of an interior phase of the pluton could explain veins within the roof of the pluton (cf. Clear

Creek in the Yukon; Marsh *et al.*, 2003). It is more difficult to attribute veins near the Hat prospect to the same intrusive source because the plutonic hostrocks there are clearly of a different composition.

Is epithermal veining related to (extensional) deformation a reasonable alternate to intrusion-related gold veins? Rapid changes in metamorphic grade and structural level, especially well displayed in the Kitsumkalum valley, are hallmarks of an extended terrain. Juxtaposition of low-grade rocks atop hotter, deeper level rocks through structural omission during extensional faulting could explain the lack of an intrusive body to which broad thermal metamorphism can be attributed. However, extension-related epithermal quartz-carbonate veins, such as those of the Republic Graben, typically contain only traces of sphalerite, galena and chalcopyrite. In contrast, veins in the Kalum area display mineralogy that is more typical of an intrusion association: base metal rich with elevated bismuth (cf. the Kalum Lake prospect). Even less equivocal is the porphyry association of veins at both the Shae occurrence and LCR/Macex, which display molybdenite mineralization in addition to chalcopyrite. At the Shae, the mineralizing biotite-quartz porphyry can be observed directly.

SUMMARY

Byproducts of geological mapping have been a preliminary evaluation of the regional structural deformational history. This history is far more complex than is indicated by existing published maps, although it appears to be similar to that recorded in the area immediately to the west by Andronicos *et al.* (2003) and in the unpublished M.Sc. thesis of Heah (1991).

Prospecting during the course of mapping resulted in notable new finds north of the LCR occurrence and near the Hat prospect. These are, respectively, porphyry and sulphide-replacement mineralization in angular boulders and outcrops along a >1 km transect, named the Shae occurrence, and several arsenopyrite and base-metal sulphide veins exposed in areas normally covered by snow and ice.

There are four styles of mineralization in the Kitsumkalum Lake area:

Type 1: porphyry-style copper-molybdenum-zinc vein stockworks in quartz-biotite granite porphyry and in adjacent country rocks

Type 2: semimassive sulphide replacement copper-molybdenum mineralization in clastic country rocks

Type 3: quartz-polymetallic sulphide veins (zinc, lead, copper-silver-gold), commonly within a carbonate envelope in an intrusive host

Type 4: lead-silver-gold veins, commonly in an argillite matrix

The abundance of type 3 veins east of the Hat occurrence and the richness of type 4 veins in the Maroon Mountain area underscore the presence of attractive intrusion-related mineralization that spans the range from proximal (type 3) to epizonal (type 4; e.g., Hart *et al.*, 2002) veins.

ACKNOWLEDGMENTS

This field project would not have been possible without the generous financial contribution from our corporate partner, Eagle Plains Resources. Eagle Plains executives, Tim Termuende and Charles Downie, conceived the project. Project geologist Chris Gallagher, despite the demands of a new drill project, made time for geological discussions. Glen Hendrickson, Brad Robison and Jesse Campbell shared their personal knowledge of the Kalum area, as well as their home base in Terrace. Jesse Campbell also proved an able field assistant and prospector.

Dave Lefebure is thanked for his excellent editing skills in reviewing the manuscript.

Geochronological work is conducted in partnership with the Pacific Centre for Isotopic and Geochemical Research at the Department of Earth and Ocean Sciences, University of British Columbia, which is funded in part by NSERC grants.

REFERENCES

- Andronicos, C.L., Chardon, D.H., Hollister, L.S., Gehrels, G.E. and Woodsworth, G.J. (2003): Strain partitioning in an obliquely convergent orogen, plutonism, and synorogenic collapse: Coast Mountains Batholith, British Columbia, Canada; *Tectonics*, Volume 22, pages 7-1-7-24.
- Baker, T. and Lang, J.R. (2001): Fluid inclusion characteristics of intrusion-related gold mineralization, Tombstone-Tungsten magmatic belt, Yukon Territory, Canada; *Mineralium Deposita*, Volume 36.
- British Columbia Ministry of Energy and Mines (2001): British Columbia Regional Geochemical Survey digital data, Terrace, 103I; *BC Ministry of Energy and Mines*.
- Breitsprecher, K. and Mortensen, J.K. (2004): BC Age 2004A – a database of isotopic age determinations for rock units from British Columbia (Release 2.0); *BC Ministry of Energy and Mines*, Open File 2004-3.
- Downie, C.C. and Stephens, J. (2003): Kalum gold-silver property; *BC Ministry of Energy and Mines*, Assessment Report 27 417, 54 pages (plus appendices).
- Duffell, S. and Souther, J.G. (1964): Geology of Terrace map-area, British Columbia; *Geological Survey of Canada*, Memoir 329, 117 pages.
- Evenchick, C.A. (1991): Geometry, evolution, and tectonic framework of the Skeena fold belt, north-central British Columbia; *Tectonics*, Volume 10, pages 527-546.
- Evenchick, C.A., Mustard, P.S., Woodsworth, G.J. and Ferri, F. (2004): Compilation of geology of Bowser and Sustut basins draped on shaded relief map, north-central British Columbia; *Geological Survey of Canada*, Open File 4638.
- Friedman, R.M. and Armstrong, R.L. (1988): Tatla Lake metamorphic complex: an Eocene metamorphic core complex on the southwestern edge of the Intermontane Belt of British Columbia; *Tectonics*, Volume 7, pages 1141-1166.
- Friedman, R.M., Diakow, L.J., Lane R.A. and Mortensen, J.K. (2001): New U-Pb age constraints on latest Cretaceous magmatism and associated mineralization in the Fawnie Range, Nechako Plateau, central British Columbia; *Canadian Journal of Earth Sciences*, Volume 38, pages 619-637.
- Gareau, S.A., Woodsworth, G.J., Friedman, R.M. and Childe, F. (1997): U-Pb dates from the northeastern quadrant of Terrace map area, west-central British Columbia; in Current Research, *Geological Survey of Canada*, Paper 1997-1A, pages 31-40.

- Harrison, T.M., Armstrong, R.L., Naeser, C.W. and Harakal, J.E. (1978): Geology and thermal history of the Coast Plutonic Complex, near Prince Rupert, British Columbia; *Canadian Journal of Earth Sciences*, Volume 16, pages 400–410.
- Hart, C.J.R., Baker, T. and Burke, M. (2000): New exploration concepts for country-rock-hosted, intrusion-related gold systems: Tintina Gold belt in Yukon; in *The Tintina Gold Belt: Concepts, Exploration and Discoveries*, Tucker, T.L. and Smith, M.T., Editors, *British Columbia and Yukon Chamber of Mines*, Special Volume 2, pages 145–172.
- Hart, C.J.R., McCoy, D.T., Goldfarb, R.J., Smith, M.T., Roberts, P., Hulstein, R., Bakke, A.A. and Bundtzen, T.K. (2002): Geology, exploration and discovery in the Tintina Gold Province, Alaska and Yukon; *Society of Economic Geologists*, Special Publication 9, Chapter 6, pages 241–274.
- Heah, T.S.T. (1991): Mesozoic ductile shear and Paleogene extension along the eastern margin of the Central Gneiss Complex, Coast Belt, Shames River area, near Terrace, British Columbia; unpublished M.Sc. thesis, *University of British Columbia*, 155 pages.
- Lang, J.R. and Baker, T. (2001): Intrusion-related gold systems: the present level of understanding; *Mineralium Deposita*, Volume 36, pages 477–489.
- Lefebvre, D.V. and Ray, G.E. (1995): British Columbia mineral deposit profiles, Volume 2 - metallics and coal; *BC Ministry of Energy and Mines*, Open File 1995-20, 135 pages.
- Lowenstern, J.B. (2001): Carbon dioxide in magmas and implications for hydrothermal systems; *Mineralium Deposita*, Volume 36.
- Marsh, E.E., Goldfarb, R.J., Hart, C.J.R. and Johnson, C.A. (2003): Geology and geochemistry of the Clear Creek intrusion-related gold occurrences, Tintina Gold Province, Yukon, Canada; *Canadian Journal of Earth Sciences*, Volume 40, pages 681–699.
- Massey, N.W.D., MacIntyre, D.G. and Desjardins, P.J. (2003): Digital map of British Columbia: Tile NM09 South-coast B.C.; *BC Ministry of Energy and Mines*, GeoFile 2003-4.
- Mihalynuk, M.G., and Ghent, E.D. (1996): Regional depth-controlled hydrothermal metamorphism in the Zymoetz River area, British Columbia; *Canadian Journal of Earth Sciences*, Volume 33, pages 1169–1184.
- Morelli, R.M. (2004): The age of gold mineralization at the Muruntau Au deposit, Uzbekistan, from Re-Os arsenopyrite geochronology; *Geological Society of America*, Annual Meeting, Program with Abstracts, page 444.
- Rowins, S.M., Groves, D.I., McNaughton, N.J., Palmer, M.R. and Eldridge, C.S. (1997): A re-interpretation of the role of granitoids in the genesis of Neoproterozoic Au mineralization in the Telfer Dome, Western Australia; *Economic Geology*, Volume 92, pages 133–160.
- Sisson, V.B. (1985): Contact metamorphism associated with the Ponder pluton, Coast Plutonic Complex, British Columbia; unpublished Ph.D. thesis, *Princeton University*, 345 pages.
- Stacey, J.S. and Kramers, J.D. (1975): Approximation of terrestrial lead isotope evolution by a two-stage model; *Earth and Planetary Science Letters*, Volume 26, pages 207–221.
- Van der Heyden, P. (1989): Jurassic magmatism and deformation; implications for the evolution of the Coast Plutonic Complex (abstract); *Geological Society of America*, Cordilleran Section, 85th annual meeting and Rocky Mountain Section, 42nd annual meeting, Abstracts with Programs, Volume 21, page 153.
- Woodsworth, G. J., Van der Heyden, P. and Hill, M. L. (1985): Terrace East Map area; *Geological Survey of Canada*, Open File 1136.
- Yukon Energy, Mines and Resources (2004): Dublin Gulch Property, *Yukon Minerals Development Department*, Mineral Property Update, 94 pages.

Heavy Mineral Sampling and Provenance Studies for Potentially Diamond-Bearing Source Rocks in the Jurassic Laberge Group, Atlin-Nakina Area (NTS 104N), Northwestern British Columbia

By Dante Canil¹, Mitchell G. Mihalynuk² and Courtney Charnell¹

INTRODUCTION

The mineralogy of clastic sedimentary rocks provides a record of the source regions uplifted and eroded during orogeny (Dickinson et al., 1983). The Jurassic Laberge Group is part of a fold and thrust belt exposed in the northern Cordillera (Fig. 1). The paleontological and sedimentary record in the Laberge Group mark the uplift and erosion of crust during the early Jurassic and the deposition and burial of detritus in a marine fore-arc basin (English et al., in press; Johannson et al., 1997). Garnet-rich horizons of immature wacke and conglomerate occurring in the Laberge Group southwest of Sloko River were first recognized during a regional mapping and magnetic survey program (Mihalynuk and Lowe, 2002). Subsequent heavy mineral sampling in the Atlin-Nakina area, aimed at tracing the source of anomalous diamonds in placer gold operations of the northern Cordillera (Casselmann and Harris, 2002), showed evidence for diamond indicator minerals, which were traced to a garnetiferous conglomerate horizon in the Jurassic Laberge Group exposed near Sloko River (Canil et al., 2004). Further detailed study of heavy minerals from one composite sample in the garnet-rich conglomerate showed it to contain clasts of eclogite, and garnets and pyroxenes from peridotite of mantle origin (Fig. 2, 3). Thermobarometric studies revealed that the detrital garnets and pyroxenes in this sample equilibrated at mantle depths approaching the diamond stability field (MacKenzie et al., in press), on geothermal gradients expected in cratonic mantle lithosphere (Fig. 4).

Detrital mantle minerals are known in other clastic sediments (McCandless and Nash, 1996). The angular nature and lack of weathering of detrital grains in the Laberge Group require proximal sources and rapid deposition (McCandless, 1990). Potential sources for the garnet and pyroxenes in the Laberge Group could be the erosion of peridotite and eclogite as xenoliths in an alkaline igneous rock such as kimberlite or lamproite, or outcrop-sized massifs exposed by uplift and exhumation. Potential source rocks of either type that are the requisite age (pre-Jurassic)

are not known in the Atlin-Nakina area. The lack of micro-ilmenite in a heavy mineral sample of the Laberge conglomerate argues against derivation from xenoliths in alkaline igneous rocks (i.e., kimberlite; MacKenzie et al., in press). No eclogite or garnet peridotite, as either xenoliths or massifs, has yet been recognized in outcrop in the Atlin-Nakina area. Furthermore, the source of peridotitic garnets and pyroxenes in the garnetiferous wacke unit of the Laberge Group is not likely to be from ophiolite and mélange that constitutes parts of the Cache Creek Terrane to the east. Mantle peridotite from ophiolite in the Cache Creek Terrane is of lower pressure origin, in which spinel, not garnet, is stable. Furthermore, the latter rocks have been investigated by field mapping, and although blueschist assemblages have been discovered in the Cache Creek Terrane near Dease Lake (Fig. 1), no eclogite has been recognized (Fig. 1; Ghent et al., 1993; Mihalynuk et al., 2004).

Thus, the source of eclogitic and peridotitic detritus in the Laberge Group sediments remains undefined, but has important implications for the crustal evolution of the northern Cordillera. In one interpretation of paleocurrent data for exposures in southern Atlin Lake, the source area for the Laberge Group sediments must lie somewhere to the west (Johannson et al., 1997). Nonetheless, further detailed study in other horizons of the Laberge Group is warranted to identify the source and provenance of mantle minerals, and whether the sources for sediment changed in space or time during deposition in the basin. The occurrence of diamond in northwestern British Columbia and southern Yukon (Casselmann and Harris, 2002) also remains enigmatic, but could be sourced in sediments that contain other detrital minerals of demonstrable high-pressure origin required for diamond formation (Fig. 4). To this end, we performed detailed paleocurrent measurements, sedimentology and a more thorough sampling for heavy minerals in different horizons of the Laberge Group. The principal goals were to examine the lateral and stratigraphic extent of the garnetiferous horizons within the Laberge Group, to understand their appearance in the sedimentary record of this basin, and to deduce the source direction for sediments containing detrital mantle minerals, and potentially diamonds.

¹ School of Earth and Ocean Sciences, University of Victoria, Victoria, BC, dcamil@uvic.ca

² Geological Survey Branch, Ministry of Energy and Mines, Victoria, BC

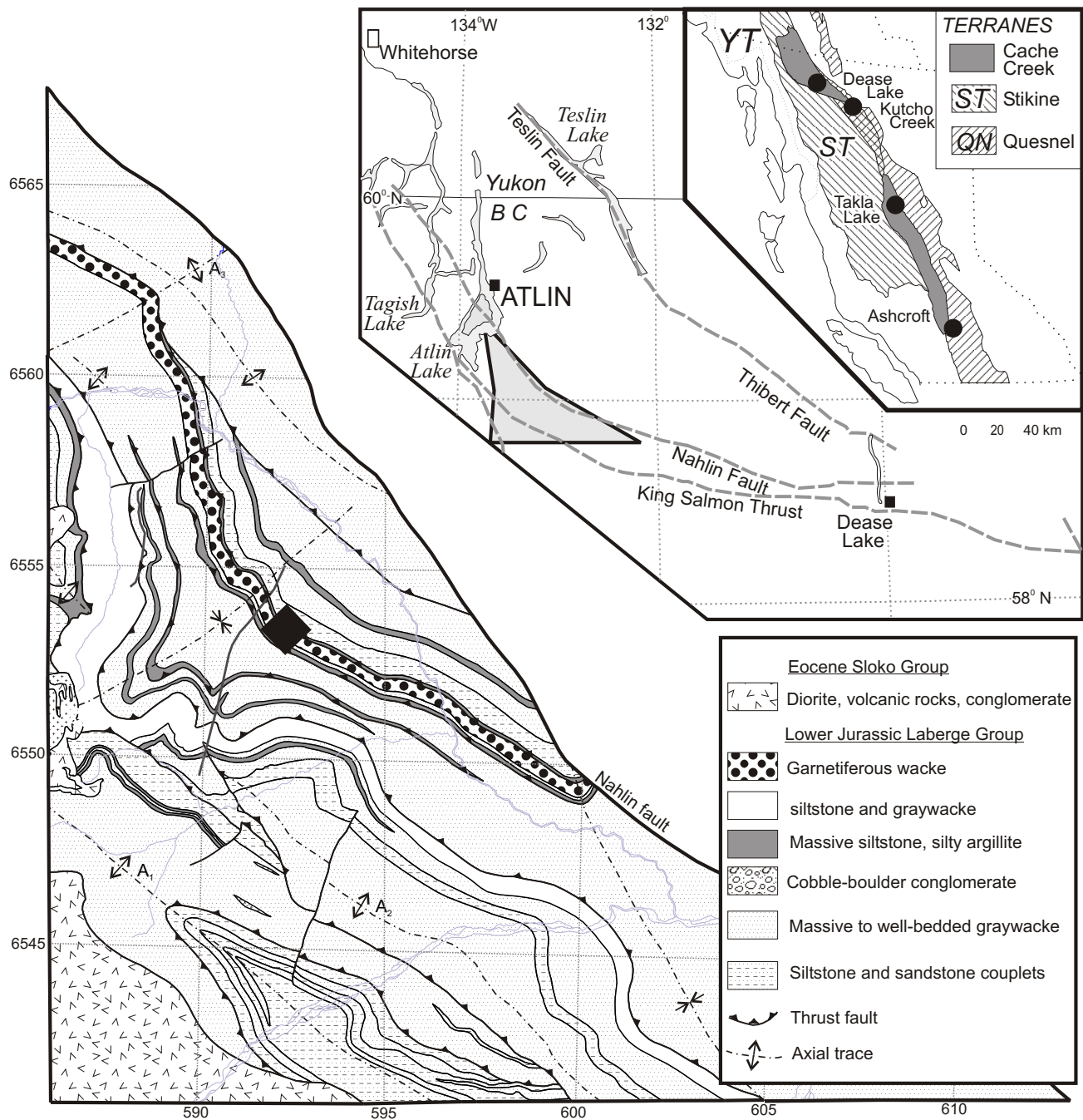


Figure 1. Geological map of part of the Laberge Group highlighting the garnetiferous wacke-pebble conglomerate. Inset shows the location of the Laberge Group in the northern Cordillera (after Johannson et al., 1997; English et al., 2002; Mihalynuk et al., 2003). Location of Eclogite Ridge is shown by the diamond.

REGIONAL GEOLOGY

The Jurassic Laberge Group is contained within the Whitehorse Trough, an early to middle Jurassic marine fore-arc basin that extends from southern Yukon into northern British Columbia in the Atlin-Nakina region. Strata in the Laberge Group near southern Atlin Lake are of Sinemurian to Pliensbachian age (197–183 Ma; Palfy et al., 2000), as constrained by biostratigraphy and U-Pb ages of tuffs and granitoid boulders in conglomerate (Johannson et

al., 1997). Sediments in the basin have been tilted, folded and thrust faulted prior to Late Cretaceous, or Middle Jurassic time. Bordering Laberge Group rocks to the east is the Nahlin Fault and rocks of the Cache Creek Terrane, an accretionary assemblage of largely Mississippian to Triassic limestone, chert, and Permian ophiolite (Monger, 1991; Mihalynuk et al., 2003). West of the Laberge Group, are Devonian to Late Triassic volcanic-arc strata of Stikinia (Fig. 1). Quartz-rich pericratonic strata of the Yukon-Tanana Terrane in part form the basement to Stikinia. Meta-

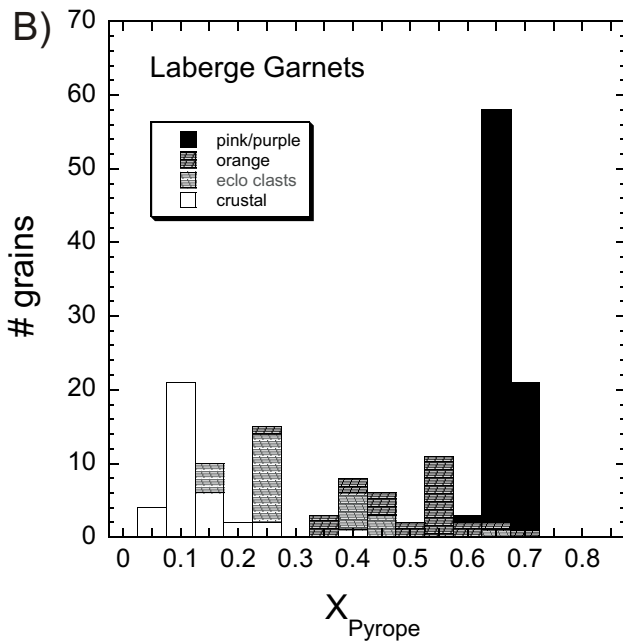
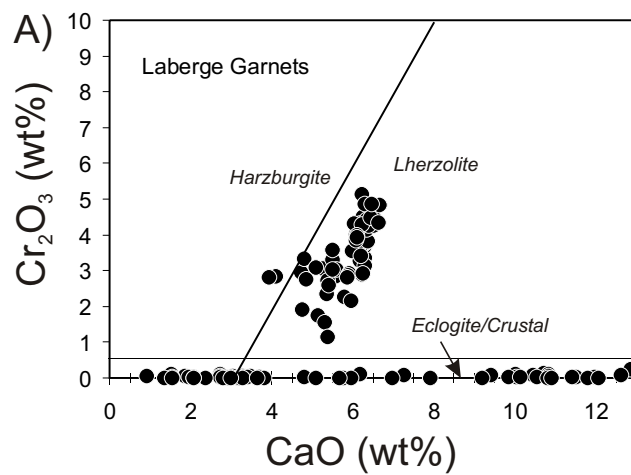


Figure 2. Plots showing compositional data for garnets from heavy mineral concentrate and eclogite clasts in the garnetiferous wacke of the Laberge Group: **A)** CaO vs. Cr₂O₃ plot used to distinguish the protolith of the detrital mantle-derived garnets; lherzolite-harzburgite division from Gurney (1984); garnets were classified as ‘crustal’, ‘eclogitic’ or ‘peridotitic’ using the approach of Schulze (2003). **B)** histogram showing mole fraction of pyrope (X_{pyr}) component (Mg₃Al₂Si₃O₁₂) in garnets.

morphosed volcanic-arc components of the Yukon-Tanana Terrane are in part correlative with Stikinia. Isotopic data from igneous and sedimentary rocks in Stikinia, and U-Pb geochronology of detrital zircons in metasediments of the Yukon-Tanana Terrane support a uniform source for quartz-rich basement strata, possibly rifted from the North American craton (Gehrels et al., 1990; Gehrels et al., 1991; Jackson et al., 1991; Mihalyuk et al., 1999).

FIELDWORK

Garnet-bearing conglomerates of the Laberge Group were examined in detail along a northwest-trending ridge,

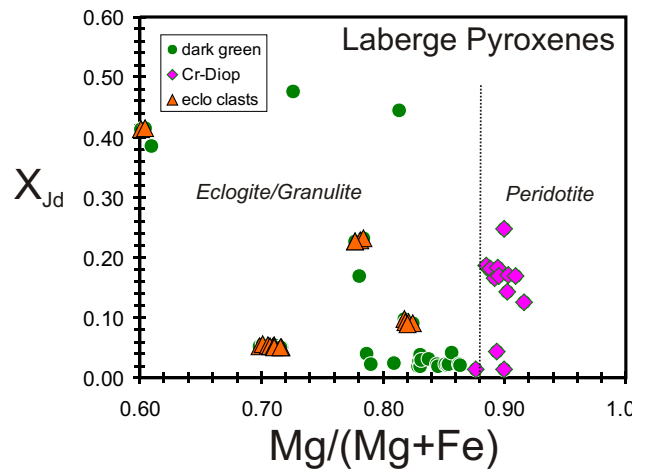


Figure 3. Compositional data for pyroxenes from the Laberge Group sediments. Note the high jadeite component in eclogitic pyroxenes from both clasts and detrital minerals. Peridotitic pyroxenes are distinguished by their emerald green colour and high Mg/Mg+Fe (> 0.9).

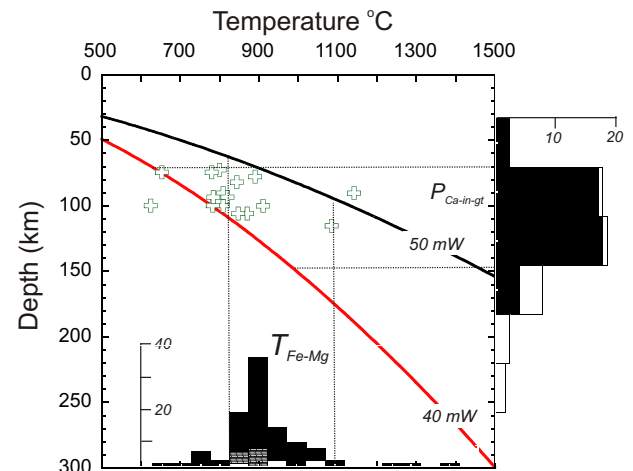


Figure 4. Plot summarizing thermobarometric calculations on detrital garnets, pyroxenes and eclogite clasts in the garnetiferous wacke (MacKenzie et al. in press). Crosses show P-T results for detrital peridotitic clinopyroxenes using the Cr-in-clinopyroxene thermometer (Nimis and Taylor, 2000). Histogram on bottom shows results of Fe-Mg exchange thermometry for eclogite clasts and peridotitic garnets, assuming they equilibrated at 3 GPa (O’Neill and Wood, 1979; Krogh, 1988), and for Ni-in-garnet thermometry (Canil, 1999). Note the dominant mode at 800–950°C and similarity to P-T results for the Cr-in-clinopyroxene method. Histogram on right shows pressures calculated based on Ca-content of garnets ($P_{Ca-in-gt}$), assuming they were in equilibrium with clinopyroxene at 900°C, the median T by the Cr-in-clinopyroxene method (Brenker and Brey, 1997). Thermobarometric pressures were converted to depths. Geothermal gradients typical of Archean (40 mW·m⁻²) and Proterozoic (50 mW·m⁻²) continental lithosphere were calculated using the approach in Canil (1999). Note the occurrence of some garnets and pyroxenes from depths below 100 km, and some as deep as the diamond stability field.

herein called Eclogite Ridge, located 8 km east of Paradise Peak in the southwest Atlin mapsheet (104N; Fig. 1). Eclogite Ridge is composed of distinct buff-weathering siltstone, sandstone and conglomerate (Fig. 5a) that form a unit ~290 m thick (Fig. 6), informally referred to here as the 'Eclogite formation'. Good outcroppings of Eclogite formation occur along the bedding-parallel ridge axis, and excellent cliff-face exposures have been created where the ridge is truncated by east-flowing stream valleys (Fig. 5a). Thickness of the Eclogite formation appears to decrease to the northwest, and possibly to the southeast, suggesting a lens-shaped cross-section that is more than 10 km long. Attempts to trace the unit north of the Sloko River have been unsuccessful, and it is presumed to be truncated to the southeast by the crustal-scale Nahlin Fault. Thus, its mapped distribution corresponds to the extents of the positive anomaly seen in the results of the aeromagnetic total field survey (Dumont et al., 2001; Lowe et al., 2003). Prominent features of the unit are depositional 'cycles' in which parallel layered argillaceous siltstone and wacke are truncated by channelized granule to cobble conglomerate in onlapping and stacked lens-shaped beds (Fig. 7a). These 'cycles' repeat every 10 to 40 m (Fig. 6).

Stratigraphically beneath the Eclogite formation is a section of dark green to brown and orange-brown weathering wacke with an average magnetic susceptibility of ~0.3. It is separated from the Eclogite formation by an ~20 m prominent recessive covered interval. Where well exposed on the north end of the ridge, the recessive unit consists of ~15 m of parallel, laminated to centimetre-scale bedded siltstone and immature, medium-grained carbonaceous arkosic sandstone with muddy matrix (wacke) showing soft-sediment deformation. No appreciable unconformity is developed where the recessive unit is in contact with the first granule conglomerate of the Eclogite formation, which has a stronger magnetic susceptibility of 15. Above the basal contact, however, angular rip-ups up to 0.5 m diameter are a lithological match for the recessive unit, suggesting that at some point the basal conglomerate cuts down into the recessive unit.

Nonconglomeratic portions of the Eclogite formation may include a conspicuous black and white banded sediment (Fig. 7b). Banding is formed by 3 to 50 mm thick intercalation of dark, organic-rich siltstone with thicker cream-coloured arkose. Dark layers are locally petroliferous. These units are incised by granule to pebble conglomerate-filled scours with axes that

trend northeasterly. Scours are commonly asymmetric in cross-section, with one steep margin (Fig. 7a). The steep-sided bedforms extend laterally into more tabular bodies that vary from 0.5 to 5 m in thickness. Differential compaction around the relatively strong conglomerate causes warping of the finer grained layers around the lens, an effect that is particularly enhanced at the steep margin. Conglomerate layers are more resistant to weathering than adjacent finer grained layers, enabling them to be traced along strike for kilometres (Fig 5b). Concentrated within these steep-sided conglomerate layers are conspicuous detrital

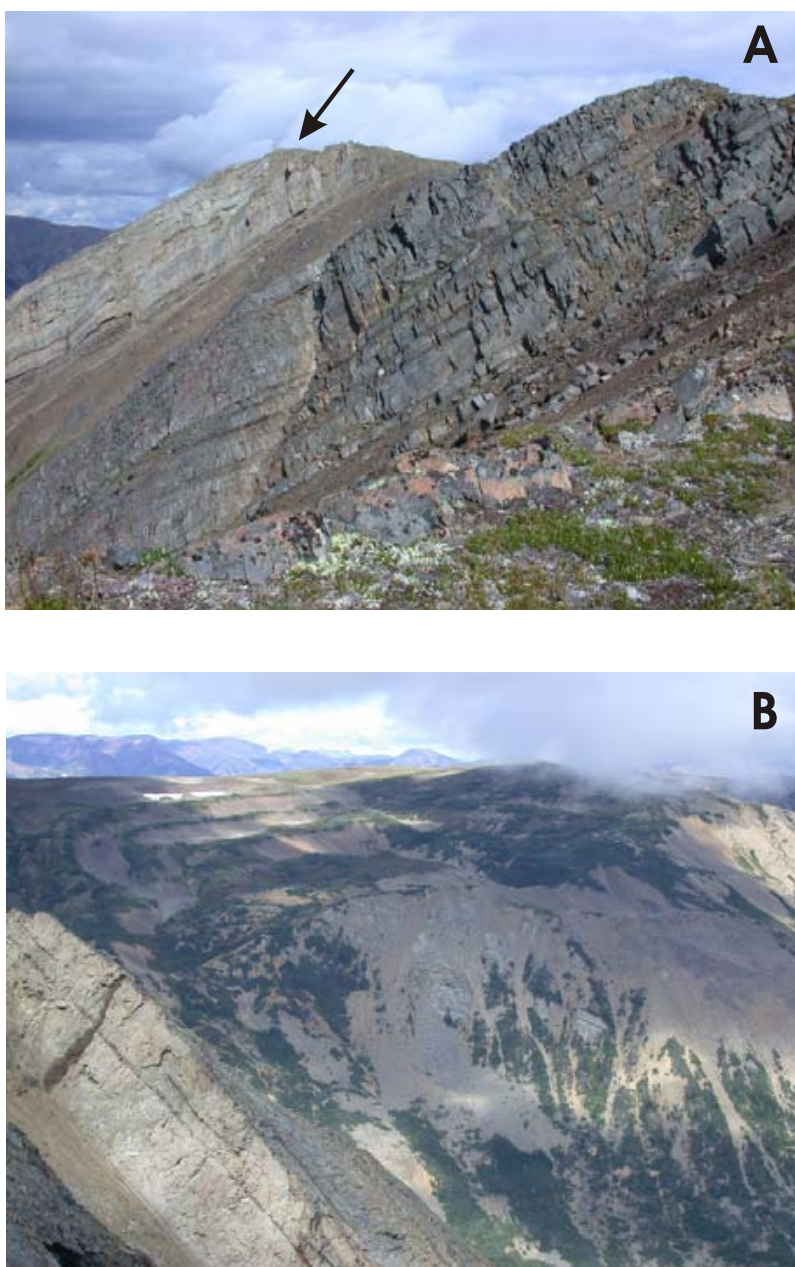


Figure 5. **A)** View of the Laberge Group to the east, showing buff-coloured ridge of garnetiferous conglomerates and wackes ('Eclogite Ridge' with arrow) underlain by garnet-free sediments (darker coloured). **B)** View from the north slope of Eclogite Ridge to the northwest, showing highly resistant conglomerate units extending laterally for kilometres along strike.

constituents including red and orange garnets up to 1 cm diameter, emerald green chrome diopside (<3 mm; Fig. 7c), olive green olivine (<3 mm) and sooty black biotite-plagioclase porphyry clasts (Fig. 7d). White-weathering hornblende-feldspar-porphyry clasts are also conspicuous (Fig. 7e), but these are not restricted to the Eclogite formation, occurring in abundance at lower stratigraphic levels. Further southeast along Eclogite Ridge, the conglomerate, sandstone and siltstone beds have similar sedimentological features, but are darker in colour (Fig. 5a), and both garnet and the sooty black porphyry clasts are scarce.

Towards the top of the section, nonconglomeratic strata include orange and black weathering coaly wacke and siltstone. Fossil plant material is dominantly swamp grass and cycad (a palm-like plant) fronds and trunks up to 20 cm in diameter.

‘ECLOGITE FORMATION’ PALEOFLOW AND DEPOSITIONAL ENVIRONMENT

Asymmetrical lens-shaped cross-sections of conglomerate beds deposited on steeply discordant to concordant erosional surfaces atop finer grained sandstones and siltstones (Fig. 7a) are interpreted as lag deposits within channel scours. Crossbedding is locally well displayed, even in coarse-grained units (Fig. 7e), and orientations of trough cross-strata could be deduced in three dimensions with certainty. Pebble-imbriation is also recognized in some places but, unless the pebbles are tiled, imbrication is difficult to distinguish from pebbles lying on ill-defined foresets. Therefore, only where they are tiled can they be used as indicators of unidirectional paleoflow. From these and other paleoflow indicators, paleocurrent directions were interpreted to flow towards the west or southwest (Fig. 8). Bidirectional flow indicators include channel scour orientation and the preferred orientation of elongate clasts, including cycad trunks, which are broadly consistent with the unidirectional indicators.

Many granules and pebbles are subrounded, but a significant portion of clasts are angular, including mineral grains like garnet, diopside and olivine, as well as porphyritic clasts of probable volcanic origin and argillaceous rip-up clasts. The presence of rip-up clasts and muddy matrix to wacke units suggest deposition by turbidity currents, not winnowing by alluvial or wave action. Some hummocky and swaley cross-strata, however, may be preserved locally within the section suggesting, the impingement of storm surge

base on the depositional environment. Channellized gravels suggest alluvial deposition, but such gravels may be deposited in an aggrading submarine channel deposit. One potential problem with the above interpretation is the presence of cycad debris, including substantial trunks, in a submarine environment. Most plant debris is buoyant and therefore not expected in a submarine depositional setting, although cycads could be susceptible to water logging.

A submarine-fan complex interpretation is consistent with previous interpretations for the depositional environment of Whitehorse Trough strata (e.g., Dickie and Hein, 1995; Johannson, 1997). A predominance of southwest-directed paleoflow indicators is, however, inconsistent with the results of previous studies, which generally showed predominantly easterly paleoflow. The data presented here are important because they indicate an east-derived source for high-P detritus, possibly an eclogitic part of the northern Cache Creek Terrane akin to the Pinchi Belt, or dextral translation of the Whitehorse Trough with respect to a high-P belt that may have included the Pinchi eclogite occurrence. Other possibilities are that the eclogite occurrences exposed within the Yukon-Tanana Terrane in the Yukon extend in a cryptic fashion into northern British Columbia and sourced the conglomerate, or that the paleoflow indicators are a local aberration and not indicative of derivation from the eastern source.

Along the shores of southern Atlin Lake are other occurrences of coarse pebble conglomerates and immature

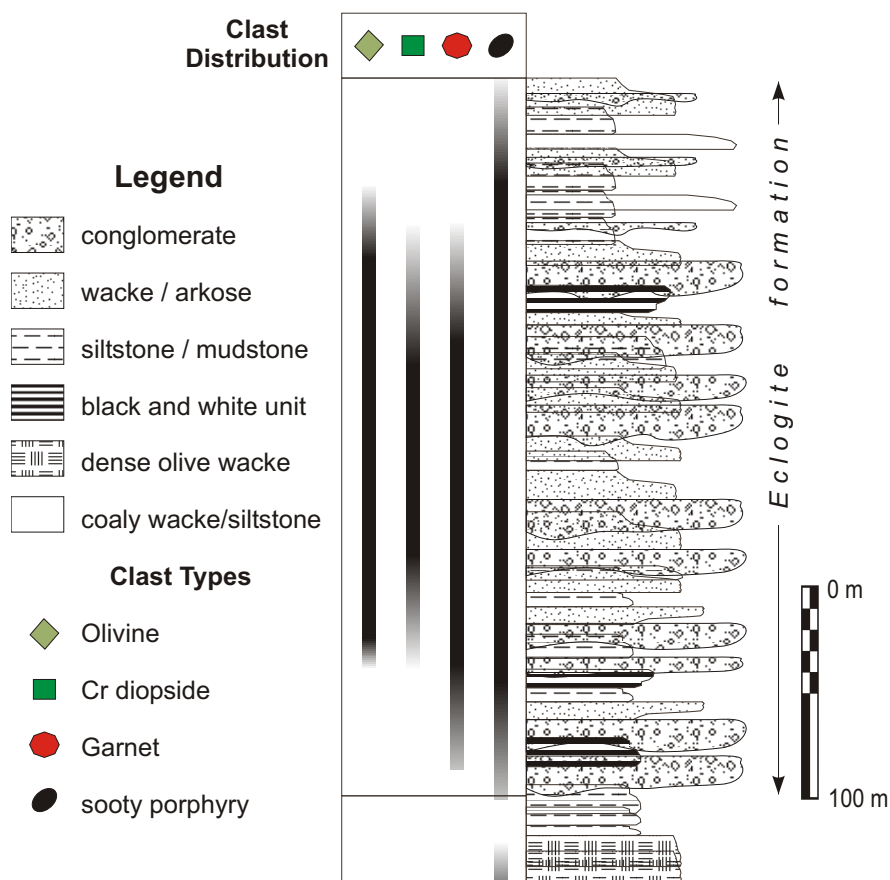


Figure 6. Stratigraphic section through the ‘Eclogite formation’ exposed on Eclogite Ridge.



Figure 7. **A)** Conglomerates and wackes viewed perpendicular to strike, showing steep-sided contact (arrow) between garnet-bearing conglomerates cutting down through underlying sandstone and siltstone units at steep sides. **B)** Banding in units below conglomerates formed by 3 to 50 mm thick intercalations of dark, organic-rich and occasionally petroliferous siltstones with thicker cream-coloured arkose. **C)** Emerald green clinopyroxene grain set in matrix of feldspar and rock fragments in the garnetiferous wacke. **D)** Fragments of rock containing phenocrysts of feldspar and biotite set in a sooty fine-grained matrix in garnetiferous wacke from the ridge. **E)** Coarse pebbles of hornblende porphyry in conglomerate. Note crossbedding in coarser units. **F)** Red pyrope garnets adhering to emerald green Cr-diopside grain from heavy mineral concentrate.

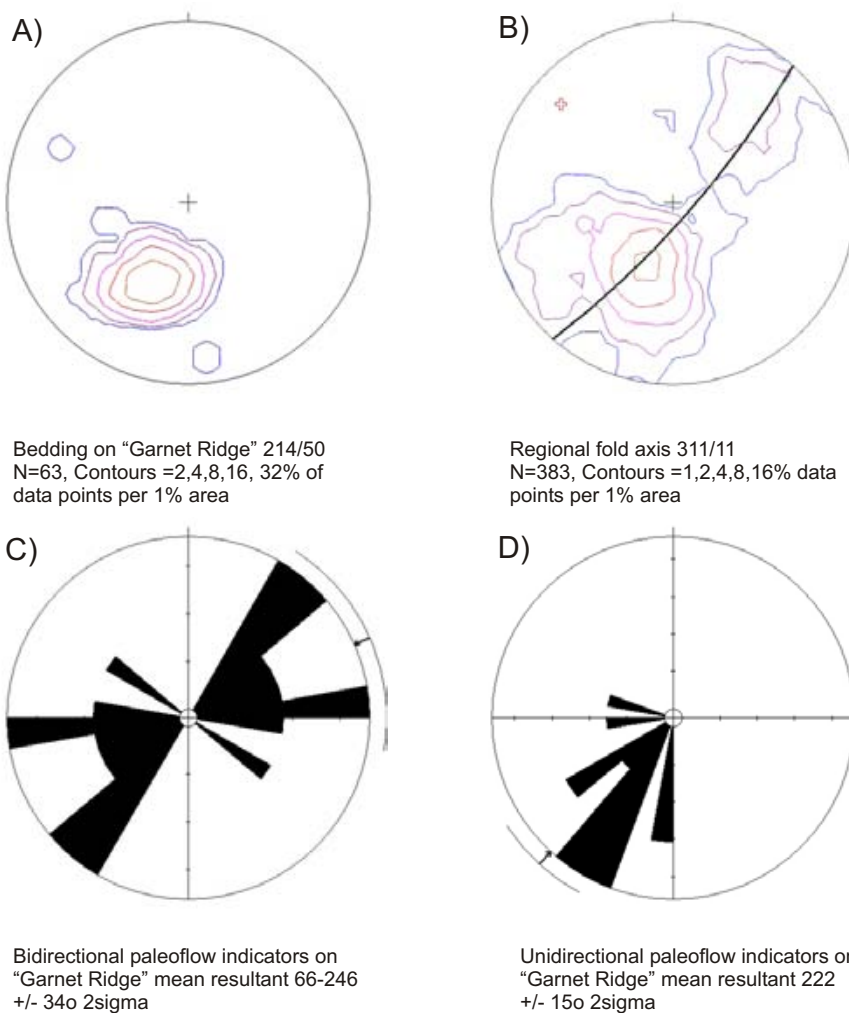


Figure 8. Measurements on bedding (A), fold axes (B) and paleoflow directions (C, D) for units exposed on Eclogite Ridge.

wackes (Johannson et al., 1997). Exposures on the northernmost islands near Janus Point contained visible garnet, but further south, on Sloko and Bastion Islands, garnet was notably absent in outcrop. Garnet-bearing units near Janus Point are along strike from those on Eclogite Ridge, 20 km to the southeast, suggesting that they are part of the Eclogite formation.

PROVENANCE

Six thin sections from samples of the wacke along Eclogite Ridge were studied petrographically and point counted ($n > 800$) to determine their modal mineralogy. The rock contains mainly feldspar and lithic fragments, notable angular detrital garnet and pyroxene, and rare olivine, amongst 3 to 8 mm clasts of pristine arc volcanics (hornblende andesite, dacite), granitoids and metamorphic rocks (mica schist, amphibolite), including rare eclogite or granulite (garnet+pyroxene+rutile). The rock has a high detrital magnetite content (~2–3%) which is likely the

source of its anomalous aeromagnetic signature (Lowe et al., 2003).

The relative proportions of lithic fragments, plagioclase, K-feldspar and quartz in clastic sediments has been used to deduce the tectonic setting of deposition and provenance in other basinal strata (Dickinson et al., 1983; Marsaglia and Ingersoll, 1992). Proportions of these components in Laberge Group garnet-bearing conglomerate is consistent across samples (Fig. 9). Detrital components of both the wacke and conglomerate suggest they were derived by early dissection of a nascent continental arc (Fig. 9). Two samples contain anomalously high K-feldspar, suggesting derivation from an exposed basement or plutonic-arc root (Boggs, 2001).

HEAVY MINERALS

Samples of coarse conglomerate and wacke weighing between 0.5 and 4.0 kg were collected from five locations along Eclogite Ridge and seven locations along the shores of southern Atlin Lake. These were processed for heavy mineral extraction at Vancouver Indicator Processors Inc., Vancouver. First, they were crushed to sand-sized particles in a jaw crusher and sieved. Sieved samples were wet screened to less than 0.25 mm fraction. The +0.25 mm fraction was passed through a magnetic separator operating at 2.1 Tesla. The magnetic fraction underwent heavy liquid separation to specific gravities greater than 3.33. Resultant concentrates were examined and hand-picked at the University of Victoria.

Heavy minerals (specific gravity > 3.33) make up between 0.004 and 0.6% of the samples. The largest percentage of heavy minerals occurs in rocks containing visible garnet and clinopyroxene in outcrop (e.g., at Eclogite Ridge and near Janus Point on Atlin Lake). Samples collected further to the south, and presumably deeper in the sedimentary section, display a rapidly decreasing percentage of heavy minerals and an absence of visible garnets in hand sample. The heavy mineral population is dominated by garnet, followed by clinopyroxene, opaque minerals and minor amounts of olivine. Garnet adheres to both clinopyroxene and olivine grains, suggesting that it is derived from both peridotite and eclogite (Fig. 7f). Further chemical analysis is in progress.

DISCUSSION

The above results require that garnet peridotite and eclogite derived from mantle lithosphere at least 100 km thick was exhumed and exposed in the northern Cordillera and shed as detritus into a fore-arc basin now preserved as the Laberge Group. Exceptional preservation of pristine mantle detritus in Laberge Group wacke and conglomerate is attributable to proximal deposition, rapid burial and an absence of metamorphism or penetrative deformation documented in this part of Whitehorse Trough during the last 170 Ma (Mihalynuk et al., 2003). Angular garnets, the presence of detrital olivine, and their mixture with pristine volcanic and feldspathic clasts indicate minimal physical or chemical attrition. This could be attributed to an arid or extremely cold climate during subaerial erosion, and rapid transport and deposition in a submarine environment. Late Early Jurassic (Toarcian) ammonite faunas in the Whitehorse Trough include the Boreal genus *Pseudolioceras*, indicating deposition from relatively cool water in high latitudes (Jakobs, 1997); however, the Jurassic was a warm period in the Earth's history, with a global lack of evidence for glaciation. An arid environment cannot be fully discounted, although the presence of coal layers, including the 20 cm diameter trunks of cycads, argues against severe aridity.

Primary alkaline igneous rocks are one potential source of the garnet peridotite and eclogite detritus. For example, Oligocene sediments in the Uinta Mountains and Green River Basin of the western United States contain garnets and pyroxenes that are thought to be sourced from Eocene kimberlite and lamproite intrusions a few hundred kilometres away, in the Wyoming Province (McCandless and Nash, 1996). The opaque fraction of heavy minerals from the Laberge Group sediments, however, contains only Mg-poor magnetite; none of the Mg- or Cr-rich spinel or ilmenite expected from an alkaline igneous source (e.g. kimberlite) are observed. Thus, an alkaline igneous source for the mantle detritus in the Laberge Group is discounted.

The only other source for the mantle detritus could be large masses of garnet peridotite and eclogite, which are volumetrically minor components of many collisional orogens, commonly occurring as septa or kilometre-size massifs within larger supracrustal metamorphic terrains (Medaris, 1999; Brueckner and Medaris, 2000). Orogenic garnet peridotite massifs have been recognized in other arcs such as the Lesser Antilles and in Sulawesi (Kadarusman and Parkinson, 2000; Abbott et al., 2001). Such massifs are often small (~1 km³), but even small masses of rocks like garnet peridotite and eclogite, which contain between 5 and 50% modal garnet, could contribute the amount of garnet observed in the heavy mineral fraction of the Laberge sediments (< 0.5 %).

Potential sources of orogenic garnet peridotite and eclogite are not known in terranes immediately adjacent to the Whitehorse Trough. Heavy durable minerals can travel far and be recycled in the sedimentary environment. River systems are known to deliver durable heavy minerals across continental-scale drainage systems (Rainbird et al.,

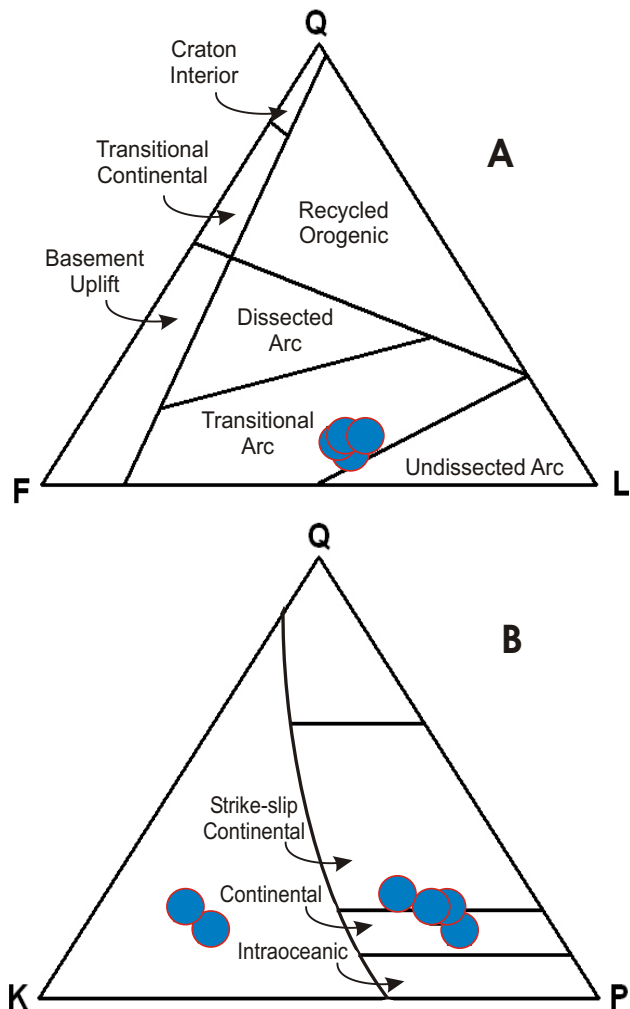


Figure 9. Ternary diagrams used to determine provenance and tectonic setting of clastic sediments: **a)** Diagram showing the proportion of quartz (Q), feldspar (F) and lithic fragments (L) of Dickinson et al (1983). **b)** Diagram showing the proportion of quartz (Q), K-feldspar (F) and plagioclase (P) of Marsaglia et al (1992). The Laberge Group wacke and conglomerates (circles) plot within newly dissected continental arc setting.

1997.), but the latter depositional setting results in mature quartz-rich clastic sediments (Roscoe, 1973), not immature poorly sorted angular detritus as observed in the Laberge Group sediments. Thus, it appears that the source region of the uplifted and exposed mantle rocks must have been proximal to the fore-arc basin in which they were deposited.

Exhumation and erosion of garnet peridotite and eclogite was apparently short lived, because the derived detritus appears in only one part of the Laberge Group that extends from Eclogite Ridge to Janus Point. This detritus was mixed with poorly sorted arc detritus, possibly including tuffaceous units. In current interpretations, these units would be some of the youngest sediments preserved in the Laberge Group at this latitude (English et al., in press). Although we have no age constraints as yet, the anticipated geochronological age determinations provided by a tuffaceous unit at Eclogite Ridge will provide age con-

straints for the sudden exposure and erosion of orogenic peridotite and eclogite at the surface.

Rapid uplift, exhumation and deposition, in the late Triassic and early Jurassic, of the Stikinia arc is substantiated by many lines of evidence in the Laberge Group and in correlative rocks along strike in the Cordillera. The U-Pb age of a granitic boulder in a conglomerate and the biostratigraphically controlled depositional age of sands adjacent to this conglomerate in the Laberge Group are dated to within a few million years, suggesting intrusion in the arc, and rapid uplift, incision and deposition (Johannson et al., 1997). Farther north in a correlative belt of rocks in Yukon, the extent and timing of early Jurassic subduction, crustal thickening, uplift and deposition are well documented. Field mapping, metamorphic isograds, and U-Pb geochronology in the Aishihik Lake area of southwestern Yukon show that crust from 30 km depths was uplifted at rates of 2 to 10 mm/year and shed into the Whitehorse Trough (Johnston and Erdmer, 1995; Johnston et al., 1996).

The strange occurrences of diamond in northwestern British Columbia (Casselman and Harris, 2002) are most likely derived from rocks that contain minerals of demonstrable high pressure origin (within the diamond stability field, Fig. 4). While we have yet to identify diamond in the heavy mineral concentrates of the Laberge Group, these garnetiferous strata are a possible source of anomalous diamond discovered during placer mining near Atlin, approximately 30 km to the northeast.

ACKNOWLEDGMENTS

In Atlin, we thank Norm Graham of Discovery Helicopters for getting us places, Gary Hill for a boat charter, and Brian Grant for good cheer and editing.

REFERENCES

- Abbott, R.N., Draper, G. and Keshav, S. (2001): Garnet peridotite found in the Greater Antilles; *EOS, Transactions of the American Geophysical Union*, Volume 82, pages 381–388.
- Boggs, S.J. (2001): Principles of Sedimentology and Stratigraphy; *Prentice-Hall*, Upper Saddle River, New Jersey, 726 pages.
- Brenker, F.E. and Brey, G.P. (1997): Reconstruction of the exhumation path of the Alpe Arami garnet-peridotite body from depths exceeding 160 km; *Journal of Metamorphic Geology*, Volume 15, pages 581–592.
- Brueckner, H.K. and Medaris, L.G. (2000): A general model for the intrusion and evolution of ‘mantle’ garnet peridotites in high-pressure and ultra-high pressure metamorphic terranes; *Journal of Metamorphic Geology*, Volume 18, pages 123–133.
- Canil, D. (1999): The Ni-in-garnet geothermometer: calibration at natural abundances; *Contributions to Mineralogy and Petrology*, Volume 136, pages 240–246.
- Canil, D., Mihalynuk, M., MacKenzie, J.M., Johnston, S.T., Ferreira, L. and Grant, B. (2004): Heavy mineral sampling of stream sediments for diamond and other indicator minerals in the Atlin-Nakina area (NTS 104N and 105N); in *Geological Fieldwork 2003, BC Ministry of Energy and Mines*, Paper 2004-1, pages 19–26.
- Casselman, S. and Harris, W. (2002): Yukon diamond rumour map and notes; *Yukon Geology*.
- Dickie, J. R. and F. J. Hein (1995): Conglomeratic fan deltas and submarine fans of the Jurassic Laberge Group, Whitehorse Trough, Yukon Territory, Canada; fore-arc sedimentation and unroofing of a volcanic island arc complex; Chough, S.K. and Orton, G.J., Editors, Fan Deltas: Depositional Styles and Controls, *Elsevier*, Amsterdam, Netherlands, pages 263–292.
- Dickinson, W.R., Beard, L.S., and Brakenridge, G.R. (1983): Provenance of North American Phanerozoic sandstones in relation to tectonic setting; *Geological Society of America Bulletin*, pages 222–235.
- Dumont, R., Coyle, M. and Potvin, J. (2001): Aeromagnetic total field map British Columbia, Sloko River, NTS 104N/3; *Geological Survey of Canada*.
- English, J., Johannson, G.G., Johnston, S.T., Mihalynuk, M.G., Fowler, M. and Wight, K.L. (in press): Structure, stratigraphy and hydrocarbon potential of the central Whitehorse Trough, northern Canadian Cordillera; *Bulletin of Canadian Society of Petroleum Geology*, in press.
- English, J.M., Mihalynuk, M.G., Johnston, S.T., Orchard, M.J., Fowler, M. and Leonard, L.J. (2002): Atlin TGI, Part VI: Early to middle Jurassic sedimentation, deformation and a preliminary assessment of hydrocarbon potential, central Whitehorse Trough and northern Cache Creek Terrane; in *Geological Fieldwork, BC Ministry of Energy and Mines*, Paper 2003-1, pages 187–201.
- Gehrels, G.E., McClelland, W.C., Samson, S.D., Patchett, P.J. and Jackson, J.L. (1990): Ancient continental margin assemblage in the northern Coast Mountains, southeast Alaska and northwest Canada; *Geology*, Volume 18, pages 208–211.
- Gehrels, G.E., McClelland, W.C., Samson, S.D., Patchett, P.J. and Jackson, J.L. (1991): U-Pb geochronology of detrital zircons from a continental margin assemblage in the northern Coast Mountains, southeastern Alaska; *Canadian Journal of Earth Sciences*, Volume 28, pages 1285–1300.
- Ghent, E. D., Stout, M. Z. and Erdmer, P. (1993): Pressure-temperature evolution of lawsonite-bearing eclogites, Pinchi Lake, British Columbia; *Journal of Metamorphic Geology*, Volume 11, pages 279–290.
- Gurney, J.J. (1984): A correlation between garnets and diamonds in kimberlites; *Kimberlites, Occurrences and Origin (University of Western Australia)*, Volume 8, pages 143–166.
- Jackson, J.L., Gehrels, G.E., Patchett, P.J. and Mihalynuk, M.G. (1991): Stratigraphic and isotopic link between the northern Stikine terrane and an ancient continental margin assemblage, Canadian Cordillera; *Geology*, Volume 19, pages 1177–1180.
- Jakobs, G. K. (1997): Toarcian (Early Jurassic) ammonoids from western North America; *Geological Survey of Canada, Bulletin* 428, 137 pages.
- Johannson, G.G., Smith, P.L. and Gordey, S.P. (1997): Early Jurassic evolution of the northern Stikinian arc: evidence from the Laberge Group, northwestern British Columbia; *Canadian Journal of Earth Sciences*, Volume 34, pages 1030–1057.
- Johnston, S.T. and Erdmer, P. (1995): Hot-side-up aureole in southwest Yukon and limits on terrane assembly of the northern Canadian Cordillera; *Geology*, Volume 23, pages 419–422.
- Johnston, S.T., Mortensen, J.K. and Erdmer, P. (1996): Igneous and metamorphic age constraints for the Aishihik meta-

- morphic suite, southwest Yukon; *Canadian Journal of Earth Sciences*, volume 33, pages 1543–1555.
- Kadarusman, A. and Parkinson, C.D. (2000): Petrology and P-T evolution of garnet peridotites from central Sulawesi, Indonesia; *Journal of Metamorphic Geology*, Volume 18, pages 193–209.
- Krogh, E.J. (1988): The garnet-clinopyroxene Fe-Mg geothermometer – a reinterpretation of existing experimental data; *Contributions to Mineralogy and Petrology*, Volume 99, pages 44–48.
- Lowe, C., Mihalynuk, M.G., Anderson, R.G., Canil, D., Cordey, F., English, J.M., Harder, M., Johnston, S.T., Orchard, M.J., Russell, J.K., Sano, H. and Villeneuve, M.E. (2003): Overview of the Atlin Integrated Geoscience Project, northwestern British Columbia, year three; *Geological Survey Canada, Current Research, 2003-A11*, pages 1–10.
- MacKenzie, J.M. and Canil, D. (1999): Composition and thermal evolution of cratonic mantle beneath the central Archean Slave Province, NWT, Canada; *Contributions to Mineralogy and Petrology*, Volume 134, pages 313–324.
- MacKenzie, J.M., Canil, D., Johnston, S.T., English, J.E., Mihalynuk, M.G. and Grant, B. (in press): First evidence for ultrahigh pressure garnet peridotite in the North American Cordillera; *Geology*, in press.
- Marsaglia, K.M. and Ingersoll, R.V. (1992): Compositional trends in arc-related, deep-marine sand and sandstone: a reassessment of magmatic-arc provenance; *Geological Society of America Bulletin*, Volume 104, pages 1637–1649.
- McCandless, T.E. (1990): Kimberlite xenocryst wear in high-energy fluvial systems: experimental studies; *Journal of Geochemical Exploration*, Volume 37, pages 323–331.
- McCandless, T.E. and Nash, W.P. (1996): Detrital mineral indicator minerals in southwestern Wyoming, U.S.A.: evaluation of mantle environment, igneous host and diamond exploration significance; *Exploration and Mining Geology*, Volume 5, pages 33–44.
- Medaris, L.G. (1999): Garnet peridotites in Eurasian high-pressure and ultrahigh-pressure terranes: a diversity of origins and thermal histories; *International Geology Reviews*, Volume 41, pages 799–815.
- Mihalynuk, M.G. and Lowe, C. (2002): Atlin TGI, Part I: an introduction to the Atlin Targeted Geoscience Initiative; in *Geological Fieldwork, BC Ministry of Energy and Mines, Paper 2001-1*, pages 1–4.
- Mihalynuk, M., Erdmer, P., Ghent, E.D., Cordey, F., Archibald, D.A., Friedman, R.M. and Johannson, G.G. (in press): Coherent French Range blueschist: subduction to exhumation in <2.5 m.y.? *Geological Society of America Bulletin*, in press.
- Mihalynuk, M.G., Johnston, S.T., English, J., Cordey, F., Villeneuve, M.E., Rui, L. and Orchard, M.J. (2003): Atlin TGI, Part III: regional geology and mineralization of the Nakina area (NTS 104N/2W and 3); in *Geological Fieldwork, BC Ministry of Energy and Mines, Paper 2002-1*, pages 9–15.
- Mihalynuk, M.G., Mountjoy, K.J., Smith, M.T., Currie, L.D., Gabites, J.E., Tipper, H.W., Orchard, M.J., Poulton, T.P. and Cordey, F. (1999): Geology and mineral resources of the Tagish Lake area (NTS 104M/ 8, 9, 10E, 15 and 104N/12W), northwestern British Columbia; *BC Ministry of Energy and Mines, Bulletin 105*, 217 pages.
- Monger, J.W.H. (1991): Upper Devonian to Middle Jurassic assemblages, Part B: Cordilleran terranes; Gabrielse, H. and Yorath, C.J., Editors, *Geology of North America, Geological Society of America*, Denver, Colorado, pages 281–327.
- Monger, J.W.H. (1969): Stratigraphy and structure of Upper Paleozoic rocks, northeast Dease Lake map-area, British Columbia (104J); *Geological Survey of Canada*, 41 pages.
- Nimis, P. and Taylor, W.R. (2000): Single clinopyroxene thermobarometry for garnet peridotites, Part 1. Calibration and testing of a Cr-in-cpx barometer and enstatite-in-cpx thermometer; *Contributions to Mineralogy and Petrology*, Volume 139, pages 541–554.
- O'Neill, H.C. and Wood, B.J. (1979): An experimental study of Fe-Mg partitioning between garnet and olivine and its calibration as a geothermometer; *Contributions to Mineralogy and Petrology*, Volume 70, pages 59–70.
- Palfy, J., Smith, P. L. and Mortensen, J. K. (2000): A U-Pb and $^{40}\text{Ar}/^{39}\text{Ar}$ time scale for the Jurassic; *Canadian Journal of Earth Sciences*, Volume 37, pages 923–944.
- Rainbird, R.H., McNicoll, V.J., Theriault, R.J., Heaman, L.M., Abbott, J.G., Long, D.G.F. and Thorkelson, D.J. (1997): Pan-continental river system draining Grenville orogen recorded by U-Pb and Sm-Nd geochronology of Neoproterozoic quartzarenites and mudrocks, northwestern Canada; *Journal of Geology*, Volume 105, pages 1–17.
- Roscoe, S.M. (1973): The Huronian Supergroup, a Paleoproterozoic succession showing evidence of atmospheric evolution; *Geological Association of Canada, Special Paper 12*, pages 31–47.
- Schulze, D.J. (2003): A classification scheme for mantle derived garnets in kimberlite: a tool for investigating the mantle and exploring for diamonds; *Lithos*, Volume 71, pages 191–213.

Toodoggone Geoscience Partnership: Preliminary Bedrock Mapping Results from the Swannell Range: Finlay River – Toodoggone River Area (NTS 94E/2 and 7), North-Central British Columbia¹

By L. Diakow, G. Nixon, B. Lane and R. Rhodes

KEYWORDS: P3, public-private partnership, Targeted Geoscience Initiative II (TGI-II), bedrock mapping, stratigraphy, Finlay River, Toodoggone River airborne gamma-ray spectrometric and magnetic survey, Toodoggone River, Finlay River, Toodoggone formation, Black Lake Intrusive Suite, Cu-Au porphyry, epithermal Au-Ag

INTRODUCTION

The Toodoggone Geoscience Partnership was initiated in 2003 to generate detailed geoscience information, including airborne geophysics and bedrock geology maps, that would support mining exploration in previously explored and more remote terrain in the east-central Toodoggone River and McConnell Creek map areas, which are considered highly prospective for Cu-Au porphyry and epithermal Au-Ag mineralization. The success of this partnership is based on the participation of all five mining companies actively exploring the program area (Stealth Minerals Ltd., Northgate Minerals Corp., Finlay Minerals Ltd., Bishop Gold Inc. and Sable Resources Ltd.), coupled with personnel from the British Columbia Geological Survey, the Geological Survey of Canada and the University of British Columbia.

In 2004, the Geological Survey of Canada released digital data and a series of maps from a low-level, high-resolution airborne gamma-ray spectrometric and magnetic survey that covered 1) most of the known porphyry and epithermal targets within the main area of prospective Early Jurassic rocks; and 2) a remote and relatively under-explored region farther east in the Swannell Ranges of the Toodoggone area (Shives *et al.*, 2004).

Bedrock mapping continued in 2004, expanding the area of detailed 1:20 000-scale map coverage in two regions: 1) the southern region, located 55 km southeast of the Kemess South Cu-Au porphyry mine and centred on Johanson Lake (Schiarizza, 2004a, b; Schiarizza and Tan, this volume); and 2) the northern region, between the Toodoggone and Finlay rivers (Diakow, 2004). This paper summarizes the results of geological mapping conducted in a 250 km² area located east of the Pillar Fault (Diakow, 2004) and bounded by the Finlay River in the south and the

Toodoggone River in the north and east (Fig. 1). The new results reported below emphasize changes in the Early Jurassic stratigraphy of the Toodoggone from west to east.

LITHOSTRATIGRAPHIC UNITS

Over the past two field seasons, nearly 600 km² of the Swannell Ranges, situated between the major drainages of the Toodoggone and Finlay rivers and their confluence, have been mapped in detail, thereby refining Jurassic stratigraphy that was, for the most part, previously assigned to an undivided Hazelton Group map unit (Diakow *et al.*, 1985, 1993). As a consequence of mapping in 2004, a region of previously undivided Jurassic rocks is now identified as part of the Toodoggone formation. These rocks have been subdivided *informally* into stratigraphic members, which collectively represent one of the most complete Early Jurassic sequences exposed anywhere in the Toodoggone River area. Volcanic rocks presumed to be near the bottom of the Toodoggone formation rest unconformably on either volcanic strata of the Late Triassic Takla Group or granitoid rocks of the Early Jurassic Black Lake Intrusive Suite. The oldest rocks consist of bedded sedimentary strata of the Upper Paleozoic Asitka Group; these are generally poorly exposed, locally intruded and thermally altered by Jurassic intrusions, and rarely observed to be overlain disconformably by the Takla Group.

The generalized geology of the study area is shown in Figures 2 and 3, and representative stratigraphic sections are given in Figure 4. The stratigraphy is transected by major northerly to north-northwesterly-trending high-angle faults, notably the Pillar and Black faults, intersected by easterly to northeasterly-trending cross-faults (Fig. 2). East of the Pillar Fault, the stratigraphy is consistently inclined to the west-southwest and has relatively shallow dips (15–25°).

Asitka Group (Unit PAs)

The Pennsylvanian to Early Permian Asitka Group comprises several large pendants resting on or adjacent to the Early Jurassic Duncan pluton near Drybrough Peak (west of the study area), where both volcanic and stratigraphically higher sedimentary rocks were mapped previously (Diakow, 2004). In this study, scattered outcrops of the Asitka Group were encountered near the

¹Contribution of the Federal-Provincial Targeted Geoscience Initiative-II (TGI-II)

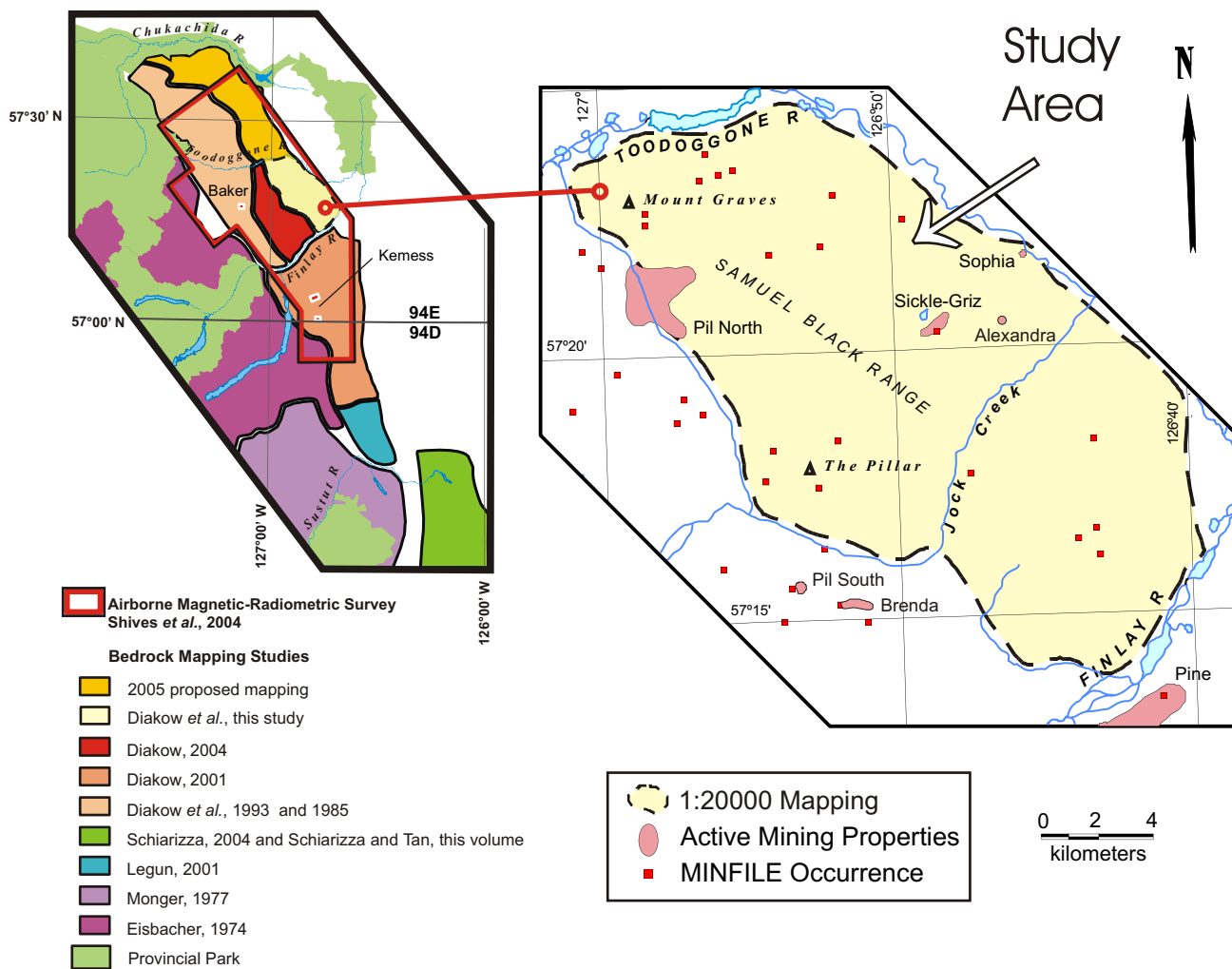


Figure 1. Location of bedrock mapping completed in 2004. Inset on the left shows published geological work in the Toodoggone River (94E) and McConnell Creek (94D) map areas (see references).

treeline in an area east of Jock Creek (Fig. 2). Here, the succession is about 130 m thick and intruded by an Early Jurassic quartz monzonite stock at the lower contact. Limestone adjacent to the intrusive contact is recrystallized and replaced locally by irregular zones of diopside-garnet-magnetite skarn, and carries patchy galena and chalcopyrite mineralization. Higher in the section, pale grey weathered limestone alternates with whitish chert in beds varying from 10 to 50 cm thick. Above the highest chert layers, siltstone interleaved with thin black mudstone partings occupies the uppermost 20 m of the section. The uppermost sedimentary strata are sharply overlain by pyroxene-bearing lavas of the Late Triassic Takla Group.

Takla Group (Unit uTTv)

The Late Triassic Takla Group is exposed along the lower north- and east-facing slopes of the mountains south of Jock Creek, and in nearby outcrops where it is juxtaposed against the Toodoggone formation by high-angle faults. South of Jock Creek, the lower contact of the Takla Group is marked by an unusually coarse clinopyroxene-

phyric basalt flow that overlies siltstones considered to represent part of the underlying Asitka Group. This contact is interpreted as a disconformity, although there is little evidence of erosion. Above this contact, lavas more typical of the Takla Group predominate, and include a variety of porphyritic basalts containing abundant, medium to coarse (<6 mm) phenocrysts of clinopyroxene. Other, volumetrically minor flow varieties include distinctive porphyritic lavas with bladed-plagioclase textures and aphanitic basalts. Pyroxene-bearing sandstones occur as sparse, thin interbeds within the volcanic succession.

Basal Toodoggone Formation Unconformity

Bedded polymictic conglomerates and sandstones (unit Tc1) occur at a number of isolated localities in the southern Toodoggone map area, and occupy the interval between mafic volcanic rocks of the Takla Group and overlying quartz-biotite-bearing volcanic rocks of the Toodoggone formation. These deposits mark a basal unconformity of regional extent in the Jurassic succession,

and record variable uplift and incision deep into pre-Jurassic strata and exhumed plutons.

The basal conglomeratic deposits may be traced discontinuously for almost 7 km west of the Pillar Fault south of Jock Creek (Diakow, 2004), and have been found farther east at two isolated localities in the study area. The conglomerates generally consist of sand-granule matrix- to clast-supported rounded cobbles and boulders derived from Takla, granitoid and, less commonly, Asitka sources. At one locality not visited by the authors, but portrayed schematically in section 1 of Figure 4, a mining company reported conglomerate dominated by granitoid debris resting atop an early quartz monzonite phase of the composite Jock Creek pluton (Fig. 2; described below). At the second locality, the unconformity is marked by a thin (<7 m) succession of basal, cobble to pebble conglomerates passing upwards into coarse to medium-grained, feldspathic to lithic sandstones containing detrital quartz.

Early Jurassic Toodoggone formation

The Toodoggone formation is an exclusively subaerial volcanic succession that comprises the sole subdivision of the Early Jurassic Hazelton Group in the Toodoggone River area. Together with cogenetic plutons of the Black Lake Intrusive Suite, these rocks host important Au-bearing epithermal and porphyry-style mineral deposits. Mapping of the Toodoggone formation has occurred episodically over several decades resulting in an evolving internal stratigraphy. A number of *informal* members have been proposed for locally mappable lithological units whose depositional ages are reasonably well constrained by more than 20 isotopic ages (Diakow, unpublished data).

Stratigraphic members of the Toodoggone formation exposed in the region between the Finlay and Toodoggone rivers include the Duncan, Metasantan and Saunders members, all of which have widespread distribution west of the Pillar Fault (Diakow, 2004). In places, rocks of the Duncan member are observed overlying Upper Triassic strata above a basal unconformity marked by erosion and typified by bedded epiclastic rocks. East of the Pillar Fault and north of Jock Creek, new stratigraphy is recognized resting upon volcanic rocks that resemble the Metasantan member. We include these new rock units as part of the Toodoggone formation and, in order of ascending stratigraphic position, *informally* name them the Quartz Lake, Graves and Pillar members. To the west, adjacent to Saunders Creek, the lower part of this new succession, tentatively correlated with the Quartz Lake member, forms several outliers, with one section resting unconformably on rocks of the Saunders member (western extremity of Fig. 2). This relationship indicates that the new stratigraphy is younger than the Saunders member, and a new U-Pb date from the study area confirms that these rocks belong in the upper part of the Toodoggone formation.

Typically, rocks of the Toodoggone formation have a narrow compositional range between high-silica andesite and dacite, and contain varying amounts of diagnostic quartz, biotite, hornblende and apatite phenocrysts. The new stratigraphy, however, is distinguished by locally

abundant basalt to andesite porphyritic flows containing clinopyroxene, flow-laminated dacite to rhyolite lavas, and a generally greater proportion of volcanoclastic rocks of various origins. Unlike most of the Toodoggone formation, quartz and biotite phenocrysts are rarely observed in these younger rocks.

DUNCAN MEMBER (UNIT Td)

The Duncan member is well exposed in the southeastern part of the study area between the Finlay River and Jock Creek. It comprises a thick, crudely layered succession of predominantly nonwelded, dacitic lithic-crystal tuffs interbedded with minor crystal-rich volcanic sandstone and siltstone. The base of the succession is marked locally by quartz-bearing sandstones in gradational contact with conglomeratic beds that mark the basal unconformity of Toodoggone strata on the Takla Group. Elsewhere, however, incipiently to moderately welded ash-flow tuffs rest directly on erosional remnants of the Takla Group. Here, within a few metres of the contact, the plane of welding is more steeply inclined (>50°) and reflects the local attitude of the rugged paleosurface.

The lithic component (<10 vol. %; <3 cm across) of the pyroclastic beds constitutes subrounded to subangular clasts of finely porphyritic to aphanitic andesitic volcanic rocks. The crystal component (typically 1–3 mm) is dominated by broken plagioclase accompanied by minor to trace amounts of rounded (resorbed) quartz and oxidized, coppery flakes of biotite.

South of the study area in the vicinity of the Kerness North Cu-Au porphyry occurrence, pyroclastic flow deposits dominate sections unconformably overlying the Triassic volcanic rocks. A similar relationship is also observed south of Attycelley Creek, where nonwelded to incipiently welded tuffs overlie nearly 100 m of layered epiclastic rocks above the basal unconformity. At both localities, U-Pb isotopic dates determined for pyroclastic rocks assigned to the Duncan member are precisely established at 199 to 200 Ma.

METSANTAN MEMBER (UNIT Tm)

The Metasantan member occupies much of the terrain north of the Finlay River, extending to the vicinity of The Pillar, where it is truncated by westerly-trending faults, and east of Mt. Graves to the Toodoggone River. The unit comprises a fairly homogeneous succession of andesitic lavas, including associated flow breccias, minor interbedded epiclastic and rare pyroclastic rocks. The basal contact with the Duncan member is abrupt and generally marked by massive flow sequences largely devoid of layering or internal flow features.

Lavas of the Metasantan member typically contain equant to subequant, blocky plagioclase phenocrysts (usually 3–5 mm), rarely found in glomeroporphyritic intergrowth (<8 mm), that commonly form 15–25 vol. % of the rock. Mafic phenocrysts include variably altered, prismatic hornblende and euhedral biotite (<5 mm) and generally constitute less than 5 vol. % of the rock. Unusually biotite-rich (8–10 vol. %) andesite lavas are comparatively rare though well exposed, for example, on a westerly-trending

ridge just south of The Pillar. Accessory minerals include small (<1 mm) grains of resorbed quartz and reddish apatite prisms (<1 mm) which, though definitive of these lavas, are sparsely distributed. Based on phenocryst mineralogy and chemical composition, these rocks are commonly referred to as trachyandesite or high-silica andesite.

East of the Black Fault in the area between the Sickle Creek and Quartz Lake cirques, andesitic flows are interbedded with, or overlain by, well-sorted sandstones and cobble to pebble conglomerates with rounded clasts of porphyritic to aphanitic andesites and monzonitic granitoid rocks. These beds are tentatively included within the Metsantan member, although some of these clastic sequences may belong to the overlying Quartz Lake member (described below) due to fault repetition (Fig. 5).

Metsantan andesites cover an extensive part of the Toodoggone region and rest on ash-flow tuff successions that appear to have slightly different ages. Argon-argon dating of this flow sequence has been hindered by the paucity of fresh hornblende and biotite. However, the two Ar-Ar dates that have been obtained yield similar isotopic ages of approximately 196 and 194 Ma.

SAUNDERS MEMBER (UNIT Ts)

The Saunders member is a homogeneous dacitic ash-flow tuff sequence best exposed in the region west of Saunders Creek and northwest toward the Toodoggone River (Diakow, 2004). Other thick accumulations are found south of the Finlay River and northeast of the Kemess South mine (Diakow, 2001). South of Jock Creek,

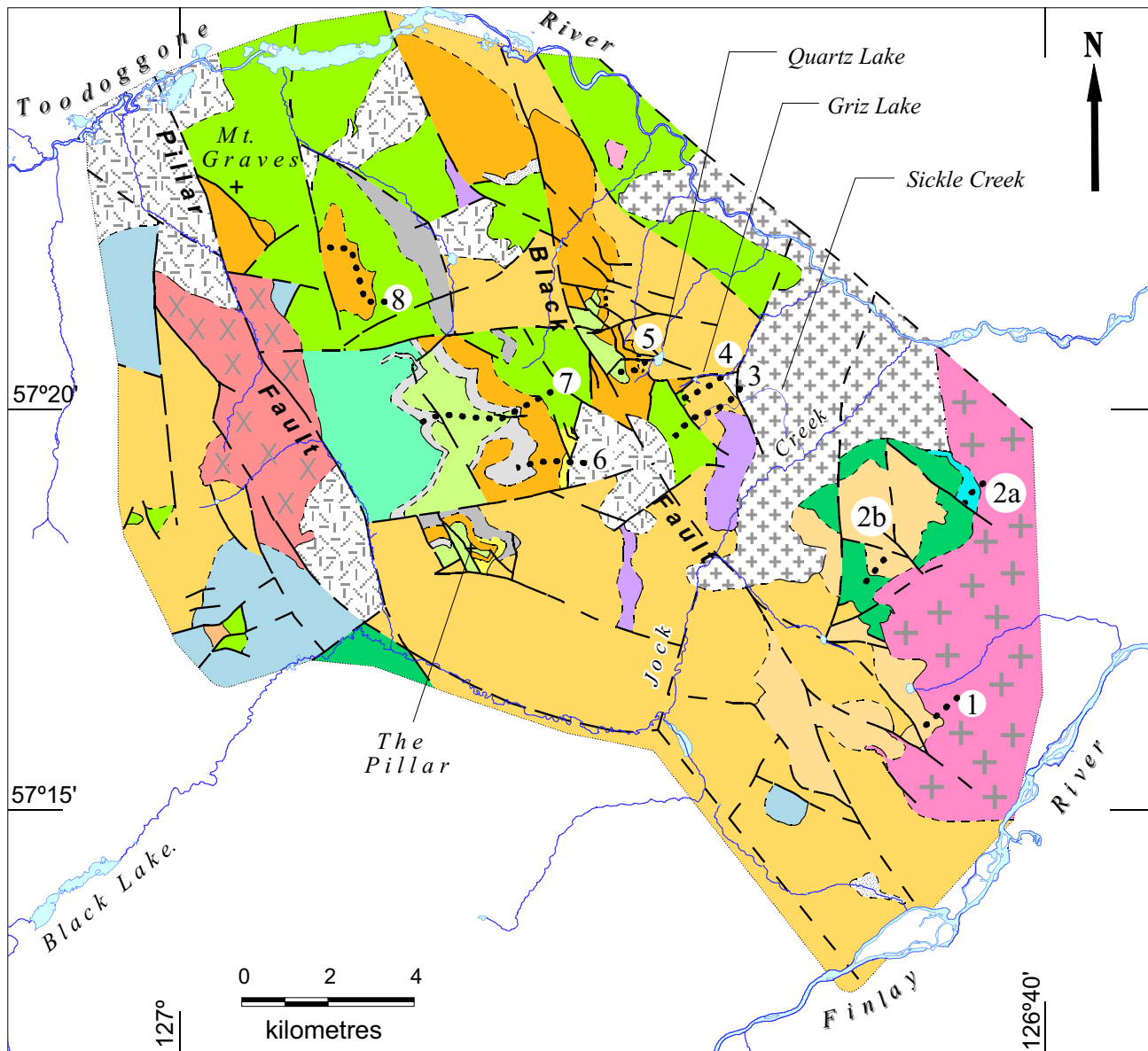


Figure 2. Generalized geology of the study area east of the Pillar Fault between the Finlay and Toodoggone rivers. Numbered transects locate the stratigraphic sections shown in Fig. 4. Informally named lakes and a creek referenced in the text are also indicated. The dash-double dot contact between early and late phases of the Jock Creek pluton is inferred from the aeromagnetic data of Shives *et al.* (2004).

an isolated occurrence of reddish oxidized pyroclastic flows form a cap less than 70 m thick on a ridge that, at lower altitude, exposes lavas of the Metsantan member. The highly variable thickness of the Saunders unit is attributed to the influence of pre-existing topography and synvolcanic faults.

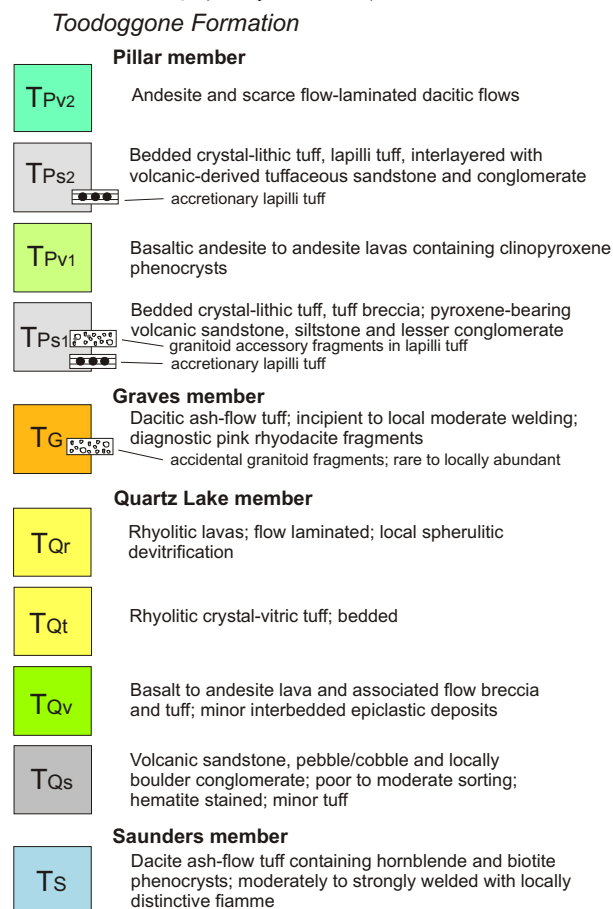
Dacite ash-flow tuffs of the Saunders member are some of the least altered rocks in the Toodoggone area. These rocks exhibit a characteristic grey color and, because of their indurated character, generally form a resistant stratigraphic marker. The tuffs are noticeably enriched in broken crystals of plagioclase (up to 40 vol. %). Splendant crystals of hornblende (up to 7 vol. %) and lesser biotite and quartz (trace to 3 vol. %) make up the majority of the remaining crystal population. Dark grey to black, cognate vitrophyre fragments (5–45% of the rock) occur throughout the ash-flow deposit and locally become densely welded to define a pronounced eutaxitic texture. Although this unit is commonly oxidized to reddish hues, the primary mineralogy and vitrophyric textures are readily identifiable.

Seven Ar-Ar and U-Pb isotopic dates indicate that the Saunders member erupted during a brief interval between 194 and 193 Ma (Diakow, unpublished data).

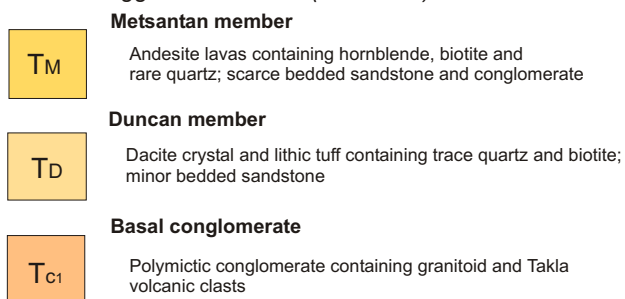
New Rock Units Forming the Uppermost Toodoggone Formation

East of the Pillar Fault, a previously undivided succession of lavas and interbedded, well-stratified pyroclastic-epiclastic rocks forms a gentle west-southwest-dipping homocline. Epiclastic strata near the base of this succession near an informally named lake, Quartz Lake, overlie hornblende- and/or biotite-bearing andesite flows provisionally assigned to the Metsantan member (section 5 in Fig. 4 and Fig. 5). Since the Saunders member is apparently missing in this area, this contact is interpreted as a disconformity. Elements of the new stratigraphy, however, demonstrably overlie the Saunders member west of the Pillar Fault, where epiclastic rocks mark an erosional contact. From these relationships and a new U-Pb date derived from near the middle of the new sequence, it is evident that these rocks are time stratigraphic, in part, with dated strata in the

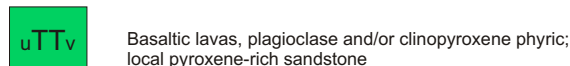
Hazelton Group (*Early Jurassic*)



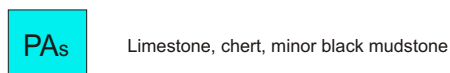
Toodoggone Formation (*continued*)



Takla Group (*Early Triassic*)



Asitka Group (*Late Carboniferous - Early Permian*)



Black Lake Intrusive Suite (*Early Jurassic*)

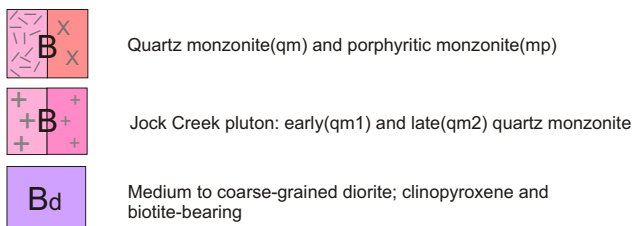


Figure 3. Legend to geology map in Figure 2 (opposite page). Additional stratigraphic elements and unit descriptions refer to sections shown in Figure 4.

bearing andesite flows (TQv, best developed elsewhere) are found at or near the hematitic base of this predominantly clastic unit (Fig. 5 and Fig. 4, section 5).

Other exposures of unit TQs, for example, are found approximately 4 km due west of Quartz Lake below the faulted base of the Graves member, in scattered outcrops along the western lower slopes of a broad valley to the northwest of the latter locality and in the vicinity of The Pillar (Fig. 2). At the former locality, these well-stratified, epiclastic and pyroclastic rocks are intercalated with variably porphyritic basaltic to andesitic lavas (TQv). The sedimentary rocks include buff to reddish brown weathering, waterlain volcanic breccias, volcanic cobble to boulder conglomerates locally enclosing large (up to 50 cm across) rounded monzonitic clasts, and coarse sandstones. Pyroclastic interbeds are dominated by grey-green lithic-crystal ash-flow tuffs of dacitic composition and their re-worked equivalents. The associated lavas are commonly

dark grey to red, finely porphyritic (<1.5 mm) plagioclase-phyric basaltic andesites with small amounts (<3 vol. %) of clinopyroxene; however, augite-rich variants (10–15 vol. %; <5 mm) and strongly amygdaloidal flows carrying subequant clinopyroxene megacrysts (<1 cm) are locally conspicuous.

At The Pillar, well-stratified sequences of volcanic conglomerates, sandstones, siltstones, ash-flow tuffs and tuffaceous breccias (TQs) underlie rhyolitic tuffs and lavas (TQr) resting directly below the Graves member. Similar rhyolitic rocks occur 3 km northeast of The Pillar and form small outliers at the top of cirque headwalls above Griz Lake and Sickle Creek (Fig. 4 and 5). Dark red to pale grey-green, spherulitic rhyolite lavas commonly exhibit flow laminations and contain plagioclase (<20 vol. %) and biotite (3 vol. %) phenocrysts. Thickly bedded sequences (<30 m) of vitric-crystal rhyolite tuff with sparse lithic fragments (<2 cm) locally underlie the rhyolite flows.

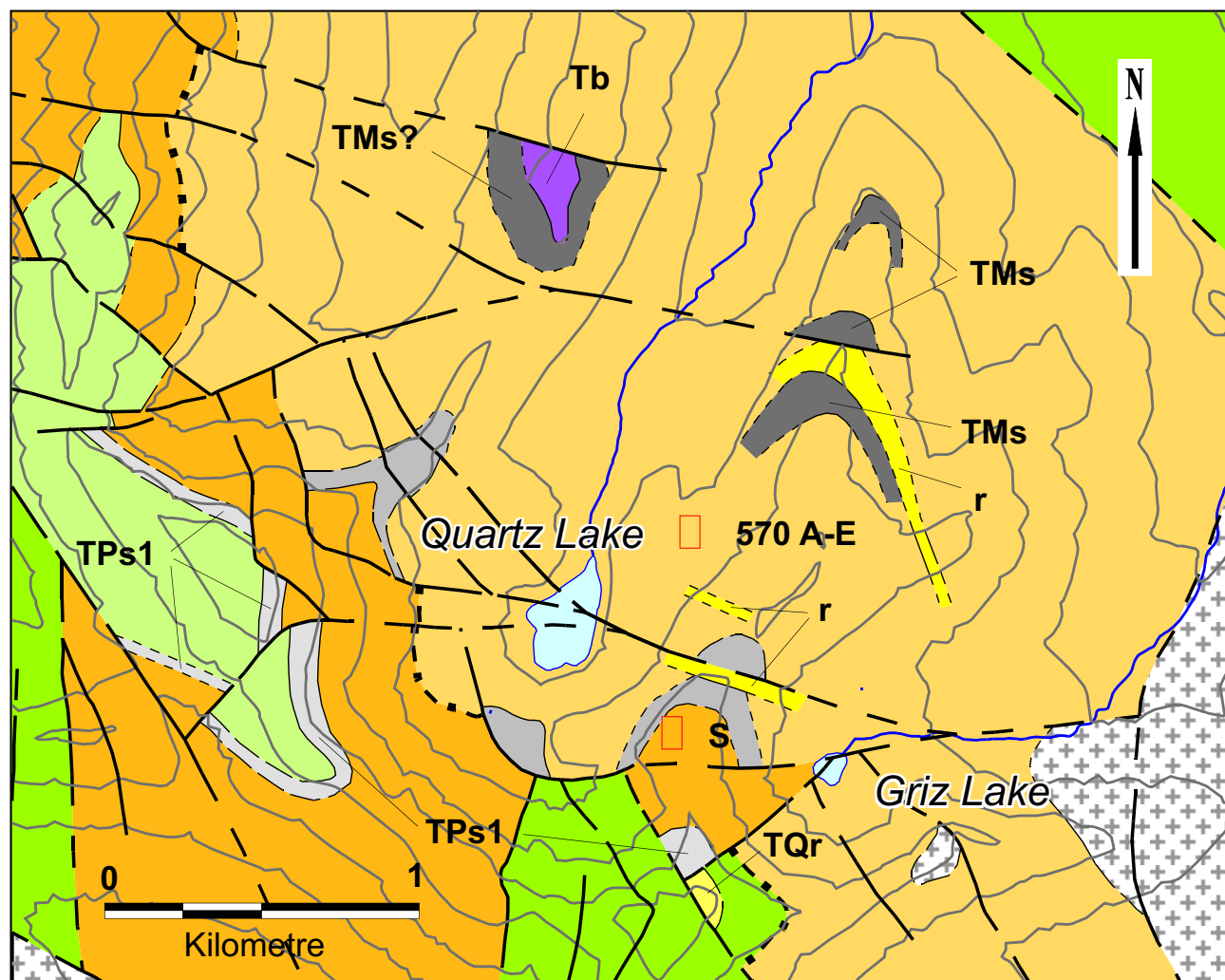


Figure 5. Geology of the Quartz Lake–Griz Lake area, showing stratigraphic elements of the Toadoggonne formation not represented in Figure 2: the location of rhyolite sills and dikes (r); and epithermal quartz-sulphide veins (570A-E) and stockworks (S) of the Sickle-Griz showing. The stratigraphy dips 20–30° degrees to the west-southwest and map units are those of Figure 3, except for epiclastic beds within the Metsantan member (TMs) and a basaltic sill (Tb). The heavy dot-dash line represents volcaniclastic and/or volcanic sequences too thin to show at map scale.

Extensive exposures of basaltic and andesitic lavas (TQv) are found on the valley slopes and ridges north and south of Mt. Graves (Fig. 2). Some flows are finely porphyritic, carrying plagioclase (<1.5 mm; up to 15–20 vol. %) and clinopyroxene (<1 mm; 1–3 vol. %). Other lavas are more distinctly porphyritic, carrying euhedral phenocrysts of clinopyroxene (<4 mm; 10–15 vol. %) and subequant plagioclase (<3 mm with rare glomerocrysts up to 7 mm; up to 20 vol. %). Rarely, flows and/or near-surface dikes are encountered with euhedral megacrysts (<1.5 cm) of clinopyroxene (<5 vol. %) rarely accompanied by subequant plagioclase (<3 vol. %). Minor interbeds of volcanic breccias of diverse origins are found locally, including monomictic laharic breccias with poorly sorted volcanic clasts (<33 cm). It is interesting to note the radical change in thickness of this flow sequence to the east toward Quartz Lake, and to the south toward the Pillar where these lavas are apparently absent (Fig. 2).

GRAVES MEMBER (UNIT Tg)

The Graves member is named for dacite ash-flow tuffs that are particularly well exposed in an isotopically dated section about 3 km southeast of Mt. Graves. These pyroclastic flows form resistant blocky exposures as much as 150 m thick, and exhibit little variability in thickness from one section to the next (Fig. 4, sections 5–8). The unit is a distinctive marker occupying a medial stratigraphic position between two internally heterogeneous members, each composed of generally similar rock types. The contacts between the Graves member and bounding rocks of the Quartz Lake and Pillar members are sharp and appear conformable throughout the reference area. The ash-flow tuff unit overlies a variety of different rock types at the top of the Quartz Lake member, including flow-laminated rhyolite (TQr), pyroxene-bearing andesite lavas interlayered with crystal tuffs and volcanic sandstone-siltstone layers containing pyroxene grains (TQv), and locally a hematite red monomictic boulder conglomerate with finer clastic interbeds or debris flow (TQs). In most sections, these massive ash flows contrast sharply with the overlying well-bedded, mixed pyroclastic-epiclastic strata (TPs1). This unit is dominated by vitric-crystal tuffs, sandstones, siltstones and conglomerates, and more localized accretionary lapilli tuff, lapilli tuff and tuff-breccia that are distinguished by abundant minute pyroxene grains. In a few places, this bedded unit is absent and stratigraphically higher pyroxene andesite lavas (TPv1) sit directly on the ash-flow deposits.

The ash-flow tuffs are rich in lithic fragments, which may constitute up to 45% of the rock. The clasts are subangular to angular and typically less than 2 cm in diameter. Zones within the ash-flow tuffs may contain concentrations of block-size fragments, but these are uncommon. The most abundant fragments are a mixture of fine-grained porphyritic and aphanitic volcanic rocks in varying hues of red, brown and green. However, pale pink to flesh-coloured dacitic fragments with minute hornblende and/or biotite grains are most diagnostic and useful for identifying this unit. Accidental fragments of pinkish biotite-hornblende

monzonite and quartz monzonite are sparsely distributed, particularly in the upper part of the ash-flow sequence. Their subrounded to rounded shapes suggest that these clasts were likely derived from subaerial drainages and incorporated during the passage of the pyroclastic flows. Fragments of plagioclase (<2 mm) dominate the crystal fraction of the matrix, locally accompanied by sparse quartz and/or biotite grains.

The Graves member is well indurated and, although it has the general appearance of a nonwelded single cooling unit, was probably emplaced as multiple flow units. Locally, lithic-rich tuffs at the top of this unit appear to have been reworked to some degree. Incipient to moderate welding is observed in places and indicated by flattened reddish brown to dark green fiamme. Although welded texture is not widespread within these ash-flow deposits, one locality was discovered at the base of the unit where dense welding and, locally, a brown devitrified vitrophyre are well displayed. The welded zone, about a metre thick, overlies an additional 10 m of bedded crystal-vitric tuff and lapilli tuff in which weak welding is again evident in a metre-thick zone just 3 m from the base of this sequence. The latter beds overlie a layer-parallel, planar-crosslaminated lithic-vitric tuff that is interpreted to represent a surge deposit.

Based on a U-Pb zircon date obtained from rocks near the middle of a section southeast of Mount Graves (Fig. 4, section 8), this ash-flow unit erupted at approximately 192 Ma. This date firmly establishes the contemporaneity of these ash-flow tuffs with compositionally similar deposits dated outside the map area (the south of Attycelley Creek) and included in the Toodoggone formation as one of the youngest known members (i.e., Kemess member, Diakow, 2001).

PILLAR MEMBER (UNITS TPS, TPV)

The Pillar member constitutes the youngest stratigraphy presently recognized in the Toodoggone area. Excellent exposures are found at the locality for which this sequence is named, as well as farther north in a downdropped fault block between The Pillar and Mt. Graves (Fig. 2, 4). The base of this unit rests on the Graves ash-flow tuff member and the top is not seen (eroded). The unit is lithologically heterogeneous and has been subdivided, where possible, into mappable volcaniclastic (TPs1, TPs2) and flow (TPv1, TPv2) stratigraphy. Secondary alteration of lavas and clastic rocks to carbonate, prehnite and a distinctive pale pink zeolite (laumontite?) is locally apparent throughout this succession.

At The Pillar, unit TPs1 is represented by at least 30 m of well-stratified, maroon to grey-green epiclastic rocks including volcanic pebble to cobble conglomerate, internally laminated sandstone, siltstone and minor mudstone, locally exhibiting crossbedding and cut-and-fill channel structures. Similar stratigraphy 2 km north-northeast of The Pillar across a major westerly-trending fault contains a high proportion of pyroclastic material including well-bedded, coarse vitric-lithic tuff of airfall origin, planar-crosslaminated lapilli tuff containing abundant angular volcanic fragments (<3 cm) of probable surge origin, and

laharic breccias with angular to subangular volcanic clasts up to 0.5 m across. Farther north, this succession is thicker (>50 m) and composed of thickly bedded, reworked volcanic breccias overlain by grey-green, thin to medium-bedded, moderately well sorted volcanic sandstones, underscoring the rapid nature of lateral facies changes.

The lower epiclastic-pyroclastic succession is conformably overlain by basaltic to andesitic lavas (TPv1) that form the peak of The Pillar and occupy lower ridges to the north. Dark reddish to purplish grey flows are moderately (10–15 vol. %) to strongly (25–30 vol. %) plagioclase phyric with subordinate clinopyroxene phenocrysts (commonly <1 mm but locally up to 3 mm, and typically comprising 1–2% but reaching 5 vol. % of the rock). The abundance and size distribution of plagioclase and clinopyroxene phenocrysts vary substantially from flow to flow. Amygdaloidal textures and thin flow breccias are observed locally.

The uppermost part of the Pillar member is preserved in the downropped fault-block north of The Pillar. The base of the upper epiclastic-pyroclastic sequence (TPs2) appears broadly conformable with the underlying lavas. The lowermost beds comprise a buff to dark brown, clast-supported, volcanic cobble to pebble conglomerate and moderately well sorted pebbly sandstone. Higher in the section, these beds are intercalated with pale grey-green to pink weathering crystal-lithic lapilli tuffs and reworked tuffs. At the northernmost exposures, the top of the succession (>130 m) is dominated by grey-green to buff, laminated to medium-bedded volcanic sandstones and pebbly sandstones with minor interbedded siltstone and mudstone.

The overlying plagioclase- and pyroxene-phyric lavas (TPv2) are texturally and mineralogically similar to the older flows (TPv1) of the Pillar member, and would be difficult to distinguish in the absence of an intervening epiclastic-pyroclastic sequence (TPs2). However, some of these flows are distinctly viscous with well-developed flow laminations and have a rhyodacitic composition. Flow breccias are generally better developed than in the andesitic lavas and flow laminae locally bear pink devitrification spots.

Black Lake Intrusive Suite (Units Bqm, Bmp, Bd)

Plutons and minor intrusions (dikes and sills) of the Early Jurassic Black Lake Intrusive Suite are found throughout the map area; the largest bodies occur at the eastern margin of the map area and along the Pillar Fault. These intrusions are temporally and probably genetically related to extrusive rocks of the Toodoggone formation.

Typical Black Lake intrusions in the study area are biotite- and hornblende-bearing quartz monzonites with a medium to coarse-grained equigranular to porphyritic texture. These plutons differ slightly in composition from those associated with Au-Cu porphyry mineralization at the Kemess deposits in that the latter intrusions are less differentiated and comprise monzodiorites and medium to coarse-grained monzonite porphyries. These mineralized plutons also have a distinctly tabular geometry, and in the

case of the Maple Leaf pluton at Kemess South, emplacement appears to be at a subvolcanic level. Monzonitic intrusions in the map area are related to porphyry-style mineralization (e.g., at the Pil North, Sophia and Alexandra prospects) and may have temporal and genetic links to epithermal precious-metal mineralization (e.g., at the Sickle-Griz showings, described below).

A large composite pluton is well exposed in the lower part of Jock Creek; to the north, this body probably underlies much of the low tree-covered region adjacent to the Toodoggone River and, to the south, it extends to the Finlay River. In order to rationalize field observations, it was necessary to subdivide the Jock Creek pluton into an older (Bqm1) and younger (Bqm2) phase. The lowermost element of the Toodoggone stratigraphy, a basal conglomerate below the Duncan ash-flow tuff member, rests nonconformably on the pluton in the extreme southeastern part of the map area, whereas monzonite intrudes the lowermost Toodoggone rocks farther north at Jock Creek. The location of the contact between younger and older phases of the Jock Creek pluton is uncertain, and has been taken to be delineated by a sharp contrast in the magnetic signature of the rocks east of Jock Creek (Fig. 2). A sample of the younger monzonite phase is currently being dated by the U-Pb technique.

The younger (Bqm2) phase of the Jock Creek Pluton is a pinkish grey, coarse-grained, equigranular to porphyritic, biotite-hornblende quartz monzonite with accessory titanite and opaque oxides. The porphyritic monzonite carries euhedral to subhedral plagioclase phenocrysts (up to 8 mm) set in a finer grained groundmass of potassium feldspar and quartz. Plagioclase crystals usually display oscillatory zoning and are flecked with sericite. Interstitial potassium feldspar is generally more strongly altered to sericite and clay minerals. Although little quartz is generally apparent in hand specimen, thin-section examination reveals some 10–15 vol. % of the mineral. The predominant ferromagnesian mineral is euhedral to subhedral hornblende (<7 mm) that is commonly altered to chlorite. Subhedral to anhedral biotite (<4 mm), also variably altered to chlorite, is present in minor amounts, along with accessory titanite (<1 vol. %) and opaque oxides.

The older phase (Bqm1) of the Jock Creek pluton is a medium-grained, equigranular quartz monzonite, mineralogically similar to the younger phase. However, the amount of quartz is notably higher (~20 vol. %) and occurs as anhedral grains clearly visible in hand sample. Anhedral potassium feldspar occurs as a late interstitial phase. Biotite is the dominant mafic mineral, accompanied by lesser amounts of hornblende and trace titanite and opaque oxides.

Plutons exposed along the Pillar Fault are quartz monzonite and porphyritic monzonite; the latter phase is associated with Cu-Au porphyry prospects in the vicinity of Pil North. The porphyritic phase of the pluton (Bmp) east of the fault cuts the youngest part of the Toodoggone stratigraphy (Fig. 2). This indicates that the intrusion is younger than 192.3 ± 0.4 Ma, the U-Pb isotopic age of the

Graves member in the upper part of the Toodoggone stratigraphy.

Small dioritic stocks and dikes of the Black Lake Intrusive Suite cut the Toodoggone formation as well as monzonitic rocks of the Jock Creek pluton. The largest diorite intrusions are northerly-trending, elongate bodies underlying valley slopes and ridge crests just west of Jock Creek. The rocks are pinkish grey to dark grey-green, fine to coarse-grained biotite-clinopyroxene diorites. Anhedral to subhedral crystals (<5 mm) of pyroxene and plagioclase are intergrown with biotite and minor (<2 vol. %) interstitial quartz and opaque oxides. Coarsely crystalline varieties locally contain fresh biotite oikocrysts up to 1.5 cm across. Secondary alteration minerals include sparse sericite, chlorite and epidote.

Minor intrusions in the form of dikes, sills and small plug-like bodies are prolific throughout the map area. The most common dikes are pinkish grey to buff weathering, medium-grained to porphyritic monzonite; pale pink to reddish weathering, aphanitic to porphyritic (rarely medium-grained) leucomonzonite (to syenite?) carrying small amounts (typically trace to 1 vol. %) of mafic minerals; and quartz± biotite porphyries. Basaltic to andesitic dikes similar in composition to pyroxene-bearing extrusive rocks in the upper part of the Toodoggone formation are also common. All dikes are generally steeply dipping and exhibit a regional, north to north-northwesterly preferred orientation.

MINERAL OCCURRENCES AND EXPLORATION

The Toodoggone area has a rich history of mineral exploration and is a successful mining district. The premier exploration targets have been, and continue to be, large tonnage Cu-Au porphyry systems and small, high-grade, precious-metal epithermal vein systems. A regional synopsis of previous exploration work is given below, along with descriptions of some of the newer discoveries and prospects in the study area.

Recent History of Toodoggone Mineral Exploration

The Toodoggone mining camp was systematically evaluated for its potential to host bulk tonnage mineral deposits in the mid-1960s by Kennco Explorations (Western) Limited. They conducted a regional geochemical sampling program that led to the discovery of the first known porphyry-style base-metal and vein-type precious metal targets in the Toodoggone region. Among the deposits found were Chappelle (Baker), Lawyers (AGB zone) and Kemess North. Follow-up exploration by Kennco and other companies began in the late 1960s and continued intermittently through the 1970s into the early 1990s. This exploration resulted in the development of small Au-Ag mines (Baker, Lawyers and Shasta) centred on epithermal quartz-vein systems and the Kemess South porphyry Au-Cu mine.

Dupont of Canada Exploration Limited commissioned the 100 tonnes/day underground Baker mine, the first mine to open in the region, in April, 1981 (Barr *et al.*, 1986). It ceased operation in November 1983, after producing 1196 kg of gold and 23 085 kg of silver from 77 596 tonnes of ore mined and milled from the A vein (MINFILE). Multinational Resources Inc. purchased the property from Dupont in 1985 and Sable Resources Limited acquired the Baker mill from Dupont in 1989. Multinational outlined a small tonnage on the B vein and, with Sable as a partner, mined and processed modest tonnages from the vein until 1996 when Sable acquired the property outright from Multinational. Since that time, Sable has, on an intermittent basis, extracted and processed limited amounts of ore from both the A and B veins.

Sable Resources Limited brought the Shasta deposit, 8 km southeast of the Baker mine, into production in October 1989, continuously extracting ore from the Creek and JM zones until April 1991. During this time, 601 kg of gold and 32 932 kg of silver were produced from 122 533 tonnes of ore processed at the Baker mill. The two ore zones were first mined by small open cuts; underground development on each followed. Small tonnages of ore were mined from the JM and Creek zones in 2000, 2003 and 2004.

In 1986, Cheni Gold Mines Ltd. purchased the Lawyers property from Kennco Western Ltd. Cheni commissioned the mine in 1989 with a combined reserve for the AGB, Cliff Creek and Duke's Ridge zones of 1.757 million tonnes grading 6.72 g/t Au and 243 g/t Ag. The AGB deposit was mined until 1991 using underground shrinkage and blast-hole stoping methods, but the Cliff Creek and Duke's Ridge zones were not mined. The steeply dipping AGB deposit, with widths of up to 12 m, had been traced north along strike for about 550 m. Mineralization consisted of native gold, native silver, electrum, acanthite and lesser chalcopyrite, sphalerite and galena in quartz veins, stockworks and chalcedony-healed breccias. Approximately 620 000 tonnes of ore were milled, although this total includes an estimated 60 000 tonnes from the AI property (MINFILE 094E 091) located north of the Toodoggone River. A total of 5042 kg of gold and 113 184 kg of silver were recovered. Cheni reclaimed the property in the late 1990s and its tenure over the site was later relinquished. The property was staked by Guardsmen Resources Inc. in 2000 and 2001, and optioned the following year to Bishop Resources Inc. In 2004, Bishop followed up encouraging float anomalies with a 1000 m trenching program on the plateau immediately west of the Cliff Creek zone.

Porphyry mineralization was first identified in the area of the Kemess South deposit in 1983. Extensive drilling programs conducted by El Condor Resources Ltd. from 1990 to 1993 outlined a geological resource for the Kemess South deposit of 250 million tonnes grading 0.62 g/t Au and 0.22 g/t Cu (Rebagliati *et al.*, 1995a). Royal Oak Mines Ltd. purchased the property and initiated site clearing and mine construction in July 1996. The mine was commissioned in October 1998. In the spring of 1999, Royal Oak became insolvent and the mine was purchased by Northgate Explora-

tion Ltd. (now Northgate Minerals Corporation). The mine presently operates at rate of approximately 50 000 tonnes per day and produces about 300 000 ounces of gold and 75 million pounds of copper per year. Recent exploration in the area of the mine has focused on the Kemess North deposit, where diamond drilling to deeper levels has expanded the size of the deposit. A feasibility study on Kemess North, completed in October 2004, identified a resource of 414 million tonnes grading 0.31 g/t Au and 0.16 g/t Cu. The proposed open pit mining project has now entered the harmonized Federal/Provincial environmental review process.

Although the Kemess South mine is outside the current map area, it has contributed significantly to the rejuvenation of exploration throughout the Toodoggone mining camp. Its importance as a remote major open-pit mining operation serviced by hydroelectricity, a modern milling facility and a substantial in-ground mineral resource cannot be understated. This infrastructure is crucial for future mine development in the Toodoggone region, as it may become a central milling complex capable of supporting numerous satellite orebodies.

Epithermal Au-Ag Veins: Sickle-Griz (MINFILE 094E 237)

Stealth Minerals Ltd. discovered the Sickle-Griz Au-Ag-base-metal epithermal vein prospect in 2003. Two physically distinct, topographically separated vein systems are recognized cutting Toodoggone volcanic rocks. Five discrete parallel veins (named 570A to 570E) are found in the bottom of the cirque occupied by Quartz Lake (Fig. 5). They have an azimuth of 155° and dip 65° to the west. Several of the most prominent veins on surface (570A and 570B) are up to 13 m in width and over 100 m in length, and transect a monotonous sequence of grey-green porphyritic andesites assigned to the Metsantan member (Fig. 5, 6). Flow-laminated rhyolitic dikes and sills, a comparatively rare occurrence in the Toodoggone camp, are also a conspicuous feature of this area (Fig. 5).

The 570 veins vary in appearance from massive, diffusely layered white quartz to multiple layers of comb-textured quartz alternating with calcite spar (Fig. 7). Potassium feldspar alteration adjacent to the veins is widespread, varying in intensity from incipient to moderate, and imparts a pale pink to brownish hue on host andesites.

The second vein system, situated about 150 m higher on the ridge above the 570 veins, exhibits more of a stockwork character, with multiple generations of quartz veins and quartz-breccia veins occupying a zone more than 75 m wide and hosted by dacitic ash-flow tuffs near the base of the Graves member (Fig. 5). Adularia sampled from narrow alteration selvages adjacent to quartz veins at both the lower and upper vein systems is being used to obtain Ar-Ar isotopic ages for the mineralization. Since the Graves member has been dated at 192.3 ± 0.4 Ma, this establishes a maximum age for emplacement of the upper vein stockwork.

Sulphide minerals in the veins occur as fine disseminations, patchy aggregates and semimassive to massive layers

up to several centimeters wide. In order of decreasing abundance, they comprise galena, sphalerite, tetrahedrite, chalcocopyrite and pyrite. Chip samples across discrete veins have yielded grades as high as 9.5 g/t Au and 407 g/t Ag over 3 m. Assay results from the first two holes drilled into the lower vein system have returned encouraging results (e.g. 3.18 g/t Au and 107.8 g/t Ag over 2.5 m from the footwall portions of the 570A vein; *see* Stealth Minerals Ltd. news release, July 16, 2004).

Au-Cu Porphyries

PIL NORTH (MINFILE 094E 083) AND VICINITY

The Pil North property is located at the western margin of the map area (Fig. 6). It is underlain by a quartz monzonite to porphyritic monzonite stock that straddles the Pillar Fault and intrudes andesitic lavas of the Metsantan member in the west and some of the youngest stratigraphic units of the Toodoggone formation in the east (Fig. 6). Exploration by Finlay Minerals Ltd. has identified a number of Cu-Au geochemical anomalies that are coincident with induced polarization chargeability anomalies. Some of these anomalies coincide with pronounced propylitic and phyllic alteration zones and are thus prime targets for porphyry-style mineralization (i.e. the Northwest and Northeast zones, Fig. 6). Other geochemical anomalies have a polymetallic signature that may be indicative of buried vein systems (i.e. East, Milky Creek, NW Extension and WG Gold zones).

The Northwest zone is characterized by a 200 by 600 m geophysical anomaly that coincides with elevated Cu-Au soil values and locally intense silicification, bleaching and pyrite-sericite alteration of the monzonitic host rock. Chalcocopyrite accompanies pyrite in narrow quartz stringers and in areas where more pervasive silica-flooding is developed. Late-stage, purple anhydrite stringers cut the mineralization. The Northeast zone lies east of the Pillar fault and is underlain by quartz-bearing flows of the Metsantan member that are weakly to moderately oxidized (Fig. 6). The hostrock displays locally intense quartz-sericite-pyrite alteration, with disseminated pyrite reaching up to 15 vol. %; in places, goethite and jarosite are well developed.

The East and Milky Creek zones have a polymetallic geochemical signature characterized by highly anomalous Au and Ag values accompanied by inconsistent Cu and Zn abundances. The East zone includes quartz stockworks and brecciated monzodiorite healed with silica; both are mineralized with small amounts of barite, galena and sphalerite. The Milky Creek zone is characterized by a potassic feldspar-magnetite-quartz stockwork within strongly clay-altered monzonite. Chip sampling across a 10 m wide segment of the Milky Creek showing averaged 0.52 g/t Au. The NW Extension, a quartz-barite stockwork anomalous in Cu and Pb, may represent a polymetallic vein on the periphery of a porphyry system. The WG Gold zone comprises quartz veins, stockworks and breccias confined to a steeply dipping, northwest-trending corridor that extends for over a kilometre. The veins are developed within quartz

monzonite and locally carry variable quantities of barite and galena. Samples of quartz float carry up to 16.8 g/t Au.

SOFIA (MINFILE 094E 238)

Porphyry-style mineralization at Sofia was discovered in the summer of 2004. The showing is restricted to a single outcrop (25 by 25 m) which is located on the west bank of the Toodoggone River, approximately 2.7 km northwest of the mouth of Jock Creek (Fig. 6). The main host rock is a medium to coarse-grained equigranular monzonite (Bqm2), although mineralization also occurs within adjacent augite-phyric lavas that exhibit pronounced alteration to chlorite and pyrite (up to 8 vol. %). These lavas have tentatively been assigned to the volcanic unit of the Quartz Lake member. Mineralization consists of subparallel magnetite veinlets and subsequent layered quartz-magne-

tite(±specularite)-chalcopyrite stockwork veins enveloped by potassium feldspar alteration (Fig. 8). Narrow, drusy quartz stringers cut the other vein types. Intense pyrite-sericite alteration occurs locally within the outcrop. Grab samples from the prospect have produced assays of up to 0.22 g/t Au and 0.05 wt. % Cu (see Stealth Minerals Ltd. news release, July 16, 2004).

ALEXANDRA PROSPECT

The Alexandra Au-Cu porphyry prospect was also discovered in 2004. It is located on a ridge 3.3 km west-southwest of the confluence of Jock Creek and the Toodoggone River, close to the *informally* named Sickle Creek (Fig. 6). The showing consists of quartz-magnetite stringers cutting intensely bleached, clay-altered andesitic volcanic rocks of the Metsantan member. The alteration zone is coincident

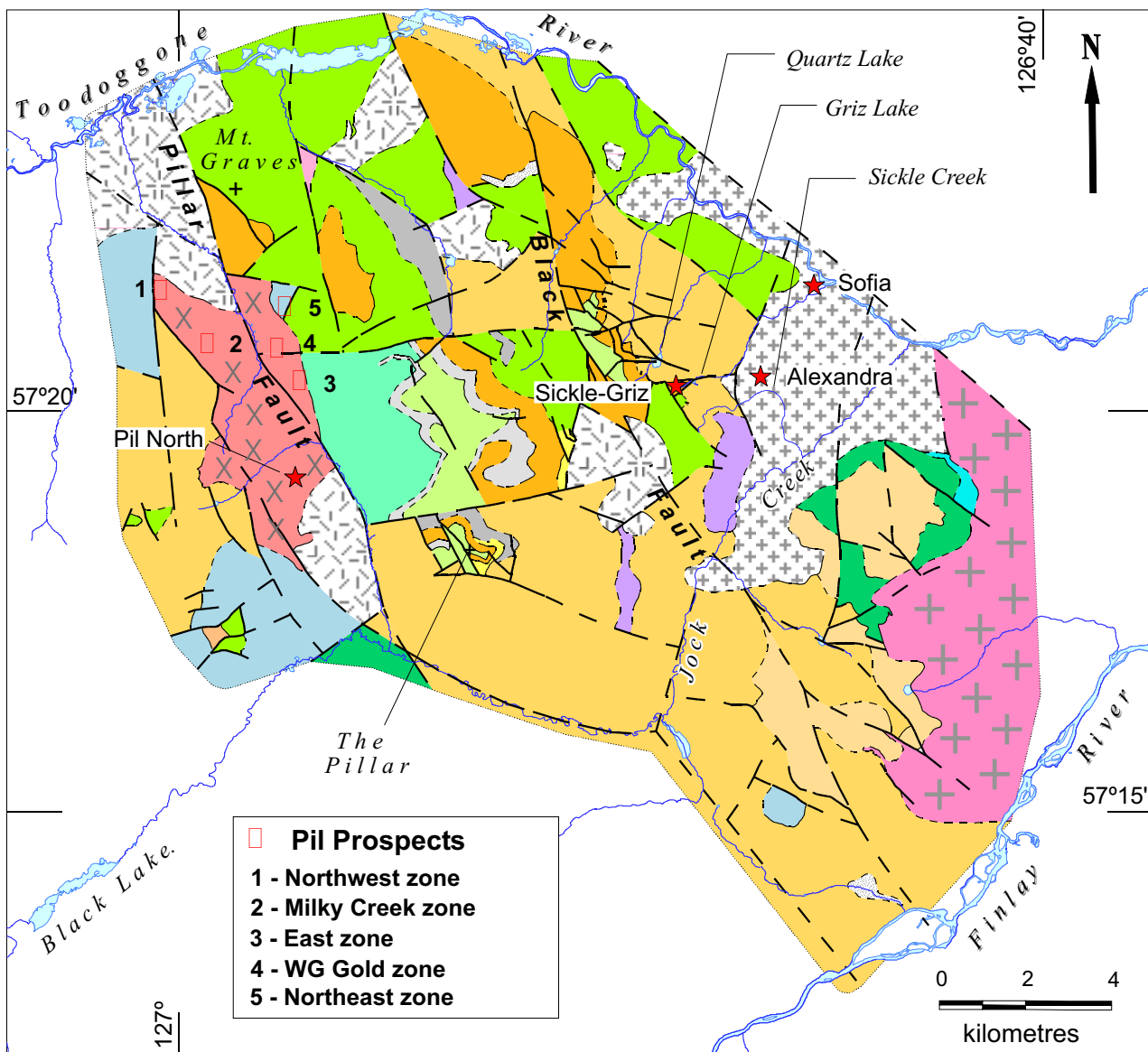


Figure 6. Location of selected Au-Cu porphyry and Au-Ag-base-metal epithermal prospects discussed in the text in relation to their geological setting as determined in this study. Legend for geological units is the same as Figure 3.



Figure 7. View of the 570A vein, displaying alternating bands of quartz and calcite spar, Quartz Lake, Sickie-Griz prospect.

with elevated Au, Cu and Ag values in soils that cover an 800 by 250 m area. The showing approaches within about 300 m of the Jock Creek monzonite (Bqm2) contact with Metsantan lavas, and extends downslope to the north and east of the ridge.

SUMMARY AND CONCLUSIONS

The main results of the 2004 field program can be summarized as follows:

The general stratigraphy of the Toodoggone region, namely rocks from the Late Carboniferous to Early Permian Asitka Group, Late Triassic Takla Group and Early Jurassic Hazelton Group, extends into the study area. The volcanic stratigraphy of the Toodoggone formation has been expanded in the upper part, stratigraphically above the Metsantan and Saunders members, to include three new *informal* members, the Quartz Lake, Graves and Pillar, from oldest to youngest, respectively. They constitute a diverse assemblage of lavas, ash-flow tuffs, and associated volcanoclastic rocks covering a wide compositional spectrum from basalt to rhyolite. Epiclastic volcanic sandstones and conglomerates interleaved with ash-flow and air-fall pyroclastic units form distinctly bedded sections within an otherwise massive flow stratig-

raphy. These new members contrast with older Toodoggone strata by the notable presence of clinopyroxene, and the scarcity of quartz, biotite and hornblende in the volcanic rocks. Their age is roughly that of the Graves member (~192 Ma), as established by U-Pb isotope systematics.

The principal intrusions in the map area are equigranular to porphyritic quartz monzonite and monzonite and minor diorite of the Early Jurassic Black Lake Intrusive Suite. A composite stock in the southeastern part of the study area, named the Jock Creek pluton, is formed by early and late monzonitic phases. Basal conglomerates of the Toodoggone formation rest nonconformably on the older phase (latest Triassic?), whereas the younger monzonite intrudes rocks as high in the Toodoggone formation as the Metsantan member (~198 Ma or slightly younger?).

These intrusions have a significant genetic association with Cu-Au porphyry mineralization south of the study area at the Kemess deposits. The new mapping extends the known distribution of potentially mineralized monzonitic intrusions north of the Finlay River, to include the Jock Creek pluton and their unnamed counterparts adjacent to the Pillar Fault at the Pil North property. The Jock Creek body apparently hosts two

new Au-Cu porphyry prospects in the map area, the Sophia and Alexandra.

Mineralized epithermal quartz-calcite veins and stockworks, such as those discovered on the Sickler-Griz property, constitute a significant exploration target. These mineralized systems affect rocks as young as the Graves member (~192 Ma). Isotopic dating, using U-Pb and Ar-Ar systematics, is currently in progress in order to constrain potential genetic relationships between porphyry and epithermal base- and precious-metal deposits.

ACKNOWLEDGMENTS

We gratefully acknowledge the generous financial and logistical support this project has received from Stealth Minerals Ltd., Northgate Minerals Corp., Finlay Minerals Ltd., Sable Resources Ltd. and Bishop Gold Inc. We have benefited from geological discussions with the geological staff, students and prospectors representing these companies in the field. Their geological contributions have led to improvements in our work. We also thank Stealth Minerals Ltd. for providing copies of their detailed outcrop maps to supplement our own mapping.

REFERENCES

- Barr, D.A., Drown, T.J., Law, T.W., McCreary, G.A., Muir, W.W., Paxton, J.M. and Roscoe, R.L. (1986): The Baker Mine Operation; *Canadian Institute of Mining and Metallurgy*, Bulletin, Volume 79, No. 893, pages 61-68.
- Diakow, L.J. (2004): Geology of the Samuel Black Range Between the Finlay River and the Toadoggone River, Toadoggone River map area, north-central British Columbia (parts of NTS 94E/2,6 and 7); *BC Ministry of Energy and Mines*, Open File Map 2004-4, 1:50 000 scale.
- Diakow, L.J. (2001): Geology of the Southern Toadoggone River and Northern McConnell Creek map areas, north-central British Columbia (parts of NTS 94E/2, 94D/15 and 16a); *BC Ministry of Energy and Mines*, Geoscience Map 2001-1, 1:50 000 scale.
- Diakow, L.J., Panteleyev, A. and Schroeter, T.G. (1993): Geology of the Early Jurassic Toadoggone Formation and gold-silver deposits in the Toadoggone River map area, northern British Columbia; *BC Ministry of Energy, Mines and Petroleum Resources*, Bulletin 86, 72 pages with maps at 1:100 000 scale.
- Diakow, L.J., Panteleyev, A. and Schroeter, T.G. (1985): Geology of the Toadoggone River area, NTS 94E; *BC Ministry of Energy, Mines and Petroleum Resources*, Preliminary Map 61, 1:50 000 scale.
- Eisbacher, G.H. (1974): Sedimentary history and tectonic evolution of the Sustut and Sifton basins, north-central British Columbia; *Geological Survey of Canada*, Paper 73-31, 57 pages.
- Legun, A. (2001): Geology of the Southern McConnell Range and Sustut River areas, British Columbia (parts of NTS 94D/3, 7, 9, 10, 15, 16); *BC Ministry of Energy and Mines*, Open File Map 2001-18, 1:50 000 scale.
- Monger, J.W.H. (1977): The Triassic Takla Group in McConnell Creek map-area, north-central British Columbia; *Geological Survey of Canada*, Paper 76-29, 45 pages.
- Rebagliati, C.M., Bowen, B.K., Copeland, D.J. and Niosi, D.W.A. (1995a): Kemess South and Kemess North porphyry gold-copper deposits, northern British Columbia; in Porphyry Deposits of the Northwestern Cordillera of North America, T.G. Schroeter, editor, *Canadian Institute of Mining and Metallurgy*; Special Volume 46, pages 377-398.

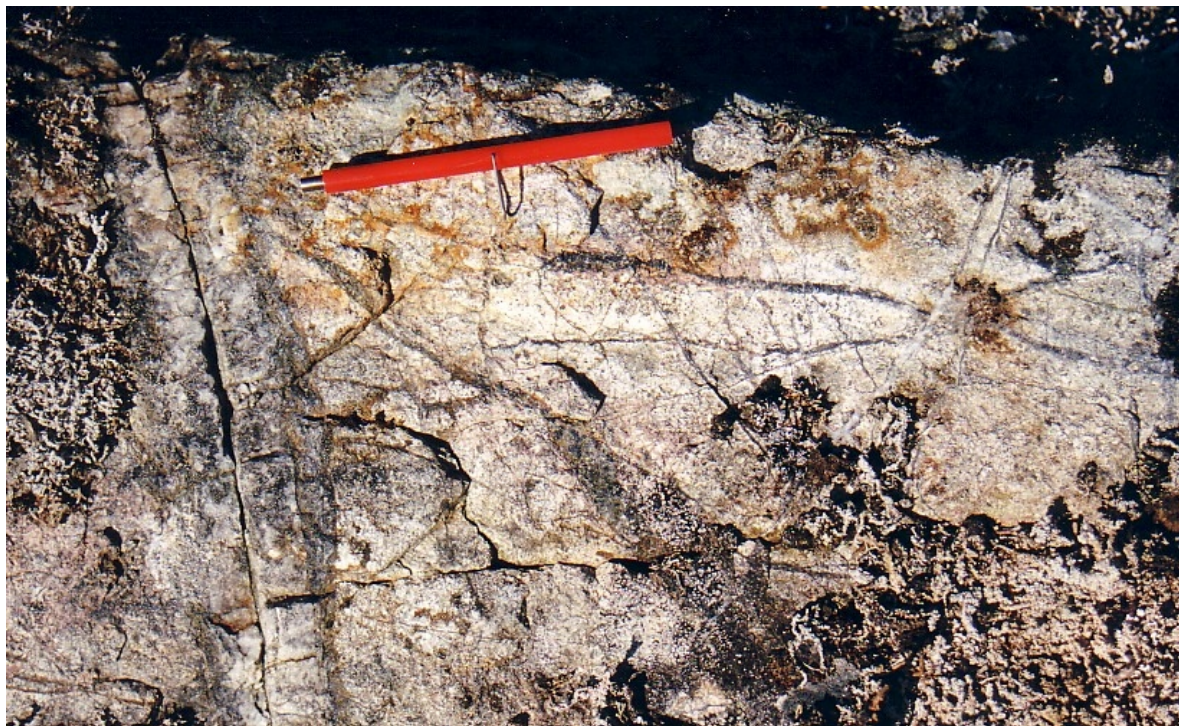


Figure 8. Stockwork Cu-Au mineralization at the Sofia showing.

- Schiarizza, P. (2004a): Geology and mineral occurrences of Quesnel Terrane, Kliyul Creek to Johanson Lake (94D/8,9); in *Geological Fieldwork 2003, BC Ministry of Energy and Mines*, Paper 2004-1, pages 83–100.
- Schiarizza, P. (2004b): Geology of Kliyul Creek–Johanson Lake area, parts of NTS 94D/8 and 9; *BC Ministry of Energy and Mines*, Open File Map 2004-5, 1:50 000 scale.
- Shives, R.B.K., Carson, J.M., Dumont, R., Ford, K.L., Holman, P.B. and Diakow, L. (2004): Helicopter-borne gamma-ray spectrometric and magnetic total field geophysical survey (parts of NTS 94D/15, E/2, 3, 6, 7, 10, 11); *Geological Survey of Canada*, Open File 4614.

Geology and Mineral Occurrences of the Quesnel Terrane between the Mesilinka River and Wrede Creek (NTS 94D/8, 9), North-Central British Columbia

By Paul Schiarizza and Sen Huy Tan

KEYWORDS: Quesnel Terrane, Takla Group, Triassic-Jurassic plutons, Hogem Batholith, volcanic sandstone, volcanic breccia, diorite, gabbro, pyroxenite, tonalite, granodiorite, copper, gold, magnetite, molybdenum

INTRODUCTION

The Johanson Lake project is a two-year bedrock mapping program initiated by the Geological Survey and Development Branch in 2003 as part of the Toodoggone Targeted Geoscience Initiative (TGI). The project is focused on a belt of Mesozoic arc volcanic and plutonic rocks of the Quesnel Terrane in the eastern part of the McConnell Creek (94D) map sheet. This area contains a number of MINFILE occurrences and numerous RGS sample sites that returned anomalously high values of gold and copper. The aim of the project is to improve the quality and detail of bedrock maps for the area and determine the setting and controls of mineral occurrences.

The initial mapping for the Johanson Lake Project was carried out in late July and August of 2003, and covered an area of about 150 km² between Kliyul Creek and Johanson Lake (Schiarizza, 2004a, 2004b). Fieldwork during the summer of 2004 extended this mapping northward to the headwaters of Wrede Creek and southward to the north margin of the Hogem Batholith, covering an additional 300 km² (Figure 1). Here, we summarize the geology of the entire project area, integrating the results of our mapping with previous geological studies within and adjacent to the area. The 2004 field program also included mapping and lithogeochemical sampling of gold occurrences in the upper Kliyul Creek and Mariposite Creek areas by contract geologists D. MacIntyre and G. Payie; the results of this work are documented separately (MacIntyre *et al.*, this volume).

The Johanson Lake project area encompasses rugged terrain within the Omineca Mountains about 350 km north-west of Prince George. The Omineca Resource Access Road provides access to a corridor through the central part of the map area, but most fieldwork was conducted from fly camps supported by the Canadian Helicopters base at the Kemess mine, 60 km north-northwest of Johanson Lake. Operating funds for the project are provided by the Toodoggone TGI and a private-public partnership agreement with Northgate Minerals Corporation.

Previous geological work within and adjacent to the Johanson Lake project area is summarized by Schiarizza (2004a). These studies include regional-scale mapping by Lord (1948) and Richards (1976a, 1976b); more detailed mapping directly east of the project area by Ferri *et al.* (1993, 2001b) and Ferri (2000a, 2000b); studies of the Takla Group by Monger (1977) and Minehan (1989a, 1989b); studies of Alaskan-type ultramafic-mafic plutons by Irvine (1974, 1976), Hammack *et al.* (1990) and Nixon *et al.* (1990, 1997); a study of granitoid intrusive rocks by Woodsworth (1976); and a study of structures related to the Finlay-Ingenika fault system by Zhang (1994), Zhang and Hynes (1991, 1992, 1994, 1995) and Zhang *et al.* (1996). In addition, the area has a history of mineral exploration dating from the early 1940s, and descriptions of many of the mineral showings are found in assessment reports on file at the offices of the British Columbia Ministry of Energy and Mines in Victoria and Vancouver.

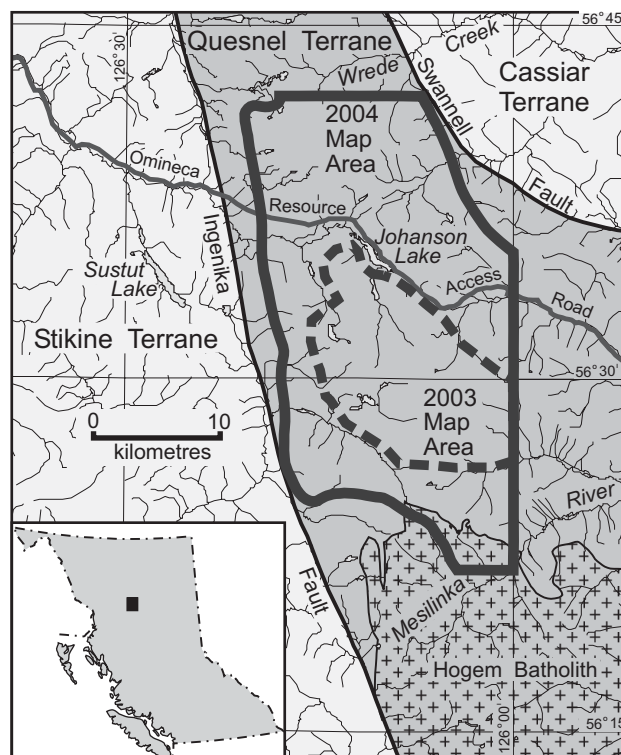


Figure 1. Location of the Johanson Lake project area, showing areas mapped during the 2003 and 2004 field seasons.

REGIONAL GEOLOGICAL SETTING

The Johanson Lake project area is underlain by the Quesnel Terrane, which includes Late Paleozoic through mid-Mesozoic volcanic, volcanoclastic and plutonic rocks formed in a system of magmatic arcs that developed along or near the western North American continental margin. East of Johanson Lake, the Quesnel Terrane is faulted against Proterozoic and Paleozoic carbonates and siliciclastics of the Cassiar Terrane, which formed part of the ancestral North American miogeocline (Fig. 2). To the south, however, the Quesnel Terrane is separated from miogeoclinal rocks by oceanic rocks of the Slide Mountain Terrane, commonly interpreted as the imbricated remnants of a Late Paleozoic marginal basin (Ferri, 1997). Along much of its length, the Quesnel Terrane is bounded to the west by the oceanic Cache Creek Terrane, which includes rocks that formed in an accretion-subduction complex related to the Quesnel magmatic arc (Travers, 1978; Struik, 1988). The Cache Creek Terrane is not present at the latitude of Johanson Lake, however, due to shuffling of terranes along Cretaceous-Tertiary dextral strike-slip faults (Gabrielse, 1985). Here, the Quesnel Terrane is juxtaposed against the Stikine Terrane, a markedly similar volcanic arc terrane, which may have originated as a northern extension of the Quesnel arc system, subsequently brought into its present position by counterclockwise oroclinal rotation and sinistral translation during the Late Triassic and Early Jurassic (Mihalyuk *et al.*, 1994).

The Quesnel Terrane is in large part represented by Upper Triassic volcanic and sedimentary rocks, which are assigned to the Takla Group in northern and central British Columbia and to the Nicola Group in the south. These rocks are locally overlain by Lower Jurassic sedimentary and volcanic rocks, and are cut by several suites of Late Triassic through Middle Jurassic plutons. In north-central British Columbia, older components of the Quesnel Terrane comprise Late Paleozoic arc volcanic and sedimentary rocks of the Lay Range assemblage, which are restricted to the eastern margin of the Quesnel belt (Ferri, 1997).

Late Triassic–Early Jurassic intrusive rocks are a prominent and economically important component of the Quesnel Terrane. These include both calcalkaline and alkaline plutonic suites, as well as Alaskan-type ultramafic intrusions. Many of these plutonic suites are found within and adjacent to the Hogem Batholith (Woodsworth, 1976; Garnett, 1978; Woodsworth *et al.*, 1991), which extends from the Johanson Lake project area more than 150 km south to the Nation Lakes area. In addition to Late Triassic–Early Jurassic rocks, the composite Hogem Batholith also includes younger granitic phases correlated with Early Cretaceous plutons that are common regionally and crosscut the Quesnel and adjacent terranes.

The structural history of the region included the development of east-directed thrust faults that juxtaposed Quesnel Terrane above Cassiar Terrane in late Early Jurassic time (Ferri, 1997, 2000a; Nixon *et al.*, 1997). To the west, east-dipping thrust faults, in part of early Middle Jurassic age, imbricate the Cache Creek Terrane and juxtapose

it above the adjacent Stikine Terrane (Monger *et al.*, 1978; Struik *et al.*, 2001). This thrusting was broadly coincident with the initiation of the Bowser basin (Ricketts *et al.*, 1992), which formed above the Stikine Terrane and contains detritus that was derived, in part, from the adjacent Cache Creek Terrane. The subsequent structural history of the region included the development of prominent dextral strike-slip fault systems in Cretaceous and Early Tertiary time. These structures include the Finlay, Ingenika and Pinchi faults, which form the western boundary of Quesnel Terrane, and may have more than 100 km of cumulative displacement (Gabrielse, 1985).

TAKLA GROUP

All stratified rocks within the Johanson Lake map area are part of the Middle to Upper Triassic Takla Group (Lord, 1948; Monger, 1977). The Takla Group is a prominent and characteristic unit of the Quesnel Terrane throughout central British Columbia, although the namesake (Takla Lake) and type area of group are found to the west of the Quesnel belt, where the name is also applied to Upper Triassic rocks of the Stikine Terrane (for a brief history of nomenclature, see Schiarizza, 2004a).

The Johanson Lake map area is at the northwest end of a belt of recent, relatively detailed mapping within the Quesnel Terrane that extends almost 250 km southward to the Nation Lakes (Ferri *et al.*, 1992, 1993, 2001a, 2001b; Ferri and Melville, 1994; Nelson and Bellefontaine, 1996). The Takla Group has not been subdivided into formal formations within this belt, although several lithologically distinct but partially coeval successions have been identified and named. The Takla rocks within the present map area are mainly or entirely Late Triassic in age, and pass eastward into equivalent rocks that Ferri *et al.* (1993, 2001b) assigned to the Plughat Mountain succession. Within the Johanson lake area, these rocks are subdivided into two main units: a heterogeneous succession of volcanoclastic, volcanic and sedimentary rocks assigned to the Kliyul Creek unit, and a more homogeneous assemblage of pyroxene-rich volcanic breccias assigned to the Goldway Peak unit (Fig. 3). Ferri *et al.* (1993, 2001b) recognized a similar subdivision of the Plughat Mountain succession to the east.

Kliyul Creek Unit

Most of the Takla Group within the Johanson Lake project area is assigned to the Kliyul Creek unit, which is equivalent to the volcanic sandstone unit of Schiarizza (2004a), and to units 1 and 2 of the Plughat Mountain succession, as subdivided by Ferri *et al.* (2001b). The Kliyul Creek unit consists mainly of volcanoclastic sandstone and breccia, but also includes limestone, siltstone and mafic volcanic rocks. Thick, somewhat arbitrarily defined packages that include conspicuous amounts of limestone have been broken out as the sandstone-carbonate subunit (in part equivalent to the sandstone-carbonate unit of Schiarizza 2004a). More discrete, relatively thin intervals dominated by thin-bedded siltstone and limestone are assigned to the

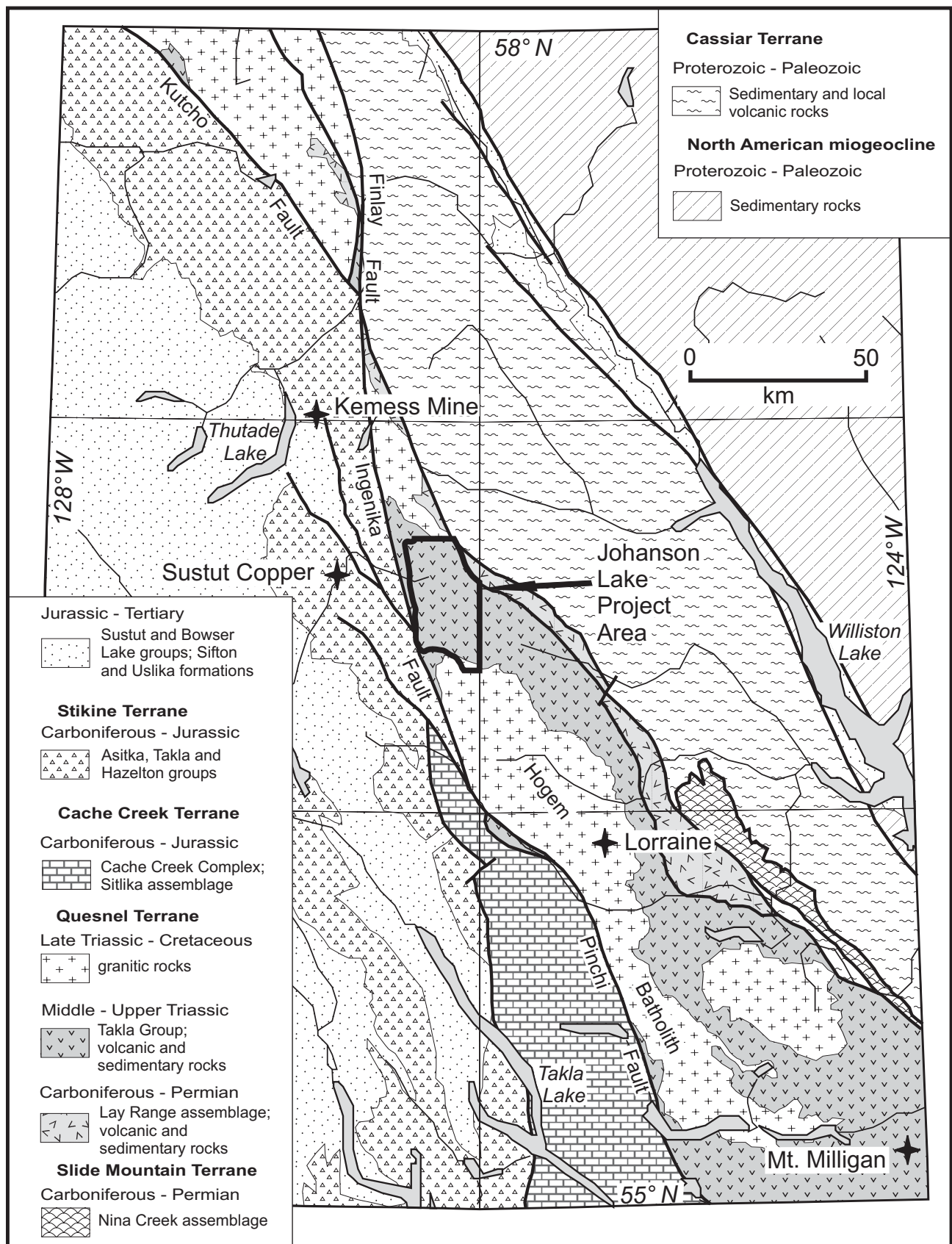


Figure 2. Regional geological setting of the Johanson Lake project area, showing locations of selected major mineral occurrences.

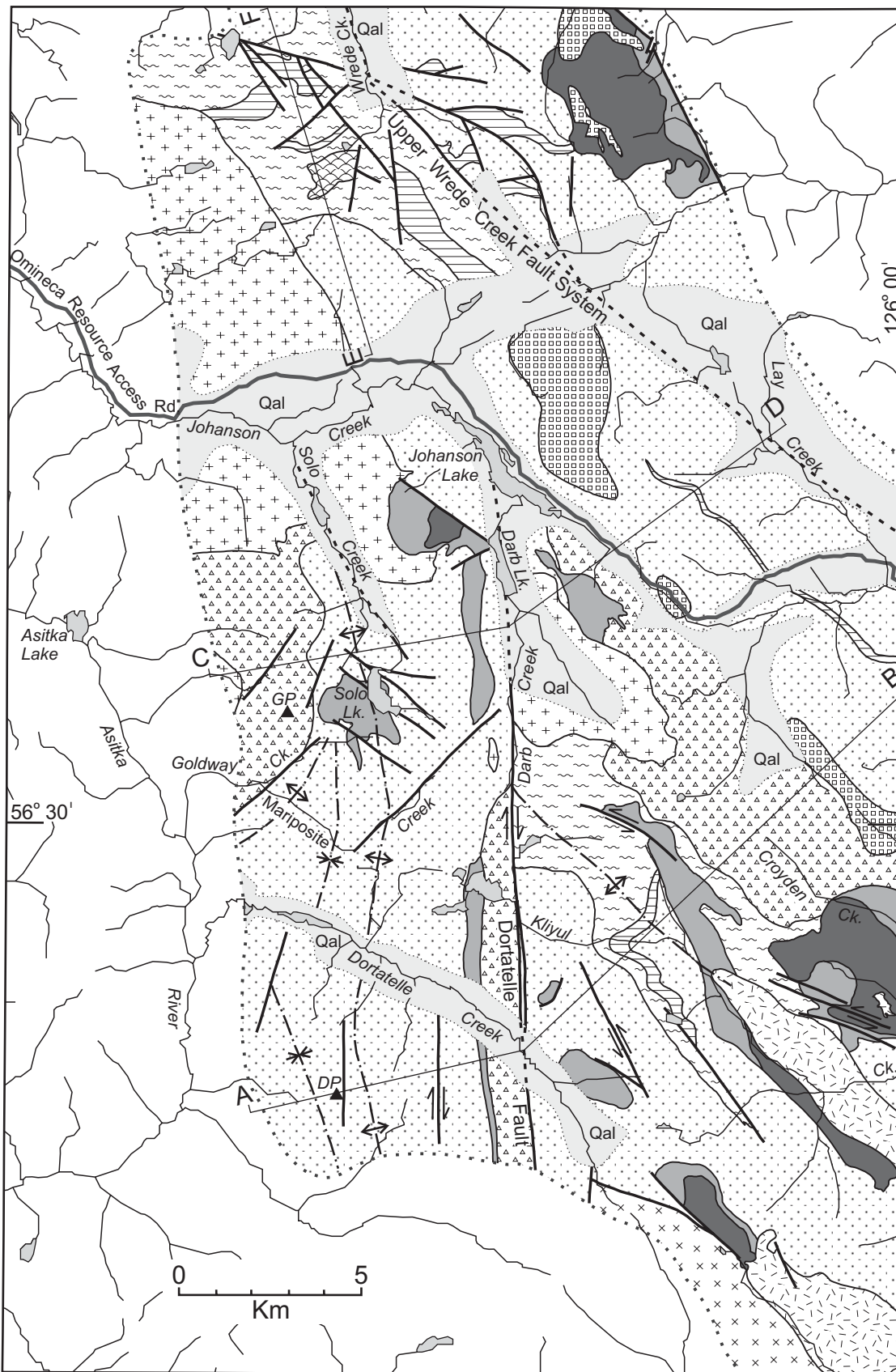


Figure 3a. Generalized geology of the Mesilinka River–Wrede Creek area, based on 2003 and 2004 fieldwork and published reports referred to in the text. Abbreviations: DP, Dortatelle Peak; GP, Goldway Peak.

siltstone-limestone subunit. These rocks generally correspond to the discontinuous sedimentary intervals within the Takla Group shown on the regional maps of Lord (1948) and Richards (1976b). The only other subunit large enough to be shown at the scale of Figure 3 is a lens of pillowed basalt that crops out in the northwest corner of the map area.

The Kliyul Creek unit is dominated by exposures of grey to green, fine to coarse-grained, commonly gritty, volcanogenic sandstone. Mineral grains of feldspar, pyroxene and less common hornblende, together with lithic fragments containing these same minerals, are the dominant constituents. The sandstone occurs partly as well-defined, thin to thick beds (Fig. 4) and partly as massive units, up to many tens of metres thick, in which bedding is not apparent. Sandstone beds within well-bedded intervals are commonly intercalated with green siltstone, also of

volcanogenic origin, and locally display graded bedding, scoured bases, flame structures and rip-up clasts.

Coarse-grained intervals, ranging from pebbly volcanogenic sandstone or lapilli tuff to coarse breccias containing fragments approaching a metre in size, are fairly common within the Kliyul Creek unit and typically form massive, resistant units tens of metres to hundreds of metres thick (Fig. 5). Volcanic rock fragments containing feldspar and/or pyroxene phenocrysts generally predominate, but clasts of aphyric volcanic rock, hornblende-feldspar porphyry, limestone, siltstone, diorite and tonalite were also observed. Locally, coarse breccia occurs as distinct layers, one to several metres thick, within intervals of much finer grained volcanic sandstone or fine breccia. These breccia units invariably contain mainly pyroxene porphyry fragments, which are supported by a matrix rich in pyroxene mineral grains. The clasts commonly range from a few centimetres to more than a metre in size, and some fragments have irregular amoeboid-like contacts and faintly chilled margins, suggesting that they were not completely cooled when they were incorporated into the breccia. These breccias probably represent mass flow deposits that tapped a different source than the finer grained sandstones with which they are intercalated.

Rocks assigned to the sandstone-carbonate subunit are generally similar to other parts of the Kliyul Creek unit, but include scattered layers and lenses of limestone. Most commonly, the limestone occurs in discontinuous intervals, from a few metres to several tens of metres thick, of interbedded limestone, grey siltstone and green volcanic sandstone to siltstone. Locally, as on the ridge south of the Darb Creek tonalite pluton, massive to bedded limestone forms lenses several tens of metres thick, but with limited strike length. Another variation occurs in the hinge area of the Kliyul Creek anticline, where dark grey limestone is mixed with volcanogenic sandstone in lenses and layers that were probably derived from slump deposits (Scharizza, 2004a). Some of these lenses comprise subequal proportions of limestone and sandstone, as patches and blocks that are intimately mixed in a chaotic fashion. In other lenses, one rock type predominates and appears to form a matrix containing clasts of the other. Similar limestone breccias form a minor proportion of the sandstone-carbonate subunit elsewhere in the area; they were noted in the northwest corner of the map area, and in a cirque basin 5.5 km north of the northwest tip of Johanson Lake.

The siltstone-limestone subunit consists mainly of thinly interbedded dark grey siltstone and limestone, although thin to thick interbeds of volcanic sandstone and calcareous sandstone are also present (Fig. 6). It typically forms distinctive reddish-weathered outcrops that are easily traced in areas of good exposure. It forms a mappable subunit that underlies the sandstone-carbonate subunit along the upper reaches of Kliyul Creek, and a possibly correlative layer that has been traced for almost 10 km on the ridges southwest of Lay Creek. In the northern part of the area, rocks assigned to the siltstone-limestone subunit occur at two (or more) stratigraphic levels, which are repeated

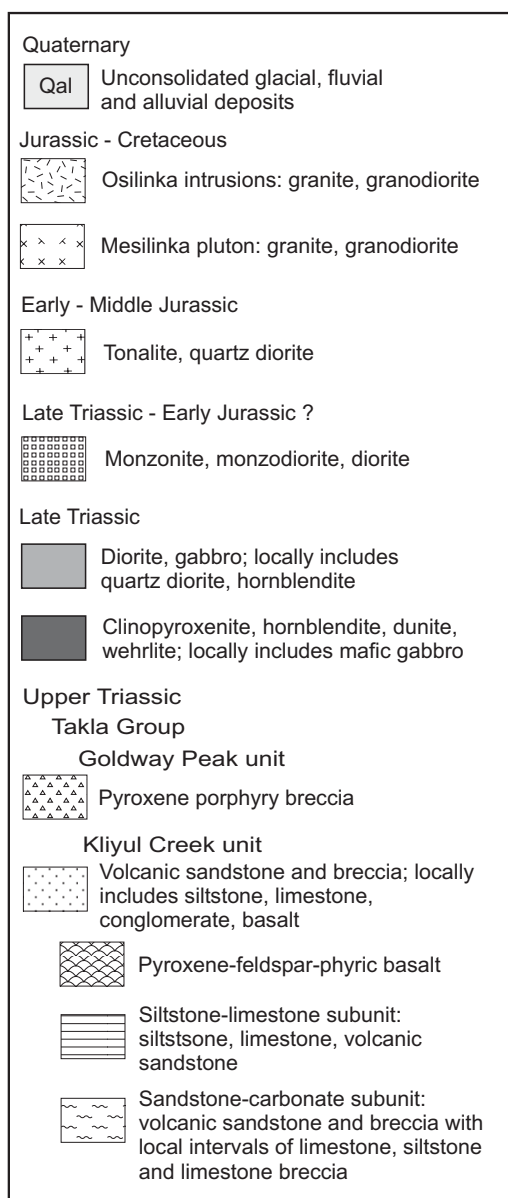


Figure 3b. Legend to accompany Figure 3a.

as numerous mappable segments that have been traced for short distances between faults related to the upper Wrede Creek system (Fig. 3).

Units of massive pyroxene porphyry and pyroxene-feldspar porphyry, derived from mafic sills, dikes and flows (?), are found at many locations within the Kliyul Creek unit but are not abundant. Pillowed basalt was observed only in the northwest corner of the map area, where it forms one mappable lens and several smaller lenses (Fig. 7). These feldspar-pyroxene-phyric pillowed flows are intercalated with volcanic sandstone, breccia and local units of siltstone and limestone of the sandstone-carbonate subunit.

Monger (1977) reported that macrofossils collected from various localities within the siltstone-limestone and sandstone-carbonate subunits of the Kliyul Creek unit are of Late Triassic (in part Late Carnian–Early Norian) age. These age assignments are corroborated by conodonts recovered from two samples collected during the 2003 field season. The samples were processed at the Geological Survey of Canada’s micropaleontology laboratory in Vancouver, and the conodonts were identified by M.J. Orchard. Both collections were from the sandstone-carbonate subdivision. One, from a limestone lens about 2 m thick on the ridge between the two main forks of upper Kliyul Creek, contained conodonts of Late Triassic (probably Carnian) age. The other sample, from a thick limestone lens on the ridge south of the Darb Creek pluton, yielded conodonts of Late Triassic (probably Early Norian) age.



Figure 4. Well-bedded volcanic sandstone of the Kliyul Creek unit, south of the west branch of Kliyul Creek.

Goldway Peak Unit

Breccias containing fragments of pyroxene-phyric basalt are fairly common within the Kliyul Creek unit, where they are intercalated with most other rock types within the unit. Pyroxene-rich volcanic breccias also occur as thick, monotonous accumulations of mappable extent in several places in the map area. These belts are assigned to the Goldway Peak unit, and are well represented on the mountain of that name, and on the ridge system north of the mountain. This unit is also well exposed in a northwest-trending belt that extends from the east edge of the map area at Croyden Creek to the southeast end of Johanson Lake, and as a narrow belt directly west of the Dortatelle fault in the southern part of the map area. In each of these exposure belts, the Goldway Peak unit rests stratigraphically above the more heterogeneous and better stratified Kliyul Creek unit, and represents the highest exposed levels of the Takla Group. The Goldway Peak unit is equivalent to the volcanic breccia unit of Schiarizza (2004a) and, at least in part, to unit 3 of the Plughat Mountain succession mapped by Ferri *et al.* (2001b) to the east.

Volcanic breccias of the Goldway Peak unit typically form resistant, blocky, green-brown to rusty-brown weathered exposures. Fresh surfaces are dark green to grey-green. Fragments are typically angular to subangular, and generally range from a few centimetres to 10 cm in diameter (Fig. 8). However, coarse, poorly-sorted breccias with fragments up to several tens of centi-



Figure 5. Volcanic breccia of the Kliyul Creek unit, on the ridge system between Dortatelle and Kliyul creeks.

metres in size are not uncommon. The breccia fragments are dominantly pyroxene and pyroxene-feldspar-phyric basalt, with considerable textural variation among different clasts based on size, abundance and feldspar versus pyroxene proportions in the phenocryst population. Other clast types include feldspar porphyry, hornblende-feldspar porphyry, aphyric basalt, diorite and pyroxenite. The matrix typically consists of pyroxene, small pyroxene-bearing lithic grains and lesser amounts of feldspar. The matrix is locally calcareous and recessive, causing the fragments to stand out in relief. In some other places, the compositional similarity between clasts and matrix obscures the fragmental texture.

Internal bedding contacts between individual breccia layers within the Goldway Peak unit are generally not evident, although a vague stratification can be observed in some cliff-face exposures. However, bedding is locally defined by thin intervals of pyroxene-rich sandstone, which occurs as thin to medium, locally graded beds. Also present in relatively minor quantities are units of massive pyroxene porphyry derived from sills, dikes and possibly flows.

The Goldway Peak unit is not directly dated. However, it overlies and interfingers with the Kliyul Creek unit, which contains Late Triassic fossils, and the lower part of the unit is locally cut by the Late Triassic Abraham Creek



Figure 6. Interbedded siltstone, limestone and volcanic sandstone of the siltstone-limestone subunit, east of Wrede Creek in the northern part of the area.

mafic-ultramafic complex. The Goldway Peak unit is therefore assigned a Late Triassic age with some confidence.

INTRUSIVE ROCKS

The Takla Group within the Johanson Lake project area is cut by a large number of intrusions. These are provisionally subdivided into four major suites, based on compositions and relative ages. These suites are 1) a Late Triassic ultramafic-mafic suite; 2) a monzonite-diorite suite of uncertain age; 3) early Middle Jurassic tonalite; 4) granite and granodiorite of, at least in part, Jura-Cretaceous age.

Late Triassic Ultramafic-Mafic Suite

The oldest intrusive suite within the map area comprises mafic and ultramafic rocks. These include typical Alaskan-type ultramafic-mafic complexes such as the Wrede Creek complex, similar but mafic-dominant complexes such as Johanson Lake and Abraham Creek, and diorite to gabbro stocks that do not include ultramafic rocks. Previously published K-Ar dates and new U-Pb dates indicate that these rocks are Late Triassic in age, consistent with Irvine's (1974) suggestion that the Alaskan-type complexes are subvolcanic intrusions associated with Takla volcanism.

WREDE CREEK ULTRAMAFIC-MAFIC COMPLEX

The Wrede Creek ultramafic-mafic complex crops out in the northwest corner of the map



Figure 7. Pillowed pyroxene-feldspar-phyric basalt from the Kliyul Creek unit, northwestern corner of map area.

area (Fig. 3). It intrudes the Kliyul Creek unit of the Takla Group along its southern and western margins, and is faulted against the Takla Group along a splay of the Lay Range fault to the northeast (Ferri, 2000a, 2000b). It is locally intruded by younger granitic rocks assigned here to the monzonite-diorite suite. The Wrede Creek complex was described briefly by Irvine (1974, 1976) and Wong *et al.* (1985), prior to being mapped in more detail by Hammack *et al.* (1990) and Nixon *et al.* (1997). It was not re-mapped during the present study, but is shown on Figure 3, and briefly summarized here, after Nixon *et al.* (1997).

The Wrede Creek complex exhibits features common to many Alaskan-type ultramafic-mafic bodies, including a crude concentric zonation and gradation of rock types, from dunite in the core to gabbro along the margins; cumulate textures in olivine clinopyroxenites; and local modal layering in gabbro. Dunite forms more than half of the ultramafic part of the complex, and is locally in direct contact with Takla country rocks along the western and southern margins. The dunite contains local narrow pods and schlieren of chromitite, and is cut by pods and dikes of pegmatite composed of hornblende and calcic plagioclase. The dunite grades outward into a narrow zone of olivine clinopyroxenite and wehrlite along the southwestern margin of the complex, and grades into a more extensive zone of clinopyroxenites in the northeastern part of the complex. The latter zone in turn grades into gabbro and diorite that form much of the eastern and southeastern margins of the complex (Fig. 3).

Wong *et al.* (1985) reported that hornblende separates from a pegmatite within dunite in the southwestern part of the Wrede Creek complex yielded K-Ar isotopic dates of 219 ± 10 Ma and 225 ± 8 Ma, and inferred that these dates approximate the crystallization age of the complex. This interpretation is corroborated by the similarity of these dates to the U-Pb isotopic dates obtained during the present study from the Abraham Creek complex and Solo Lake stock.

DORTATELLE ULTRAMAFIC-MAFIC COMPLEX

The Dortatelle ultramafic-mafic stock crops out 2 km east of the divide at the head of Dortatelle Creek (Fig. 3). It intrudes the Kliyul Creek unit of the Takla Group to the north and northeast, is bounded by a fault and the Mesilinka phase of the Hogem Batholith to the southwest, and is truncated by the Osilinka phase of the Hogem Batholith at its southeast end. The southern part of the complex was described briefly by Irvine (1976) and was also mapped during the 2004 field season. The north end of the complex is shown after Cooke (1972).



Figure 8. Pyroxene porphyry breccia, Goldway Peak unit, upper Croyden Creek.

The Dortatelle ultramafic-mafic complex displays an imperfect zonation that is truncated by the fault and granitic rocks on its south and southwest margins. It is dominated by wehrlitic rocks that locally grade into dunite along the southwestern edge of the complex, and into clinopyroxenite to the northeast. The clinopyroxenite in turn passes northeastward into strongly linedated hornblende gabbro that forms the outer margin of the complex. Northeast-striking layering was observed at several locations within the wehrlitic zone, where it is defined by centimetre to decimetre-thick layers with contrasting modal proportions of olivine and clinopyroxene. Lord (1948) noted that there are grains and blebs of chromite within the Dortatelle complex; the presence of chromite grains within dunite was confirmed during the present study, but no significant concentrations (*i.e.*, chromitite) were noted.

ABRAHAM CREEK MAFIC-ULTRAMAFIC COMPLEX

Ultramafic and mafic rocks exposed near the eastern edge of the map area, along Croyden and Porphyry creeks, form the northwestern end of a large, markedly elongate pluton, referred to as the Abraham Creek complex, that extends for 24 km into the adjacent Aiken Lake map area (Ferri *et al.*, 1993, 2001b). Within the Johanson Lake map area, the Abraham Creek complex has been subdivided into a central unit of mainly clinopyroxenite, hornblende and mafic gabbro, and a unit dominated by diorite, gabbro and microdiorite that flanks the ultramafic rocks to the north and south. Dikes of diorite, microdiorite, diabase, pyroxene porphyry, hornblende-feldspar porphyry and monzodiorite are common within both mappable units, and are thought to be an integral part of the intrusive complex (Schiarizza, 2004a). Although ultramafic rocks and associated mafic

gabbro constitute about 50% of that part of the pluton exposed in the Johanson Lake area, these rocks are distinctly subordinate to dioritic rocks elsewhere within the complex (Ferri *et al.*, 2001b).

A sample of diorite from the southern part of the Abraham Creek complex was collected during the 2003 field season and submitted to the geochronology laboratory at the University of British Columbia for isotopic dating. Zircons extracted from this sample yielded a U-Pb date of 219.5 ± 0.6 Ma (R. Friedman, University of British Columbia, personal communication, 2004), which is interpreted as a crystallization age for this part of the complex.

KLIYUL CREEK MAFIC-ULTRAMAFIC COMPLEX

The Kliyul Creek mafic-ultramafic complex is a narrow pluton, 13 km long, that extends from the ridges south of Kliyul Creek, near the eastern edge of the map area, northwestward to the headwaters of the creek (Fig. 3). It intrudes the Kliyul Creek unit of the Takla Group, and is itself cut by a granitic stock at its southeast end. The southeastern end of the Kliyul Creek complex was mapped by Irvine (1976) as mainly peridotite, locally with a border phase of hornblende gabbro. These rocks are inferred to continue northwestward, across the drift-covered lower reaches of two major tributaries of Kliyul Creek, into exposures of peridotite, gabbro, diorite and monzodiorite that crop out along the southwest slopes of Kliyul Creek (Noel, 1971b; Gill, 1994). From there the pluton crosses to the northeast side of Kliyul Creek and extends to the headwaters of the creek. The northwestern part of the pluton consists mainly of diorite, microdiorite, monzodiorite and gabbro, but includes local patches of clinopyroxenite and hornblendite (Schiarrizza, 2004a).

JOHANSON LAKE MAFIC-ULTRAMAFIC COMPLEX

The Johanson Lake mafic-ultramafic complex is located in the central part of the map area, about 1.5 km southwest of Johanson Lake. These rocks were described briefly by Irvine (1976) and were subsequently studied in more detail by Nixon *et al.* (1990, 1997). They were not remapped during the present study, but are shown on Figure 3 after Nixon *et al.*, who subdivided the complex into two units: a core of mainly clinopyroxenite and hornblendite, and a more voluminous outer unit consisting mainly of gabbro and diorite.

The Johanson Lake complex intrudes the Kliyul Creek unit of the Takla Group, and is itself cut by tonalite of the Johanson Creek pluton. Stevens *et al.* (1982, sample GSC 80-46) reported that unaltered hornblende from coarse-grained hornblendite of the Johanson Lake complex yielded a K-Ar isotopic date of 232 ± 13 Ma. This date has large analytical uncertainty but is, within error, the same as the Late Triassic K-Ar and U-Pb dates that have been obtained from the Wrede, Abraham Creek and Solo Lake complexes (Wong *et al.*, 1985; this study).

DIORITE-GABBRO PLUTONS

Most of the diorite to gabbro plutons included within the ultramafic-mafic suite occur in the central part of the map area and are described by Schiarizza (2004a). These include a stock south of the east end of Johanson Lake, an elongate stock west of Darb Creek, the Solo Lake stock, and a sill-like body that occurs along the contact between the Kliyul and Goldway Peak units west of the Dortatelle fault (Fig. 3). A fairly large diorite stock that was mapped along a major west-flowing tributary to upper Dortatelle Creek during the 2004 field season is also included in this suite. These plutons are lithologically similar to the dioritic phases within the composite ultramafic-mafic intrusive bodies, and some host copper-gold mineralization similar to that associated with diorite of the Abraham Creek and Kliyul Creek complexes. Their inclusion in the ultramafic-mafic suite is corroborated by a U-Pb zircon date of 223.6 ± 0.8 Ma that was obtained on a sample of diorite collected from the Solo Lake stock in 2003 (Richard Friedman, University of British Columbia, personal communication, 2004).

Triassic-Jurassic Monzonite-Diorite Suite

Intrusive rocks assigned to the monzonite-diorite suite are represented by a fairly large monzonite pluton northeast of Johanson Lake, a small stock of similar composition that crops out along the Omineca Resource Access Road 3 km to the southeast, and an elongate diorite to monzodiorite pluton still farther to the southeast, along the eastern boundary of the map area (Fig. 3). Also tentatively included in this suite are dioritic and monzonitic rocks that intrude the Takla Group and Wrede Creek ultramafic-mafic complex in the northeast corner of the map area.

The Johanson Lake pluton and the small stock exposed along the road consist mainly of light grey to pinkish grey weathered, medium to coarse-grained hornblende monzonite, commonly with pink feldspar phenocrysts from 1 to 2 cm in size. Magnetite is a common accessory, and the Johanson Lake pluton has a prominent expression on regional aeromagnetic maps. Contacts with the adjacent Takla Group are generally sharp, but a zone of monzodiorite and diorite dikes extends for up to 1 km east of the Johanson Lake pluton. These monzonite bodies are not dated, but samples have been collected and submitted to the geochronology laboratory at the University of British Columbia for U-Pb isotopic dating. Monzonitic intrusions that have been dated by the U-Pb method elsewhere in the region include a latest Triassic stock at the Cat copper-gold porphyry deposit, and Early Jurassic stocks at the Mount Milligan copper-gold porphyry deposit (Mortensen *et al.*, 1995).

The elongate pluton that intrudes the Takla Group at the eastern edge of the map area consists of medium-grey hornblende diorite, quartz diorite and quartz monzodiorite. The texture is typically medium grained, isotropic and equigranular to plagioclase porphyritic. Dikes of similar composition are fairly common within the Takla Group for several kilometres north of the pluton.

The rocks assigned to the monzonite-diorite suite in the northeast corner of the area were not examined during the present study, but are shown after Nixon *et al.* (1997), who described them as hornblende-bearing quartz monzonite, monzonite, quartz diorite and diorite. The northern intrusive body within this area may be continuous with the southern end of the Fleet Creek pluton, which extends for 25 km to the northwest and consists mainly of monzodiorite and diorite (Richards, 1976b). Wong *et al.* (1985) reported that hornblende from a diorite dike that cuts the Takla Group south of the Wrede Creek ultramafic-mafic complex yielded a K-Ar isotopic date of 172 ± 6 Ma. Farther north, biotite and hornblende separates from diorite collected from the main body of the Fleet Creek pluton have yielded discordant K-Ar dates of 156 ± 5 Ma and 142 ± 12 Ma, respectively (Wanless *et al.*, 1979, samples GSC 78-14 and GSC 78-15). None of these K-Ar dates are likely to reflect crystallization ages for this intrusive suite.

Early Middle Jurassic Tonalite Suite

The tonalite intrusive suite is represented by two large plutons in the central and northwestern part of the map area, and by a number of smaller plugs of similar composition in the same geographic area. These rocks intrude the Takla Group as well as older plutonic rocks of the ultramafic-mafic suite.

DARB CREEK PLUTON

The Darb Creek pluton comprises light grey weathered, medium to coarse-grained hornblende-biotite tonalite that is well exposed on the slopes surrounding the prominent eastern tributary of Darb Creek (Schiarizza, 2004a). The pluton cuts the contact between the Kliyul Creek and Goldway Peak units of the Takla Group along its southern margin, and on its northeast margin truncates the southern margin of a dioritic stock that straddles this same stratigraphic contact (Fig. 3). Where observed, the contacts are sharp, although the tonalite commonly contains abundant xenoliths of country rock for a few tens of metres along its outer margin. The Darb Creek pluton is apparently truncated by the Dortatelle fault to the west, but this contact was not observed.

Zircon extracted from a tonalite sample from the southern part of the Darb Creek pluton has yielded a preliminary U-Pb isotopic date of 177 Ma, and titanite from the same sample gives a U-Pb date of 174.0 ± 2.0 Ma (R. Friedman, University of British Columbia, personal communication, 2004). These dates indicate that the pluton crystallized in the earliest Middle Jurassic (using the Jurassic time scale of Pálffy *et al.*, 2000).

JOHANSON CREEK PLUTON

The Johanson Creek pluton is a large tonalitic intrusion with an outcrop extent of about 12 by 6 km along the northwest edge of the map area. It cuts the Kliyul Creek and Goldway Peak units of the Takla Group, and locally the Johanson Lake mafic-ultramafic complex. The western margin of the pluton is largely obscured by drift, but regional maps suggest that it is truncated by the Ingenika

fault. The southern boundary of the pluton shows an apparent dextral offset of 2 km along the drift-filled valley of Solo Creek; a post-pluton dextral fault is therefore inferred to follow the valley.

The Johanson Creek pluton consists mainly of light grey, medium to coarse-grained hornblende-biotite tonalite, locally grading to quartz diorite. The texture is isotropic through most of the pluton, but locally it displays a weak, steeply dipping, west to northwest-striking foliation defined by the alignment of mafic grains and tabular feldspar crystals. Where observed, external contacts are sharp; xenoliths of country rock typically occur only within the outer few metres of the pluton, and narrow dikes of tonalite likewise extend for only a few metres into the adjacent country rock. At one locality along the pluton's eastern margin, however, the contact is defined by a border phase, about 200 m wide, of medium grey hornblende diorite cut by tonalite and quartz monzonite dikes.

Wanless *et al.* (1979, samples GSC 78-12 and GSC 78-13) reported that biotite and hornblende separates from a sample of the Johanson Creek pluton yielded discordant K-Ar dates of 121 ± 4 Ma and 142 ± 12 Ma, respectively. A sample collected during the 2004 field season is currently being processed for U-Pb dating of zircons. We suspect that the pluton will yield an Early to Middle Jurassic crystallization age, similar to that of the Darb Creek pluton.

Jurassic-Cretaceous Granite and Granodiorite

Exposures of granite and granodiorite are restricted to the southern part of the map area, where they constitute part of the northern tip of the Hogem Batholith and several related stocks and plugs north of the batholith. These granitic rocks are subdivided into two phases, the Mesilinka pluton and the Osilinka stocks, following Woodsworth (1976).

MESILINKA PLUTON

The western exposures of granitic rock at the south end of the Johanson Lake project area are part of the Mesilinka pluton, a prominent component of the northwestern part of the Hogem Batholith (Woodsworth, 1976). Within the Johanson Lake map area, the pluton consists mainly of coarse-grained biotite monzogranite to quartz monzonite, commonly with K-feldspar and plagioclase phenocrysts up to 2 cm in size. These rocks are characterized by a strong north-plunging lineation, defined by elongate biotite clots and stretched feldspar and quartz grains, and a less pronounced northeast-dipping foliation. The monzogranite is cut by numerous dikes of aplite and pegmatite along its northeast margin, some of which crosscut the foliation and lineation. It is not clear whether these dikes are related to the Mesilinka pluton or to the adjacent Osilinka stock. Where observed, the contact with adjacent ultramafic rocks of the Dortatelle complex is a steeply-dipping, northwest-striking fault defined by mylonitic granitic rocks. However, there are screens and xenoliths of ultramafic rocks within the northeastern margin of the pluton, suggesting an original intrusive relationship. The contact between the Mesilinka pluton and the Takla Group to the north was not

observed, but is mapped as a fault after Woodsworth (1976).

The Mesilinka pluton was assigned an Early Jurassic age by Woodsworth (1976), but this was revised to Cretaceous by Woodsworth *et al.* (1991), in part because Eadie (1976) obtained K-Ar biotite dates of 101 ± 4 Ma and 112 ± 4 Ma from samples collected to the south and southeast of the Johanson Lake map area. A sample collected from the northern part of the pluton during the 2004 field season has been submitted to the geochronology laboratory at the University of British Columbia for U-Pb dating of zircons in order to determine a crystallization age for this part of the pluton.

OSILINKA STOCKS

Woodsworth (1976) considered several small, commonly elongate stocks of granite and granodiorite that he mapped within and adjacent to the northern Hagem Batholith to be the youngest granitic phases in the area, and Woodsworth *et al.* (1991) referred to these small plutons as the Osilinka stocks. Within the Johanson Lake project area, the Osilinka stocks are represented by the eastern part of the Hagem Batholith, an elongate pluton along Kliyul Creek and the small Davie Creek plug farther north, as well as by small plugs and dikes elsewhere in the southeastern part of the area that are too small to be shown on Figure 3. Collectively these stocks intrude the Takla Group and ultramafic-mafic plutons of the Dortatelle, Kliyul Creek and Abraham Creek complexes. The southern stock is also in contact with the Mesilinka pluton, but the relative ages of these two granitic bodies was not established by observed crosscutting relationships.

The Osilinka stocks within the Johanson Lake map area consist mainly of grey to pinkish weathered, medium to coarse-grained, equigranular biotite granodiorite to monzogranite. The stock within the Hagem Batholith locally includes a marginal phase of aplitic biotite-muscovite granite, and contains numerous dikes of aplite and pegmatite. Textures are for the most part isotropic, but the western part of the stock within the Hagem Batholith is weakly to moderately lineated and foliated, as are adjacent rocks of the Mesilinka pluton and Dortatelle ultramafic-mafic complex.

An Osilinka stock to the east-southeast of the Johanson Lake map area has yielded a biotite K-Ar date of 122 ± 6 Ma (Wanless *et al.*, 1972, sample GSC70-11), and a stock to the south yielded a biotite K-Ar date of 120 Ma (G. Woodsworth, unpublished data, reported in Woodsworth *et al.*, 1991). However, the latter stock has recently yielded a much older U-Pb zircon date of 192.3 ± 2.1 – 4.8 Ma (Nelson *et al.*, 2003; J. Nelson, personal communication, 2003), indicating an Early Jurassic crystallization age, whereas the Davie Creek stock, which was sampled in 2003 (Schiarizza, 2004a), has yielded a preliminary U-Pb zircon date of 132 to 150 Ma, indicating Late Jurassic or Early Cretaceous crystallization (R. Friedman, University of British Columbia, personal communication, 2004). These U-Pb dates suggest that the Osilinka stocks include rocks of at least two different ages. A sample collected from the

Osilinka stock at the north end of the Hagem Batholith in 2004 has been submitted to the geochronology laboratory at the University of British Columbia for U-Pb dating in order to further constrain the crystallization ages of this suite of plutons.

STRUCTURE

Mesoscopic Structure and Metamorphism

The Takla Group within most of the map area is at greenschist-facies metamorphic grade. Mafic volcanoclastic rocks are characterized by the metamorphic assemblage chlorite-epidote-actinolite, commonly accompanied by carbonate and leucocene. These minerals partially to completely replace original pyroxene crystals. Relict feldspar grains are albitized, at least in part, and partially replaced by epidote, calcite and white mica. The metamorphic assemblages observed within the Takla Group are also found within plutonic rocks of the Late Triassic mafic-ultramafic suite. Younger plutons show variable chlorite-epidote alteration but are generally not conspicuously metamorphosed. It is not clear whether this reflects the predominant age of metamorphism or the more felsic composition and massive nature of the younger plutons.

Outcrops within the project area are characterized by abundant fractures and brittle faults. These structures have highly variable orientations, although northwest to north strikes and steep dips predominate. Many of the northwest to north-striking faults show indications of dextral strike-slip movement, although northwest-striking faults in the Croyden Creek–Kliyul Creek area are mainly sinistral. Many east to northeast-striking mesoscopic faults also show a sinistral sense of displacement; these may be conjugate riedel shears related to the more abundant north to northwest-striking dextral faults.

Penetrative foliations occur mainly within high-strain zones associated with faults. However, a weak slaty cleavage of more regional aspect is apparent locally. In the southwestern part of the area, this cleavage is axial planar to mesoscopic folds that occur on the limbs of larger macroscopic folds. Mesoscopic folds are not common elsewhere in the area, and those seen are typically localized along faults.

Map-scale Structure

The macroscopic structure of the Johanson Lake map area will be discussed in terms of four domains and two fault systems that separate these domains. The southern part of the area is divided into southeast and southwest domains by the north-striking Dortatelle fault. The northern part of the area is divided into northeast and northwest domains by the northwest-trending upper Wrede Creek fault system.

DORTATELLE FAULT

The Dortatelle fault is a prominent north-trending structure in the south-central part of the map area. It has a prominent topographic expression and marks the trunca-

tion of the Darb Creek pluton and Kliyul Creek anticline on its east side, and localizes a narrow sliver of the Goldway Peak unit on its west side. Rocks adjacent to the fault are commonly strongly foliated for several hundred metres beyond the fault trace. Parts of the fault were studied in detail by Zhang and Hynes (1994), who demonstrated that it was a dextral strike-slip fault on the basis of the geometric relationships between S and C surfaces and associated folds. Richards (1976a, 1976b) showed the fault being truncated by, or merging with, the Ingenika fault 20 km south of Dortatelle Creek. The fault does not appear to continue as a prominent structure north of Johanson Lake (Fig. 3).

SOUTHEAST DOMAIN

The structure east of the Dortatelle fault is dominated by the northwest-trending Kliyul Creek anticline, which is defined by opposing dips and facing directions in the Kliyul Creek unit of the Takla Group (Fig. 9, section A-B). The extensive exposures of the overlying Goldway Peak unit to the northeast are presumed to be preserved in the core of an adjacent syncline, but this structure is not well defined due to the few bedding measurements obtained from the Goldway Peak unit.

Steeply dipping, northwest to west-northwest-striking faults with kinematic indicators showing predominantly

sinistral strike-slip displacements are prominent features of the southeast domain (Fig. 10). Most of these were described by Schiarizza (2004a), but additional sinistral faults were mapped east of upper Dortatelle Creek during the 2004 field season, and MacIntyre et al. (this volume) show that a prominent structure cutting the north end of the Kliyul Creek mafic-ultramafic complex was also the locus of sinistral displacement. Most of the sinistral faults are within or peripheral to plutons of the Late Triassic mafic-ultramafic suite, which show a marked elongation parallel to the faults. It is suspected that the sinistral faults are broadly contemporaneous with intrusion of these plutons.

In the southern part of the domain, in the area of mutual contact between the two phases of the Hagem Batholith and the Dortatelle ultramafic-mafic complex, all rocks commonly display a strong L-tectonite fabric that plunges gently to moderately northward. Map-scale structures in this area include a north-northwest-striking brittle fault that marks an apparent dextral offset of the northern margin of the Osilinka phase, and a steep northwest-striking fault, locally defined by a narrow mylonite zone, that in part separates the Mesilinka pluton from the Dortatelle ultramafic-mafic complex. The latter fault, or a major splay from it, is inferred to extend to the west-northwest and define the contact between the Mesilinka pluton and the Takla Group,

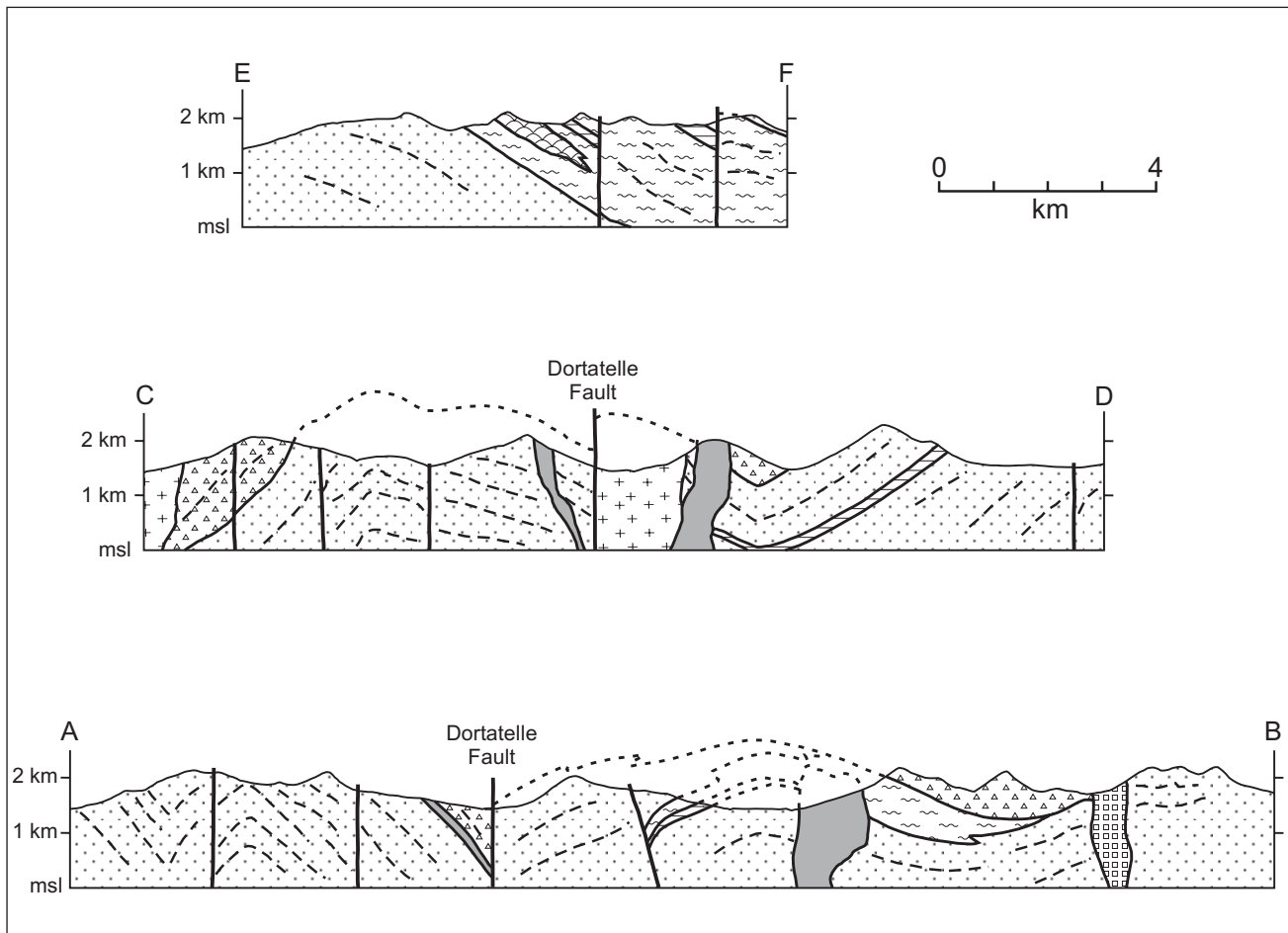


Figure 9. Schematic vertical cross-sections along lines shown on Figure 3a. See Figure 3b for legend.



Figure 10. Sinistral fault cutting south margin of the Abraham Creek mafic-ultramafic complex near eastern edge of map area, north of Kliyul Creek.

based on the observations of Woodsworth (1976), who reported that rolled K-feldspar megacrysts within mylonitized plutonic rock along this contact show that the Takla rocks moved southward over the pluton.

SOUTHWEST DOMAIN

The structure west of the Dortatelle fault is dominated by the north-trending Solo Lake anticline (Fig. 9, sections A-B and C-D). In the south, the eastern limb of the anticline consists of a homoclinal panel of the Kliyul Creek unit several kilometres wide that is overlain by the Goldway Peak unit adjacent to the Dortatelle fault. To the north, from Mariposite Creek to Solo Lake, this panel is disrupted by northeast and northwest-striking faults, and northward from there it comprises rocks that dip and face mainly to the north or northeast. The western limb of the Solo Lake anticline is folded across several, mainly north-plunging, subsidiary folds, including an anticline-syncline pair that is mapped south of Goldway Creek. These folds seem to die out to the north, and northwest of Solo Lake the Kliyul Creek unit forms a west-facing, locally overturned panel that is stratigraphically overlain to the west by the Goldway Peak unit.

Steeply dipping, north to north-northeast-striking faults are a prominent feature of the southern and western portions of the southwest domain. Many of these are marked by conspicuous orange-weathered zones of Fe-Mg carbonate alteration. Others exhibit quartz-pyrite alteration or are defined by zones, up to tens of metres wide, of strongly foliated chlorite schist. Shear bands cutting chlorite schist within one north-striking fault zone in the southern part of the domain indicate dextral strike-slip movement.

Northwest to west-northwest-striking faults are prominent structures around Solo Lake. A history of dextral movement along these faults is indicated by geometrical relationships at the Solo and Bruce mineral occurrences, where northwest-striking fault zones within the Solo Lake stock locally host en echelon arrays of more northerly striking gold-bearing quartz veins (Richards, 1991). Farther north, a north-northwest-striking dextral fault is inferred to occupy the drift-covered valley of Solo Creek, based on an apparent dextral offset of the southern margin of the Johanson Creek pluton (Fig. 3).

Zhang and Hynes (1991) inferred that a northeast-striking fault along the upper reaches of Mariposite Creek was the locus of sinistral displacement, based on the offset of local stratigraphy within the Takla Group. An east-northeast-striking fault west of Darb Lake may also be sinistral, if the elongate diorite stock to the south correlates with the diorite unit at the south end of the Johanson Lake mafic-ultramafic complex (Fig. 3). These sinistral faults, and northeast-striking sinistral faults elsewhere in the map area (Zhang and Hynes, 1991; Schiarizza, 2004a) are interpreted as conjugate riedel shears (R' of Tchalenko, 1970) within the system of mainly northwest to north-striking dextral faults that formed during regional motion along the Finlay-Ingenika fault system (Zhang and Hynes, 1991, 1994).

UPPER WREDE CREEK FAULT SYSTEM

A system of mainly northwest-striking faults, informally referred to as the upper Wrede Creek fault system, extends from the northwest corner of the map area southeastward to the broad drift-covered valley north of the Johanson Lake monzonite pluton (Fig. 3). Individual faults within this system are locally defined by abrupt truncations of subunits within the Kliyul Creek unit of the Takla Group. Unequivocal indications of movement sense were not documented during the present study, although Zhang and Hynes (1991) interpreted most northwest-striking faults in this area as dextral strike-slip faults. The fault system is inferred to extend southeastward along the upper reaches of Lay Creek to the eastern boundary of the map area, although it is not exposed over this distance. At the eastern edge of the map area, it apparently connects with a collinear system of faults mapped by Ferri *et al.* (2001b) as the Polaris Creek dextral strike-slip fault system.

NORTHWEST DOMAIN

The Kliyul Creek unit in the northwestern part of the map area, southwest of the upper Wrede Creek fault system, generally dips moderately to gently northward (Fig. 9,

section E-F) but displays many local truncations and disruptions along north to northwest-striking faults. Most of these faults are spatially associated with the upper Wrede Creek system and are thought to be subsidiary dextral or extensional faults related to that system. A northeast-striking fault, defined by the apparent truncation of several northwest-trending structures, is shown as a sinistral fault by Zhang and Hynes (1991), and may be an antithetic riedel shear related to the dextral system.

NORTHEAST DOMAIN

The Takla Group northeast of the upper Wrede Creek fault system is represented by moderately to gently dipping strata of the Kliyul Creek unit. Dip direction is variable but, in contrast to the northwest domain, is mainly to the south. Steeply dipping, east-striking faults of unknown sense of displacement were mapped in several places, and are commonly marked by zones of orange-weathered carbonate-altered rock. A steeply dipping, northwest-striking fault near the north boundary of the map area is marked by several tens of metres of fractured and sheared chlorite-epidote-calcite-altered rock. Accretion steps associated with gently plunging mineral fibres on some fault surfaces within the zone indicate dextral displacement.

Ingenika Fault

The Ingenika fault marks the boundary between the Quesnel and Stikine terranes at the latitude of the Johanson Lake project area, and occupies a series of low, drift-covered valleys directly west of the map area. It forms part of a major system of dextral strike-slip faults that also includes the Finlay fault to the north and the Pinchi fault to the south (Fig. 2). Within the map area, the westernmost exposures of Takla rocks between Goldway Peak and the Johanson Creek pluton are characterized by a strong foliation that dips at moderate to steep angles toward the east. This foliation rapidly dies out eastward, and is suspected to be related to the adjacent Ingenika fault.

Zhang and Hynes (1994) analyzed the orientations of early-formed conjugate shear sets within and adjacent to the present map area, and concluded that fault-bounded domains had rotated clockwise about subvertical axes in response to progressive displacement along the Ingenika and related faults. Their analysis indicates rotations of up to 59° adjacent to the Finlay-Ingenika fault, decreasing systematically to zero about 20 km away from the main fault.

Timing of Deformation

The timing of deformation within the Johanson Lake project area is not well constrained, but is suspected to range from Late Triassic to Tertiary in age. The dominant structures within and adjacent to the map area are dextral fault systems. These include the north to northwest-striking Dortatelle and Upper Wrede Creek–Polaris Creek systems, as well as numerous smaller faults with similar orientations and documented dextral displacements. Dextral faults are known to cut the youngest rocks within the Johanson Lake project area, the Jura-Cretaceous Osilinka granites (Fig. 3;

Richards, 1976b). They are related to the Finlay-Ingenika fault system (Zhang and Hynes, 1994), which is part of a Cordillera-wide system of dextral faults that was active mainly in Late Cretaceous through Late Eocene time (Gabielse, 1985; Struik, 1993; Umhoefer and Schiarizza, 1996).

Macroscopic folds within the Johanson Lake project area deform the Upper Triassic Takla Group, and one of them, the Kliyul Creek anticline, is truncated by the Dortatelle fault. Most of the folding may have been related to the Late Cretaceous–early Tertiary dextral strike-slip faults of the area, as suggested by Zhang and Hynes (1994). However, some of the folds might be vestiges of older events, such as the late Early Jurassic thrusting of the Quesnel Terrane over terranes to the east.

The northwest-striking sinistral faults of the southeast domain show a strong spatial relationship with mafic-ultramafic plutons of the Late Triassic suite, which are typically markedly elongate parallel to the faults. Some sinistral faults are localized along dikes of the mafic-ultramafic suite, and some host copper mineralization that is thought to be genetically related to this suite of plutons (Schiarizza, 2004a). The sinistral faults are therefore thought to be mainly or entirely of Late Triassic age, and thus to predate the dextral faults.

Nelson *et al.* (2003) interpreted structures at the Hawk showing, 50 km southeast of the Johanson Lake project area, in terms of sinistral faulting overprinted by younger dextral faults related to the Pinchi system. There, however, the faults cut Early Jurassic granodiorite of the Hogen Batholith, so the sinistral faults are Early Jurassic or younger. An episode of sinistral faulting that predates the major dextral faults of the region was also proposed by Nixon *et al.* (1997) along the western boundary of Quesnel Terrane, 300 km north of the Johanson Lake area. There, the distribution of rocks correlated with the King Salmon allochthon suggests that the western strand of the Thibert fault accommodated about 100 km of sinistral displacement prior to its reactivation as a dextral fault. A general theme to the structural interpretations of Nixon *et al.* (1997), Nelson *et al.* (2003) and the present study is that there were one or more episodes of orogen-parallel sinistral faulting prior to formation of the Late Cretaceous–Tertiary dextral strike-slip faults that dominate much of the structural pattern of the region. These relationships are consistent with the analysis presented by Avé Lallemand and Oldow (1988), who suggested that the cordilleran margin was undergoing left-oblique convergence during Triassic to mid-Cretaceous time, and right-oblique convergence from the Late Cretaceous to the present.

MINERAL OCCURRENCES

The known mineral occurrences within the Johanson Lake map area are shown on Figure 11. These include a wide variety of occurrence types, which are grouped and discussed in the following sections according to their primary plutonic and/or structural controls. The occurrences

that are not mentioned in this report are described by Schiarizza (2004a).

Chromite and Platinum Group Elements in Ultramafic Rocks

Lord (1948) noted that ultramafic rocks of the Wrede Creek and Dortatelle ultramafic-mafic complexes locally contain grains and blebs of chromite. He also described seams of chromite, up to 2.5 cm wide, within talus blocks of smooth-surfaced, buff-weathering serpentine from the Wrede Creek complex. These observations formed the basis for the Wrede Creek Chromite (094D 026) and Mesilinka River (094D 022) MINFILE occurrences (Fig. 11).

Nixon *et al.* (1997) documented in situ pods and schlieren of chromite at several localities within dunite of the Wrede Creek complex. They range from 0.1 to 5 cm in width, from 5 to 40 cm in length, and commonly occur in clusters, forming chromite-rich zones up to several metres wide. Five samples of chromite were analysed for their noble element contents. All five samples were markedly enriched in platinum (from 123 to 2388 ppb), some had significant concentrations of rhodium (up to 72 ppb) and one contained anomalous gold (29 ppb). No subsequent studies have been undertaken to determine the extent and detailed grade characteristics of these PGE-enriched chromites. However, Lett and Jackaman (2002) analyzed archived stream sediment samples from around the Wrede Creek complex for platinum, palladium and gold, and found anomalous platinum concentrations in a number of these samples.

Copper-Gold Mineralization Associated with the Late Triassic Mafic-Ultramafic Plutonic Suite

Copper-gold mineralization associated with plutons and related dioritic dikes of the Late Triassic mafic-ultramafic suite occurs in a belt that extends from the eastern edge of the map area between Kliyul and Croyden creeks northwestward to Johanson Lake (Fig. 11). Individual intrusive bodies known to host mineralization include the Abraham Creek, Kliyul Creek and Johanson Lake mafic-ultramafic complexes, the elongate diorite stock west of Darb Lake, and the diorite stock east of the Darb Creek tonalite pluton. The mineral occurrences within this belt have been described by Schiarizza (2004a) and are only briefly summarized in the following paragraphs.

The most common style of mineralization within the Kliyul Creek–Johanson Lake belt consists of pyrite-chalcopyrite disseminations and blebs within and along fractures, in narrow quartz and quartz-carbonate veins, and within local, commonly silicified shear zones. These modes of occurrence are commonly spatially associated, and porphyry-style mineralization of this type is documented over substantial areas within and peripheral to dioritic rocks near the south margin of the Abraham Creek complex (Grexton and Roberts, 1991), within the Kliyul Creek complex northeast of the major fork in the creek (Wilson, 1984b; Cross, 1985), and within the diorite stock

east of Darb Creek (Leriche and Luckman, 1991a, 1991b; Gill, 1994). Significant gold values are associated with the copper mineralization in all of these areas (Schiarizza, 2004a).

The Croy occurrence comprises massive to disseminated magnetite-pyrrhotite-pyrite-chalcopyrite mineralization associated with quartz-calcite-chlorite gangue. It occurs as lenses within steeply dipping northwest-trending shear zones that cut the Takla Group near the north margin of the Abraham Creek complex. Copper-gold skarns at the Kliyul and Pacific Sugar occurrences comprise magnetite-pyrite-chalcopyrite mineralization within limestone-bearing sections of the Kliyul Creek unit of the Takla Group, and are associated with dioritic rocks related to the Kliyul Creek mafic-ultramafic complex. Stratabound layers of magnetite-pyrite-chalcopyrite at the Soup North and Soup South occurrences are likewise found in an area containing numerous dioritic dikes between the Abraham Creek and Kliyul Creek mafic-ultramafic complexes.

A zone of quartz-pyrite±sericite alteration encompasses the north end of the Kliyul Creek mafic-ultramafic complex, and extends intermittently for 5 km to the west-northwest, to the head of Darb Creek (Schiarizza, 2004a, 2004b). This zone includes the Kliyul skarn occurrence, and also hosts a number of gold-bearing quartz veins (Schiarizza, 2004a; MacIntyre *et al.*, this volume). Gold-bearing quartz veins, commonly containing pyrite and chalcopyrite, also occur within the northwestern part of the Abraham Creek mafic-ultramafic complex.

Porphyry Copper-Molybdenum Mineralization Associated with the Monzonite-Diorite Suite of Plutons

Porphyry-style mineralization documented at the Nik, Grapes and Breccia occurrences is associated with dikes that are part of the monzonite-diorite plutonic suite. Copper is the main commodity of economic interest but, in contrast to showings associated with the ultramafic-mafic suite, molybdenum is also present.

NIK (MINFILE 094D 109), GRAPES (MINFILE 094D 163) AND REDGOLD (MINFILE 094D 162)

The Nik claims were staked by BP Minerals Limited in 1976 to cover mineralization along the southwest margin of the Wrede Creek ultramafic-mafic complex. The claims were explored with geophysical, geochemical, trenching and drilling programs from 1976 to 1986. Porphyry-style copper-molybdenum mineralization was documented by diamond-drilling at the Nik showing (Bates, 1976), and by more extensive percussion and diamond-drilling programs covering the Grapes showing (Bates, 1977, 1979). The Redgold occurrence to the southeast lies in an area that yielded high contents of copper and molybdenum in overburden. An extensive trenching program, however, showed only rare traces of chalcopyrite and molybdenite in bedrock (Mustard and Wong, 1979).

Sulphide mineralization at the Nik and Grapes occurrences comprises pyrite, chalcopyrite, molybdenite and

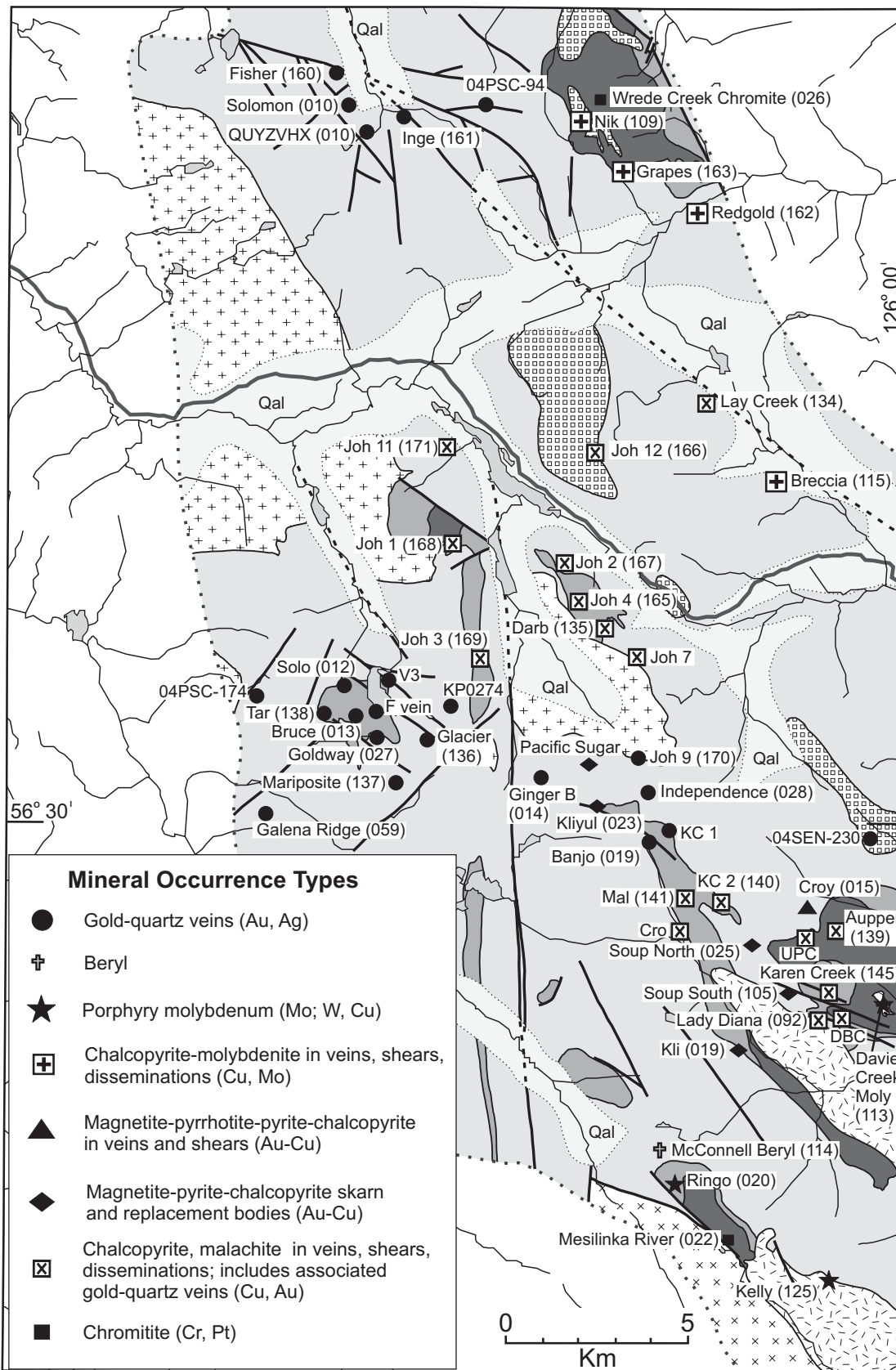


Figure 11. Locations of mineral occurrences in the Mesilinka River–Wrede Creek area. Occurrences found in the MINFILE database are shown with the 094D MINFILE number appended in brackets. Base map is derived from Figure 3, with only plutonic rocks and faults shown.

bornite as disseminations and fracture fillings (Wong *et al.*, 1985). Mineralization occurs within dioritic to quartz dioritic dikes, here assigned to the monzonite-diorite suite, and within associated rocks of the Wrede Creek complex and Takla Group. Propylitic alteration characterizes pyritic zones and potassic alteration, consisting of sericite and biotite, is associated with chalcopyrite and molybdenite-bearing rocks. Wong *et al.* (1985) obtained K-Ar dates of 172 ± 6 Ma on hornblende from one of the diorite dikes, and 157 ± 5 Ma on secondary biotite from sulphide-mineralized pegmatite of the Wrede Creek complex.

BRECCIA (094D 115) AND LAY CREEK (094D 134)

The Breccia occurrence is located on the southwest side of the Lay Creek valley, 2.5 km north of the Omineca Resource Access Road. It was discovered in 1981, and subsequent exploration included geochemical and geophysical surveys and a three-hole diamond-drill program by Lornex Mining Corporation in 1982 (Christopher, 1982). This program demonstrated that porphyry-style copper-molybdenum mineralization occurs over a substantial area.

The mineralization at the Breccia showing is well exposed over an area about 100 m long, within and adjacent to a small creek, where natural exposures have been augmented by blasting. The mineralized rock is a distinctive sheeted breccia comprising angular slabs and plates within a matrix of chlorite, pink calcite and quartz. The sheet-like fragments within the breccia are mainly Takla volcanoclastic rock, but also include diorite and bleached/altered rock of uncertain protolith. Mineralization consists of pyrite and chalcopyrite, in part accompanied by malachite and azurite, as clots and veinlets within the matrix, as disseminations within chlorite-rich parts of the matrix, and as disseminations within some of the breccia fragments. The sheeted nature of the breccia is apparently the result of alteration having been focused along, but also crosscutting, a system of more or less planar joints spaced 2 to 10 cm apart. This jointing is well displayed in weakly altered Takla sandstone and breccia a short distance northwest of the mineralized outcrops, where it dips at moderate angles to the southwest.

A 152 m vertical diamond-drill hole, collared adjacent to the mineralized outcrops, encountered variably mineralized breccia throughout the entire length of the hole (Christopher, 1982). Hole 2, drilled 325 m to the east-southeast, cut Takla rocks and quartz diorite dikes, and was variably mineralized with pyrite, chalcopyrite and molybdenite, the latter occurring in narrow quartz veins and as coatings on fracture and shear surfaces. A third hole, collared 580 m southeast of the mineralized breccia outcrops, encountered Takla rocks mineralized with pyrite but only local traces of molybdenite and chalcopyrite. All core was analyzed in 10-foot sections. The highest copper (0.53%) and silver (0.14 oz./ton) assays came from a 10-foot section in hole 2, and the highest molybdenum assay of 0.012% came from 30 feet lower in the same hole (Christopher, 1982). The samples were also analyzed for gold, but no significant values were returned. The drillholes and mineralized outcrops of the Breccia showing occur within a northwest-trending

zone, about 1500 m long and 300 m wide, of anomalous IP chargeability and copper in soils geochemistry (Christopher, 1982), suggesting that the area has untested exploration potential.

The Lay Creek showing is located 3 km northwest of the Breccia occurrence. This mineralization was discovered by Lornex Mining Corporation in 1983, during a program of prospecting and geochemical and geophysical surveys along a northwest extension of the Breccia exploration grid. Mineralization occurs in two in situ veins and numerous float occurrences scattered over a northeast-trending zone about 500 m long within mafic volcanic sandstone and breccia of the Kliyul Creek unit (Serack, 1983). The largest vein is vertical, strikes northwest and is about 70 cm wide. It contains coarse pyrite and chalcopyrite in a quartz-carbonate gangue. One grab sample of float contained 9500 ppb Au, 2.3 ppm Ag and 1190 ppm Cu (Serack, 1983, sample F47).

JOH 12 (MINFILE 094D 166)

The Joh 12 showing is located 2.5 km east of Johanson Lake, along the eastern margin of the Johanson Lake monzonite pluton. It was discovered in 1991 during exploration of the Joh property by Reliance Geological Services Inc. for Swannell Minerals Corporation (Leriche and Luckman, 1991a). Mineralization consists of several occurrences of pyrite-chalcopyrite-malachite along fractures within variably chloritized and potassically altered monzonite. Samples of this material yielded assay values of up to 3329 ppm Cu and 47 ppb Au. A float sample from a stream draining the Joh 12 area contained molybdenite, in addition to chalcopyrite and pyrite, along a dry fracture (Leriche and Luckman, 1991a).

Porphyry Molybdenum Occurrences Associated with the Osilinka Stocks

Porphyry molybdenum occurrences are restricted to the southern part of the map area, where they are associated with the Jura-Cretaceous Osilinka stocks. This type of occurrence is best represented by the Davie Creek Moly prospect (MINFILE 094D 113), comprising molybdenum mineralization within and peripheral to the small Davie Creek stock that intrudes hornblende and associated rocks of the Abraham Creek complex on the south side of lower Porphyry Creek. The mineralized stock was discovered by Rio Tinto in 1963, and intermittent diamond-drill programs by various companies between then and 1982 have demonstrated that low-grade molybdenite mineralization occurs through much of the granite (Folk, 1979; Bowen, 1982; Norman, 1982). Molybdenite occurs in quartz veinlets with pyrite and local traces of chalcopyrite, and along dry fractures; it is commonly associated with strong K-feldspar alteration.

The Ringo showing (MINFILE 094D 020) comprises molybdenite disseminated in felsite, quartz and pegmatite veins at the north end of the Dortatelle ultramafic-mafic complex. The veins are probably related to the nearby Osilinka stock. The mineralization was first described by Lord (1948), who noted disseminated molybdenite in frag-

ments of altered pyroxenite and quartz within the moraine at the north end of Dortatelle complex. Subsequent exploration by Stellac Exploration Ltd. between 1971 and 1973 outlined several dispersion trains of molybdenite-bearing material in float, and a single in situ occurrence, comprising a mineralized felsite dike about 1 m wide and 30 m long (Cooke, 1972). This exploration also led to the discovery of two quartz veins containing pyrite and chalcopyrite within the Takla Group about 800 m west of the in situ molybdenite occurrence. There has been no subsequent exploration recorded on the showing.

The Kelly MINFILE occurrence (094D 125) is located along the northern margin of the Osilinka phase of the Hogem Batholith, 5 km southeast of the Ringo showing. It is described as "molybdenite in pegmatite" on a Canadian Superior Exploration Ltd. map dating from the early 1970s (BC Ministry of Energy and Mines property file). There is no other information available regarding this showing.

Structurally Controlled Gold-Quartz Veins

Most mineral occurrences within the Johanson Lake project area have a spatial and inferred genetic relationship to one of three plutonic suites, as described in the previous sections. In contrast, gold-bearing quartz veins in the upper Wrede Creek area are not apparently related to plutonic rocks, but are localized along minor shear zones spatially related to the upper Wrede Creek dextral strike-slip fault system. These vein showings are therefore inferred to be relatively young occurrences that formed during Late Cretaceous–early Tertiary dextral strike-slip faulting in the region. Gold-quartz veins in the Solo Lake area are hosted by the Late Triassic Solo Lake stock but are controlled by dextral faults and have similar mineralogy to the Wrede Creek occurrences; it is suspected that they may also be of Late Cretaceous–early Tertiary age.

UPPER WREDE CREEK VEIN SYSTEMS

The QUYZVHX gold-bearing quartz vein (MINFILE 094D 010), located in the western headwaters of Wrede Creek, was discovered in the mid-1940s (White, 1948). The showing was restaked as part of the Inge Group in 1980 by Golden Rule Resources Limited, who conducted exploration programs on the claim group until 1990. This exploration led to the discovery of the Solomon vein and several other veins in the immediate vicinity of the original QUYZVHX vein, as well as the Fisher vein (MINFILE 094D 160), 2 km to the north-northwest, and the Inge vein (MINFILE 094D 161), 1 km to the east-northeast (Wilson, 1984a; Smith, 1985; Cruickshank, 1990).

The gold occurrences in the upper Wrede Creek area are hosted by volcanoclastic and local sedimentary rocks of the sandstone-carbonate subunit of the Takla Group. The general characteristics of the vein systems were summarized by Cruickshank (1990). Most comprise multiple lenses and veins of quartz (locally quartz-carbonate) within steeply dipping, mainly west-northwest-striking shear zones marked by variably schistose rocks altered with chlorite, sericite, epidote and carbonate. Individual shear zones are commonly several metres wide and locally more

than 10 m wide, and have been traced for 50 to 60 m at the QUYZVHX and Solomon occurrences. Mineralized quartz veins within the shear zones are generally less than a metre wide but locally up to 5 m wide, and tend to splay, coalesce and terminate abruptly. Mineralization typically consists of erratically distributed pyrite and chalcopyrite, but the Fisher and Solomon veins also contain galena, and native gold has been reported from the Solomon vein (Wilson, 1984a; Smith, 1985). The best gold values have been reported from the Solomon vein system. These include a grab sample that returned 7.933 oz./ton Au, 2.46 oz./ton Ag, 0.19% Cu, 1.51% Pb and 1.40% Zn (Wilson, 1984a), and a 15 cm chip sample across vein material heavily mineralized with galena and chalcopyrite that yielded 3.14 oz./ton Au and 2.0 oz./ton Ag (Smith, 1985).

SOLO LAKE VEIN SYSTEMS

Gold-bearing quartz veins associated with the Solo Lake stock include the Solo (MINFILE 094D 012), Bruce (MINFILE 094D 013) and Goldway (MINFILE 094D 027) occurrences, discovered in the mid-1940s (White, 1948), and the F vein, V3 and Tar (MINFILE 094D 138) occurrences, discovered during renewed exploration in the 1980s and 1990s (Pawliuk, 1985; von Rosen, 1986; Richards, 1991). The vein systems associated with the Solo Lake stock were well described by Richards (1991). Each occurrence shown on Figure 9 comprises a number of veins, with individual veins ranging from several metres to more than 100 m in length, and from a few centimeters to several metres in width. Gold and silver ratios are commonly near one to one, and the precious metals are associated with pyrite, and locally galena and sphalerite. Visible gold has been reported from the A and C veins of the Bruce occurrence. The A vein has returned assay values up to 74.19 g/t Au over 29 cm (Phendler, 1984).

The geometry of the vein systems is most apparent at the Solo and Bruce occurrences, where individual veins are arranged en echelon within northwest-striking zones that approach 1 km in length. Individual veins strike more northerly than the overall system, and are inferred to occupy extensional fractures within dextral shear systems (Richards, 1991). Alteration related to the veins is minimal, and Richards (1991) suggested that the veins may be related to fault movements during the late stages of emplacement and cooling of the Solo Lake stock. Alternatively, the veins may be considerably younger, and the Solo Lake stock may have been a favourable mechanical and chemical host for vein systems that were localized along components of the regional system of Late Cretaceous–early Tertiary dextral strike-slip faults.

Other Occurrences

MCCONNELL BERYL (MINFILE 094D 114)

The McConnell beryl occurrence comprises a single float block located in a moraine a short distance north of the Dortatelle ultramafic-mafic complex (Fig. 11). The block was derived from a pegmatite dike at least 1 m wide and contains scattered grains of garnet and a few crystals of pale green beryl up to 2 cm in diameter (Lord, 1948). Similar

pegmatite dikes (without beryl) occur in situ within the Dortatelle complex and adjacent Takla group; they are presumably related to the nearby Osilinka stock at the north end of the Hogem Batholith. Associated aplitic dikes host molybdenite mineralization of the Ringo (MINFILE 094D 020) occurrence.

The spatial association of beryl-bearing pegmatites with chromium-bearing ultramafic rocks suggests that there was potential for the formation of emeralds within or adjacent to the Dortatelle complex. Legun (2004) conducted a brief survey of the original discovery area to evaluate this potential, but did not find any beryl or anomalous beryllium concentrations in stream sediments collected from the basin. The south end of the Dortatelle complex was mapped during our 2004 field program. Aplitic and pegmatitic dikes, apparently derived mainly from the Osilinka stock, were observed cutting the ultramafic rocks, but none of these contained beryl.

04PSC-94

Sample 04PSC-94 was collected from a mineralized quartz vein that cuts the Takla Group on the ridge crest east of the head of Wrede Creek (Fig. 11). The vein is about 50 cm wide, strikes north-northwest, and dips steeply. It consists mainly of white bull quartz cut by rusty hairline fractures, but also includes scattered vugs containing quartz crystals and patches of pyrite-chalcopyrite-azurite mineralization. The sample of well-mineralized vein material contained 1771 ppb Au, 61.529 ppm Ag and greater than 10 000 ppm Cu. It also yielded anomalous values of Zn (257 ppm), Mo (14.46 ppm), As (41.5 ppm), Sb (2.74 ppm) and Hg (133 ppb).

04PSC-174

A northerly-striking fault zone identified during the 2004 field season, on the ridge about 900 m northwest of Goldway Peak, is marked by 3 m of quartz-pyrite-altered rock. A grab sample of this material (sample 04PSC-174, Fig. 11) yielded 1134 ppb Au and 3.496 ppm Ag. A different northerly-trending alteration zone, 360 m to the south-east, comprises about 5 m of foliated quartz-sericite-chlorite-pyrite-altered volcanic sandstone. A sample of this material contained 138 ppb Au, 1.821 ppm Ag and 240 ppm Cu.

04SEN-230

Sample 04SEN-230 was collected from a system of subhorizontal mineralized quartz veins that cut the southeastern part of the elongate monzodiorite pluton along the eastern margin of the map area near Croyden Creek (Fig. 11). Individual veins are up to 15 cm thick and are locally mineralized with pyrite, galena, chalcopyrite and malachite. The grab sample collected from mineralized vein material yielded 940 ppb Au, greater than 100 ppm Ag, greater than 10 000 ppm Pb, 2562.8 ppm Cu and 26.2 ppm Mo.

SUMMARY

The Takla Group within the Johanson Lake project area comprises Upper Triassic rocks that have been separated into two major units. Most of the group is assigned to the Kliyul Creek unit, which consists of massive to well-bedded, feldspar±pyroxene-rich volcanic sandstones, intercalated with volcanic breccias and local mafic flows. A sandstone-carbonate subunit includes significant amounts of limestone, either as a component of slump breccias or as coherent layers interbedded with the volcanoclastic rocks. Another mappable subunit consists mainly of thin-bedded siltstone and limestone. The Kliyul Creek unit is overlain by the Goldway Peak unit, which consists mainly of massive pyroxene-rich volcanic breccias.

The Takla Group is cut by numerous plutons that are tentatively subdivided into four suites. The oldest intrusive suite includes Alaskan-type ultramafic-mafic complexes as well as diorite-gabbro stocks that are similar to the mafic phases within the Alaskan complexes. These rocks are Late Triassic in age and probably represent subvolcanic intrusions associated with Takla volcanism. Younger intrusive rocks include a monzonite-diorite suite of suspected Late Triassic–Early Jurassic age; an early Middle Jurassic tonalite suite; and granite to granodiorite stocks and plutons that are, at least in part, of Jura-Cretaceous age.

The oldest structures in the area are northwest-striking sinistral shear zones that are common around Kliyul Creek in the southwestern part of the map area. These faults are spatially associated with a belt of Late Triassic ultramafic-mafic plutons that show marked elongation parallel to the faults. It is suspected that sinistral faulting was broadly contemporaneous with Late Triassic plutonism and therefore with construction of the Takla volcanic-plutonic arc. Younger structures are dominated by steeply dipping, north to northwest-striking dextral strike-slip faults. These faults probably formed during displacement along the Ingenika fault to the west, which is part of a regional system of dextral strike-slip faults that was active mainly during the Late Cretaceous and early Tertiary. North to northwest-trending folds occur between, and are locally truncated by, dextral strike-slip faults. These may be broadly contemporaneous with the dextral faulting or be vestiges of older deformation events, such as the early Middle Jurassic thrust faulting that is documented at this latitude along the eastern margin of the Quesnel Terrane.

The Johanson Lake project area hosts a large number of mineral occurrences with a variety of plutonic and structural controls. Dunite of the Wrede Creek ultramafic-mafic complex contains chromitite pods that are enriched in platinum. Dioritic rocks of the Late Triassic mafic-ultramafic suite host porphyry-style copper-gold mineralization as pyrite-chalcopyrite disseminations in veins and fractures. Magnetite-pyrite-chalcopyrite lodes occur in shear zones peripheral to the Late Triassic suite, and copper-gold skarns and replacement bodies occur where these intrusions cut calcareous units of the Takla Group. Porphyry copper-molybdenum mineralization is locally associated with the monzonite-diorite suite, and porphyry molybdenum

occurrences are associated with Jura-Cretaceous granitic rocks. Systems of structurally controlled gold-quartz veins are spatially associated with dextral strike-slip fault systems that are thought to be Late Cretaceous or early Tertiary in age.

ACKNOWLEDGMENTS

We are grateful to Carl Edmunds and Chris Rockingham of Northgate Minerals Corporation for their continued interest in the area, and for renewing the partnership agreement that provided the funding necessary for fieldwork. We thank Ryan Hinds of Canadian Helicopters Limited for safe and reliable helicopter transportation. Discussions in the field with Dave Lefebure, Richard Friedman, Don MacIntyre and Garry Payie were helpful and are gratefully acknowledged. We also thank Mike Orchard and Steve Irwin for conodont processing and identification, and Richard Friedman for radiometric dating.

REFERENCES

- Avé Lallemand, H.G. and Oldow, J.S. (1988): Early Mesozoic southward migration of cordilleran transpressional terranes; *Tectonics*, Volume 7, pages 1057–1075.
- Bates, C.D.S. (1976): Drilling report on the Ingenika Range property, Nik mineral claims, Omineca Mining Division (NTS 94D9); *BC Ministry of Energy, Mines and Petroleum Resources*, Assessment Report 6015, 4 pages.
- Bates, C.D.S. (1977): Drilling report on the Ingenika Range property, Nik mineral claims, Omineca Mining Division (NTS 94D9); *BC Ministry of Energy, Mines and Petroleum Resources*, Assessment Report 6452, 2 pages.
- Bates, C.D.S. (1979): Drilling report on the Ingenika Range property, Nik mineral claims, Omineca Mining Division (NTS-94D9); *BC Ministry of Energy, Mines and Petroleum Resources*, Assessment Report 7451, 7 pages.
- Bowen, B.K. (1982): Diamond drilling report on the Kliylu 1 group of claims, Omineca Mining Division, N.T.S. 94C/5W; 94D/8E; *BC Ministry of Energy, Mines and Petroleum Resources*, Assessment Report 10 009, 9 pages.
- Christopher, P. (1982): Geological, geochemical, geophysical and diamond drilling report on the Breccia, Breccia 2, Breccia 3 and Breccia 4 claims, Lay Creek area, Omineca Mining Division (94D/9E); *BC Ministry of Energy, Mines and Petroleum Resources*, Assessment Report 10 686, 10 pages.
- Cooke, D.L. (1972): Geological and geochemical report on the Ringo claim group, fifteen miles SE of Sustut Lake, Omineca Mining Division; *BC Department of Mines and Petroleum Resources*, Assessment Report 3839, 10 pages.
- Cross, D.B. (1985): Geological, geophysical and geochemical report, KC 1 and 2 claims, Omineca Mining Division, British Columbia, N.T.S. 94D/8E, 9E; *BC Ministry of Energy, Mines and Petroleum Resources*, Assessment Report 14 416, 18 pages.
- Cruikshank, R.D. (1990): Geological and trenching report on the Inge 1 to 4 mineral claims, Omineca Mining Division, British Columbia, NTS 94D/9; *BC Ministry of Energy, Mines and Petroleum Resources*, Assessment Report 21 358, 27 pages.
- Eadie, E.T. (1976): K-Ar and Rb-Sr geochronology of the northern Hogen Batholith, BC; unpublished B.Sc. thesis, *University of British Columbia*, 46 pages.
- Ferri, F. (1997): Nina Creek Group and Lay Range Assemblage, north-central British Columbia: remnants of late Paleozoic oceanic and arc terranes; *Canadian Journal of Earth Sciences*, Volume 34, pages 854–874.
- Ferri, F. (2000a): Devonian-Mississippian felsic volcanism along the western edge of the Cassiar Terrane, north-central British Columbia (NTS 93N, 94C and 94D); in *Geological Fieldwork 1999*, *BC Ministry of Energy and Mines*, Paper 2000-1, pages 127–146.
- Ferri, F. (2000b): Preliminary geology between Lay and Wrede ranges, north-central British Columbia (NTS 94C/12; 94D/9, 16); *BC Ministry of Energy and Mines*, Geofile 2000-1, 1:50 000 scale.
- Ferri, F. and Melville, D.M. (1994): Bedrock geology of the Germansen Landing–Manson Creek area, British Columbia (94N/9, 10, 15; 94C/2); *BC Ministry of Energy, Mines and Petroleum Resources*, Bulletin 91, 147 pages.
- Ferri, F., Dudka, S., and Rees, C. (1992): Geology of the Uslika Lake area, northern Quesnel Trough, B.C. (94C/3, 4, 6); in *Geological Fieldwork 1991*, *BC Ministry of Energy Mines and Petroleum Resources*, Paper 1992-1, pages 127–145.
- Ferri, F., Dudka, S., Rees, C. and Meldrum, D. (1993): Geology of the Aiken Lake and Osilinka River areas, northern Quesnel Trough (94C/2, 3, 5, 6, 12); in *Geological Fieldwork 1992*, *BC Ministry of Energy Mines and Petroleum Resources*, Paper 1993-1, pages 109-134.
- Ferri, F., Dudka, S., Rees, C., Meldrum, D. and Willson, M. (2001a): Geology of the Uslika Lake area, north-central British Columbia (NTS 94C/2, 3, 4); *BC Ministry of Energy and Mines*, Geoscience Map 2001-4, 1:50 000 scale.
- Ferri, F., Dudka, S., Rees, C. and Meldrum, D. (2001b): Geology of the Aiken Lake area, north-central British Columbia (NTS 94C/5, 6, 12); *BC Ministry of Energy and Mines*, Geoscience Map 2001-10, 1:50 000 scale.
- Folk, P. (1979): Diamond drill report, Kliylu claim, #1581 (12), 20 units, Omineca Mining Division, Map 94D/8E, 94C/5W; *BC Ministry of Energy, Mines and Petroleum Resources*, Assessment Report 7743, Part 1, 3 pages.
- Gabrielse, H. (1985): Major dextral transcurrent displacements along the northern Rocky Mountain Trench and related lineaments in north-central British Columbia; *Geological Society of America Bulletin*, Volume 96, pages 1–14.
- Garnett, J.A. (1978): Geology and mineral occurrences of the southern Hogen Batholith; *BC Ministry of Mines and Petroleum Resources*, Bulletin 70, 67 pages.
- Gill, D.G. (1994): Geological, geochemical assessment report on the Darb property, N.T.S. mapsheet 94D/8; *BC Ministry of Energy, Mines and Petroleum Resources*, Assessment Report 23 545, 15 pages.
- Grextion, L. and Roberts, P. (1991): Porphyry Creek Property, 1990 prospecting, mapping and sampling, N.T.S. 94C/5, 2; 94D/8, 9, Omineca Mining Division; *BC Ministry of Energy, Mines and Petroleum Resources*, Assessment Report 21 521, Part 1, 68 pages.
- Hammack, J.L., Nixon, G.T., Wong, R.H. and Paterson, W.P.E. (1990): Geology and noble metal geochemistry of the Wrede Creek Ultramafic Complex, north-central British Columbia (94D/9); in *Geological Fieldwork 1989*, *BC Ministry of Energy, Mines and Petroleum Resources*, Paper 1990-1, pages 405–415.
- Irvine, T.N. (1974): Ultramafic and gabbroic rocks in the Aiken Lake and McConnell Creek map-areas, British Columbia; in *Report of Activities, Part A, Geological Survey of Canada*, Paper 74-1A, pages 149–152.
- Irvine, T.N. (1976): Studies of cordilleran gabbroic and ultramafic intrusions, British Columbia; in *Report of Activi-*

- ties, Part A, *Geological Survey of Canada*, Paper 76-1A, pages 75–81.
- Legun, A. (2004): The potential for emeralds in B.C. – a preliminary overview; in *Geological Fieldwork 2003, BC Ministry of Energy and Mines*, Paper 2004-1, pages 219–229.
- Leriche, P.D. and Luckman, N. (1991a): Geological and geochemical report on the Joh property, Johanson Lake area, Omineca Mining District, British Columbia; *BC Ministry of Energy, Mines and Petroleum Resources*, Assessment Report 21 781, 22 pages.
- Leriche, P.D. and Luckman, N. (1991b): Geological and geochemical report on the Darb property, Johanson Lake area, Omineca Mining District, British Columbia; *BC Ministry of Energy, Mines and Petroleum Resources*, Assessment Report 21 782, 23 pages.
- Lett, R. and Jackaman, W. (2002): PGE stream sediment geochemistry in British Columbia; in *Geological Fieldwork 2001, BC Ministry of Energy and Mines*, Paper 2002-1, pages 365–375.
- Lord, C.S. (1948): McConnell Creek map-area, Cassiar District, British Columbia; *Geological Survey of Canada*, Memoir 251, 72 pages.
- Mihalynuk, M.G., Nelson, J. and Diakow, L.J. (1994): Cache Creek terrane entrapment: oroclinal paradox within the Canadian Cordillera; *Tectonics*, Volume 13, pages 575–595.
- Minchan, K. (1989a): Takla Group volcano-sedimentary rocks, north-central British Columbia: a summary of fieldwork (94D/9); in *Geological Fieldwork 1988, BC Ministry of Energy, Mines and Petroleum Resources*, Paper 1989-1, pages 227–232.
- Minchan, K. (1989b): Paleotectonic setting of Takla Group volcano-sedimentary rocks, Quesnellia, north-central British Columbia: unpublished M.Sc. thesis, *McGill University*, 102 pages.
- Monger, J.W.H. (1977): The Triassic Takla Group in McConnell Creek map-area, north-central British Columbia; *Geological Survey of Canada*, Paper 76-29, 45 pages.
- Monger, J.W.H., Richards, T.A. and Paterson, I.A. (1978): The Hinterland Belt of the Canadian Cordillera: new data from northern and central British Columbia; *Canadian Journal of Earth Sciences*, Volume 15, pages 823–830.
- Mortensen, J.K., Ghosh, D.K. and Ferri, F. (1995): U-Pb geochronology of intrusive rocks associated with copper-gold porphyry deposits in the Canadian Cordillera; in *Porphyry Deposits of the Northwestern Cordillera of North America*, Schroeter, T.G., Editor, *Canadian Institute of Mining, Metallurgy and Petroleum*, Special Volume 46, pages 142–158.
- Mustard, D.K. and Wong, R.H. (1979): Geological and geochemical assessment report on the Nik mineral claims, Nos. 6, 7 and 8, Ingenika Range area, Omineca Mining Division, B.C., NTS 94D/9E; *BC Ministry of Energy, Mines and Petroleum Resources*, Assessment Report 7249, 17 pages.
- Nelson, J.L. and Bellefontaine, K.A. (1996): The geology and mineral deposits of north-central Quesnellia: Tezzeron Lake to Discovery Creek, central British Columbia; *BC Ministry of Energy, Mines and Petroleum Resources*, Bulletin 99, 112 pages.
- Nelson, J., Carmichael, B. and Gray, M. (2003): Innovative gold targets in the Pinchi Fault/Hogem Batholith area: the Hawk and Axelgold properties, central British Columbia (94C/4, 94N/13); in *Geological Fieldwork 2002, BC Ministry of Energy and Mines*, Paper 2003-1, pages 97–113.
- Nixon, G.T., Hammack, J.L. and Paterson, W.P.E. (1990): Geology and noble metal geochemistry of the Johanson Lake Mafic-Ultramafic Complex, north-central British Columbia (94D/9); in *Geological Fieldwork 1989, BC Ministry of Energy, Mines and Petroleum Resources*, Paper 1990-1, pages 417–424.
- Nixon, G.T., Hammack, J.L., Ash, C.H., Cabri, L.J., Case, G., Connelly, J.N., Heaman, L.M., Laflamme, J.H.G., Nuttall, C., Paterson, W.P.E. and Wong, R.H. (1997): Geology and platinum-group-element mineralization of Alaskan-type ultramafic-mafic complexes in British Columbia; *BC Ministry of Employment and Investment*, Bulletin 93, 141 pages.
- Noel, G.A. (1971b): Geological-geophysical-geochemical report on the Kli mineral claims, Kliyul Creek area; *BC Department of Mines and Petroleum Resources*, Assessment Report 3264, 30 pages.
- Norman, G.E. (1982): Diamond drilling report on the Kliyul 1 group of claims, Omineca Mining Division, N.T.S. 94C/5W; 94D/8E; *BC Ministry of Energy, Mines and Petroleum Resources*, Assessment Report 10 730, 8 pages.
- Pálffy, J., Smith, P.L. and Mortensen, J.K. (2000): A U-Pb and $^{40}\text{Ar}/^{39}\text{Ar}$ time scale for the Jurassic; *Canadian Journal of Earth Sciences*, Volume 37, pages 923–944.
- Pawliuk, D.J. (1985): Report on assessment work on the Goldway Peak property, Omineca Mining Division, Johanson Lake, British Columbia; *BC Ministry of Energy, Mines and Petroleum Resources*, Assessment Report 14 105, 17 pages.
- Phendler, R.W. (1984): Report on assessment work (sampling and assaying) on Vi 1 and Vi 2 (Record Nos. 1948 and 1949), Johanson Lake area, Omineca Mining Division, British Columbia; *BC Ministry of Energy, Mines and Petroleum Resources*, Assessment Report 13 175, 9 pages.
- Richards, T.A. (1976a): Takla Project (Reports 10-16): McConnell Creek map-area (94D, east half), British Columbia; in *Report of Activities, Part A, Geological Survey of Canada*, Paper 76-1A, pages 43-50.
- Richards, T.A. (1976b): Geology, McConnell Creek map-area (94D/E); *Geological Survey of Canada*, Open File 342, 1:250 000 scale.
- Richards, T.A. (1991): Geologic setting and sampling of vein systems, Solo Group of mineral claims, Omineca Mining Division, 94D/9; *BC Ministry of Energy, Mines and Petroleum Resources*, Assessment Report 21 394, 39 pages.
- Ricketts, B.D., Evenchick, C.A., Anderson, R.G. and Murphy, D.C. (1992): Bowser basin, northern British Columbia: Constraints on the timing of initial subsidence and Stikinia-North America terrane interactions; *Geology*, Volume 20, pages 1119–1122.
- Schiarizza, P. (2004a): Geology and mineral occurrences of Quesnel Terrane, Kliyul Creek to Johanson Lake (94D/8, 9); in *Geological Fieldwork 2003, BC Ministry of Energy and Mines*, Paper 2004-1, pages 83–100.
- Schiarizza, P. (2004b): Geology of the Kliyul Creek–Johanson Lake area, parts of NTS 94D/8 and 9; *BC Ministry of Energy and Mines*, Open File 2004-5, 1:50 000 scale.
- Serack, M.L. (1983): Geology, geochemistry, geophysics prospecting report on the Breccia and Breccia 2-4 claims in the Omineca Mining Division, 94D/9E; *BC Ministry of Energy, Mines and Petroleum Resources*, Assessment Report 11 842, 14 pages.
- Smith, A.R. (1985): Geological, geochemical and prospecting report, Inge 1 and 2 mineral claims, N.T.S. 94D/9E & W, Omineca Mining Division, British Columbia; *BC Ministry of Energy, Mines and Petroleum Resources*, Assessment Report 14 630, 23 pages.
- Stevens, R.D., Delabio, R.N. and Lachance, G.R. (1982): Age determinations and geological studies, K-Ar isotopic ages,

- Report 15; *Geological Survey of Canada*, Paper 81-2, 56 pages.
- Struik, L.C. (1988): Crustal evolution of the eastern Canadian Cordillera; *Tectonics*, Volume 7, pages 727–747.
- Struik, L.C. (1993): Intersecting intracontinental Tertiary transform fault systems in the North American Cordillera; *Canadian Journal of Earth Sciences*, Volume 30, pages 1262–1274.
- Struik, L.C., Schiarizza, P., Orchard, M.J., Cordey, F., Sano, H., MacIntyre, D.G., Lapierre, H. and Tardy, M. (2001): Imbricate architecture of the upper Paleozoic to Jurassic oceanic Cache Creek Terrane, central British Columbia; *Canadian Journal of Earth Sciences*, Volume 38, pages 495–514.
- Tchalenko, J.S. (1970): Similarities between shear zones of different magnitudes; *Geological Society of America Bulletin*, Volume 81, pages 1625–1640.
- Travers, W.B. (1978): Overtaken Nicola and Ashcroft strata and their relations to the Cache Creek Group, southwestern Intermontane Belt, British Columbia; *Canadian Journal of Earth Sciences*, Volume 15, pages 99–116.
- Umhoefer, P.J. and Schiarizza, P. (1996): Latest Cretaceous to Early Tertiary dextral strike-slip faulting on the southeastern Yakalom fault system, southeastern Coast Belt, British Columbia; *Geological Society of America Bulletin*, Volume 108, pages 768–785.
- von Rosen, G. (1986): Assessment geological report on mapping, sampling and bulk sampling program on the Good (4155) - Prospects (4147) - Much (4149) - Pro (4150) - Fit (4151) - Dar (4154) mineral claims (Gold group), Goldway Peak - Johanson Lake area, Omineca Mining Division; *BC Ministry of Energy, Mines and Petroleum Resources*, Assessment Report 15 313, 35 pages.
- Wanless, R.K., Stevens, R.D., Lachance, G.R. and Delabio, R.N. (1972): Age determinations and geological studies, K-Ar isotopic ages, Report 10; *Geological Survey of Canada*, Paper 71-2, 96 pages.
- Wanless, R.K., Stevens, R.D., Lachance, G.R. and Delabio, R.N. (1979): Age determinations and geological studies, K-Ar isotopic ages, Report 14; *Geological Survey of Canada*, Paper 79-2, 67 pages.
- White, W.H. (1948): Sustut-Aiken-McConnell Lake area; in Annual Report of the Minister of Mines for 1947, *B.C. Department of Mines*, pages A100–A111
- Wilson, G.L. (1984a): Geological and geochemical report, Inge 1 and 2 mineral claims, N.T.S. 94D/9E, Omineca Mining Division, British Columbia; *BC Ministry of Energy, Mines and Petroleum Resources*, Assessment Report 12 803, 13 pages.
- Wilson, G.L. (1984b): Geological, geochemical and geophysical report, KC 1 and 2 mineral claims, N.T.S. 94D/8E and 9E, Omineca Mining Division, British Columbia; *BC Ministry of Energy, Mines and Petroleum Resources*, Assessment Report 13 580, 17 pages.
- Wong, R.H. and Godwin, C.I. (1980): K/Ar age determinations, Wrede Creek zoned ultramafic complex (94D/E); in Geological Fieldwork 1979, *BC Ministry of Energy, Mines and Petroleum Resources*, pages 156–157.
- Wong, R.H., Godwin, C.I. and McTaggart, K.C. (1985): Geology, K/Ar dates, and associated sulphide mineralization of Wrede Creek zoned ultramafic complex (94D/E); *BC Ministry of Energy, Mines and Petroleum Resources*, Geology in British Columbia 1977–1981, pages 148–155.
- Woodsworth, G.J. (1976): Plutonic rocks of McConnell Creek (94D west half) and Aiken Lake (94C east half) map-areas, British Columbia; in Report of Activities, Part A, *Geological Survey of Canada*, Paper 76-1A, pages 69–73.
- Woodsworth, G.J., Anderson, R.G. and Armstrong, R.L. (1991): Plutonic regimes; Chapter 15 in Geology of the Cordilleran Orogen in Canada, H. Gabrielse and C.J. Yorath, editors, *Geological Survey of Canada*, Geology of Canada, no. 4, pages 491–531; also *Geological Society of America*, The Geology of North America, Volume G-2.
- Zhang, G. (1994): Strike-slip faulting and block rotations in the McConnell Creek area, north-central British Columbia: structural implications for the interpretation of paleomagnetic observations; unpublished Ph.D. thesis, *McGill University*, 238 pages.
- Zhang, G. and Hynes, A. (1991): Structure of the Takla Group east of the Finlay-Ingenika Fault, McConnell Creek area, north-central B.C. (94D/8, 9); in Geological Fieldwork 1990, *BC Ministry of Energy, Mines and Petroleum Resources*, Paper 1991-1, pages 121–129.
- Zhang, G. and Hynes, A. (1992): Structures along Finlay-Ingenika Fault, McConnell Creek area, north-central British Columbia (94C/5; 94D/8, 9); in Geological Fieldwork 1991, *BC Ministry of Energy, Mines and Petroleum Resources*, Paper 1992-1, pages 147–154.
- Zhang, G. and Hynes, A. (1994): Fabrics and kinematic indicators associated with the local structures along Finlay-Ingenika Fault, McConnell Creek area, north-central British Columbia; *Canadian Journal of Earth Sciences*, Volume 31, pages 1687–1699.
- Zhang, G. and Hynes, A. (1995): Determination of position-gradient tensor from strain measurements and its implications for the displacement across a shear zone; *Journal of Structural Geology*, Volume 17, pages 1587–1599.
- Zhang, G., Hynes, A. and Irving, E. (1996): Block rotations along the strike-slip Finlay-Ingenika Fault, north-central British Columbia: implications for paleomagnetic and tectonic studies; *Tectonics*, Volume 15, pages 272–287.

Geological Setting and Economic Potential of Gold Occurrences in the Kliyul Creek-Solo Lake Area, North-Central British Columbia

By D.G. MacIntyre and G. Payie

KEYWORDS: lithogeochemistry, gold-quartz veins, quartz-sericite-pyrite alteration, quartz-carbonate alteration, gold skarn

INTRODUCTION

This report summarizes the results of lithogeochemical sampling completed in the Kliyul Creek-Solo Lake area of north central British Columbia. The study area is part of the larger Johanson Lake project (Fig. 1). The purpose of this work was to confirm the widespread distribution of gold in quartz veins as recognized by previous workers and to assess the potential for economically viable deposits in the area. Geochemical sampling and geologic mapping was done in early August from two strategically located fly camps one located at Divide Lake, the other near the headwaters of Mariposite Creek (Fig. 2). A total of 95 samples were collected and submitted to Acme Analytical Laboratories in Vancouver for multi-element inductively coupled plasma (ICP) analysis. Stations were established using a Garmin GPS unit and databases and maps were created using Manifold 6.0 GIS software.

The work discussed in this report was done as part of the Johanson Lake project. This project, which is now in its second year, is primarily a bedrock mapping program initiated by the Geological Survey Branch as part of the Toadogone Targeted Geoscience Initiative (TGI). The project focuses on a belt of Mesozoic arc volcanic and plutonic rocks in the eastern part of the McConnell Creek (94D) map sheet. This area contains a number of gold, copper and molybdenum mineral occurrences and Regional Geochemical Survey sample sites that returned anomalously high values of gold and copper. The aim of the project is to improve the quality and detail of bedrock maps for the area and determine the setting and controls of mineral occurrences. This will help guide exploration strategies on known mineral occurrences and focus exploration for new occurrences. Operating funds were provided by the Toadogone TGI and a private-public partnership agreement with Northgate Exploration Ltd. A more complete description of the project and the results of mapping completed in 2003 are provided in a previous report (Schiarizza, 2004). Results of work done in 2004 are contained in an accompanying report in this volume.

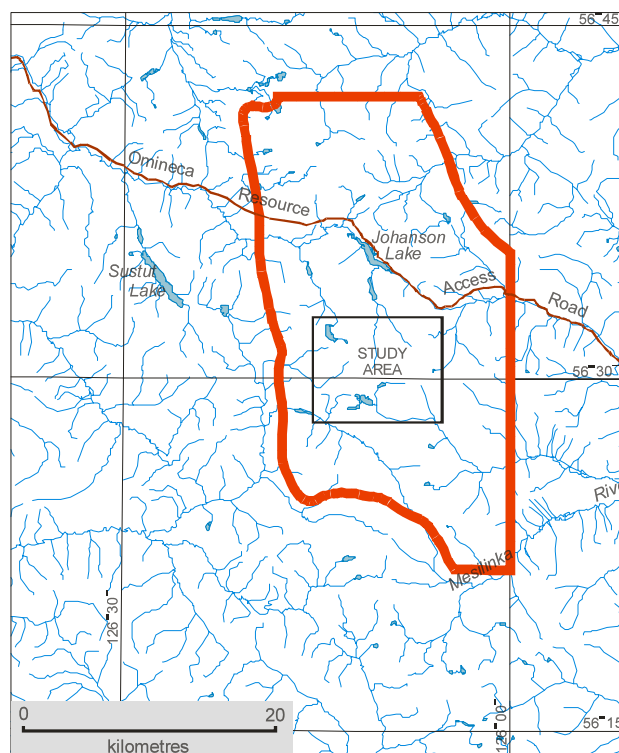


Figure 1. Location of the Johanson Lake project (thick line) and the current study area (rectangle).

PREVIOUS WORK

The history of geologic mapping and mineral exploration in the Johanson Lake project area is described in a previous report (Schiarizza, 2004). Table 1 is a summary of recorded mineral exploration in the study area. The earliest recorded exploration activity was in 1949 when Goldway Peak Mines Ltd. began working on prominent gold-quartz veins near Goldway Peak. Although a small amount of work was done intermittently over the next 20 years it was not until 1970 that Kennco Exploration discovered skarn mineralization near the headwaters of Lay Creek. Sumac Mines Ltd. optioned the Kliyul property from Kennco and completed 11 diamond-drill holes in 1973 and 1974 resulting in the discovery of additional gold-bearing skarn mineralization. Meanwhile, El Paso Mining continued to explore quartz veins at

Goldway Peak, San Jacinto Explorations Ltd. did regional exploration for skarn mineralization in the Lower Kliyul Creek area and BP Minerals explored a large quartz-sericite-pyrite alteration zone south of the Kliyul property (Bap property). Kennco Explorations resumed work on the Kliyul property in 1981 completing four NQ drillholes. BP minerals did more work on the Bap property in 1982 and in 1984 they mounted an aggressive exploration program that saw them work on a number of different properties in the area including the Kliyul property. At the same time various operators did work on showings in the Goldway Peak area. In 1990, Placer

Dome optioned the Kliyul property and did some additional mapping and sampling. In 1992, Noranda Exploration acquired the property and in 1993 they drilled six reverse circulation percussion holes. They also did extensive lithochemical sampling in the Mariposite Creek area (Gill, 1994) which resulted in the discovery of a significant number of gold-bearing veins. Battle Mountain Canada (Hemlo Gold Mines Ltd.) subsequently completed two drillholes on this property (Gill, 1996) but the results were discouraging and no further work was done.

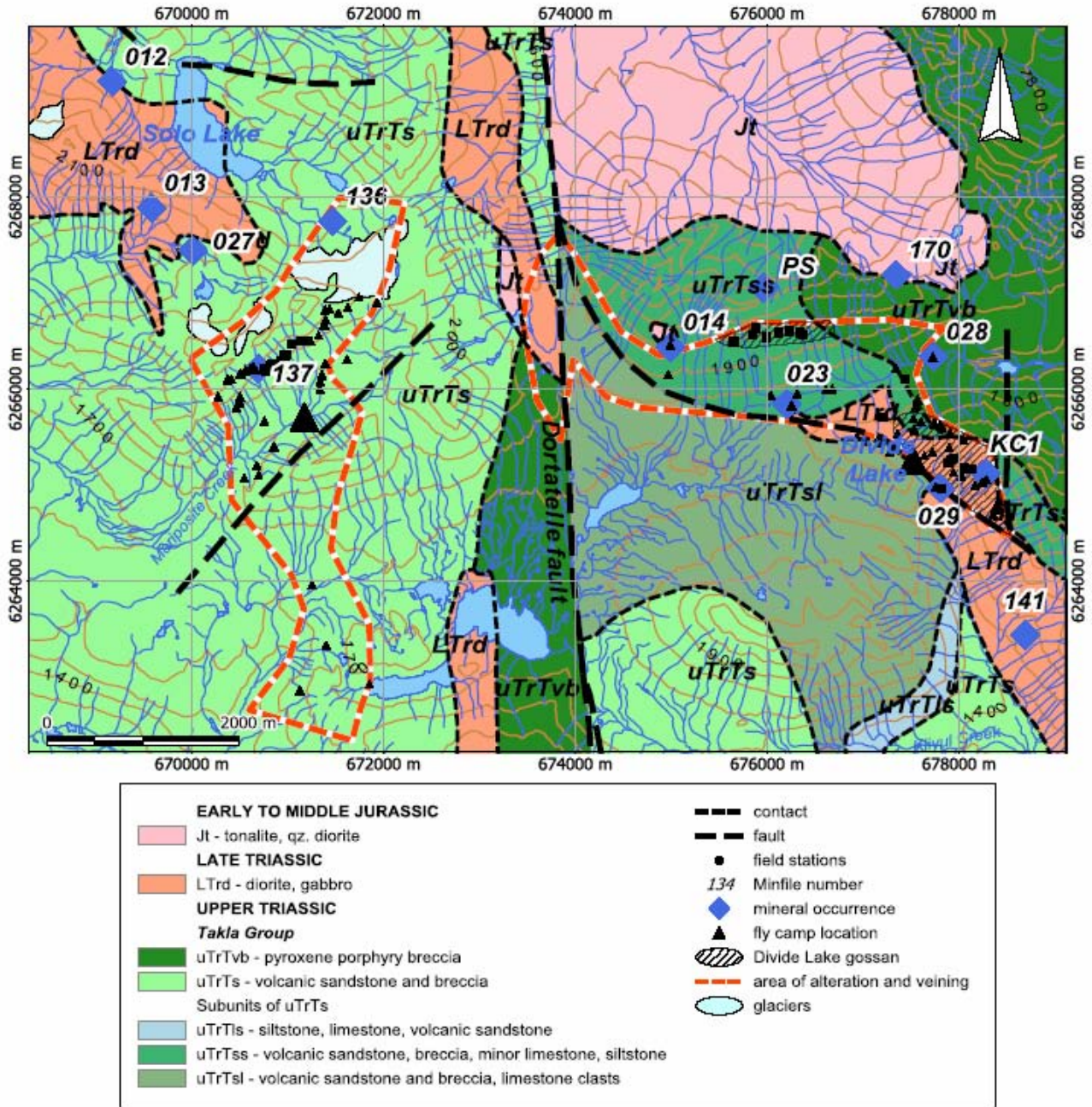


Figure 2. Geological map of the study area showing location of field stations, fly camps and mineral occurrences. Geology after Schiarizza (2004a).

TABLE 1. HISTORY OF EXPLORATION IN THE SOLO LAKE-KLIYUL CREEK AREA

Year	Operator	Area/Property	Work Done	Target	Result
1949	Goldway Peak Mines Ltd.	Goldway Peak	preliminary work	Au quartz veins	
1970-72	Kennco Explorations	Kliyul property	property staked; geochemical and geophysical surveys	zone of skarn mineralization	delineated 2.5X1.0 km IP chargeability anomaly and coincident but smaller Cu soil and magnetic anomalies
1971-72	El Paso Mining & Milling Co.	lower Kliyul Creek	prospecting	skarn mineralization	discovered skarn zones along sheared contact between ultramafics and volcanics
1973	Sumac Mines Ltd. (option from Kennco?)	Kliyul property	3 x-ray DDH	zone of skarn mineralization	unknown
1973	San Jacinto Explorations Ltd.	Goldway Peak	geochemical soil survey	Au quartz veins	unknown
1974	Sumac Mines Ltd. (option from Kennco?)	Kliyul property	6 BQ DDH	West & East zone Cu anomalies	
1974	Sumac Mines Ltd. (option from Kennco?)	Kliyul property	5 BQ DDH	magnetic high	intersected magnetite-Cu-Au mineralization in well fractured sericite, chlorite, epidote, carbonate, quartz, pyrite skarn hosted by calcareous andesite tuffs and agglomerates and lesser diorite. Estimated size of resource calculated to be 2.5 million tons grading 0.3% Cu and 0.03 opt Au
1974-75	BP Minerals Ltd.	Bap claims	geological mapping; geochemical and mag/JEM surveys	intensely sheared clay-sericite altered feldspar phyrlic volcanics/intrusives and Au quartz veins	
1976	BP Minerals Ltd.	Bap claims	Maxmin EM survey		
1981	Dupont of Canada Ltd.	AS 1 claim, Goldway Creek area	geological mapping and geochemical survey		
1981	Kennco Explorations and Vital Pacific Ltd.	Kliyul property	4 NQ DDH totaling 603 m all in southerly direction	central skarn zone	
1982	BP Minerals Ltd.	Bap claims	trace element study on previously collected samples	intensely sheared clay-sericite altered feldspar phyrlic volcanics/intrusives and Au quartz veins	
1982	Dermot Fahey and Laramie Mining Corp.	Goldway Peak	geochemical survey		
1983	Laramie Mining Corp	Goldway Peak	preparatory study to determine road access	Au quartz veins	
1984	BP Minerals Ltd.	Kliyul property	re-logged and sampled portions of core; geological mapping; geochemical sampling	skarn mineralization	
1984	Laramie Mining Corp	Goldway Peak	geological mapping; rock sampling and assaying; VLF geophysical survey	Au quartz veins	

TABLE 1 (CONTINUED)

1984	BP Minerals Ltd.	lower Kliyul Creek	geological mapping and geochemical survey		
1984	Golden Rule Resources Ltd.	KC 1 & 2	obtained claims; preliminary sampling and prospecting; further geological mapping, geochemical and magnetic surveys		
1985	BP Minerals Ltd.	Goldway Peak	geological mapping and geochemical survey	Au quartz veins	delineated Au quartz veins and fractures in quartz-carbonate-pyrite altered zone
1985	Golden Rule Resources Ltd.	KC 1 & 2	geological mapping, geochemical, magnetic and VLF surveys		
1985-1986	Laramie Mining Corp	Goldway Peak	prospecting, geological mapping, trenching and sampling	Au quartz veins	
1986	Lemming Mining Resources for BP Resources	Bap claims	soil geochemical survey	intensely sheared clay-sericite altered feldspar phyrlic volcanics/intrusives and Au quartz veins	
1986	Ritz Resources Ltd. For Golden Rule Resources Ltd.	KC 1 & 2	geological mapping, geochemical, magnetic and VLF surveys		
1990	Placer Dome	Kliyul property	line cutting, prospecting, magnetic, VLF-EM, soil and rock geochemical surveys	delineate magnetic anomalies similar to the known skarn zone, possible porphyry style mineralization and/or mineralized structures parallel to the large glacial valley	
1992	Noranda Exploration Company Ltd.	Kliyul property	1:5000 scale geological mapping, rock and minor soil sampling	alteration assemblages	
1993	Hemlo Gold Mines Inc.	Kliyul property	6 reverse circulation drill holes totaling 560 m	main skarn zone	gold bearing skarn intersected
1994	Hemlo Gold Mines Inc.	Kliyul property	10 diamond-drill holes; 1120 m	main skarn zone	gold-bearing skarn intersected
1995	gold bearing skarn intersected	Mariposite Creek property	Geochemical and geological surveys	extensive area of alteration and veining	
1996	Battle Mountain Canada	Mariposite Creek property	2 diamond-drill holes; 461 m; litho-geochemistry, 743 samples	quartz veins	drilling failed to intersect significant Au values; 70 of 743 rock samples contained >500 ppb Au

GEOLOGICAL SETTING

The geological setting of the study area is described in a previous report (Schiarizza, 2004). Only minor revisions and additional information are presented here. The geology of the study area, as mapped by Schiarizza (2004a) is shown on Figure 2. The reader should refer to an accompanying report in this volume for a current description of the regional stratigraphic units recognized in the project area.

The study area is underlain by Middle and Upper Triassic volcanic and sedimentary rocks of the Takla Group. These rocks, which are part of the Quesnel Terrane, are cut by economically important Late Triassic-Early Jurassic calc-alkaline and alkaline intrusive rocks.

The study area is situated within a belt of folded and faulted Takla Group rocks. The map pattern is strongly influenced by the development of prominent dextral strike-slip fault systems in Cretaceous and Early Tertiary time. These structures include the Finlay-Ingenika and

Pinchi faults located west and south of the study area. The north-trending Dortatelle fault, which transects the study area is believed to be related to this fault system.

Takla Group

Schiarizza (this volume) subdivides the Takla Group into a lower unit of volcanic sandstone and breccia (uTrTs) and an upper unit of predominantly pyroxene porphyry breccia (uTrTvb). The lower unit is further divided into subunits. These are

1. volcanic sandstone and breccia with local fragments, lenses and slump-blocks of limestone (TrTs)
2. volcanic sandstone and breccia with local intervals of thin-bedded limestone and siltstone (uTrTss)
3. siltstone, limestone and volcanic sandstone (uTrTls)
4. pyroxene-feldspar phyric basalt (does not occur in the study area).

For a more complete description of these lithologic units see Schiarizza (2004) and Schiarizza (this volume).

Mafic Intrusive Complexes West of the Dortatelle Fault

Gabbro, diorite and microdiorite, with minor amounts of quartz diorite and tonalite, form a narrow, northerly trending unit that has been traced for about 6 km within the volcanic sandstone and breccia unit of the Takla Group just west of the Dortatelle fault where it follows Darb Creek (Fig. 2). Similar rocks form a north-striking, sill-like body that marks the contact between the volcanic sandstone and volcanic breccia units a short distance to the south.

North Kliyul Creek Microdiorite

A separate body of mainly microdiorite, crops out in the southeast corner of the study area. These exposures are near the northern end of a northwest-trending body of diorite to gabbro that is exposed along the slopes east of the north branch of Kliyul Creek (Schiarizza, 2004). Near Divide Lake this intrusion is foliated and has pervasive quartz-sericite-pyrite alteration. Where it is less deformed and altered the rock is seen to be feldspar phyric with 40 to 60%, 1 to 2 mm feldspar phenocrysts. Numerous dikes of similar composition and trend cut Takla Group rocks west of this intrusion.

Solo Lake Stock

The Solo Lake stock intrudes the volcanic sandstone unit of the Takla Group in the northwest corner of the study area, along and southwest of Solo Lake (Fig. 2). The intrusion consists mainly of light to medium grey,

medium-grained, equigranular hornblende quartz diorite to diorite. Melanocratic hornblende-rich diorite, locally grading to hornblendite, occurs locally, as do patches and dikes of mafic-poor tonalite. Dikes showing a similar range of composition are common within the Takla Group peripheral to the stock. A sample collected during the 2003 field season gave a U-Pb isotopic age of 223.6 ± 0.8 Ma (Schiarizza, 2004a).

DARB CREEK PLUTON

A pluton of massive, light grey weathering, medium- to coarse-grained hornblende-biotite tonalite crops out on the slopes surrounding the prominent eastern tributary of Darb Creek (Fig. 2). Along its south margin the pluton cuts an east-dipping succession of the Takla Group; where observed this contact is sharp, although the tonalite contains abundant xenoliths of country rock for a few tens of metres along its outer margin. A small, presumably related pluton crops out near the Ginger B vein and shows similar abundance of xenoliths. The Darb Creek pluton is apparently truncated by the Dortatelle fault to the west. Preliminary U-Pb dating of the Darb Creek stock has given ages of 174 ± 2.0 Ma and 177 Ma on titanite and zircon respectively (Schiarizza, 2004a).

Hornblende-Feldspar Phyric Dikes

A number of northwest trending, grey weathering hornblende-feldspar phyric dikes cut pervasively altered and sheared microdiorite southeast of Divide Lake. These dikes have weak chlorite-epidote alteration but for the most part appear to be post-mineral and post-deformation. A sample was collected from one of these dikes and has been submitted for whole rock Ar-Ar isotopic age dating.

STRUCTURE

The structure of the Johanson Lake project area has been discussed in a previous report (Schiarizza, 2004). Some of this information is repeated here as regional structures are deemed to play an important role in the localization of mineral occurrences.

The structure of most outcrops within the study area is characterized by brittle to brittle-ductile faults. A large proportion of these outcrop-scale faults strike northwest to north and dip steeply; some show evidence for dextral strike-slip displacement, consistent with the interpretation that these structures are related to Cretaceous-Tertiary dextral strike slip faults that are prominent regional structures (Zhang and Hynes, 1994). However, a significant number of northwest-striking, relatively ductile faults with sinistral displacement were also observed; these may relate to an earlier period of sinistral faulting that has not been well-documented in the region. Penetrative foliations are for the most part restricted to local high strain zones associated with faults. However, a

weak slaty cleavage of more regional aspect is apparent locally, mainly in the southern part of the area. This cleavage is axial planar to local mesoscopic folds and, in the area west of the Dortatelle fault, is associated with larger folds with wavelengths of several hundred metres. The age of these structures is unknown; they may be related to the Cretaceous-Tertiary dextral strike slip faults that dominate the structure of much of the area (Zhang and Hynes, 1994), or might be vestiges of an older event, such as the late early Jurassic thrusting of the Quesnel Terrane over terranes to the east.

The Kliyul Creek–Johanson Lake map area is separated into two domains by the north-striking Dortatelle fault. The area east of the fault is broadly anticlinal in nature, with a poorly defined hinge occurring within the western part of the sandstone-carbonate unit (uTrTsl) of the Takla Group. Along its northeast margin interbedded volcanic sandstone and breccia with minor limestone and siltstone dips and faces to the northeast at moderate to gentle angles and is in turn overlain by a thick section belonging to the volcanic breccia unit. West of the Dortatelle fault the volcanic sandstone and breccia unit strikes mainly north and dips moderately to the east. Rocks exposed near the headwaters of Mariposite Creek have moderate to strong ductile deformation

Dextral Fault Systems

The structural geology of the Johanson Lake project area was studied by Zhang and Hynes (1991, 1992, 1994), who concluded that most of the deformation was related to dextral transcurrent movement on the Finlay–Ingenika fault system. They found that most faults were subvertical, and were either dextral strike-slip faults with northwest, north-northwest or north strikes, or sinistral strike-slip faults with east-northeast strikes. This suite of faults corresponds closely with the predicted orientations of structures that would form in a stress field resulting from dextral displacement along the Finlay–Ingenika fault (Tchalenko, 1970; Figure 18 of Zhang and Hynes, 1994). Zhang and Hynes also concluded, based on variations in the orientation of conjugate shear sets that formed early in the deformation history, that fault-bounded domains had rotated clockwise about subvertical axes in response to progressive displacement. Their analysis indicates rotations of up to 59 degrees adjacent to the Finlay–Ingenika fault, decreasing systematically to zero about 20 km away from the main fault. The suite of structures described by Zhang and Hynes (1994) was recognized during the 2003 mapping program (Schiarizza, 2004), but almost exclusively at the outcrop scale. With a few exceptions, such as the Dortatelle fault, individual faults could not be traced confidently beyond a single ridge or cirque basin.

The Dortatelle fault was mapped by Richards (1976), who shows it extending from the Ingenika fault northward about 40 km to just beyond Johanson Lake. Parts of the fault were studied in detail by Zhang and Hynes (1994),

who demonstrated that it was a dextral strike-slip fault on the basis of the geometric relationships between S and C surfaces and associated folds. The fault is easily mapped on the basis of its prominent topographic expression and the apparent truncation of map units along it. Rocks adjacent to the fault, particularly on its west side, are commonly strongly foliated for several hundred metres beyond the fault trace. The foliation typically strikes north-northwest and dips steeply, consistent with the interpretation of dextral displacement along the fault.

Sinistral Faults

Faults with sinistral strike-slip displacement were documented by Schiarizza (2004) within the southeastern part of the Johanson Lake project area. Three of these strike east to northeast and are reasonably interpreted as conjugate riedel shears within a dextral fault system related to the Cretaceous-Tertiary Finlay–Ingenika fault (Zhang and Hynes, 1994). Most of the sinistral faults strike west-northwest to northwest, however, and probably represent a separate deformation event. Observations made during the current study suggest that a northwest- to west-trending sinistral strike slip fault follows the north arm of Kliyul Creek, passes just west of Divide Lake and extends westward under fluvial-glacial cover towards the Dortatelle fault. The sinistral sense of displacement along this fault is inferred from the angular relationship between the shear zone boundaries and the associated flattening foliation.

Schiarizza (2004) notes that sinistral shear zones are in general more ductile than many outcrop-scale faults observed in the area, and that in two areas the shear zones were localized along pyroxene porphyry dikes. It is suspected that sinistral faulting may have been broadly contemporaneous with the latter stages of mafic magmatism in the area.

MINERAL OCCURRENCES

The following description of mineral occurrences in the study area has been abridged from an earlier report by Schiarizza (2004). Many of the occurrences in the Solo Lake–Kliyul Creek area that were described in this earlier report were visited and sampled as part of the current study.

Mineral occurrences within the Kliyul Creek–Solo Lake study area are shown on Figure 2. Most contain copper and gold, and are spatially associated with mafic plutons and related dikes. These include pyrite-chalcocopyrite in shear zones and veins within and peripheral to the plutonic rocks; magnetite-pyrite-chalcocopyrite lodes in shear zones peripheral to the plutonic rocks, and magnetite-pyrite-chalcocopyrite skarn and replacement bodies where calcareous units of the Takla Group are intruded by diorite dikes. Gold-bearing

TABLE 2. MINERAL OCCURRENCES IN THE KLIYUL CREEK–SOLO LAKE STUDY AREA.

MINFILE No.	Name	Easting	Northing	Status	Commodities	Deposit Type
012	Solo F-K veins	669170	6269201	Showing	Au Ag	Au-quartz vein
013	Bruce, A-vein	669582	6267886	Showing	Au Ag Pb	Au-quartz vein
014	Ginger B	674753	6266147	Showing	Au Ag Cu Pb	Au-quartz vein
023	Kliyul, Klisum, Kli, Kennco	676617	6266999	Developed Prospect	Au Cu Fe Ag	Skarn
027	Goldway, Mo, Ps, Solo	670011	6267439	Showing	Au Ag Pb	Au-quartz vein
028	Independence, FL, KC North, KC	677487	6266261	Showing	Au Ag Cu Pb	Au-quartz vein
029	Banjo, Bap, KC 1, KC 2	677739	6264755	Showing	Au Cu Ag Pb Zn	Au-quartz vein
136	Glacier, Joh	671470	6267746	Showing	Au	Au-quartz vein
137	Johan, Dort, Mariposite	670614	6265204	Showing	Au	Au-quartz vein
141	Mal, Cro 2	678396	6263389	Showing	Cu Au Ag	Porphyry Cu
170	Joh 9, Joh, Joh 3-10, Darb, Jo 3	677548	6267254	Showing	Au Cu	Skarn
--	KC1	678282	6265119	Showing	Au	Au-quartz vein
--	Pacific Sugar	675958	6267054	Showing	Au-Cu	Au Skarn

Note: Minfile numbers prefixed by 094D; UTM coordinates are NAD83, Zone 9

quartz veins occur within shear zones in the Solo Lake stock. Similar veins occur in the Divide Lake area and near the headwaters of Mariposite Creek. Schiarizza (2004) suggested these major alteration zones reflected the area's potential for large porphyry-style copper-gold mineralizing systems and thus, became the primary focus for the current study.

Gold Quartz Veins in the Divide Lake Area

A series of bright red and yellow outcrop bluffs and talus slopes define an irregular zone of quartz-pyrite ±sericite alteration that extends from the head of Darb Creek for about 5 km southeast, to the head of the north fork of Kliyul Creek (Photo 1). This conspicuous alteration attracted early prospectors in the area, who discovered the Ginger B (MINFILE 094D 014), Independence (094D 028) and Banjo (094D 029) gold-bearing quartz vein systems within and peripheral to the zone (White, 1948). The KC 1 occurrence, northeast of the Banjo, was discovered within the alteration zone at a later date (Fox, 1982).

Mineralization within the North Kliyul Creek Dioritic Stock

The dioritic stock that crops out on the slopes east of the north fork of Kliyul Creek hosts mineralization represented by the KC 2 (094D 140) and Mal (094D 141) MINFILE occurrences. The Cro 2 occurrence is along the southwest margin of the stock about 1 km south of the Mal. Mineralization at the KC 2 occurrence covers a broad area along the northeast margin of the stock and extends into the Takla country rocks. It includes quartz veins and silicified or quartz-carbonate-altered shear zones mineralized with magnetite, pyrite, chalcopyrite, malachite and azurite, and locally galena and sphalerite (Wilson, 1984; Cross, 1985). Shear zones trend northwest, north and northeast. Samples of mineralized material have yielded assay values of up to 5484 ppb Au and 14.5 ppm Ag (Cross, 1985). The Mal occurrence comprises variably oriented quartz-carbonate veins associated with fractures and shear zones that occur over several hundred metres along a major tributary to the north fork of Kliyul Creek. Some

of the veins and shears are mineralized with pyrite, galena and malachite. A sample of one rusty quartz-carbonate vein containing disseminated pyrite yielded 16200 ppb Au and 3.10 ppm Ag (Wilson, 1984). At the Cro 2 occurrence, rocks of the Takla Group are cut by silicified, chloritized and pyritized shear zones for at least several tens of metres along the southwest margin of the diorite stock. The zone contains small quartz-pyrite veins, and a sample of one of these veins contained 294 ppb Au and 5.40 ppm Ag (Fox, 1991).

Magnetite-Pyrite-Chalcopyrite Skarn Occurrences

The Kliyul magnetite-pyrite-chalcopyrite occurrence (MINFILE 094D 023) is located in an area of poor bedrock exposure within the broad valley, bounded by gossanous bluffs and talus slopes, at the head of Kliyul Creek. Geology projected from the south and north suggests that the volcanoclastic rocks that host the mineralization are within the sandstone-carbonate unit of the Takla Group. The area was staked in 1970 and explored with silt, soil and geophysical surveys. Copper-gold mineralization associated with magnetite was discovered in 1974 by a drill program that tested a magnetic anomaly. Exploration by various companies subsequent to the initial discovery included diamond drilling in 1981 and reverse circulation drilling in 1993. The latter program extended the known skarn mineralization and suggested that the resource estimate of 2.5 million tons grading 0.3% Cu and 0.03 ounces per ton (oz/T) Au from the initial drilling could be increased (Gill, 1993). Two samples were collected from outcrop in Lay Creek which drains through the area of skarn mineralization.

The Pacific Sugar skarn showing, located about 1 km north of the Kliyul occurrence, was discovered in the mid 1990s. It is hosted by the volcanic sandstone unit of the Takla Group, which at this location includes an interval of calcareous siltstones and limestones. Exploration work to date has outlined a magnetite-pyrite-epidote-garnet skarn unit measuring 40 by 100 m and 3 to 6 m thick (Gill, 1995). Mineralization consists of massive magnetite and pyrite containing disseminations, impregnations and clots of pyrrhotite and chalcopyrite. Endoskarned diorite in the footwall of the unit is inferred to be the source of the skarn mineralization. The skarn was tested with 5 diamond-drill holes, with a cumulative length of 154.8 m, in 1996. Significant drill results include 2048 ppm Cu and 625 ppb Au over 3.97 m (Leriche and Harrington, 1996).

Gold Quartz Veins Associated with the Solo Lake Stock

Gold-bearing quartz veins within, and along the margins of, the Solo Lake stock are among the oldest documented mineral exploration targets within the study area. The Solo (MINFILE 094 D 012), Bruce (MINFILE 094D 013) and Goldway (MINFILE 094D 027) occurrences were explored in the mid 1940s and are described by White (1948). Exploration has continued intermittently to the present time, and new vein systems have been discovered, including the F vein (Pawliuk, 1985), the V3 occurrence (V1, V2 and V3 samples of von Rosen, 1986) and the Tar occurrence (MINFILE 094D 138; L veins of Richards, 1991).

The vein systems associated with the Solo Lake stock are well described by Richards (1991). Each occurrence comprises a number of veins, with individual veins ranging from several metres to several hundred metres in length, and from a few centimetres to several metres in width. Gold and silver ratios are commonly near one to one, and the precious metals are associated with pyrite, and locally galena and sphalerite. Visible gold has been reported from the A and C veins of the Bruce occurrence. The A vein has returned assay values up to 74.19 g/t Au over 29 cm (Phendler, 1984).

The geometry of the vein systems is most apparent at the Solo and Bruce occurrences, where individual veins are arranged in echelon within northwest-striking zones that approach 1 km in length. Individual veins strike more northerly than the overall system, and are inferred to occupy extensional fractures within dextral shear systems (Richards, 1991). Alteration related to the veins is minimal, and Richards (1991) suggests that the veins may be related to fault movements during the late stages of emplacement and cooling of the Solo Lake stock.

Gold Quartz Veins and Stockwork within the Mariposite Creek Alteration Zone

A zone of quartz-ankerite-pyrite alteration, marked in part by conspicuous orange-brown-weathered outcrops, extends north and south of upper Mariposite Creek for a total length of about 5 km (Fig. 2). Quartz veins are an integral part of this alteration, and exploration at the Glacier (MINFILE 094D 136) and Mariposite (MINFILE 094D 137) occurrences, where veins are particularly dense, has been directed towards evaluating the area's potential to host a bulk tonnage gold deposit. Gill (1996) reports that 743 rock samples

TABLE 3. LITHOGEOCHEMICAL SAMPLE DESCRIPTIONS.

Sample	Easting	Northing	Material sampled	Vein width	Mineralization	Alteration	Showing
DMA04-001	677640	6265306	quartz vein	5 cm			
DMA04-001A	677640	6265306	quartz vein	5 cm			
DMA04-002	677725	6265337	quartz vein	3-4 cm			
DMA04-002A	677725	6265337	quartz vein	3-4 cm			
DMA04-003	677897	6265392	microdiorite		trace pyrite	chlorite-epidote	
DMA04-005	678048	6265474	quartz vein				
DMA04-007	677801	6265625	microdiorite			chlorite-epidote	
DMA04-011	677942	6265130	sheared microdiorite		pyrite	oxidized	
DMA04-012	678029	6265090	microdiorite		pyrite	quartz-sericite	
DMA04-013	678168	6264990	microdiorite		pyrite	quartz-sericite	
DMA04-014	678243	6265023	microdiorite		pyrite	quartz-sericite	
DMA04-015	678289	6265051	quartz vein	up to 40 cm			
DMA04-017	678399	6264794	microdiorite		pyrite	quartz-sericite	
DMA04-019	678358	6264687	sheared microdiorite		malachite	chlorite-epidote	
DMA04-019A	678358	6264687	sheared microdiorite		malachite	chlorite-epidote	
DMA04-020	677564	6265276	sheared microdiorite		malachite, pyrite	chlorite-epidote	
DMA04-021	677281	6265343	quartz vein	40 cm	malachite, pyrite		
DMA04-021A	677281	6265343	quartz vein	40 cm			
DMA04-022	677165	6265432	quartz vein				
DMA04-023	677033	6265461	qz-carbonate vein			chlorite-epidote	
DMA04-026	676037	6265933	microdiorite		pyrite	quartz-sericite	
DMA04-027	674990	6266457	quartz vein	3-5 m			
DMA04-027A	674990	6266457	quartz vein	3-5 m	pyrite		Ginger B
DMA04-027B	674990	6266457	quartz vein	3-5 m	malachite, pyrite		Ginger B
DMA04-027C	674990	6266457	volcanic with qtz veinlets	3-5 m	pyrite	chlorite-epidote	Ginger B
DMA04-028	674967	6266149	quartz vein	30 cm			
DMA04-028A	674967	6266149	fd. phytic volcanic	30 cm	pyrite	chlorite-epidote	
DMA04-029	676315	6265951	skarn		pyrite	chlorite-epidote	Kliyul
DMA04-031	676679	6265998	quartz vein	1 m			
DMA04-032	677344	6266215	quartz vein	2-10 cm			
DMA04-033	677729	6266334	quartz vein	1 m	pyrite		Independence
DMA04-033A	677729	6266334	volcanic with qz veinlets	1 m		quartz-carbonate	Independence
DMA04-034	677572	6265887	quartz vein	2 m			
DMA04-038	677359	6265534	microdiorite		pyrite	quartz-sericite	
DMA04-040	677757	6264975	quartz vein				Banjo
DMA04-042	670734	6266198	quartz vein				
DMA04-044	670638	6266233	quartz vein	30 cm			
DMA04-045	670607	6266208	quartz vein				
DMA04-045A	670607	6266208	volcanic with qz veinlets				
DMA04-046	670559	6266192	quartz vein	10 m			
DMA04-047	670508	6266157	quartz vein	1.5 m			
DMA04-049	670373	6266096	quartz vein	2 cm			
DMA04-050	670274	6265918	quartz vein	5-7 m			
DMA04-051	670507	6265918	quartz vein	1 m			
DMA04-052	670500	6265856	volcanic with qz veinlets			quartz-carbonate	
DMA04-053	670464	6265811	quartz vein	80 cm			
DMA04-053A	670464	6265811	volcanic			quartz-carbonate	
DMA04-055	671743	6266956	quartz vein	.5-5 cm	pyrite		
DMA04-056	671627	6266846	quartz vein	10 cm	pyrite		
DMA04-057	671527	6266789	quartz vein				

DMA04-059	671391	6266823	quartz vein	2-5 cm		
DMA04-060	671399	6266718	quartz vein			
DMA04-060A	671399	6266718	quartz vein	10-20 cm		
DMA04-061	671383	6266669	quartz vein	1-5 cm		
DMA04-062	671321	6266559	quartz vein			
DMA04-064	671340	6265995	metased		pyrite	silicified
DMA04-064A	671340	6265995	quartz vein	1-2 cm		
DMA04-065	671338	6266079	quartz vein			
DMA04-065A	671338	6266079	metased		pyrite	quartz-carbonate
DMA04-065B	671338	6266079	metased with qz veinlets		pyrite	quartz-sericite
DMA04-066	671356	6266143	quartz vein	5-15 cm		
DMA04-067	671395	6266265	quartz vein			
DMA04-069	670858	6265396	quartz vein	30 cm		
DMA04-070	670678	6265201	quartz vein			
DMA04-071	670695	6265100	quartz vein	3-5 m		
DMA04-072	670550	6265072	quartz vein	2-3 m		
DMA04-073	670755	6265665	quartz vein	60-100 cm		
DMA04-074	671222	6265634	quartz vein			
DMA04-075	671255	6263961	quartz vein	7 cm		
DMA04-076	671402	6263325	volcanic with qz veinlets			quartz-carbonate
DMA04-078	671854	6262923	quartz vein	15-25 cm		
GPA04-001	677949	6265276	microdiorite		pyrite	quartz-sericite
GPA04-002	677890	6265230	microdiorite		pyrite	quartz-sericite
GPA04-004	678052	6265173	microdiorite		pyrite	quartz-sericite
GPA04-005	678140	6265170	microdiorite		pyrite	quartz-sericite
GPA04-007	675849	6266563	microdiorite		pyrite	chlorite-epidote
GPA04-008	675878	6266634	microdiorite		pyrite	chlorite-epidote
GPA04-009	675994	6266541	microdiorite		pyrite	quartz-sericite
GPA04-012	676234	6266594	microdiorite		pyrite	quartz-sericite
GPA04-014	676374	6266563	microdiorite		pyrite	quartz-sericite
GPA04-015	677440	6266098	quartz vein			
GPA04-015A	677440	6266098	quartz vein			
GPA04-016	677208	6265707	rhyolite dike		pyrite	
GPA04-017	677820	6264961	qz-fd porph. dike		pyrite, chalcopyrite	
GPA04-017A	677820	6264961	volcanic with qz veinlets			silicified
GPA04-018	670757	6266218	quartz-carbonate vein	up to 85 cm		
GPA04-020	670813	6266231	quartz vein	2-5 cm	pyrite	
GPA04-021	670819	6266249	quartz-carbonate vein	60 cm		
GPA04-022	670830	6266255	quartz-carbonate vein	up to 60 cm		
GPA04-026	670944	6266290	quartz vein	12 cm		
GPA04-029A	671041	6266472	metased			
GPA04-031	671217	6266497	quartz vein			

Note: UTM coordinates are zone 9, NAD83

TABLE 4. ANALYTICAL DATA.

Sample	Au ppb	Cu ppm	Ag ppm	Pb ppm	Zn ppm	As ppm	Mo ppm	Ni ppm	Co ppm	Cr ppm	Mn ppm	Ba ppm	Fe %	Ca %	Mg %	S %
DMA04-001	18.5	13.3	0.1	1.4	97	1	1.9	5.4	13.7	7.8	636	67	5.03	0.22	1.9	2.15
DMA04-001A	17.3	12.5	0.1	1.6	87	0.8	1.8	4.4	12.8	6.4	604	52	4.86	0.2	1.77	1.97
DMA04-002	0.6	5.1	0	0.8	24	1.6	0.2	7.4	6.2	35.6	544	3	1.48	0.81	0.67	0
DMA04-002A	8.9	21.7	0.1	1.5	30	1.6	0.2	7.1	15.4	4	252	32	5.06	0.24	1.4	4.52
DMA04-003	23	79.6	0.2	2.1	91	2.7	0.6	4.7	4.9	4.1	592	47	4.13	0.26	1.84	0.17
DMA04-005	32.4	10.9	0.6	0.8	62	0	0.2	2.9	2.6	4.3	325	6	0.64	0.07	0.01	0
DMA04-007	9.7	32	0.3	40.7	201	6.2	1	6.3	16.5	5.4	1638	45	4.07	0.56	1.8	1.75
DMA04-011	11.3	11.3	0.2	1.4	154	1.5	0.6	5.3	2.4	6.3	730	119	2.38	0.27	1.37	0.09
DMA04-012	11.1	14.9	0.1	3	63	2.8	1.3	4.9	8.7	5.6	356	32	4.43	0.18	1.22	2.97
DMA04-013	6.2	22	0.1	6.2	63	5.6	0.8	3.4	6.1	12.6	491	25	5.05	0.04	1.89	2.11
DMA04-014	33.1	11.4	0.6	16.2	22	3.9	0.8	2.5	7.4	1.3	114	38	3.66	0.01	0.35	2.58
DMA04-015	326.6	259.4	3.1	12.1	131	0.8	0.5	2.7	7.2	2.6	641	11	2.58	0.01	0.02	0
DMA04-017	10.7	21.2	0.2	0.9	57	3.8	0.5	4.8	5.3	4.6	832	36	2.64	0.5	1.23	1.22
DMA04-019	21.9	9246.9	0.3	1.6	120	0	0.2	5	15.3	18.9	795	142	3.38	2.03	1.5	0
DMA04-019A	9.5	3188.7	0.1	1.2	94	0	0.1	5.5	13.6	5.6	734	81	2.32	0.18	0.86	0
DMA04-020	286.4	3830.9	3.3	1.1	178	0	0.2	49.2	57.6	188.9	2273	2	6.99	1.57	4.2	0.06
DMA04-021	24.4	350.8	0.4	1.8	7	0	2	5.4	2.3	7.1	418	15	1.54	1.15	0.05	0.26
DMA04-021A	6.2	12.4	0.1	0.7	2	0	0.5	2.2	1	5.6	182	5	0.67	0.1	0.01	0.12
DMA04-022	38.5	10.7	0.3	1.5	13	0	0.9	2.8	3.2	3.5	472	15	1.43	0.08	0.02	0.13
DMA04-023	4	5.8	0	1.5	9	0.5	5.7	5.2	2.3	5.7	458	10	0.94	1.75	0.19	0
DMA04-026	39.6	225.9	0.3	8.9	295	4.5	1.3	12.2	8.5	17.7	688	72	2.12	0.72	1.61	0.73
DMA04-027	14.3	23.2	0.1	0.8	1	0	1.3	1.3	0.4	3.9	60	14	0.46	0.01	0	0
DMA04-027A	11360.8	21.9	18.1	5.7	11	0	59.4	3.8	3	12.1	538	4	1.74	0.1	0.42	0.35
DMA04-027B	9136.8	106.2	17.7	4.8	11	0	8	3	2.2	8.6	499	5	1.23	0.45	0.41	0.35
DMA04-027C	57	163.5	0.4	3.6	97	0.8	0.8	10.2	22	10.2	2004	58	4.27	2.26	2.17	1.48
DMA04-028	39	31.4	0.1	1.2	2	0	23.6	1.6	5.3	1.8	155	3	0.62	0.31	0.05	0.06
DMA04-028A	9.5	21.8	0	0.8	69	3.2	0.7	15.5	19.7	27.4	812	69	3.28	0.58	1.71	1.45
DMA04-029	1009.5	933.9	2.3	7.2	430	0	0.9	6.4	21.3	4.6	804	16	13.51	0.2	1.38	0.13
DMA04-031	51.4	11.8	0.2	2	23	0.8	0.7	3.3	6.5	3.7	283	20	1.64	0.39	0.08	0.51
DMA04-032	7.1	10	0	4.6	18	0.6	0.2	3	3.1	4.5	582	727	0.99	1.17	0.04	0.15
DMA04-033	1194.8	53.1	1.5	1.8	14	0	2.5	8.1	14.9	7	466	21	1.86	0.47	0.03	0.81
DMA04-033A	57.3	166.1	0.5	4.9	71	0	0.4	6.6	30.2	1.2	1278	97	4.3	4.58	1	1.11
DMA04-034	115.4	7.1	0.7	30.1	8	0	69.1	1.9	1.8	3.8	172	33	1.12	0.06	0.03	0.18
DMA04-038	13.4	26.1	0.1	2.3	34	0	0.9	3.1	6	4.1	264	15	4.82	0.33	1.62	3.24
DMA04-040	62.5	167.7	3.6	454.6	13	0.7	2.5	32	4.6	36.8	248	86	1.22	0.08	0.27	0.17
DMA04-042	194.7	101.7	1.3	8.4	29	14.3	0.8	2.2	7.2	2.7	917	24	1.77	4.47	0.05	0.25
DMA04-044	14	11.6	0.2	12.8	13	0.8	0.7	3.1	2.2	3.3	420	14	1.1	1.83	0.02	0
DMA04-045	265.2	7.5	1.5	111.8	25	3.7	4.7	11.6	1.4	7.8	699	7	0.73	4.62	0.04	0
DMA04-045A	183.8	67.8	0.6	11.6	77	0.9	2.4	14.8	24.1	7.9	1522	108	5.62	6.3	2.25	0.84
DMA04-046	30.4	15	0.4	2.4	8	0.7	1.4	1.8	1.5	4	101	3	0.62	0.04	0.01	0
DMA04-047	15.3	10.3	0.1	5	73	1.3	7.3	4.8	1.3	4.5	567	6	0.88	3.75	0.02	0
DMA04-049	7.2	11.5	0.1	23.6	14	1.1	0.6	3.4	3.1	4.7	1575	47	1.32	9.38	0.19	0.24
DMA04-050	6.9	5.6	0.1	0.7	2	0	0.4	1.7	0.8	7.1	140	3	0.82	0.08	0	0
DMA04-051	6	24.8	0.1	1.2	5	1.1	2.7	2.6	2.7	5.6	223	14	0.94	0.3	0.01	0
DMA04-052	58.9	441.9	1.6	2.5	6	4.6	0.2	3.7	5.6	2.5	1420	8	1.13	11.03	0.14	0.1
DMA04-053	21.5	26.9	0.4	4.7	21	0.9	3.1	1.9	1.5	5.2	140	12	0.78	0.11	0.02	0.06
DMA04-053A	24.5	65.9	0.3	2.7	78	0.8	0.7	14.4	22.5	20.4	969	33	5.24	3.65	1.73	0.31
DMA04-055	312.5	54.3	0.8	11.2	3	0	0.1	3.4	5.4	3.2	173	7	1.76	0.67	0.02	0.93
DMA04-056	904.8	21.5	0.3	0.7	2	6.9	0.2	3	5.6	4.4	183	8	1.23	0.29	0.01	0.18

DMA04-057	2.8	2.3	0.1	21.2	15	0	0.1	2.6	1.3	2	3453	14	1	28.34	0.25	0.06
DMA04-059	4.4	8.6	0.1	0.9	3	1.4	0.1	2.8	2.5	3.9	261	9	1.1	0.2	0.01	0.06
DMA04-060	228.1	70.7	0.8	7.4	42	57.1	0.9	6.4	16	3.4	993	68	3.38	4.02	0.67	1.27
DMA04-060A	10.2	27.5	0.1	1.4	7	0.8	0.2	8	4.5	4.5	222	9	1.13	0.65	0.04	0.07
DMA04-061	30.3	20.8	0.2	7.3	13	5.2	2.9	4.5	5.4	3.8	2053	57	1.33	17.49	0.3	0.09
DMA04-062	227.6	9.5	1.2	21.5	16	1.3	3.8	8.5	4	6.3	1043	18	1.47	6.94	0.66	0.07
DMA04-064	72.8	96.2	0.8	5.5	97	23.9	1.1	46.3	22.9	71.1	1008	120	4.75	4.25	2.17	0.69
DMA04-064A	93.8	57.9	0.5	9.6	112	5.1	0.6	43.9	25.8	43.7	1150	95	5.06	4.13	1.61	0.5
DMA04-065	48.7	31.3	0.3	10.6	20	4.2	0.1	2.6	3.2	3.4	913	27	1.42	8.69	0.23	0.32
DMA04-065A	9.5	117.8	0.3	4.4	62	1.9	1.4	30.9	24.3	22.8	1232	39	5.24	5.01	2	0.93
DMA04-065B	826.3	173	1.3	9.7	107	173.4	1.3	69.6	24.7	15.2	1042	86	5.66	4.85	1.96	2.11
DMA04-066	27.1	9.2	0.3	59.8	16	5.4	0.2	2	1.9	4.6	291	15	1.22	3.13	0.08	0.19
DMA04-067	45.7	18.8	0.3	5.6	7	2.3	0.5	1.5	1.9	3.2	1342	30	1.08	10.49	0.08	0.11
DMA04-069	1.8	4.8	0	0.7	7	0.6	0.2	1.6	0.5	5.9	131	3	0.94	0.04	0	0
DMA04-070	5	4.2	0.1	1	3	0	0.2	2.1	0.7	6.2	136	2	0.53	0.21	0	0
DMA04-071	116.2	41.8	0.4	4	22	0.6	0.2	4.7	1.7	5.8	170	6	0.8	0.48	0.03	0
DMA04-072	338.5	5.9	1.4	1.5	266	0.8	0.2	2.6	1.2	5.1	163	1	0.56	0.48	0.02	0
DMA04-073	155.1	8.2	10.6	207.1	301	0.7	0.2	1.5	1.3	3.6	226	9	0.71	0.35	0.01	0
DMA04-074	4.3	4.8	0.3	13.5	23	0.6	0.2	1.3	0.6	4.6	128	10	0.67	0.12	0	0.09
DMA04-075	52.8	15.1	0.2	3.5	28	6.7	0.2	10	10	10	610	52	2.16	2.4	0.61	0.14
DMA04-076	378.6	25.8	0.3	2.1	24	10.9	0.2	4.2	8.5	3.2	792	30	2.49	3.64	0.9	0.36
DMA04-078	2.4	13.6	0.1	1	2	2.9	0.3	4.6	2.5	5.5	68	5	0.75	0.04	0.01	<0.05
GPA04-001	19.6	110.5	0.2	3.5	103	0.5	1.4	4	7.7	2.7	636	30	3.67	0.23	1.73	1.07
GPA04-002	1	23.7	0	1.2	36	0.6	0.2	4	2.1	9.4	324	15	2.2	0.14	1.86	0.24
GPA04-004	17.7	22.3	0.2	2	44	0	0.7	2.6	1	3.2	494	29	3.49	0.25	1.38	0.07
GPA04-005	6.4	37.5	0.1	1.8	151	2.5	0.5	5.4	7.1	7.3	1466	25	3.34	0.44	1.99	0.49
GPA04-007	3.3	34	0.1	3.7	98	1.8	0.7	7.5	10.1	10.6	935	121	3.89	0.59	2.17	1.1
GPA04-008	6.9	38	0.1	1.3	44	2.5	1.2	4.4	8.8	2.8	440	52	3.58	0.16	0.63	1.81
GPA04-009	2.1	21.2	0.1	7	85	1.4	0.5	16.4	5.6	67.1	476	101	3.61	0.26	1.63	1.52
GPA04-012	4.6	16.7	0.1	2.1	15	0	0.6	4.7	2.3	13.2	234	42	3.28	0.03	0.88	0.61
GPA04-014	15.3	30.2	0.2	2.8	26	0.6	1.1	3.4	5.8	2.3	126	75	2.15	0.08	0.43	0.51
GPA04-015	102	6.9	1.3	4.4	11	0	1.7	25.9	7.7	5.7	618	10	1.53	0.06	0.02	0.14
GPA04-015A	399.9	150.8	13.1	13.5	88	5.3	0.3	330.4	43.3	115.2	3658	44	5.29	10.15	5.31	2.08
GPA04-016	9	9.1	1.3	30.5	31	2.5	0.1	1.1	1	1	149	4	0.49	0.02	0.01	0.08
GPA04-017	2.9	569.2	0.6	23.4	16	0	6.7	43.8	7.1	50.2	400	42	1.47	1.02	0.77	0.33
GPA04-017A	20.4	33.3	0.2	21.7	69	1.1	9.5	191.8	31.2	525.8	1099	327	3.81	5.38	4.15	0.54
GPA04-018	58.1	30.4	0.6	22	16	0.7	2.6	18.6	3.6	10.1	808	14	1.13	5.03	0.15	0
GPA04-020	689.7	8.8	1.1	1.8	6	5.8	1.3	3.5	2.8	6.8	444	57	1.15	2.29	0.1	0.17
GPA04-021	43.7	38.9	0.3	4	55	3.3	1.1	12	12	10.8	1115	37	3.6	6.46	0.93	0.18
GPA04-022	41.2	8.9	0.3	9.6	29	1.3	0.9	12.6	2.6	8.8	283	7	0.97	1.24	0.1	0
GPA04-026	100.1	5.1	0.1	5.1	27	1.2	0.2	2.4	1.3	6	122	6	0.76	0.07	0.01	0
GPA04-029A	34.1	90.1	0.5	17.9	35	6.5	0.5	15.8	18.4	7.9	1294	150	2.99	8.88	0.64	0.44
GPA04-031	229.5	6.2	1.9	74.4	34	1.3	14.9	26.8	2.8	16.5	340	16	1.13	1.37	0.33	0

Analytical done by Acme Analytical Laboratories, Vancouver B.C. Analytical method: ICP-MS, 30 gram sample, hot acid leach.

collected in the area of the Mariposite and Glacier occurrences included 70 samples (9%) that contained greater than or equal to 500 ppb Au. Two diamond-drill holes on the Mariposite occurrence intersected high density quartz-carbonate vein and stockwork intervals, but these contained only weak gold mineralization (Gill, 1996).

RESULTS OF THE CURRENT STUDY

The primary focus of the current study was to collect a suite of lithogeochemical samples from two areas of extensive alteration and veining that were identified as prospective during the 2003 field season. The first of these areas, referred to here as the Divide Lake area, ex-

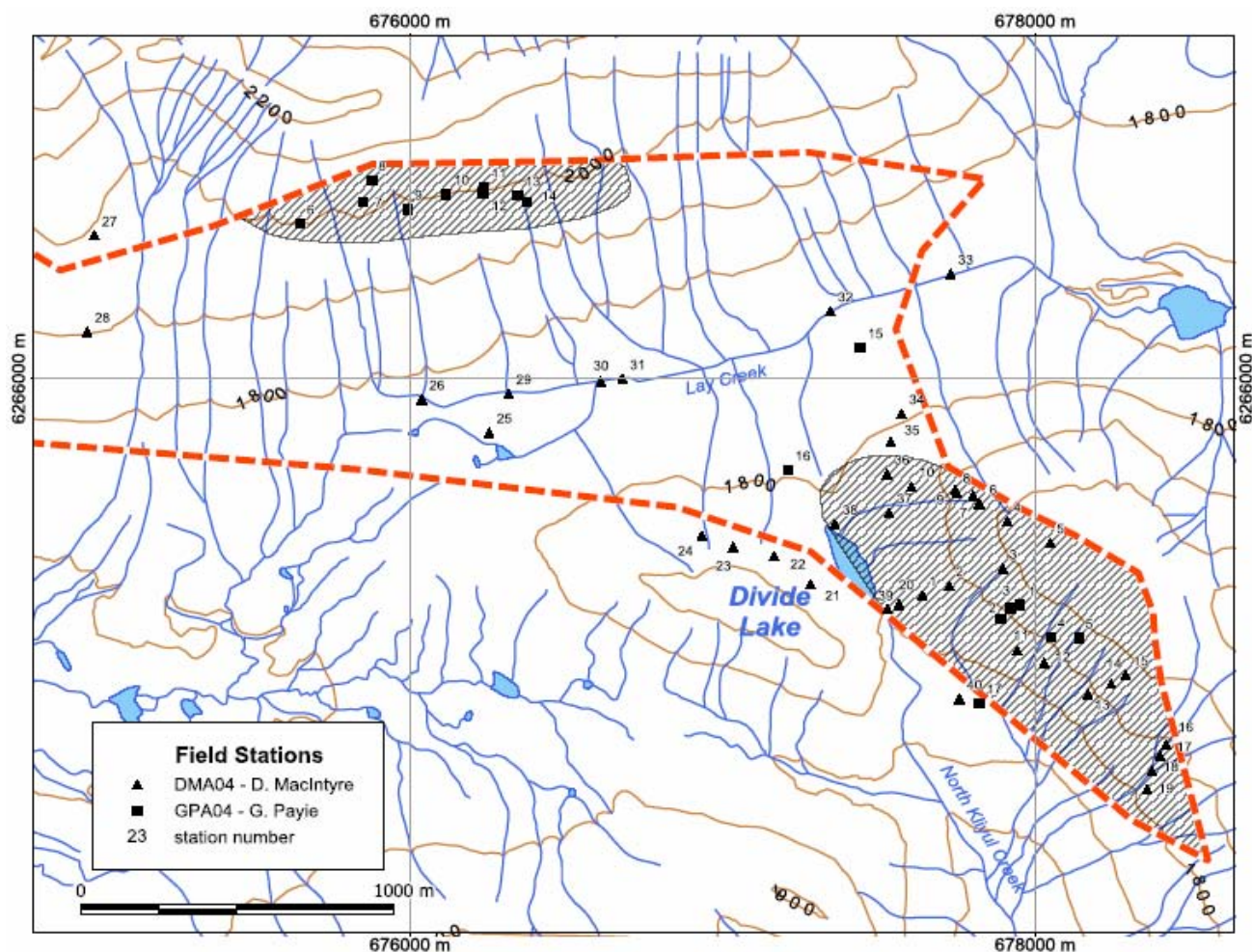


Figure 3. Field station locations, Divide Lake area.

tends from the headwaters of the north arm of Kliyul Creek westward to the Dortatelle fault (Fig. 2). At the southern end of this zone is a prominent gossan that is well exposed on steep southwest-facing slopes southeast of Divide Lake (Fig. 2). The second area, referred to here as the Mariposite Creek area, extends from the headwaters of Mariposite Creek southward toward Dortatelle Creek. Sampling done within these two areas was primarily of quartz veins and altered wall rocks. Sample descriptions are presented in Table 3 and analytical results are given in Tables 4 and 5.

Divide Lake Area

As described in an earlier section, mineral occurrences in the Divide Lake area can be categorized into 3 main groups – gold quartz veins such as the Banjo, Independence, Ginger B and KC1, shear-hosted copper mineralization such as the Mal and magnetite-pyrite-chalcopyrite skarn such as the Kliyul and Pacific Sugar (Table 2). In addition an extensive gossanous zone of foliated microdiorite and Takla volcanic rocks with per-

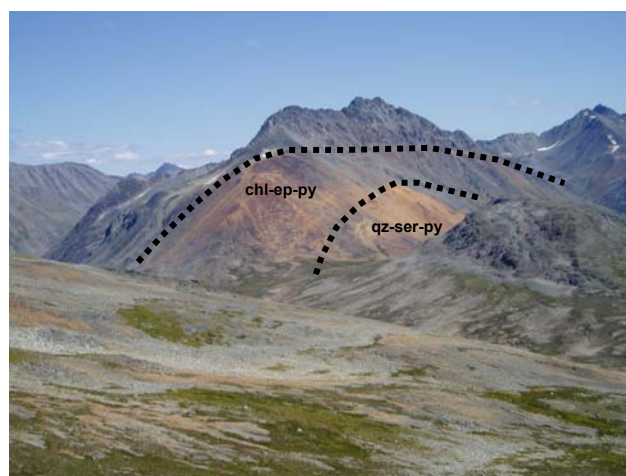


Photo 1. View southeast toward the Divide Lake gossan showing approximate boundaries of chlorite-epidote-pyrite and quartz-sericite-pyrite alteration zones. Altered rocks are mainly microdiorite. Divide Lake is located in the pass near the base of the gossan. The headwaters of Lay Creek are in the foreground. The prominent ridge east of the gossan is composed of resistant, east-dipping volcanic breccias of the Takla Group (unit uTrTv).

vasive quartz-sericite-pyrite and chlorite-epidote-pyrite alteration crops out on the steep southwest-facing slope southeast of Divide Lake (Photo 1). This zone is referred to here as the Divide Lake gossan. As shown on Figure 3, the majority of field stations in the Divide Lake area were located within this zone of alteration and mineralization.

GOLD QUARTZ VEINS

The gold-quartz veins at the Ginger B, Independence, Banjo and KC1 showings, which are on the order of 1 to 5 m in width, typically occur within massive volcanoclastic or dioritic intrusive rocks that locally show evidence of shearing. The veins are steeply dipping to vertical and strike northwest, northeast and east (Fig. 4). Although sulphide content is generally low, sulphides do sometimes occur as bands near the outer margins of the veins with various combinations of pyrite, chalcopyrite and rare galena (Photo 2). Significant gold and silver values have been reported from all of the occurrences (White, 1948; Fox, 1982; Christopher, 1986). A sample collected from a pyrite-chalcopyrite-bearing quartz vein on the Banjo showing during the 2003 mapping program contains 2251 ppb Au and more than 100 ppm Ag (Schiarizza, 2004a: sample 03PSC-93). Samples collected as part of the current project (Table 3, Fig. 3) confirm anomalous gold values at all of these showings (Table 4, Fig. 5). Copper values, on the other hand, are generally low to weakly anomalous for quartz veins but higher in sheared microdiorite along the trend of the North Kliyul Creek fault (Table 4, Fig. 6).

All major quartz veins in the Divide Lake area were re-examined as part of the current study. The best results came from two samples of the Ginger B quartz vein (DMA04-027A, DMA04-027B) which were assayed and gave values of 10.38 and 9.12 g/t Au respectively (Table 5). Both of these grab samples contained pyrite and one contained malachite. A third sample of barren quartz from the centre of the vein (DMA04-027) contained low Au, Cu and Ag values. This suggests that the Au values in the Ginger B vein are associated with the occurrence of pyrite.

Another major quartz vein in the area, the Independence vein, is exposed in a trench along the south bank of Lay Creek (Photo 3). A sample from this vein (DMA04-033), which contained minor amounts of pyrite, was assayed and gave a value of 1.25 g/t Au (Table 5). However, a sample of quartz-carbonate-pyrite altered wall rock (DMA04-033A) contained low Au and slightly anomalous copper values.

Although good gold values have been reported for the Banjo vein (Schiarizza, 2004), a sample collected as part of this study only contained slightly anomalous gold and copper and 454 ppm lead. Such variation in values from the same vein reflects the notorious “nugget effect” which makes sampling and evaluation of quartz veins very difficult.



Photo 2. View southwest toward the Ginger B gold-quartz vein. Rock hammer for scale. Note banding and Fe oxide staining near vein contact. A sample collected from this material assayed 10.38 g/t Au.

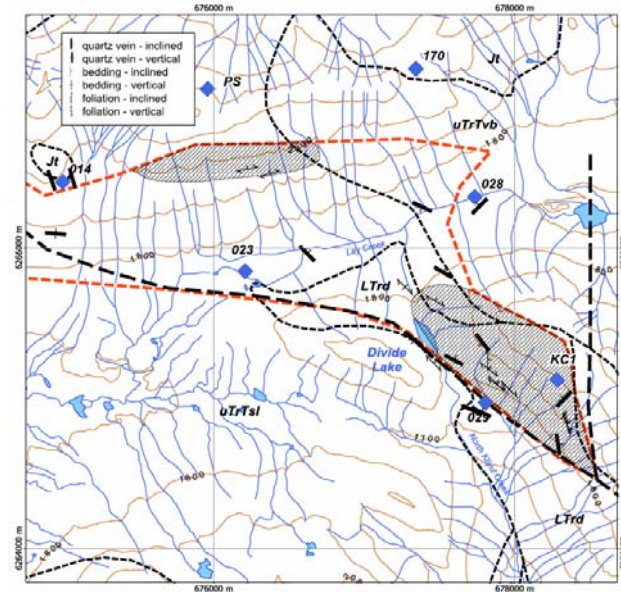


Figure 4. Structural trends of gold-quartz veins, bedding and foliation in the Divide Lake area. See Figure 2 for legend.

A prominent quartz vein, up to 40 cm in width, has been exposed by trenching near the top of the ridge east of Divide Lake. This vein occurs within an area of pervasive chlorite-epidote alteration and is thought to be

TABLE 5. FIRE ASSAY RESULTS.

Sample	Showing	g/t Au
DMA04-027A	Ginger B quartz vein	10.38
DMA04-027B	Ginger B quartz vein	9.12
DMA04-029	Kliyul skarn	1.04
DMA04-033	Independence quartz vein	1.25

Assays done at Acme Analytical Laboratories, Vancouver, British Columbia; fire assay, analysis by ICP-ES.



Photo 3. View southwest across a trench on the Independence vein. The vein (under Gary Payie's right foot) is about a metre wide and is mainly massive, white quartz. Brown to orange weathering volcanic rocks exposed on the walls of the trench have strong quartz-carbonate-pyrite alteration, typical of alteration associated with quartz veins in the study area.

the KC1 showing. A chip sample across the vein (DMA04-15) gave slightly anomalous Au and Cu values.

A number of other quartz veins crop out along the northeast facing slope of the ridge west of Divide Lake (DMA04-021-024). Although these veins locally contain sulphides, samples submitted for analyses did not return any significant gold values (Table 4).

GOLD SKARN OCCURRENCES

The Kliyul magnetite-pyrite-chalcopyrite occurrence (MINFILE 094D 023) is located in an area of poor bedrock exposure within the broad valley, bounded by gossanous bluffs and talus slopes, at the head of Lay Creek. An historical resource estimate of 2.5 million tons grading 0.3% Cu and 0.03 oz/T Au has been calculated for the deposit and could potentially be increased (Gill, 1993).

As shown in Photo 4, outcrop is very limited in the vicinity of the Kliyul skarn deposit with most of the area

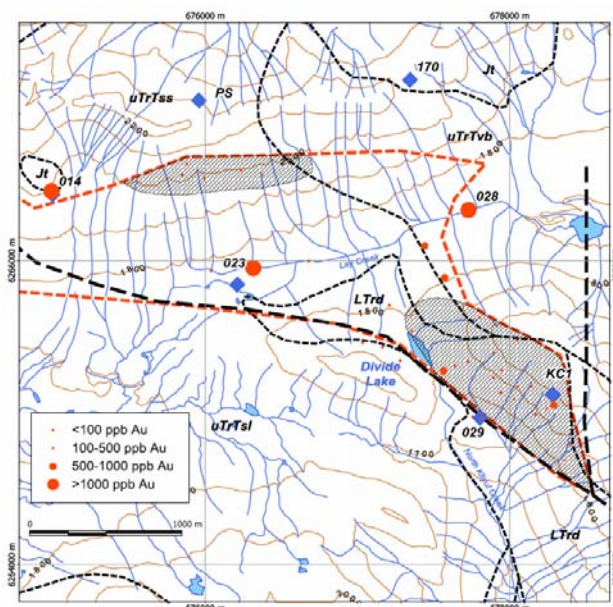


Figure 5. Gold values for samples collected in the Divide Lake area as part of the current study. See Figure 2 for legend.

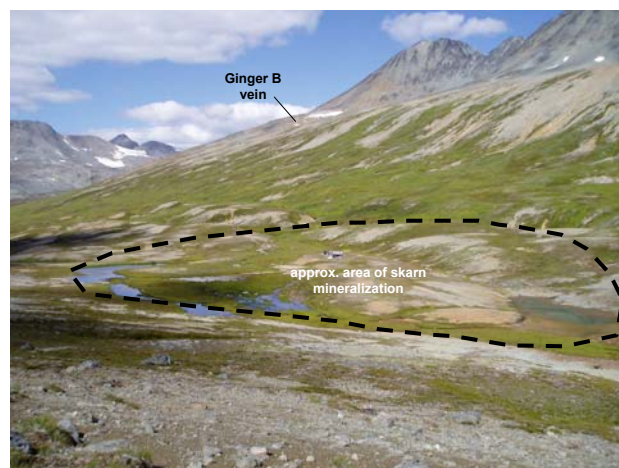


Photo 4. View northwest across the Kliyul skarn deposit. The building in the middle of the area of skarn mineralization is the remains of an old exploration camp. Also shown is the location of the Ginger B gold-quartz vein on the ridge northwest of the camp..

covered by mounds of glacial transported material. However, two samples were collected from outcrop in Lay Creek. The first of these was from quartz-sericite-pyrite altered microdiorite that crops out northwest of the area of skarn mineralization. This sample (DMA04-026) contained low Au and only slightly elevated Cu and Zn values. The second sample is from chlorite-epidote-magnetite skarn that crops out along the south bank of Lay Creek, northeast of the old camp. This sample (DMA04-029) contained 1.04 g/t Au (Table 5), 933 ppm Cu and 430 ppm Zn (Table 4).

Another skarn showing, the Pacific Sugar (labeled PS on Fig. 4, 5 and 6) is located about 1 km north of the

Kliyul occurrence. The skarn was tested with 5 diamond-drill holes, with a cumulative length of 154.8 m, in 1996. Significant drill results include 2048 ppm Cu and 625 ppb Au over 3.97 m (Lerliche and Harrington, 1996). This showing was not visited as part of the current study.

DIVIDE LAKE GOSSAN

A prominent gossan has developed on the steep southwest-facing slope of the ridge southeast of Divide Lake (Photo 1). This gossan is over a kilometre long and extends from the 1700 m level to the top of the ridge. Several days were spent examining and sampling this area with a total of 29 stations recorded within the gossan zone (Fig. 3). The strongest gossan coincides with a lower zone of pervasive quartz-sericite-pyrite alteration in foliated microdiorite. Up slope this alteration grades into chlorite-epidote alteration with a corresponding decrease in disseminated pyrite. Quartz veining is rare within the alteration zone and those that were sampled did not carry any appreciable gold values. The only mineralization of note occurs along the southwest margin of the gossan where chlorite-epidote altered diorite is cut by northwest-trending shear zones containing malachite and chalcopyrite. Two samples (DMA04-019, 019A) collected at station DMA04-019 (Fig. 3) near the southeast end of the gossan returned Cu values of 9247 and 3831 ppm respectively but had low Au values. Another sample (DMA04-020) collected from similarly sheared, propylitically altered microdiorite that crops out near the Divide Lake fly camp contained 3831 ppm Cu and slightly anomalous Au (286 ppb). These copper-bearing shear zones are close to a major northwest-trending fault (Fig. 6) that swings westward toward the Dortatelle fault. The alignment of occurrences along this trend as shown by the orientation of anomalous copper samples in Figure 6 suggests this may be the most prospective part of the Divide Lake gossan.



Photo 5. View southeast across the Divide Lake gossan. Orange weathering rocks have pervasive quartz-sericite-pyrite alteration that grades up slope into a zone of propylitic alteration.

A number of samples of quartz-sericite-pyrite and chlorite-epidote altered microdiorite were collected within the Divide Lake gossan (Table 3). None of these samples contained significant concentrations of precious or base metals with most values at background or, at the most, slightly anomalous (Table 4, Fig. 5 and 6).

LAY CREEK GOSSAN

A smaller, less pronounced gossan, located up slope from the Kliyul skarn deposit, was also sampled during the current study (Fig. 3). This gossan is mainly due to the presence of disseminated pyrite in propylitically altered feldspar phyrlic volcanic or intrusive rocks. Locally, these rocks have strong quartz-sericite-pyrite alteration possibly associated with the development of shear zones. None of the samples of microdiorite collected from this zone contained anomalous Au or Cu.

Mariposite Creek Area

Rocks exposed on the steep southeast- and northwest-facing slopes that straddle the headwaters of Mariposite Creek weather a conspicuous orange-brown colour due to extensive zones of quartz-ankerite-pyrite alteration associated with numerous quartz veins. The size of the area of alteration and the density of quartz veining attracted companies like BP Resources (Meyers and Smit, 1985) and Hemlo Gold Mines (Gill, 1996) to test the area for possible bulk tonnage Cu-Au deposits. This area was targeted for follow-up work as part of the current project after regional mapping in 2003 confirmed the extensive nature of alteration and veining (Schiarizza, 2004).

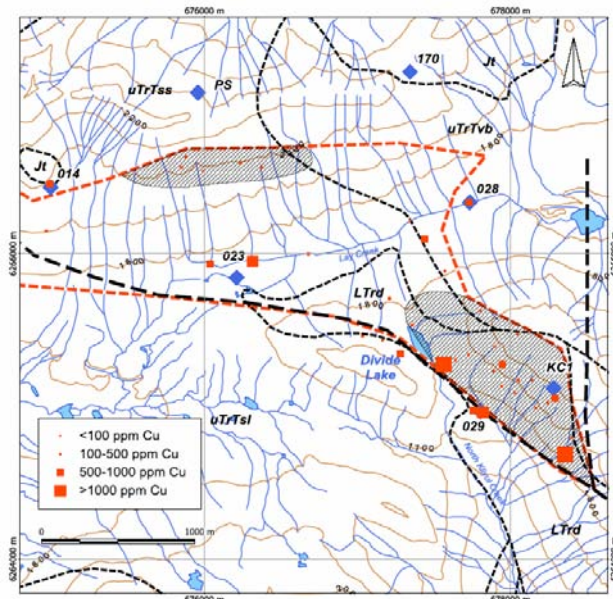


Figure 6. Copper values for samples collected in the Divide Lake area as part of the current study. See Figure 2 for legend.



Photo 6. View northwest toward the Lay Creek gossan (dotted outline). Rocks in the foreground are pervasively altered and foliated microdiorite that crops out near the northern end of the Divide Lake gossan..



Photo 7. View northwest toward the Mariposite quartz veins and lenses (white areas in the middle of the slope) that are well-exposed on the southwest-facing slope of the ridge northwest of the headwaters of Mariposite Creek. Hemlo Gold Mines drilled two holes into these veins in 1996. Note orange-brown weathering due to oxidation of quartz-ankerite alteration zones associated with the veins. Dark to medium grey weathering outcrops are relatively unaltered Takla volcanic rocks.

As part of the current study, a suite of samples were collected from quartz veins exposed on the steep slopes

above the headwaters of Mariposite Creek (Table 3, Fig. 7). This is the area of strongest alteration and highest abundance of veins. Scattered areas of quartz-ankerite alteration and narrow, discontinuous quartz veins do occur further south and several of these were sampled as well (Fig. 7).

Quartz veins in the Mariposite Creek area range from a few centimetres to several metres in width with some, like those at the Mariposite showing occurring as large irregular lenses (Photo 7). However, most veins are tabular, steeply dipping (Photo 8) and strike predominantly to the northwest (Fig. 8). Some veins can be traced for several hundred metres; others only a few metres before they pinch out. Overall, the veins, which vary from pure quartz to mixed quartz and carbonate, contain no or only very minor amounts of sulphide minerals. Alteration envelopes are also variable. Some envelopes extend several metres out from the vein contact, others only a few centimetres and some veins appear not to have any alteration associated with them at all. From a

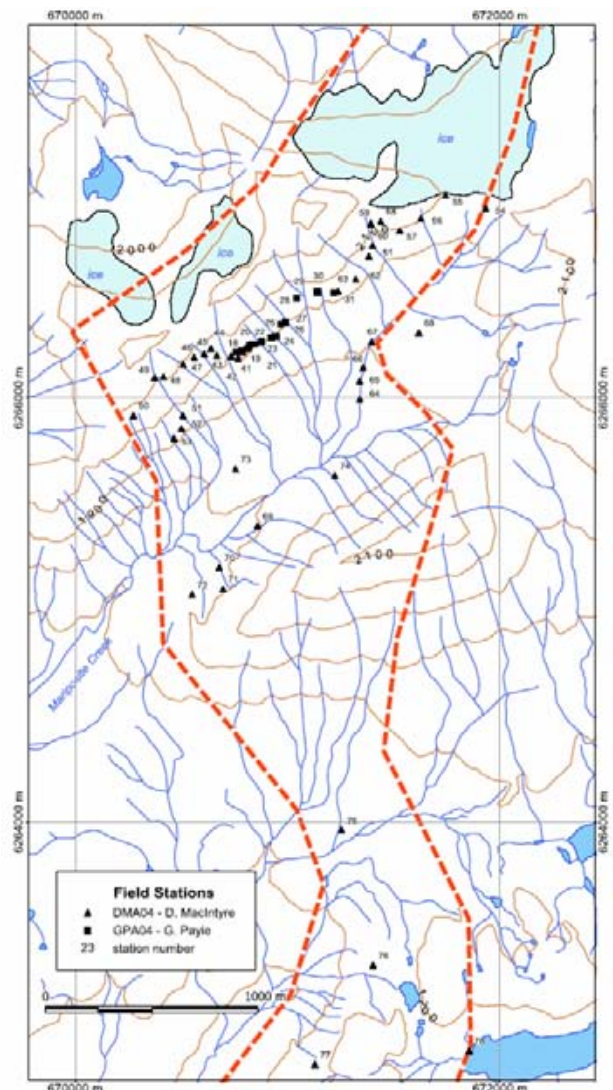


Figure 7. Station locations in the Mariposite Creek area.

distance, the extent of alteration is misleading as much of the colour anomaly is due to altered talus sitting on relatively unaltered rocks. The writers estimate that less than 20% of the rock exposed on the slope north of Mariposite Creek, is actually altered. The rest is relatively unaltered Takla volcanics and metasediments.

A number of samples collected in the Mariposite Creek area contained anomalous gold concentrations (Table 4, Fig. 9) but many others only contained background. These results are not dissimilar from those reported by Gill (1996) where of 743 samples collected in the area, 70 (9%) contained greater than 500 ppb Au. The location of Gill's samples is also shown on Figure 9 for comparison. Although the number of samples containing anomalous gold is encouraging, the erratic distribution and grade is a concern. In part, this reflects the difficulty of determining gold concentrations using grab and chip samples. Bulk sampling is required to effectively determine the overall concentration and distribution of gold, especially in some of the larger veins.

Some of the strongest, most continuous wallrock alteration occurs in metasedimentary rocks that crop out along the upper, northernmost branch of Mariposite Creek (Photo 9). Although most of the alteration is quartz-ankerite, locally there is also strong quartz-sericite-pyrite alteration especially where quartz vein stockworks have developed. A sample collected from one of these zones



Photo 8. Typical steeply dipping quartz veins in the Mariposite Creek area. This vein was sampled (DMA04-053) but contained low concentrations of gold as did a sample of the quartz-ankerite altered wallrock (DMA04-053A).

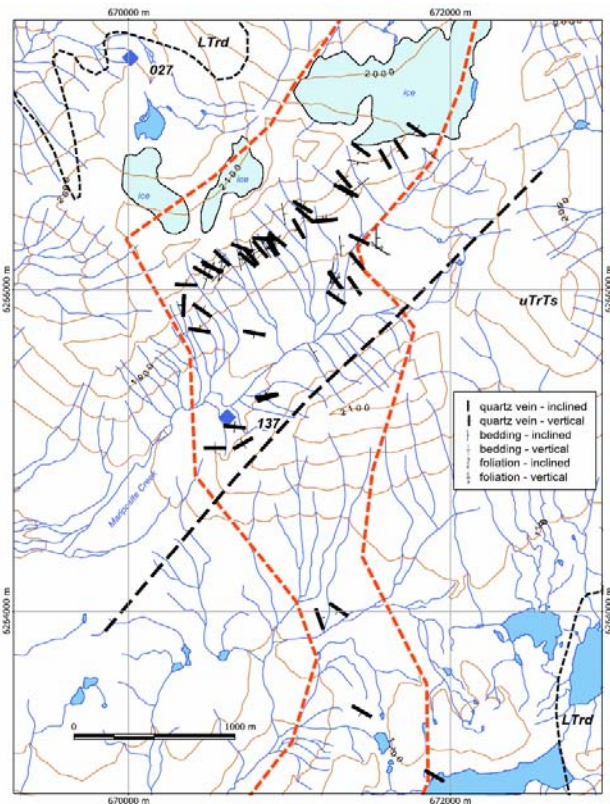


Figure 8. Structural trends of gold-quartz veins, bedding and foliation in the Mariposite Creek area. See Figure 2 for legend.

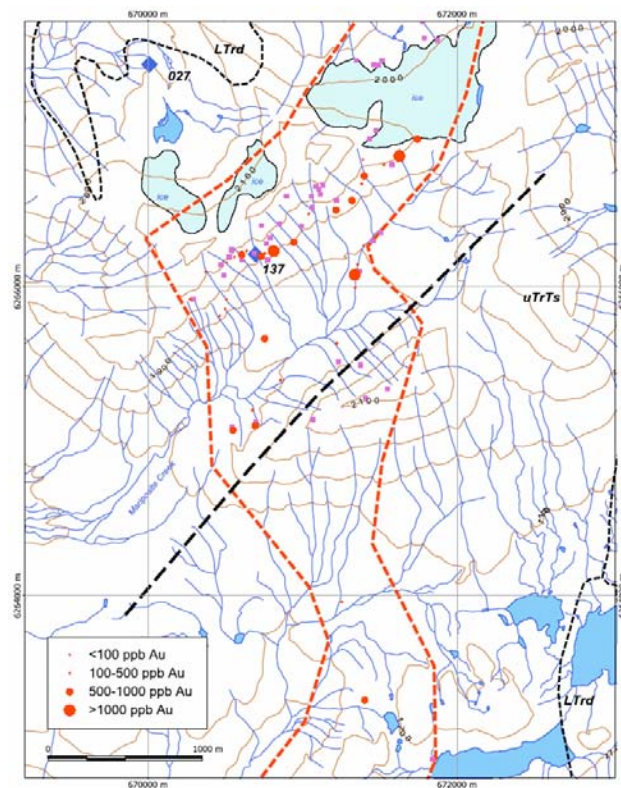


Figure 9. Gold values for samples collected in the Mariposite Creek area as part of the current study. See Figure 2 for legend. Purple squares show samples collected by Gill (1994) that had >500 ppb Au.

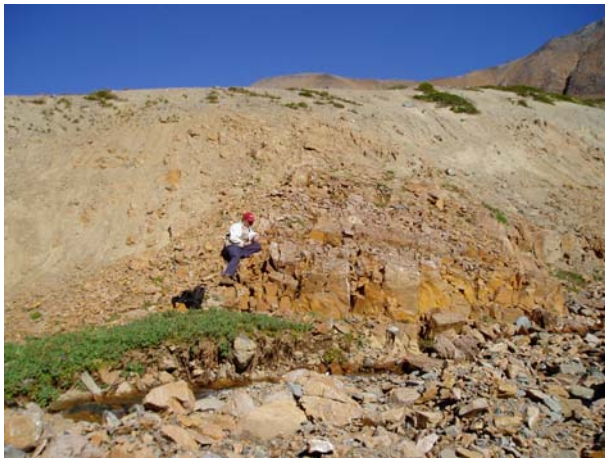


Photo 9. View northwest toward an outcrop of pervasive quartz-ankerite-pyrite altered metasediments exposed on the west bank of Mariposite Creek near station DMA04-064



Photo 10. Quartz vein stockwork in pervasive quartz-ankerite altered metasediments. These rocks crop out in Mariposite Creek near station DMA04-065A where a sample with similar veining contained 826 ppb Au.

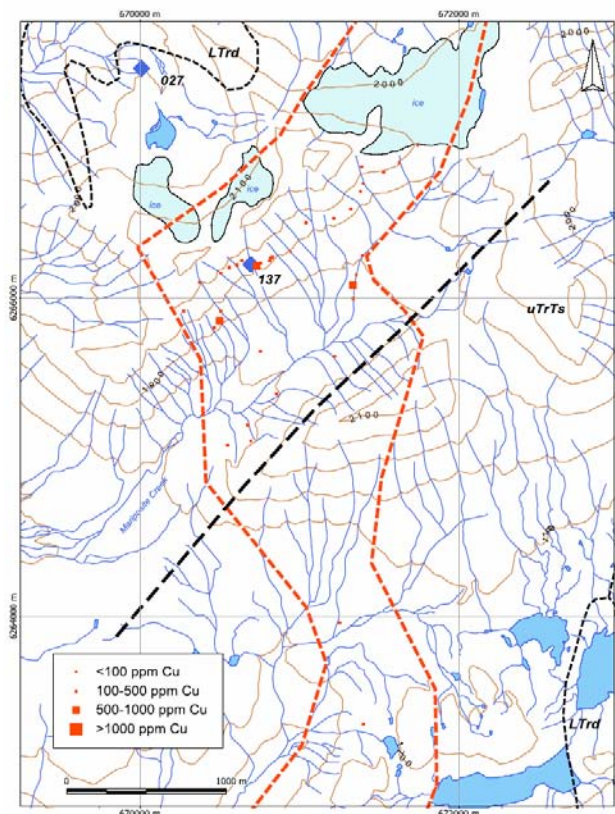


Figure 10. Copper values for samples collected in the Mariposite Creek area as part of the current study. See Figure 2 for legend.

(DMA04-065B) contained 826 ppb Au and slightly anomalous Cu (173 ppm). This was the highest Cu value determined for the samples from the Mariposite Creek area (Table 4; Fig. 10).

CONCLUSIONS

Based on the results of this study and previous exploration work, the main exploration targets in the area are gold-quartz veins, gold-bearing skarn and copper associated with shear zones near Divide Lake. Gold-quartz veins are most abundant near the headwaters of Mariposite Creek where hundreds of predominantly northwest-trending, steeply dipping veins crop out over a distance of 1.5 km. Although these veins locally contain significant gold concentrations, the distribution of gold is erratic and evaluation of the veins is difficult without bulk sampling. Better gold values appear to be associated with the presence of pyrite and/or galena. Previous drilling of the Mariposite showing produced disappointing results but dioritic to monzonitic intrusive rocks with associated stockwork veining were intersected at depth... In the writers' opinion, the best target in this area is not the massive quartz-carbonate lenses at the Mariposite showing but rather strongly altered and veined metasedimentary rocks exposed in Mariposite Creek itself. The alteration here is more pervasive, locally grades into strong quartz-sericite-pyrite alteration and in places quartz vein stockworks with anomalous gold concentrations have developed (Photo 10). An intrusive body similar to that intersected in drilling up slope at the Mariposite showing may be present at depth.

Although rocks in the Mariposite area are locally sheared and ductily deformed, quartz veins show no sign of deformation and appear to have crystallized within open fractures, possibly tension gashes (Richards, 1991). Most of these fractures trend northwest, while others are

lensoidal structures with a northeast orientation. Formation of tension gashes and northwest-trending fractures may be related to extension in a southwest-northeast direction, possibly related to strike-slip movement on the nearby Dortatelle fault. Northwest-trending shear zones may also be related to this period of faulting, which is believed to be Late Cretaceous or Early Tertiary. If formation of quartz veins is indeed related to this fault movement then these veins are unrelated to the older Late Triassic and Early Jurassic intrusive bodies in the study area. However, there may be younger intrusive bodies, not yet recognized or dated that have a genetic association with formation of the quartz veins. Alternatively quartz vein formation is related to hydrothermal activity that accompanied strike-slip faulting.

The Divide Lake gossan is related to an extensive zone of pervasive quartz-sericite-pyrite and chlorite-epidote alteration. Samples collected from this alteration zone contained only background or slightly elevated precious and base metal concentrations. However, the extent and style of alteration is typical of phyllic and propylitic alterations assemblages found peripheral to porphyry copper deposits and the possibility that such a deposit exists at depth should be considered. The occurrence of hornblende-feldspar phyrlic dikes cutting the alteration zones may be further evidence of an intrusive body at depth. Copper mineralization in shear zones along the southwest edge of the gossan may also be related to a porphyry system.

Although gold occurs sporadically in many of the quartz veins in the area, to date, the best target for a bulk tonnage deposit remains the Kliyul gold skarn. Although results of exploration to date have been encouraging, much additional exploration will be needed to determine more precisely the ultimate size and economic potential of this deposit.

ACKNOWLEDGMENTS

The writers would like to thank Paul Schiarizza for assisting in arranging logistics and providing much useful information.

REFERENCES

- Cross, D.B. (1985): Geological, geophysical and geochemical report, KC 1 and 2 claims, Omineca Mining Division, British Columbia, N.T.S. 94D/8E, 9E; *B.C. Ministry of Energy, Mines and Petroleum Resources*, Assessment Report 14416, 18 pages.
- Gill, D.G. (1993): Drilling assessment report on the Kliyul property, N.T.S. 94D/8, 9; *B.C. Ministry of Energy, Mines and Petroleum Resources*, Assessment Report 23033, 12 pages.
- Gill, D.G. (1994): Geological and geochemical assessment report on the Joh property, N.T.S. map sheet 94D/9; *B.C. Ministry of Energy, Mines and Petroleum Resources*, Assessment Report 23543, 15 pages.
- Gill, D.G. (1994): Assessment report on the Joh, Darb, Croydon, Mariposite & Kliyul Properties, *B.C. Ministry of Energy, Mines and Petroleum Resources*, Assessment Report 23379.
- Gill, D.G. (1995): Geological assessment report on the Joh 3 group of claims, N.T.S. map sheet 94D/9; *B.C. Ministry of Energy, Mines and Petroleum Resources*, Assessment Report 23842, 16 pages.
- Gill, D.G. (1996): Drilling report on the Mariposite property, N.T.S. 94D/8, 9; *B.C. Ministry of Energy, Mines and Petroleum Resources*, Assessment Report 24778, 23 pages.
- Fox, M. (1982): Geological and geochemical report, KC 1 and 2 mineral claims, N.T.S. 94D/8E and 9E, Omineca Mining Division, British Columbia; *B.C. Ministry of Energy, Mines and Petroleum Resources*, Assessment Report 10346, 14 pages.
- Fox, M. (1991): Geological and geochemical exploration report, Jo 1-8 and Cro 1-5 mineral claims, N.T.S. 94D/8E and 9E, Omineca Mining Division, British Columbia; *B.C. Ministry of Energy, Mines and Petroleum Resources*, Assessment Report 21502, 18 pages.
- Leriche, P.D. and Harrington, E. (1996): Diamond drilling report on the Joh property, Johanson Lake area, Omineca Mining Division, British Columbia; *B.C. Ministry of Energy, Mines and Petroleum Resources*, Assessment Report 25099, 22 pages.
- Meyers, R.E. and Smit, H.Q. (1985): 1984 assessment report of the geological and geochemical exploration program on the Goldway 1-8 claims, Omineca Mining Division, NTS 94D/8, 9; *B.C. Ministry of Energy, Mines and Petroleum Resources*, Assessment Report 13697, 83 pages.
- Pawliuk, D.J. (1985): Report on assessment work on the Goldway Peak property, Omineca Mining Division, Johanson Lake, British Columbia; *B.C. Ministry of Energy, Mines and Petroleum Resources*, Assessment Report 14105, 17 pages.
- Phendler, R.W. (1984): Report on assessment work (sampling and assaying) on Vi 1 and Vi 2 (Record Nos. 1948 and 1949), Johanson Lake area, Omineca Mining Division, British Columbia; *B.C. Ministry of Energy, Mines and Petroleum Resources*, Assessment Report 13175, 9 pages.
- Richards, T.A. (1976): Geology, McConnell Creek map-area (94D/E); *Geological Survey of Canada*, Open File 342, scale 1:250 000.
- Schiarizza, P. (2004): Geology and Mineral Occurrences of Quesnel Terrane, Kliyul Creek to Johanson Lake (94D/8,9) in Geological Fieldwork 2003, *B.C. Ministry of Energy and Mines*, Paper 2004-1, pages 83-100.
- Schiarizza, P. (2004a): Geology of the Kliyul Creek-Johanson Lake area, Parts of NTS 94D/8 and 9, *B.C. Ministry of Energy and Mines*, Open File Map 2004-5, scale 1:50,000.
- Tchalenko, J.S. (1970): Similarities between shear zones of different magnitudes; *Geological Society of America, Bulletin*, Volume 81, pages 1625-1640.
- von Rosen, G. (1986): Assessment geological report on mapping, sampling and bulk sampling program on the Good (4155) - Prospects (4147) - Much (4149) - Pro (4150) - Fit (4151) - Dar (4154) mineral claims (Gold

- group), Goldway Peak - Johanson Lake area, Omineca Mining Division; *B.C. Ministry of Energy, Mines and Petroleum Resources*, Assessment Report 15313, 35 pages.
- Wilson, G.L. (1984): Geological, geochemical and geophysical report, KC 1 and 2 mineral claims, N.T.S. 94D/8E and 9E, Omineca Mining Division, British Columbia; *B.C. Ministry of Energy, Mines and Petroleum Resources*, Assessment Report 13580, 17 pages.
- Zhang, G. and Hynes, A. (1991): Structure of the Takla Group east of the Finlay-Ingenika fault, McConnell Creek area, north-central B.C. (94D/8, 9); in *Geological Fieldwork 1990*, *B.C. Ministry of Energy, Mines and Petroleum Resources*, Paper 1991-1, pages 121-129.
- Zhang, G. and Hynes, A. (1992): Structures along Finlay-Ingenika fault, McConnell Creek area, north-central British Columbia (94C/5; 94D/8, 9); in *Geological Fieldwork 1991*, *B.C. Ministry of Energy, Mines and Petroleum Resources*, Paper 1992-1, pages 147-154.
- Zhang, G. and Hynes, A. (1994): Fabrics and kinematic indicators associated with the local structures along Finlay-Ingenika fault, McConnell Creek area, northcentral British Columbia; *Canadian Journal of Earth Sciences*, Volume 31, pages 1687-1699.
- White, W.H. (1948): Sustut-Aiken-McConnell Lake area; in *Annual Report of the Minister of Mines for 1947*, *B.C. Department of Mines*, pages A100-A111.

U-Pb and K-Ar Isotopic Dates from the Beece Creek – Tatlayoko Lake Area (NTS 92N/9, 92O/5, 6), Southwestern British Columbia

By Richard Friedman¹, Janet Gabites¹ and Paul Schiarizza²

KEYWORDS: geochronology, U-Pb, K-Ar, zircon, muscovite, Fish Lake porphyry Cu-Au deposit, Skinner gold-quartz vein, Anvil Mountain pluton, Jackass Mountain Group

INTRODUCTION

The geology of the eastern Coast Belt in parts of the Mount Waddington (92N) and Taseko Lakes (92O) map areas was updated during the Tatlayoko bedrock mapping project, carried out by the British Columbia Geological Survey Branch in the early to mid-1990s. The results of this program are summarized in a geological report by Schiarizza and Riddell (1997) and a 1:100 000-scale geoscience map by Schiarizza *et al.* (2002). The geological mapping was supported by isotopic dating carried out at the University of British Columbia. In this paper we present previously unpublished data and age interpretations on four samples that were collected during fieldwork associated with the Tatlayoko project.

GEOLOGICAL SETTING

The geology of the central part of the Tatlayoko project area, simplified from Schiarizza *et al.* (2002), is shown in Figure 1. The area encompasses the boundary between the Coast and Intermontane morphogeological belts, which corresponds approximately with the trace of the Yalakom fault, a major linear feature that extends for about 300 km and was the locus of more than 100 km of Late Cretaceous (?) to early Tertiary dextral strike-slip displacement (Umhoefer and Schiarizza, 1996). The oldest rocks in the map area are assigned to three separate terranes: Cadwallader-Methow, Bridge River and Stikine. Younger rocks comprise the Jura-Cretaceous Tyaughton-Methow basin and overlying Upper Cretaceous subaerial volcanic rocks of the Powell Creek formation. Late Cretaceous and Eocene intrusive rocks are common in the Beece Creek and Fish Lake areas.

The Cadwallader-Methow Terrane comprises Middle Triassic to Middle Jurassic arc-related volcanic, plutonic and sedimentary rocks that are exposed southwest of the Yalakom fault in a belt that extends from west of Tatlayoko Lake southeastward to the Nemaia valley. These rocks are

stratigraphically overlain by sedimentary rocks of the Tyaughton-Methow basin, including the Jura-Cretaceous Relay Mountain Group and the mid-Cretaceous Jackass Mountain Group. This belt is truncated south of the Nemaia valley by the Taseko fault. The bedrock geology south of the Taseko fault is dominated by exposures of mid-Cretaceous sedimentary rocks of the Taylor Creek Group (equivalent in age but lithologically distinct from the Jackass Mountain Group) and overlying Upper Cretaceous volcanic rocks of the Powell Creek formation. The basement to these exposures is inferred to be the oceanic Bridge River Terrane (Schiarizza *et al.*, 1997), a Mesozoic accretion-subduction complex that is locally represented by a thin belt of chert and greenstone along the south side of the Taseko fault.

Outcrop is poor, and geological relationships are consequently less well understood, in the area of subdued topography northeast of the Yalakom fault. Pre-Neogene strata along the Chilko River comprise volcanic and volcanoclastic rocks that have been correlated with the Lower to Middle Jurassic Hazelton Group of the Stikine Terrane (Tipper, 1969a,b). To the southeast, in the Chaunigan Lake – Fish Lake area, pre-Neogene bedrock consists of mainly Lower Cretaceous sedimentary and volcanic rocks that are correlated with the upper part of the Relay Mountain Group and the overlying Jackass Mountain Group (Schiarizza *et al.*, 2002).

GEOCHRONOLOGY

Conventional isotope-dilution thermal-ionization mass spectrometry (ID-TIMS) U-Pb data are reported and interpreted for zircons from three rock samples from the Anvil Mountain and Fish Lake areas, and K-Ar data are reported from a single sample collected near Tatlayoko Lake. All sample preparation and analyses were carried out at the Department of Earth and Ocean Sciences, University of British Columbia. Sample preparation and U-Pb analytical techniques are given in Friedman *et al.* (2001). The U-Pb data are listed in Table 1 and plotted on concordia diagrams in Figure 2. The K-Ar data are listed in Table 2.

Fish Lake Dacite

Sedimentary and volcanic rocks that crop out along and near the lower reaches of the creek that drains Fish Lake include pebbly sandstone and pebble conglomerate containing volcanic and granitoid clasts, tuffaceous sand-

¹University of British Columbia, Vancouver, BC

²British Columbia Ministry of Energy and Mines, Victoria, BC

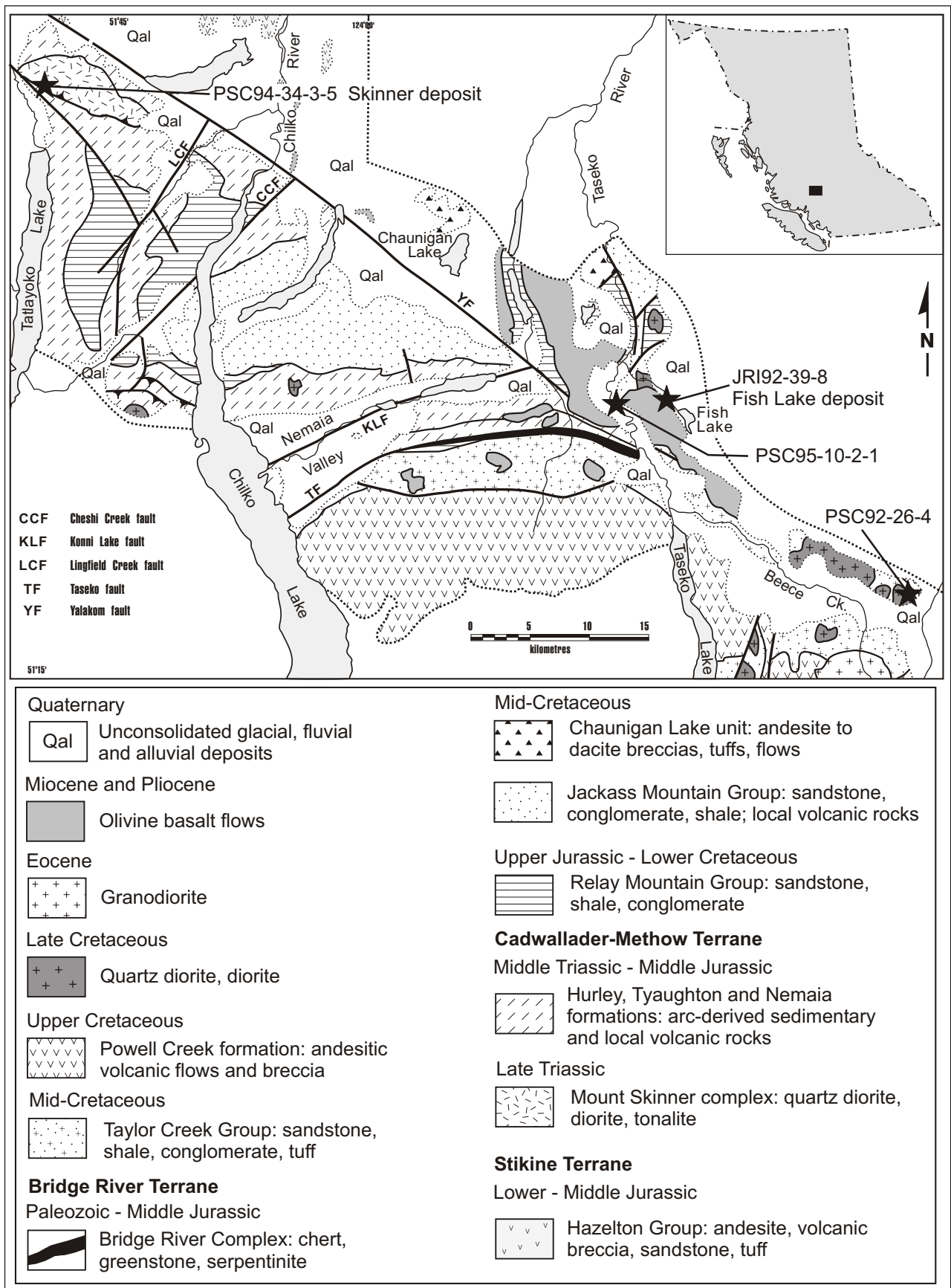


Figure 1. Simplified geological map of the Beece Creek – Tatlayoko Lake area, showing locations of samples discussed in this report.

TABLE 1. URANIUM-LEAD ANALYTICAL DATA.

Fraction ¹	Wt (mg)	U ² (ppm)	Pb ³ (ppm)	Pb ⁴			Isotopic ratios (1, %) ⁷			Apparent ages (2, Ma) ⁷		
				²⁰⁶ Pb ⁴ ²⁰⁴ Pb	Pb ⁵ ²⁰⁸ Pb ⁶ (pg)		²⁰⁶ Pb/ ²³⁸ U	²⁰⁷ Pb/ ²³⁵ U	²⁰⁷ Pb/ ²⁰⁶ Pb	²⁰⁶ Pb/ ²³⁸ U	²⁰⁷ Pb/ ²³⁵ U	²⁰⁷ Pb/ ²⁰⁶ Pb
PSC95-10-2-1 Fish Lake dacite: 100.5 +7.2/-0.6 Ma; weighted ²⁰⁷ Pb/ ²⁰⁶ Pb and one concordant analysis												
A	0.080	230	3.7	1185	15	11.4	0.01571 (0.10)	0.1040 (0.34)	0.04803 (0.27)	100.5 (0.2)	100.5 (0.6)	101 (13)
B	0.113	336	5.1	2465	23	12.8	0.01451 (0.17)	0.09608 (0.29)	0.04802 (0.22)	92.9 (0.3)	93.2 (0.5)	100 (11)
C	0.069	441	6.1	1052	24	14.1	0.013169 (0.18)	0.0872 (0.43)	0.04803 (0.37)	84.3 (0.3)	84.9 (0.7)	101 (17/18)
PSC92-26-4 Anvil Mountain pluton: ca. 93 Ma; one concordant analysis												
A	0.161	105	1.4	448	35	6.7	0.01432 (0.18)	0.0955 (0.69)	0.04839 (0.61)	91.6 (0.3)	92.6 (1.2)	119 (29)
B	0.156	106	1.5	1101	14	7.1	0.01460 (.06)	0.0964 (0.24)	0.04789 (0.22)	93.4 (0.1)	93.4 (0.4)	94 (11)
JRI92-39-8: Fish Lake quartz diorite: 91.5 +1.1/-5.6 Ma; lower intercept age												
A	0.779	265	3.9	2214	85	9.8	0.01460 (0.11)	0.0974 (0.18)	0.04837 (0.11)	93.5 (0.2)	94.4 (0.3)	117 (5)
G	0.043	285	4.1	1003	11	10.8	0.01571 (0.09)	0.0954 (0.35)	0.04803 (0.31)	92.2 (0.2)	92.5 (0.6)	101 (15)
H	0.046	286	4.1	1103	11	10.8	0.01571 (0.12)	0.0969 (0.32)	0.04796 (0.24)	93.8 (0.2)	93.9 (0.5)	97 (11)

¹ Upper case letter = zircon fraction identifier. All zircon fractions were air abraded to remove grain facets; PSC95-10-2-1: zircon nonmagnetic at 20 degrees sideslope and 1.8 amperes field strength on Franz™ magnetic separator; (front slope 15 degrees for all samples). Fraction A +134 m, B -134+74 m, C-74 m. PSC92-26-4: zircon nonmagnetic at ~2 degrees sideslope and 1.8 amperes field strength on Franz™ magnetic separator; All grains >134 m picked and strongly abraded. JRI92-39-8: zircon nonmagnetic at 1 degree sideslope and 2.0 amperes field strength on Franz™ magnetic separator; >134 m, H comprises tips broken off of these grains.

² U blank correction of 1pg ± 20%; U fractionation corrections were measured for each run with a double ²³³U-²³⁵U spike (about 0.004/amu).

³Radiogenic Pb

⁴Measured ratio corrected for spike and Pb fractionation of 0.0043/amu ± 20% (Daly collector) which was determined by repeated analysis of NBS Pb 981 standard throughout the course of this study.

⁵Total common Pb in analysis based on blank isotopic composition.

⁶Radiogenic Pb

⁷Corrected for blank Pb (1-4 pg, throughout the course of this study), U (1 pg) and common Pb concentrations based on Stacey Kramers (1975) model Pb at the age of the rock or the ²⁰⁷Pb/²⁰⁶Pb age of the rock.

stone, hornblende-feldspar-phyric andesite, and dacite containing quartz and feldspar phenocrysts. These rocks may correlate with the volcanic and sedimentary package (observed only in drillcore) that hosts the Fish Lake porphyry copper-gold deposit a few kilometres to the east. They were assigned to the informal Fish Creek succession (unit IKsv) by Schiarizza and Riddell (1997), but Schiarizza *et al.* (2002) separated them into a lower shale-sandstone unit, assigned to the lower Cretaceous Relay Mountain Group, and an upper unit of sandstone, conglomerate and volcanic rocks that was included in a volcanic-bearing facies of the mid-Cretaceous Jackass Mountain Group. Columnar-jointed quartz-feldspar-phyric dacite that crops out along the Taseko Lakes road is part of the sedimentary-volcanic succession that is included in the Jackass Mountain Group. Sample PSC95-10-2-1 was collected from this dacite exposure to determine the age of the volcanic rocks in this succession.

Sample PSC95-10-2-1 yielded a modest quantity of good-quality, clear, pale pink, stubby prismatic and equant multifaceted zircon grains. Zircons with diameters of about 150 to 60 μm were selected and air abraded to remove all facets. The grains were then subdivided into three fractions on the basis of size. Results for these three fractions, plotted in Figure 2, define a linear array, with the coarsest grains concordant at ca. 100 Ma and finer grains discordant with younger Pb/U and Pb/Pb dates. This array is interpreted to result from Pb loss with no evidence of older inherited zircon. An interpreted age of 100.5 +7.2/-0.6 Ma is based on

the weighted mean of ²⁰⁷Pb/²⁰⁶Pb dates for the three fractions; the ²⁰⁶Pb/²³⁸U date for concordant fraction A provides a minimum age for the sample.

The sedimentary-volcanic succession along Fish Creek is assigned to the Jackass Mountain Group on the basis of characteristic rock types, including granitoid-bearing conglomerates and pebbly sandstones. The occurrence of volcanic rocks is unusual for the Jackass Mountain Group, but the mid-Cretaceous age obtained from the dacite sample supports the inclusion of these volcanic rocks in the group. Volcanic rocks exposed to the north and northwest, assigned to the Chaunigan Lake unit by Schiarizza and Riddell (1997) and Schiarizza *et al.* (2002), may be correlative, although these rocks are assigned to the age-equivalent Spences Bridge Group by Hickson and Hignman (1993).

Anvil Mountain Pluton

Hornblende diorite, quartz diorite and hornblende-feldspar porphyry occur as stocks, plugs and dikes that are common within the Taylor Creek Group east of Taseko Lake (Fig. 1). These intrusive rocks are associated with porphyry copper-molybdenum mineralization at the Chita showing (MINFILE 092O 049) east of Taseko Lake, and with epithermal-style mineralization at the Knight showing (MINFILE 092O 002) near the headwaters of Nadila Creek (Schiarizza *et al.*, 2002). The largest pluton in this area comprises diorite to quartz diorite that underlies the Anvil Mountain ridge system, northeast of Beece Creek. Sample

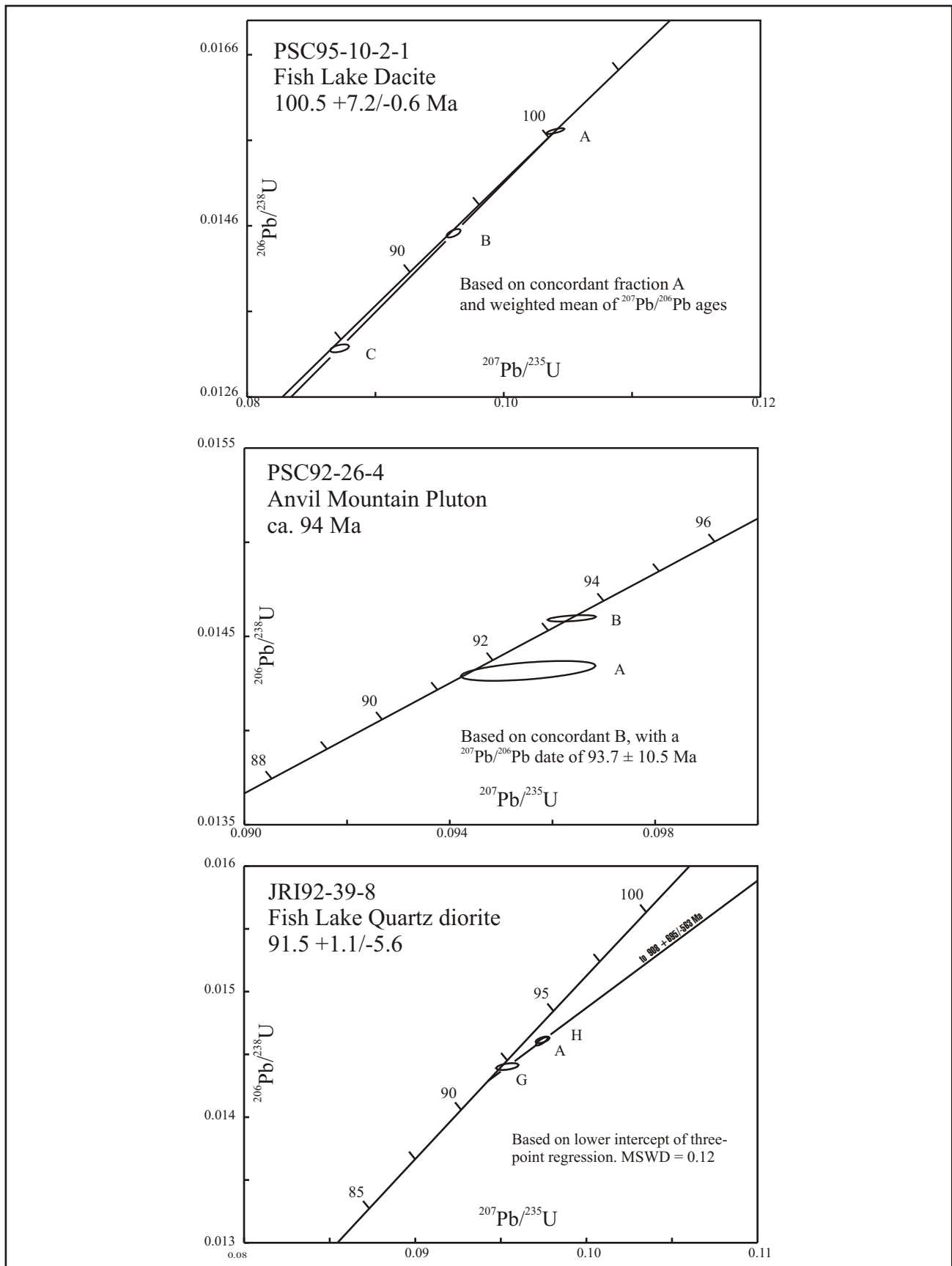


Figure 2. Concordia plots with results displayed at the 2 level of uncertainty.

PSC92-26-4, comprising hornblende quartz diorite, was collected from the eastern part of this ridge system in order to determine the crystallization age of this pluton.

Clear, colourless, equant rounded to stubby prismatic multifaceted zircons were recovered from sample PSC92-26-4. The modest amount of material present was only sufficient for two fractions. An age of ca. 94 Ma is suggested on the basis of concordant fraction B, with a $^{206}\text{Pb}/^{238}\text{U}$ date of 93.4 ± 0.1 Ma. Fraction A is discordant, just below the concordia curve at ca. 92 Ma, due to Pb loss and/or the presence of minor inherited zircon. It is difficult to suggest an age with associated precision on the basis of one concordant result. However, a conservative estimate would be 93.7 ± 10.5 Ma, based on the $^{207}\text{Pb}/^{206}\text{Pb}$ date for concordant fraction B.

The date obtained from the Anvil Mountain pluton compares closely with an Ar-Ar date of 92 ± 1.3 Ma obtained from volcanic rocks near the base of the Powell Creek formation by J.A. Maxson (reported in Wynne *et al.*, 1995) in the Mount Tatlow area. It suggests that the intrusive rocks cutting the Taylor Creek Group in this area may be comagmatic with the overlying Powell Creek formation.

Fish Lake Quartz Diorite

The Fish Lake porphyry copper-gold deposit is located in an area of virtually no bedrock exposure about 5 km east of the Taseko River (Fig. 1). Based on 143 945 m of drilling in 326 holes, Independent Mining Consultants calculated a mineable reserve of 633 million tonnes at an average grade of 0.253% Cu, 0.466 g/t Au and 0.5 g/t Ag (Taseko Mines Limited, press release, March 16, 1998). The deposit is described by Wolfhard (1976) and Caira *et al.* (1995). According to Caira *et al.*, the Fish Lake deposit is spatially and genetically related to a steeply dipping lenticular body of porphyritic quartz diorite that is surrounded by an east-west elongate complex of steep, southerly-dipping, subparallel quartz-feldspar porphyry dikes. These rocks, referred to as the Fish Lake Intrusive Complex, cut volcanic and volcanoclastic rocks, as well as an older intrusive body of porphyritic diorite that may be coeval with the volcanics. Mineralization occurs within both the intrusive complex and adjacent volcanic, volcanoclastic and plutonic country rocks. Core sample JRI92-39-8, of hornblende-quartz-feldspar porphyry from the Fish Lake Intrusive Complex, was collected in order to determine a crystallization age for the synmineralization intrusions.

Zircons recovered from sample JRI92-39-8 are primarily clear, colourless, euhedral prisms with length-width ratios of ~2.5–3.5. Results for three analyzed fractions are discordant to marginally concordant and define a linear array. Although cores were not observed during grain selection, all fractions are interpreted to contain minor inheritance, even fraction H, which comprised tips broken from more elongate prisms. The interpreted age of $91.5 +1.1/-5.6$ Ma is based on the lower intercept of a three-point regression (MSWD = 0.12). A very poorly constrained upper intercept of $908 +695/-563$ Ma

provides an estimate for the average age of inheritance in analyzed grains.

The $91.5 +1.1/-5.6$ Ma date presented here for the Fish Lake Intrusive Complex is about 10 million years older than the preliminary 80 Ma estimate from the same sample presented by Schiarizza and Riddell (1997). It is also older than a previous whole-rock K-Ar date of 77.2 ± 2.8 Ma obtained from a hornfels containing 40% secondary biotite, which was interpreted as the date of mineralization (Wolfhard, 1976). It is very similar to the date obtained from the compositionally similar Anvil Mountain pluton, suggesting that the two intrusive suites are related.

Skinner Gold-Quartz Vein

The Skinner mineral occurrence (MINFILE 092N 039), located 5 km north of the north end of Tatlayoko Lake (Fig. 1), comprises a system of gold-bearing quartz veins within Late Triassic quartz diorite and diorite of the Mount Skinner Igneous Complex. Individual veins are arranged en echelon within a structurally controlled lineament that trends 070 (Berniolles, 1991). Development has focused on the Victoria vein, at the southwest end of the system, which has been traced for more than 130 m and ranges up to 1.4 m thick. It strikes between 050 and 060 and dips steeply to the northwest. The vein walls are defined by slickensided faults, and the veins themselves are cut by parallel faults, at least some of which accommodated sinistral movement. The vein consists almost entirely of quartz, with minor amounts of pyrite, chalcocopyrite, malachite and rare visible gold. Gold values are variable, and concentrations as high as 136 g/t across 0.65 m have been recorded (Berniolles, 1991). A 172 t bulk sample extracted from the vein by Ottarasko Mines Limited in 1992 and 1993 produced 11 351 g of gold (Northern Miner, June 6, 1994).

White mica locally lines vugs and open fractures in quartz of the Victoria vein. Sample PSC94-34-3-5, of muscovite-bearing vein material, was collected for K-Ar dating of the mica. The mica separate yielded an Early Eocene date of 51.9 ± 2.6 Ma (Table 2). This provides a minimum age for the vein and most likely dates the late stages of the hydrothermal system responsible for the veining. If this interpretation is correct, then the veining was probably coincident with dextral movement along the Yalakom fault, which is just 5 km northeast of the Skinner occurrence (Fig. 1). This suggests that the Skinner vein system formed along an antithetic sinistral fault system related to dextral movement along the Yalakom fault. The Lingfield Creek and Cheshi Creek faults to the southeast may have had a

TABLE 2. K-AR ANALYTICAL DATA.

Sample	Size fraction (mesh)	K (%)	^{40}Ar rad (mole/g $\times 10^{-10}$)	^{40}Ar rad (% of total)	Age (Ma; 2 error)
PSC94-34-3-5					
Muscovite	-40+80	7.98	16.3	72.4	51.9 ± 2.6

Notes: Samples analysed in the Geochronology Laboratory, Department of Earth and Ocean Sciences, U.B.C., by Janet Gabites (potassium) and Joe Harakal (argon).

Decay constants $\lambda_e = 0.1581 \times 10^{-10} \text{ yr}^{-1}$, $\lambda_b = 4.962 \times 10^{-10} \text{ yr}^{-1}$,

$^{40}\text{K}/\text{K} = 1.167 \times 10^{-4}$ mole/mole.

similar origin, although these structures and the Skinner vein system are oriented slightly more easterly than would be expected for antithetic riedel shears in an ideal simple shear model (e.g. Wilcox *et al.*, 1973). These departures may reflect varying degrees of clockwise rotation in the structural blocks southwest of the Yalakom fault, as is suggested by the structural analysis of Umhoefer and Kleinspehn (1995), who relate this block rotation to the area's position between the Tchaikazan and Yalakom faults.

ACKNOWLEDGMENTS

Janet Riddell, in cooperation with Nadia Caira of Taseko Mines Limited, collected the core sample from the Fish Lake deposit. Louis Berniolles provided the muscovite-bearing vein material from the Skinner occurrence.

REFERENCES

- Berniolles, L. (1991): Prospecting report - Skinner Group; *BC Ministry of Energy, Mines and Petroleum Resources*, Assessment Report 22007.
- Caira, N.M., Findlay, A., DeLong, C. and Rebagliati, C.M. (1995): Fish Lake porphyry copper-gold deposit, central British Columbia; in *Porphyry Deposits of the Northwestern Cordillera of North America*, Schroeter, T.G., Editor, *Canadian Institute of Mining, Metallurgy and Petroleum*, Special Volume 46, pages 327–342.
- Friedman, R.M., Diakow, L.J., Lane, R.A. and Mortensen, J.K. (2001): New U-Pb age constraints on latest Cretaceous magmatism and associated mineralization in the Fawnie Range, Nechako Plateau, central British Columbia; *Canadian Journal of Earth Sciences*, Volume 38, pages 619–637.
- Hickson, C.J. and Hignman, S. (1993): Geology of the northwest quadrant, Taseko Lakes map area, west-central British Columbia; in *Current Research, Part A*, *Geological Survey of Canada*, Paper 93-1A, pages 63–67.
- Schiarizza, P. and Riddell, J. (1997): Geology of the Tatlayoko Lake – Beece Creek area (92N/8, 9, 10; 92O/5, 6, 12); in *Interior Plateau Geoscience Project: Summary of Geological, Geochemical and Geophysical Studies*, Diakow, L.J. and Newell, J.M., Editors, *BC Ministry of Employment and Investment*, Paper 1997-2, pages 63–101.
- Schiarizza, P., Gaba, R.G., Glover, J.K., Garver, J.I. and Umhoefer, P.J. (1997): Geology and mineral occurrences of the Taseko – Bridge River area; *BC Ministry of Employment and Investment*, Bulletin 100, 291 pages.
- Schiarizza, P., Riddell, J., Gaba, R.G., Melville, D.M., Umhoefer, P.J., Robinson, M.J., Jennings, B.K. and Hick, D. (2002): Geology of the Beece Creek – Niut Mountain area, British Columbia (NTS 92N/8, 9, 10; 92O/5, 6, 12); *BC Ministry of Energy and Mines*, Geoscience Map 2002-3, 1:100 000 scale.
- Stacey, J.S. and Kramer, J.D. (1975): Approximation of terrestrial lead isotope evolution by a two-stage model; *Earth and Planetary Science Letters*, Volume 26, pages 207–221.
- Tipper, H.W. (1969a): Mesozoic and Cenozoic geology of the northeastern part of Mount Waddington map area (92N), Coast District, British Columbia; *Geological Survey of Canada*, Paper 68-33.
- Tipper, H.W. (1969b): Geology, Anahim Lake; *Geological Survey of Canada*, Map 1202A, 1:253 440 scale.
- Umhoefer, P.J. and Kleinspehn, K.L. (1995): Mesoscale and regional kinematics of the northwestern Yalakom Fault System: major Paleogene dextral faulting in British Columbia, Canada; *Tectonics*, Volume 14, pages 78–94.
- Umhoefer, P.J. and Schiarizza, P. (1996): Latest Cretaceous to Early Tertiary dextral strike-slip faulting on the southeastern Yalakom fault system, southeastern Coast Belt, British Columbia; *Geological Society of America Bulletin*, Volume 108, pages 768–785.
- Wilcox, R.E., Harding, T.P. and Seely, D.R. (1973): Basic wrench tectonics; *American Association of Petroleum Geologists Bulletin*, Volume 57, pages 74–96.
- Wolfhard, M.R. (1976): Fish Lake; in *Porphyry Deposits of the Canadian Cordillera*, Sutherland Brown, A., Editor, *Canadian Institute of Mining and Metallurgy*, Special Volume 15, pages 317–322.
- Wynne, P.J., Irving, E., Maxson, J.A. and Kleinspehn, K.L. (1995): Paleomagnetism of the Upper Cretaceous strata of Mount Tatlow: evidence for 3000 km of northward displacement of the eastern Coast Belt, British Columbia; *Journal of Geophysical Research*, Volume 100, pages 6073–6091.

Aley Carbonatite: A Paleozoic Iron Oxide Copper Gold (IOCG) Deposit in North-Central British Columbia?

By Stephen T. Johnston¹ and Leanne Pyle¹

INTRODUCTION

Iron oxide copper gold (IOCG) deposits are recognized world-wide and include a number of world-class, high-tonnage, low-grade Cu-Au deposits that are typically hosted in intrusive-hydrothermal breccias and include the Mesoproterozoic Olympic Dam (Australia) and Igarape-Bahia Alemão (Brazil) deposits (Hitzman *et al.*, 1992). In the Canadian Cordillera, numerous Mesoproterozoic breccia bodies in the Yukon, collectively known as the Wernecke Breccias, have associated IOCG mineralization (Fig. 1; Thorkelson *et al.*, 2001). Despite their economic significance, the origins and paragenesis of IOCG deposits, and hence mineral deposit models and related exploration strategies for IOCG deposits, continue to be debated (Hauck, 1990). In the Canadian Cordillera, exploration for IOCG deposits has focused on Proterozoic strata in the Yukon and adjacent portions of the Northwest Territories.

We report on recent mapping of the western margin of the Aley carbonatite complex of northeastern British Columbia (Fig. 1, 2). The Aley carbonatite is one of a series of carbonatite complexes that intrudes little-metamorphosed continental margin strata of the Canadian Cordillera foreland belt (Fig. 1). Of these complexes, the Aley carbonatite complex is of particular interest due to its anomalously high concentrations of Nb₂O₅ and its spatial association with the Ospika pipe, an ultramafic lamprophyric diatreme breccia pipe that has been previously investigated as a possible diamond exploration target (Fig. 2). Although carbonatites have traditionally been explored primarily for their rare earth element (REE) potential, Groves and Vielreicher (2001), based on their work on the Palabora carbonatite of South Africa, recently proposed a link between IOCG deposits and carbonatites. After summarizing the characteristics of carbonatites and IOCG deposits, we present the results of recent detailed (1:5000-scale) mapping across the western margin of Aley carbonatite. Should the Aley carbonatite prove to host significant IOCG mineralization, it would suggest that the series of carbonatite complexes that characterize the Canadian Cordilleran Foreland Belt may constitute a significant, newly recognized IOCG province.

CARBONATITES AND IOCG DEPOSITS

Carbonatites are igneous rocks consisting of >50% magmatic carbonate. Although most common in Precambrian cratonic regions, carbonatites are known world-wide, range in age from the Archean to the present (Woolley, 1989) and are interpreted to be genetically and spatially associated with continental rifts (Bailey, 1977). Burke *et al.* (2003), based on a compilation of African carbonatite occurrences, have suggested that deformed carbonatite complexes occur along and characterize relict sutures where oceans adjacent to rifted continental margins have been closed. Johnston *et al.* (2003) suggested that carbonatite complexes of the Cordilleran foreland may lie along and mark a cryptic suture separating a far-travelled ribbon continent to the west (Johnston, 2001) from autochthonous North American strata to the east. Repeated carbonatite magmatism spanning hundreds of millions of years characterizes some small regions (Bailey, 1977). All carbonatites commonly occur together with alkaline igneous rocks as part of an alkaline intrusive series that includes olivine-free nephelinites, syenites and pyroxenites. Rarely, carbonatites are spatially associated with kimberlite.

Carbonatite mineralogy ranges from calcite (soivite) to dolomite carbonatites (raugaugite). Zoned carbonatite intrusions with calcite rims and dolomite cores have been documented. Important accessory phases commonly include pyroxene, magnetite and hematite, and apatite. Finitization, consisting of Na metasomatic alteration of the host wallrocks, is commonly observed adjacent to carbonatite intrusions. Economic concentrations of REE, particularly Nb, used in the production of stainless steel and high-strength metallic alloys, make carbonatites attractive exploration targets. The Palabora carbonatite of South Africa hosts an economic magnetite-copper-phosphate-REE deposit (Eriksson, 1989).

Iron oxide copper gold deposits occur in a variety of brecciated hostrocks, but are all associated with potassic anorogenic granitoid plutons, and are spatially associated with crustal-scale faults that mark cratonic margins (Hitzman *et al.*, 1992). Most known IOCG deposits are Paleo- to Mesoproterozoic. Host breccia bodies are typically steeply plunging pipe-like bodies that consist of fresh to entirely metasomatized country-rock fragments. Metasomatism locally extends into unbrecciated wallrocks. Hostrocks range from older sedimentary and volcanic strata to much older gneiss complexes, and rarely

¹ School of Earth & Ocean Sciences, University of Victoria, PO Box 3055 STN CSC, Victoria, BC V8W 3P6, e-mail

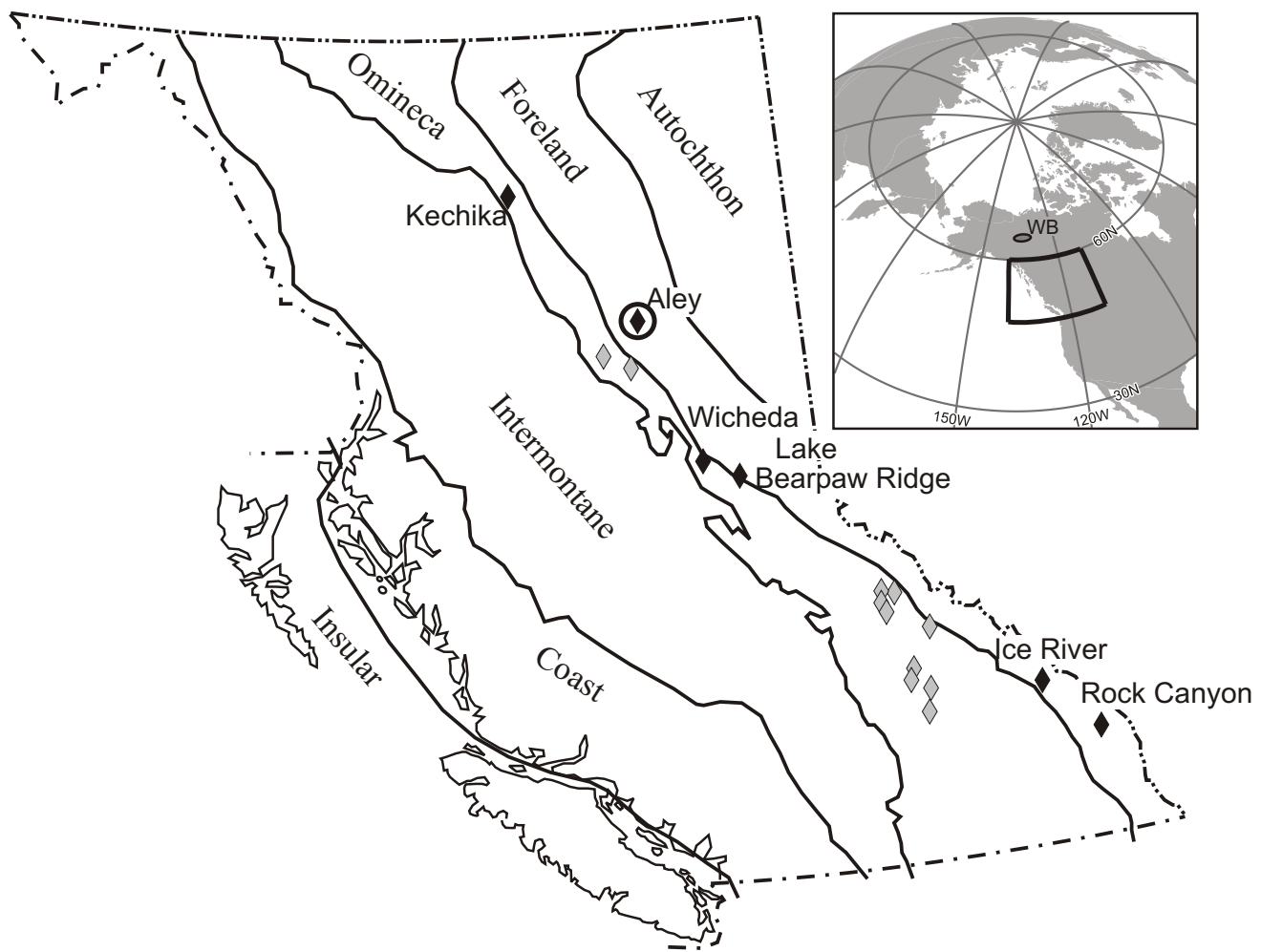


Figure 1 – Distribution of known carbonatite complexes in the Foreland and Omineca belts of British Columbia, in part after Pell (1994). Black diamonds indicate carbonatites emplaced into layered strata thought to have been deposited along the ancient continental platform and slope of western North America, and include the Aley carbonatite (circled). Grey diamonds indicate carbonatites hosted by metamorphosed strata of probable Precambrian age. Distribution of the Wernecke Breccia bodies is indicated on the inset map.

comprise coeval anorogenic granitoids. Mineralization is characterized by low-grade copper and gold mineralization in magnetite and hematite. Magnetite and hematite occur as a cement binding together breccia fragments, as breccia fragments, and as a texture-destroying metasomatic alteration of wallrock fragments. Anomalous enrichment in light REE, F and P, and Ag, As, Ba, Co, Mo, Nb, Ni, Th, and U is common. Evidence of early carbonate alteration is rare, although carbonates are commonly replaced by younger sulphide minerals, and the extent of early carbonate fluxing may be underestimated. Carbon dioxide is a common component of the ore fluids (Groves and Vielreicher, 2001)

ALEY CARBONATITE

The Aley carbonatite complex was mapped as part of a regional-scale (1:250 000) mapping program by Thompson (1989) and in detail by Maeder (1986, 1987). The main components of the complex are 1) an oval shaped intrusion 3.0 km in diameter along its long north-south axis and char-

acterized by a massive, coarsely crystalline dolomite carbonatite core; 2) spatially associated lamprophyre dikes; 3) a mantle of rocks that have previously been referred to as ‘amphibolite’ (Mader, 1987; Pell, 1994) and mapped as a continuous body that completely encloses the intrusion; 4) an outer fenite zone, previously interpreted as Na-metasomatized wallrocks; and 5) cleaved argillaceous limestone and dolomitic limestone of the host wallrocks (Fig. 2). We first discuss the wallrocks, then the ‘amphibolite’ mantle, and finally the carbonatite and its associated lamprophyres.

Regional mapping has established the stratigraphic succession into which the carbonatite was intruded, and the relationship of the carbonatite to regional facies boundaries (Thompson, 1989). Slaty limestones and calcareous slate of the Cambrian to Ordovician Kechika Formation host the carbonatite complex. Stratigraphically overlying the Kechika Formation in the vicinity of the Aley carbonatite are light grey dolostones of the Middle Ordovician Skoki Formation (Fig. 2). The dolostones include a dark green

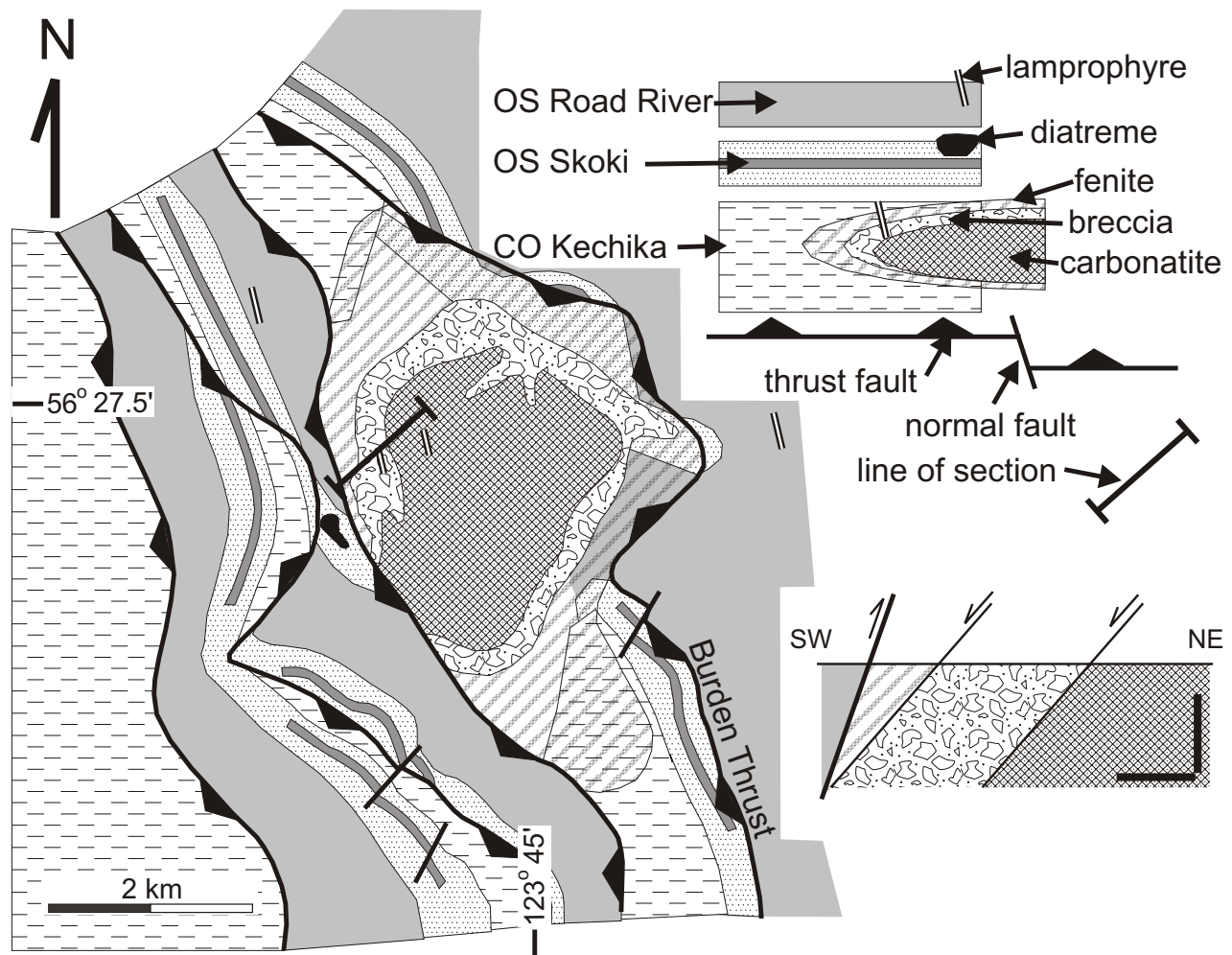


Figure 2 – Detailed geology of the Aley carbonatite (in part after Mader, 1987 and Thompson, 1989). See Figure 1 for location. The grey marker unit contained in the Skoki Formation is an alkalic basalt layer. The diatreme that intrudes the Skoki Formation west of the carbonatite is the Ospika Pipe. Schematic cross-section at lower right shows the relationships between the fenite, breccia and carbonatite; black bars represent 250 m on the cross-section. Abbreviations: OS, Ordovician-Silurian; CO, Cambrian-Ordovician.

weathering alkaline basalt that thins away from the Aley carbonatite to the north and south (Fig. 2). Pyle and Barnes (2001) identified carbonatite ocelli in samples of the basalt collected to the north of the Aley carbonatite (D. Canil, personal communication, 2001). The Skoki Formation passes both upsection and to the west into shales, calcareous shales and sandstones of the basinal Road River Group (Fig. 2). The transition from carbonates of the Skoki Formation to shales of the Middle Ordovician to Middle Devonian Road River Group has been interpreted as a facies boundary where shallow-water platform and shelf carbonates pass westward into deep water shales of the continental slope and adjacent basin (Cecile and Norford, 1979; Pyle and Barnes, 2001). Hence, the Aley carbonatite intruded along or close to the ancient western margin of the North American continent.

FENITE ZONE

Kechika Formation rocks within 500 m map distance of the intrusion are characterized by a bleached to cream-

white weathering colour, have been mapped as ‘fenites’, and have been interpreted as sedimentary rocks metasomatized during carbonatite intrusion by the addition of Na_2O , K_2O , MgO and Fe_2O_3 (Mader, 1987; Pell, 1994). Two distinct rock types characterize the fenite zone: coarsely crystalline dolomite and finely laminated dolostone. Coarsely crystalline dolomite is texturally and mineralogically identical to the dolomitic carbonatite intrusion and occurs as massive, lamination-parallel layers 5 to 100 cm thick that we interpret as intrusive carbonatite sills. Finely laminated dolostones that host the sills are characterized by wavy, anastomosing laminations that appear mylonitic. Contacts with unaltered and nonlaminated (nonmylonitized?) Kechika Formation rocks are gradational over short distances and are commonly sharp. These relationships suggest to us that the fenitized zone is a structurally distinct package of rocks with an uncertain relationship to adjacent rocks of the Kechika Formation. We believe that at least some of the fenitized rocks are mylonitized carbonatite of the intrusion. Interleaving of massive and mylonitized carbonatite suggests that

intrusion was synkinematic and involved the development of highly strained rocks.

MANTLING BRECCIA

The carbonatite intrusion is mapped as being everywhere isolated from the fenite zone by a mantle of amphibolite (Fig. 2; Mader, 1987). Pell (1994) noted that, locally at least, the amphibolite was characterized by breccia. Our mapping focused on the western margin of the carbonatite, where the intrusion is separated from the fenite zone by a thick and continuous breccia body that forms a steeply west-dipping sheet. The breccia is grey, matrix supported and heterogeneous (Fig. 3). Clasts range in size from sand-sized particles to blocks >1 m in diameter, are well rounded but not spherical, and are commonly characterized by bleached (altered) margins (Fig. 3a). A weak foliation defined by alignment of the largest clasts is locally evident and parallels the steep west dip of the breccia body. The majority of the clasts consist of quartzite or microcrystalline leucosyenite. Limestone clasts, presumably derived from the adjacent country rocks, are common. Neither the quartzite nor the leucosyenite is mapped in the vicinity of the Aley carbonatite and the source of these abundant clasts is unknown. Clasts of hematite-magnetite, carbonatite and aphanitic 'greenstone' are rare.

The matrix varies between a magmatic microsyenite and a clastic mix of sand-sized particles of quartzite and grey, aphanitic lithic clasts of uncertain lithology. The microsyenite consists of interlocking, euhedral feldspar (or possibly nepheline) microlites that appear igneous in origin. Both the clastic and microsyenite matrix are commonly characterized by hematite and hematite-magnetite cement. Hematite forms asymmetric, laminated mantles on many of the clasts and locally penetrates into clasts along fractures (Fig. 3b,c) that cut across matrix and clasts. Previous geochemical studies, summarized in Pell (1994), indicate that the syenite clasts are characterized by light REE enrichment similar to, but not as strongly developed as, the that of Aley carbonatite. The matrix is anomalously Na and K-rich, but otherwise geochemically similar to fenite zones marginal to many carbonatite intrusions (Pell, 1994).

Sheets of highly foliated and lineated, orange-weathering carbonatite are common in the breccia. These carbonatite sheets appear to locally host rare singular clasts. The foliation is defined by wavy laminations and by discontinuous layers rich in rods of white, coarsely crystalline saddle dolomite. The lineation is defined by 1–10 mm long rods of saddle dolomite that plunge steeply down-dip to the west (Fig. 3d). At one locality, the foliation was defined by alignment of abundant, highly altered orthopyroxene 'plates' 1 cm across. The sheet-like geometry of the foliated carbonatites and the presence of altered orthopyroxene crystals imply that the carbonatite sheets originated as dikes or sills that intruded the breccia. In one instance a sheet of foliated carbonatite rooted into a west-dipping extensional shear zone (Fig. 3e). The close spatial relationship between shear zones and foliated carbonatite sheets may indicate that carbonatite intrusion was synkinematic with extensional (top down to the west)

shearing and that the presence of the carbonatite magma promoted and localized shear zones within the breccia. In addition to the sheared carbonatite sheets, orange-weathering, discordant dikes and sills of massive carbonatite are common throughout the breccia body, although they appear more abundant adjacent to the contact with the main body of the underlying Aley carbonatite. These carbonatite dikes narrow and branch upward away from the underlying intrusion (Fig. 3f), suggesting that the breccia body predated and formed the roof above the intruding Aley carbonatite.

Argillaceous limestones of the Ordovician Skoki Formation immediately west of and in fault contact with the mantling breccia are intruded by a breccia pipe (Ospika pipe). Although distinguishable from the mantling breccia due to the presence of abundant phlogopite, the Ospika pipe breccia is otherwise similar to and probably genetically related to the mantling breccia. Both breccias are characterized by a similar suite of clasts, the presence of bleached reaction rims on the clasts, a heterogeneous igneous matrix that locally consists of pyroxene-phyric carbonatite, and crosscutting carbonatite dikes that postdate breccia emplacement.

ALEY CARBONATITE

The Aley intrusion consists of bright orange weathering crystalline dolomite, and sits structurally beneath and is in sharp contact with the overlying breccia body. The carbonatite-breccia contact consists of a highly sheared zone, ranging from 1 to >10 m wide, of structurally intermixed breccia, green schist, hematite layers and carbonatite. Kinematic indicators, including asymmetric folds, extensional shears, and a crenulation cleavage, imply that deformation occurred during top-down-to-the-west shearing. The presence of interfoliated layers of highly strained and unstrained carbonatite indicates that extensional shearing was coeval with intrusion. The core of the intrusion consists of weakly foliated to unstrained, coarsely crystalline dolomite. The orange colour appears to result from abundant disseminated hematite. The foliation commonly dips steeply to the west to northwest, parallel to the contact with the overlying breccia body. Previous geochemical studies (Pell, 1994) have established that the carbonatite is strongly enriched in phosphorus (>11% P₂O₅) and light REE. Concentrations of Nb₂O₅ alone locally exceed 2%.

The age of the carbonatite intrusion is constrained as being younger than the enclosing Late Cambrian to Middle Ordovician Kechika Formation. An alkalic volcanic layer in the Ordovician Skoki Formation, which is locally characterized by carbonatite ocelli, thins away from the carbonatite to the north and south. The spatial association of this alkalic volcanic unit with its carbonatitic affinity may indicate that volcanism and intrusion were cogenetic, requiring a mid-Ordovician age for the Aley carbonatite. Alternatively, the close spatial association of the volcanic layer and the intrusion may be another example of repeated carbonatitic magmatism in one locality over long periods of time.



Figure 3. **a)** Rounded, elongate syenite clasts (light grey) in dark grey, hematitic microsyenite matrix. **b)** Syenite and quartzite clasts enclosed in laminated hematite-magnetite mantles within a hematitic microsyenite matrix; note that hematite-magnetite mantles are asymmetric and appear to penetrate into the clasts along fracture planes. **c)** Close-up of laminated hematite-magnetite mantle. **d)** Foliated and lineated orange-weathering carbonatite sheet within the mantling breccia; light grey saddle dolomite forms resistant, elongate lenses that define a steeply westward plunging, down-dip lineation. **e)** Breccia cut by down-dip to the west extensional shear zone (asymmetric arrows indicate sense of shear); note extensional domino-faulting of breccia in the hangingwall of the extensional shear, and the carbonatite sheet (black arrow) at lower left that defines the down-dip continuation of the extensional shear; **f)** 30 m high cliff face exposure of breccia immediately above the upper contact of the Aley carbonatite intrusion; upward-branching carbonatite dikes that root downward into the carbonatite pluton intrude the grey-weathering breccia.

Lamprophyre dikes intrude the breccia body and Ordovician to Devonian Road River Group to the east of the carbonatite. If attributable to the same magmatic event that gave rise to the carbonatite, these lamprophyres would indicate a Devonian or younger age of intrusion. Two K-Ar ages on phlogopite separates the lamprophyre dikes yielded ages of 339 ± 12 and 349 ± 12 Ma (Maeder, 1986). We interpret these ages as reflecting cooling through the closure temperature for Ar in biotite-phlogopite and therefore interpret 345 Ma (Mississippian) as the minimum possible age of the lamprophyres.

STRUCTURAL GEOLOGY

The complex and its wallrocks are imbricated along a series of steeply west-dipping, east-verging thrust faults. The carbonatite occurs in the immediate hangingwall of the Burden thrust (Fig. 2), a major northwest-trending thrust fault that merges with the north-trending mountain front to the south where it defines the east limit of the Rocky Mountain structural province (Thompson, 1989). Kechika Formation rocks in the hangingwall of the Burden thrust north and south of the Aley carbonatite are folded, forming an overturned anticline with a steeply west-dipping axial surface. It remains unclear if the carbonatite is itself tightly folded in the core of this fold; although the dolomitic carbonatite in the core of the intrusion is weakly foliated, there is no indication of significant strain that one would commonly associate with the hinge of a tight, overturned fold. In addition, the symmetric ovoid shape of the carbonatite body and lack of any significant penetrative deformation or flow within the body argue against the intrusion having been tightly folded, and the upward branching geometry of carbonatite dikes that root into the roof of the intrusion all point to the intrusion being the right way up. How then to reconcile the folded nature of the Kechika Formation wallrocks north and south of the intrusion with the apparent lack of folding of the intrusion itself? It may be that the tight overturned fold roots into the fenite zone, which may be a mylonitic thrust, as opposed to a metasomatic aureole.

The Aley carbonatite and its host Kechika Formation rocks are thrust east over an overturned panel of shale of the Road River Group (Fig. 2). A biotite lamprophyre dike that intrudes the footwall Road River Group shales provides a link with lamprophyres that characterize the Aley carbonatite. To the west, Kechika Formation rocks carried in the Burden thrust sheet are interpreted as being overthrust by younger argillaceous limestones and calcareous shales of the Road River Group. Interpretation of this contact as a fault is consistent with the presence of fault rocks (gouge and disrupted and folded strata) and with the absence of the Skoki Formation, which is known to lie between and separate the Kechika Formation and Road River Group regionally. Interpreting the contact as a thrust fault, however, requires that younger (Road River) strata were thrust over older (Kechika) strata. Interpretation of the fault as a normal fault would be consistent with the younger over older relationship and with the absence of the Skoki Formation. Extensional, top down to the west shear zones have

been observed in the breccia above the carbonatite and along the breccia-carbonatite contact (Fig. 3f). Interleaving of sheared and unstrained carbonatite, the rooting of sheared carbonatite into discrete shear zones, and truncation of extensional shears by unstrained carbonatite dikes imply that shearing was synintrusive and may have accommodated emplacement of the Aley carbonatite intrusion. It may be, therefore, that the fault zone bounding the Burden thrust sheet to the west is a Paleozoic extensional fault that developed during Aley carbonatite magmatism. Alternatively, the observed younger over older relationships and the absence of the Skoki Formation could be accomplished by having a thrust fault cut structurally upsection through an already overturned panel of rock, although this conflicts with our interpretation of the Aley carbonatite being right way up.

An isolated area underlain by rocks of the Skoki Formation, immediately west of the Aley carbonatite in the hangingwall of the fault forming the western margin of the Burden thrust sheet, hosts an ultramafic diatreme pipe, referred to as the Ospika diatreme. The diatreme has been prospected for diamond potential. Depending upon the nature of the fault bounding the western margin of the Burden thrust sheet, the Ospika pipe either originated to the west of the carbonatite (if the fault is a thrust) or structurally above the carbonatite (if the fault is a normal fault).

ECONOMIC GEOLOGY

Extensive exploration of the Aley carbonatite and the adjacent Ospika pipe, including surface mapping and diamond-drilling, has focused on the Nb_2O_5 and diamond potential, respectively. Concentrations of $>0.6\%$ Nb_2O_5 characterize large volumes of the carbonatite intrusion, with local concentrations of $>2\%$, comparable to the 0.5–0.7% Nb_2O_5 grade of carbonatite mined near at St. Honoré, Quebec (Pell, 1994). High concentrations of light REE and phosphates further enhance the economic viability of the Aley carbonatite.

Ultrabasic diatremes similar to the Ospika pipe, located to the south (Golden) and north (Kechika), have yielded microdiamonds (Simandl, 2004). Exploration of the Ospika pipe has, however, so far failed to yield diamonds or diamond-indicator minerals (e.g., G8–G10 garnets).

Creeks draining the Aley carbonatite and the mantling breccia comprise an isolated placer gold province; no other significant placer gold deposit is known in British Columbia east of the Rocky Mountain Trench. Placer gold provinces elsewhere in the eastern Cordillera are commonly spatially associated with mid-Cretaceous granitoid plutons (Dawson *et al.*, 1991). No mid-Cretaceous plutons are known east of the Rocky Mountain Trench in northeastern British Columbia. The presence of the Aley carbonatite at the head of the creeks characterized by placer gold makes it likely that the carbonatite intrusion or its wallrocks is the source of the gold.

DISCUSSION AND CONCLUSIONS

The Aley carbonatite complex shares many of the traits of IOCG deposits. Intrusion was accommodated by and synkinematic with crustal extension. Spatial association with a long-lived, Paleozoic carbonate-to-shale facies boundary implies proximity to a major, continent-bounding fault system. The carbonatite postdated and was emplaced into and beneath a steeply plunging body of magmatic breccia. The spatially and genetically related Ospika pipe, located to the west of the carbonatite, also forms a steeply plunging breccia pipe. Significant metasomatism attended breccia emplacement: clasts of country rock exhibit bleached altered rims, and are mantled by, shot through and partially to wholly replaced by laminated to massive hematite and hematite-magnetite. Hematite and hematite-magnetite also occur as discrete fragments within the breccia, and as a ubiquitous cement phase present throughout the matrix. Locally, the breccia matrix consists of sheared carbonatite, implying significant carbonate-fluxing during breccia emplacement. The presence of a 'fenite zone' hosting the breccia may indicate that metasomatism extended into the unbrecciated country rock. Although potassic anorogenic granitoid plutons were not mapped in the vicinity of the carbonatite body, the presence of abundant microsyenite clasts in the breccia and the syenite-nephelinite character of the breccia matrix imply the presence of associated anorogenic magmatism. Previous exploration has demonstrated that the carbonatite is anomalously enriched in light REE, as well as phosphorus. No visible gold mineralization has been reported in the carbonatite or the mantling breccia. Low-grade gold mineralization is, however, implied by the presence of significant gold placers on the creeks draining the intrusive complex.

Interpretation of the Aley carbonatite as host to significant IOCG mineralization remains a largely untested model. The extent of related copper mineralization, a hallmark of IOCG deposits, remains entirely unknown, as does the amount of enrichment in other IOCG-associated elements (F, Ag, As, Ba, Co, Mo, Th and U). Fundamental constraints, such as the age of breccia formation and subsequent carbonatite intrusion, are lacking. It seems likely that the structural evolution of the carbonatite and the mantling breccia involves a synmagmatic extensional event and Late Cretaceous displacement along east-verging thrust faults. The geometry of extensional and thrust structures is, however, only broadly constrained, and the relationship of the carbonatite to these structures remains poorly understood.

Our observations from the Aley carbonatite lend support to the suggestion, first made by Groves and Vielreicher (2001), that carbonatites are an end member of the IOCG family of mineral deposits. All previously documented occurrences of IOCG mineralization are Proterozoic or older. Confirmation of significant IOCG mineralization at the Paleozoic Aley carbonatite would make it the youngest known IOCG occurrence in the world, and would imply that exploration for IOCG deposits should expand into post-Proterozoic terranes. From a Canadian perspective, the Aley carbonatite is but one of a series of Paleozoic

carbonatites and alkaline complexes that extend the length of the Foreland Belt of the Cordilleran orogen, all of which may potentially host IOCG mineralization. Hence, exploration programs for IOCG deposits, which have to date focused on the Mesoproterozoic Wernecke Breccias of the Yukon and Northwest territories, might now find encouragement to expand into Paleozoic strata along the length of the Cordilleran Foreland.

ACKNOWLEDGMENTS

This research was supported by a British Columbia Ministry of Energy and Mines – University of Victoria Partnership: Energy and Minerals Projects grant to the senior author. The endorsement of the proposed research by Brian Grant and George Simandl of the BCGS was much appreciated. Our interest in carbonatites was stimulated by Kevin Burke, Lewis Ashwal and Sue Webb. Discussions with Bob Thompson regarding the geology of northeastern British Columbia, Gerry Carlson and Bob Anderson regarding IOCG deposits, and Dante Canil regarding carbonatite magmatism helped clarify our ideas. Pacific Western Helicopters is thanked for safe and efficient transportation, and for a dramatic evening rescue from four angry grizzly bears.

REFERENCES CITED

- Bailey, D.K. (1977): Lithosphere control of continental rift magmatism; *Journal of the Geological Society of London*, Volume 133, pages 103–106.
- Burke, K., Ashwal, L.D. and Webb, S.J. (2003): New way to map old sutures using deformed alkaline rocks and carbonatites; *Geology*, Volume 31, pages 391–394.
- Cecile, M.P., and Norford, B.S. (1979): Basin to platform transition, lower Paleozoic strata of Ware of Trutch map-areas, northeastern British Columbia; in Current Research, Part A, *Geological Survey of Canada*, Paper 79-1A, pages 219–226.
- Dawson, K.M., Panteleyev, A., Sutherland-Brown, A. and Woodsworth, G.J. (1991): Regional metallogeny; Chapter 19 in *Geology of the Cordilleran Orogen in Canada*, Gabrielse, H. and Yorath, C.J., Editors, *Geological Society of America*, Volume G-2, pages 709–768.
- Eriksson, S.C. (1989): Phalabowra: a saga of magmatism, metasomatism and miscibility; in *Carbonatites: Genesis and Evolution*, Bell, K., Editor, *Unwin Hyman*, London, pages 221–254.
- Groves, D.I., and Vielreicher, N.M. (2001): The Phalabowra (Palabora) carbonatite-hosted magnetite-copper sulfide deposit, South Africa: an end-member of the iron-oxide copper-gold-rare earth element deposit group? *Mineralium Deposita*, Volume 36, pages 189–194.
- Hauk, S.A. (1990): Petrogenesis and tectonic setting of middle Proterozoic iron-oxide-rich deposits: an ore deposit model for Olympic Dam-type mineralization; *United States Geological Survey*, Bulletin 1932, pages 4–39.
- Hitzman, M.W., Oreskes, N. and Einaudi, M.T. (1992): Geological characteristics and tectonic setting of Proterozoic iron oxide (Cu-U-Au-REE) deposits; *Precambrian Research*, Volume 58, pages 241–287.
- Johnston, S.T. (2001): The great Alaskan terrane wreck: reconciliation of paleomagnetic and geological data in the north-

- ern Cordillera; *Earth and Planetary Science Letters*, Volume 3, pages 259–272.
- Johnston, S.T., Burke, K., Ashwal, L.D. and Webb, S.J. (2003): Examples of deformed alkaline rocks and carbonatites (DARCS) in suture zones and as sources of alkaline rocks and carbonatites (ARCS) in overlying rifts from the north-western Cordilleran continental margin and elsewhere; *Geological Society of America*, Annual Meeting, Volume 35, pages 230–233.
- Mader, U.K. (1986): The Aley carbonatite complex; unpublished M.Sc. thesis, *University of British Columbia*, Vancouver, British Columbia.
- Mader, U.K. (1987): The Aley carbonatite complex, northern Rocky Mountains, British Columbia (94B/5); in *Geological Fieldwork 1986, BC Ministry of Energy, Mines and Petroleum Resources*, Paper 1987-1, pages 283–288.
- Pell, J. (1994): Carbonatites, nepheline syenites, kimberlites and related rocks in British Columbia; *BC Ministry of Energy, Mines and Petroleum Resources*, Bulletin 88, 136 pages.
- Pyle, L.J., and Barnes, C.R. (2001): Ordovician-Silurian stratigraphic framework, MacDonald Platform to Ospika Embayment transect, northeastern British Columbia; *Canadian Society of Petroleum Geologists Bulletin*, Volume 49, pages 513–535.
- Simandl, G.J. (2004): Concepts for diamond exploration in ‘on/off craton’ areas, British Columbia, Canada; *Lithos*, Volume 77, pages 749–764.
- Thompson, R.I. (1989): Stratigraphy, tectonic evolution and structural analysis of the Halfway River map area (94B), northern Rocky Mountains, British Columbia; *Geological Survey of Canada*, Memoir 42, 119 pages.
- Thorkelson, D.J., Mortensen, J.K., Davidson, G.J., Creaser, R.A., Perez, W.A. and Abbott, J.G. (2001): Early Mesoproterozoic intrusive breccias in Yukon, Canada: the role of hydrothermal systems in reconstructions of North America and Australia; *Precambrian Research*, Volume 111, pages 31–55.
- Woolley, A.R. (1989): The spatial and temporal distribution of carbonatites; in *Carbonatites: Genesis and Evolution*, Bell, K., Editor, *Unwin Hyman*, London, pages 15–37.

New Observations on the Geology of the Turnagain Alaskan-Type Ultramafic Intrusive Suite and Associated Ni-Cu-PGE Mineralization, British Columbia

By J.E. Scheel¹, G.T. Nixon² and J.S. Scoates¹

KEYWORDS: Turnagain, ultramafic, sulphide, Alaskan-type, Ni-Cu-PGE mineralization

INTRODUCTION

The Turnagain Alaskan-type ultramafic intrusive suite – a type originally recognized in Duke Island, Alaska (Irvine, 1962, 1967b) – lies 65 km east of Dease Lake, north-central British Columbia. It is a fault bounded, 3.5 by 8 km ultramafic intrusion located on the margin of Ancestral North America and is part of the Mesozoic accreted island-arc terrane of Quesnellia. Alaskan-type intrusions have been recognized in the Alaskan Panhandle, in the accreted terranes of the British Columbian Cordillera (Fig. 1), and in the Ural Mountains in Russia. The term Alaskan-type is synonymous with Uralian-type, zoned, or concentrically zoned, the latter being descriptive of the geometrical arrangement of rock units present in various Alaskan-type intrusive suites. These bodies are exploration targets for chromite and associated platinum-group-element (PGE) mineralization (*e.g.*, Nixon *et al.*, 1991, 1993). The Turnagain intrusion is unique, however, in that it contains appreciable contents of magmatic sulphides.

Alaskan-type intrusions are typically composed of cumulate dunite, wehrlite, olivine clinopyroxenite, clinopyroxenite, hornblende clinopyroxenite, hornblendite and diorite, and minor leucocratic feldspar-rich rocks such as granodiorite and syenite. The complete range of rock units is rarely present (Nixon, pers comm, 2004). The Turnagain Alaskan-type ultramafic intrusive suite has been explored for economic Ni-Cu-PGE mineralization since its initial discovery in 1956 (Nixon, 1997). Falconbridge Limited conducted extensive exploration on the ultramafic body in the late 1960s and early 1970s. Currently, the property is owned and operated by Hard Creek Nickel Corporation (formerly Canadian Metals Exploration/Bren-Mar Resources Limited). Recent mapping and sampling by the principal author was undertaken during the summer of 2004 to help better un-

derstand the petrogenesis of the Turnagain intrusive suite and the physiochemical processes responsible for its associated Ni-Cu-PGE mineralization.

REGIONAL GEOLOGY

Many Alaskan-type ultramafic intrusions in the Canadian Cordillera occur in Quesnellia, an Upper Paleozoic to Early Mesozoic arc terrane accreted to the margin of Ancestral North America during the Early Jurassic. The Quesnellia Terrane forms a part of the Omineca Belt in British Columbia and extends south into Washington State and north into the Yukon Territory. The regional geology of the Cry Lake and Dease Lake map areas (Fig. 2), including the Turnagain intrusion, has been mapped by Gabrielse (1998).

The Turnagain intrusion lies to the north of the Mesozoic Kutcho fault and Hottah-Thibert fault system. Although the dextral strike-slip Kutcho fault separates Quesnellia from Ancestral North America in northern BC (Gabrielse, 1998), the amount of displacement is uncertain. The Kutcho fault is not exposed near the Turnagain intrusion (Clark, 1975; Nixon, 1997) but is marked by two large valleys on either side of the Turnagain River. It is part of a major regional fault system that extends southward towards Washington State and northwards towards the Yukon (Gabrielse, 1998).

There are numerous clastic sedimentary rocks, ranging from Cambrian to Mississippian in age, which are proximal to the Turnagain ultramafic suite (Fig. 3). The lower Ordovician Road River Formation and the Mississippian Earn Group are two such examples. Both of these units are juxtaposed against the western, northern and eastern margins of the Turnagain intrusion and comprise the bulk of the regional geology north of the Kutcho fault. These units are dominantly composed of graphitic phyllite with intercalated calc-silicate and quartz-rich tuff layers (Photo 1), and are fairly recessive units that crop out mainly along the Turnagain River and in the alpine areas east of the intrusion. Both stratigraphic packages are commonly pyritic and unfossiliferous near the Turnagain intrusion and have graphite contents reaching up to 80% of the rock. Numerous quartz veins cut through the phyllite. They are commonly only a few millimetres in thickness, and rarely reach up to a metre

¹ Pacific Centre of Isotopic and Geochemical Research, Department of Earth and Ocean Sciences, University of British Columbia

² British Columbia Ministry of Energy and Mines

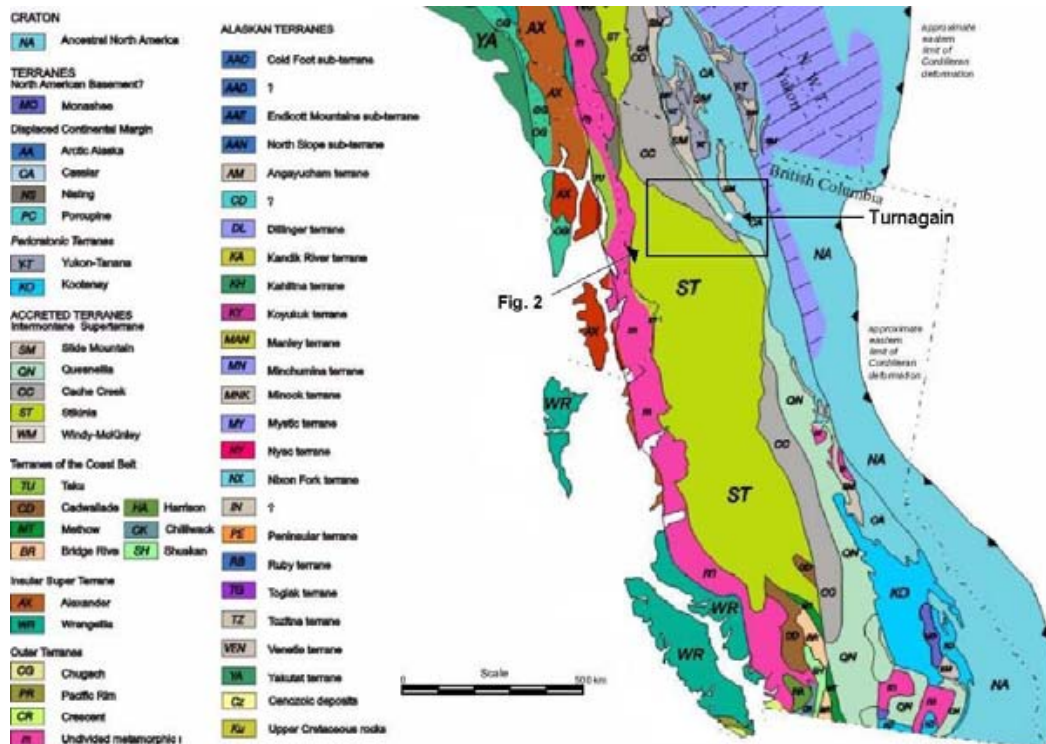


Figure 1. Terrane map of British Columbia and southern Alaska showing the location of the Turnagain ultramafic intrusive suite (white dot). Modified from Wheeler *et al.* (1991).

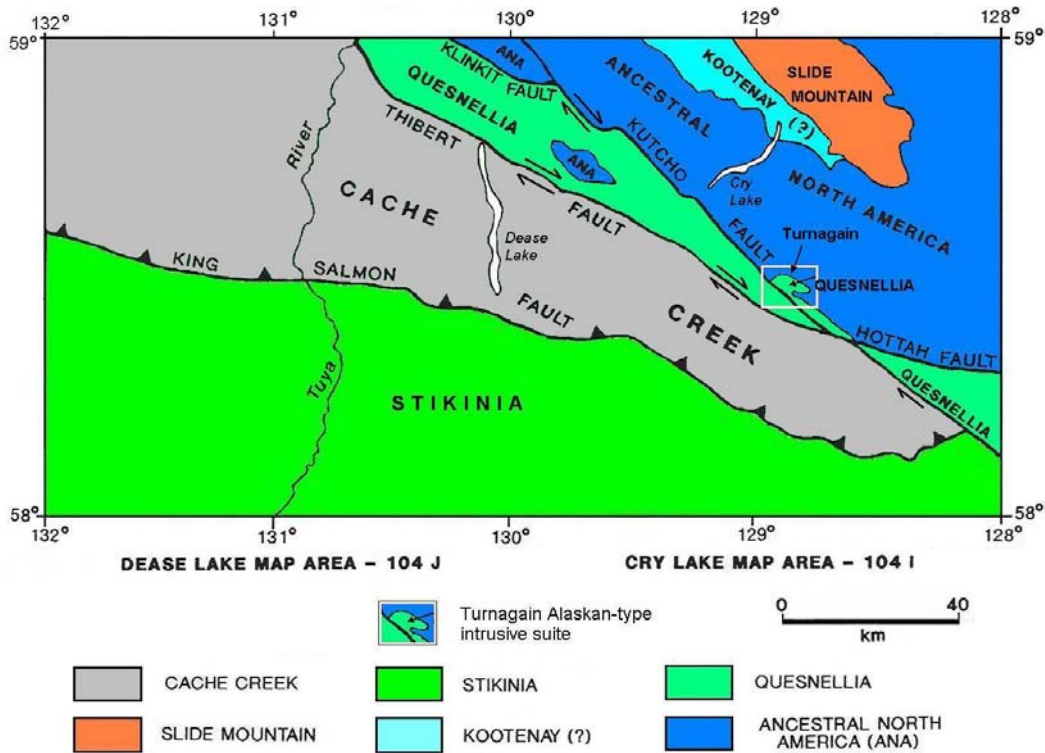


Figure 2. Simplified map of the Dease Lake and Cry Lake map areas, modified from Gabrielse (1998). The area of the Turnagain ultramafic intrusive suite is outlined.

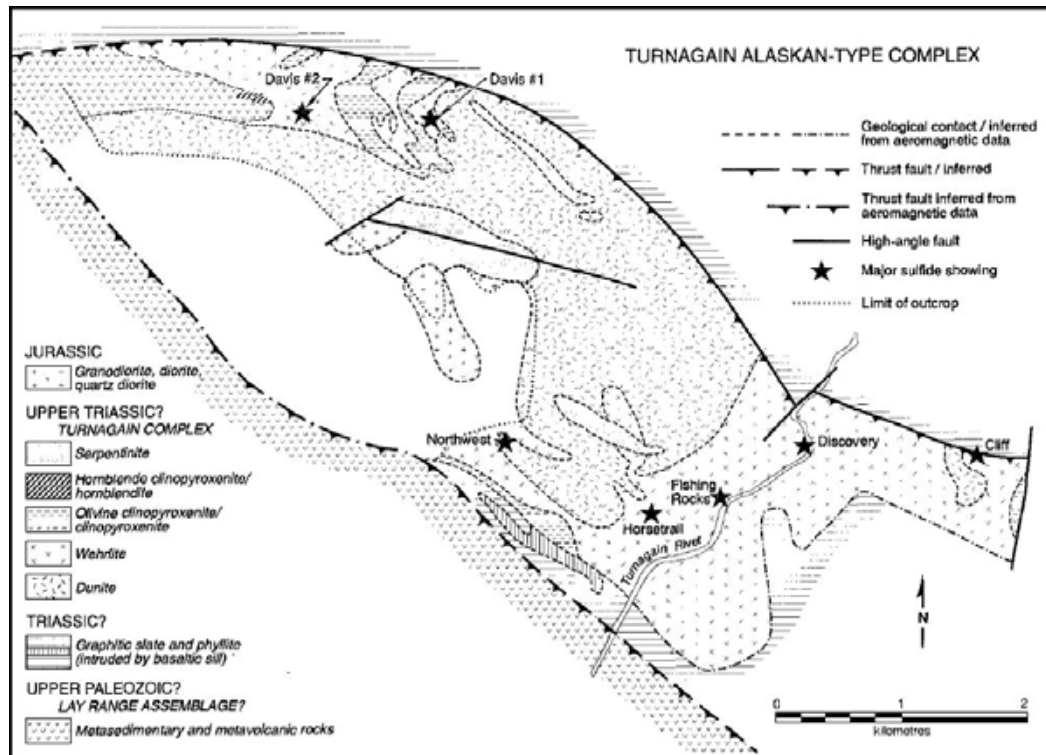


Figure 3. Simplified geological map of the Turnagain intrusion. Modified from Nixon (1997).



Photo 1. Quartz-rich tuff interbedded with graphitic phyllite, east of the Turnagain intrusion. Note the poor cleavage in the bed. Hammer is approximately 30 cm in length. UTM NAD 87, Zone 9 – Easting 513132 Northing 6479300.

thick. These veins do not show any evidence of propagation into the ultramafic cumulate rocks of the Turnagain body. Locally the phyllite is complexly folded (Photo 2), which is attributed to its position within a regional fold axis verging west-northwest.

The phyllite shows no hornfelsing or other contact metamorphism adjacent to the northern and eastern contacts of the Turnagain intrusion. Its texture and grade are primarily due to the regional greenschist-facies metamorphism that affected the area during the middle Cretaceous (Gabrielse, 1998). The northern faulted contact of the Turnagain intrusion with the phyllite of the Road River Formation and Earn Group is not exposed, but proximal to the contact the rocks are highly altered to talc, serpentine and carbonate (Photo 3).

To the north of the Road River Formation and the Earn Group lies the Upper Cambrian Kechika Formation which is described by Gabrielse (1998) as comprising a "highly cleaved, soft, light to dark grey phyllite" that is conformable with the overlying Road River Formation (Fig. 3). Although it is rarely exposed, a small outcrop of this formation was found near the Turnagain River to the north of the ultramafic rocks. It appeared no different from the graphitic phyllite of the Road River Formation or the Earn Group despite the fact it was mapped by Gabrielse (1998) as the Kechika Formation.

An unnamed group of rocks lies to the southeast of the Turnagain ultramafic suite. The rock units comprise sedimentary rocks of unknown origin, possibly volcanoclastic, with variable amounts of interbedded carbonate (Fig. 3). The group is undated, and assumed to be late Triassic in age (Gabrielse, 1998). Exposures of these rocks are minimal as much of the unit is apparently buried by eolian and glaciofluvial sediments deposited at the confluence of three valleys. The volcanoclastic rocks are thought to be part of the Quesnellia Terrane (Fig. 2), and are probably the remnants of a small Mesozoic fore-arc basin (Gabrielse, 1998). A large hornfelsed raft, presumably a piece of this unit (1 by 0.5 km) is located in the northwestern part of the Turnagain ultramafic suite and will be discussed in detail in the section to follow.

The Eaglehead Pluton dominates much of the geology south of the Kutcho fault. It is generally dioritic to granodioritic in composition and contains phenocrysts of hornblende and rare potassium feldspar. The Eaglehead Pluton is considered to be early Jurassic in age (Gabrielse, 1998). It hosts a marginal porphyry copper deposit and related gold placers (Gabrielse, 1998) and represents the bulk of the rock units southwest of the Turnagain intrusion. Numerous ophiolitic complexes have been thrust on top of this unit.

GEOLOGY OF THE TURNAGAIN

The geology of the Turnagain ultramafic rocks has been previously described by Clark (1975) and Nixon (1989, 1997), but new additions and modifications were

made during field mapping in the summer of 2004. The Turnagain intrusion is broadly composed of a central dunite core in the north with peripheral units of wehrlite, olivine clinopyroxenite, clinopyroxenite, and rare hornblende clinopyroxenite and hornblendite (Fig. 3). Feldspathic varieties of the latter are extremely rare and both hornblende clinopyroxenite and magmatic hornblendite are poorly exposed. Representative samples of these rock units were recovered in recent drillcore (Aug-Sept 2004) from the southwestern part of the intrusion. Based on the southward dipping nature of the mineralized zones and the megascopic distribution of the ultramafic rock units present in the Turnagain, these more evolved rocks are believed to be located at the roof of the intrusion.

Orthopyroxene is not present in the Turnagain cumulate rocks, a characteristic feature of all Alaskan-type intrusions and conventionally explained by the silica-undersaturated nature of the parental magma (*e.g.*, Irvine, 1967; Garuti *et al.*, 2001). The dunite and wehrlite host disseminated chromite grains, but only the dunite contains discontinuous layers, pods and schleiren of chromitite (Photo 4). Chromitites are typically small, about 30 cm long by a few centimetres thick, and have an erratic distribution. They are commonly complexly folded and discontinuous and appear to be the result of cumulate remobilization after slumping or gravity flow events.

The dunite is mainly composed of cumulus olivine, minor amounts of chromite, intercumulus olivine, and pyroxene, and trace amounts of primary phlogopite. One exposure contains secondary euhedral uvarovite that is spatially associated with multiple parallel black serpentine veinlets (Photo 5) over a thickness of roughly 50 cm. Serpentinization is highly variable in the Turnagain rock units but commonly represents no more than about 10 vol % of the rock. Dunite is distinguished from wehrlite by its dun-coloured weathered surface and its lack of pyroxene cleavages on fresh surfaces. Some dunite from drillcore has olivine with a green colour almost comparable to olivine grains found in mantle xenoliths. Olivine grains in the larger mass of fresh dunite, located in the northern part of the intrusion (Fig. 3), commonly have a very well developed parting.

Dunite commonly hosts grains of poikilitic green diopside, either as discrete, centimetre-scale crystals or elongate aggregations. The latter are interpreted to be small dikes resulting from the escape of trapped liquid but the origin of discrete diopside is still debatable. Such crystals may result from the *in situ* crystallization of trapped melt or later stage injection along zones of weakness or pre-existing fractures. Larger dikes of grey-green clinopyroxenite, commonly pegmatitic, intrude much of the dunite and wehrlite. Such dikes are considered to be injections of evolved magma into the relatively cool olivine cumulates during a syn-crystallization deformational event.

Some dunite that is proximal to massive sulphide mineralization is commonly altered to grey tremolite.



Photo 2. Complex folding, which is especially apparent in quartzite layers, within graphitic phyllite east of the Turnagain intrusion. Pencil end is approximately 4 cm long. E 513605 N 6478887.



Photo 3. Heterogeneous talc-serpentine-carbonate alteration of ultramafic rock from the northern contact of the Turnagain ultramafic intrusive suite. Distribution of the most altered rocks lies within the black lines. Hammer is approximately 30 cm long. E 506151 N 6484799.



Photo 4. Multiple discontinuous chromitite pods and schleiren in dunite. Hammer is approximately 40 cm long. E 507767 N 6483550.

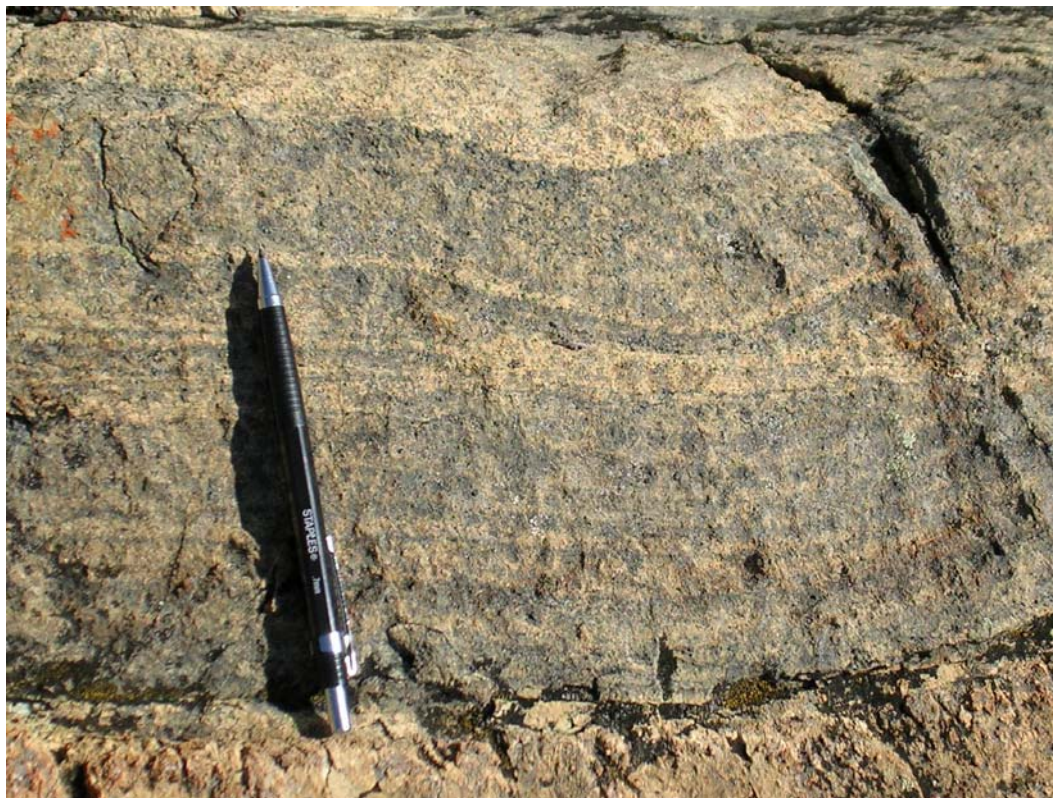


Photo 5. Pervasive magnetite-serpentine alteration of dunite, and spatially associated secondary uvarovite crystals. Pencil is approximately 12 cm long. E 507824 N 6483614.

Individual crystals pseudomorph olivine, are very fine-grained and are indistinguishable in hand sample. Under crossed-polarized light, however, tremolite is optically continuous and is presumed to be in the same optical orientation as the original olivine grains which it replaces. Larger tremolite needles commonly grow in crystallographically controlled fractures or partings within olivine. These tremolite-altered dunites are characterized by the same dun-brown weathering colour, but differ in the fresh surface. The rock appears matte-black on fresh surface with no distinguishable grains. Tremolite-altered dunite is also much harder than fresh dunite, and may be part of the reason for the outcroppings of such material in the Horsetrail Zone (Fig. 3). This zone has been identified as the main area of Ni-sulphide mineralization, although its deformational and magmatic history have yet to be resolved. Dunite-hosted sulphide mineralization is rare, comprising no more than 2 vol % of the rock. Pyrrhotite, possibly troilite, pentlandite, and trace chalcopyrite are commonly found as disseminated grains in the dunite. Rare net-textured aggregations of sulphides occur locally, including examples at the Discovery showing (Fig. 3).

Wehrlite, the second most abundant rock type in the intrusion, can be generally expressed by two distinct textural subtypes. On the west side of the Turnagain River, where the bulk of the intrusion resides, it is mainly composed of cumulus olivine with a sizable proportion of intercumulus clinopyroxene and minor amounts of cumulus pyroxene. This type of wehrlite is the most common and appears to be associated with Fe-Ni sulphide mineralization throughout the intrusion. On the east side of the river, and in the far northwest of the intrusion, cumulus clinopyroxene reaches approximately 40 vol %. Wehrlite with cumulus pyroxene is commonly mineralized with disseminated grains of Ni-poor pyrrhotite. Wehrlite containing only intercumulus pyroxene, such as that found in the Horsetrail showing, tends to contain extensive pentlandite mineralization.

Contacts between wehrlite and dunite are sharp to gradational over short distances, represented by a slight change in the size and modal abundance of pyroxene, and appear to reflect magmatic layering (Photos 6 and 7). As stated above, chromite grains are found only as disseminations in this unit. Large amounts of secondary magnetite are found where serpentinization is pervasive. Clinopyroxenite dikes also intrude the wehrlitic units in the Turnagain intrusive suite.

Olivine clinopyroxenite and clinopyroxenite are two rock units that are of relatively minor abundance in the Turnagain intrusion. They mainly occur in the northwestern part of the intrusion and commonly comprise around 85 vol % cumulus pyroxene and small amounts of cumulus olivine. In this area, these units appear to be differentiates of the original Turnagain magma as opposed to brecciated and intrusive clinopyroxenite found elsewhere. Further east, however, where large amounts of coarse to pegmatitic pyroxenites are found, the clinopyroxenites appear intrusive. This type

of pyroxenite is commonly found in all Alaskan-type intrusions (Nixon, pers comm, 2004). Olivine clinopyroxenite also exhibits rare magmatic layering where it is intercalated with wehrlitic rock units.

Pegmatitic variants of clinopyroxenite, both intrusive and *in situ*, have large crystals that rarely reach up to 20 cm in length. Pegmatitic dikes are commonly found adjacent to the cumulate clinopyroxenite. *In situ* pegmatitic variants within the cumulate pyroxenite are uncommon and confined to the northwestern part of the intrusion (Fig. 3). Clinopyroxenite from the northwest, which is juxtaposed against cumulate dunite, is commonly intruded by multiple thin dikes of fine-grained dunite (Photo 8). These dikes are randomly oriented and are no wider than 20 cm. The forsterite component of olivine within these dikes, based on optical observations, is relatively high. The origin of such Mg-rich olivine in late-stage dikes is problematic and currently unresolved. These dikes may have similar geneses to the pothole structures and dunite pipes observed in the Merensky reef in the Bushveld Complex (*e.g.*, Scoon and Mitchell, 2004).

Hornblende clinopyroxenite and clinopyroxenite are very poorly exposed and their relationships to other units in the Turnagain intrusion are not well constrained. Their occurrence coincides with a Cu-Pt-Pd soil anomaly near the southwestern margin of the intrusion. Mineralization within these hornblende-rich rocks appears to be due to the segregation of magmatic sulphides during the co-crystallization of hornblende and magnetite.

Magmatic hornblendite and hornblende clinopyroxenite found in the southwestern area of the intrusion have amphibole crystals that typically range from less than 1 cm to up to 3 cm in length. These crystals appear to be cumulus, but in some cases they replace pyroxene. Most hornblende-bearing ultramafic rocks in the Turnagain intrusion are associated with large amounts of cumulus(?) magnetite, such that these units can be identified using aeromagnetic surveys. However, the many faults that are associated with complete serpentinization of nearby ultramafic rock units are also associated with large amounts of secondary magnetite. The faults, however, do not pose significant problems for the interpretation of airborne magnetic surveys since they form distinctly linear features.

Float samples collected near the southwestern margin (Fig. 3) of the intrusion are composed almost entirely of hornblende and magnetite with large amounts of secondary pyrite. Preliminary study of drillcore from this area, the only known occurrence of these *in situ* magmatic hornblende-bearing rocks, has revealed pervasive brecciation and erratic chalcopyrite mineralization. Investigations into the nature of the Cu-Pt-Pd mineralization are underway, and preliminary results show that high PGE values do not correlate with sulphide content. Although it is possible the PGE are not present in the sulphides, it is more likely that their distribution in sulphide minerals is highly erratic.

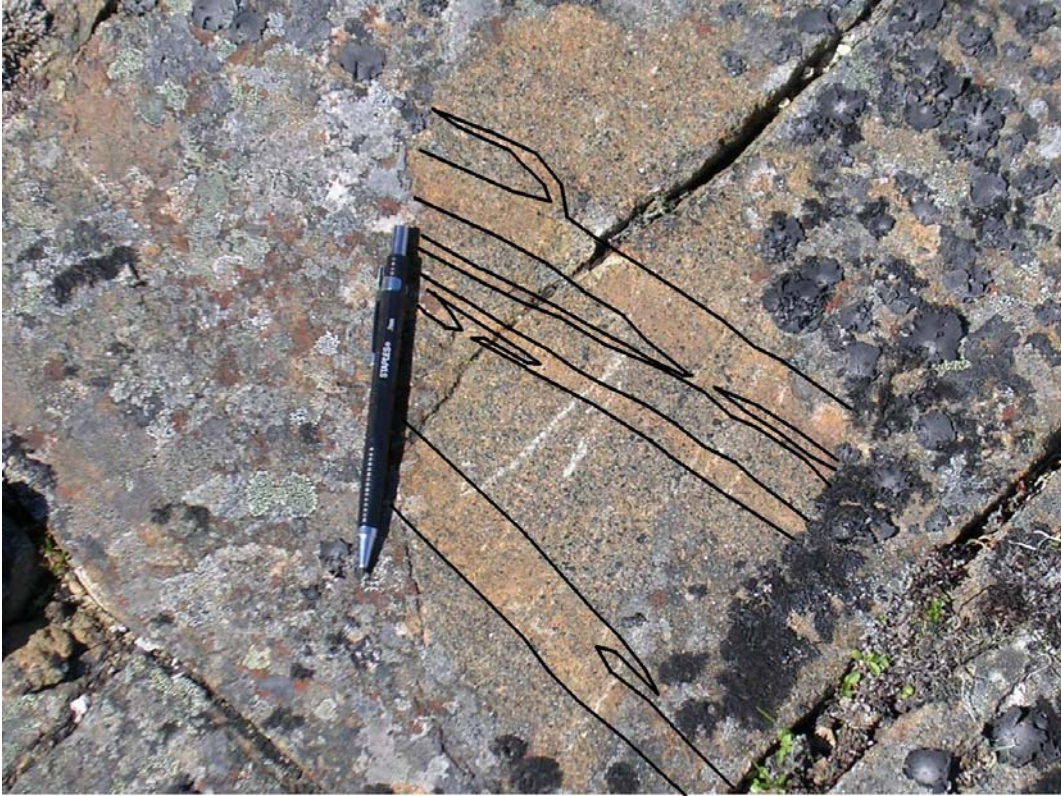


Photo 6. Magmatic layering, defined by distribution and size of cumulus diopside, in wehrlite. Pencil is approximately 12 cm long. E 507127 N 6484162.



Photo 7. Magmatic layering, defined by alternating layers of dunite and wehrlite. Dunitic layers are outlined in black. Hammer is approximately 30 cm in length. E 506777 N 6484487.



Photo 8. Dunite dikes intruding cumulate clinopyroxenite. Hammer is approximately 30 cm long. E 506830 N 6483988.

One previously unrecognized unit of hornblendite was found during the past field season and appears to be metasomatic in origin. This unit is characterized by a rusty weathered surface and increased strength compared to the metavolcanics that host it. Crystals of fine-grained hornblende are intergrown within the metavolcanic raft (Fig. 3) and are observed at the northeastern contact with cumulate wehrlite in the northwestern corner of the intrusion. Distal veins, which are found several tens of metres away from the contact and are considered to be genetically associated with the hornblendite, show fine-grained quartz margins and coarse-grained hornblende crystals in the centre.

The main hornblendite zone is characterized by planar hornblende altered areas. Hot magmatic fluids that flowed through the metavolcanic raft are considered to be responsible for its alteration. Other areas appear completely bleached and contain quartz and sericite. Clark (1975) mapped a hornblendite unit in the same vicinity, approximately 100 m to the northwest, but no exposures of this unit were found in 2004. This hornblendite appears to be completely covered by talus. It is possible that the hornblendite present here is either greisenous in origin, *i.e.*, it formed by the reaction of the *in situ* Turnagain magma(s) with fluids released from the raft, or it is a magmatic cumulate. Fluids released from the cumulate hornblendite may be responsible for the metasomatic hornblendite, thus the two lithological styles may be co-genetic.

A large 1.5 by 0.5 km metavolcaniclastic raft, which may be part of the unnamed formation to the southeast of the Turnagain ultramafic intrusion, is found in the northwestern part of the intrusion (Fig. 3). It is in intrusive contact with wehrlite at its northern margin, and dunite at its eastern and southern margins. The western margin is not exposed, although it appears to extend to the western bounding fault of the Turnagain. The raft is largely composed of plagioclase and quartz with minor hornblende and biotite. Tightly folded layers are observed in the raft and it has been hornfelsed to a significant degree. This unit, like the phyllite surrounding the Turnagain intrusion, is pervasively crosscut by numerous white quartz veins. These veins are commonly only 10 cm wide but may decrease down to millimetre scale. Present within the volcaniclastic unit are small, 5 cm-wide pods of granitic material, which can connect to centimetre-scale granitic dikes. These pods and dikes are characterized by pink potassium feldspar, cream-coloured plagioclase, white quartz, brown hornblende, brown-black biotite and clear muscovite. Many dikes and pods are randomly oriented, but the bulk of them are preferentially oriented parallel to bedding. The contacts between dikes/pods and the host metavolcaniclastic appear intrusive, but show partial assimilation of the host rock at their margins. This material appears to have formed by partial melting of the raft as it was heated up to magmatic temperatures by the Turnagain parental magma. Middle Cretaceous greenschist-facies metamorphism and deformation occurred after the intrusion was (partially) solidified.

CURRENT AND FUTURE RESEARCH

The Turnagain Alaskan-type ultramafic intrusive suite is the subject of current research for an MSc thesis by the principal author at the University of British Columbia. The goal of this study is to help better constrain the petrogenesis of the Turnagain intrusion and to gain a greater understanding of the physiochemical processes involved in the formation of its Ni-Cu-PGE mineralization.

During the summer of 2004, 172 samples were collected and 150 of these were cut into thin sections, mostly polished sections. Both transmitted and reflected light petrographic investigations of all 150 samples are currently underway. These observations will aid in constraining the crystallization and evolutionary history of the Turnagain intrusion. They will also reveal cryptic and subtle details regarding comagmatic and later-stage alteration, microstructural styles, and the nature of Ni-Cu sulphide mineralization.

Chromite chemistry, as well as associated olivine and pyroxene chemistry, can be used as a petrological indicator in mafic-ultramafic rocks (e.g., Irvine, 1965; Irvine, 1967a; Roeder and Reynolds, 1991; Sack and Ghiorso, 1991; Barnes and Roeder, 2001). In late 2004, the principal author began using the electron microprobe to investigate the spinel chemistry of various representative samples taken from the Turnagain ultramafic intrusive suite. Microprobe analyses of olivine and pyroxene will follow in 2005. Sulphur isotopic analyses of sulphides from the Turnagain Alaskan-type ultramafic intrusive suite and its wallrocks will help to constrain the origin of sulphide. Geochronological studies (U-Pb zircon/baddeleyite, Ar-Ar hornblende/biotite) of four samples collected this past summer will help to constrain the age of the Turnagain intrusion and its associated Ni-Cu-PGE mineralization. Finally, Nd isotopic studies across a transect of the Turnagain intrusion will constrain the amount of crustal input in each lithology to better develop a petrogenetic model for the origin and evolution of the Turnagain ultramafic intrusive suite.

ACKNOWLEDGMENTS

The authors would like to thank Barry Whelan, Tony Hitchins and Chris Baldys of the Hard Creek Nickel Corporation for their help in the preliminary stages of the project as well as in the field this summer, and for funding, lodging and sample transportation. Pacific Western Helicopters must also be thanked for their exemplary service and support during the 2004 field season. Finally, we thank the Ministry of Energy and Mines at the British Columbia Geological Survey for access to their library and the invaluable information within.

REFERENCES

- Barnes, S.J., and Roeder, P.L. (2001): The range of spinel compositions in terrestrial mafic and ultramafic rocks; *Journal of Petrology*, Volume 42, no 12, pages 2279-2302.
- Clark, T. (1975): Geology of an ultramafic complex on the Turnagain River, northwestern B.C.; unpublished PhD thesis, *Queens University*, 454 pages.
- Gabrielse, H. (1998): Geology of Cry Lake and Dease Lake map areas, north-central British Columbia; *Geological Survey of Canada*, Bulletin 504, 147 pages.
- Garuti, G., Pushkarew, E.V., Zaccarini, F., Cabella, R. and Anikina, E. (2003): Chromite composition and platinum-group mineral assemblage in the Uktus Uralian-Alaskan-type complex (Central Urals, Russia); *Mineralium Deposita*, Volume 38, no 3, pages 312-326.
- Irvine, T.N. (1965): Chromian spinel as a petrogenetic indicator. Part I. Theory; *Canadian Journal of Earth Sciences*, Volume 2, no 6, pages 648-672.
- Irvine, T.N. (1967a): Chromian spinel as a petrogenetic indicator. Part II. Petrological applications; *Canadian Journal of Earth Sciences*, Volume 4, no 1, pages 71-103.
- Irvine, T.N. (1967b): The Duke Island Ultramafic Complex, southeastern Alaska; in *Ultramafic and Related Rocks*, Wyllie, P.J., Editor, *John Wiley and Sons*, New York, pages 84-97.
- Nixon, G.T. (1997): Ni-sulphide mineralization in the Turnagain Alaskan-type complex: A unique magmatic environment; *Ministry of Energy, Mines and Petroleum Resources*, Paper 1998-1, pages 18-1 – 18-12
- Nixon, G.T., Hammack, J.L., Ash, C.H., Cabri, L.J., Case, G., Connelly, J.N., Heaman, L.M., Laflamme, J.H.G., Nuttall, C., Paterson, W.P.E. and Wong, R.H. (1993): Geology and platinum-group-element mineralization of Alaskan-type ultramafic-mafic complexes in British Columbia; *Geological Survey of British Columbia*, Bulletin 93, 141 pages.
- Nixon, G.T., Cabri, L.J., and Laflamme, J.H.G. (1990): Platinum-group-element mineralisation in lode and placer deposits associated with the Tulameen Alaskan-type complex, British Columbia; *The Canadian Mineralogist*, Volume 28, no 3, pages 503-535.
- Roeder, P.L., and Reynolds, I. (1991): Crystallization of chromite and chromium solubility in basaltic melts; *Journal of Petrology*, Volume 32, no 5, pages 909-934.
- Scoon, R.N. and Mitchell, A.A. (2004): Petrogenesis of discordant magnesian dunite pipes from the central sector of the eastern Bushveld Complex with emphasis on the Winnaarshoek Pipe and disruption of the Merensky Reef; *Economic Geology*, Volume 99, no 3, pages 517-541.
- Sack, R.O. and Ghiorso, M.S. (1991): Chromite as a petrogenetic indicator; *Reviews in Mineralogy*, Volume 25, pages 323-354.
- Wheeler J.O., Brookfield A.J., Gabrielese H., Monger J.W.H., Tipper H.W. and Woodsworth G.J. (1991): Terrane map of the Canadian Cordillera; *Geological Survey of Canada*, Map 1713, scale 1:1,000,000.

Contribution to the Mineralogy of the Arthur Point Rhodonite Deposit, Southwestern British Columbia

By Z.D.Hora¹, A.Langrova² and E.Pivec³

KEYWORDS: *rhodonite, sedimentary manganese minerals, chert, braunite, pyroxmangite, metamorphism, replacement mineralization*

INTRODUCTION

The Arthur Point rhodonite deposit near Bella Coola has been known since 1982, when discovered by the prospector Tony Karup. The property was later described by Hancock (1992). This paper expands upon the information presented in Hancock's description.

Rhodonite is exposed on the shoreline of a small peninsula in two outcrops some 200 m apart, separated by 150 m of heavy vegetation cover.

The rhodonite occurs as stratabound zones within a unit of chert and argillaceous chert several hundred metres thick. While most of the rhodonite outcrop exhibits massive, fine-grained banding in a yellow-green chert, locally along the footwall of the main zone there is a lenticular band, up to 10 cm thick, containing irregular lenses and bands of a metallic-looking mineral, mostly surrounded by pink-coloured rims of manganese silicates (Fig. 1).

ANALYTICAL PROCEDURES

Mineralogy was investigated using optical microscopy, X-ray powder diffractometry and electron microprobe techniques at the Institute of Geology Academy of Science of the Czech Republic in Prague.

Mineral analyses were made with a CAMECA SX-100 electron microprobe using the wavelength dispersive technique. The beam diameter was 10 μ m with an accelerating potential of 15 kV; a beam current of 20 nA was measured on a Faraday cup. A counting time of 10 s was used for all elements. The standards employed were synthetic SiO₂, TiO₂, Al₂O₃, Fe₂O₃ and MgO, and natural jadeite, leucite, apatite, diopside, spinel (all K) and barite (L). The data were reduced using the X-PHI correction. Total Mn and Fe



Figure 1. Sample of chert with braunite lenses and rhodonite-pyroxmangite rims.

are given as MnO and FeO (Table 1), although small amounts of Mn₂O₃ and Fe₂O₃ cannot be excluded.

Mineral phases were also identified by X-ray diffraction, using a Phillips X'Pert APD (automatic powder diffractometer), employing CuK α radiation and graphite monochromator. The following conditions were employed: scanning speed 1 $^{\circ}$ /min, generator voltage 40 kV and current 40 mA.

¹ British Columbia Geological Survey (retired)

² Geological Institute, Academy of Sciences of the Czech Republic, Prague, Czech Republic

³ Geological Institute, Academy of Sciences of the Czech Republic, Prague, Czech Republic (retired)

TABLE 1. REPRESENTATIVE ANALYSIS OF MINERALS FROM THE ZONE RIMMING BRAUNITE LENSES IN
CHERT, ARTHUR POINT, BRITISH COLUMBIA.

	Braunite			Rhodonite				Pyroxmangite				K-feldspar				Albite
	6	19	18	11	5	12	26	8	4	13	15	9	16	22	17	21
SiO ₂	10.45	10.30	10.12	46.30	46.46	45.97	46.39	48.47	49.48	48.79	49.44	64.12	64.38	63.05	64.67	68.66
TiO ₂	0.04	0.04	0.17	0.02	0.00	0.00	0.00	0.00	0.01	0.00	0.00	0.00	0.00	0.00	0.01	0.01
Al ₂ O ₃	0.00	0.01	0.02	0.00	0.00	0.00	0.00	0.00	0.02	0.00	0.02	18.33	18.27	18.43	18.36	19.68
Cr ₂ O ₃	0.00	0.00	0.00	0.00	0.00	0.00	0.00	0.00	0.00	0.00	0.00	0.00	0.00	0.03	0.05	0.00
V ₂ O ₃					0.00	0.00		0.00	0.01			0.01				
FeO	0.03	1.21	1.05	0.02	0.00	0.00	0.00	0.00	0.00	0.08	0.09	0.09	0.04	0.00	0.00	0.03
MgO	0.01	0.00	0.00	0.15	0.29	0.15	0.07	0.38	0.58	0.34	0.13	0.00	0.01	0.00	0.00	0.01
MnO	82.07	78.12	79.22	49.72	48.42	49.79	50.84	45.75	45.22	45.63	45.36	1.08	0.87	0.69	0.63	0.19
CaO	0.05	0.20	0.89	3.39	5.04	3.78	3.77	0.96	1.37	0.97	0.82	0.02	0.00	0.00	0.00	0.00
ZnO	0.00	0.00	0.04	0.00			0.06			0.01	0.04		0.01	0.00	0.07	0.00
BaO	0.00	0.00	0.00	0.00	0.00	0.00	0.00	0.05	0.00	0.00	0.02	0.57	0.33	1.57	0.15	0.03
Na ₂ O	0.01	0.01	0.00	0.00	0.03	0.01	0.04	0.95	1.01	0.93	0.97	0.48	0.54	0.52	0.49	11.42
K ₂ O	0.00	0.01	0.00	0.00	0.00	0.01	0.00	0.00	0.00	0.00	0.00	16.14	15.96	15.60	15.89	0.16
Rb ₂ O	0.04	0.00	0.00	0.00			0.01	0.00		0.00	0.00		0.02	0.08	0.00	0.00
Total	92.70	89.90	91.50	99.59	100.29	99.71	101.20	96.56	97.68	96.75	96.88	100.84	100.42	99.97	100.33	100.84

Sample descriptions: 6, solid lens; 19, grain in chert; 18, grain in pyroxmangite; 11, rhodonite from the contact with braunite; 5, rhodonite in chert; 12, rhodonite from small veins in braunite; 26, continuous zone on the contact with braunite; 8, prevailing pyroxmangite from the rim between chert and braunite; 4, pyroxmangite grains from the chert; 13, pyroxmangite from the small veins in braunite; 15, zone of pyroxmangite without rhodonite; 9, K-feldspar in braunite; 16, K-feldspar in pyroxmangite; 22, K-feldspar in rhodonite; 17, K-feldspar in chert; 21, albite in chert together with K-feldspar

SAMPLE DESCRIPTION

The studied sample is a banded metasediment consisting of parallel lenticular bands of dark grey chert up to 1 cm thick. It contains lens-shaped layers of a metallic-looking, dark steel grey mineral up to 5 mm thick. This mineral was identified as braunite (Fig. 1).

Such lenses frequently have pink rims, which were found to be a mixture of rhodonite and pyroxmangite. Locally, these pink bands form independent layers in the chert as well as crosscutting veinlets. In rare cases, the braunite lenses are observed in direct contact with chert.

The rock structure indicates a ductile deformation, during which the braunite lenses behaved as plastic bodies, but occasionally they crosscut the linear texture of cherty layers.

During later brittle deformation, fracture and foliation planes were filled with Mn silicates.

Crosscutting relationships, observed with the aid of a microscope, indicate that braunite and chert are older constituents while the pink Mn silicates result from a younger replacement process.

CHERT

Dark grey to black, thinly laminated siliceous rock is composed of isometric, xenomorph grains of quartz up to 160 μm in diameter. The rounded shapes indicate that this rock may consist of recrystallized radiolarians (Snyder, 1978). In addition to graphitic particles, the chert contains disseminated xenomorph grains of braunite, in part as interstitial filling and also as inclusions 0.01 to 0.03 μm in size. These particles give the chert an overall grey appearance,

while local accumulations in the form of smears enhance parallel structure (Fig. 6, 7).

Quartz represents 70 to 80% of the chert. Other minerals in the chert are K-feldspar, possibly in two generations, with the dominant one having higher Ba content (>1%). Also identified was relatively high purity, well-crystallized albite. The size of feldspar grains is similar to that of the surrounding quartz grains (Fig. 12, 13).

Under the microscope, the chert seems to be intensively replaced by rhodonite and pyroxmangite. This process took place after the recrystallization of silica and after the braunite was deformed jointly with quartz and feldspars. As a curiosity, one tiny grain of Ca antimonate with a composition similar to romeite (Ca, Fe, Mn, Na)₂(Sb, Ti)₂O₆(O, OH, F) was observed in the chert silica. Due to its small size, and the quality of the polish, the incomplete microprobe analysis gave following results: 4.78% SiO₂, 15.32% CaO, 2.29% Na₂O, 6.04% MnO and ~60% Sb₂O₅.

BRAUNITE

Braunite is not known from recently forming submarine Mn minerals, which could be considered as a similar protolith to the Arthur Point occurrence. These are usually poorly crystalline oxide phases such as todorokite and birnessite (Crerar *et al.*, 1982). Studies of Mn deposits in Japan by Choi and Hariya (1992) showed that braunite may form as a result of postdepositional reactions between primary Mn compounds and hydrothermal or biogenic silica. These reactions probably take place during diagenesis and/or low-temperature and high-pressure metamorphism.



Figure 2. Photomicrograph (25x) of braunite lens with Mn-silicate rim in chert.

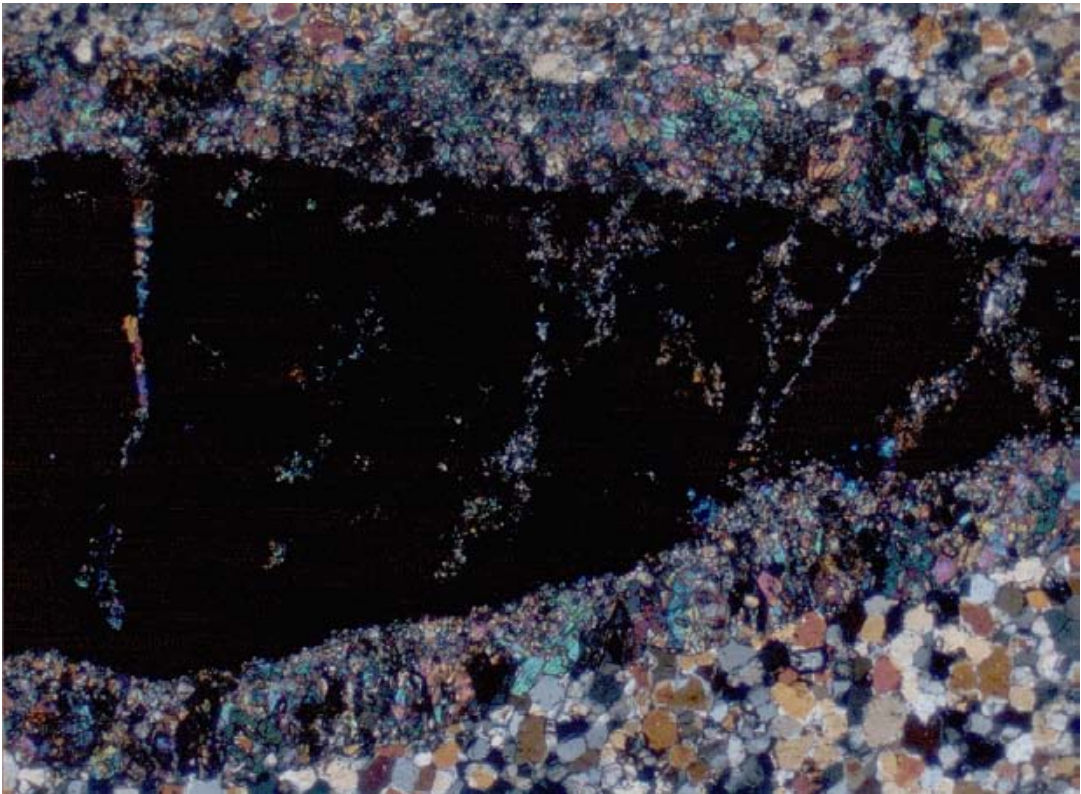


Figure 3. Same view as in Figure 2, in polarized light.

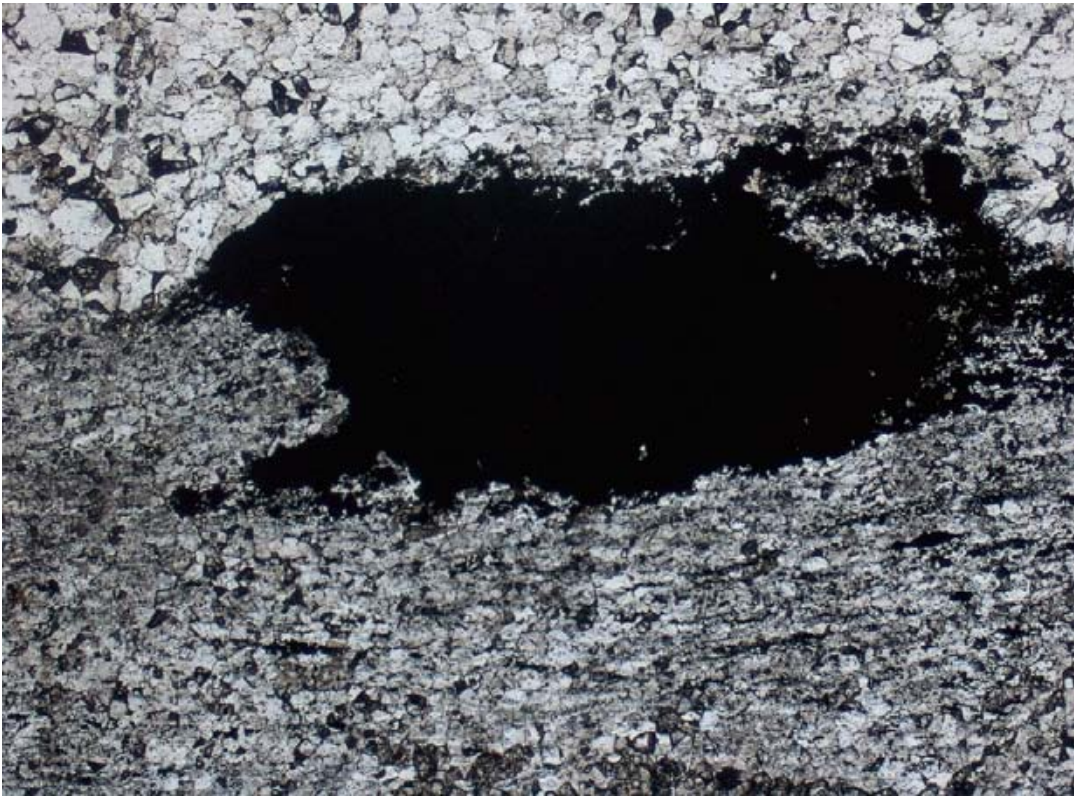


Figure 4. Photomicrograph (25x) of braunite lens in contact with chert on upper rim and with Mn-silicate on bottom rim.

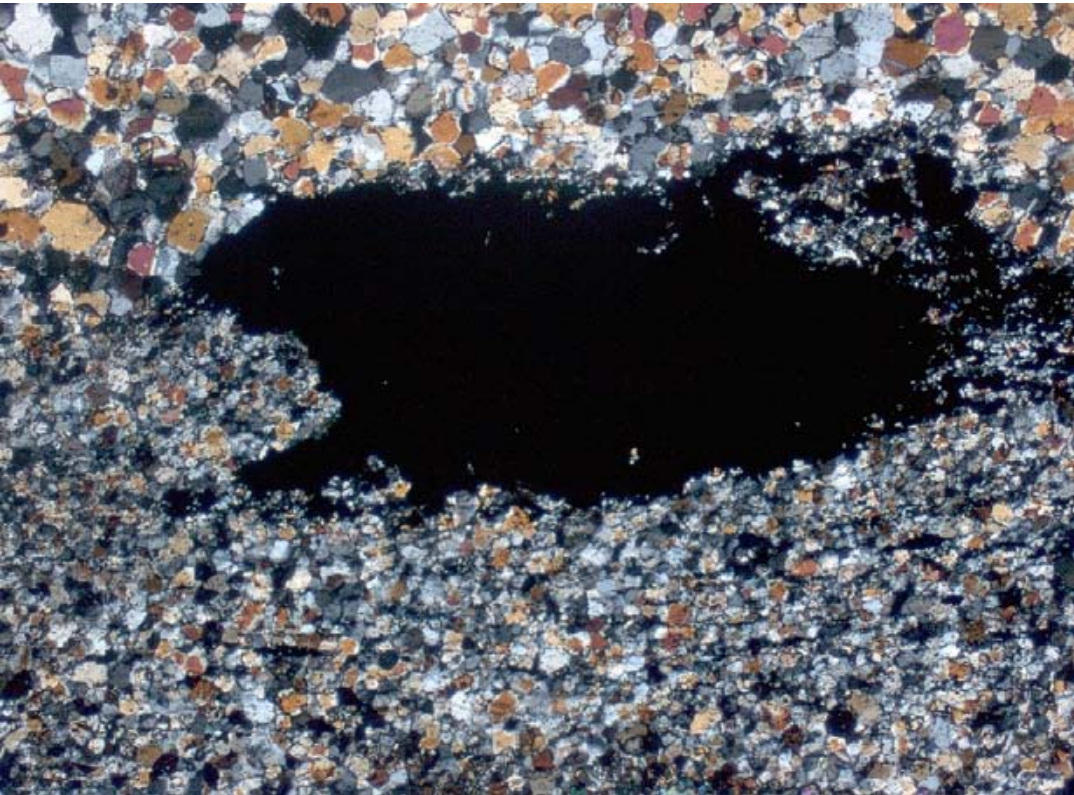


Figure 5. Same view as in Figure 4, in polarized light.



Figure 6. Photomicrograph (25x) of chert with disseminated braunite.



Figure 7. Same view as in Figure 6, in polarized light



Figure 8. Photomicrograph (100x) of chert with disseminated braunite.

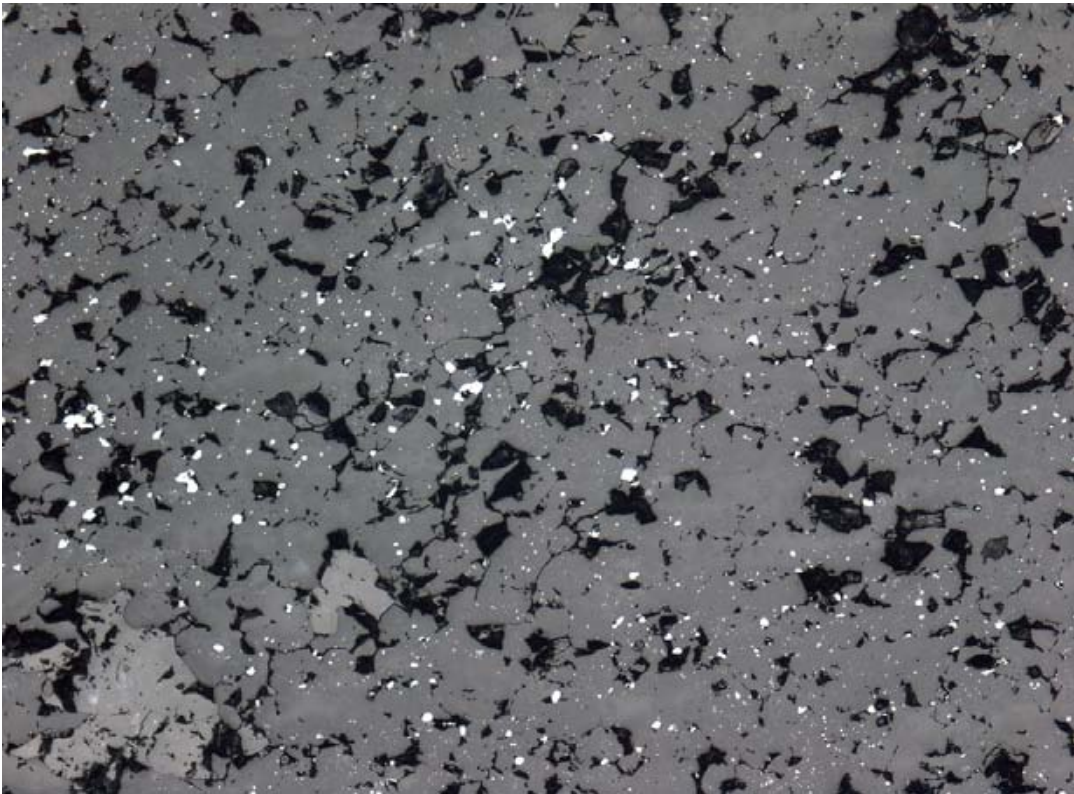


Figure 9. Same view as in Figure 8, in reflected light.

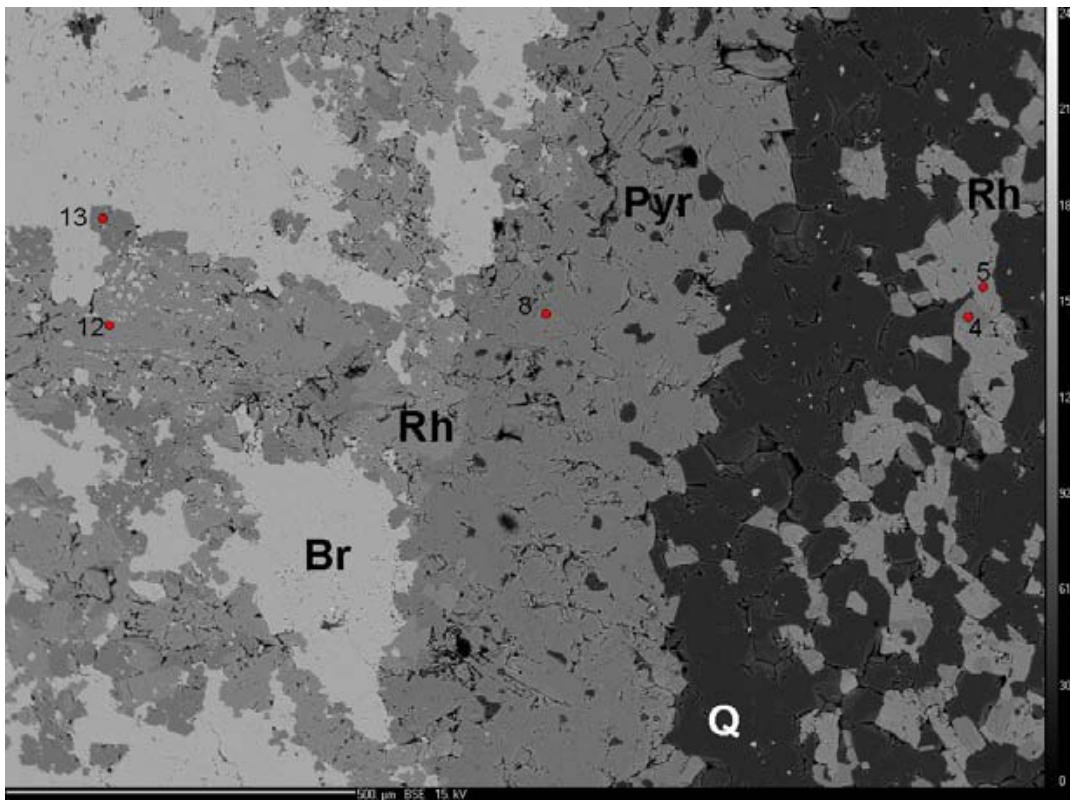


Figure 10. Location of microprobe tests 4, 5, 8, 12 and 13.

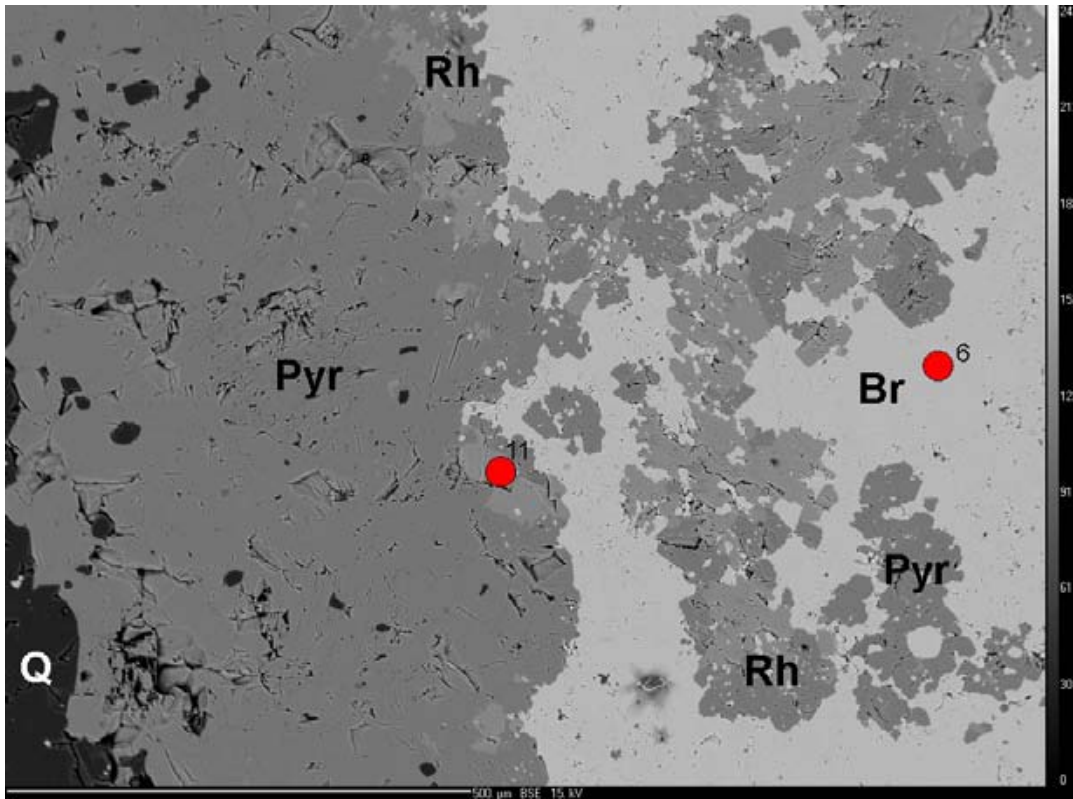


Figure 11. Location of microprobe tests 6 and 11.

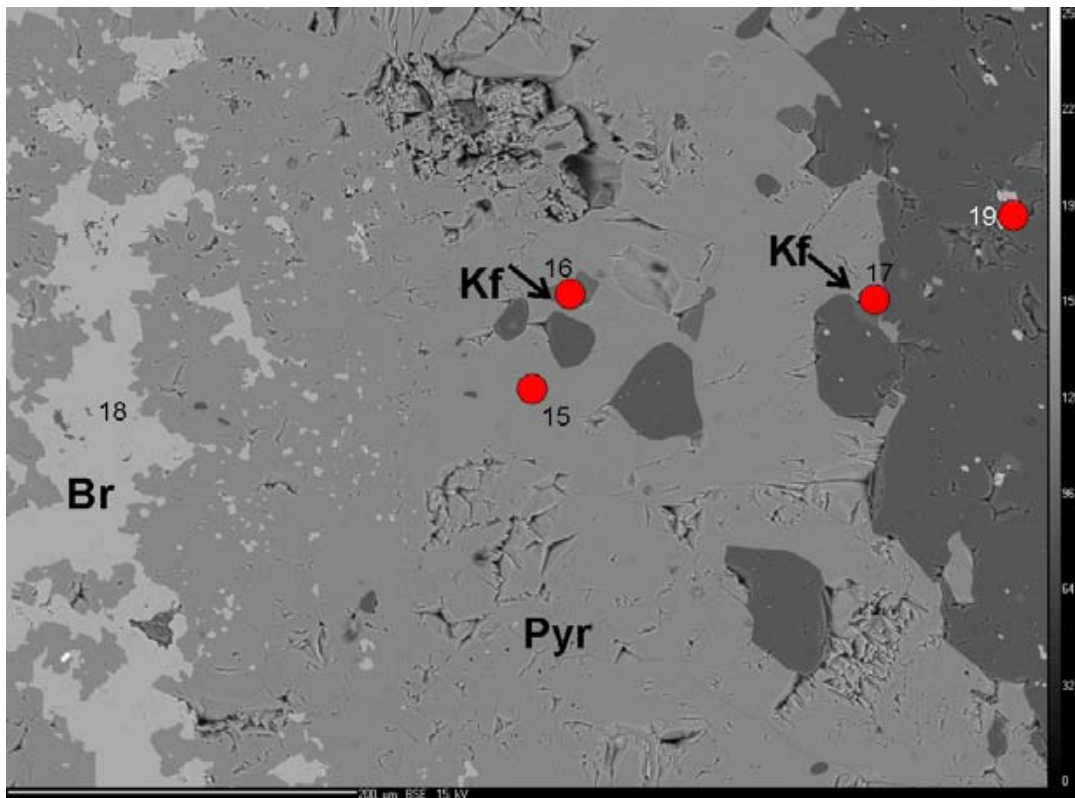


Figure 12. Location of microprobe tests 15, 16, 17, 18 and 19.

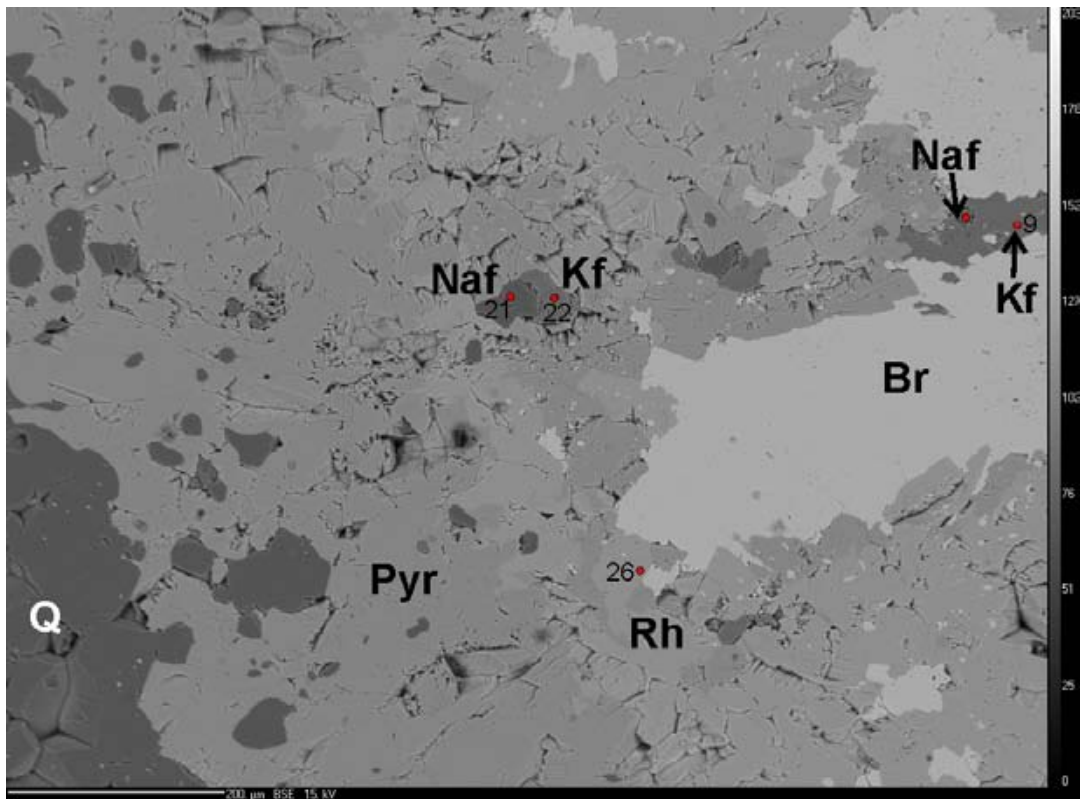


Figure 13. Location of microprobe tests 9, 21, 22 and 26.

The Arthur Point braunite was identified using the combination of reflex and transmission microscopy, XRD and electron microprobe.

In most natural occurrences, braunite contains approximately 10% SiO₂, while synthetically by substituting Si⁺⁴ for Mn⁺⁴ it can accommodate up to 40% SiO₂ without the lattice constants changing (Huebner, 1967). Our tested sample corresponds to the formula 3Mn₂O₃·MnSiO₃, but this may also be written (Mn,Si)₂O₃.

The Arthur Point samples contain both small lenses of massive braunite and disseminated grains within the chert matrix (Fig. 3, 5, 9). Lenses are usually 30 to 50 mm in length and 3 to 5 mm thick. Later fractures were filled with veinlets of rhodonite and pyroxmangite (Fig. 2, 3). Such veinlets are up to 0.01 mm thick and sometimes contain remobilized braunite.

Based on our study, the oldest minerals at Arthur Point site are braunite and quartz. The composition of earlier phases of the Arthur Point sedimentary sequence cannot be established.

RHODONITE AND PYROXMANGITE

Pinkish coloured lenses, bands and braunite rims within the Arthur Point deposit are not a single mineral. By using a combination of optical and XRD analysis combined with local microprobe analysis, they were identified as a mixture of rhodonite and pyroxmangite.

As is mentioned in Simandl and Church (1996), these two minerals are difficult to distinguish from each other. Considering the optical properties, pyroxmangite exhibits higher birefringence and a smaller angle of optical axis than rhodonite. However, since the size of isometrical grains in the samples is under 40 μm, the difference is so small that the two minerals are optically indistinguishable. Nevertheless, under the electron microprobe, the two minerals exhibit different backscattered electron images (Fig. 10, 11). Also, the interpretation of XRD diagrams confirmed the presence of both minerals. In relationship to braunite lenses, both minerals are younger and form rims to, and fill the fractures within, the braunite lenses (Fig. 2, 3). Rhodonite is dominant and pyroxmangite appears younger in direct contact with massive braunite (Fig. 10, 11).

In chemical composition, the rhodonite is lower in SiO₂ and higher in MnO and CaO compared to pyroxmangite. The Mn content of rhodonite decreases with distance from massive braunite lenses. It appears that the Mn in these rims results from a younger process of hydrothermal replacement. Pyroxmangite replaces rhodonite and its Mn content is independent of where it occurs. The origin of pyroxmangite may be explained by the increase in P-T conditions during the replacement process (Candia *et al.*, 1975).

Microprobe tests on rhodonite from Arthur Point by the British Museum (Natural History) reported MnO content between 42.1 and 48.0% (Hancock, 1992). Since the higher end corresponds to pyroxmangite, it is conceivable that this mineral has escaped attention and its presence in the deposit is more widespread than previously expected.

SUMMARY

In conclusion, our study led us to believe that the Arthur Point deposit exhibits two separate metamorphic processes. The first, probably a high-pressure – low-temperature process, converted the original sea bottom sedimentary protolith into a braunite-chert assemblage. The second mobilized some manganese and silica and resulted in the formation of Mn silicates, at least in part at the expense of original product. This second phase could be the one described by Hancock (1992) as being between 400 and 500 °C with a pressure range of 500 to 2000 bars.

Also, the so-called deposits of ‘rhodonite’ in British Columbia (Leaming, 1966) are most probably mineralogically more diverse than originally thought.

ACKNOWLEDGMENTS

The authors wish to thank A. Karup and F. Ayers for many samples from the deposit and for copies of their correspondence with the British Museum (Natural History). J. Pavkova and Z. Korbelova provided technical help; J. Brozek and V. Srein helped with photodocumentation; and J. Dobrovolny helped with X-ray records. Constructive comments and editorial improvements were provided by B. Grant and M. Mihalynuk.

REFERENCES

- Candia, M.A.F., Peters, T. and Valarelli, J.V. (1975): The experimental investigation of the reactions MnCO₃+SiO₂ = MnSiO₃+CO₂ and MnSiO₃+MnCO₃ = Mn₂SiO₄+CO₂ in CO₂/H₂O gas mixtures at a total pressure of 500 bars; *Contributions to Mineralogy and Petrology*, Volume 52, pages 261–266.
- Choi, J.H. and Hariya, Y. (1992): Geochemistry and depositional environment of Mn oxide deposits in the Tokoro Belt, northeastern Hokkaido, Japan; *Economic Geology*, Volume 87, pages 1265–1274.
- Crerar, D.A., Namson, J., Chyi, M.S., Williams, L. and Feigenson, M.D. (1982): Manganiferous cherts of the Franciscan Assemblage: I. general geology, ancient and modern analogues, and implications for hydrothermal convection at oceanic spreading centers; *Economic Geology*, Volume 72, pages 519–540.
- Hancock, K.D. (1992): Arthur Point (Sea Rose) rhodonite; in *Exploration in British Columbia 1991, BC Ministry of Energy, Mines and Petroleum Resources*, pages 89–98.
- Huebner, J.S. (1967): Stability relations of minerals in the system Mn-Si-C-O; unpublished Ph.D. thesis, *John Hopkins University*, 279 pages.
- Leaming, S.F. (1966): Rhodonite in British Columbia; *The Canadian Rockhound*, February 1966, pages 5–11.
- Roy, S. (1968): Mineralogy of the different genetic types of manganese deposits; *Economic Geology*, Volume 63, pages 760–786.
- Simandl, G.J. and Church, B.N. (1996): Clearcut pyroxmangite/rhodonite occurrence, Greenwood area, southern British Columbia (82/E2); in *Geological Fieldwork 1995, BC Ministry of Energy, Mines and Petroleum Resources*, Paper 1996-1, pages 219–222.

Snyder, W.S. (1978): Manganese deposited by submarine hot springs in chert-greenstone complexes, western United States; *Geology*, Volume 6, pages 741–744.

Towards a British Columbia Rock Geochemical Atlas

By Ray Lett¹ and Christine Ronning²

KEYWORDS: British Columbia Geological Survey, bedrock geochemistry, lithochemochemistry, analytical methods, database, atlas

INTRODUCTION

Past release of geoscience data by the Geological Survey Branch (GSB) from mapping, mineral deposits studies and geochemical surveys have stimulated exploration activity in British Columbia. Bedrock geochemistry, in particular, is an important tool for identifying rock samples that could enhance the minerals potential of an area. For example, those with anomalous metal contents are commonly close to mineralization whereas samples depleted in elements can indicate hydrothermal alteration. Point bedrock geochemical anomalies commonly indicate a local mineralized source whereas regional trends confirm the extension of favourable host rock for a particular style of mineralization from map sheet to map sheet. Other applications of lithochemochemical data are for interpreting bedrock geology and the results of stream geochemical surveys.

British Columbia Geological Survey geoscientists have generated a large volume of lithochemochemical and mineral identification data from the analysis of rock samples and minerals collected throughout the province over the past 20 years. While much of this information has been reported in BC Ministry of Energy and Mines publications, these analyses have never been collected into a single database. This paper describes the development of a database intended to capture the rock geochemical information and create a lithochemochemical atlas for the Province. Other Canadian geological surveys such as Ontario, Newfoundland and Saskatchewan have lithochemochemical databases (Adcock *et al.*, 1994, Saunders, 1996) and there is also a Canadian Geosciences Knowledge Network (CGKN) initiative for establishing a Canadian network of geoscience databases that would include lithochemochemical information (Adcock *et al.*, 2003).

¹ British Columbia Ministry of Energy and Mines, PO Box 9333 Stn. Prov. Govt., Victoria, BC, V8W 9N3

² Department of Geography, University of Victoria, PO Box 1700 STN CSC, Victoria, BC, V8W 2Y2

DATABASE DESIGN

One of the complexities in creating a database for geochemical data collected over a long time period is that the information will invariably be produced by a variety of analytical techniques, sample preparation methods and may also come from several, different laboratories. The structure must therefore be able to relate these variables to the results in the database so that extracted information is consistent with a particular method and/or source. The GSB lithochemochemical database is designed to recognize the multiple analytical methods and data sources used to generate the information over a period of 20 years by creating a number of related Microsoft Access™ tables. The structure is shown in Figure 1. Typically, a primary key that is a unique number assigned to every sample analyzed through the GSB laboratory links the tables. The two key database tables are

- **Master Data Table:** This is the main table representing the hub of most of the relationships and containing such key fields such as *Lab ID*, *Field ID*, *Batch ID*, *Rock Type*, *Latitude* and *Longitude*. The Master data table contains all of the records in the database, sample collector, the rock type, sample location coordinates and the NTS map sheet. *Lab ID* is the primary database key. *Field ID* is the identification number assigned to the sample by the collector whereas *Batch ID* is number given by the GSB laboratory to a batch of samples submitted for analysis.
- **Analysis:** This table contains direct analytical data or is linked to tables with information about the identity of the elements determined, the method used, and the laboratory responsible for producing the results.

Other database tables include *Analysis_Code*, *Analysis_Code_Metadata* (a more detailed description of method), *Prep_Code* (e.g., sample milling by either tungsten carbide or steel swing mill), *Geologists_Code* (geoscientist responsible for submitting the sample) and *Interference* (inter-element analytical interference). *Analysis_Code* identifies 23 methods (Table 1) that have been used to analyse rock samples since 1985.

There are twelve tables for raw data in which elements are grouped according a commonality of methods used for analysis. For example, *Values_oxide*

TABLE 1. ANALYTICAL METHODS IDENTIFIED IN THE ANALYSIS_CODE DATABASE TABLE

Method Code	Method Summary
_XRF1	x-ray fluorescence - fused disc
_XRF2	x-ray fluorescence - pressed pellet
_AAS	Aqua Regia-Flame atomic absorption spectrometry
_CAA	Cold vapour - atomic absorption spectrometry
_FAA	Lead fire assay_atomic absorption finish/ICP
_FAG	Lead fire assay graphite furnace atomic absorption finish
_FAM	Lead fire assay_atomic absorption finish/ICPM
_GRAV	Gravimetric determination
_HAA	Hydride generation atomic absorption spectrometry (HAAS)
_ICP	Aqua regia digestion-Inductively Coupled Emission Spectrometry (ICP/ES)
_ICPM	Mixed acid (HF) digestion (ICP/ES)
_LE	Leco combustion
_LIC	Lithium metaborate fusion-Inductively Coupled Emission Spectrometry (ICP/ES)
_LICM	Lithium metaborate fusion-Inductively Coupled Mass Spectrometry (ICP/MS)
_MAA	Mixed acid (HF) digestion-Flame atomic absorption spectrometry (FAAS)
_MS	Aqua regia digestion -Inductively Coupled Mass Spectrometry (ICP/MS)
_MSM	Mixed acid (HF) digestion (ICP/MS)
_NA	Instrumental neutron activation (INAA)
_NFNA	Nickel sulphide fire assay_neutron activation finish
_PMS	Peroxide fusion_Inductively Coupled Mass Spectrometry (ICP/MS)
_SE	Ion selective electrode
_SPEC	Spark emission spectroscopy
_TI	Titration

contains a combination of major oxides, loss on ignition, carbon and sulphur results. Values_minor indicates a suite of elements determined by x-ray fluorescence rather than the more conventional term for a geochemical element association or a concentration range (e.g., minor elements).

Some of the tables have an element suite where multi-element results were produced by a single technique such as instrumental neutron activation analysis (Values_INA) or rare earth elements by a sodium peroxide sinter and inductively coupled plasma mass spectrometry (Values_REE). In other tables, the elements are grouped according to when the analysis was completed because methodologies changed over time. For example, to accommodate older (pre 1990) results there

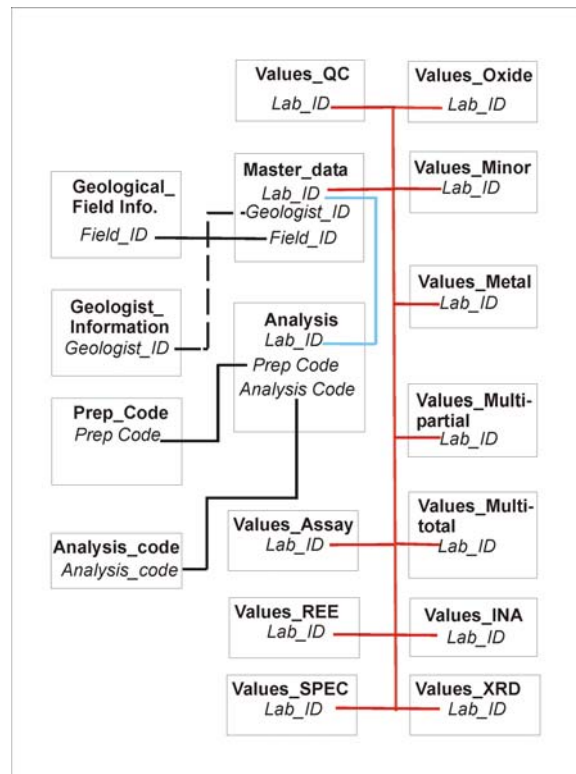


Figure 1. Lithochemical database structure. Some of the tables have been omitted.

are tables for metals measured by hydrofluoric acid digestion-atomic absorption spectrophotometry (Values_Metal), Spark Emission Spectroscopy (Values_Spec) and for minerals identified by x-ray Diffraction (Values_XRD). The Values_Spec and Values_XRD tables have qualitative rather than quantitative information.

For more recent (post 1990) results tables have been created (e.g., Multi_Partial, Multi_Total) because element analyses were more commonly generated by multi-element methods such as inductively coupled plasma emission spectrometry and inductively coupled plasma mass spectrometry. The sample decomposition method is also indicated in these tables by the modifier Multi_total (lithium metaborate fusion) or Multi_partial (acid digestion). Results of standard and replicate sample analyses are collected in the Values_QC table. Extraction of specific data (e.g., results for 1995 samples analyzed by a combination of lead fire assay and neutron activation) from the database is accomplished using Microsoft Access™ filters and queries.

INFORMATION SOURCES

The database is currently being populated primarily with data from Geological Survey Branch files and re-

ports. More specifically, the sources of information are

- Digital dBASE format reports downloaded from the Geological Survey Branch laboratory information tracking system implemented in 1985.
- Scanned copies of analytical reports in the laboratory archives and tables and appendices in Ministry of Energy and Mines Papers, Open Files and Bulletins.
- Digital copies of final analytical reports submitted by the laboratory to Geological Survey Branch geoscientists.

In December 2004, the database had 18,590 sample records although of these only an estimated 10,000 have location coordinates. The distribution of these samples is shown in Figure 2. The database will be updated with information from future Geological Survey Branch projects and for other sources such as Ministry of Energy and Mines assessment reports.

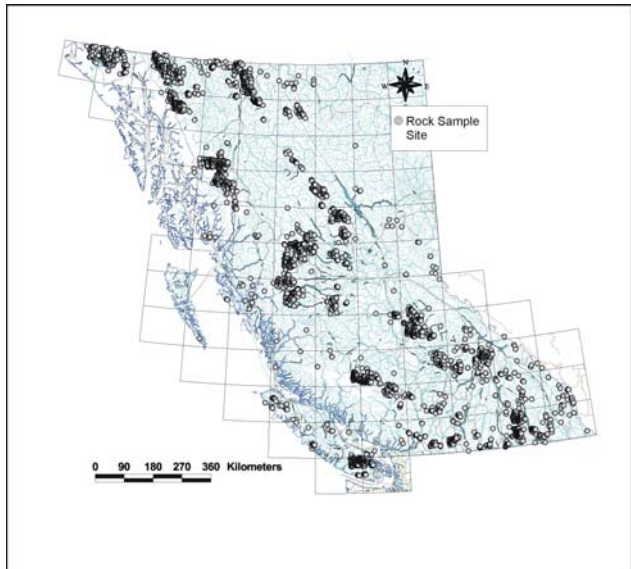


Figure 2. Geological Survey Branch rock samples with locations and lithochemical data.

CONCLUSIONS

A Microsoft Access™ database containing almost 19,000 analytical and mineral identification records from rock samples collected by the British Columbia Ministry of Energy and Mines is in the process of completion. Rapid and simple access to rock geochemical data at this broad scale will encourage mining companies to apply new exploration concepts for evaluating larger areas of British Columbia. The database will be produced as a CD version and also as an atlas of element maps showing as themes on the Geological Survey Map Place portal allowing the lithochemical analyses to be viewed on a province-wide scale.

ACKNOWLEDGMENTS

The authors appreciate helpful comments from Stephen Adcock and Eric Grunsky, Geological Survey of Canada during early stages of the database design. Brian Grant is thanked for encouraging this project and for his editorial advice on the text of this paper.

REFERENCES

- Adcock, S.W., Grunsky, E., Laframboise, P. and Sirito, W.A. (2003): Association of Mathematical Geology Conference, Portsmouth, United Kingdom, September 7th to 12th, 2003, Abstract.
- Adcock, S.W., Dunn, C.E. and Sirito, W.A. (1994): Lithochemical database of Cretaceous Strata in Central Saskatchewan; *Government of Saskatchewan Open File OF 2491*, 222 pages.
- Saunders, C. (1996): Volcanic Rock Geochemical Database - Version 2.0; *Newfoundland Department of Natural Resources*, Report 96-1, pages 175-180.

Alkalic Cu-Au Deposits of British Columbia: Sulfur Isotope Zonation as a Guide to Mineral Exploration

By C.L. Deyell^{1,2} and R.M. Tosdal¹

KEYWORDS: alkalic porphyry, sulfur isotopes, Lorraine, Mt Polley, Red Chris, Afton, Galore Creek.

INTRODUCTION

Cu-Au porphyry deposits associated with alkalic igneous rocks are known in only a few mineral provinces worldwide and some of the best-known examples are from British Columbia (*e.g.*, Galore Creek, Mt Polley, Afton/Ajax, Copper Mountain). The Lachlan Fold Belt of New South Wales (Australia), the other major alkalic porphyry province (*e.g.*, Cadia, Goonumbla), and other isolated alkalic systems are known from the Philippines (Dinkidi), Greece (Skouries) and Colorado (Allard Stock).

Alkalic porphyry deposits are of economic significance and represent some of the world's highest grade porphyry gold resources (*e.g.*, Ridgeway: 53 Mt @ 2.5 g/t Au, 0.77% Cu or 4.26 Moz Au; Cadia Far East: 290 Mt @ 0.98 g/t Au, 0.36% Cu or 9.13 Moz Au). In British Columbia, the alkalic porphyry systems at Copper Mountain, Mount Milligan and Galore Creek have a combined resource of over 900 Mt (Lang *et al.*, 1995). New exploration at Afton, Galore Creek and Lorraine has added significant resources.

Alkalic porphyry deposits present difficult exploration targets for several reasons. The high-grade metal concentrations are typically associated with small volume pipe-like intrusions that may have areal extents of only a few hundred square metres (Wilson *et al.*, 2002). The alkalic systems also have no associated advanced argillic alteration assemblages, and phyllic alteration is late and typically restricted to fault zones. Supergene enrichment is poorly developed due to the low pyrite contents of the hypogene alteration assemblages (Cooke *et al.*, 2002). Furthermore, the lack of extensive peripheral hypogene alteration hinders identifying the focus for fluid flow more than several hundred metres away from the mineralized porphyry centre. Effective exploration therefore requires tools to

recognize subtle or cryptic alteration zones or geochemical dispersion halos that highlight proximity to a mineralized intrusive centre. The focus of this study is the application of sulfur isotope analyzes to alkalic Cu-Au systems in British Columbia to test whether this technique can aid in the exploration of porphyry-style mineralization in this region.

BACKGROUND

Initial research in alkalic porphyry deposits of Australia and the Philippines has suggested that systematic vertical and lateral sulfur isotopic zonation surrounds several mineralized porphyry complexes (*e.g.*, Goonumbla and Cada, NSW; Lickfold, 2001; Wilson, 2003; Didipio, Philippines; Wolfe, 2001). Data collected by the Centre for Ore Deposit Research (CODES) at the University of Tasmania indicates sulfide compositions in these systems range from -2 to -10‰. The most negative values typically occur towards the top of the mineralized monzonite pipes, with a return to near-zero values with distance upward and/or outwards from the pipe. Several enigmatic sulfide compositions between -16 and -19‰ have been detected in the core of the Goonumbla quartz monzonite porphyries at depths of 1 km below the surface (Lickfold, 2001). These low values cannot be explained by contamination by biogenic sulfur, as has been argued for the Galore Creek deposit, British Columbia (Shannon *et al.*, 1983), since the Goonumbla sulfides occur in the core of an intrusive complex hosted by a near-coeval volcanic sequence.

The initial studies described above led to the obvious question of whether sulfur isotopes can provide a "magic-bullet" for exploration and a means to vector toward sulfide when faced with chloritic and propylitically altered rocks that are distal to the ore. Despite the suggestive evidence, the temporal controls on the isotopic zonation have not been tested adequately in either the Australian examples or elsewhere in the world. The trend towards negative sulfur isotopic compositions of sulfide minerals upwards through the monzonite bodies is thought to relate at least in part to sulfide deposition from an oxidized (sulfate predominant) fluid. Whether this mechanism in

¹ CODES, University of Tasmania, Hobart, Tasmania, Australia

² MDRU, University of British Columbia, Vancouver, BC

conjunction with cooling can account for the isotope systematics of alkalic porphyry deposits remains to be tested. It is furthermore still unclear what causes the zonation. It is possible that mixing of two sulfur sources may have occurred, and/or that wall rock buffering of redox conditions may have been influential in controlling the observed sulfur isotope zonation (D. Cooke, pers comm, 2004). Regardless, the zonation has been shown to be a robust, predictable phenomenon, and at least one major exploration company has had success using sulfur isotopes as a vector to delineate new Cu-Au occurrences. However, before sulfur isotope mapping can be applied widely, it must be established whether the zonation is a phenomenon common, or not, to these deposits on a worldwide basis.

THIS STUDY

In contrast to the Australian and Philippine deposits, very little data is currently available regarding the sulfur isotope signature of alkalic systems in British Columbia. The goals of this study are therefore to determine whether systematic sulfur isotopic zonation of sulfide minerals might also characterize alkalic porphyry deposits in this region.

This study has been completed over a two-year period and has been funded through the Rocks to Riches program, managed by the British Columbia and Yukon Chamber of Mines (BCYCM). Preliminary research conducted in the 2003 field season consisted of investigations at several major deposits including Galore Creek, Afton, Red Chris, Mt Polley, and Lorraine (Fig. 1). Initial results uncovered some interesting trends (Deyell *et al.*, 2004). In particular, data for Mt Polley showed a trend of decreasing $\delta^{34}\text{S}_{\text{sulfide}}$ values with increasing Au grades, suggesting redox controls were significant for Au deposition. Similar trends were noted in the Bishop Zone at Lorraine, although samples from the Lower Main Zone in this same deposit appear to have an opposite trend with a positive correlation between Au grade and $\delta^{34}\text{S}_{\text{sulfide}}$ values. As a follow-up, research in the 2004 field season was focused only on the Lorraine and Mt Polley deposits. The aim was to fully test the origin and significance of the zonation and relation to Cu-Au mineralization at specific alkalic porphyry deposits.

In this paper, we report results from the 2003 and 2004 studies, which includes the combined research at Lorraine and Mt Polley as well as a summary of the preliminary investigations at the Red Chris, Galore Creek and Afton deposits. The sulfur isotopic data is only summarized in the chapter; the complete analytical data is available at <http://www.em.gov.bc.ca/Mining/Geosurv/Publications/catalog/catfldwk.htm> or at www.mdru.ubc.ca.



Figure 1. Location map showing the location of selected alkalic porphyry Cu-Au deposits in British Columbia.

METHODS

The 2004 study included ten days of fieldwork at Lorraine and Mt Polley during July and August. This work consisted primarily of core logging and sampling with specific focus on the distribution of sulfide species and sampling over a range of rock types, alteration assemblages, and metal grades. The sulfides were extracted manually using a hand-held drill (Dremel tool). Care was taken to ensure pure mineral separates although in the case of very fine-grained samples and intergrown sulfides, some contamination or mixed sulfide samples could not be avoided.

Sulfur isotopic analyses were completed at the United States Geological Survey (USGS) Isotope Laboratory in Denver (Colorado, USA) and the University of Tasmania Central Science Laboratory in Hobart (Australia). The USGS lab $\delta^{34}\text{S}$ analyses were completed using an on-line method with an elemental analyzer coupled to a Micromass Optima mass spectrometer following the method of Giesemann *et al.* (1994). The University of Tasmania lab uses conventional sulfur isotope techniques according to Robinson and Kusakabe (1975) and measurements are performed on a VG Sira Series II mass spectrometer. Analytical uncertainties for both techniques are estimated at ± 0.1 per mil (‰).

RESULTS

Lorraine

The Lorraine deposit is located in the northern Intermontane Belt approximately 280 km northwest of Prince George (Fig. 1). The bulk of the previously de-

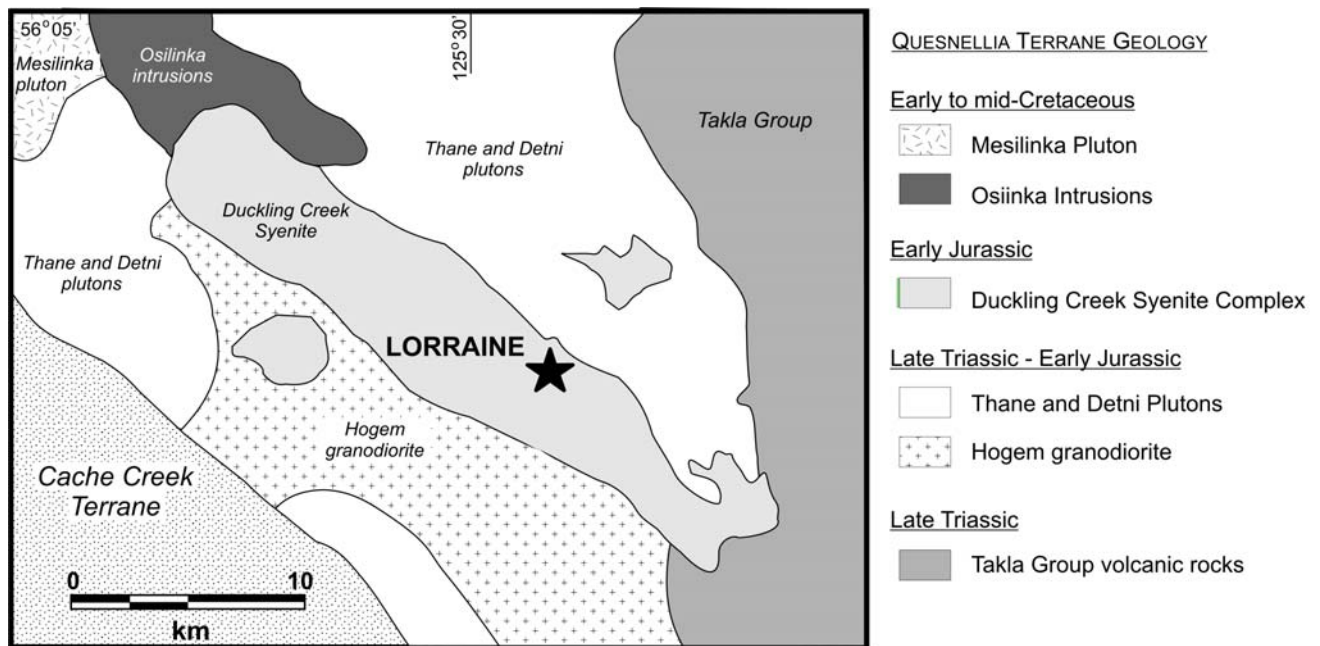


Figure 2. Location and regional geological setting of the Lorraine deposit. Modified from Nixon and Peatfield (2003).

fined resource (32 Mt at 0.66% Cu, 0.25 g/t Au; Morton, 2003) occurs within a roughly circular area comprising the Lower Main, Main and Bishop zones. Several other peripheral mineral occurrences have also been identified (e.g., Copper Peak, All Alone Dome). The property is hosted entirely by the Hogem Batholith, a late Triassic to Middle Jurassic intrusion of calc-alkalic to alkalic composition (Garnett, 1978). All known mineralization is associated with alkalic rocks of the Duckling Creek Syenite Complex (Fig. 2), which is a discrete unit within the composite (182 to 162 Ma) Hogem Batholith (Bishop *et al.*, 1994).

The Duckling Creek Suite forms a northwesterly trending, elongate unit approximately 35 km long and averaging 8 km wide (Morton, 2003). In the Lorraine area, the syenite complex was originally subdivided into a foliated syenite 'migmatite' that enveloped and partially intruded a suite of pyroxenites and monzonitic to dioritic rocks (Garnett, 1978). Younger crosscutting leucocratic syenite and potassium feldspar porphyry dikes and sills are common.

The geology of the Lorraine area was reviewed by Nixon and Peatfield (2003) who made several significant revisions. They subdivided the Duckling Creek Syenite Complex into two distinct intrusive phases (Fig. 3). Phase 1 is an early plutonic suite of feldspathic pyroxenite, mela-syenite and monzonite. Phase 2 is a younger suite of leuco-syenites and potassium feldspar megacrystic porphyries. The 'migmatite' described previously is thought to represent local zones of metasomatic compositional layering and veining in more extensive areas of minor intrusive

activity and potassic alteration (Nixon and Peatfield, 2003).

Alteration related to Cu-Au mineralization at Lorraine has been documented in several studies (Wilkinson *et al.*, 1976; Garnett, 1978; Bishop *et al.*, 1995; Nixon and Peatfield, 2003). This alteration is dominated by alkalic, particularly potassium, metasomatism consisting of an early stage of secondary biotite development and pervasive potassium feldspar deposition that affects all rock units. Local sodium metasomatism is a pervasive replacement of plagioclase by albite and conversion of augite pyroxene to aegirine pyroxene (Morton, 2003). Late-stage weak sericite and propylitic (chlorite-epidote-carbonate) alteration is also recognized (Bishop *et al.*, 1994). Late quartz veins occur locally. An unusual calc-silicate assemblage of diopsidic clinopyroxene, garnet, albite, epidote, biotite and apatite was also recognized in the BM area by Nixon and Peatfield (2003).

TABLE 1. METAL RATIOS* FOR MINERALIZED ZONES AT LORRAINE.

	Au/Cu	Ag/Cu	Ag/Au
Lower Main	28.6	15.1	18.9
Upper Main	0.8	11.4	37.7
Bishop	1.1	32.5	116.1

*based on mean assay results from Eastfield Resources drill programs from 1993 to 2002. Ratios are calculated on the basis of % Cu, g/t Au, g/t Ag. Data below detection assigned values of 50% of detection limit for the purposes of these calculations.

Sulfide minerals are chalcopyrite and bornite with secondary chalcocite, digenite and rare covellite. Pyrite is a minor constituent. The sulfides are fine- to medium-grained disseminations with lesser sulfide-bearing veinlets and fractures fillings (Bishop *et al.*, 1994). No systematic spatial zonation of sulfide mineralogy has been recognized. Average gold (grams per tonne) to copper (weight percent) ratios are much lower than those at other alkalic deposits (*e.g.*, Afton, Copper Mountain, Mt Polley: Stanley, 1993) with values of about 0.8 in the Lower Main zone and 1.1 in the Bishop zone (Table 1). It has been suggested that at least part of the mineralization is magmatic in origin, due to the occurrence of copper sulfides as blebs and “net-textured” semi-massive sulfide in pyroxenite (Bishop *et al.*, 1994; Morton, 2003).

SULFUR ISOTOPE STUDY

Prior to the study in 2003, no sulfur isotope data were available for the Lorraine property. Samples for the 2003 study were selected from skeleton core held by Eastfield Resources in Vancouver. These samples consisted mainly of material from the Lower Main and Bishop zones with a few additional samples from the Upper Main zone and peripheral mineral showings. Reported sulfur isotope data for sulfides ranged from -0.2 to -10.2‰, with average values of -4.1‰ in the Lower Main zone and -2.3‰ in the Bishop zone (Deyell *et al.*, 2004). These data could not be correlated reliably with different rock or alteration types, since only the skeleton core was available at that time. However, the

Phase 1 (pre-mineralization)

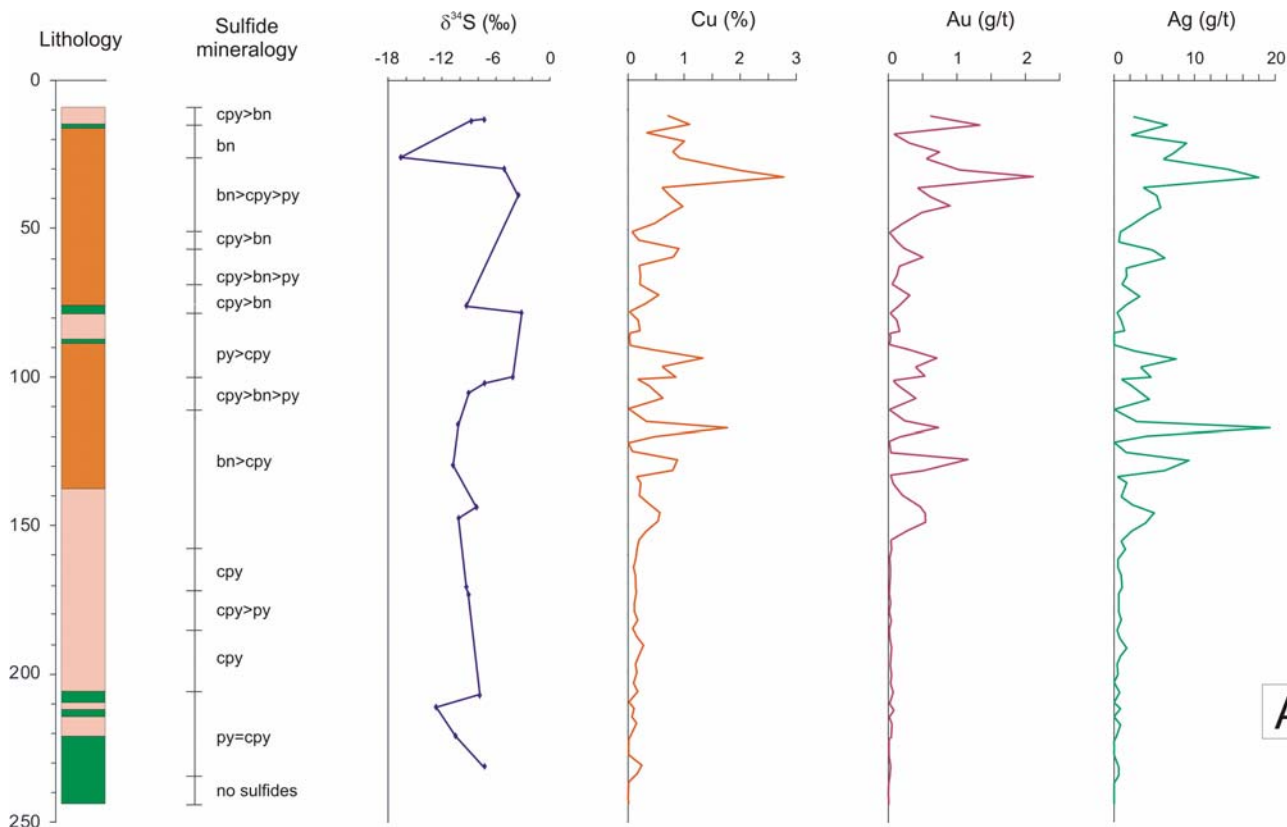
- **Mesocratic monzonite-syenite**
Pinkish grey, medium-grained, roughly equigranular plutonic rocks ranging from monzonitic to syenitic compositions. Distinguished from mela-syenites by lower abundance of mafics (typically 15-20%) consisting of pyroxene, biotite, +/- amphibole.
- **Mela-syenite**
Greenish-grey, medium to coarse-grained, biotite-clinopyroxene Kspar syenite with 25-40% mafics.
- **Feldspathic pyroxenite**
Dark greenish black, medium to coarse-grained biotite clinopyroxene to melanocratic syenodiorite (with variable feldspar component). This unit includes the three varieties described by Nixon and Peatfield (2003); clinopyroxene with interstitial feldspar, oikocrystic pyroxenite, and pyroxenite with large, roughly tabular, Kspar crystals.

Phase 2 (pre- to syn- mineralization)

- **Kspar megacrystic porphyry dykes**
Coarse-grained, grey to white (rarely pale pink) tabular to blocky Kspar crystals with local accessory clinopyroxene and/or magnetite.
- **Quartz vein**
Coarse white quartz vein with chalcopyrite-bornite.
(Not a significant lithological unit, but does occur as a mapable zone in DDH L95-13; Fig. 4).

Figure 3. Summary of major geological units at Lorraine (and legend for lithological drill logs shown in Figure 4). Geological information is summarized from Nixon and Peatfield (2003) with additional observations from this study.

correlation of $\delta^{34}\text{S}_{\text{sulfide}}$ data to metal grades was significantly different for samples from the Lower Main and Bishop zones. The Bishop zone samples have a strong correlation between decreasing $\delta^{34}\text{S}$ values and Au grade, but nearly an opposite, although less well defined, trend was suggested for samples from the Lower Main zone.



A

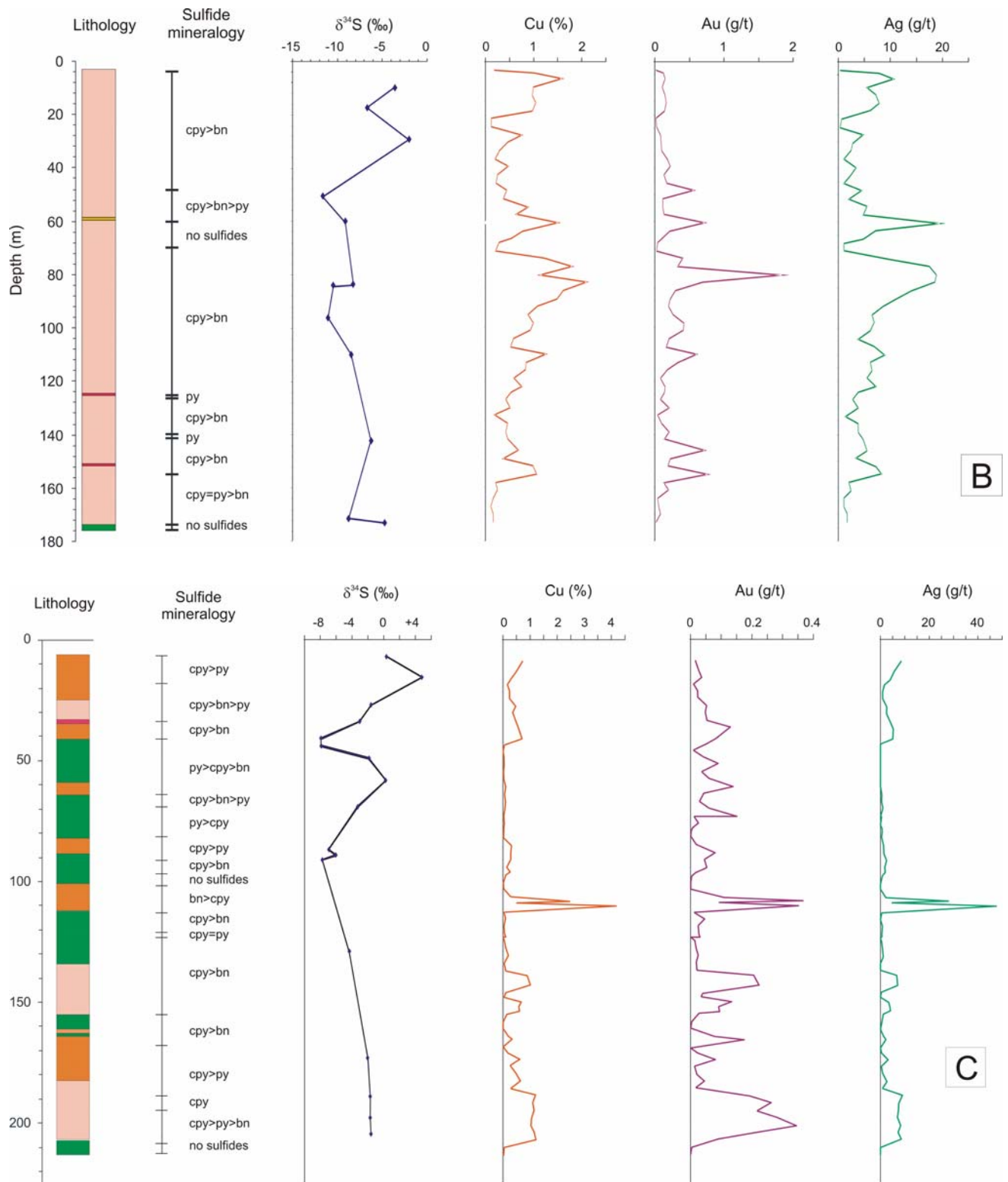


Figure 4. Schematic logs for selected drillholes through each of the major mineralized zones at Lorraine. A: Lower Main, DDH 2002-62; B: Upper Main, DDH L-95-13; C: Bishop, DDH 2001-58. See Figure 3 for geological legend. Assay values summarized from Eastfield Resources data.

Schematic drillhole logs were constructed for one hole in each of the Lower Main, Upper Main, and Bishop zones (Fig. 4). These logs illustrate the relationship between rock type, dominant sulfide

mineral species, $\delta^{34}\text{S}_{\text{sulfide}}$ values, and metal grades, although locally intense but extremely variable potassic alteration proximal to mineralized zones commonly made it difficult to identify primary rock types. The re-

relationship between $\delta^{34}\text{S}_{\text{sulfide}}$ data and Au grades as well as Cu-Au metal ratios is shown in Figure 5. There is some indication of increasing $\delta^{34}\text{S}$ values with Cu-Au

ratios at both the Upper Main and Bishop zones, but there is also significant scatter in the data.

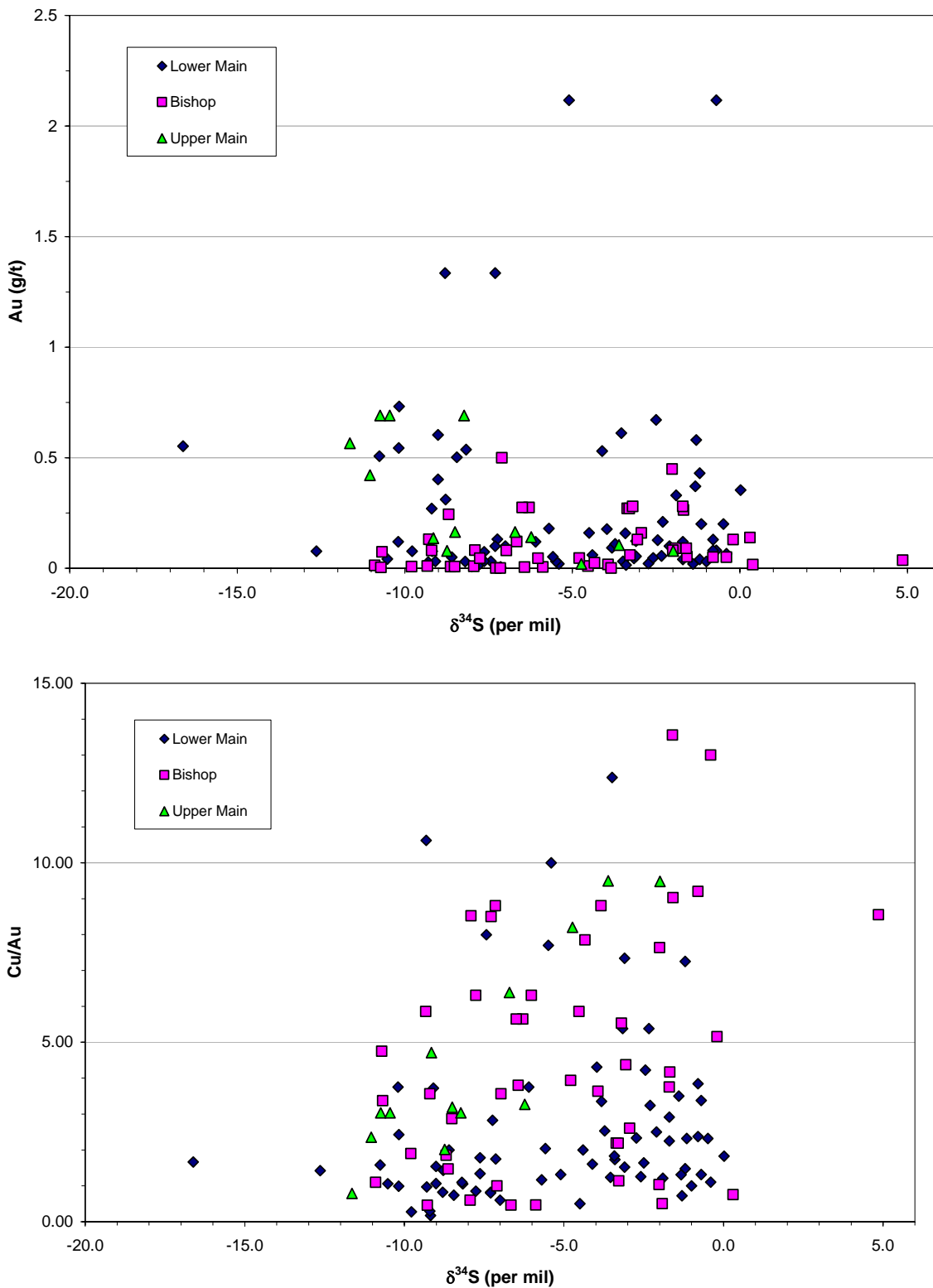


Figure 5. A (top): Lorraine $\delta^{34}\text{S}$ data plotted against Au (g/t) values. B (bottom): Lorraine $\delta^{34}\text{S}$ data plotted against Cu/Au values (Cu as %, Au as g/t). All metal values taken from assay intervals provided by Eastfield Resources.

TABLE 2. SUMMARY OF $\delta^{34}\text{S}$ DATA (AS PER MIL) FOR LORRAINE.

Area	Range $\delta^{34}\text{S}$	Average $\delta^{34}\text{S}$
Lower Main	0 to -16.6	-5.3
Bishop	+4.9 to -10.9	-5.0
Upper Main	-2.0 to -11.6	-7.8

Overall, the sulfur isotope data indicate that most of the analyzed material from Lorraine is not primary magmatic sulfides, as originally proposed by Bishop *et al.* (1994), since the data vary over a range of nearly 20%. Furthermore, magmatic values are generally assumed to be consistently near zero, which is not the case here. The available data are consistent, however, with a hydrothermal origin and are comparable to magmatic-hydrothermal sulfide compositions from porphyry Cu-Au systems. More detailed analysis of the dataset will be required to understand the relationship between sulfur isotope values and mineralization, alteration types, and/or igneous units.

Mt Polley

The Mt Polley deposit is located in the Quesnel terrane (Fig. 1) near Likely, British Columbia. The deposit was mined between 1997 and 2001 and produced 27.7 Mt of ore from the Cariboo and Bell pits (Fig. 6). The property has been inactive since 2001 but still contains an estimated 31.9 Mt of ore in the Bell and unexploited Springer deposits (Imperial Metals, pers comm, 2004). In August 2003, the discovery of a previously unknown, high-grade copper-gold zone, the NE zone, located approximately 1.5 km to the northeast of the Bell pit, initiated a major exploration and drilling program which led to the identification of several mineralized zones (Fig. 6). On-going exploration continues to intersect significant Cu and Au grades (*see* Imperial Metals for details).

The Mt Polley area is underlain by Jurassic and Triassic intrusive rocks of the Mt Polley intrusive complex. This complex consists of multiple intrusions of diorite to plagioclase porphyry to monzonite compositions that intruded sedimentary and volcanic rocks of the Nicola Group (Fraser *et al.*, 1995). The intrusions are associated with several intrusion breccias, which is a breccia with igneous matrix. The igneous breccias and numerous hydrothermal breccias form the main host for Cu-Au mineralization. In the Bell, Cariboo and Springer zones, the hydrothermal breccias are dominated by either actinolite, biotite, magnetite or albite, although the relationships between the different phases are unclear (Fraser *et al.*, 1995). Alteration consists of a core zone, coincident with the hydrothermal and intrusion breccias (Fig. 7), that is characterized by pervasive potassic alteration surround-

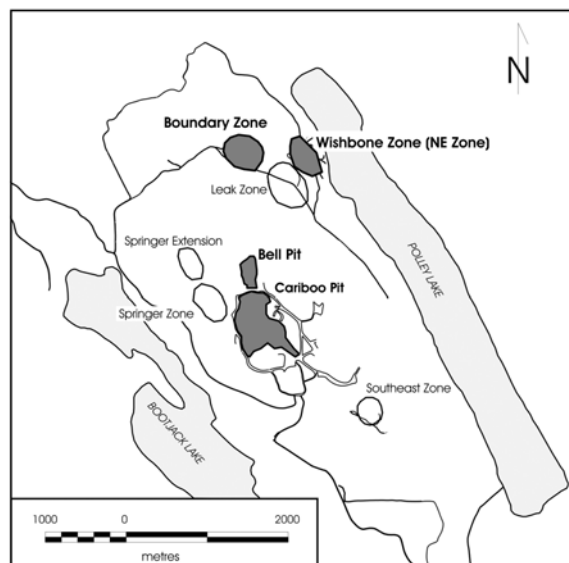


Figure 6. The Mt Polley deposit showing locations of major mineralized zones.

ed by a garnet-epidote zone, and rimmed by propylitic (epidote-pyrite-calcite) assemblages (Hodgson *et al.*, 1976). Mineralization occurs primarily as disseminations of chalcopyrite-magnetite-bornite, with increasing pyrite and diminishing bornite outwards from the core of the deposit. Sulfides also occur as blebs in the matrix of the hydrothermal breccias and abundant veins. Copper and gold values are closely correlated, and generally correspond to high magnetite concentration (Fraser *et al.*, 1995).

The recently discovered NE zone has several significant differences to the Bell and Cariboo areas. The geology of this region is dominated by plagioclase and potassium feldspar-pyritic intrusions that are locally megacrystic. In addition, there are lesser monzonite with late augite porphyry and mafic dykes. Mineralization is spatially associated with intrusion breccias (Fig. 8a) that are heterolithic, matrix- to clast-supported, with a fine- to medium-grained, equigranular monzonite matrix. Sulfide minerals are dominated by bornite, chalcopyrite and lesser pyrite. The sulfides are coarse-grained clots, irregular veins, or fine disseminations overprinting the matrix of the intrusion breccias and locally the breccia clasts as well. Sulfide minerals are also in veins and as disseminations in coherent intrusive phases. A sulfide zonation was recognized in cross-section with a core of bornite±chalcopyrite, rimmed by chalcopyrite-dominant sulfide assemblages, with pyrite ± chalcopyrite at the margins (*see* Fig. 10c).

Alteration in the NE zone (K. Ross, pers comm, 2004) consists of an early, pervasive, potassium metasomatism associated with little to no biotite. A distinct magnetite-garnet-apatite assemblage is pre- to

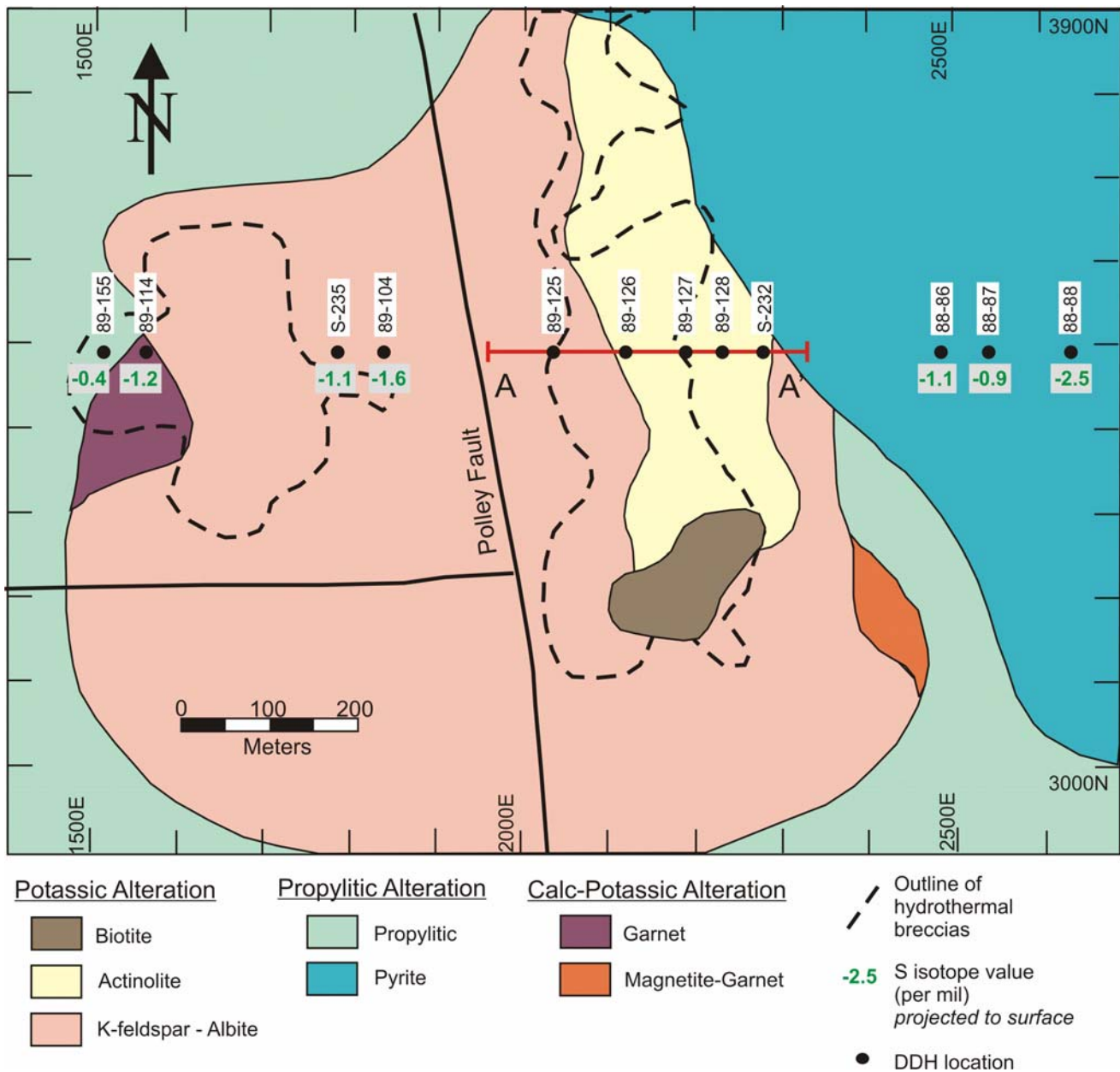


Figure 7. Alteration map of 'central zone', Mt Polley (slightly modified from Fraser *et al.*, 1995) showing line of section 3460N that was selected for detailed $\delta^{34}\text{S}$ sampling (see Fig. 9). Also shown are locations of DDH that were sampled in 2003 for preliminary sulfur isotope investigations and $\delta^{34}\text{S}$ results as per mil values (see Supplemental data for sample depths).

syn-mineral. This assemblage may overlap with a slightly later syn- to post-mineral assemblage dominated by a Ca-Al silicate (clinozoisite or prehnite?) and is associated with albite-calcite, lesser garnet, and minor diopside. Late alteration consisting of calcite-sericite-albite-chlorite is widespread. Chlorite-carbonate-pyrite alteration is rare but occurs locally peripheral to the brecciated zones and within the country rocks to the east of the main mineralized centre.

The Nordic zone, which is part of the Boundary Zone (Fig. 6), was examined briefly. Samples of one

drillhole (ND-04-01) have some similarities to the NE zone, although several significant differences were noted. In particular, sulfide minerals are primarily associated with a magnetite±garnet, clinozoisite or prehnite(?) +calcite breccia matrix (Fig. 8b). It is unclear whether this assemblage overprints an original intrusive matrix. Pyrite in association with chalcopyrite is more abundant in the core of the mineralized zone than in the NE zone. Bornite was not observed. In general, the Nordic zone is significantly more gold- and silver-rich than the NE zone (Imperial Metals, pers comm, 2004).

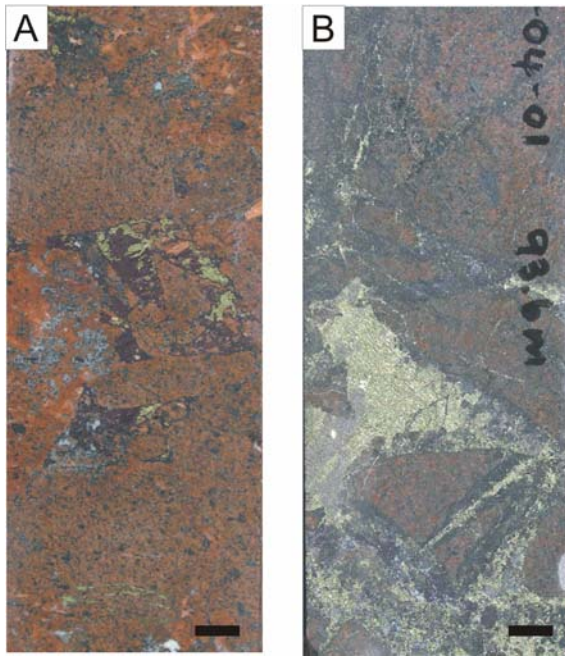


Figure 8. Photos of Mt Polley drillcore. A. NE Zone, bornite-chalcopyrite mineralization in matrix of intrusion breccia (DDH 04-29, 100.5m). B. Nordic Zone, chalcopyrite-pyrite-magnetite \pm garnet breccia cement (ND-04-01, 93.6m). Scale bars = 1 cm.

SULFUR ISOTOPE STUDY

Prior to the initiation of this study, no sulfur isotope data were available for the Mt Polley deposit. Samples for the preliminary 2003 study were obtained from a collection archived at MDRU from the study of Fraser *et al.* (1995) and from a short field visit in October 2003 by S. Ebert. The majority of the 2003 samples were selected from the Cariboo and Bell deposits (along section 3460N; Fig. 7). At that time, only three samples were taken from the NE zone.

The $\delta^{34}\text{S}_{\text{sulfide}}$ results ranged between +1.5 and -3.4‰, and $\delta^{34}\text{S}$ data for the Cariboo and Bell deposits were generally higher than those for samples from the NE zone (with average values of -0.4 and -3.2‰, respectively). In the Cariboo deposit, the highest $\delta^{34}\text{S}_{\text{sulfide}}$ data appeared to be spatially associated with a small body of plagioclase porphyry and intrusion breccia that forms the core of this zone. However outside of this area, the sulfur isotope data was limited and further work was required to define the details of any zonation trends present in the dataset. Further work was also necessary to determine the nature and source of $\delta^{34}\text{S}_{\text{sulfide}}$ variation throughout the Mt Polley region.

Samples from 2004 were focused on section 3460N in the Cariboo zone (in five selected drillholes; Fig. 9). Detailed sampling was also completed along one cross-section (section 18) through the core of the NE zone (Fig. 10). Only one drillhole (ND-04-01) was sampled in the Nordic zone.

Sulfur isotope results from Cariboo zone (Fig. 9) range from -2.3 to +2.4‰. An average $\delta^{34}\text{S}_{\text{sulfide}}$ value of +0.2‰ for the Cariboo samples is significantly higher than that for samples in the NE zone (*see* Fig. 10). A distinct sulfur isotope zonation is apparent in cross-section (Fig. 9B), with the Cu ore zone surrounded by high $\delta^{34}\text{S}_{\text{sulfide}}$ values. Negative $\delta^{34}\text{S}$ values are spatially associated with the top and middle of the plagioclase porphyry and intrusion breccia as mapped by Fraser *et al.* (1995). These results agree with the conclusions of Fraser *et al.* (1995) who suggested that the porphyry and associated breccia are the source of fluids responsible for mineralization in the Cariboo zone.

In contrast to the Cariboo deposit, chalcopyrite with lesser pyrite and bornite from the NE zone have significantly lower $\delta^{34}\text{S}_{\text{sulfide}}$ values, which range from -1.1 to -7.0‰. In cross-section (Fig. 10b), $\delta^{34}\text{S}_{\text{cpy}}$ values appear to be zoned with minimum values concentrated at depth to the east-northeast, slightly offset from the core of bornite mineralization. The more negative $\delta^{34}\text{S}$ values are coincident with intrusion and hydrothermal brecciation, although a range of values is recognized through these rock types. It is possible that the data reflect the path of oxidized, mineralizing fluids from depth although further investigations should identify any structural controls and/or alteration zonation associated with this area.

Red Chris

The Red Chris Cu-Au deposit is located in the Stikine Terrane of northwestern British Columbia (Fig. 1), in the Totogga Lake area approximately 80 km south of Dease Lake. Exploration for Cu-Au in this area is recorded as early as 1956 (Baker *et al.*, 1997), although it has never been mined. The property was acquired by bcMetals Corporation in 2003, who have since defined an inferred resource of 28.2 Mt at 0.62% Cu and 0.5 g/t Au (data from bcMetals website, Nov. 2003).

The geology and nature of Cu-Au mineralization of the Red Chris area is summarized from Baker *et al.* (1997). The geology of the region is dominated by Mesozoic volcanic rocks that include the Middle to Upper Triassic Stuhini Group and the overlying Lower Jurassic Hazelton Group. Cu-Au mineralization is associated with the Red Stock, which is an elongate, Early Jurassic subvolcanic intrusion that cuts the volcano-sedimentary suite of the Stuhini Group. The Red Stock is a multi-phase porphyritic to equigranular, hornblende quartz monzodiorite to monzonite. Alteration is characterized by abundant early potassic assemblages overprinted by later sericitic and argillic alteration. Sulfide minerals are dominantly vein-hosted chalcopyrite, lesser bornite, and negligible pyrite. Bornite becomes more abundant than chalcopyrite with increasing depth. Minor galena and sphalerite are late phases (Baker *et al.*, 1997). Unusual features of the de-

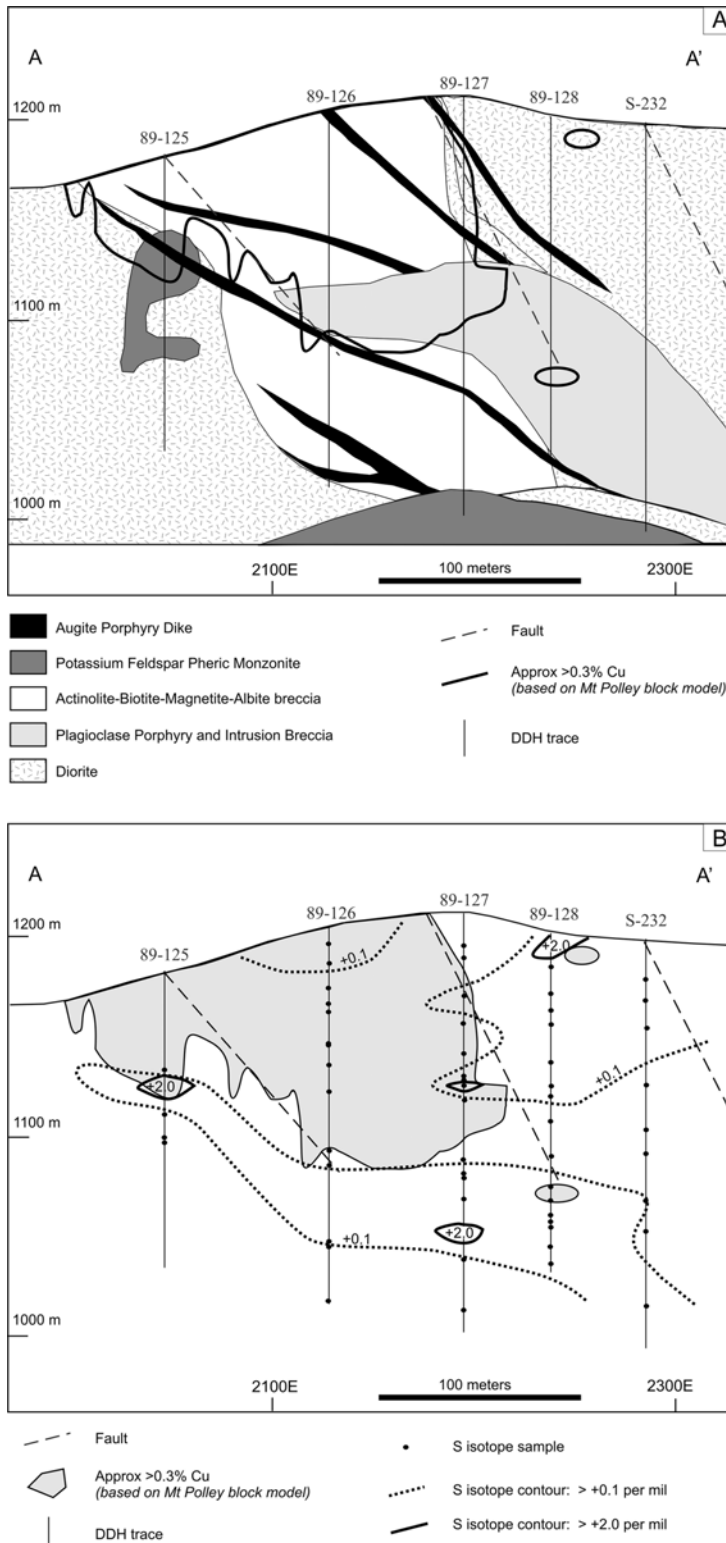


Figure 9. Mt Polley section 3460N. A. General geology after Fraser *et al.* (1995) with approximately outline of > 0.3% Cu. B. Sulfur isotope sample locations and contours of $\delta^{34}\text{S}_{\text{sulfide}}$ values (see Supplemental data for tabulated data).

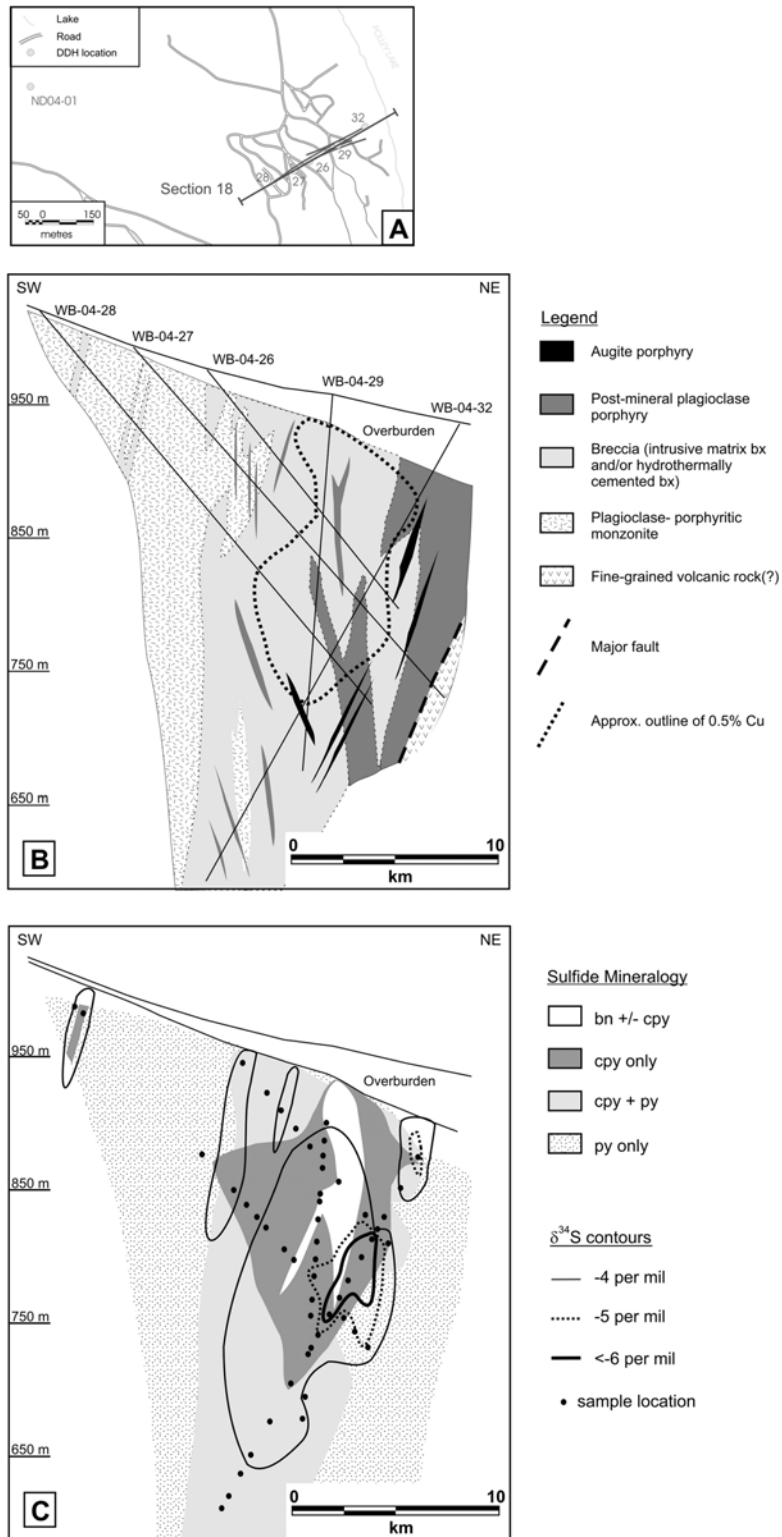


Figure 10. Schematic cross-section through the NE zone, Mt Polley. A. General location of Section 18 (mine grid) across the NE zone that was sampled for this study. General geology (modified from K. Ross, pers comm, 2004) and outline of Cu mineralization. C. Sulfide mineral zonation and contours of $\delta^{34}\text{S}_{\text{cpy}}$ data from this study.

posit include the abundance of carbonate alteration and veins, and the occurrence of mineralized quartz vein stockwork in the Main Phase of the Red Stock. Red

Chris also lacks Na- and Ca-bearing silicate alteration assemblages. Both features are more typical of calc-alkalic porphyry deposits than other alkalic deposits of

British Columbia (Baker *et al.*, 1997). Despite those differences, Red Chris is more similar in many ways to the alkalic porphyry deposits of New South Wales in Australia (*e.g.*, Goonumbla, Lickfold *et al.*, 2003; Cadia, Wilson *et al.*, 2003), which also contain well-mineralized quartz vein stockwork.

SULFUR ISOTOPE STUDY

Only limited sulfur isotope data for sulfides and sulfates from the Red Chris property were available prior to this study (T. Baker and J. Thompson, pers comm, 1997). This data indicated that the sulfide $\delta^{34}\text{S}$ values range from -3.6 to $+0.6\text{‰}$ with sulfate $\delta^{34}\text{S}$ values ranging from $+12.5$ to $+16.0\text{‰}$. This current study sought to test the variability in sulfur isotope compositions with different alteration styles and with Cu/Au ratios. Unfortunately, only a small number of samples were available for this work and were gathered from a collection held by T. Baker (James Cook University, Australia) and MDRU.

The $\delta^{34}\text{S}_{\text{sulfide}}$ determined during this study are similar to the initial results (T. Baker and J. Thompson, pers comm, 1997) with values ranging from $+0.9$ to -5.0‰ . Most samples are from the Main Zone and the results are shown in cross-section in Figure 11 (section 50000E). The data is relatively sparse, although in general, positive $\delta^{34}\text{S}_{\text{sulfide}}$ values form the core of the strong quartz-sulfide stockwork zones and at depth. There is significant variability at the margins and tops

of the intense stockwork zones, although $\delta^{34}\text{S}_{\text{sulfide}}$ data are generally negative.

Results from this study are consistent with decreasing temperature outwards from the core of the mineralized zones and/or with decreasing depth. Preliminary fluid inclusion data from T. Baker and J. Thompson (pers comm, 1997) suggest a temperature range from over 500° to 300°C , or over at least 200°C during the potassic and quartz-sericite-carbonate vein and associated sulfide events. At these temperatures (from 500° to 300°C), calculated $\Delta^{34}\text{S}_{\text{sulfate-pyrite}}$ values based on fractionation equations in Ohmoto and Rye (1979) would decrease by approximately 7‰ under equilibrium conditions. Although no $\delta^{34}\text{S}_{\text{sulfate}}$ data are available for anhydrite associated with the mineralizing event, a 7‰ $\Delta^{34}\text{S}_{\text{sulfate-pyrite}}$ difference could reasonably account for the 4 to 5‰ range in $\delta^{34}\text{S}_{\text{sulfide}}$ data indicated in Figure 11. A more comprehensive study would be required to confirm the role of cooling as the source of $\delta^{34}\text{S}_{\text{sulfide}}$ variation, and determine the extent of the $\delta^{34}\text{S}$ zonation in the adjacent unmineralized wall rocks.

Galore Creek

The Galore Creek porphyry system is located in the Stikine terrane of northwestern British Columbia at the western margin of the Intermontane Belt (Fig. 1). The region contains Cu-Au mineralization in several discrete zones. The largest zones, the Central, Southwest and

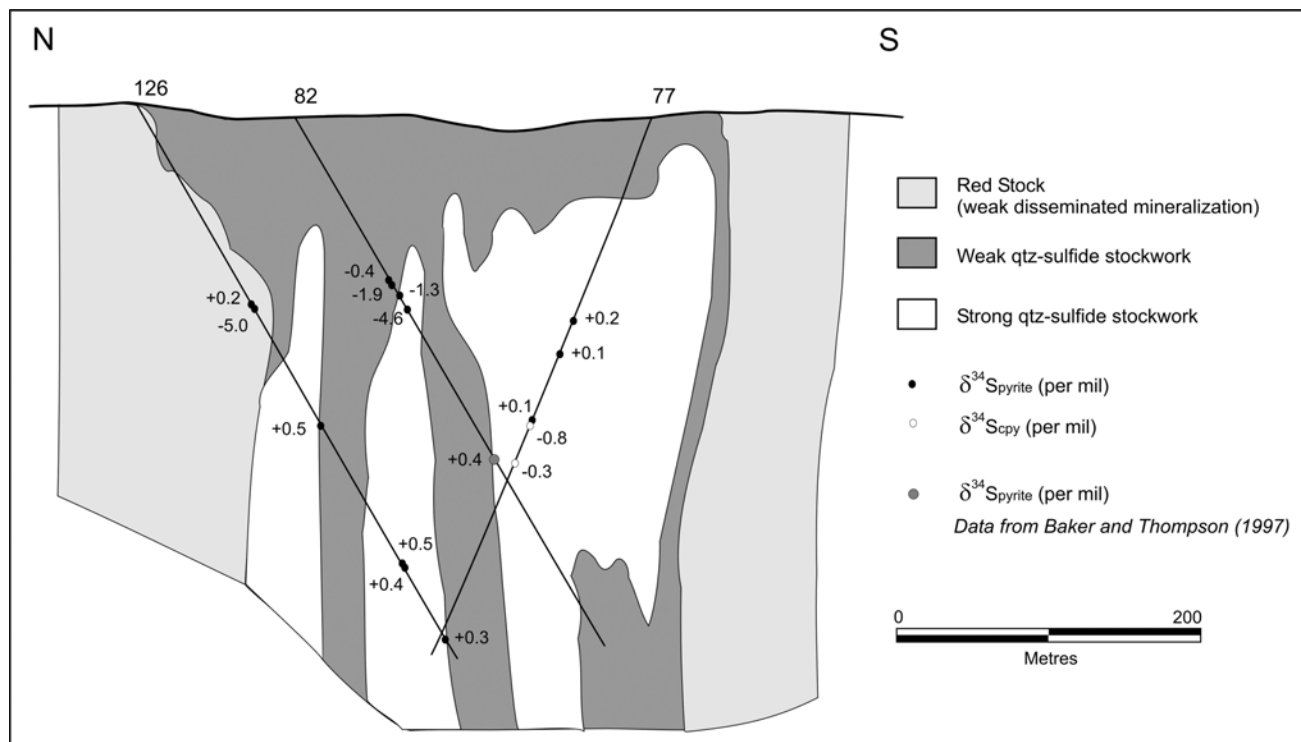


Figure 11. Schematic cross-section (Section 50000E; looking east) through the Main Zone of the Red Chris deposit (modified from Blanchflower, 1995). $\delta^{34}\text{S}_{\text{sulfide}}$ data from this study (with approximate sample locations) are shown, as well as one data point located on this sections from Baker and Thompson (pers comm, 1997). See Baker *et al.* (1997) for section location and local geology.

Junction zones (Fig. 12), contain an identified resource of 284 Mt at 0.67% Cu (Enns *et al.*, 1995). The Galore Creek area is dominated by Upper Triassic to Lower Jurassic alkalic volcanic rocks and syenite intrusions (Enns *et al.*, 1995). Multiple intrusive phases are recognized, and include pre-, inter-, late- and post-mineral phases (Enns *et al.*, 1995; Simpson, 2003). The intrusions are dominantly silica-undersaturated, alkalic and metaluminous, although the youngest intrusive phase is weakly silica-saturated. Numerous breccias are also present and locally host significant sulfide mineral concentrations, particularly in the Southwest Zone (Enns *et al.*, 1995). In general, Cu and Au are associated most closely with pervasive K-silicate and lesser Ca-K silicate alteration as replacement, disseminated and

fracture-controlled chalcopyrite with locally abundant bornite. Higher Au values are normally associated with bornite (Simpson, 2003).

Copper to gold ratios are variable throughout the Galore Creek deposit. In the Central Zone, copper concentrations are fairly consistent although gold concentrations are variable and are closely associated with abundant bornite, magnetite and hematite in the northern and southern portions of this zone (Enns *et al.*, 1995). As a result, Cu/Au ratios are variable and are lowest to the north and south of the Central Zone core (Fig. 12). In the Southwest Zone, Cu/Au are variable and higher Au concentrations locally correspond to an increase in pyrite content (Enns *et al.*, 1995).

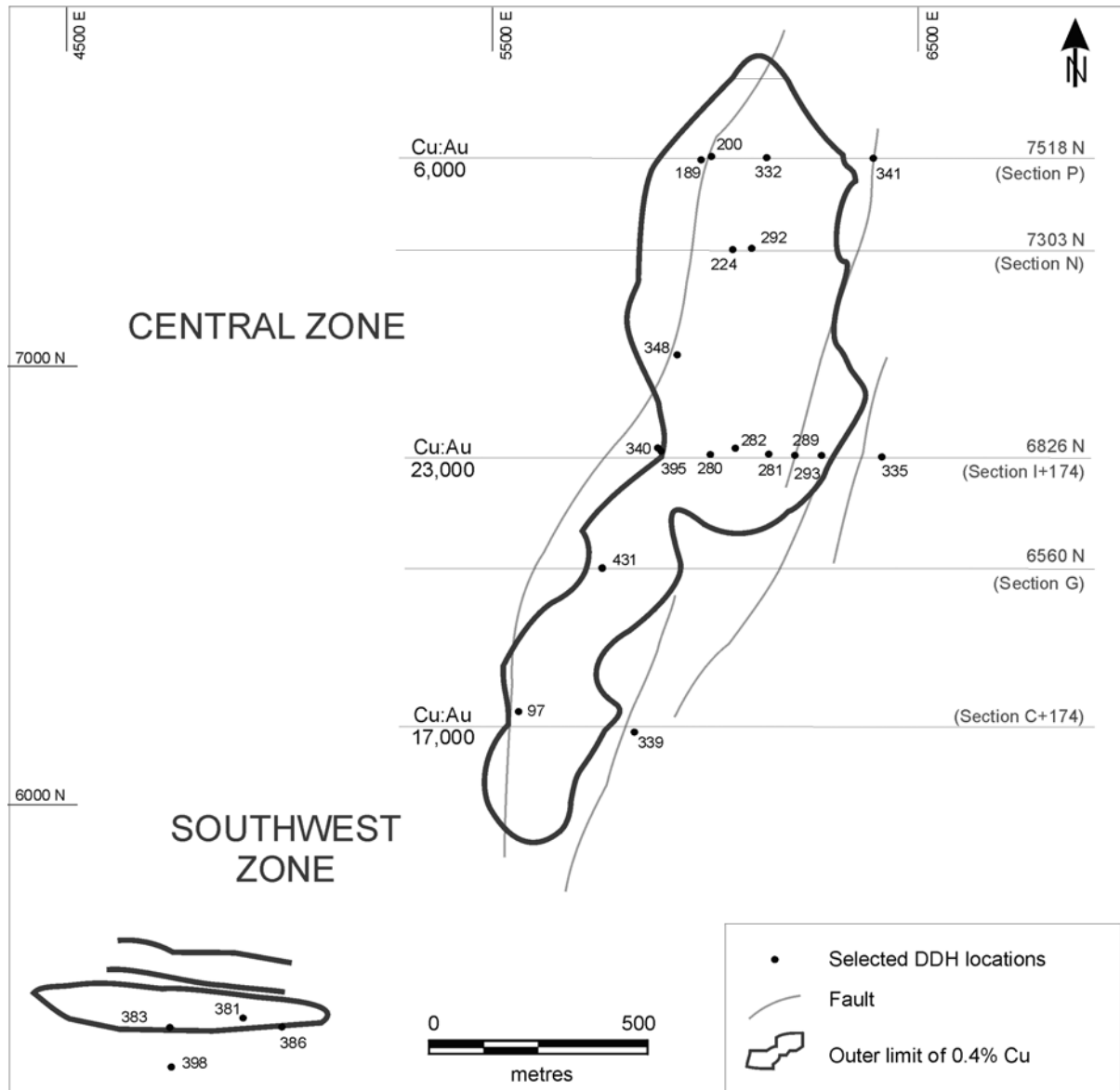


Figure 12. Map of the Galore Creek area showing location of the major mineralized areas (Central and Southwest Zones), diamond-drill hole locations from which the isotope samples were collected, and lines of section (adapted from Enns *et al.*, 1995).

SULFUR ISOTOPE STUDY

Prior to this study, limited sulfur isotope data for sulfides and sulfates at Galore Creek were acquired by J. Thompson and C. Stanley (MDRU). Their data suggest a range of $\delta^{34}\text{S}$ values from -9.9 to -6.4% for sulfides and $+5.0$ to $+7.4\%$ for sulfates (J. Thompson, pers comm, 2003) but sampling was restricted to the Central Zone.

In the current project, sulfide samples were obtained from a suite archived at MDRU. Twenty-nine samples of drillcore were selected along five cross-sections through the Central Zone, with an additional seven samples from the Southwest zone (Fig. 12). Sulfide $\delta^{34}\text{S}$ data range from -3.5 to -11.3% . Data for sulfides in the Central and Southwest zones are similar. Average $\delta^{34}\text{S}$ values are -7.3% and -6.5% , respectively. Copper and gold grades are not available for individual samples from these deposits, thus we are unable to comment on the correlation of isotope values with grade. However, the spatial distribution of isotope results (Fig. 13) does illustrate relatively higher average $\delta^{34}\text{S}$ values for sulfides at the northern and southern parts of the Central Zone, compared to the core of this zone. This core area contains on average lower Au grades in association with intense Ca-K silicate alteration (Enns *et al.*, 1995). In general, the sulfur

isotope zoning in the Galore Creek deposit is weak and is probably related to, or complicated by, the multi-phase intrusive-hydrothermal history in this district (Enns *et al.*, 1995). At this stage, not enough is known regarding the timing and relationship of the multiple intrusive-hydrothermal phases to constrain the origin or significance of the sulfur isotope results. A systematic paragenetic study of the magmatic and hydrothermal history would be required to fully understand the implications of the data.

Afton

The Afton property, located near Kamloops, British Columbia (Fig. 1), is the largest Cu-Au deposit in the Iron Mask Batholith district. The Afton mine produced 22.1 Mt of ore at 0.91% Cu and 0.67 g/t Au (Ross *et al.*, 1995) while in operation from 1977 to 1987. The property is currently owned by DRC Resources who have delineated an additional resource of over 51 Mt Cu (measured and indicated; DRC Resources, pers comm, 2004). The bulk of this resource is contained within a southwest trending lens that is roughly 200 to 250 m in thickness. The sulfide resource extends below and to the southwest of the current Afton pit (Fig. 14). Other nearby deposits include Ajax, Pothook and Crescent.

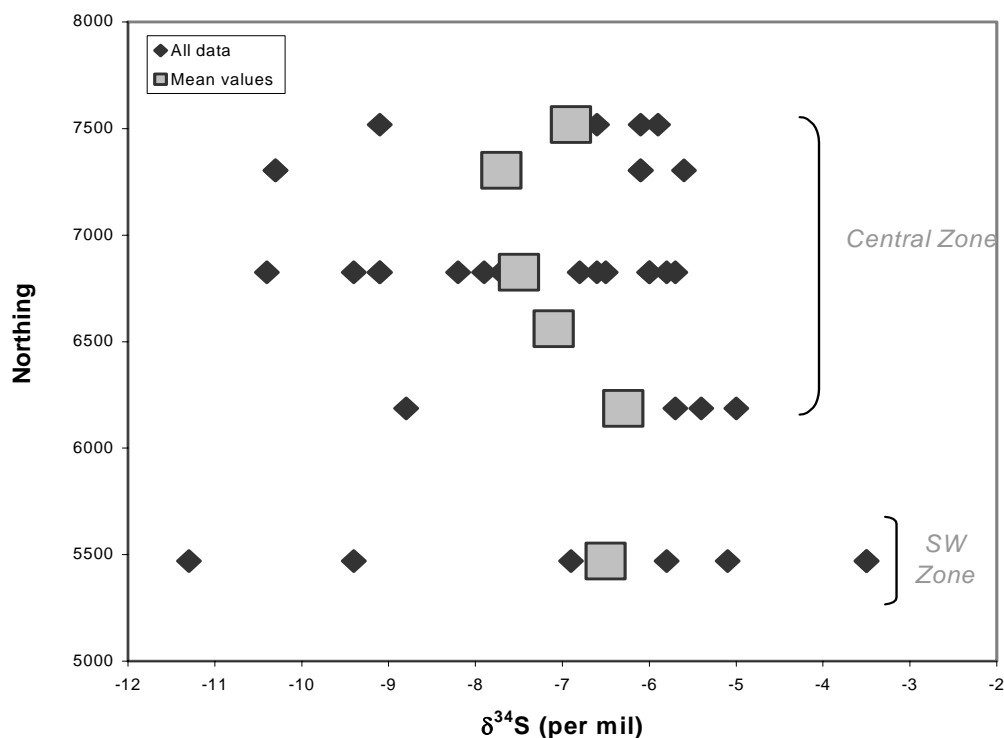


Figure 13. Distribution of Galore Creek $\delta^{34}\text{S}$ results from the 2003 study. Data are plotted according to their northing location. Individual data points are shown, as well as mean $\delta^{34}\text{S}$ values for each line of section.

All porphyry systems are hosted by the Iron Mask Batholith, an Early Jurassic composite alkalic intrusion that was emplaced into the Late Triassic Nicola Group composed of volcanic, volcanoclastic and minor sedimentary rocks. The batholith consists of two major plutons, the Cherry Creek pluton and the Iron Mask pluton; the latter is dominant around the Afton mine. The Iron Mask pluton includes four major intrusive phases; the Pothook diorite, Hybrid unit, Cherry Creek diorite-monzonite-syenite and the Sugarloaf diorite (after Ross *et al.*, 1995; Snyder and Russell, 1995). Minor picrite also occurs in several deposits in the Iron Mask Batholith, including Afton (Ross *et al.*, 1995). Volcanic and sedimentary rocks of the Tertiary Kamloops Group (Ewing, 1981) unconformably overlie the batholith.

The bulk of ore originally mined from the Afton pit was from a thick supergene zone that extended to depths of about 400 to 500 m (Kwong, 1987). This ore consisted primarily of native copper and chalcocite with minor cuprite, malachite and azurite. Hypogene ore consists of bornite and chalcopyrite with lesser chalcocite and covellite. Sulfides occur as disseminations and veinlets, with variable K-feldspar, albite, epidote, hematite, magnetite and carbonate (Kwong, 1987).

SULFUR ISOTOPE STUDY

Prior to this study, no $\delta^{34}\text{S}$ data were available for the Afton deposit. Sampling was completed on-site in July 2003, and no additional work was carried out in the 2004 study. The initial sulfur isotope sampling was focused along one long section, oriented roughly southwest along the length of known mineralization (Fig 15), including the Southwest zone (*see* Fig. 14). Several samples were also taken from smaller occurrences peripheral to the Afton pit to test the regional sulfur isotope signature.

The $\delta^{34}\text{S}$ data for the main mineralized area and the Southwest zone range from +3.6 to -8.0‰. Samples peripheral to the Afton pit, taken from Ajax, Big Onion and the Magnetite showings, also occur within this range. There are no obvious correlations of $\delta^{34}\text{S}_{\text{sulfide}}$ values to either Cu and Au grade, although less than half of the samples analyzed have associated assay data. Figure 15 shows the distribution of $\delta^{34}\text{S}$ data in cross-section and relative to the estimated position of the ore zone (0.5% Cu cut-off: DRC Resources, pers comm, 2003). There is considerable variability in the data although a zone of strongly depleted or negative $\delta^{34}\text{S}_{\text{sulfide}}$ values is apparent in the core of the known

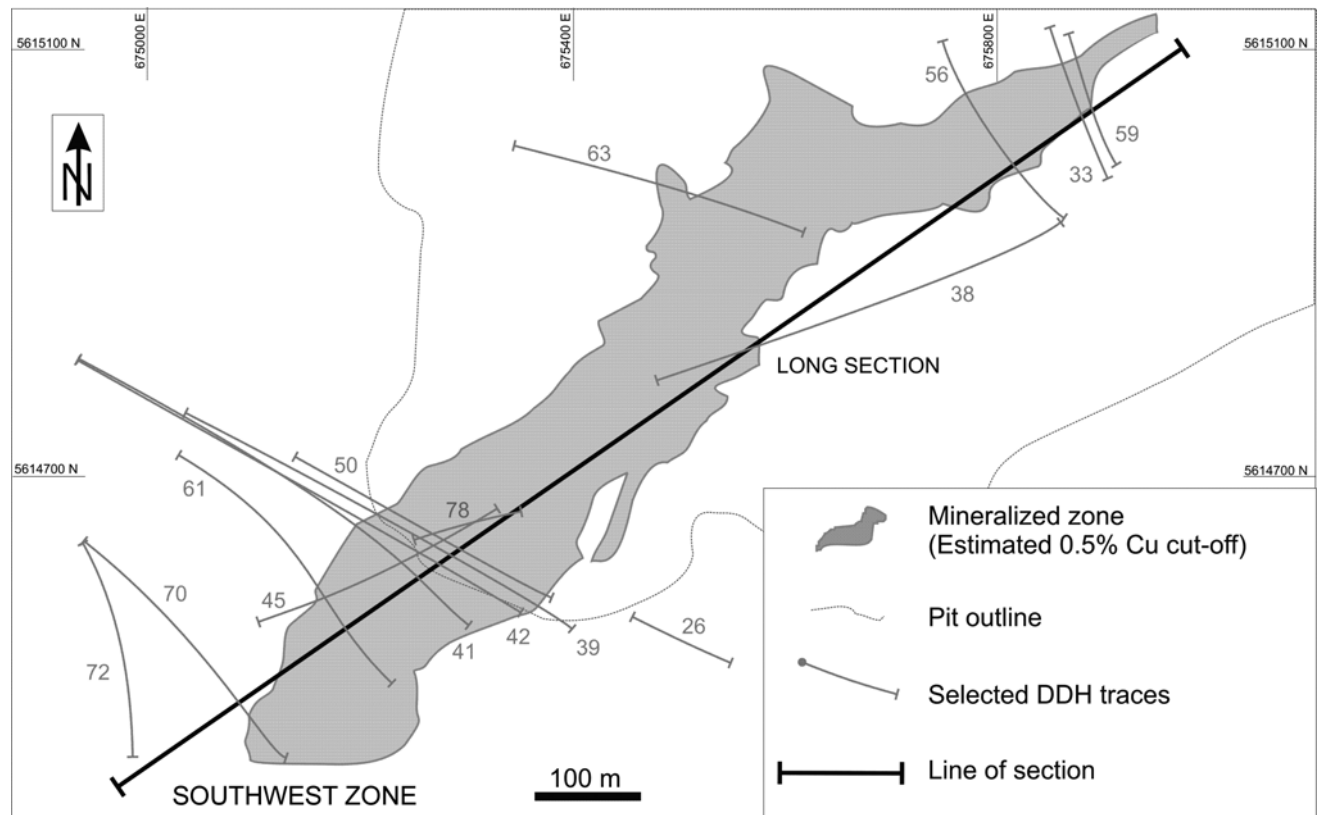


Figure 14. Plan view of the Afton area showing location of the hypogene mineralized zone delineated by DRC Resources. Also shown is the location of the cross-section detailed in Figure 15.

mineralized zone. This anomalous zone extends further to the southwest in DDH-70 (-7.1‰), although this drillhole has not been tested by assays. Negative $\delta^{34}\text{S}_{\text{sulfide}}$ values are also concentrated at the eastern margin of the mineralized zone, where they extend to surface. Only one anomalously positive $\delta^{34}\text{S}_{\text{sulfide}}$ value of +3.2‰ is recorded in the longitudinal section. It occurs at depth, at the margin of what has been modeled as a thin wedge of ore grade material (DRC Resources, pers comm, 2003) that likely lies along a fault or fracture zone.

Overall, the sulfur isotope zonation at Afton is well defined through the core of the main mineralized body. Discrete zones of anomalously high and low $\delta^{34}\text{S}_{\text{sulfide}}$ values may indicate domains of reduced and oxidized fluids, respectively, suggesting that fluid mixing along structural intersections may have contributed to ore deposition. A more thorough investigation into the nature of the ore and alteration assemblages, and the geometry of associated structures, would be required to fully understand the origin and significance of the sulfur isotope zonation.

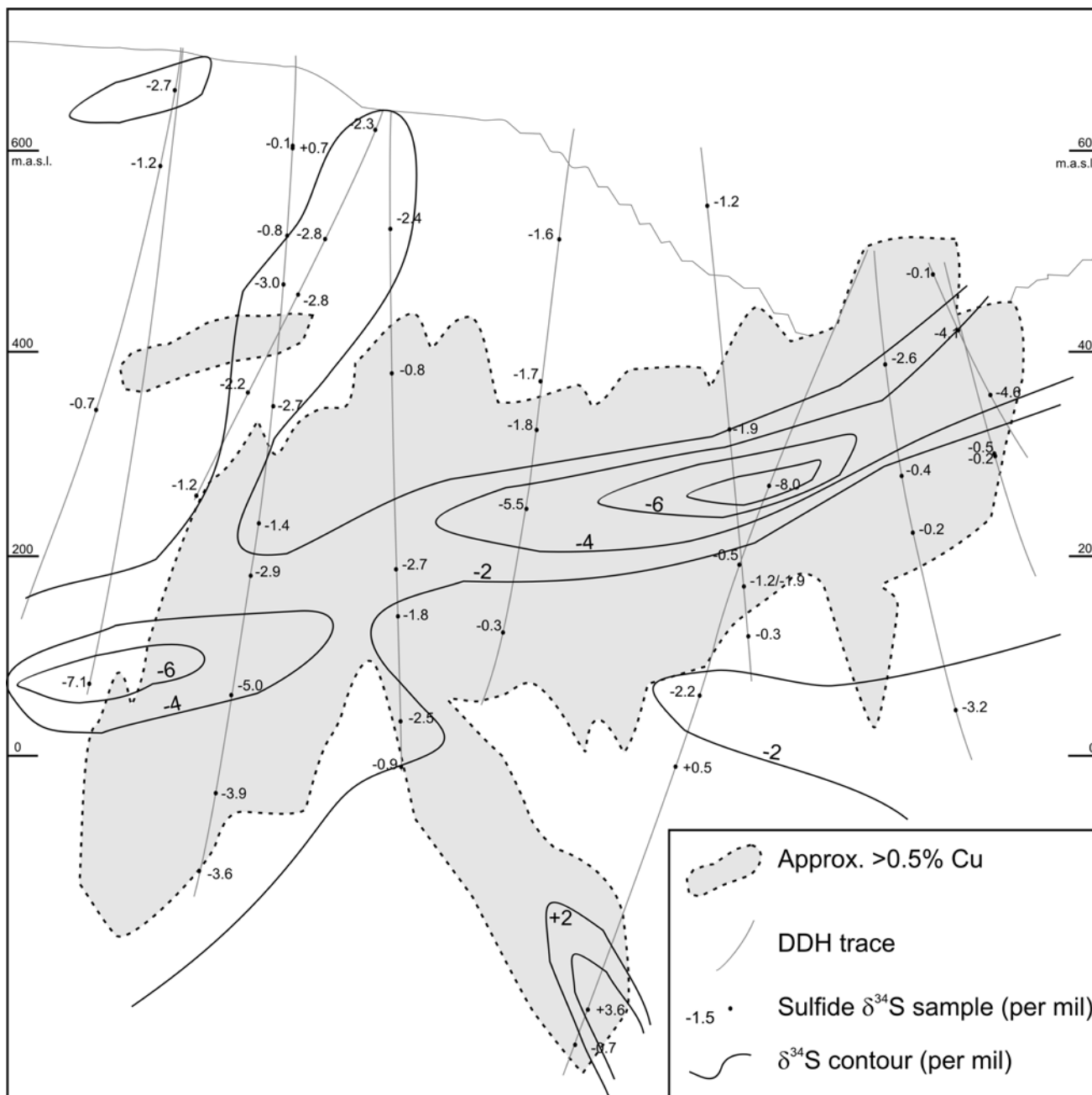


Figure 15. Afton long section showing $\delta^{34}\text{S}$ results and approximate position of ore zone outlined by 0.5% Cu cut-off (from DRC Resources, pers comm, 2003). Contours of $\delta^{34}\text{S}$ data at 2 per mil intervals are shown.

SUMMARY

This report summarizes data from a two-year study of sulfur isotope zonation in selected alkalic porphyry deposits in British Columbia. Preliminary data were collected for the Lorraine, Mt Polley, Red Chris, Afton and Galore Creek deposits in this first year of this study (2003). Initial results for Lorraine and Mt Polley in particular were of sufficient interest to warrant further work, and detailed sampling was completed on-site at these two deposits in July-August of 2004. Major findings are summarized as follows:

- Data from the Lorraine deposit are consistent with a magmatic-hydrothermal origin for mineralization, and not a strictly primary magmatic sulfide source. There is some indication of increasing $\delta^{34}\text{S}$ values with Cu-Au ratios in a few mineralized zones, but the relationship of $\delta^{34}\text{S}$ data with lithology, sulfide mineralogy, and metal grades needs to be tested further.
- At Mt Polley, detailed sulfur isotope analyses from the Cariboo zone suggests that the Cu ore zone is surrounded by high $\delta^{34}\text{S}_{\text{sulfide}}$ values. Negative $\delta^{34}\text{S}_{\text{sulfide}}$ values are spatially associated with plagioclase porphyry and related intrusion breccia. Similarly, the spatial distribution of $\delta^{34}\text{S}$ data at the NE zone suggests a strong relationship to intrusion and/or hydrothermal brecciation, and anomalous or negative values are slightly offset relative to a core of bornite \pm chalcopyrite deposition. In general, results indicate a consistent sulfur isotope zonation in both mineralized areas and suggest that the path of oxidized, and potentially metal-bearing fluid, can be traced from their source.
- At Red Chris, the data collected was limited to an existing sample suite from T. Baker and sample coverage is limited. In general, results are consistent with decreasing depositional temperature outwards from the core of the mineralized zones and/or with decreasing depth. Further work would be required to determine the extent of the $\delta^{34}\text{S}$ zonation into relatively unaltered and unmineralized wall rocks.
- Sulfur isotope data from the Galore Creek deposit do not exhibit any obvious spatial zonation, although there is some indication of more negative $\delta^{34}\text{S}$ values associated with lower Au grades in the core of the Central Zone. Further work would be required to understand the multi-phase intrusive-hydrothermal history of this district and their relation to sulfide deposition.
- Results from the Afton deposit indicate a distinct sulfur isotope zonation occurs within the deposit. There is a core of anomalous and strongly negative values in the centre of the main hypogene

mineralized zone. Local positive $\delta^{34}\text{S}$ values at depth may indicate the introduction of a different, more reduced, fluid source along structural features.

In summary, systematic sulfur isotopic zonation has been recognized within several alkalic Cu-Au deposits in British Columbia. While this technique may not be universally applicable, it may still prove to be a valuable exploration tool in those deposits where a predictable zonation pattern can be identified.

ACKNOWLEDGMENTS

This project was funded through the Rocks to Riches program managed by the British Columbia and Yukon Chamber of Mines and this financial support is gratefully acknowledged. This work would not have been possible without the assistance and additional support of all the companies involved. We would particularly like to thank G. Garrett and G. Peatfield (Eastfield Resources), and extend sincere thanks to J. Paige and the Lorraine camp crew for all their assistance – both geological and mechanical. Special thanks also to Patrick McAndless and Leif Bjornson (Imperial Metals), and the Mt Polley exploration crew for all their help. Additional assistance and discussions provided by S. Ebert, T. Baker, D. Cooke and K. Ross are thankfully acknowledged. We also would like to sincerely thank R.O. Rye and C. Bern at the USGS Stable Isotope Lab for their assistance in providing extremely rapid analytical results. Special thanks to D. Cooke for his editorial contributions. This paper is MDRU publication P179.

REFERENCES

- Baker, T., Ash, C.H. and Thompson, J.F.H. (1997): Geological setting and characteristics of Red Chris porphyry copper-gold deposits, northwestern British Columbia; *Exploration and Mining Geology*, Volume 6 no 4, pages 297-316.
- Bishop, S.T., Heah, T.S., Stanley, C.R. and Lang, J.R. (1995): Alkalic intrusion hosted copper-gold mineralization at the Lorraine deposit, north-central British Columbia; *in: Porphyry Deposits of the Northwestern Cordillera of North America*, Schroeter, T.G., Editor, *Canadian Institute of Mining, Metallurgy, and Petroleum*, Special Volume 46, pages 623-629.
- Blanchflower, J.D. (1995): 1995 exploration report on the Red Chris property; unpublished report to American Bullion Minerals Ltd., 93 pages.
- Cooke, D.R., Wilson, A.J., Lickfold, V. and Crawford, A.J. (2002): The alkalic Au-Cu porphyry province of NSW; AusIMM 2002 Annual Conference, Auckland, New Zealand, pages 197-202.
- Deyell, C.L., Tosdal, R. and Ebert, S. (2004): Sulfur Isotopic Zonation in Alkalic Porphyry Cu-Au Systems:

- Applications to Mineral Exploration in British Columbia; Final Report to the BCYCM, Rocks to Riches Program, Year 1.
- Enns, S.G., Thompson, J.F.H., Stanley, C.R. and Yarrow, E.W. (1995): The Galore Creek porphyry copper-gold deposits, northwestern British Columbia; *in* Porphyry Deposits of the Northwestern Cordillera of North America, Schroeter, T.G., Editor, *Canadian Institute of Mining, Metallurgy, and Petroleum*, Special Volume 46, pages 630-644.
- Ewing, T.E. (1981): Regional stratigraphy and structural setting of the Kamloops Group, south-central British Columbia; *Canadian Journal of Earth Sciences*, Volume 19, pages 1464-1477.
- Fraser, T.M., Stanley, C.R., Nikic, Z.T., Pesalj, R. and Gorc, D. (1995): The Mount Polley alkalic porphyry copper-gold deposit, south-central British Columbia; *in* Porphyry Deposits of the Northwestern Cordillera of North America, Schroeter, T.G., Editor, *Canadian Institute of Mining, Metallurgy, and Petroleum*, Special Volume 46, pages 609-622.
- Garnett, J.A. (1978): Geology and mineral occurrences of the southern Hogen batholith; *B.C. Ministry of Energy, Mines and Petroleum Resources*, Bulletin 70, 75 pages.
- Giesemann, A., Jager, H.J., Norman, A.L., Krouse, H.R. and Brand, W.A. (1994): On-line sulfur-isotope determination using and elemental analyzer coupled to a mass spectrometer; *Analytical Chemistry*, Volume 65, pages 2816-2819.
- Hodgson, C.J., Bailes, R.J. and Verzosa, R.S. (1976): Cariboo-Bell; *in* Porphyry Deposits of the Canadian Cordillera, Sutherland Brown, A., Editor, *Canadian Institute of Mining, Metallurgy, and Petroleum*, Special Volume 15, pages 338-396.
- Kwong, Y.T.J. (1987): Evolution of the Iron Mask batholith and its associated copper mineralization; *B.C. Ministry of Energy, Mines and Petroleum Resources*, Bulletin 77, 55 pages.
- Lang, J. R., Stanley, F.R., Thompson, J. F. H. and Dunne, K. F. (1995): Na-K-Ca magmatic-hydrothermal alteration in alkalic porphyry Cu-Au deposits, British Columbia; *in* Magmas, Fluids, and Ore Deposits, Thompson, J.F.H., Editor, *Mineralogical Association of Canada*, Short Course Volume 23, pages 339-366.
- Lickfold, V. (2001): Volatile evolution and intrusive history at Goonumbla, central western NSW; unpublished PhD thesis, *University of Tasmania*, Australia.
- Morton, J.W. (2003): Summary report on the Lorraine-Jajay property, Omineca Mining Division, B.C; internal report for Eastfield Resources, 20 pages.
- Nixon, G.T., and Peatfield, G.R. (2003): Geological setting of the Lorraine Cu-Au porphyry deposit, Duckling Creek Syenite Complex, North-central British Columbia; *B.C. Ministry of Energy and Mines*, Open File 2003-4, 24 pages.
- Ohmoto, H. and Rye, R.O. (1979): Isotopes of sulfur and carbon; *in* Geochemistry of Hydrothermal Ore Deposits, Barnes, H.L., Editor, *John Wiley & Sons*, New York, pages 509-567.
- Robinson, B.W. and Kusakabe, M. (1975): Quantitative preparation of sulfur dioxide for $^{34}\text{S}/^{32}\text{S}$ analyses, from sulfides by combustion with cuprous oxide; *Analytical Chemistry*, Volume 47, pages 1179-1181.
- Ross, K.V. (2004): Alteration study of the Northeast Zone, Mount Polley Mine, British Columbia; report prepared for Imperial Metals Corporation, April 25, 2004.
- Ross, K.V., Godwin, C.I., Bond, L. and Dawson, K.M. (1995): Geology, alteration and mineralization of the Ajax East and Ajax West copper-gold alkalic porphyry deposits, southern Iron Mask Batholith, Kamloops, British Columbia; *in* Porphyry Deposits of the Northwestern Cordillera of North America, Schroeter, T.G., Editor, *Canadian Institute of Mining, Metallurgy, and Petroleum*, Special Volume 46, pages 565-580.
- Shannon, S.S., Finch, R.J., Ikramuddin, M. and Mutschler, F. E. (1983): Possible sedimentary sources of sulfur and copper in alkaline-suite porphyry-copper systems; *in* Abstracts with Programs, *Geological Society of America* (September 1983), Volume 15, no 6, page 684.
- Simpson, R.G. (2003): Independent technical report for the Galore Greek Property; internal report for SpectrumGold Inc., 65 pages.
- Snyder, L.D. and Russell, J.K. (1995): Petrogenetic relationships and assimilation processes in the alkalic Iron Mask Batholith; *in* Porphyry Deposits of the Northwestern Cordillera of North America, Schroeter, T.G., Editor, *Canadian Institute of Mining, Metallurgy, and Petroleum*, Special Volume 46.
- Stanley, C.R. (1993): A thermodynamic geochemical model for the co-precipitation of gold and chalcopyrite in alkalic porphyry copper-gold deposits; MDRU Annual Technical Report for "Copper-Gold Porphyry Systems of British Columbia", Year 2, *The University of British Columbia*, Vancouver, B.C.
- Wilson, A. (2003): The genesis and exploration context of porphyry copper-gold deposits in the Cadia district, NSW; unpublished PhD thesis, *University of Tasmania*, Australia.
- Wilson, A., Cooke, D.R. and Thompson, J.F.H. (2002): Alkalic and high-K calc-alkalic porphyry Au-Cu deposits: A summary; *in* Giant Ore Deposits: Characteristics, Genesis and Exploration, Cooke, D.R., and Pongratz, J., Editors, *CODES Special Publication 4*, pages 51-55.
- Wolfe, R.C. 2001, Geology of the Didipio region and paragenesis of the Dinkidi Cu-Au porphyry deposit; unpublished PhD thesis, *University of Tasmania*, Australia, 200 pages.

Wrangellia Terrane on Vancouver Island, British Columbia: Distribution of Flood Basalts with Implications for Potential Ni-Cu-PGE Mineralization in Southwestern British Columbia

By A.R. Greene¹, J.S. Scoates¹ and D. Weis¹

KEYWORDS: Wrangellia, large igneous province, basalt, contamination, Ni-Cu-PGE mineralization

INTRODUCTION

Wrangellia consists largely of an oceanic plateau, a vast outpouring of basalt and more Mg-rich magma that erupted onto the ocean floor and was subsequently accreted to the western margin of the North American plate. Flood basalts form extensive sequences on Vancouver Island and are believed to have formed by melting in a mantle plume (an upwelling zone of hot mantle rock). They form the oceanic variety of a Large Igneous Province (LIP). A peculiarity of the Wrangellia plateau is that it erupted into an extinct island arc.

The continental equivalents of oceanic plateaus are the hosts of world-class ore deposits. The Ni-Cu-PGE (platinum group elements) deposit of the Noril'sk-Talnakh region in Siberia, arguably the richest ore deposit in the world, is located in intrusions related to the Siberian LIP. Here the assimilation of S-bearing sedimentary rocks by picritic (high-MgO) magma led to the segregation of Ni- and PGE-rich magmatic sulphides. Other examples are the deposits of the Raglan region in northern Quebec, and possibly those of the Manitoba Ni belt, where komatiitic magmas interacted with argillaceous sediments, again leading to the formation of large and rich magmatic sulphide deposits.

Although many showings of Ni-sulphides are present in Wrangellia, no major ore deposits are known. Hulbert (1997) undertook a long-term appraisal of the intrusive complexes in the Yukon segment of the terrane. Although he showed that the mineralization resembles that at Noril'sk and Raglan, no large economically exploitable accumulations have as yet been found. This is surprising, because the essential ingredients required to form a Noril'sk-type deposit — the emplacement of hot, Ni- and PGE-rich picritic magmas into S-bearing sediments —

appear to be present. In this respect, Wrangellia is a much more reasonable exploration target than many other oceanic and continental plateaus where the underlying crust consists mainly of granitic or ultramafic rocks.

The ongoing study seeks to provide insight into the potential for Ni-Cu-PGE mineralization for the portion of the Wrangellia Terrane on Vancouver Island. This overview is a preliminary report of fieldwork and a summary of previous research. This study represents one important aspect of a larger study on the significance of the Wrangellia Terrane as a giant accreted oceanic plateau. Oceanic plateaus are enigmatic phenomena that represent the largest known magmatic events on Earth. Such enormous volumes of magma erupt over geologically short time intervals (several million years) and, in addition to potentially generating world-class ore deposits, their formation may have catastrophic effects on the climate and biosphere. There are few well-preserved examples of accreted oceanic plateaus. Exposures of Triassic Wrangellia flood-volcanic sequences represent one of the finest examples of an accreted oceanic plateau worldwide. These lava sequences offer an exceptional opportunity to closely examine the on-land remains of an oceanic plateau and to assess criteria for evaluating Ni-Cu-PGE mineralization potential.

TECTONIC SETTING OF THE WRANGELLIA TERRANE

The Wrangellia Terrane is a complex and variable terrane that extends from Vancouver Island to central Alaska (Fig. 1). Wrangellia is most commonly characterized by widespread exposures of Triassic flood basalts and complementary intrusive rocks (Jones *et al.*, 1977). Triassic flood basalts extend in a discontinuous belt from Vancouver and Queen Charlotte Islands (Karmutsen Formation), through southeast Alaska and the Kluane Ranges in southwest Yukon, and into the Wrangell Mountains and Alaska Range in east and central Alaska (Nikolai Formation). This belt of flood basalt sequences has distinct similarities and is recognized as representing a once-contiguous terrane (Jones *et al.*, 1977).

¹ Pacific Centre for Isotopic and Geochemical Research, Department of Earth and Ocean Sciences, University of British Columbia

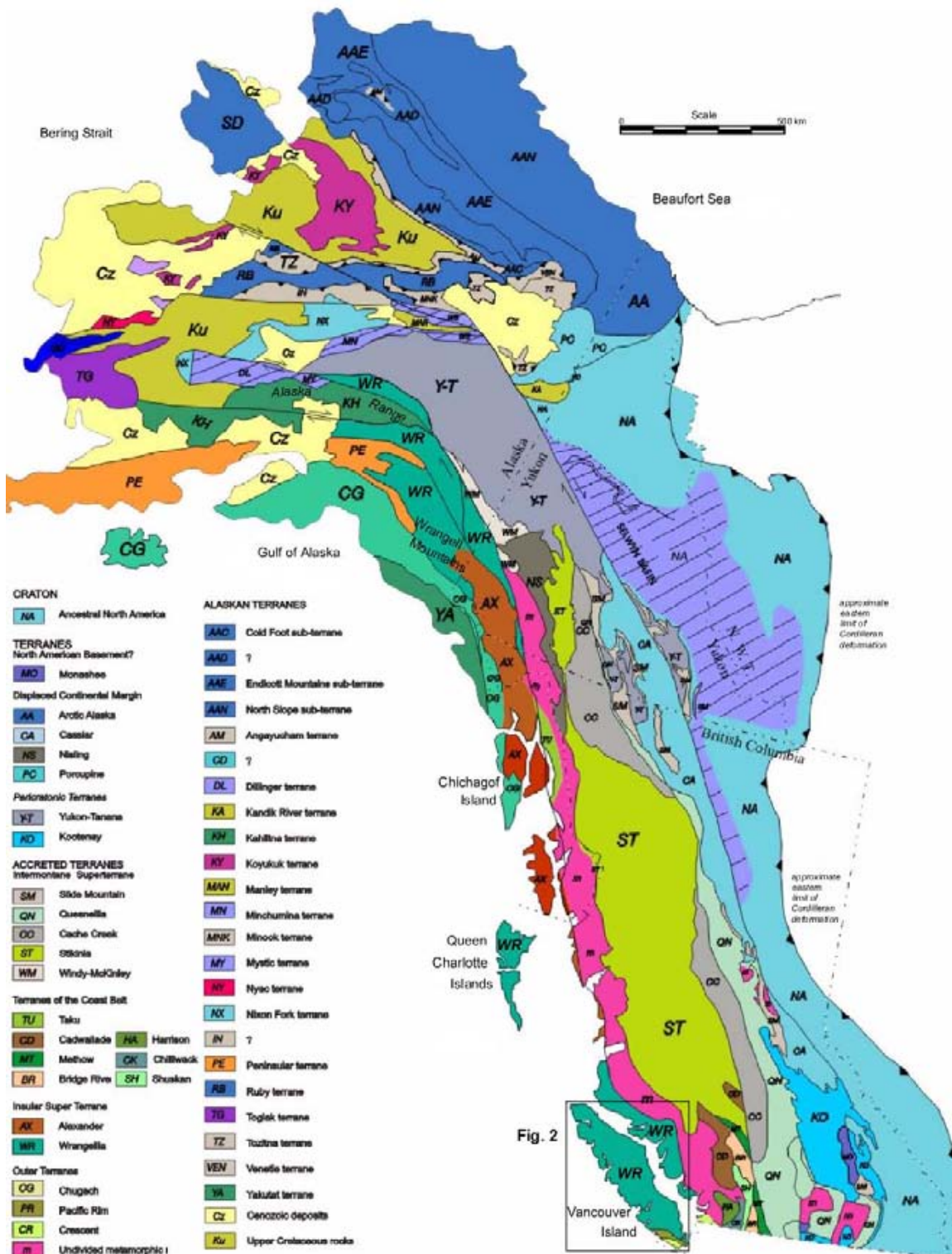


Figure 1. Terrane map of western Canada and Alaska (modified after Wheeler *et al.* [1991]) showing the distribution of the Wrangellia Terrane (WR) in British Columbia, the Yukon and Alaska.

Wrangellia has a long and diverse geologic history spanning much of the Phanerozoic. On Vancouver Island, the oldest rocks of Wrangellia, which lie at the top of an imbricated stack of northeast-dipping thrust sheets (Monger and Journeay, 1994), are Late Silurian to Early Permian arc sequences (Muller, 1980; Brandon *et al.*, 1986; Sutherland Brown *et al.*, 1986). In the Late Triassic, rapid uplift associated with a rising plume head lead to eruption of voluminous flood basalts as part of an extensive oceanic plateau (Richards *et al.*, 1991). As volcanism ceased, the oceanic plateau soon began to subside and accumulate deep-water carbonate sediments (Jeletzky, 1970; Carlisle and Suzuki, 1974). Sedimentation within the Wrangellia Terrane lasted until the Early Jurassic, when the resurgence of arc volcanism developed in response to subduction, forming the Bonanza arc (Armstrong and MacKevett, 1977; DeBari, 1990)

The enormous exposures of the Karmutsen appear to represent a single flood basalt event (Richards *et al.*, 1989). A mantle plume initiation model has been proposed for the Wrangellia flood basalts based on (1) relatively limited geochemical data, (2) the nature of the underlying and overlying formations, (3) rapid uplift prior to volcanism, (4) the lack of evidence of rifting associated with volcanism and (5) the short duration and high eruption rate of volcanism (Richards *et al.*, 1991). The basalt flows are estimated to have erupted a minimum volume of $1 \times 10^6 \text{ km}^3$ (Panuska, 1990) within a maximum of five million years (Carlisle and Suzuki, 1974).

During the 80 million years or so between arc activity and emergence of oceanic plateau flood basalts, as the continents gathered into a great landmass, Wrangellia became part of a composite terrane (Plafker *et al.*, 1989). By the Middle Pennsylvanian, Wrangellia may have joined with the Alexander Terrane (Gardner *et al.*, 1988) or been in close proximity (stratigraphic continuity) with the Alexander Terrane (Yorath *et al.*, 1985). The ocean-bound Wrangellia Terrane amalgamated with the Taku Terrane of southeast Alaska and the Peninsular Terrane of southern Alaska by as early as the Late Triassic (Plafker *et al.*, 1989). Paleomagnetic and faunal evidence indicate the Wrangellia Terrane originated far to the south of its present position (Hillhouse, 1977; Yole and Irving, 1980; Hillhouse *et al.*, 1982; Hillhouse and Gromme, 1984). Wrangellia accreted to the North American craton by the Late Jurassic or Early Cretaceous (Monger *et al.*, 1982; Tipper, 1984; Plafker *et al.*, 1989; Gehrels and Greig, 1991; van der Heyden, 1992; Monger *et al.*, 1994).

GEOLOGIC SETTING OF THE KARMUTSEN FORMATION

Widespread areas of British Columbia are underlain by the distinctive flood basalt sequences of the Karmutsen Formation (Fig. 2). Approximately 35% of northern and central Vancouver Island consists of Karmutsen basalt (Barker *et al.*, 1989). Exposures of the Karmutsen are also

extensive on the southern Queen Charlotte Islands, although the base of the formation is not exposed. On Vancouver Island, both underlying island arc rocks of the Paleozoic Sicker Group and the Karmutsen Formation are intruded by mafic sills thought to be associated with the Karmutsen (Barker *et al.*, 1989). The Karmutsen Formation is commonly intercalated with small lenses of marine sediments and is capped by shallow-water limestone (Carlisle and Suzuki, 1974).

The earliest in-depth studies of the Karmutsen Formation on Vancouver Island were made by J.E. Muller and co-workers (Muller, 1967; Muller and Carson, 1969; Muller *et al.*, 1974; Muller, 1977, 1981; Muller *et al.*, 1981) and D. Carlisle and his students (Carlisle, 1963; Surdam, 1968; Carlisle, 1972; Kuniyoshi, 1972; Carlisle and Suzuki, 1974). This initial work established the location, characteristics, and depositional history of the Triassic volcanic sequences. Units were subsequently mapped and described in further detail by G.T. Nixon and co-workers (Nixon *et al.*, 1993; Nixon *et al.*, 1994; Nixon *et al.*, 1994) on northern Vancouver Island and N.W.D. Massey and co-workers (Massey and Friday, 1988, 1989; Massey, 1995a, 1995b, 1995c) on central Vancouver Island.

The Karmutsen Formation forms thick flood-volcanic sequences throughout the densely-forested regions of northern and central Vancouver Island. The predominantly extrusive, marine sequences locally exceed 6000 m in thickness (Carlisle and Suzuki, 1974), however, extensive faulting throughout the Karmutsen makes reconstruction of the stratigraphic thickness challenging. Diagnostic units of the Karmutsen are often divided into (1) a lower member of exclusively pillow lava ($2500 \pm 150 \text{ m}$) (2) a middle member of pillow breccia and aquagene tuff (600–1100 m) and (3) an upper member of massive basalt flows ($2600 \pm 150 \text{ m}$) (Carlisle & Suzuki, 1974) (Fig. 3).

Basalts of the Upper Triassic Karmutsen preserve both a submarine and subaerial history of eruption for the oceanic plateau. The Karmutsen Formation contains a much larger proportion of submarine basalts than the predominantly subaerial Nikolai “Greenstone” in Alaska, however, there are subaerial flows in the uppermost sequences of the Karmutsen and submarine basalts near the base of the Nikolai (Muller *et al.*, 1974; Jones *et al.*, 1977). Concordant massive subaerial flows preserve no evidence of erosional surfaces between flows and lack any significantly thick or laterally continuous trace of intravolcanic sediments. The “essentially homogeneous” flood basalts (Barker *et al.*, 1989; Richards *et al.*, 1991; Lassiter *et al.*, 1995; Yorath *et al.*, 1999) formed as an enormous lava pile beneath, close to, and above the surface of the ocean within a geologically short time span.

The age of flood basalts of the Karmutsen is bracketed by fossils in the underlying and overlying sedimentary units. Eruption of Wrangellia flood basalts possibly occurred in their entirety within 2.5 to 3.5 million years (early Upper Ladinian to early Upper Car-

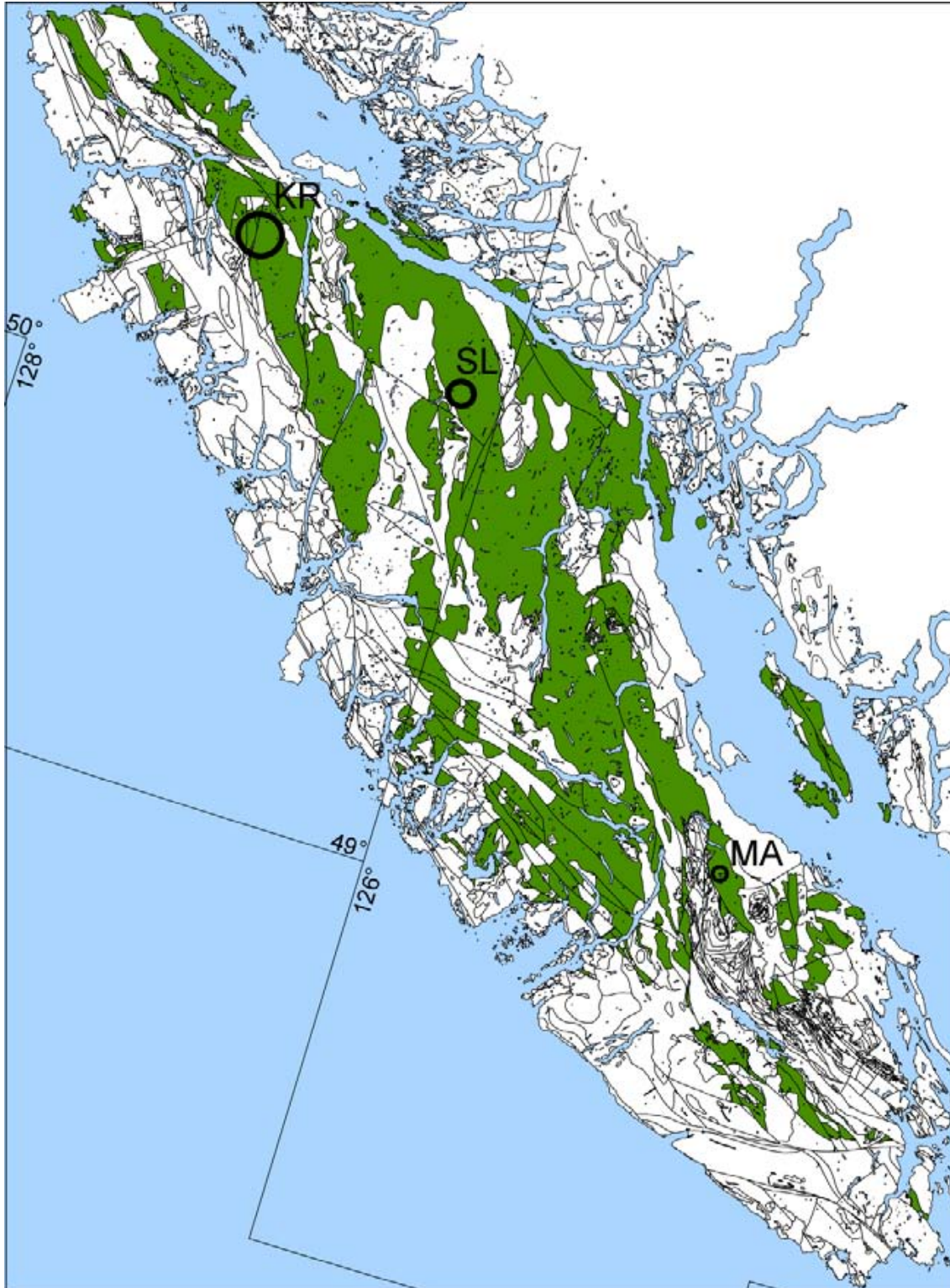


Figure 2. Map of Vancouver Island showing exposures of flood basalt from the Karmutsen Formation (green) (after Massey *et al.*, [2003a, 2003b]). Areas of field study discussed in the text are outlined with black circles, from north to south (west of the Karmutsen Range [KR], east of Schoen Lake [SL], and Mount Arrowsmith [MA]).

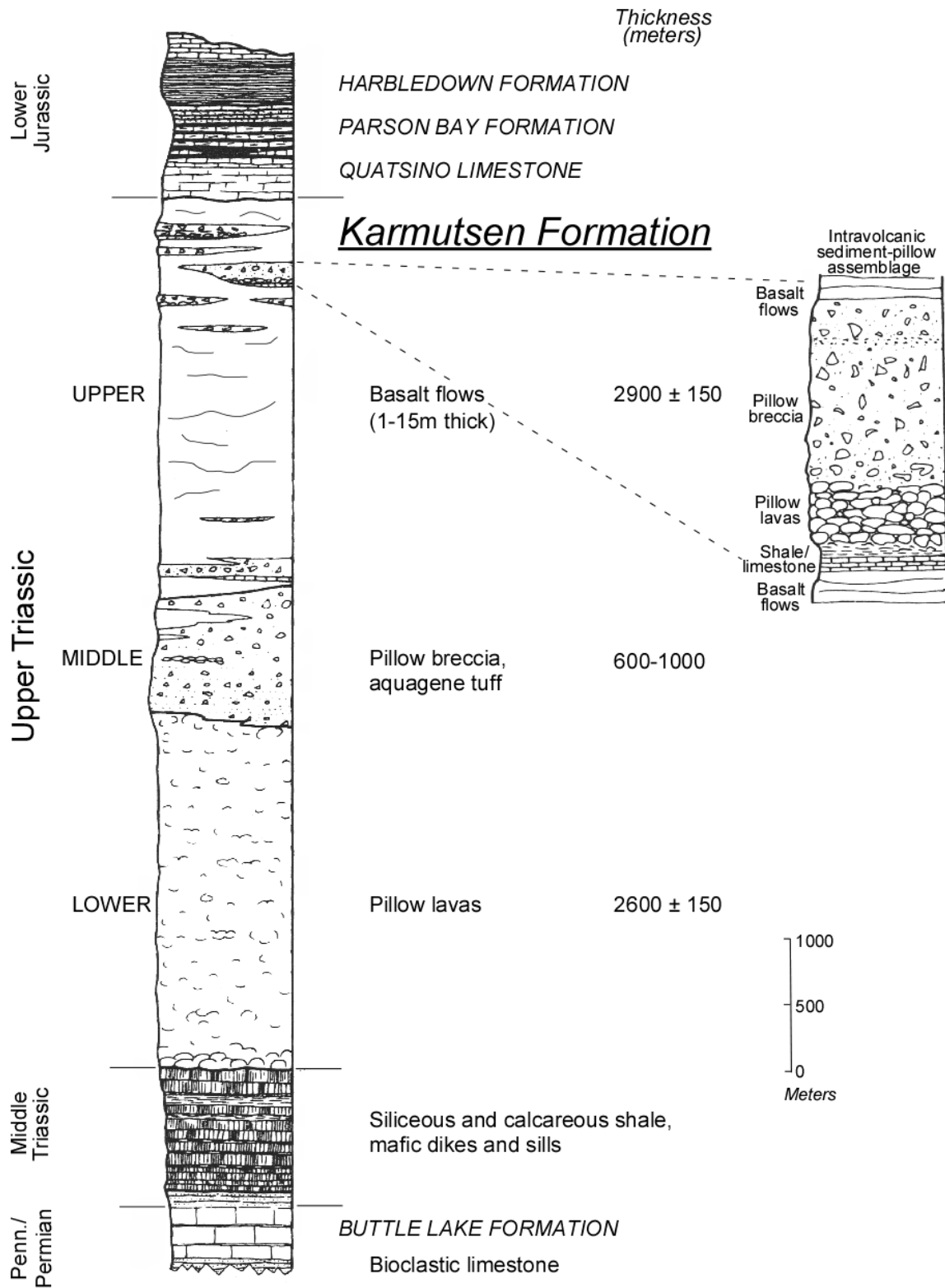


Figure 3. Composite stratigraphic column depicting flood basalt sequences of the Karmutsen Formation and major sedimentary sequences on northern Vancouver Island (modified after Carlisle and Susuki [1974]).

nian—middle Triassic) (Carlisle and Suzuki, 1974). Zircon ages for related intrusive units on Vancouver Island corroborate these bracketing ages (217–222 Ma [Isachsen *et al.*, 1985]; 227 ± 3 Ma [Parrish and McNicoll, 1992]). Conodonts and zircons dated in Nikolai volcanics in Alaska and the Yukon also indicate a Carnian age (Plafker *et al.*, 1989; Mortensen and Hulbert, 1991).

The size of the area sampled in this study represents a small portion of the overall exposure of Wrangellia flood basalts. However, these areas consist of exposures of each of the three members in previously unsampled areas for high-precision isotopic and trace-element analyses. In addition, field observations and sampling in the Yukon and Alaska will be beneficial for comparison to relationships on Vancouver Island.

DESCRIPTION OF THE STUDY AREA

Field studies were undertaken in July, 2004 to investigate Wrangellia flood basalts on Vancouver Island. Prior to undertaking fieldwork, published literature and maps were evaluated for the selection of target areas. Discussions with Nick Massey and Graham Nixon, of the British Columbia Ministry of Energy and Mines Geological Survey Branch, were also beneficial for selecting optimal field areas. The selection of areas was based on accessibility, potential for exposure of thick stratigraphic sequences, and minimal faulting. The three areas chosen were Mount Arrowsmith on the central part of Vancouver Island, and east of Schoen Lake Provincial Park and west of the Karmutsen Range on the northern third of Vancouver Island (Fig. 2). With the exception of Mount Arrowsmith, these areas have not seen extensive sampling for geochemical studies.

Reconnaissance of these areas indicates that complete sections of the volcanic flood basalt sequences are not present in any one area. However, thick sections and isolated exposures of pillow lavas, pillow breccias and massive flows are well-exposed and accessible, primarily along logging roads. The degree of faulting, dense vegetation cover and the steep nature of the terrain made assessment of the stratigraphy difficult in particular areas. Fifty evenly distributed samples were collected for petrographic and geochemical analysis. Special care was taken to sample the freshest appearing basalts and cover the extent of the exposed Triassic stratigraphy.

Of the three study areas, exposures on Mount Arrowsmith preserve the most extensive stratigraphy. The thickness of the exposure (~3000 m) is approximately half that exposed at Buttle Lake (~6000 m), however, proportions of each of the members are comparable (Yorath *et al.*, 1985). The basal pillow lavas are easily distinguished by their globular form, selvage rims and interstitial filling (Photos 1 and 2). Pillow basalt is overlain by accumulations of broken pillow fragments (pillow breccia) with no easily-recognizable bedding (Photo 3). This unit is thick (~1000 m), widespread and

fairly uniform in thickness in the area (Yorath *et al.*, 1985). The pillow breccia may have formed as the result of a varied eruptive stage where stacks of pillows emerging from young lava centres collapsed due to an increased level of magma flux or seismic activity (Yorath *et al.*, 1985).

Exposures of basalt in the area east of Schoen Lake Provincial Park are densely vegetated and difficult to access. This area was explored in detail by D. Carlisle (Carlisle, 1972), but has not been the focus of any geological investigation since. All three members of the Karmutsen are exposed in roadcuts in this area. On the west side of the Karmutsen Range, between Nimpkish Lake and Victoria Lake, the terrain is dissected by an extensive network of logging roads with exposures in roadcuts primarily preserving massive lava flows and isolated exposures of pillow basalt lower in the section.

Massive lava flows, exposed in each of the previously described areas, are generally 1 to 15 m thick and exhibit coarser grain size than the pillow basalt unit (Photo 4). Amygdules are prevalent throughout individual flows, which commonly reveal uneven contacts with no discernible erosional surface, columnar jointing or substantial thickness of intercalated sediment. Comagmatic dikes or sills are rare in these areas and difficult to distinguish. The basalt flows are found to be rarely interbedded with thin, lenticular beds of both marine and non-marine sediments, however, most of the flows appear to have erupted subaerially or in shallow water, which precluded significant deposition (Carlisle and Suzuki, 1974).

MAGMATIC SULPHIDE DEPOSITS IN THE WRANGELLIA TERRANE OF BRITISH COLUMBIA?

The intrusive centres linked to the overlying Wrangellia flood basalts represent one of the largest belts of Ni-Cu-PGE-bearing mafic and ultramafic rocks in North America (Hulbert, 1997). Geochemical variations in the Wrangellia flood basalts preserve a record, as yet undeciphered, of the evolution of magmas within upper crustal magma chambers or sills and interactions with local contaminants and deep crustal contaminants during ascent. At Noril'sk, the geochemistry of the flood basalts has been used as an indication of the likelihood that complementary intrusive rocks contain Ni-Cu-PGE deposits (*e.g.*, Naldrett and Lightfoot, 1993) and the geochemistry of the intrusive rocks has been successfully used to constrain the role of staging chambers for crustal contamination and sulphide segregation within magmas prior to eruption (*e.g.*, Arndt *et al.*, 2003). In contrast, there has been limited geochemical examination of the intrusive complexes of the Wrangellia Terrane, other than the Kluane Mafic-Ultramafic Belt (Hulbert, 1997). More importantly, in proportion to their vast aerial exposure,



Photo 1. Cross-section of a stack of closely packed, asymmetric basalt pillows with what were originally glassy pillow rinds west of the Karmutsen Range (626835 E, 5586081 N). The pillows have features indicating formerly chilled rims and more massive interiors. These features indicate eruption in a relatively deep marine setting. Geologic hammer (~80 cm) for scale.



Photo 2. Close-up of Photo 1, showing pillow basalt with areas of concentrations of vesicles. Geologic hammer (~80 cm) for scale.



Photo 3. Pillow breccia with angular, blocky clasts in a fine-grained matrix east of Schoen Lake (709745 E, 5567557 N). Geologic hammer (~40 cm) for scale.



Photo 4. Massive basalt flows near Keogh Lake, west of the Karmutsen Range (627605 E, 5595029 N). Arrows (~2 m) indicate possible contacts between flows. Most flows have concentrations of amygdules (~5-15% volume) filled with chlorite, quartz and calcite. Flow tops do not appear brecciated.

minimal attention has been given to the thick sequences of flood basalts (*e.g.*, Barker *et al.*, 1989; Lassiter *et al.*, 1995).

In this ongoing study, detailed geochemical (major and trace elements, PGE) and isotopic studies (Pb-Sr-Nd-Hf) of the Wrangellia flood basalts on Vancouver Island will be used to critically test the relative importance of different components on the formation of magmatic sulphide deposits (*e.g.*, magma composition, nature and relative age of wallrock, extent of contamination, prior sulphide segregation, tectonic setting). Hulbert (1997) stated the possibility that olivine-rich basalt flows (picritic basalts) and mafic and ultramafic intrusions may be restricted to the Yukon segment of Wrangellia as a result of their formation in proximity to the hotter axial "jet" of the mantle plume. However, this aspect of the Wrangellia flood basalt province is poorly understood due to the lack of comparative studies. To assess the significance of primitive S-undersaturated magmas, crustal contamination, and high-level magmatic processes, it is important to understand the relative contributions to the magmas from the plume source and the lithosphere (Lightfoot and Hawkesworth, 1997). This, in turn, will provide insight into the potential for Ni-Cu-PGE mineralization in the British Columbia part of the Wrangellia Terrane.

The nature of the basement rock is likely crucial to the formation of magmatic Ni-Cu-PGE deposits in flood basalt provinces. Late Paleozoic sediments underlie Wrangellia flood basalts on Vancouver Island, as well as in the Kluane Ranges and Wrangell Mountains (Muller, 1967; Jones *et al.*, 1977). Zoned, sill-like mafic and ultramafic bodies, representing subvolcanic magma chambers for the overlying Triassic flood basalts, appear to preferentially intrude particular sequences of Late Paleozoic sediments within the Kluane Ranges (Hulbert, 1997). These relationships indicate that S- and Ba-rich sediments may have been integral to contaminating magmas and initiating sulphide immiscibility (Hulbert, 1997). Is this the case for flood basalts and intrusive sills within the Wrangellia Terrane in British Columbia? What does the geochemistry of the Wrangellia flood basalts and intrusions in British Columbia tell us about the likelihood of Ni-Cu-PGE deposits in this part of the terrane? And on a regional scale, what is the relationship between magma composition, wallrock, age and tectonic setting throughout the entire Wrangellia Terrane?

ONGOING AND PLANNED RESEARCH

We are presently preparing 50 samples for high-precision analytical work to help answer these questions. Presently, samples are being prepared for analysis of major and trace elements, and radiogenic isotopes at the Pacific Centre for Isotopic and Geochemical Research (PCIGR) at the University of British Columbia (UBC). Careful procedures are being used to avoid any

contamination of samples during crushing. Petrographic thin-sections for all the samples are also currently being analyzed for their mineralogy and texture.

We plan a thorough evaluation of the petrology, geochronology and geochemistry of flood basalts in the Wrangellia Terrane. Particular emphasis will be placed on determining the extent of crustal contamination in the Wrangellia magmatic suite by local sedimentary sources and/or by lower crustal material. Due to the lack of a comprehensive geochemical database for Wrangellia, especially for the British Columbia portion, this requires the acquisition of a large, internally consistent geochemical database with element concentrations and isotopic ratios measured in the same laboratory. Ratios of low-abundance trace elements are very sensitive to differences in sources and contaminants (*e.g.*, Nb/La, La/Sm, Ba/Th, Sr/Nd, Pb/Nd), while combining different radiogenic isotopic systems (*e.g.*, Pb-Pb, Rb-Sr, Sm-Nd, Lu-Hf) with different geochemical behaviours and relative ratios for the parent and daughter isotopes can precisely fingerprint source components (*e.g.*, enriched mantle, depleted mantle, arc crust, sediments). Select samples will be precisely dated (Ar-Ar) to provide absolute time constraints on magmatism in the Wrangellia Terrane of British Columbia. It will also be essential to evaluate relative PGE enrichment-depletion in the basalts and intrusions. Finally, the Ni contents of olivine will be systematically determined in all olivine-bearing lavas and intrusions to monitor the effects of sulphide segregation in this large magmatic system.

We plan to complete the compilation of geological information for the entire Wrangellia Terrane (British Columbia, Yukon and Alaska). The major goal of the compilation work is to constrain the location, areal significance and stratigraphic location of intrusions and sedimentary sequences. Additional field studies planned in the Yukon and Alaska during the summer of 2005 will be beneficial to the work on Vancouver Island. Insights gained here, in regions of relatively minor faulting, will be applied to Wrangellia exposures in British Columbia where structural complexity is more evident.

The ultimate goal of this project is the establishment of criteria for evaluating the Ni-Cu-PGE mineralization potential of the Wrangellia Terrane in British Columbia. This will be accomplished through integration of field, petrologic, geochemical and geochronologic constraints of volcanic sequences. The criteria for magmatic Ni-Cu-PGE sulphide mineralization in the Wrangellia Terrane established in this project should help to attract mineral exploration programs in British Columbia and aid mineral exploration companies in refining their existing exploration models.

ACKNOWLEDGMENTS

Funding for this project has been generously provided by the Rocks to Riches Program administered by

the British Columbia and Yukon Chamber of Mines. We would also like to thank Nick Massey and Graham Nixon, of the British Columbia Ministry of Energy and Mines Geological Survey Branch, for their insightful discussions and Nick Arndt for helping to initiate the mineralization potential study.

REFERENCES

- Armstrong, A.K. and MacKevett, E.M., Jr. (1977): The Triassic Chitstone Limestones, Wrangell Mountains, Alaska; *United States Geological Survey*, Open File Report 77-217, pages D49-D62.
- Arndt, N.T., Czamanske, G.K., Walker, R.J., Chauvel, C. and Fedorenko, V.A. (2003): Geochemistry and origin of the intrusive hosts of the Noril'sk-Talnakh Cu-Ni-PGE sulfide deposits; *Economic Geology*, Volume 98, pages 495-515.
- Barker, F., Brown, A.S., Budahn, J.R. and Plafker, G. (1989): Back-arc with frontal-arc component origin of Triassic Karmutsen basalt, British Columbia, Canada; *Chemical Geology*, Volume 75, pages 81-102.
- Brandon, M.T., Orchard, M.J., Parrish, R.R., Brown, A.S. and Yorath, C.J. (1986): Fossil ages and isotopic dates from the Paleozoic Sicker Group and associated intrusive rocks, Vancouver Island, British Columbia; Current Research, Part A, *Geological Survey of Canada*, Paper 86-1A, pages 683-696.
- Carlisle, D. (1963): Pillow breccias and their aquagene tuffs, Quadra Island, British Columbia; *Journal of Geology*, Volume 71, pages 48-71.
- Carlisle, D. (1972): Late Paleozoic to Mid-Triassic sedimentary-volcanic sequence on Northeastern Vancouver Island; *Geological Society of Canada*, Paper, 72-1, Part B, pages 24-30.
- Carlisle, D. and Suzuki, T. (1974): Emergent basalt and submergent carbonate-clastic sequences including the Upper Triassic Dilleri and Welleri zones on Vancouver Island; *Canadian Journal of Earth Sciences*, Volume 11, pages 254-279.
- DeBari, S.M., Anderson, R.G. and Mortensen, J.K. (1999): Correlation Among Lower to Upper Crustal Components in an Island Arc: the Jurassic Bonanza arc, Vancouver Island, Canada; *Canadian Journal of Earth Sciences*, Volume 36, pages 1371-1413.
- Gardner, M.C., Bergman, S.C., Cushing, G.W., MacKevett, E.M., Plafker, G., Campbell, R.B., Dodds, C.J., McClelland, W.C. and Mueller, P.A. (1988): Pennsylvanian pluton stitching of Wrangellia and the Alexander terrane, Wrangell Mountains, Alaska; *Geology*, Volume 16, pages 967-971.
- Gehrels, G.E. and Greig, C.J. (1991): Late Jurassic detrital zircon link between the Alexander-Wrangellia terrane and Stikine and Yukon-Tanana terranes; *Geological Society of America*, Abstracts with Programs, Volume 23, page A434.
- Hillhouse, J.W. (1977): Paleomagnetism of the Triassic Nikolai Greenstone, McCarthy Quadrangle, Alaska; *Canadian Journal of Earth Sciences*, Volume 14, pages 2578-3592.
- Hillhouse, J.W. and Gromme, C.S. (1984): Northward displacement and accretion of Wrangellia: New paleomagnetic evidence from Alaska; *Journal of Geophysical Research*, Volume 89, pages 4461-4467.
- Hillhouse, J.W., Gromme, C.S. and Vallier, T.L. (1982): Paleomagnetism and Mesozoic tectonics of the Seven Devils volcanic arc in northeastern Oregon; *Journal of Geophysical Research*, Volume B. 87, pages 3777-3794.
- Hulbert, L.J. (1997): Geology and metallogeny of the Klauane mafic-ultramafic belt, Yukon Territory, Canada: eastern Wrangellia - a new Ni-Cu-PGE metallogenic terrane; *Geological Survey of Canada*, Bulletin, 506, 265 pages.
- Isachsen, C., Armstrong, R.L. and Parrish, R.R. (1985): U-Pb, Rb-Sr, and K-Ar geochronometry of Vancouver Island igneous rocks; *Geological Association of Canada*, Victoria Section Symposium (abstr.), pages 21-22.
- Jeletzky, J.A. (1970): Some salient features of Early Mesozoic history of Insular Tectonic Belt, western British Columbia; *Geological Survey of Canada*, Paper 69-14, 26 pages.
- Jones, D.L., Silberling, N.J. and Hillhouse, J. (1977): Wrangellia; a displaced terrane in northwestern North America; *Canadian Journal of Earth Sciences*, Volume 14, pages 2565-2577.
- Kuniyoshi, S. (1972): Petrology of the Karmutsen (Volcanic) Group, northeastern Vancouver Island, British Columbia; unpublished PhD thesis, *University of California*, 243 pages.
- Lassiter, J.C., DePaolo, D.J. and Mahoney, J.J. (1995): Geochemistry of the Wrangellia Flood Basalt Province: Implications for the Role of Continental and Oceanic Lithosphere in Flood Basalt Genesis; *Journal of Petrology*, Volume 36, pages 983-1009.
- Lightfoot, P.C. and Hawkesworth, C.J. (1997): Flood basalts and magmatic Ni, Cu, and PGE sulphide mineralization: Comparative geochemistry of the Noril'sk (Siberian Traps) and West Greenland sequences; in Large igneous provinces: continental, oceanic, and planetary flood volcanism, Mahoney, J.J. and Coffin, M.F., Editors, *American Geophysical Union*, Geophysical Monograph 100, pages 357-380.
- Massey, N.W.D. (1995a): Geology and mineral resources of the Alberni-Nanaimo Lakes sheet, Vancouver Island 92F/1W, 92F/2E, and part of 92F/7E; *British Columbia Ministry of Energy, Mines and Petroleum Resources*, Paper 1992-2, pages 1-132.
- Massey, N.W.D. (1995b): Geology and mineral resources of the Cowichan Lake sheet, Vancouver Island 92C/16; *British Columbia Ministry of Energy, Mines and Petroleum Resources*, Paper 1992-3, pages 1-112.
- Massey, N.W.D. (1995c): Geology and mineral resources of the Duncan sheet, Vancouver Island 92B/13; *British Columbia Ministry of Energy, Mines and Petroleum Resources*, Paper 1992-4, pages 1-112.
- Massey, N.W.D. and Friday, S.J. (1988): Geology of the Chemainus River-Duncan Area, Vancouver Island (92C/16; 92B/13); in Geological Fieldwork 1987, *British Columbia Ministry of Energy, Mines and Petroleum Resources*, Paper 1988-1, pages 81-91.
- Massey, N.W.D. and Friday, S.J. (1989): Geology of the Alberni-Nanaimo Lakes Area, Vancouver Island (91F/1W, 92F/2E and part of 92F/7); in Geological Fieldwork 1987, *British Columbia Ministry of Energy, Mines and Petroleum Resources*, Paper 1989-1, pages 61-74.

- Massey, N.W.D., MacIntyre, D.G., Desjardins, P.J. (2003a): Digital Map of British Columbia: Tile NM9 Mid Coast, B.C.; *B.C. Ministry of Energy and Mines*, Geofile 2003-4.
- Massey, N.W.D., MacIntyre, D.G., Desjardins, P.J. (2003b): Digital Map of British Columbia: Tile NM10 Southwest B.C.; *B.C. Ministry of Energy and Mines*, Geofile 2003-3.
- Monger, J.W.H. and Journeay, J.M. (1994): Basement geology and tectonic evolution of the Vancouver region; in *Geology and Geological Hazards of the Vancouver Region, Southwestern British Columbia*, Monger, J.W.H., Editor, *Geological Survey of Canada*, Bulletin 481, pages 3-25.
- Monger, J.W.H., Price, R.A. and Tempelman-Kluit, D.J. (1982): Tectonic accretion and the origin of the two major metamorphic and plutonic belts in the Canadian Cordillera; *Geology*, Volume 10, pages 70-75.
- Monger, J.W.H., van der Heyden, P., Journeay, J.M., Evenchick, C.E. and Mahoney, J.B. (1994): Jurassic-Cretaceous basins along the Canadian Coast Belt: Their bearing on pre-mid-Cretaceous sinistral displacements; *Geology*, Volume 22, pages 175-178.
- Mortensen, J.K. and Hulbert, L.J. (1991): A U-Pb zircon age for a Maple Creek gabbro sill, Tatamagouche Creek area, southwestern Yukon Territory; *Geological Survey of Canada*, Paper 91-2, pages 175-179.
- Muller, J.E. (1967): Kluane Lake map area, Yukon Territory; *Geological Survey of Canada*, Memoir, 137 pages.
- Muller, J.E. (1977): Evolution of the Pacific Margin, Vancouver Island, and adjacent regions; *Canadian Journal of Earth Sciences*, Volume 14, pages 2062-2085.
- Muller, J.E. (1980): The Paleozoic Sicker Group of Vancouver Island, British Columbia; *Geological Survey of Canada*, Paper 79-30, 22 pages.
- Muller, J.E. (1981): Insular and Pacific Belts; in *Cordilleran Cross-section- Calgary to Victoria*, Field Guide 1981, Price, R.A., Monger, J.W.H. and Muller, J.E., Editors, *Geological Association of Canada*, pages 261-334.
- Muller, J.E., Cameron, B.E.B. and Northcote, K.E. (1981): Geology and mineral deposits of Nootka Sound Map-Area, Vancouver Island, British Columbia; *Geological Survey of Canada*, Paper 80-16.
- Muller, J.E. and Carson, D.J.T. (1969): Geology and mineral deposits of the Alberni area, British Columbia; *Geological Survey of Canada*, Paper 68-50, 35 pages.
- Muller, J.E., Northcote, K.E. and Carlisle, D. (1974): Geology and mineral deposits of Alert Bay - Cape Scott map area, Vancouver Island, British Columbia; *Geological Survey of Canada*, Paper 74-8, 77 pages.
- Naldrett, A.J. and Lightfoot, P.C. (1993): A model for giant magmatic sulphide deposits associated with flood basalts; in *Giant Ore Deposits*, Whiting, B.H., Mason, R. and Hodgson, C.J., Editors, *Society of Economic Geologists*, Special Publication, pages 81-123.
- Nixon, G.T., Hammack, J.L., Hamilton, J.V. and Jennings, H. (1993): Preliminary geology of the Mahatta Creek area, northern Vancouver Island (92L/5); in *Geological Fieldwork 1992*, Grant, B. and Newell, J.M., Editors, *British Columbia Ministry of Energy, Mines and Petroleum Resources*, Paper 1993-1, pages 17-35.
- Nixon, G.T., Hammack, J.L., Koyanagi, V.M., Payie, G.J., Panteleyev, A., Massey, N.W.D., Hamilton, J.V. and Haggart, J.W. (1994): Preliminary Geology of the Quatsino - Port McNeill map areas, northern Vancouver Island (92L/12, 11); in *Geological Fieldwork 1993*, Grant, B. and Newell, J.M., Editors, *British Columbia Ministry of Energy, Mines and Petroleum Resources*, Paper 1994-1, pages 63-85.
- Nixon, G.T., Hammack, J.L., Payie, G.J., Snyder, L.D., Archibald, D.A. and Barron, D.J. (1994): Quatsino-San Josef map area, Northern Vancouver Island (92L/12W, 102I/8,9); in *Geological Fieldwork 1994*, Grant, B. and Newell, J.M., Editors, *British Columbia Ministry of Energy, Mines and Petroleum Resources*, Paper 1995-1, pages 9-21.
- Panuska, B.C. (1990): An overlooked, world class Triassic flood basalt event; *Geological Society of America*, Abstracts with Programs, Volume 22, page A168.
- Parrish, R.R. and McNicoll, V.J. (1992): U-Pb age determinations from the southern Vancouver Island area, British Columbia; in *Radiogenic Age and Isotopic Studies: Report 5*, *Geological Survey of Canada*, Paper 91-2, pages 79-86.
- Plafker, G., Nokleberg, W.J. and Lull, J.S. (1989): Bedrock geology and tectonic evolution of the Wrangellia, Peninsular, and Chugach terranes along the Trans-Alaskan Crustal Transect in the northern Chugach Mountains and southern Copper River basin, Alaska; *Journal of Geophysical Research*, Volume 94, pages 4,255-4,295.
- Richards, M.A., Duncan, R.A. and Courtillot, V. (1989): Flood basalts and hotspot tracks: plume heads and tails; *Science*, Volume 246, pages 103-107.
- Richards, M.A., Jones, D.L., Duncan, R.A. and DePaolo, D.J. (1991): A mantle plume initiation model for the Wrangellia flood basalt and other oceanic plateaus; *Science*, Volume 254, pages 263-267.
- Surdam, R.C. (1968): The stratigraphy and volcanic history of the Karmutsen group, Vancouver Island, British Columbia; *University of Wyoming*, Contributions to Geology, Volume 7, pages 15-26.
- Sutherland Brown, A., Yorath, C.J., Anderson, R.G. and Dom, K. (1986): Geological maps of southern Vancouver Island, LITHOPROBE I 92C/10, 11, 14, 16, 92F/1, 2, 7, 8; *Geological Survey of Canada*, Open File 1272.
- Tipper, H.W. (1984): The allochthonous Jurassic-Lower Cretaceous terranes of the Canadian Cordillera and their relation to correlative strata of the North American craton; *Geological Association of Canada*, Special Paper 27, pages 113-120.
- van der Heyden, P. (1992): A middle Jurassic to early Tertiary Andean-Sierran arc model for the coast belt of British Columbia; *Tectonics*, Volume 11, pages 82-97.
- Yole, R.W. and Irving, E. (1980): Displacement of Vancouver Island, paleomagnetic evidence from the Karmutsen Formation; *Canadian Journal of Earth Sciences*, Volume 17, pages 1210-1228.
- Yorath, C.J., Clowes, R.M., Green, A.G., Sutherland Brown, A., Brandon, M.T., Massey, N.W.D., Spencer, C., Kanasewich, E.R. and Hyndman, R.D. (1985): Lithoprobe - Phase 1: Southern Vancouver Island: Preliminary analyses of reflection seismic profiles and surface geological studies; in *Current Research*, part A, *Geological Survey of Canada*, Paper 85-1A, pages 543-554.

Yorath, C.J., Sutherland Brown, A. and Massey, N.W.D. (1999): LITHOPROBE, southern Vancouver Island, British Columbia; *Geological Survey of Canada*, Bulletin 498, 145 pages.

Wheeler, J.O., Brookfield, A.J., Gabrielese, H., Monger, J.W.H., Tipper, H.W. and Woodsworth, G.J. (1991): Terrane map of the Canadian Cordillera; *Geological Survey of Canada*, Map 1713, scale 1:1,000,000.

Spatsizi River Stream Sediment and Water Survey, Northwestern British Columbia (NTS 104H/1, 2, 3, 4, 5, 6, 7, 11, 12 & 13)

By Wayne Jackaman¹

KEYWORDS: mineral exploration, multi-element, stream sediment, stream water, National Geochemical Reconnaissance Program, Spatsizi Plateau

INTRODUCTION

During June 2004, a helicopter and truck supported drainage sediment and water survey was successfully completed in parts of the Spatsizi River map sheet (NTS 104H). The reconnaissance-scale program covered a 5000 km² area southwest of the Spatsizi Plateau Wilderness Provincial Park in northwestern British Columbia (Fig. 1). Funded by the BC and Yukon Chamber of Mines' Rocks to Riches program, all aspects of the sample collection, preparation and analysis activities have been conducted according to current National Geochemical Reconnaissance (NGR) program standards and specifications (Ballantyne, 1991). Survey results are expected to fit seamlessly into the existing provincial NGR and BC Regional Geochemical Survey (RGS) databases and will compliment the Bowser Lake (NTS 104A) NGR program that was also completed in 2004 (Lett *et al.*, 2005).

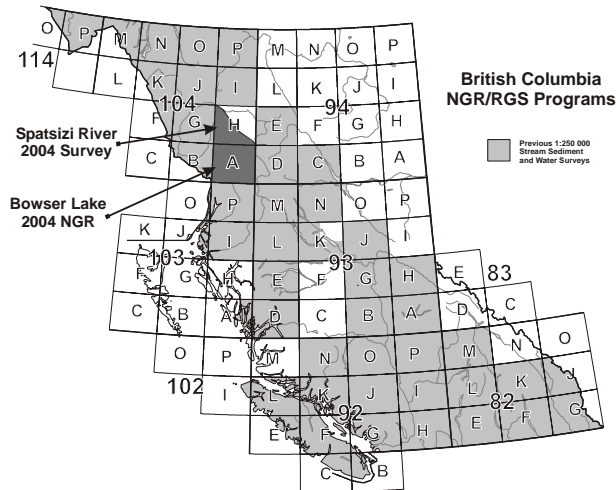


Figure 1: Location map of NGR surveys.

¹ 3011 Felderhof Road, Sooke, BC, V0S 1N0

REGIONAL SUMMARY

Situated approximately 300 km north of Terrace, the Spatsizi River map sheet can be accessed from Highway 37. Bordering the region to the west is the Iskut River Valley and the Klappan River Valley follows the park boundary along the northeast edge of the survey area. Helicopter support services are available at the Bob Quinn airstrip and limited road access exists at Coyote Creek and extends along an abandoned rail grade. Located within the Northern Skeena Mountain Range, the region is characterized by extreme variations in elevation, which range from high mountainous and heavily glaciated peaks (2500 to 2800 m) to low river valleys (less than 750 m).

The map sheet lies within the Stikinia Terrane of the Intermontane Belt (Fig. 2). The regional geology consists of the east-trending Stikine arch rocks along the northern portion of the map sheet and by the Bowser and Sustut basins over the remainder of the sheet. Mineralization found in the area includes vein and porphyry-style copper (gold, molybdenum) deposits, limestone bodies found along the southern flank of the Stikine arch and coal found in the Groundhog coalfield of the Bowser basin.

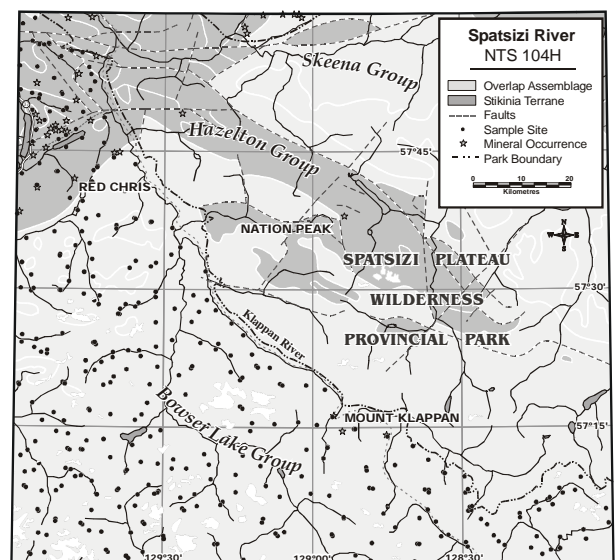


Figure 2: Generalized geology map showing sample sites and known mineral occurrences.

TABLE 1. DETECTION LIMITS: ICPMS (SEDIMENTS).

VARIABLE	D.L.	UNITS
Aluminium	0.01	%
Antimony	0.02	ppm
Arsenic	0.1	ppm
Barium	0.5	ppm
Bismuth	0.02	ppm
Cadmium	0.01	ppm
Calcium	0.01	%
Chromium	0.5	ppm
Cobalt	0.1	ppm
Copper	0.01	ppm
Gallium	0.2	ppm
Iron	0.01	%
Lanthanum	0.5	ppm
Lead	0.01	ppm
Magnesium	0.01	%
Manganese	1	ppm
Mercury	5	ppb
Molybdenum	0.01	ppm
Nickel	0.1	ppm
Phosphorus	0.001	%
Potassium	0.01	%
Scandium	0.1	ppm
Selenium	0.1	ppm
Silver	2	ppb
Sodium	0.001	%
Strontium	0.5	ppm
Sulphur	0.02	%
Tellurium	0.02	ppm
Thallium	0.02	ppm
Thorium	0.1	ppm
Titanium	0.001	%
Tungsten	0.1	ppm
Uranium	0.1	ppm
Vanadium	2	ppm
Zinc	0.1	ppm

The BC MINFILE database identifies only 37 known mineral occurrences in the map sheet including the Red Chris (104H 005) developed prospect. The porphyry-style copper-gold mineralization found at the East and Main zones of the Red Chris deposit is hosted by Tsaybahe Group volcanics, which have been intruded by hornblende-feldspar porphyry of monzonite composition. Indicated reserves of the combined zones are 39.6 million tonnes grading 0.28 g/t gold and 0.56% copper (Ash *et al.*, 1996).

SURVEY DETAILS

At an average sample site density of one site every 14 km², field observations, site location information and a total of 379 sediment and water samples were systematically collected from 360 sample sites (Fig. 2). In addition, 72 water samples (one in every five sites) were collected, filtered and acidified.

Aqua regia digestion-inductively coupled plasma mass spectroscopy (ICPMS) and epithermal instrumental neutron activation analysis (INAA) are the analytical methods being used to determine elements in stream sediments. Natural stream water samples were analyzed for pH and conductivity in the field and will be further analyzed for uranium. Multi-element ICP anal-

TABLE 2. DETECTION LIMITS: INAA, F AND LOI IN SEDIMENTS, AND NATURAL WATERS.

VARIABLE	D.L.	UNITS
Antimony	0.1	ppm
Arsenic	0.5	ppm
Barium	50	ppm
Bromine	0.5	ppm
Cerium	5	ppm
Cesium	0.5	ppm
Chromium	20	ppm
Cobalt	5	ppm
Europium	1	ppm
Gold	2	ppb
Hafnium	1	ppm
Iron	0.2	%
Lanthanum	2	ppm
Lutetium	0.2	ppm
Rubidium	5	ppm
Samarium	0.1	ppm
Scandium	0.2	ppm
Sodium	0.02	%
Tantalum	0.5	ppm
Terbium	0.5	ppm
Thorium	0.2	ppm
Tungsten	1	ppm
Uranium	0.2	ppm
Ytterbium	2	ppm
Fluorine	10	ppm
Loss on Ignition	0.1	%
pH		
Uranium	0.01	ppb
Conductivity	0.01	uS

TABLE 3. DETECTION LIMITS: TRACE AND MAJOR ELEMENTS IN PROCESSED WATERS.

VARIABLE	D.L.	UNITS
Aluminium	2	ppb
Antimony	0.01	ppb
Arsenic	0.1	ppb
Barium	0.2	ppb
Beryllium	0.005	ppb
Boron	0.5	ppb
Cerium	0.01	ppb
Cesium	0.01	ppb
Chromium	0.1	ppb
Cobalt	0.05	ppb
Copper	0.1	ppb
Dysprosium	0.005	ppb
Erbium	0.005	ppb
Gadolinium	0.005	ppb
Lanthanum	0.01	ppb
Lead	0.01	ppb
Lithium	0.02	ppb
Manganese	0.1	ppb
Molybdenum	0.05	ppb
Neodymium	0.005	ppb
Nickel	0.2	ppb
Praseodymium	0.005	ppb
Rubidium	0.05	ppb
Samarium	0.005	ppb
Strontium	0.5	ppb
Titanium	0.5	ppb
Uranium	0.005	ppb
Vanadium	0.1	ppb
Ytterbium	0.005	ppb
Yttrium	0.01	ppb
Zinc	0.5	ppb
Calcium	0.02	ppm
Iron	0.005	ppm
Magnesium	0.005	ppm
Potassium	0.05	ppm
Silicon	0.02	ppm
Sodium	0.05	ppm
Sulphur	0.05	ppm

ysis of trace and major element constituents will be completed on the processed water samples that were collected at every fifth sample site. A complete list of elements and stated detection limits are provided in Tables 1, 2 and 3.

Results from the Spatsizi survey will be published in the spring of 2005. The information will be released as a CD-ROM and will include complete data listings, statistical summaries, sample location map and single element plot maps for each of the geochemical variables. The data will be provided in digital and printable hardcopy formats.

ACKNOWLEDGMENTS

Individuals and companies that contributed to the successful completion of the Spatsizi field program include Peter Friske (GSC), Ray Lett (BCGS), McElhanney Consulting (Vancouver), Lakelse Air (Terrace) and Bell II Lodge.

REFERENCES

- Ash, C.H., Stinson, P.K., Fraser, T.M., MacDonald R.W.J. and Nelson, K.J. (1996): *Geology of the Todagin Plateau - Red Chris area, northwest British Columbia, B.C. Ministry of Energy, Mines and Petroleum Resources*, Open File 1996-4.
- Ballantyne, S.B. (1991): *Stream geochemistry in the Canadian Cordillera: convention and future applications for exploration*; in *Exploration Geochemistry Workshop, Geological Survey of Canada*, Open File 2390.
- Lett, R.E., Friske, P.W.B. and Jackaman, W. (2005): *The national geochemical reconnaissance Program in NW British Columbia: the Bowser Lake (NTS 104A) regional geochemical survey*; in *Geological Fieldwork, 2004, B.C. Ministry of Energy and Mines*, Open File 2005-1.
- MINFILE 104H (1992): *Researched and compiled by Gravel, J.L.; Spatsizi River Mineral Occurrence Map; B.C. Ministry of Energy, Mines and Petroleum Resources*, Release date: January 1992.

Geology and Mineral Potential of the Grand Forks Map Sheet (082E/01), Southeastern British Columbia

By Trygve Höy¹ and Wayne Jackaman²

KEYWORDS: Regional geology, Grand Forks complex, Granby fault, Kettle River fault, metallogeny, mineral deposits

INTRODUCTION

The Grand Forks map sheet (082E/01) in southern British Columbia lies between the Rossland area in the east and the Greenwood area in the west (Fig. 1). The sheet was proposed as a Rocks to Riches mapping/compilation project due to its potential for discovery of gold mineralization, particularly epithermal gold. Exploration in the Republic District of northern Washington, southwest of the Grand Forks sheet, has led to the discovery of several epithermal gold deposits, and recent prospecting northeast of the Grand Forks sheet has also identified several epithermal gold targets that appear to be related to Eocene Coryell intrusive rocks. Both the Rossland and Greenwood camps are historical gold producers that are currently undergoing renewed interest and exploration, as is the Franklin gold camp north of Grand Forks. Some recent exploration has also focused in the Grand Forks map sheet, in part due to the similarities in styles of mineralization, lithologies and structures that characterize the Rossland and Greenwood camps, and the Republic district. This report, and the newly released 1:50,000 geological map (Høy and Jackaman, 2005) will hopefully spur and direct future exploration in the Grand Forks-Christina Lake area.

The Grand Forks area is part of the Kettle River (east-half) sheet, mapped at a scale of one inch to four miles (1:253,440) by Little (1957). It is included in the 1:250,000 scale compilation by Tempelman-Kluit (1989). This latter work stressed the importance of extensional tectonics throughout southern British Columbia and, within the Grand Forks area, supported a model proposed by Preto (1970) that recognized a Proterozoic core complex between extensional normal faults. Preto's detailed mapping clearly defined the limits of these inferred Proterozoic rocks, and outlined lithologic and structural units within the complex.

Several other more detailed studies include parts of the Grand Forks map sheet. The western edge of the sheet is part of the Greenwood camp that has been mapped by Fyles (1990) and Church (1986). A thesis by Laberge (Laberge *et al.*, 2004) focused on the western edge of the complex, and in particular on the Granby fault. Acton *et al.* (2002) studied the area east of Christina Lake, focusing on the nature of late Paleozoic basement rocks and several previously unrecognized mafic intrusive complexes.

This study has compiled and reinterpreted all previously published geological maps of the area, including considerable data that has been released in industry assessment reports. Approximately one month was spent in the field, mainly focusing on the southeastern part of the map sheet as this area had not been previously mapped at a detailed (1:50,000) scale.

All geological data has been compiled on 1:20,000 trim maps. These have been combined and will be released as a 1:50,000 map in both digital and hardcopy format (Høy and Jackaman, 2005). An update of BC MINFILE data is also in progress and will be released at a later date.

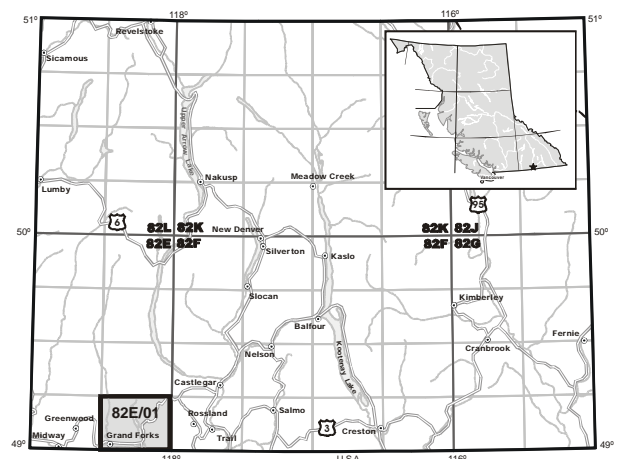


Figure 1: Map showing the location of the Grand Forks map sheet.

¹ 2450 Dixon Road, Sooke, BC, V0S 1N0

² 3011 Felderhof Road, Sooke, BC, V0S 1N0

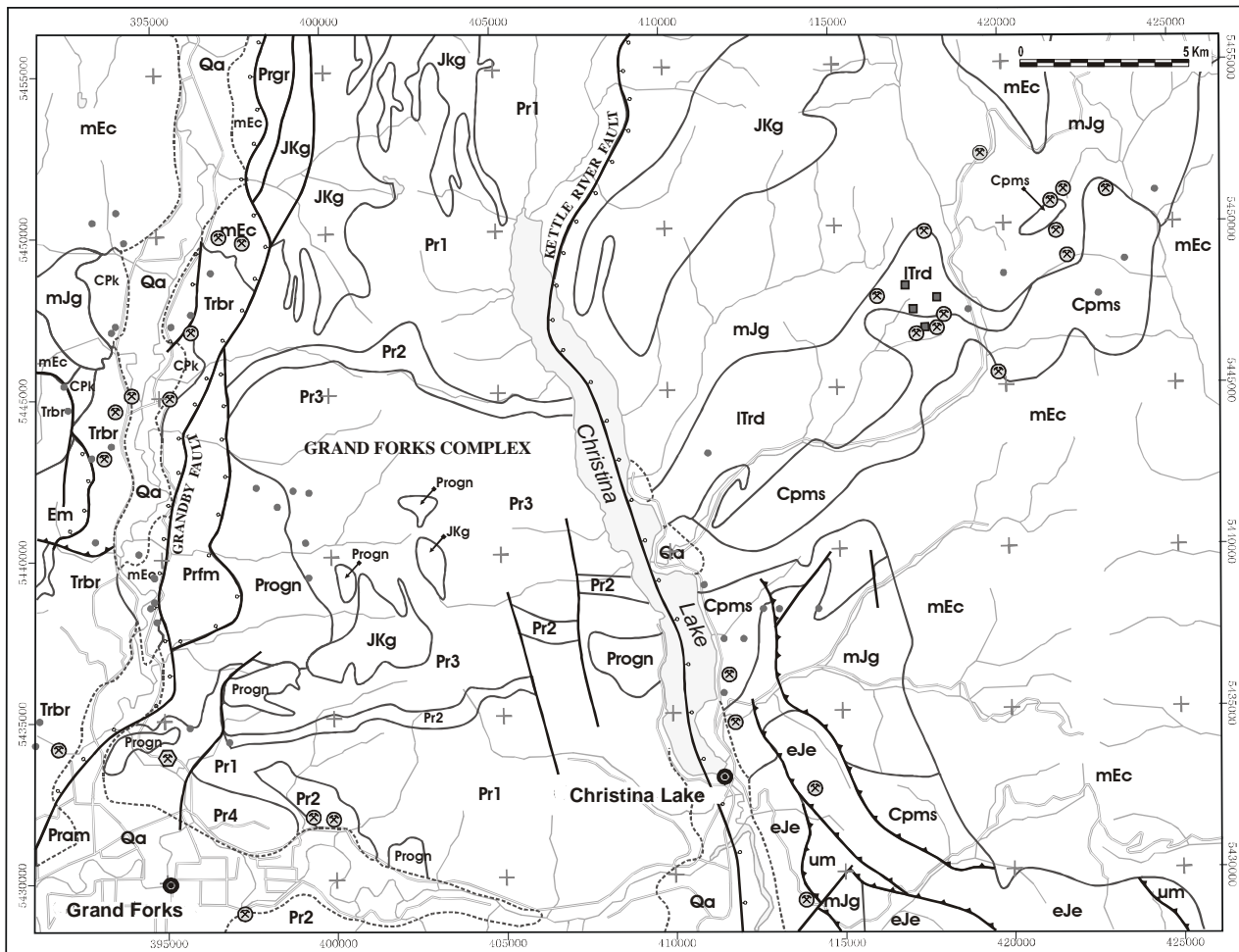


Figure 2: Geological map of the Grand Forks area (see text for sources of mapping).

REGIONAL GEOLOGY

The Grand Forks complex is one of several metamorphic complexes in the southern Omineca that appears to be related to Eocene extension, faulting and denudation (Parrish *et al.*, 1988). It is bounded on the west by the Granby fault, a west-dipping normal fault, and on the east by the east-dipping Kettle River fault (Fig. 2). Within the complex are a suite of mainly high-grade metasedimentary rocks that are intruded by a variety of mainly felsic stocks and dikes.

Hanginwall Assemblages, Granby Fault

An interfolded and faulted succession of late Paleozoic oceanic rocks of the Knob Hill and Anarchist groups, and mainly middle Triassic volcanoclastic rocks of the Brooklyn Formation, Nicola Group (Fyles, 1990; Preto, 1970; Laberge *et al.*, 2003) occur in the hangingwall of the Granby fault, along the western edge of the map area (Fig. 2).

The bounding Granby fault dips variably to the west, placing these mainly low-grade rocks of Quesnellia and Slide Mountain against the higher grade

rocks of the Grand Forks complex. The fault is marked by a zone of brittle shearing and brecciation, typically a few hundred metres wide. It appears to truncate and shear Coryell syenites of the Granby pluton (Preto, 1970). The Granby pluton is dated at 51.1 ± 0.5 Ma, U/Pb zircon (Carr and Parkinson, 1989) and therefore normal movement on the fault must have occurred during or post middle Eocene time. Wingate and Irving (1994), based on geomagnetic data, present a model of Eocene tilting of hangingwall rocks (mean tilt of approximately 30° east) due to normal movement on the west-dipping, listric Granby fault. Assuming synchronous metamorphism and a similar geothermal gradient across the fault, Laberge *et al.* (2003) estimate a minimum vertical displacement of 4 km across the Granby fault.

Hanginwall Assemblages, Kettle River fault

Hangingwall rocks of the Kettle River fault, exposed east of Christina Lake (Fig. 2), include mainly syenites and monzonites of the Eocene Coryell batholith and granites and granodiorites of the Middle Jurassic Nelson plutonic suite. A granodiorite of probable

Grand Forks Complex

The Grand Forks complex is bounded by Eocene-age normal faults. It is structurally similar to several other metamorphic complexes in the southern Omineca belt that typically expose penetratively deformed and highly metamorphosed mid-Proterozoic to mid-Paleozoic rocks. These are interpreted to correlate with ancestral North America or with marginal miogeoclinal rocks of the Kootenay terrane.

Details of the geology of the Grand Forks complex, as schematically illustrated in Figure 2, are taken mainly from Preto (1970). The complex includes a lower succession of highly deformed sillimanite paragneiss and schist, amphibolite, calcisilicates and marbles of unit Pr1. They are intruded by abundant pegmatite and, locally, granodiorite orthogneisses in the form of stocks and sills (unit Progn).

A succession of quartzites (Pr2), locally interlayered with white marble, structurally overlies the older? paragneiss complex. These are in turn structurally overlain by garnet-biotite-sillimanite schists, marbles and calcisilicates of unit Pr3 (unit III, Preto, *op. cit.*). As in underlying units, pegmatites are locally abundant, and in places comprise more than 25 % of the succession. Unit Pr3 is exposed in the central part of the complex, within a large synformal structure that is bounded to the north and south by the quartzites of Pr2 (Fig. 2). Amphibolites and amphibole gneisses of Pr4 are exposed in the southern part of the complex, as well as in stratabound lenses in Pr3. Their structural position, mainly above unit Pr3, implies a younger age, although this is not known with certainty.

A variety of deformed and locally differentiated intrusive units occur throughout the Grand Forks complex. Only the largest of these orthogneisses or foliated granitic rocks are shown on Figure 2, and are collectively included in unit Progn. As well, many post-kinematic intrusions, correlated with Jurassic-Cretaceous granodiorites, are exposed in the complex.

The age of paragneisses and schists of the Grand Forks complex is not known, although most workers have suggested correlations with Proterozoic to Paleozoic (?) rocks exposed in the Monashee complex farther north. Detailed mapping of Monashee complex rocks in both the Thor-Odin and Frenchman cap domes south and north of Revelstoke have established a fairly well constrained stratigraphy as shown in Hoy (1987). This succession includes a core gneiss complex comprising intercalated paragneiss and orthogneiss, unconformably overlain by a cover sequence comprising a basal quartzite succession and overlying paragneisses, schists, calcisilicates, marbles and amphibolites (*see* Summary and References in Höy, 2001). A regionally extensive carbonatite tuff and several large stratabound lead-zinc-silver deposits occur in the cover succession. Several of these have been compared to the Broken Hill-type deposit (Höy, 2001).

Comparison of the Grand Forks succession with that in the Monashee complex shows a general similarity (Fig. 3), with the structurally lowest unit, Pr1, correlating with the core gneisses of the Monashee complex, the quartzitic sequence, Pr2, with the basal quartzites of the cover succession, and overlying dominantly paragneisses, schists, amphibolites and marble with the similar overlying cover sequence in the

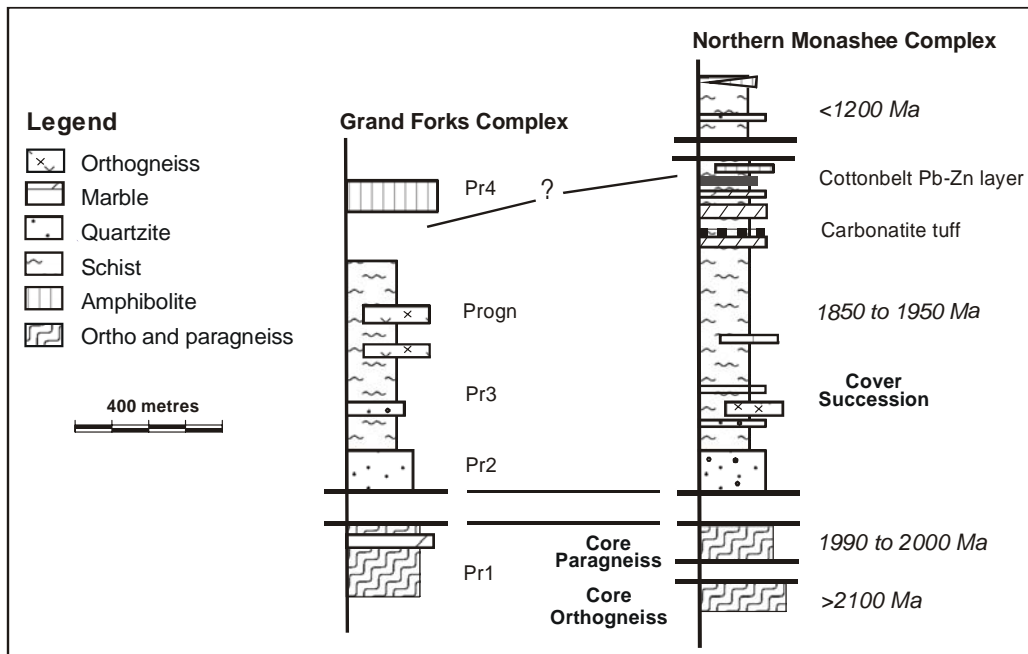


Figure 3: Correlation of main lithologic units of the Grand Forks complex with those of the Monashee Complex; data modified from Preto (1970) and Höy (2001).

Monashee complex. Furthermore, this correlation, if valid, implies that the quartzitic unit (Pr2) may define an unconformity separating early Proterozoic basement (Pr1) from an overlying Middle Proterozoic stratigraphic succession.

MINERAL POTENTIAL

A variety of mineral deposit types occur throughout the Grand Forks map sheet, including several types of gold veins, numerous gold, molybdenite and copper skarns, rare-earth pegmatites and industrial minerals. This diversity and abundance of deposits reflect both the structural complexity of the area and the variety of host rock types.

Some recent exploration, particularly north and east of the Grand Forks map sheet, has focused on epithermal-style mineralization. This is due, in part, to the successful exploitation by Echo Bay Mines (now Kinross Gold Corp.) of the K-2 gold deposit in the Republic Graben in northern Washington State and to the recent successful drill results from the Emanuel Creek deposit. These are structurally controlled low-sulphidation epithermal gold deposits that appear to be related to an unconformity at the top of the Eocene Sanpoil Formation.

Similar north-trending structures extend into southern British Columbia and have been the focus of considerable exploration. Epithermal style gold mineralization is recognized in the Franklin gold camp, located along the Granby Fault north of the Grand Forks map sheet. Farther west, the Dusty Mac and Vault deposits, both low-sulphidation epithermal deposits, are within the White Lake basin along the north-trending Okanagan fault system. North of Christina Lake, in the Lower Arrow Lake area, prospecting has focused on north-trending structures and on Eocene age intrusive and volcanic rocks and has led to the discovery of several new occurrences with characteristics typical of epithermal gold mineralization.

A new thrust belt has been identified in the southeastern part of the Grand Forks sheet, east of Christina Lake, that is probably related to thrust faulting that has been documented at the Rosslund (Höy and Dunne, 2001) and Greenwood camps (Fyles, 1990). The thrust faults in the Christina Lake area locally extend through Eocene Coryell rocks resulting in zones of widespread sericite-silica alteration and dispersed pyrite mineralization. This Eocene reactivation of earlier faults, associated hydrothermal activity, and Coryell host has similarities to epithermal mineralization that is currently being investigated at Lower Arrow Lake (Kootenay Gold Corp.). Hence, it is suggested that the large exposures of Coryell intrusive rock to the north, generally considered a barren host for mineralization, warrant further prospecting and exploration.

A number of other exploration targets in the eastern part of the Grand Forks map sheet have been identified. Preliminary work on several north- and northeast-trending shear zones in Middle Jurassic intrusive rocks located just northeast of the map area have identified anomalous gold (Kootenay Gold Corp.). Mapping (this study and Acton *et al.*, 2002) has identified a number of other similar shears that cut unit mJg just east of Christina Lake and in the northeast part of the map area. Pyrite and variable high-level alteration assemblages along these shears, including sericite and quartz, suggest potential for gold mineralization.

Several massive sulphide occurrences in metasediments just north of Sunderland Creek, east of Christina Lake, have similarities to the massive sulphide veins at Rosslund. Preliminary investigation of these suggests that they are structurally controlled and related to a mafic intrusion, and have skarn envelopes and a mineralogy dominated by pyrrhotite, chalcopyrite and magnetite. The recognition of several structural panels of Elise metavolcanic rocks in the southeast part of the map sheet (Fig. 2), similar to host rocks of many of the Rosslund veins, enhances the potential for Rosslund-type veins in the southern part of the Grand Forks sheet.

These discoveries, the considerable exposure of under-explored Eocene-age rocks, and recognition of several mineralized faults underscore the potential for discovery of epithermal gold mineralization in the Grand Forks map sheet. As well, recognition of a thrust belt that has been traced for more than 15 km in Elise Formation metavolcanic rocks, and massive sulphide mineralization related to mafic intrusive activity, also indicates potential for Rosslund-type gold-copper mineralization.

SUMMARY

The Grand Forks map sheet includes highly deformed and metamorphosed Proterozoic paragneiss and orthogneiss exposed in the core of the Grand Forks complex. These rocks appear to correlate with lithologically similar rocks of the Monashee complex farther north. The Grand Forks complex is bounded by extensional normal faults, the Granby fault along the western margin and the Kettle River fault along the eastern.

Hangingwall rocks above the Granby fault, exposed along the western edge of the map sheet, include mainly lower metamorphic grade rocks of Quesnellia that are intruded by Jurassic-Cretaceous and Eocene Coryell rocks. Farther west in the Greenwood area, Quesnel rocks and probable Slide Mountain Terrane mafic and ultramafic rocks are repeated by a series of apparent southwest-verging thrust faults.

Hangingwall rocks of the Kettle River fault, exposed east of Christina Lake, include metavolcanic rocks of the Early Jurassic Rosslund Group and a

metasedimentary succession that is tentatively correlated with the Carboniferous-Permian Mount Roberts Formation, both part of Quesnel Terrane. These are repeated by several high angle thrust faults, locally marked by serpentinites that may be remnants of Slide Mountain terrane lithologies.

There is considerable potential for discovery of new gold occurrences in the Grand Forks and Christina Lake areas. Important new exploration targets include Rosslund-type intrusive-related gold-copper veins in Early Jurassic Elise Formation rocks east of Christina Lake and epithermal gold mineralization in late structures that cut Coryell intrusive rocks farther north.

The Grand Forks project has involved mapping and compilation of geology of the Grand Forks map sheet. This map will be released in digital format and 1:50,000 hard copy format early in 2005.

ACKNOWLEDGMENTS

The British Columbia and Yukon Chamber of Mines Rocks to Riches program is thanked for support of this project. Ian Webster, Larry Jones and Brian Grant of the British Columbia Geological Survey Branch are thanked for their technical help and support.

Discussions with Linda Caron, Craig Kennedy, Tom Kennedy, Kathryn Dunne and Jim MacDonald on various aspects of the geology and mineral occurrences of the area are gratefully acknowledged.

Finally, I would like to thank G.M. Defields and L. Höy for their help and support in the field.

REFERENCES

- Acton, S.L., Simony, P.S. and Heaman, L.M. (2002): Nature of the basement to Quesnel Terrane near Christina Lake, Southeastern British Columbia; *Canadian Journal of Earth Sciences*, Volume 39, pages 65-78.
- Carr, S.D. and Parkinson, D.L. (1989): Eocene stratigraphy, age of the Coryell batholith, and extensional faults in the Granby valley, southern British Columbia; *Tectonics*, Volume 6, pages 175-196.
- Chenney, E.S. (1980): Kettle dome and related structures of northeastern Washington; *Geological Society of America*, Memoir 153, pages 463-482.
- Church, B.N. (1986): Geological setting and mineralization in the Mount Attwood-Phoenix area of the Greenwood mining camp, BC; *BC Ministry of Energy, Mines and Petroleum Resources*, Paper 1986-2.
- Fyles, J.T. (1990): Geology of the Greenwood-Grand Forks area, British Columbia; NTS 82E/1,2; *BC Ministry of Energy, Mines and Petroleum Resources*, Open File 19.
- Höy, T. (1987): Geology of the Cottonbelt Lead-Zinc-Magnetite Layer, Carbonatites and Alkalic Rocks in the Mount Grace Area, Frenchman Cap Dome, Southeastern British Columbia; *BC Ministry of Energy and Mines*, Bulletin 80, 100 pages.
- Höy, T. (2001): Sedex and Broken Hill-type deposits, northern Monashee Mountains, southern British Columbia; *BC Ministry of Energy and Mines*, Geological Fieldwork 2000, Paper 2001-1, pages 85-114.
- Höy, T. and Jackaman, W. (2005): Geology of the Grand Forks map sheet (082E/01); *BC Ministry of Energy and Mines*, Geoscience map 2005-1.
- Höy, T. and Dunne, K.P.E. (1997): Early Jurassic Rosslund Group, southeastern British Columbia; *BC Ministry of Energy and Mines*, Bulletin 102.
- Höy, T. and Dunne, K.P.E. (2001): Metallogeny and mineral deposits of the Nelson-Rosslund map area; *BC Ministry of Energy and Mines*, Bulletin 109.
- Laberge, J.D., Pattison, D.R.M. and Simony, P.S. (2004): Geology of the Granby fault, an Eocene extensional fault in southeast British Columbia; *BC Ministry of Energy and Mines*, Geological Fieldwork 2003, pages 33-47.
- Little (1957): Kettle River, British Columbia; *Geological Survey of Canada*, Map 6-1957.
- Parrish, R.R., Carr, S.D. and Parkinson, D.L. (1988): Eocene extensional tectonics and geochronology of the southern Omineca belt, British Columbia and Washington; *Tectonics*, Volume 7, pages 181-212.
- Preto, V.A. (1970): Structure and petrology of the Grand Forks Group, British Columbia; *Geological Survey of Canada*, Paper 69-22, 80 pages.
- Tempelman-Kluit, D.J. (1989): Geology, Penticton, British Columbia; *Geological Survey of Canada*, Map 1736A, scale 1:250,000.
- Wingate, M.T.D. and Irving, E. (1994): Extension in high-grade terranes of the southern Omineca Belt, British Columbia: evidence from paleomagnetism; *Tectonics*, Volume 13, pages 686-711.

MapPlace.ca Image Analysis Toolbox, British Columbia – Phase 2

By Ward E. Kilby¹

KEYWORDS: MapPlace, Image Analysis, Landsat, ASTER, HYPERION, AVIRIS, Spectral Angle Mapper, Tasseled Cap

INTRODUCTION

Phase 1 of this project established the framework of the Image Analysis Toolbox (IAT) that has now been operational for one year. In Phase 2, the IAT was completed with the addition of more analysis tools, imagery and imagery types. Near-complete coverage of the province with Landsat 7 (ETM+) imagery is now available. One new ASTER image was purchased and 45 new ASTER images located along the boarder with the United States were obtained and loaded into the system. All the existing and new ASTER images were orthorectified to improve their spatial accuracy. One HYPERION hyperspectral image was purchased and added to the site requiring a new style of map presentation. Two new analysis tools were added to the IAT. A variety of program modifications were made to increase the efficiency of the site's operation and provide full access to all the ASTER bands for any given analysis.

The established IAT framework has proven robust during the past year of operation and capable of incorporating new imagery and analysis tools. The IAT is now an integral part of the Exploration Assistant component of the MapPlace.

IMAGE ANALYSIS TOOLBOX TOOLS

Two new tools, the Tasseled Cap Transformation and the Spectral Angle Mapper (SAM) were added to the IAT (Fig. 1). Program enhancements were also made to the existing IAT programs to increase their efficiency and capability.

ASTER Program Enhancement

ASTER imagery contains 14 image bands, three bands from the visual near infra-red region (VNIR), six from the shortwave infrared region (SWIR) and five

from the thermal infrared region (TIR) of the electromagnetic spectrum (Kilby *et al.* 2004). Each of these three groups of bands has a different pixel resolution. The VNIR bands have 15 m sample spacing; the SWIR bands have 30 m spacing and the TIR 90 m spacing. IAT tools provided in Phase 1 were only capable of operating on any one of these groupings at one time. In Phase 2, all tools that could access more than one image band were adjusted to resample any ASTER band on-the-fly so that any combination of bands could be utilized by any of the tools. Now when bands from more than one spectral group are used in an analysis they are all resampled to a 15 m resolution. If all the bands are from the SWIR or from the TIR groups then the resolution will be the original sample size of 30 and 60 m, respectively.

Image Analysis Tools

Select the type of analysis desired.

Zoom to at least 1:1 000 000 to see image.

- One-Band Analysis
- Three-Band Analysis
- Two-Band Ratio
- FCC
- NDVI Vegetation Analysis
- Tasseled Cap Transformation
- Spectral Angle Mapper

Focus Images

[Back to Exploration Assistant](#)

Figure 1. Analysis tools control panel.

Tasseled Cap Transformation

The Tasseled Cap Transformation is a traditional Landsat analysis technique used to compress spectral data into a few bands to reveal key forest attributes. It was originally developed for use with the early Landsat

¹ Cal Data Ltd.

Thematic Mapper data in the early 1980s. It has more recently been modified to utilize Landsat 7 Enhanced Thematic Mapper Plus (ETM+) data. (Huang *et al.* 2002). The Tasseled Cap Transform uses a predetermined 6X6 transformation matrix to convert the Landsat 7 (ETM+) bands (1, 2, 3, 4, 5 and 7) into six new bands. This transformation was determined for at-satellite reflectance but the imagery in the IAT is in radiance values. As a result, the result will be less discriminating than if reflectance values were available but it is nonetheless a valuable method. The IAT Tasseled Cap tool displays the first three of these bands which together usually explain about 97% of the variance in the image. These three bands are referred to as the 'Brightness', 'Greenness' and 'Wetness' bands and are displayed as the red, green and blue bands of the resultant RGB analysis image, respectively. Figure 2 displays the control panel for this tool. The tool only works on Landsat images, when transformation matrices for the other image types become available the tool could be expanded to work on them as well. Most of the parameters required to operate this tool are preset. All the user is required to do is select the size of the analysis area by filling in the 'Analysis Area Pixel Width' entry box. Then the user clicks on the 'Digitize Centre of Interest' button and moves to the reference image and clicks on the point that will form the centre of the analysis image. The resultant image will highlight bare

ground as red, wetness as blue and vegetation as shades of green and yellow (Fig. 3). The analysis highlights many image features that are not apparent in a natural colour image. Note the difference between wet and dry material in the tailings. Also the relative amount of vegetation in logging cut blocks can be visualized. This tool is excellent for highlighting outcrops and identifying differences in vegetation that could be the result of the underlying geology.

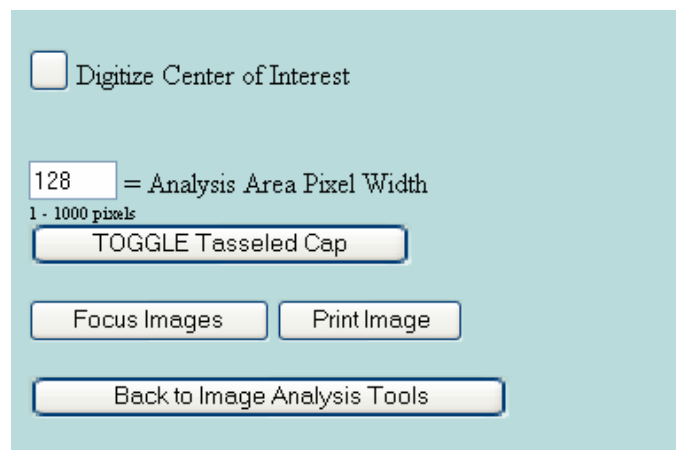


Figure 2. The Tasseled Cap Transformation control panel.

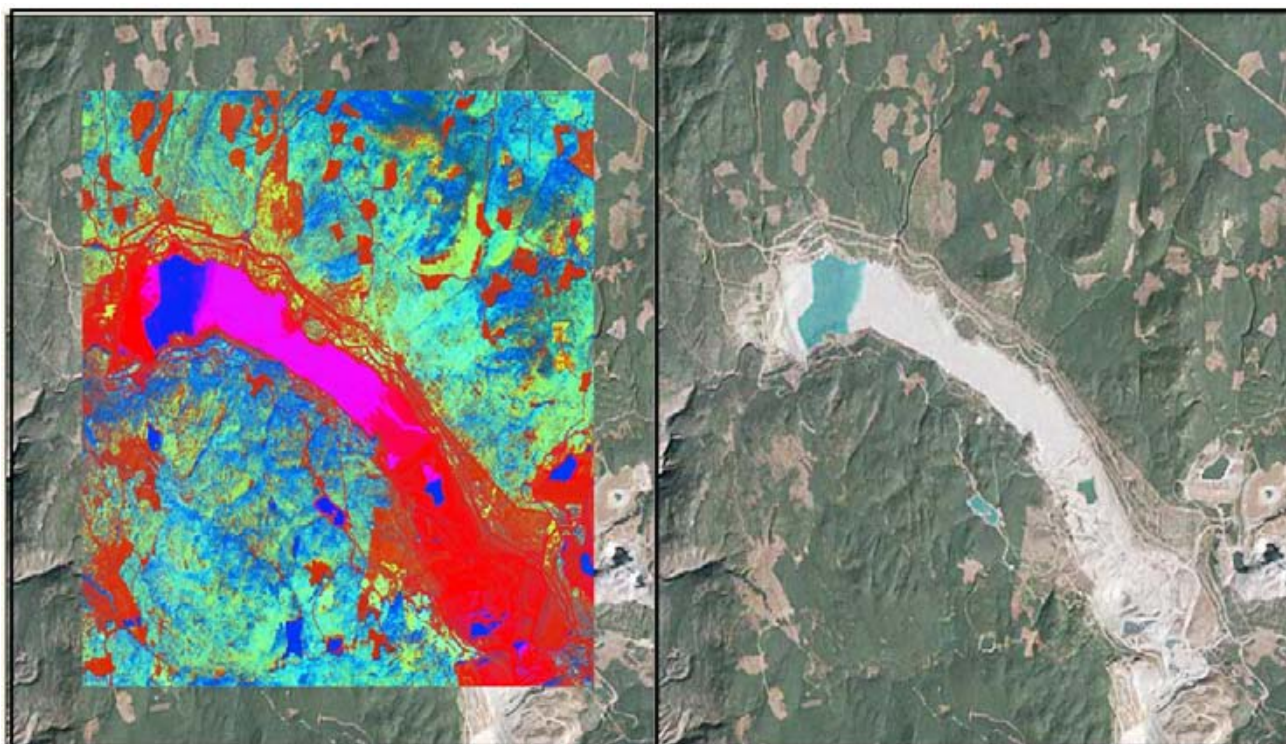


Figure 3. Results of the Tasseled Cap Transformation analysis over the Highland Valley operation.

Spectral Angle Mapper

The spectral angle mapper (SAM) generates an analysis image where each pixel contains the vector

angle between a reference spectrum and the spectrum at each pixel location. In the IAT, the reference spectrum is selected by the user from a pixel on the reference image. The spectral angle may be calculated for any

number of contiguous image bands. This tool requires significant computation effort so the fewer bands and smaller analysis area that are used the quicker the result will be returned. Analysis based on large numbers of image bands could require several minutes to calculate. The best results are often obtained by selecting only the band range that is relevant to the target feature one is attempting to map. To use the SAM tool the user first selects the range of contiguous image bands that will form the spectrum by selecting the maximum and minimum bands of the range. Then a reference or target spectrum is selected by clicking on the 'Digitize Target Pixel' button and then digitizing a pixel on the reference image that contains the desired reference spectrum. The user may also select a colour scheme for the resultant analysis image from the 'Colour Map' selection box. The size of the analysis area may be selected by modifying the value in the 'Analysis Area Pixel Width' entry field. Then the user selects the area to be mapped with the SAM tool by clicking on the 'Digitize Centre of Interest' button and digitizing a location on the reference image. Different areas of the image may be mapped with the same reference spectrum simply by clicking on the 'Digitize Centre of Interest' button in the control panel and then selecting a new position on the reference image. This tool is useful when the user knows what exists at one position and wants to map all the areas with a similar spectral response. The spectrum

for a single pixel is the result of the integration of all the individual spectrum received by the measuring instrument from the pixel area. Therefore pixels which contain only a partial amount of the target substance will still have a smaller spectral angle with the reference spectrum than pixels with none of the target substance so in this way some characteristics can be mapped at the sub pixel level.

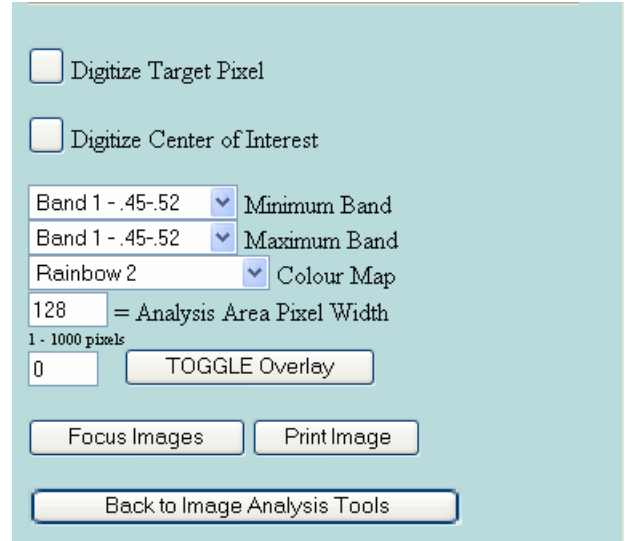


Figure 4. Spectral Angle Mapper control panel.

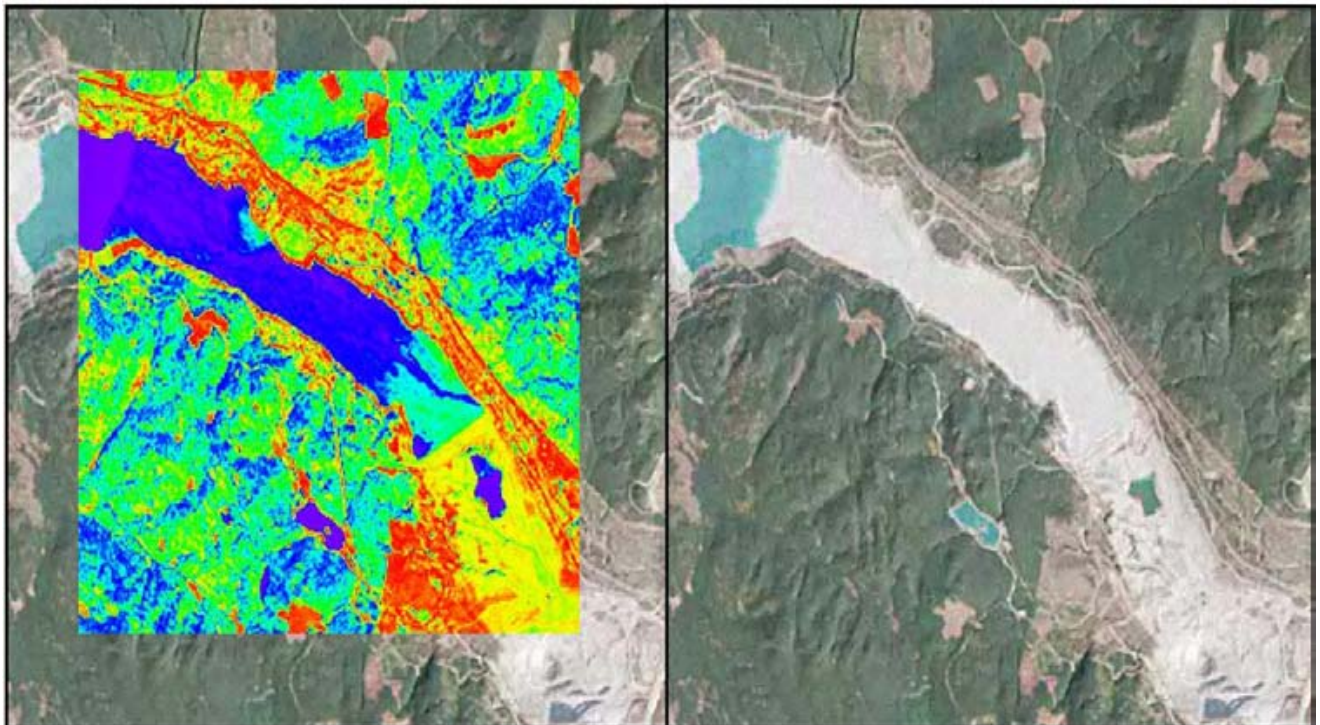


Figure 5. Results of a SAM analysis. The red colours have the smallest spectral angle with the reference spectrum that was obtained from the logging cut block in the upper centre of the image. The reference spectrum represented a mix of vegetation and soil.

IMAGE ANALYSIS TOOLBOX IMAGES

Landsat 7 (ETM+)

During Phase 2, 48 additional Landsat images were obtained and added to the system for a total of 68 images providing near complete coverage of the province (Fig. 6). The source and description of the Landsat 7 (ETM+) imagery is described in Kilby *et al.* (2004).

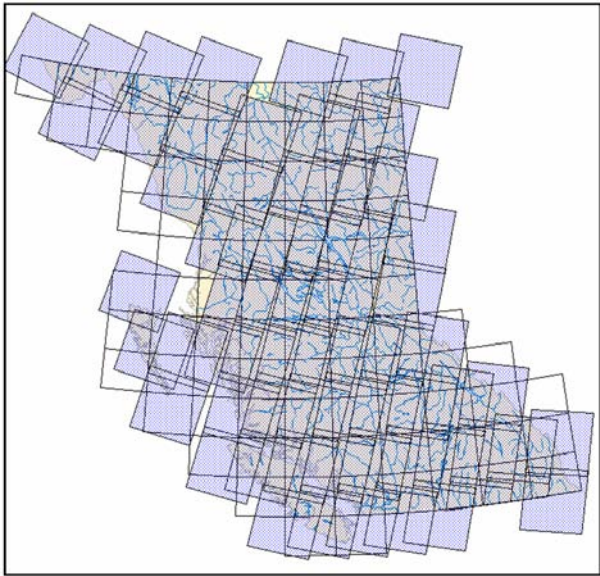


Figure 6. Distribution of Landsat 7 (ETM+) imagery.

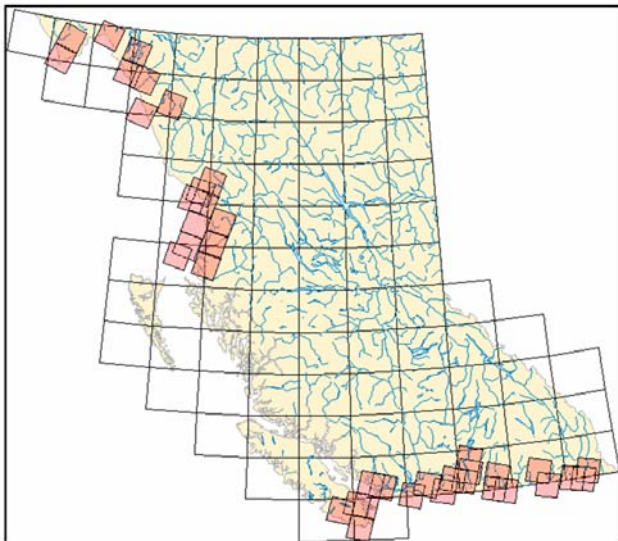


Figure 7. Distribution of ASTER imagery.

ASTER

During Phase 2, 46 new ASTER images were added to the system for a total of 51 images (Fig. 7). The images are primarily along the BC-US border as these images could be obtained at no cost. One image from the Okanagan Lake region was purchased. For a complete description of the imagery source and band characteristics see Kilby *et al.* (2004). All the ASTER images were orthorectified during this phase of the project to improve their spatial accuracy. The ASTER sensor can have cross track look angles of up to 8° which can cause a significant amount of image distortion. The orthorectification process removed this distortion and compensated for the topographic relief in the image area.

HYPERION

One HYPERION image was purchased and added to the system during Phase 2. HYPERION images have 242 bands that cover the VNIR, SWIR and TIR range of the electromagnetic spectrum, 355.57 to 2577.18 nm in approximately 10 nm increments (Fig. 8). The image purchased covers an area of 7 km wide by 88 km long in the Cariboo region. Part of the Equity Silver operation is captured in the northern part of the image (Fig. 9). The image was ordered through the United States Geological Survey website at <http://eol.usgs.gov/index.php> and purchased from the EROS Data Center in Sioux Falls, South Dakota. Due to the very large size of the image and to reduce storage and processing requirements, a new map configuration was developed to hold the image during analysis. The map is oriented relative to the satellite orbit path rather than true north (Fig. 10). All of the usual map functions and information are available in the normal manner. The only caution is that the map is not in a UTM projection so the coordinate readout should be set to display latitudes and longitudes if accurate positions are to be determined from the map display.

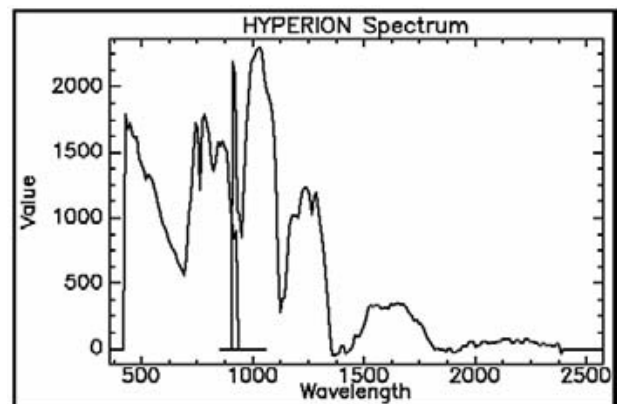


Figure 8. HYPERION spectrum from a conifer tree slope.

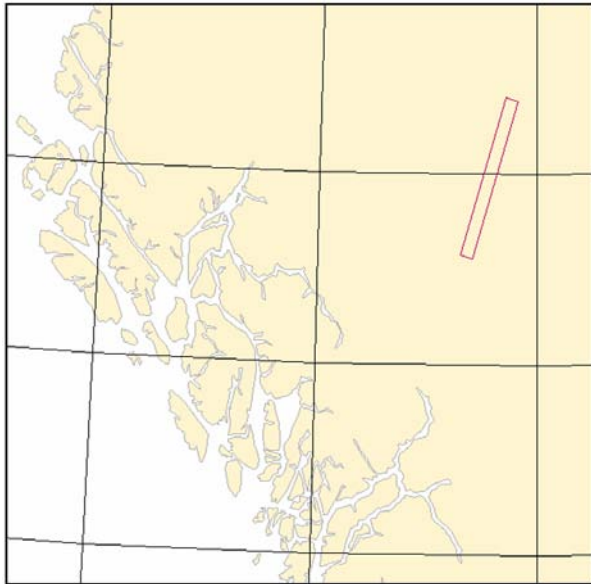


Figure 9. Location of the HYPERION image. Note orientation of the image.



Figure 10. HYPERION image in analysis map that is oriented parallel to the satellite orbit.

AVIRIS

The same single AVIRIS image is available for investigation as was available from the Phase 1 portion of the project. The image is from the Canal Flats area in southeastern British Columbia (Fig. 11). A complete

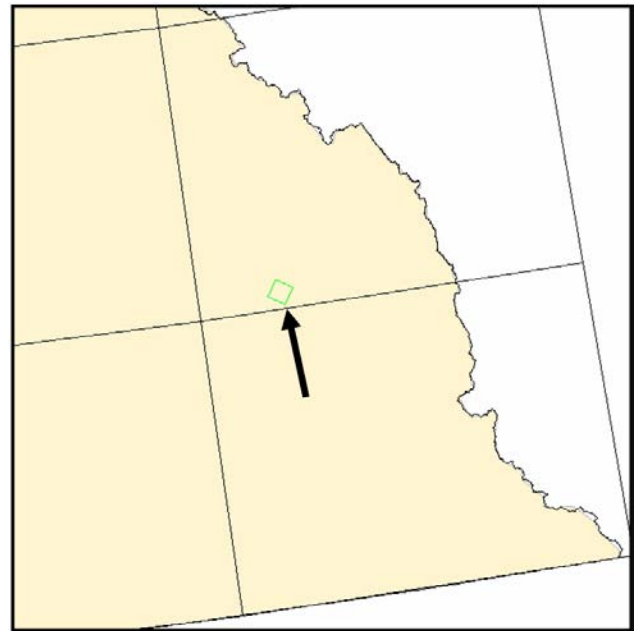


Figure 11. Location of the AVIRIS image.

description of the image is provided in Kilby *et al.* (2004).

ACKNOWLEDGMENTS

This project was made possible by a grant from the Rocks to Riches program managed by the British Columbia and Yukon Chambers of Mines. The British Columbia Ministry of Energy and Mines provided funding for this program.

Larry Jones of the British Columbia Geoscience, Research and Development Branch provided invaluable assistance in migrating the IAT onto the MapPlace web server.

REFERENCES

- Huang, C., Wylie, B., Homer, C., Yang, L. and Zylstra, G. (2002): Derivation of a Tasseled cap transformation based on Landsat 7 at-satellite reflectance; *International Journal of Remote Sensing*, Volume 23, no 8, pages 1741-1748.
- Kilby, W.E., Kliparchuk, K. and McIntosh, A. (2004): Image Analysis Toolbox and Enhanced Satellite Imagery Integrated into the MapPlace; *British Columbia Ministry of Energy and Mines*, Geological Fieldwork 2003, Paper 2004-1, pages 209-215.

Alkaline Magmatism and Porphyry Cu-Au Deposits at Galore Creek, Northwestern British Columbia

By James M. Logan

KEYWORDS: geology, mineralization, geochronology, alkaline, porphyry copper-gold, Stikinia, Stuhini Group, Copper Mountain intrusive suite, copper, gold, magnetite, garnet, biotite, pseudoleucite, Central zone, Junction zone, Butte zone, Southwest zone, Copper Canyon

INTRODUCTION

Porphyry deposits and prospects containing copper, molybdenum and gold are important historical contributors to the metallic mining industry in British Columbia. Elevated metal prices and recent exploration successes have renewed interest in British Columbia's copper-gold porphyry deposits, in particular the alkalic Cu-Au porphyry class of deposits (e.g., Galore Creek, Mount Polley and Afton-Ajax). These and cospatial calcalkaline Cu-Mo and Cu-Mo-Au porphyry deposits formed outboard of ancestral North America in island-arc tectonic settings in the Late Triassic to Early Jurassic. The alkalic Cu-Au deposits in both the Stikine and Quesnel terranes are the products of a discrete alkaline magmatic event (210–200 Ma) at the end of the Triassic.

In order to better understand the controls on mineralization and maximize exploration efficiencies, a partnership was struck between the British Columbia Ministry of Energy and Mines and exploration companies with a direct interest in refining the alkaline Cu-Au porphyry exploration model (Abacus Mining and Exploration Corp., Imperial Metals Corp., NovaGold Resources Inc.) as it applies to the Iron Mask, Mount Polley and Galore Creek magmatic complexes. Additional funding was obtained through a Rocks to Riches grant provided by the British Columbia and Yukon Chamber of Mines. The new information provided by these studies will update the provincial database and mineral deposit models, and promote Cu-Au porphyry exploration, all of which will ultimately lead to new discoveries and resources in the province.

The Galore Creek project objectives are to determine the spatial and temporal relationships between the alkaline (feldspathoid-bearing) volcanic rocks, mineralization and the various intrusive phases of the alkalic Galore Creek magmatic complex; characterize mineral zones located peripheral to, and as much as 1000 m vertically above, the Central zone; acquire a suite of samples from the various mineralized zones, as well as a suite of least altered volcanic and intrusive rocks, for major and trace element analysis, and

compare with published data and data from the Mount Polley and Iron Mask suites; and

compare these results with those from other alkalic intrusive centres in the province to establish a metallogenic model that will direct exploration.

The Galore Creek camp is located within the lower Stikine River region of northwestern British Columbia, approximately 150 km northeast of Stewart. The property is 75 km northwest of the Eskay Creek gold-silver mine, on the west side of the Cassiar Highway (Fig. 1). It contains twelve known Cu-Au occurrences (MINFILE 104G/90 through 99), that are distributed across an area measuring 5 km by 4 km, and over a vertical range of 1000 m. Three of these, the Central, Junction and Southwest zones, contain resources of 284 million tonnes at 0.67% Cu. NovaGold Resources Inc is currently in an option agreement to earn 100% ownership of the property. In 2003, SpectrumGold completed a 3000 m drill program to test for the presence of increased gold and copper grades in the Central deposit. At that time, a new zone of Cu-Au mineralization, the 'Bountiful zone', was discovered beneath the Central zone and has spurred re-evaluation of the Galore Creek property.

This report summarizes the regional geology and presents some of the preliminary field observations from the 2004 field mapping. The Galore Creek component of the Cu-Au Porphyry Project conducted 1:20 000-scale field mapping and sampling of the western and southern portions of the Galore Creek basin, where overburden is thin and outcrop exposure is good. In addition, regional-scale traverses were started outside the main intrusive complex and traced stratigraphy back into the Galore Creek basin, where potassium metasomatism has typically obliterated primary protoliths. Magnetic susceptibilities of intrusive and volcanic units were measured to better utilize the low-level airborne geophysical survey and aid map compilation. A map of the intrusive complex, together with geochemical analytical results and petrography, will be released as a GeoFile.

PREVIOUS WORK

Forrest Kerr carried out the first geological mapping along the Stikine and Iskut rivers from 1924 to 1929, but it was not until 1948 that his data were published (Kerr, 1948a, b). Kerr proposed the original Permian and pre-Permian subdivision of Paleozoic strata and, from his work in the Taku River valley of the Tulsequah map area, he de-

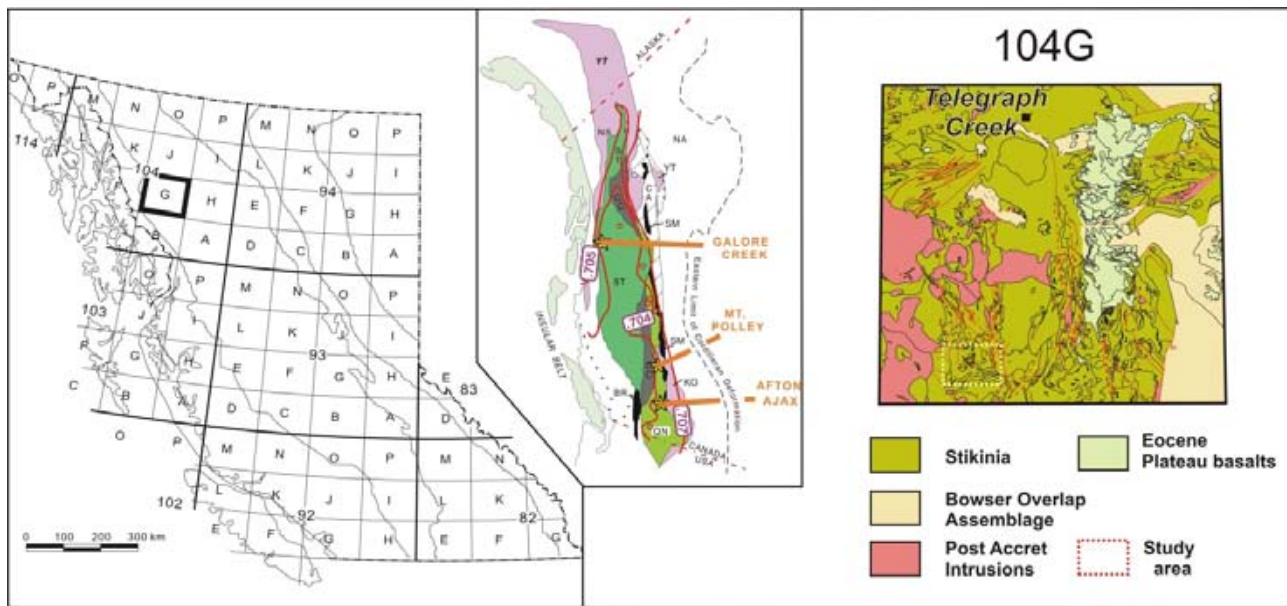


Figure 1. Location of the Galore Creek component of the Cu-Au Porphyry Project in northwestern British Columbia (NTS 104G). Inset is a terrane map of northern Cordillera (*modified from* Wheeler and McFeely, 1991), showing the tectonostratigraphic setting of the three study areas. Mesozoic initial strontium isopleths are from Armstrong (1988). Box on the right shows detailed terrane relationships for NTS 092I and the project area.

fined the Late Triassic Stuhini Group, much of which underlies the current study area. In 1956, a helicopter-supported reconnaissance of the Telegraph Creek map area was conducted by the Geological Survey of Canada (1957, Operation Stikine). Jack Souther masterminded Operation Stikine and produced 1:250 000-scale geological maps of the Telegraph Creek sheet (104G), Tulsequah sheet (104K) and 1:50 000-scale detailed studies of Mount Edziza (1988, 1992). Other work by the Geological Survey of Canada (Fig. 1) includes that of Monger (1970, 1977), Souther (1971, 1972, 1992) and Anderson (1984, 1989).

A. Panteleyev carried out mapping in the immediate area of Galore Creek, in conjunction with a study of the deposit between 1973 and 1975 (Panteleyev, 1973, 1974, 1975, 1976, 1983). Geological mapping was completed at 1:50 000 scale in the Galore Creek area (Sphaler Creek and Flood Glacier map sheets) in 1988 (Logan *et al.*, 1989; Logan and Koyanagi, 1994). Concurrent British Columbia Geological Survey projects have completed 1:50 000-scale map coverage north and west of the Iskut north project area in the Scud River, Yehiniko Lake, Chutine River and Tahltan Lake map areas (Brown *et al.*, 1996).

REGIONAL GEOLOGY

The study area straddles the boundary between the Intermontane Belt and the Coast Belt, and is underlain mainly by rocks of the Stikine Terrane (Stikinia), the westernmost terrane of the Intermontane Belt (Fig. 1). The stratigraphic and plutonic framework of northwestern Stikinia is summarized by Anderson (1993), Gunning (1996) and Logan (2000). It consists of a Paleozoic to Mesozoic sedimentary and volcanoplutonic arc assemblage that includes the Devonian to Permian Stikine assemblage,

the Late Triassic Stuhini Group and the Early Jurassic Hazelton Group. These are overlain by Middle Jurassic to early Tertiary successor-basin sediments of the Bowser Lake and Sustut Groups, Late Cretaceous to Tertiary continental volcanic rocks of the Sloko Group, and Late Tertiary to Recent bimodal shield volcanism of the Edziza and Spectrum ranges.

The Stikine Terrane is a composite allochthonous (?) terrane made up of an amalgamation of volcanic island arcs ranging in age from late Paleozoic through Early Jurassic. Modern analogs include the Pacific island arcs from Japan south through the Philippines, or New Guinea to New Zealand. Recent studies suggest that the Stikine terrane developed adjacent to the ancestral margin of North America (McClelland, 1992; Mihalynuk *et al.*, 1994; Gunning 1996) and that parts of the Paleozoic Stikine assemblage are correlative with and depositionally tied to Paleozoic rocks of the Yukon-Tanana Terrane. Depositional ties between the Quesnel and Yukon-Tanana terranes are also known and this, together with the hook-like geometry of the 0.706 initial $^{87}\text{Sr}/^{86}\text{Sr}$ line around the northern end of Stikinia (Fig. 1), led Nelson and Mihalynuk (1993) and Mihalynuk *et al.* (1994) to propose a single arc model consisting of the Quesnel, Yukon-Tanana, Nisling and Stikine terranes.

Upper Triassic volcanic rocks and paired, alkaline-calcalkaline Cu-Au deposits extend the length of the Canadian Cordillera (Barr *et al.* 1976). In the south, in Quesnellia, the Nicola and Takla groups lie east of the Cache Creek Terrane. Farther north, in Stikinia, the Stuhini and Lewis River groups lie west of the Cache Creek. There is little difference in age, lithology or chemistry of the Triassic strata from one tectonostratigraphic terrane to the next (Barr *et al.*, 1976; de Rosen-Spence, 1985; Mortimer, 1987;

Logan and Koyanagi, 1994; Panteleyev *et al.*, 1996; Nelson and Bellefontaine, 1996). Unconformities separate the Upper Triassic Stuhini Group, which is mainly submarine volcanic rocks, from the Jurassic Hazelton Group, which is mainly subaerial volcanic and sedimentary rocks in north-western British Columbia. A paraconformity separates the Triassic from Early Jurassic volcanism in north-central Quesnellia (Nelson and Bellefontaine, 1996). A similar hiatus is interpreted at Mount Polley (Logan and Mihalynuk, this volume), where Lower Jurassic sedimentary rocks overlie the Triassic volcanic sequence; however, in southern Quesnellia, the Early Jurassic volcanic rocks of the Rossland Group (Höy and Dunne, 1997) indicate a substantial eastward shift of volcanism from the Triassic magmatic axis.

Galore Creek is one of a number intrusion-related Cu-Au deposits that developed in the Upper Triassic to Lower Jurassic (?) volcanoplutonic-arc rocks of the Quesnel-Stikine arc (Barr *et al.*; 1976; Nelson and Mihalynuk, 2004). Similar deposits extend the length of the Intermontane Belt (Fig. 1). The Cu-Au deposits are associated, in the south, with the Iron Mask batholith (Afton, Ajax, and Crescent) and Copper Mountain intrusives (Copper Mountain, Ingerbelle); to the north, with the Hogem batholith (Lorraine); and, in the Stikine Terrane, with Galore Creek intrusives (Galore Creek).

The deposits at Galore Creek are hosted within shoshonitic submarine volcanic rocks and coeval subvolcanic syenite intrusions of the Upper Triassic Stuhini Group. It is a high-level, silica-undersaturated alkaline porphyry Cu-Au system of latest Triassic age (210 Ma; Mortensen *et al.*, 1995) that lies 38 km southwest of the large calcalkaline Cu-Mo-Au Schaft Creek system.

STUHINI GROUP ROCKS

Upper Triassic Stuhini Group flows, tuffs, volcanic breccias and sedimentary rocks define a volcanic edifice centred on Galore Creek. Contemporaneous sedimentary rocks flank the volcanic centre and, east of the South Scud River fault, a sequence of metavolcanic breccias and massive volcanic rocks is intruded by the coeval calcalkaline Hickman pluton. Stuhini stratigraphy ranges in age from early Carnian to late Norian, based on radiometric dates (Anderson, 1983) and fossil ages (Souther, 1972; Logan and Koyanagi, 1994; Brown *et al.*, 1996).

Volcanic rocks constitute the bulk of the Upper Triassic stratigraphy at Galore Creek, and three different calcalkaline volcanic suites are recognized: a lower subalkaline hornblende-bearing basaltic andesite; a medial subalkaline to alkaline augite-porphyrific basalt; and an uppermost alkaline orthoclase and pseudoleucite-bearing shoshonitic basalt. Stratified, sedimentary facies equivalent units of the lavas were deposited on the flanks of the edifice and contain diagnostic fossils. Carnian fossils are preserved within the lower sedimentary package; the medial and upper sedimentary packages are characterized by conodonts and bivalves of Norian age (Logan and Koyanagi, 1994). Rocks of the medial and upper volcanic

subdivisions underlie the Galore Creek basin, host multiple syenite intrusions and Cu-Au mineralization that make up the intrusive-volcanic complex and are, in part, extrusive equivalents of these subvolcanic intrusions.

The Lower volcanic subdivision consists of aphyric and sparse hornblende and plagioclase-phyric flows, breccia and tuff that underlie extensive areas south of Galore Creek and constitute most of the Middle to Upper Triassic country rock that hosts the Hickman batholith (Logan and Koyanagi, 1994; Brown *et al.*, 1996).

The Medial volcanic subdivision is dominated by polyolithic volcanic conglomerate, wacke, sandstone, siltstone and fine tuffaceous rocks, and distinctive but subordinate pyroxene-phyric basalt flow breccias and dikes. The clast composition is variable, including pale green, grey or purple, sparsely porphyritic plagioclase andesite, pyroxene porphyry basalt, coarse-bladed plagioclase-pyroxene porphyritic basalt and rarely limestone. The clasts are angular to subrounded and constitute from 15 to 80% of the rock in an arkosic matrix of similar composition. Graded sandstone and siltstone beds and local, thinly laminated, black and orange, calcareous argillite horizons are interbedded with the conglomerate on the ridge west of the head of Galore Creek. They are characterized by soft-sediment slumping, faulting and scour-and-fill structures, and crosscut by sedimentary dikes (Fig. 2). Interlayered



Figure 2. Well-laminated calcareous argillite rip-ups in a chaotic lahar-conglomerate unit. This unit marks the transition from volcanic conglomerates of the Medial subdivision upward into the alkaline volcanic tuffaceous rocks.

with the dominantly epiclastic rocks are pyroxene porphyry flow breccias, pyroxene crystal tuff, and reworked volcanic sandstone containing vitreous pyroxene crystals. The medial unit generally coarsens upwards. Lower units are thin, repetitively graded AE-turbidites. Higher in the section are thick-bedded, chaotic to normally graded lahar-conglomerate and pyroxene-phyric lava flows. The turbidites and paucity of lava flows suggest a distal depositional environment.

The Upper alkaline volcanic subdivision is best exposed west of Copper Canyon. Volcanic rocks at the base of the section (Logan and Koyanagi, 1994, Fig. 12) are pervasively potassium metasomatized and, in some places, may be intrusive in origin. The lower unit is cut by pseudoleucite, potassium feldspar syenite porphyry bodies and younger felsic and diabase dikes. Overlying the lower package are less altered intermediate tuff-breccia, tuffaceous wacke and rare, interbedded orange-weathering grit containing shale rip-up clasts. The unit fines and becomes well bedded upward; the volcanic component also reflects a change to more alkaline magmatism. The top of the section consists of orthoclase and biotite crystal tuffs and fine epiclastics, lithic crystal tuffs, lapilli tuffs and polymictic volcanic conglomerates that are interbedded with well-laminated siltstone and fine-grained sandstone beds. A distinctive accretionary lapilli horizon was recognized near the base of the section (Fig. 3). The epiclastic



Figure 3. Accretionary lapilli horizon marks the transition from a lower package of heterolithic breccias and lapilli tuff upwards into potassium feldspar and biotite-rich airfall crystal tuffs, west of Copper Canyon.

and tuffaceous beds are characteristically potassium feldspar rich, crossbedded and show both normal and reverse grading. Graded bedding, interpreted to be normal, indicates that the beds are overturned in places (Fig. 4). Interbedded with the silts and tuffs are slump deposits of massive to chaotic maroon silt and sand containing cross-bedded rip-up clasts and large angular breccia blocks of fine-grained tuff, some showing soft-sediment plastic deformation. Among the sediments are polyolithic conglomerates that contain syenite clasts of the Galore Creek intrusives. Rare clasts of mineralized syenite porphyry occur within the potassium feldspar crystal-rich lapilli tuff unit west of Copper Canyon. A grab sample from a 40 cm block of well mineralized potassium feldspar pseudoleucite porphyry syenite from a lapilli tuff bed returned exceedingly high copper, silver and gold values (6.53 % Cu, 0.21 g/t Au and 174 g/t Ag; JLO04-44-504, *see* Table 1). Orthoclase crystal tuffs contain large potassium feldspar crystals up to 1 by 2 cm in size. Subhedral to euhedral clots and crystals of detrital biotite constitute 2–5% of a number of crystal lithic tuff beds. The euhedral crystals provide evidence for a pyroclastic origin for these rocks, as does the presence of accretionary lapilli. The crosslamination, rip-up clasts, soft-sediment deformation features and presence of accretionary lapilli could be interpreted as evidence of a base surge or airfall deposit. Argon-argon step heating of biotite from this unit gives a plateau age of 212 Ma (Logan and Koyanagi, 1994).



Figure 4. Potassium feldspar-rich graded crystal tuff, west of Copper Canyon.

Pseudoleucite trachyte breccia flows crop out on the ridge between the Anuk River valley and the head of Galore Creek (Fig. 5). The tuffs consist of a sequence of orthoclase crystal tuffs and crystal-lithic tuffs and flow-banded sills or welded tuffs. The rocks are potassically altered and cut by a pronounced and strong penetrative deformation that has produced foliated and schistose rocks. The north-trending extent of these potassium-rich volcanic units is evident on the potassium radiometric image derived from the low-level airborne geophysical survey (Yarrow and Taylor, 1990).

ORTHOCLASE PORPHYRY SYENITE

The Galore Creek magmatic complex is located in the headwaters of Galore Creek. It comprises a series of orthoclase-porphyratic syenite intrusions that intrude coeval Upper Triassic Stuhini Group volcanic rocks and related sediments. At least 12 main equigranular and orthoclase porphyritic feldspathoid-bearing syenite intrusive units can be identified and have been described (Enns *et al.*, 1995).

The early intrusive suite is premineral to intermineral and includes pseudoleucite porphyry and megaporphyry dikes (I-1 and I-2), grey syenite porphyry (I-3), dark syenite porphyry (I-4a, I-4b), and dikes of fine-grained orthoclase syenite megaporphyry (I-5). The early suite is exposed in the south part of the complex. Intrusives I-1, I-2

and I-3 are only exposed in drillcore. Due to their intense hydrothermal alteration, they have been interpreted as the causative intrusion for the main stage of copper mineralization (Sillitoe, 1991a, 1991b; Enns *et al.*, 1995). The I-3 outcrop in lower Dendritic Creek could not be substantiated. I-4 is the most common intrusive in the southern part of the deposit. It is a medium dark grey porphyry with 10–20% white stubby orthoclase phenocrysts (5–20 mm in length) and rare euhedral pseudoleucite phenocrysts up to 5 cm in diameter (Fig. 6). The matrix to I-4 is a mixture of fine-grained orthoclase, biotite and chlorite.

The remaining phases are considerably less altered, crosscut mineralization and are considered to be postmineral. Most of these phases were defined in drillcore from the Central zone, where crosscutting relationships could be observed and projected between holes. In the field, the most commonly encountered phases are the medium-grained equigranular syenite (I-8), an intergrowth of orthoclase, hornblende and epidote and rarely 2–5 mm orthoclase phenocrysts; and the medium-grained orthoclase syenite megaporphyry (I-9a and I-9b), which is equivalent to the epidote syenite megaporphyry of Allen *et al.* (1976) and is the most abundant intrusive phase at Galore Creek. It forms thick (up to 50 m) subhorizontal dikes that dilute the ore in the Central, North Junction, Butte and West Rim zones. It is characterized by 10–30% euhedral orthoclase megacrysts, 10–30 mm in length, in a medium to rarely coarse-grained matrix. Chlorite and biotite pseudo-



Figure 5. I-4 porphyry syenite, showing stubby orthoclase phenocrysts and rare euhedral pseudoleucite phenocrysts, southern part of the Central zone.

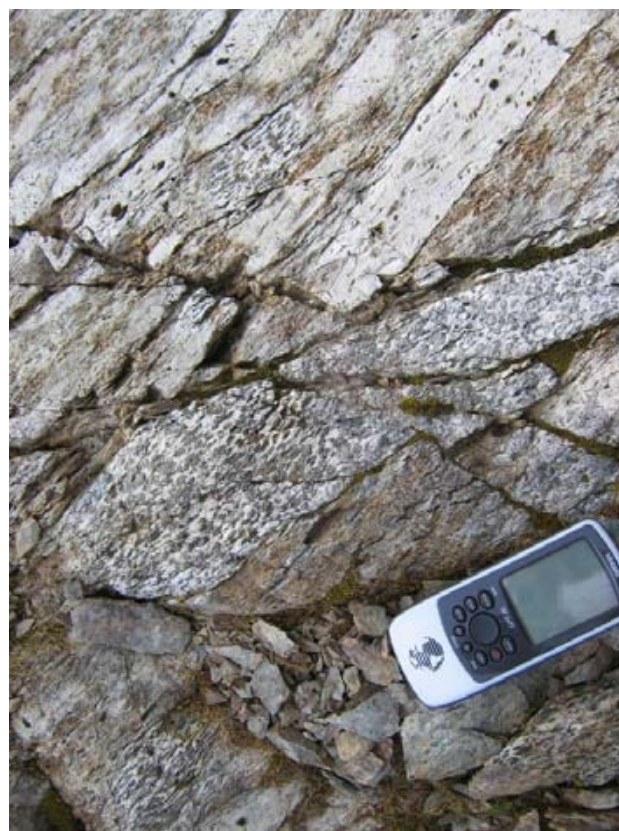


Figure 6. Pseudoleucite trachyte breccia flow on the ridge between the Anuk River Valley and the head of Galore Creek.

morphs hornblende, and variable amounts of epidote and garnet characterize the unit. I-9b can be distinguished from I-9a in hand specimen by the presence of coarse plagioclase and magnetite in the matrix and commonly very large orthoclase phenocrysts (up to 20 cm). I-9a is also typically more potassically altered and pyritic. I-11 is a medium-grained, equigranular, grey to brown intergrowth of orthoclase, biotite and pyroxene, with sparse, acicular white orthoclase phenocrysts (2–7%). It contains miarolitic cavities filled with epidote and garnet. Lavender porphyry (I-12) is a quartz-bearing (Enns *et al.*, 1995) syenite. It is characterized by strongly aligned trachytic orthoclase phenocrysts (50–70%) in a lavender-coloured orthoclase matrix.

Uranium-lead ages (Mortensen *et al.*, 1995) from intrusive rocks at Galore Creek range from 210 ± 1 Ma (Pb-Pb isochron, titanite) for an early intermineral syenite porphyry (I-4) to 197.2 ± 1.2 Ma (Pb-Pb isochron, titanite) for a postmineral potassium feldspar porphyry (I-9). These span the Triassic-Jurassic boundary (~200 Ma), using the time scale of Palfy (2000), and suggest a protracted magmatic history for the Galore Creek magmatic complex.

MINERALIZATION AND ALTERATION

Ten porphyry copper-gold deposits are known on the Galore Creek property. The Central and North Junction zones have drill-indicated reserves; the remaining deposits are considerably smaller and less well tested. The deposits are interpreted to be high-level synvolcanic mantos related to alkaline plutonic rocks that intrude and breach the volcanic edifice (Allen *et al.*, 1976).

Central Zone

The alteration mineralogy and zonation developed around the Central zone have been well documented and described by Barr (1966), Allen *et al.* (1976), Panteleyev (1976) and Enns *et al.* (1995), and references therein. The zone extends 1800 m north-northeasterly and varies in width from 200 to 500 m. The deposit dips steeply to the west. It is divided into a core zone and north and south zones. Although the metasomatic overprint (calcsilicate mineral assemblage) at Galore Creek is unusual, the distribution of sulphides, precious metals and magnetite is consistent with the expected zoning pattern for alkalic porphyry deposits (Jones and Leveille, 1989; McMillan, 1991).

Prograde and retrograde alteration mineral assemblages characterize the hydrothermal system that was centred on the Central zone. Early, hot, dominantly magmatic fluids caused potassium silicate alteration and the deposition of biotite, magnetite, orthoclase, bornite and chalcopyrite (Fig. 7). The potassium silicate alteration is preserved in the northern and southern parts of the Central zone. Cooling and collapse of the hydrothermal system downward produced patchy propylitic alteration (epidote, chlorite, calcite and pyrite), which is developed peripheral to the mineralization. This was followed by a late-stage (?) or separate hydrothermal fluid that caused calcic-potassic

alteration. This assemblage consists of pervasive white orthoclase, coarse biotite, garnet, anhydrite, diopside and apatite (Fig. 8). The calcic-potassic alteration is centred above the magmatic breccia in Dendritic Creek at the core of the Central zone and is interpreted to have emanated from this centre. A late, lower temperature (?) alteration (SAC), characterized by an assemblage of sericite, anhydrite, carbonate and pyrite±hematite (specular) is developed along the margins of the Central, Junction and Butte zones (Fig. 9).

Disseminated pyrite is the most abundant sulphide mineral. Chalcopyrite and bornite, in the ratio 10:1, are the main copper minerals. Sphalerite and galena are associated within garnet-rich areas, and trace amounts of molybdenite, native silver, native gold and tetrahedrite have been noted (Allen, 1966). Magnetite occurs in veinlets with or without chalcopyrite and often cements breccias. Chalcocite, cuprite, native copper and tenorite are secondary copper minerals (Logan and Koyanagi, 1994).

Gold is generally associated with higher grades of copper mineralization. There is not always a strong correlation; many areas of high copper lack appreciable gold. However, higher gold grades are associated with bornite in the north and south parts of the Central zone.



Figure 7. Potassium silicate alteration of a volcanic breccia altered and preferentially replaced by biotite, magnetite and orthoclase, southern end of Central Zone. Inset shows enlargement of bornite and chalcopyrite mineralization



Figure 8. Calcic-potassic alteration in the orthomagmatic breccia located on the west side of the Central Zone, Dendritic Creek. Pervasive white potassium metasomatism, with coarse intergrowths of biotite, garnet, anhydrite and apatite, replace the matrix of the breccia.

Copper Canyon

The Copper Canyon showing is located approximately 8 km due east of the Galore Creek deposit. It is owned by Eagle Plains Resources. It was tested by seven diamond-drill holes (1010 m) in 1957 by the American Metal Company Limited. At that time, geological reserves of 27 million tonnes with an average grade of 0.72% copper and 0.43 g/t gold were inferred (Spencer and Dobell, 1958). In 1990, Consolidated Rhodes Resources Ltd. completed 3784 m of diamond-drilling in thirteen holes. NovaGold, under an option agreement with Eagle Plains Resources, completed eight diamond-drill holes totalling 3017 m in 2004. Drilling confirmed and expanded the near-surface copper-gold-silver mineralization on the property, which is associated with a syenite porphyry and a hydrothermal system that is similar to but smaller than that at Galore Creek. The Copper Canyon area has been mapped in detail by Leary (1990) and Otto and Smithson (2004).

The deposit is hosted by Late Triassic alkaline flows, tuffs, epiclastics and syenite intrusives. To the east, Middle Triassic sediments and Lower Permian limestones are thrust westward over these volcanics at the head of Copper Canyon Creek. Two northwesterly-trending dikes of syenite porphyry crop out in the lower part of the creek. The



Figure 9. Alteration characterized by an assemblage of sericite, anhydrite, carbonate (SAC) and pyrite±hematite (specular) overprints an I-5 at the portal to the North Junction Zone.

porphyry is similar to the dark syenite porphyry at Galore Creek. It contains potassium feldspar megacrysts up to 4 cm in length, abundant biotite and disseminated pyrite. An intrusive breccia phase or brecciated intrusive is developed locally. Biotite was collected from the magmatic breccia for radiometric dating; results are pending.

STRUCTURE

The orientations of layered rocks around the Galore Creek magmatic complex outline a broad domal structure, possibly related to intrusion but probably reflecting younger deformational events. The Galore Creek area is flanked on the east by the north-trending, east-dipping Copper Canyon thrust fault, which forms the west-verging component of the regional Scud River fault, which has been interpreted to represent a positive flower structure (Logan and Koyanagi, 1994). The western flank is characterized by north-trending upright folds and a well-developed north-trending, west-dipping mylonite zone. Penetrative deformation of the Triassic rocks is rare and restricted to discrete shear zones or folds in sedimentary rocks. Shear sense gives an apparent top-to-the-west sense of motion (Fig. 10). Folds are broad, open structures and generally plunge southerly. These structures postdate mineralization. The Cone Mountain thrust fault is a northwest-trending, east-dipping mylonite zone with similar tops-to-the-west-directed thrusting (Brown *et al.*, 1996). The footwall to the mylonite is foliated granodiorite (185 Ma), which provides a lower limit to the age of thrusting.

Well-bedded sedimentary and water-lain crystal tuffaceous rocks, exposed along the western edge of the complex and at Copper Canyon, permit a structural analysis of the rocks in the area. With the exception of a thick pack-



Photo 9. Discrete brittle shear zone developed in volcanic conglomerates along the western wall of the Galore Creek basin. Rotation of clasts gives an apparent tops-to-the-west sense of shear.

age of crystal-rich tuffs at Copper Canyon, all other bedding measurements are upright.

Thrusts at Copper Canyon postdate mineralization and may coincide with shears to the west of the complex.

Late dikes, D-1 through D-4, trend 90° and 125°, have north and south dips, and crosscut alteration, mineralization and all I-1 through I-12 syenite dikes.

CHEMISTRY

Samples were steel milled at the British Columbia Geological Survey Branch Laboratory in Victoria. Splits were shipped for analysis to TeckCominco Laboratories, Vancouver for major and trace element abundances (Ba, Rb, Sr, Nb, Zr and Y) by X-ray fluorescence (XRF); ACME Analytical, Vancouver for trace element analyses using inductively coupled plasma – emission spectrometry (ICP-

ES); and Actlabs, Ancaster, Ontario for trace element analyses using instrumental neutron activation analysis (INAA). A subset of these samples has also been sent to Memorial University, Newfoundland for trace element analysis using inductively coupled plasma – mass spectrometry (ICP-MS). Results are pending.

CONCLUSIONS

A Late Triassic volcanic centre is preserved at Galore Creek. Sulphide deposition within it was related to a dynamic system of synvolcanic faults, syenite intrusions, explosive breccias and comagmatic extrusive volcanics. Because dikes, sills and explosive breccias dominate, together with pseudoleucite-bearing intrusives, this is envisioned to have taken place in a high-level setting, possibly within the throat of a volcano. Radiometric ages (Mortensen *et al.*, 1995) indicate a prolonged alkaline magmatic history for the intrusive complex, with the bulk of copper-gold mineralization occurring early. Intense potassium metasomatism and copper-gold mineralization are synvolcanic and latest Triassic in age (Logan and Koyanagi, 1994). Extrusive equivalent rocks of the potassium porphyritic syenite constitute the upper stratigraphy package of the Stuhini Group at Galore Creek (Fig. 11). These rocks are predominantly potassium feldspar and biotite crystal-rich pyroclastic and epiclastic rocks. Accretionary lapilli and depositional bed forms are interpreted to be base surge deposits and indicate subaerial deposition.

No single mineralization-alteration zonation pattern is apparent that would tie all the mineral occurrences at Galore to a single central hydrothermal system (i.e., centred over the Central Zone), nor is there any apparent relation between elevation and either sulphide or alteration mineral assemblages.

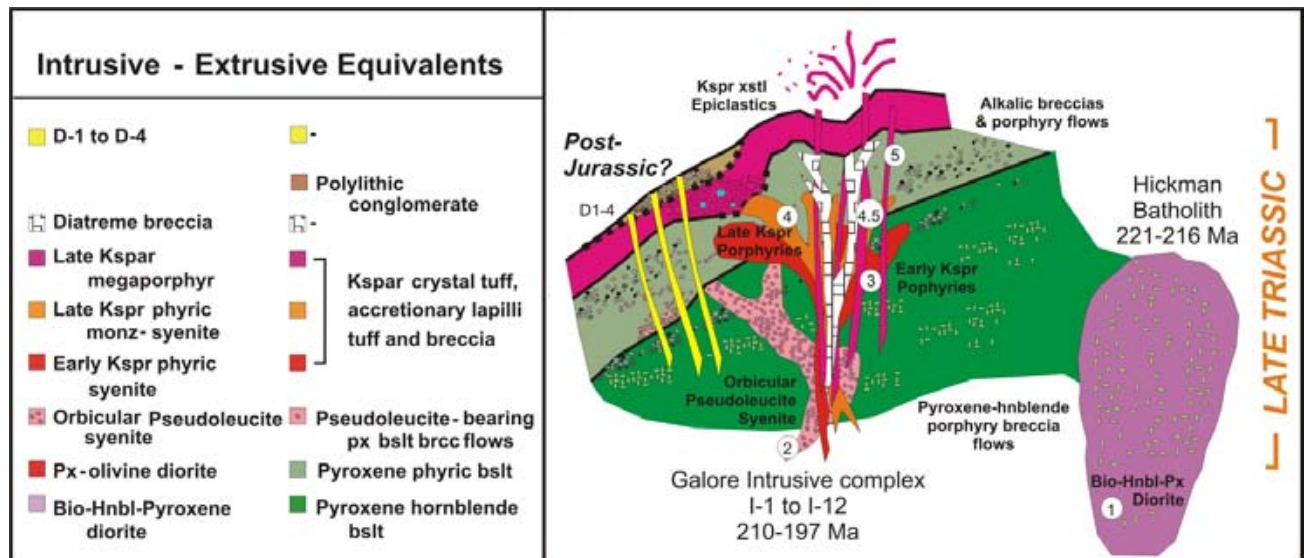


Figure 11. Schematic representation of the Late Triassic volcanic and magmatic complex at Galore Creek, showing relative ages of events.

ACKNOWLEDGMENTS

The Galore Creek component of the Cu-Au Porphyry Project was conceived through discussions with Joe Piekenbrock of NovaGold Resources Inc., Scott Petsel Project Geologist for the Galore Project, and the Ministry of Energy and Mines. It was jointly funded and supplemented by funding from a Rocks to Riches grant. Jim Muntzert and Frank Gish are both heartily thanked for providing such positive and cheerful, in fact infectiously enthusiastic, logistical support. Special thanks are extended to John Proffett, who shared his observations and interpretations of the geology at Galore Creek and numerous other porphyry deposits. Valuable discussions in the field with Stuart Moriss, Bruce Otto and Dave Smithson reintroduced the author to the Galore Creek area and its mineral occurrences. These were helpful and much appreciated. Philip Gordon and a number of the 'core logging elite' shared their knowledge of stratigraphy and alteration-mineralization from the North Junction, Copper Canyon and Gap zones.

Dave Lefebure visited the camp during the course of fieldwork. Brian Grant is thanked for rubber sheeting the submission date and providing editorial comments and help that ensured this paper saw the light of day.

REFERENCES

- Allen, D.G., Panteleyev, A. and Armstrong, A.T. (1976): Galore Creek; in Porphyry Deposits of the Canadian Cordillera, Sutherland Brown, A., Editor, *Canadian Institute of Mining and Metallurgy*, Special Volume 15, pages 402–414.
- Anderson, R.G. (1984): Late Triassic and Jurassic magmatism along the Stikine Arch and the geology of the Stikine Batholith, North-Central British Columbia; in Current Research, Part A, *Geological Survey of Canada*, Paper 84-1A, pages 67–73.
- Anderson, R.G. (1989): A stratigraphic, plutonic, and structural framework for the Iskut River map area, northwestern British Columbia; in Current Research, Part E; *Geological Survey of Canada*, Paper 89-1E, pages 143–151.
- Anderson, R.G. (1993): A Mesozoic stratigraphic and plutonic framework for northwestern Stikinia (Iskut River area), northwestern British Columbia; in Mesozoic paleogeography of the western United States, II: Los Angeles, CA; Dunne, G., and McDougall, K., Editors, *Society of Economic Paleontologists and Mineralogists*, Pacific Section, pages 477–494.
- Barr, D.A., Fox, P.E., Northcote, K.E. and Preto, V.A. (1976): The alkaline suite porphyry deposits: a summary; in Porphyry Deposits of the Canadian Cordillera, Sutherland Brown, A., Editor, *Canadian Institute of Mining and Metallurgy*, Special Volume 15, pages 359–367.
- Bloomer, S.H., Stern, R.J., Fisk, E. and Gerschwind, C.H. (1989): Shoshonitic volcanism in the Northern Mariana Arc, 1. mineralogic and major and trace element characteristics; *Journal of Geophysical Research*, Volume 94, Number B4, pages 4469–4496.
- Brown, D.A., Gunning, M.H. and Greig, C.J. (1996): The Stikine project: geology of western Telegraph Creek map area, northwestern British Columbia; *BC Ministry of Energy, Mines and Petroleum Resources*, Bulletin 95, 175 pages.
- Brown, D.A., Logan, J.M., Gunning, M.H., Orchard, M.J. and Bamber, E.W. (1991): Stratigraphic evolution of the Paleozoic Stikine assemblage in the Stikine Iskut rivers area, northwestern British Columbia (NTS 104G and 104B); in Contributions to the Geology and Geophysics of Northwestern British Columbia and Southeastern Alaska, Anderson, R.G., Editor, *Canadian Journal of Earth Sciences*, Volume 28, pages 958–972.
- de Rosen-Spence, A. (1985): Shoshonites and associated rocks of central British Columbia; in Geological Fieldwork 1984, *BC Ministry of Energy, Mines and Petroleum Resources*, Paper 1985-1, pages 426–442.
- Enns, S.G., Thompson, J.F.H., Stanley, C.R. and Yarrow, E.W. (1995): The Galore Creek porphyry copper-gold deposits, northwestern British Columbia; in Porphyry Deposits of the Northern Cordillera, Schroeter, T.G., Editor, *Canadian Institute of Mining and Metallurgy*, Special Volume 46, pages 630–644.
- Gabrielse, H., Monger, J.W.H., Wheeler, J.O. and Yorath, C.J. (1991): Part A: Morphogeological belts, tectonic assemblages, and terranes; Chapter 2 in Geology of the Cordilleran Orogen in Canada, Gabrielse, H. and Yorath, C.J., Editors, *Geological Survey of Canada*, Geology of Canada, Number 4, pages 15–28 (also Geological Society of America, The Geology of North America, Volume G-2).
- Geological Survey of Canada (1957): Operation Stikine; Map 9-1957.
- Gill, J. and Whelan, P. (1989): Early rifting of an oceanic island arc (Fiji) produced shoshonitic to tholeiitic basalts; *Journal of Geophysical Research*, Volume 94, Number B4, pages 4561–4578.
- Gunning, M.H. (1996): Definition and interpretation of Paleozoic volcanic domains, northwestern Stikinia, Iskut River area, British Columbia; unpublished Ph.D. thesis, *University of Western Ontario*, 389 pages.
- Höy, T. and Dunne, K.P.E. (1997): Early Jurassic Rossland Group, southern British Columbia, Part I – stratigraphy and tectonics; *BC Ministry of Energy and Mines*, Bulletin 109, 196 pages.
- Kerr, F.A. (1948a): Lower Stikine and Iskut River areas, British Columbia; *Geological Survey of Canada*, Memoir 246, 94 pages.
- Kerr, F.A. (1948b): Taku River map area, British Columbia; *Geological Survey of Canada*, Memoir 248, 84 pages.
- Leary, G. (1990): Report on 1990 Phase I mapping and drilling on the Copper Canyon property, northwestern British Columbia; *BC Ministry of Energy, Mines and Petroleum Resources*, Assessment Report 21 062.
- LeMaitre, R.W., Editor (1989): Classification of igneous rocks and glossary of terms; *Blackwell Scientific Publications*, Oxford, 193 pages.
- Logan, J.M. and Koyanagi, V.M. (1994): Geology and mineral deposits of the Galore Creek area, northwestern British Columbia (104G/3 and 4); *BC Ministry of Energy, Mines and Petroleum Resources*, Bulletin 92, 96 pages.
- Logan, J.M., Koyanagi, V.M. and Rhys, D.A. (1989): Geology and mineral occurrences of the Galore Creek area (104G/3 and 4); *BC Ministry of Energy, Mines and Petroleum Resources*, Open File 1989-8.
- Logan, J.M., Drobe, J.R. and McClelland, W.C. (2000): Geology of the Forrest Kerr – Mess Creek area, northwestern British Columbia (NTS 104B/10, 15 and 104G/2 & 7W); *BC Ministry of Energy and Mines*, Bulletin 104, 164 pages.
- McClelland, W.C. (1992): Permian and older rocks of the southwest Iskut River map area, northwestern British Columbia; in Current Research, Part A, *Geological Survey of Canada*, Paper 92-1A, pages 303–307.

- McMillan, W.J. (1991): Porphyry deposits in the Canadian Cordillera; in *Ore Deposits, Tectonics and Metallogeny in the Canadian Cordillera*, BC Ministry of Energy, Mines and Petroleum Resource, Paper 1991-4, pages 253–276.
- Monger, J.W.H. (1970): Upper Paleozoic rocks of the Stikine arch, British Columbia; *Geological Survey of Canada*, Paper 70-1, Part A, pages 41–43.
- Monger, J.W.H. (1977): Upper Paleozoic rocks of northwestern British Columbia; *Geological Survey of Canada*, Paper 77-1A, pages 255–262.
- Mortensen, J.K., Ghosh, D.K. and Ferri, F. (1995): U-Pb geochronology of intrusive rocks associated with copper-gold porphyry deposits in the Canadian Cordillera; in *Porphyry Deposits of the Northwestern Cordillera of North America*, T. G. Schroeter (Editor), *Canadian Institute of Mining, Metallurgy and Petroleum*, Special Volume 46, pages 142–158.
- Mortimer, N. (1986): Late Triassic, arc-related, potassic igneous rocks in the North American Cordillera; *Geology*, Volume 14, pages 1035–1078.
- Mortimer, N. (1987): The Nicola Group: Late Triassic and Early Jurassic subduction-related volcanism in British Columbia; *Canadian Journal of Earth Sciences*, Volume 24, pages 2521–2536.
- Mutschler, F.E., Griffin, M.E., Stevens, D.S., Shannon, S.S. (1985): Precious metal deposits related to alkaline rocks in the North American Cordillera – an interpretive review; *Transactions of the Geological Society South Africa*, Volume 88, pages 355–377.
- Mutschler, F.E., Mooney, T.C. and Johnson, D.C. (1990): Precious metal deposits related to alkaline igneous rocks – a space-time trip through the Cordillera; in *Proceedings of the Fourth Western Regional Conference on Precious Metals and the Environment*, *American Institute of Mining Engineers*, Society for Mining, Metallurgy, and Exploration, pages 43–59.
- Nelson, J. (1991): The tectonic setting of alkaline porphyry suite copper-gold deposits in the Canadian Cordillera (abstract); *Canadian Institute of Mining, Metallurgy and Petroleum*, 93rd Annual General Meeting, Vancouver, April, 1991, page 57.
- Nelson, J. and Bellefontaine, K.A. (1996): The geology and mineral deposits of north-central Quesnellia: Tezzeron Lake to Discovery Creek, central British Columbia; *BC Ministry of Energy, Mines and Petroleum Resources*, Bulletin 99, 112 pages.
- Nelson, J. and Mihalynuk, M.G. (1993): Cache Creek Ocean: closure or enclosure? *Geology*, Volume 21, pages 173–176.
- Nixon, G.T., Archibald, D.A., and Heaman, L.M. (1993): ^{40}Ar - ^{39}Ar and U-Pb geochronometry of the Polaris Alaskan-type complex, British Columbia: precise timing of Quesnellia-North America interaction; *Geological Association of Canada – Mineralogical Association of Canada*, Joint Annual Meeting, Waterloo, ON, Program with Abstracts, p. 76.
- Palfy, J., Smith, P.L. and Mortensen, J.K. (2000): A U-Pb and ^{40}Ar - ^{39}Ar time scale for the Jurassic; *Canadian Journal of Earth Sciences*, Volume 37, pages 923–944.
- Orchard, M.J. (1991): Report on conodonts and other microfossils from the Telegraph Creek – Iskut River, northwestern British Columbia; *Geological Survey of Canada*, Conodont Data File, Report OF-1991-13.
- Pearce, J.A. and Cann, J.R. (1973): Tectonic setting of basic volcanic rocks determined using trace element analyses; *Earth and Planetary Science Letters*, Volume 19, pages 290–300.
- Pearce, J.A., Harris, N.B.W. and Tindle, A.G. (1984): Trace element discrimination diagrams for the tectonic interpretation of granitic rocks; *Journal of Petrology*, Volume 25, Part 4, pages 956–983.
- Panteleyev, A. (1973): GC, HAB, BUY (Stikine Copper); in *Geology in British Columbia 1972*, BC Ministry of Energy, Mines and Petroleum Resources, pages 520–526.
- Panteleyev, A. (1974): GC, HAB, BUY (Stikine Copper); in *Geology in British Columbia 1973*, BC Ministry of Energy, Mines and Petroleum Resources, pages 501–504.
- Panteleyev, A. (1975): Galore Creek map area; in *Geological Fieldwork 1974*, BC Ministry of Energy, Mines and Petroleum Resources, Paper 1975-1, pages 59–62.
- Panteleyev, A. (1976): Galore Creek map area; in *Geological Fieldwork 1975*, BC Ministry of Energy, Mines and Petroleum Resources, Paper 1976-1, pages 79–81.
- Panteleyev, A. (1983): GC, HAB, BUY (Stikine Copper); in *Geology in British Columbia 1976*, BC Ministry of Energy, Mines and Petroleum Resources, pages 122–125.
- Panteleyev, A., Bailey, D.G., Bloodgood, M.A. and Hancock, K.D. (1996): Geology and mineral deposits of the Quesnel River – Horsefly map area, central Quesnel Trough, British Columbia (NTS map sheets 93A/5, 6, 7, 11, 12, 13; 93B/9, 16; 93G/1; 93H/4); *BC Ministry of Energy, Mines and Petroleum Resources*, Bulletin 97, 156 pages.
- Ricketts, B.D., Evenchick, C.A., Anderson, R.G. and Murphy, D.C. (1992): Bowser basin, northern British Columbia: constraints on the timing of initial subsidence and Stikinia-North America Terrane interactions; *Geology*, Volume 20, pages 1119–1122.
- Sillitoe, R.H. (1991a): Geological reassessment of the Galore Creek porphyry Cu-Au deposit, British Columbia, unpublished company report, *Kennecott Canada Inc.*, Vancouver, British Columbia, 12 pages.
- Sillitoe, R.H. (1991b): Further comments on the geology and exploration of the Galore Creek porphyry Cu-Au deposit, British Columbia, unpublished company report, *Kennecott Canada Inc.*, Vancouver, British Columbia, 12 pages.
- Souther, J.G. (1971): Geology and mineral deposits of Tulsequah map area; *Geological Survey of Canada*, Memoir 362, 76 pages.
- Souther, J.G. (1972): Telegraph Creek map area, British Columbia; *Geological Survey of Canada*, Paper 71-44, 38 pages.
- Souther, J.G. (1992): The Late Cenozoic, Mount Edziza Volcanic Complex, British Columbia; *Geological Survey of Canada*, Memoir 420, 320 pages.
- Streckeisen, A. (1975): To each plutonic rock its proper name; *Earth-Sciences Review*, Volume 12, pages 1–33.
- Sutherland Brown, A. (1976): Morphology and classification; in *Porphyry Deposits of the Canadian Cordillera*, Sutherland Brown, A., Editor, *Canadian Institute of Mining and Metallurgy*, Special Volume 15, pages 44–51.
- Tozer, E.T. (1988): Report on Triassic fossils from Telegraph Creek map area, British Columbia; *Geological Survey of Canada*, Report Tr-1-ETT 1988, 3 pages.
- Watson, J.L. (1969): Garnets of Stikine Copper's Galore Creek property; unpublished B.Sc. thesis, *University of British Columbia*, 27 pages.
- Wheeler, J.O. and McFeely, P. (1991): Tectonic assemblage map of the Canadian Cordillera and adjacent parts of the United States of America; *Geological Survey of Canada*, Map 1712A, scale 1:2 000 000.

White, W.H., Harakal, J.E. and Carter, N.C. (1968): Potassium-argon ages of some ore deposits in British Columbia; *Canadian Institute of Mining and Metallurgy Bulletin*, Volume 61, pages 1326–1334.

Yarrow, E. and Taylor, K.J. (1990): Report on soil, rock geochemical sampling, VLF-EM, magnetometer and diamond drill

surveys on the Galore Creek Group I, II, III claims, Liard Mining Division; *BC Ministry of Energy, Mines and Petroleum Resources*, Assessment Report 20 558.

Regional Geology and Setting of the Cariboo, Bell, Springer and Northeast Porphyry Cu-Au Zones at Mount Polley, South-Central British Columbia

By James M. Logan and Mitchell G. Mihalynuk

KEYWORDS: geology, mineralization, alkaline, porphyry copper-gold, Quesnellia, Mount Polley, Cariboo, Bell, Springer, Northeast zone, Nicola, hydrothermal breccia, magnetite, Likely

INTRODUCTION

Porphyry deposits and prospects containing copper, molybdenum, gold and tungsten are the most important historic contributors to the metallic mining industry in British Columbia. Elevated metal prices and recent exploration successes have rekindled interest in British Columbia's copper-gold porphyry deposits. In particular, the alkaline Cu-Au porphyry class of deposits, such as Galore Creek, Mount Polley and Afton-Ajax, are key exploration targets. These and co-spatial calcalkaline Cu-Mo, Cu-Mo-Au porphyry deposits formed outboard of ancestral North America in island-arc settings in Late Triassic to Early Jurassic time. Two major components of this arc, the Stikine and Quesnel terranes, were the locus of a discrete alkaline mag-

matic event that gave rise to alkaline Cu-Au deposits at the end of the Triassic period (210 to 200 Ma).

In order to better understand the controls on mineralization and maximize exploration efficiencies, a partnership was struck between the British Columbia Ministry of Energy and Mines and exploration companies with a direct interest in refining the alkaline Cu-Au porphyry exploration model (Abacus Mining and Exploration Corporation, Imperial Metals Corporation, NovaGold Resources) as it applies to the Iron Mask, Mount Polley and Galore Creek magmatic complexes. The new information provided by these studies will update the provincial database and mineral deposit models, and promote Cu-Au porphyry exploration that will ultimately lead to new discoveries and resources in the province.

The Mount Polley Cu-Au porphyry deposit is located 56 km northeast of Williams Lake on the west side of Quesnel Lake (Fig. 1), approximately 8 km southwest of Likely (MINFILE 093A/008, 093A/164). It is currently owned and operated by Imperial Metals Corporation.

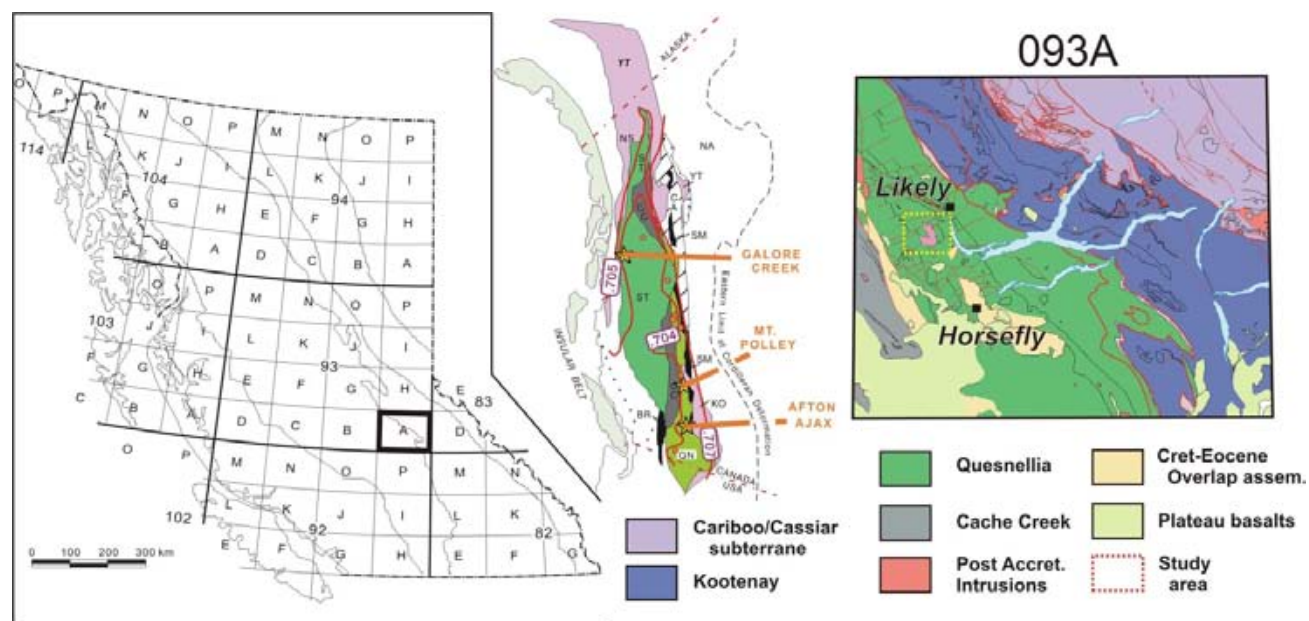


Figure 1. Location of the Mount Polley component of the Cu-Au Porphyry Project in south-central British Columbia (NTS 092I). Inset is terrane map of the northern Cordillera (modified from Wheeler and McFeely, 1991), showing the tectonostratigraphic setting of the three study areas. Mesozoic initial Sr isopleths are from Armstrong (1988). Box on right shows detailed terrane relationships for NTS 093A and the project area.

Production at Mount Polley began in October 1997 (Cariboo-Bell) and continued until 2001, with an overall production of 60 735 000 kg of copper; 11 517 000 g of gold and 2 347 000 g of silver from a total of 35.5 million tonnes mined and 27.6 million tonnes of material milled (BC Ministry of Energy and Mines, MINFILE). In 2003, discovery of a new zone of high-grade Cu-Au mineralization, the 'Northeast zone', spurred re-evaluation of the Mount Polley property and a resurgence in porphyry exploration east of Williams Lake.

Ongoing assessment of the previously produced (Springer and Bell zones) and newly identified (Northeast zone) resources on the property indicates the total proven and probable reserves to be: 24 733 044 t of 0.362% Cu and 0.31 g/t Au for the Springer zone; 9 784 689 t of 0.264% Cu and 0.297 g/t Au for the Bell; and 6 202 814 t of 0.9782% Cu, 0.324 g/t Au and 6.978 g/t Ag for the Northeast zone (Imperial Metals Corporation, press release, August 3, 2004). In anticipation of restarting operations at Mount Polley, Imperial Metals has applied, and been approved, for a mine permit amendment to allow mining of the Northeast zone. The Northeast zone has been renamed the 'Wright pit' after the late George Wight, mine manager at Cariboo-Bell from 1996–2003.

The Mount Polley field component of the Cu-Au porphyry study comprised reconnaissance geological mapping and sampling of the 200 km² area centred on the Cariboo pit. Key objectives of the project are to elucidate the stratigraphic and petrochemical relationships between the volcanic, subvolcanic and plutonic rocks that constitute the alkaline complex and to evaluate relationships between the newly discovered Northeast zone mineralization and the main hydrothermal system responsible for the Central zone (Cariboo and Bell) and West zone (Springer) mineralization. Uranium-lead dates for intrusive phases in the Mount Polley complex show Late Triassic crystallization ages (204.7 ± 3 Ma; Mortensen *et al.*, 1995) using the time scale of Palfy (2000). However, previously defined stratigraphy based on regional correlations, fossil determinations and imprecise radiometric-dating techniques, which gave cooling rather than crystallization ages, are Early Jurassic for the country rocks. Mapping around Mount Polley and additional alkaline magmatic centres (Shiko Lake, Bullion Pit and Bootjack West) was conducted to help reconcile this inconsistency.

PREVIOUS WORK

Regional geological studies in the Quesnel River area by the Geological Survey of Canada were carried out in the 1950s and 1960s (Tipper, 1959, 1978; Campbell, 1961, 1963; Campbell and Campbell, 1970), but it was not until the work by Fox (1975) that the alkaline composition of the volcanic rocks was recognized in the Quesnel area. Detailed mapping and mineral deposit studies in the Horsefly area by Morton (1976) and by Bailey (1978) in the area around Morehead Lake provided the first stratigraphic subdivisions and descriptions of the geology encompassing Mount Polley.

Regional studies of the contact relationships between the Intermontane-Omineca belts have been the focus of numerous university thesis studies (e.g., Rees, 1987; Ross *et al.*, 1985, 1989; McMullin *et al.*, 1990 and references therein; Struik, 1986, 1987, 1988a, b). Bailey (1988, 1989, 1990), Panteleyev (1987, 1988), and Panteleyev and Hancock (1989) carried out regional-scale geological mapping and mineral evaluation in the area located between Quesnel and the Horsefly River as part of the 1985–1990 Canada-British Columbia Mineral Development Agreement. The focus of their studies was to remap and re-interpret the central Quesnel volcanic belt and test the economic potential for gold and copper deposits along its volcanic-intrusive axis (Panteleyev *et al.*, 1996). Deposit studies at Mount Polley by Fraser (1994, 1995) and Fraser *et al.* (1995) recognized three stages of breccia emplacement (pre, syn and post-mineralization) and distinct alteration assemblages that separate the deposit into two distinctive zones.

REGIONAL GEOLOGY

The study area lies along the eastern margin of the Intermontane Belt, close to its tectonic boundary with the Omineca Belt, in south-central British Columbia. At this latitude, the Intermontane Belt is underlain mainly by Upper Paleozoic to Lower Paleozoic arc-volcanic, plutonic and sedimentary rocks of the Quesnel Terrane. Farther west are coeval rocks of the oceanic Cache Creek Terrane (Fig. 1). The Quesnel Terrane consists of a Late Triassic to Early Jurassic magmatic-arc complex that formed above an east-dipping subduction zone (Mortimer, 1987). The Cache Creek Terrane, with its Late Triassic to Middle Jurassic blueschist-facies rocks, represents the remnants of this subduction-accretionary complex (Travers, 1977; Mihalynuk *et al.*, 2004). Quesnellia is fault bounded, juxtaposed on the west with Paleozoic and Mesozoic rocks of the Cache Creek complex and on the east with Mesozoic to Paleozoic and older metasedimentary, metavolcanic and metaplutonic rocks of the pericratonic Kootenay Terrane. The Barkerville and Cariboo Subterrane of the Kootenay Terrane separated Quesnellia from North America until the Middle Jurassic, at which time they were imbricated and thrust eastward onto the North American craton. The tectonic boundary between the Kootenay and Quesnel terranes is intruded by the Jura-Cretaceous Raft Batholith to the south. Tertiary volcanic rocks and feeder dikes of the Chilcotin Group are the youngest rocks in the region.

Mount Polley is one of a chain of alkalic intrusion-related Cu-Au deposits that developed in the Upper Triassic to Lower Jurassic volcanic-plutonic arc rocks of the Quesnel Terrane (Barr *et al.*, 1976). It is hosted by a high-level alkalic intrusive complex within the Central Quesnel Belt that is of latest Triassic age (202 Ma; Mortensen *et al.*, 1995). A chain of similar deposits extends the length of the Intermontane Belt (Fig. 1). In the south, they are associated with the Iron Mask batholith (Afton, Ajax, and Crescent) and Copper Mountain intrusives (Copper Mountain, Ingerbelle) and, to the north, with the Hogem batholith (Lorraine) and, in the Stikine Terrane, with Galore Creek intrusives (Galore Creek).

Triassic Nicola Group

In the vicinity of Quesnel Lake, the Nicola Group consists of a lower, dominantly metasedimentary unit and an upper, dominantly volcanic-arc assemblage (Fig. 2). The older Middle to Late Triassic (Anisian to Norian) sedimentary unit forms a northwest-trending belt exposed east of Quesnel Lake. It has been estimated to comprise at least 2500 m (Rees, 1987) to locally 4000 m (Bloodgood, 1990) of fine-grained sedimentary rocks that grade upward into (Carnian to Norian) basal units of the upper volcanic unit. The overlying volcanic rocks define a parallel northwest-trending belt up, to 20 km wide, of subaqueous and subordinate subaerial volcanic rocks with an estimated thickness on the order of 5 to 6.5 km (Rees, 1987; Panteleyev *et al.*, 1996). Thickest accumulations of volcanic rocks and coeval subvolcanic intrusions define the magmatic axis of the Quesnel arc.

Panteleyev *et al.* (1996) adopted the stratigraphy of Bailey (1978) and recognized three volcanic units in the study area: a subaqueous pyroxene-phyric basalt unit of predominantly flows and breccias; pyroclastic and laharic deposits of more evolved 'felsic compositions; and an upper subaerial analcime-bearing olivine basalt unit. Ages of these three units were interpreted to span the Upper Triassic to Early Jurassic boundary. The main basaltic unit was reported as Carnian to Norian in age, the felsic more differentiated volcanoclastic unit, Sinemurian, and the upper analcime-bearing basalt reported as Sinemurian to pre-Pliensbachian (Panteleyev *et al.*, 1996 and references therein). Subsequent U-Pb isotopic dating of the various intrusive phases of the Polley and Bootjack stocks indicates that these intrusives are Upper Triassic in age (Palfy, 2000) and therefore can not be intruding rocks younger than 200 Ma.

The stratigraphy presented below summarizes the results of 3 weeks of mapping; it does not benefit from any new radiometric or fossil constraints and is therefore preliminary in scope and intent (Fig. 3). A detailed multisensor airborne survey (Shives *et al.*, 2004) aided stratigraphic and structural analysis (Fig. 4).

AUGITE±OLIVINE BRECCIA FLOWS AND TUFFACEOUS ROCKS.

Green, grey and dark maroon pyroxene-phyric alkali olivine basalt flows, breccias and minor pillow basalt crop out near Jacobie Lake, west of Morehead Lake and south of Mount Polley. The flows are commonly massive with amygdaloidal brecciated tops. Massive coherent flows are interlayered with block and lapilli-flow breccias. Textures vary and include aphyric and trachytic varieties, but most commonly are coarsely porphyritic. Phenocrysts of pyroxene and plagioclase (up to 10 mm) and olivine (5 mm) constitute from 30 to 75% of the rock. The groundmass consists of very fine grained plagioclase (microlites), clinopyroxene, olivine, magnetite and alteration minerals, including iddingsite, calcite, chlorite, pyrite and epidote. Vesicles are rimmed by analcime and filled by calcite.

Copper mineralization occurs within interlayered maroon and green, pyroxene-olivine-phyric flow breccias

near Jacobie Lake (Fig. 2). Here, 2 cm wide veins of chalcocite, malachite and azurite are localized at the contact zone between the base of one flow and the top of another. Zeolites commonly replace the matrix or fill voids within the volcanic units.

PYROXENE PORPHYRY BRECCIAS AND CRYSTAL-RICH SEDIMENTS

Pyroxene-phyric basalt flows, breccias and tuffaceous rocks display volcanic textures and depositional forms similar to those of the augite-olivine basalts, differing only by the absence of olivine and the greater abundance of plagioclase. Pyroxene basalts are more extensive, although they are locally interdigitated with augite-olivine basalt.

These rocks are maroon, green and grey in colour. Thick flows have massive centres and brecciated tops and/or bottoms. Breccias are clast supported to matrix rich. Lapilli to block tuff flows and fluidal ejecta are interlayered with juvenile pyroxene and plagioclase crystal-rich sandstones and finer grained green and grey siltstones. Well-preserved, thin-bedded, waterlain crystal and ash tuffs crop out along the Ditch road, west of Quesnel Lake and southeast of Jacobie Lake (Fig. 5). West of Quesnel Lake, submarine debris flows disrupt the strata and incorporate poorly preserved horn corals. Near Jacobie Lake, a complete (?) eruptive cycle is preserved in outcrop, beginning with coarse breccia blocks of purple vesicular pyroxene-plagioclase-phyric basalt that fine upward through lapilli and ash to crystal-rich horizons of pyroxene and plagioclase (Fig. 3). Normal graded bedding, crossbedding and load features are common in the sediments; all indicate upright facing beds and a subaqueous environment of deposition.

ANALCIME-BEARING PYROXENE BASALT BRECCIAS

Analcime-bearing mafic flows crop out near Trio Lake, Mount Polley and west of Morehead Lake (Fig. 2). However, easily accessible and excellent exposures are found along the highway north of Prior Lake within an ~260 m thick volcanic section dominated by dark grey-green to maroon, vesicular augite-porphyrus flows. Analcime content varies from one flow to the next, as do pyroxene and olivine contents. Typical flows comprise 30% medium to coarse-grained euhedral pyroxene (up to 60%); 20–50% fine to coarse plagioclase, locally including coarse trachytically aligned, bladed phenocrysts; 2–10% medium-grained olivine, commonly replaced by bright red iddingsite (Fig. 6); up to 10% amygdules, mostly filled with calcite and chlorite; and 0–20% euhedral, salmon pink analcime up to 3 cm in diameter (Fig. 7). The volcanic section extends along strike to the north and, at Sister Mountain, is intruded by a <1 km² subvolcanic hornblende-plagioclase-phyric monzonite body. Other parts of the section include well-bedded tuffite and debris flows, including metre-size blocks of limestone. These features point to a submarine depositional environment.

Correlative maroon olivine-pyroxene-phyric basalt flows, breccias and poorly bedded ash and crystal tuff, located west of Morehead Lake, also contain conspicuous

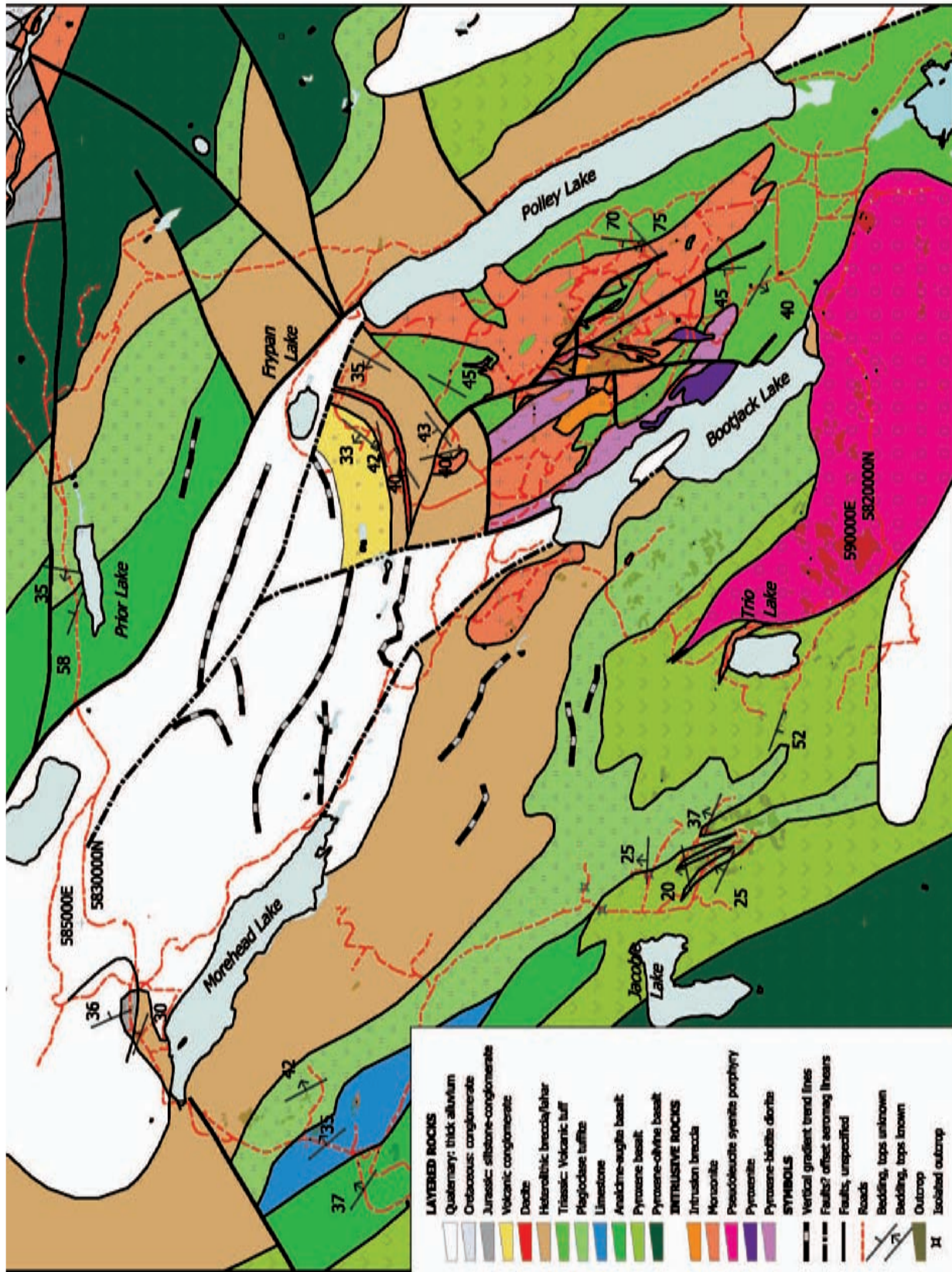


Figure 2. Compilation map of the Mount Polley area. Incorporates unpublished assessment work and published work by Bailey (1990), Hodgson *et al.* (1976), Panteleyev *et al.* (1996), Shives *et al.* (2004) and Wild (1999).

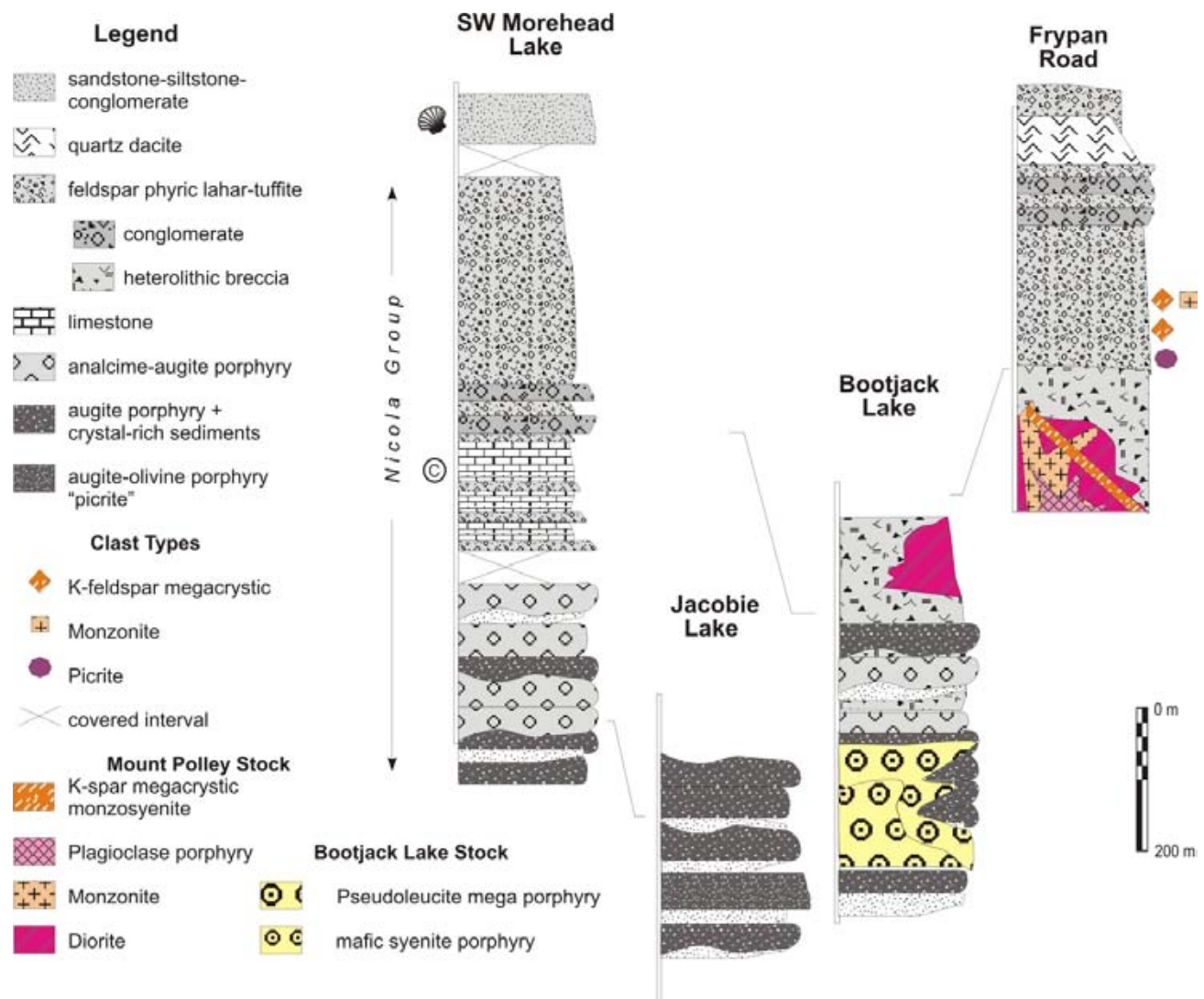


Figure 3. Stratigraphic sections for Nicola Group volcanic and sedimentary rocks in the Morehead Lake, Jacobie Lake, Bootjack Lake and Frypan Road areas.

analcime (Fig. 3). Flow rock comprises coarse tabular crystals of pyroxene; subrounded olivine (3–5 mm, altered to iddingsite); plagioclase laths; and pink or brownish, rounded to euhedral analcime crystals (2–5mm, 10–20%). Some of the flow tops contain amygdulose of analcime, calcite, chlorite and minor epidote. In thin-section, euhedral to subhedral analcime crystals (0.25 mm) and plagioclase laths are interstitial to larger euhedral (2–3 mm) zoned clinopyroxene crystals and altered olivine grains (<1 mm).

Massive, dark green to black, analcime-bearing pyroxene±olivine–phyric flows and breccias south and east of Trio Lake are intruded and hornfelsed by pseudoleucite porphyritic syenite of the Bootjack stock. In addition to pyroxene, plagioclase and olivine phenocrysts, the basalt contains up to about 20% euhedral to rounded, white analcime crystals. The basalt is interlayered with thick heterolithic volcanoclastic breccias dominated by pyroxene-plagioclase– and pyroxene-olivine–phyric fragments. Similar, coarsely porphyritic grey-green analcime-

bearing olivine-pyroxene basalts are exposed in the containment ditch south of the mine, and on the Polley Lake road, west of the mine.

NORIAN – LIMESTONE AND INTERBEDDED MAROON EPICLASTICS

Light to medium-grey, recrystallized micritic limestone is exposed on two hillsides south of the highway, west of Morehead Lake (Fig. 2). The unit is no more than a few hundred metres thick and is discontinuous along strike. It dips moderately northeast and is interbedded with maroon epiclastic and conglomeratic units. Deposition of limestone and reworked clastic rocks probably mark a hiatus in volcanic activity.

The lower sections of the limestone are interbedded with 0.5 to 1.5 m thick maroon and limonitic weathering lapilli and fine, ash-rich tuff beds that overlie (across a 100 m covered section), pink analcime-bearing, pyroxene-olivine–phyric volcanic breccias and massive basalt flows.

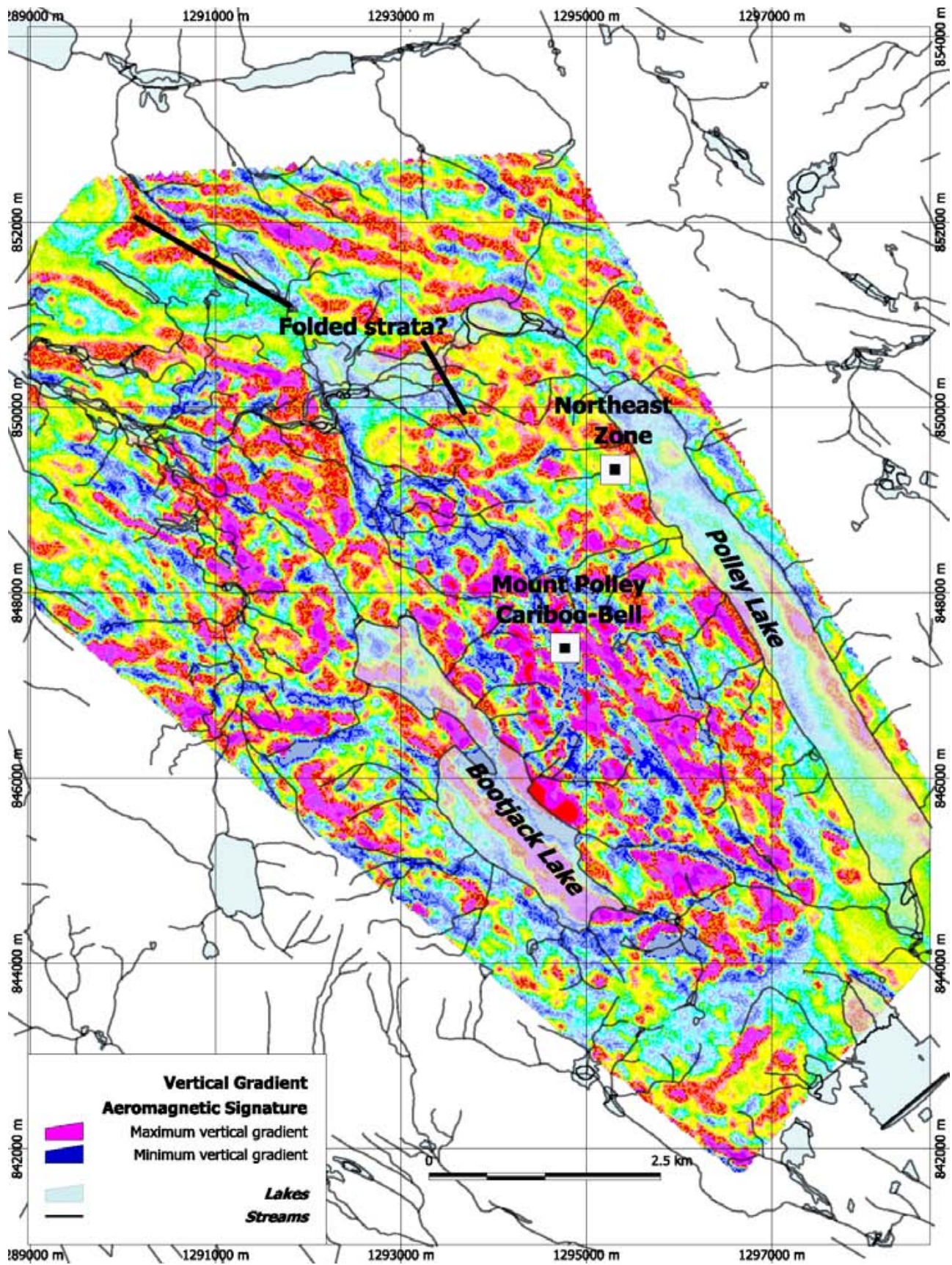


Figure 4. Vertical-gradient magnetic lineaments adapted from Shives *et al.* (2004).



Figure 5. Picritic basalt breccia interbedded with volcaniclastic units of the Nicola Group, southeast of Jacko Lake

Up section, the limestone is characterized by 5 to 10 cm thick beds of medium-grey micrite. The limestone is brecciated, recrystallized and cut by white calcite and limonitic iron carbonate veinlets; traces of pyrite and malachite occur locally where the limestone crops out along highway (Fig. 3).

At this locality, the limestone is reported to contain fossils of uncertain Lower Jurassic age (GSC- 93216, Sinemurian?; *in Panteleyev et al.*, 1996); however, it is correlated with other discontinuous lenses of grey limestone unequivocally dated as Norian based upon conodont fauna (H.W. Tipper *in Panteleyev et al.*, 1996). This limestone datum marks the top of the Triassic volcanic-volcaniclastic section on the west side of the central axis of the Quesnel belt (Bailey, 1988; Panteleyev *et al.*, 1996).

LAHAR AND TUFFITE

A red to brown-weathering, tuffaceous lahar is exposed along the Frypan road (between Bootjack and northern Polley Lake) and around the northern end of Morehead Lake (Fig. 2). It is characterized by a dark hematitic ash matrix and conspicuous, locally abundant white and pink zeolites (laumontite) that replace the matrix and coat fractures. Clasts are polyolithic and primarily angular lapilli with rare rounded boulders that show a complete lack of sorting. Clast compositions are dominated by green and maroon, crowded tabular feldspar porphyry basalts. The lahar is chaotic and massive; rarely are bedding attitudes observed.

Near Morehead Lake, the unit is heterolithic (Fig. 8). Common clast types include: maroon, fine tabular feldspar porphyry; aphanitic dark green basalt, locally with sparse coarse pyroxene crystals; olivine-magnetite (\pm chromite) dunite; fine to medium-grained, holocrystalline pink syenite (?) or K-metasomatized monzonite; polygenetic tuff and/or tuffite. At apparently deeper stratigraphic levels (assuming no fault displacements across numerous covered



Figure 6. Typical flow, comprising euhedral pyroxene, plagioclase and olivine replaced by bright red iddingsite.

intervals), the lahar gives way to well-bedded maroon sandstone with sparse conglomerate lenses less than 10 cm thick. Clasts are tabular feldspar porphyry, lesser feldspar-hornblende porphyry, and sparse but conspicuous pyroxene clasts. Still farther down section, these become more tuffaceous in character and end abruptly at a covered contact with limestone (Fig. 3). Correlative units to the tuffaceous rocks are reported to contain Late Triassic fossils (GSC- 117609, 10 and 117621, Norian, probably upper Norian; *in Panteleyev et al.*, 1996).

Clasts from an isolated outcrop of polyolithic block to lapilli tuff located southwest of Morehead Lake consist of 90% crowded feldspar porphyries with equal abundances of trachytic and felted textures. Aphanitic mafic clasts and rare pyroxene-phyric clasts constitute the remaining 10%.

Exposures of the unit along the Frypan road are also heterolithic. Clasts include maroon, fine tabular feldspar porphyry; aphanitic green basalt; grey plagioclase-pyroxene-phyric basalt; and subvolcanic pyroxene microdiorite and monzonite. It is matrix supported with angular clasts, some of which display thin reaction rims. In one locality, the lahar is incised by a channel containing polyolithic volcanic conglomerate (Fig. 3).

EARLY JURASSIC SEDIMENTARY UNIT

East of Morehead Lake, shallowly dipping dirty brown sandstone, black siltstone and lesser calcareous granule conglomerate contain abundant fossil fauna that all point to an Early Jurassic age (GSC- 93215b, Lower Sinemurian, Canadensis Zone; *in Panteleyev et al.*, 1996). These strata may have been deposited atop the maroon lahar unit. Although contacts are covered, bedding orientations suggest a simple stratigraphic succession. If this is correct, the con-



Figure 7. Atypically coarse analcime-bearing pyroxene±olivine-phyric flow, highway north of Prior Lake.

glomerate is between Norian and Sinemurian in age, deposited near the Jurassic-Triassic boundary (Fig. 3).

CONGLOMERATES AND TUFFITE

Conglomerate and tuffite are apparently most extensive where they crop out near Morehead Lake and east of Polley Lake (Fig. 2). At these localities, a clear separation of this unit from the lahar-tuffite unit may not be possible. Lithologically similar units can be observed at other localities, such as the highway cutbanks north of Prior Lake, near Jakobie Lake, and along the eastern cliffs of northern Quesnel Lake; however, at these localities, the volcanic sandstone and volumetrically subordinate conglomerate tend to be intercalated with coarse tuffaceous or flow units and are clearly part of the arc construction phase.

The conglomerate unit is a variegated polymictic cobble to boulder conglomerate, best exposed on low glaciated outcrops and small knobs on both sides of the Frypan road. The unit apparently rests atop the tuffaceous lahar exposed in the Frypan roadcuts and around the northern end of Morehead Lake (see above). Polymictic conglomerate is massive to locally well bedded (Fig. 9). It contains subangular to well-rounded clasts up to large boulder size (70 cm).

Clast composition is variable, including monzonite (Fig. 3), possibly derived from the 'Polley volcanic succession' and a variety of plagioclase porphyries that contain hornblende or pyroxene. Pyroxene porphyry clasts are



Figure 8. Hematitic, maroon weathering tuffaceous lahar, comprised dominantly of angular to subrounded clasts of crowded tabular feldspar porphyry basalt in a crystal-rich ash matrix. Exposure on highway southwest Morehead Lake.

probably derived from the more deeply incised part of the arc. These conglomerate units could mark a significant hiatus in volcanic deposition, although unit thickness is a poor proxy for elapsed time in dynamic volcanic environments. Note that heterolithic volcanic breccia and lahar-conglomeratic units are intruded by monzonite in the area between the Cariboo pit and Polley Lake, near the Au zone and possibly also west of Bootjack Lake. These are older volcanoclastic rocks that lie stratigraphically lower in the pile.

QUARTZ-PHYRIC MAUVE DACITE.

Dense, quartz-phyric, white to mauve-weathering lapilli tuff is exposed in two outcrops between Bootjack Lake and northern Polley Lake (Fig. 2). We have used the field term 'mauve dacite' for this unit even though the SiO₂ content is not quite high enough to place it squarely within the dacite field. Based upon bedding in enclosing strata, the thickness of this unit can be estimated as at least 70 m



Figure 9. Jurassic (?) conglomerate south of Frypan Road and north of Mount Polley.

(Fig. 3). It is crystal rich, composed of tabular and broken plagioclase laths (40%, <3 mm), hornblende (3% altered 2–3 mm prisms), light grey quartz eyes (up to 1%, 5 mm in diameter) and biotite (<1%, altered 2–3 mm booklets). A vague compaction fabric is preserved locally, but clear evidence of collapsed pumice fragments or welding is absent.

Bedding orientations of enclosing strata are parallel to the trend of the mauve dacite unit. A poorly exposed, probable gradational southern contact with the maroon laharic conglomerate suggests that this unit is part of the volcanic stratigraphy and not a hypabyssal intrusion, although a tuff dike or sill origin cannot be ruled out. Areas south of the unit have been penetrated by diamond-drilling. No unit like the mauve dacite is described in drillcore logs (Tennant, 1997, 1998, 2000). A sample of mauve dacite was collected for U-Pb geochronology; results are pending.

Mount Polley Intrusive Complex

The Mount Polley stock is a north to northwest-trending, high-level, composite alkalic intrusive complex (Fig. 2). The stock is 5.5 by 4 km in size and comprises primarily fine-grained porphyritic diorite and monzonite, plagioclase porphyry and syenite dikes with abundant screens of metavolcanic rocks and hydrothermal breccias, features characteristic of a subvolcanic environment. Bordering it to the southwest is an ~1 km thick panel of volcanic strata that separates it from the 2.3 by 7 km, northwest-elongated Bootjack stock, which is also a composite intrusive body and includes an unusual orbicular pseudoleucite syenite. Subvolcanic textures are lacking in the Bootjack stock.

A hornblende ^{40}Ar - ^{39}Ar plateau age from the coarse-grained syenite phase of the Bootjack stock yielded a well-defined age of 203.1 ± 2.0 Ma (Bailey and Archibald, 1990). Uranium-lead ages (Mortensen *et al.*, 1995) from the Polley stock (201.7 \pm 4 Ma; zircon, diorite and 204.7 \pm 3 Ma; zircon, plagioclase porphyry) are similar to ages from the Bootjack stock (202.7 \pm 7.1 Ma; zircon orbicular syenite and 200.7 \pm 2.8 Ma; Pb-Pb, titanite, pseudoleucite syenite). However, Fraser (1995) inferred that the Bootjack stock is younger on the basis of diorite xenoliths present within the nepheline pseudoleucite and orbicular syenite units.

PYROXENITE

Hornblende pyroxenite and biotite gabbro have been intersected in drillholes collared near the east shore of Bootjack Lake (Hodgson *et al.*, 1976) and recognized as xenoliths within diorite, and clasts within intrusive breccia in the Bell pit (Fraser, 1995). Foliated hornblendite xenoliths and accidental clasts are common within volcanic units east of the Cariboo pit.

DIORITE

In the mine area, diorite is the earliest phase and comprises the majority of the Mount Polley stock. It is a homogeneous, medium to fine-grained equigranular rock that weathers pale grey. A large body of weakly altered, fine to medium-grained diorite is exposed north of the Cariboo pit

and in the west wall of the Bell pit (Fig. 2). At this locale, it is cut by tight epidote-lined fractures that have albite-epidote \pm K-feldspar alteration envelopes. Unaltered, equigranular, medium-grained biotite-pyroxene diorite crops out along the Bootjack Lake road, west of the mine. Mafic minerals consist of medium-grained (3–6 mm) altered pyroxene (30%) and an additional 15% large poikilitic biotite crystal. In thin section, the diorite consists of euhedral (1–2 mm) plagioclase laths (40–50%), green clinopyroxene (1 mm) crystals (15–20%) and poikilitic biotite (10–15%) that encloses plagioclase, pyroxene and magnetite grains. Accessory minerals include magnetite, sphene and apatite.

MONZONITE

Monzonite, where unaltered, is grey to pink, fine to medium grained, porphyritic or rarely seriate. It is composed of roughly equal amounts of plagioclase (3–5 mm tabular laths) and K-feldspars (subhedral 2–3 mm grains and matrix material) and 10–15% mafic minerals (pyroxene and/or hornblende and less biotite). Accessory minerals include magnetite, sphene and apatite. In outcrop, the monzonite resembles a potassium enriched, medium-grained diorite. Its distribution, particularly around the mine, has been overestimated in part due to the pervasive potassium alteration in this area but also because monzonite was used as a field term or catch-all for pink to orange-altered rocks that could not be designated as diorite, plagioclase porphyry or potassium megacrystic monzosyenite.

Small (<1 km²), high-level, stocks of hornblende monzonite crop out north of Prior Lake and northwest of Bootjack Lake. These intrusions consist of holocrystalline plagioclase-hornblende-pyritic subvolcanic monzodiorite and pink equigranular monzonite. Both stocks contain abundant rounded xenoliths of pyroxene porphyry and diorite. The stock northwest of Bootjack Lake consists of a crackle or autobrecciated, fine-grained monzonite. At its southern margin, it is a pink breccia with clasts defined by a tight, anastomosing network of chlorite fractures; however, toward its centre, the stock is dominated by a potassic-albite-altered breccia resembling the hydrothermal breccias at the Springer zone and on Mount Polley.

PLAGIOCLASE PORPHYRY

Plagioclase porphyry is a grey to green, fine to medium-grained, seriate-textured subvolcanic intrusion. It is characterized by 1–4 mm, white, stubby plagioclase phenocrysts (up to 70%), subhedral 2–3 mm mafic minerals including biotite, hornblende and less abundant pyroxene set in a groundmass that is commonly potassic altered. Accessory minerals include magnetite, sphene and apatite. Plagioclase porphyry are pre, syn and post-mineral intrusions. They appear to be associated with a pervasive potassium metasomatic event. A common occurrence of plagioclase porphyry (and monzonite) is as matrix to brecciated diorite in the intrusive breccias, which are common within mineralized zones

In drillcore from beneath (?) the Bell pit (BD-04-26), 2–3 m wide dikes of crowded plagioclase porphyry with



Figure 10. Plagioclase porphyry dike, chilled margin against pervasive potassium metasomatized monzodiorite. Drillcore from beneath Bell pit.

chilled sharp contacts and internal trachytic textures intrude equigranular potassium-altered diorite or monzonite (Fig. 10). Plagioclase porphyry containing xenoliths of biotite diorite is exposed halfway down the main haulage ramp in the Cariboo pit. The plagioclase porphyry (dyke?) is chilled against mineralized and altered medium-grained monzonite, clearly postdating potassic-albite fractures and patchy chalcopyrite mineralization.

POTASSIUM FELDSPAR PORPHYRITIC SYENITE

Potassium feldspar porphyritic monzonite-syenite occurs as dikes within the core of the Central zone, as a stock on the top of Mount Polley (Fraser, 1994) and as fragments in mineralized breccias at the Northeast zone (Fig. 11) and Lloyd-Nordic zone (Fig. 2). It is characterized by the presence of salmon pink coloured tabular K-feldspar (orthoclase) phenocrysts. An inverse relationship between the proportion of feldspar phenocrysts and their size results in crowded trachytic varieties that contain 20–25% phenocrysts averaging less than 7 mm in size, and those monzosyenites that contain fewer phenocrysts (2–10%), but which can be greater than 2 cm in length. The groundmass consists of weakly aligned plagioclase crystals with interstitial clinopyroxene, biotite and lesser magne-

tite, sphene and apatite. Plagioclase crystal inclusions within the potassium megacrysts indicate that the two crystallized simultaneously. Late deuteric alteration has sericitized the feldspars and replaced mafic minerals with a mixture of chlorite, white mica and carbonate.

In the high wall between the Bell and Cariboo pits is a set of east-southeast-trending, south-dipping dikes of K-feldspar porphyritic syenite. The dikes are 0.25–5 m thick, have chilled margins and a weak trachytic fabric, and are overprinted by weak chlorite-pyrite alteration. A sample was collected for radiometric dating; results are pending.

A southeast-trending intrusive breccia characterized by pervasive potassic alteration and frothy albite replacement along clast margins defines the western contact of the Mount Polley monzosyenite stock. Lithology closely resembles that of the dikes described above. The stock contains about 5% large equant potassium megacrysts in a plagioclase-rich groundmass containing pyroxene altering to hornblende, biotite, and magnetite. It is overprinted by discrete alteration zones containing one or more of albite, epidote, magnetite, chlorite and pyrite and locally chalcopyrite. A grab sample of chalcopyrite mineralization returned low Cu (~0.2%) and Au (207 ppb) values (JLO04-25-127; see Table 1).

BRECCIAS

Intrusion breccias and hydrothermal breccias are associated with a number of high-level alkalic intrusive centres



Figure 11. Mineralized fragments of K-feldspar porphyritic monzonite-syenite in breccias at the Northeast zone.

in the study area (Mount Polley, all mineral zones; Shiko Lake and the small stock located northwest of Bootjack Lake). Intrusion breccias are matrix supported; plagioclase porphyry in the Cariboo pit (Fig. 12) or quartz syenite at Shiko Lake contain approximately 30% angular to rounded, rotated clasts of monzonite-diorite country rock in addition to more exotic xenoliths (pyroxene-olivine-phyric volcanic rock, mafic subvolcanic intrusive, foliated hornblende gabbro, or diorite clasts). Hydrothermal breccias are heterolithic, often with clasts of intrusion breccia, volcanic rocks, diorite and monzonite. These breccias contain either rounded (pebble dikes) or angular clasts that are partially replaced, and have their interstices filled, by alteration minerals (Springer zone, Fig. 13). Fraser (1994) divided the hydrothermal breccias at Mount Polley into four types, based on dominant matrix mineralogy: biotite, actinolite, albite and magnetite. The potassic-albite breccia west of Mount Polley and at the Springer zone are characterized by the presence of tabular albite and lesser biotite crystals filling vugs in the breccia matrix. Biotite breccia and actinolite breccia in the Cariboo and magnetite breccias occur northwest of the Northeast zone.

Bootjack Stock

The Bootjack stock is a silica undersaturated, layered syenite pluton (Hodgson *et al.*, 1976; Fraser *et al.*, 1993), located south of Bootjack Lake (Fig. 2). In contrast to the fine-grained porphyritic textures of the rocks that make up



Figure 12. Intrusion breccia, plagioclase porphyry in the Cariboo pit

the Polley stock, the Bootjack phases exhibit coarse-grained plutonic textures. It has an easterly to northwesterly trend and is separated from the Mount Polley stock by a narrow belt of northwest-trending mafic metavolcanic flows, breccias and fine-grained bedded volcanoclastic units. To the south (and deeper), the stock intrudes stratigraphically lower analcime-bearing pyroxene-olivine-phyric basalt and volcanoclastic breccias. Compositional layering within the main body of the syenite strikes westerly and dips moderately north (consistent with the majority of regional bedding measurements), although, at the west end of the body (Trio Lake), the layering trends northwesterly with steep easterly dips (Hodgson *et al.*, 1976). The stock comprises a mafic pseudoleucite syenite, a crowded orbicular syenite and a coarse-grained granophyric syenite (Fraser, 1994).

MAFIC PSEUDOLEUCITE SYENITE PORPHYRY

A melanocratic porphyritic syenite comprises ~40% of the stock and crops out primarily along the stock's western margin. It contains up to 20% 2 cm euhedral phenocrysts of pseudoleucite (mixture of nepheline, K-feldspar and sericite) in a medium to coarse-grained salt and pepper textured groundmass (Fig. 14) comprising K-feldspar, nepheline, albite, clinopyroxene, hornblende and magnetite. Mafic minerals constitute 15 to 25% of the rock. Narrow chilled



Figure 13. Intrusive breccia characterized by pervasive potassic alteration and frothy, albite replacement along clast margins. Breccia defines the western contact of the Mount Polley monzo-syenite stock located on Mount Polley.

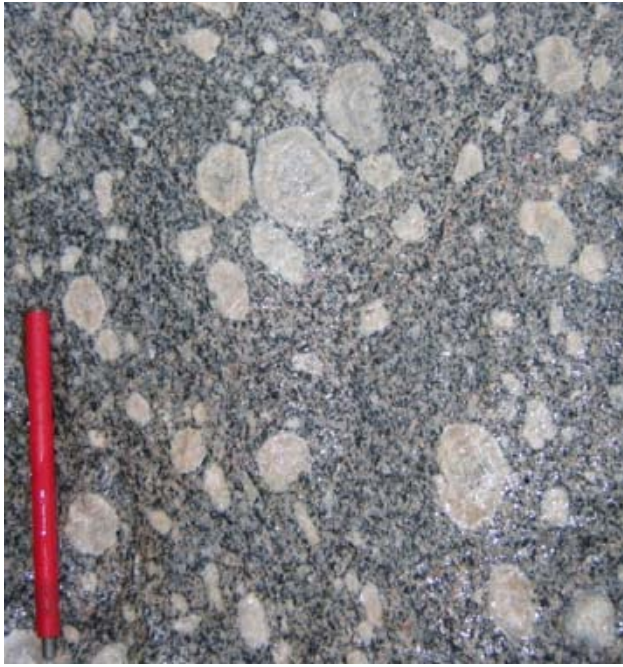


Figure 14. Porphyritic syenite, containing up to 20% 2 cm euhedral phenocrysts of pseudoleucite (mixture of nepheline, K-feldspar and sericite).

apophyses of the mafic syenite porphyry intrude mafic analcime-bearing basalt near Trio Lake.

A large (18 m wide), north-trending, east-dipping tabular block of pyroxene porphyritic metabasalt is exposed in the northeast wall of the borrow pit, approximately 2 km northwest of the tailings impoundments. The syenite is chilled adjacent to the xenolith and, to the west, the metabasalt is faulted against leucocratic orbicular nepheline syenite. In addition, the pyroxene porphyry is veined by pink potassic alteration (orthoclase flooding), epidote and minor pyrite. It is important to note that, although this augite porphyry resembles some of the youngest crosscutting 'AP'dikes, observations indicate that it predates the syenite.

FELSIC ORBICULAR NEPHELINE SYENITE

The orbicular nepheline syenite is a leucocratic rock consisting of 30 to 90% orbicules of pseudoleucite up to 4 cm in diameter. Interstitial to the orbicules is a medium-grained equigranular matrix of nepheline, clinopyroxene, biotite, sphene and magnetite. The orbicules contain subhedral pseudoleucite cores and have concentric overgrowths of K-feldspar. This unit constitutes approximately 55% of the Bootjack stock.

The northeastern margin of the stock (southeast end of Bootjack Lake) has been overprinted by biotite and fluorite. (Fraser, 1995). In a structurally restored section, where regional dips have been removed by assuming that all parts of the crust were tilted equally, the northern part of the stock would be the roof zone (see 'Structure' section).

QUARTZ-PLAGIOCLASE PORPHYRITIC MONZOSYENITE

Coarse-grained quartz and feldspar-phyric monzonite and monzosyenite dikes intrude the pseudoleucite syenite southwest of Bootjack Lake. Panteleyev *et al.* (1996) included these as part of their Triassic-Jurassic suite of rocks (unit 7). Hodgson *et al.* (1976) correlated them with a younger suite of calcalkaline, quartz-bearing stocks of probable Cretaceous age. We follow Hodgson's correlation.

AUGITE PORPHYRY DIKES

Augite porphyry dikes are ubiquitous throughout the area. They are typically recessive, rubbly weathering, 10–100 cm thick and consist of 30–50% euhedral 1–5 mm clinopyroxene phenocrysts in a black to dark green aphyric groundmass of plagioclase laths, magnetite and interstitial K-feldspar (indicated by staining samples with sodium cobaltinitrate). The youngest intrusions occur as northerly striking, moderately east-dipping swarms of generally thin (centimetre to metre-scale) dikes that crosscut all of the igneous and breccia units at the deposit (Fraser, 1994).

They are compositionally like Nicola Group basalt flows and feeder dikes. They also cut mineralized monzonite intrusions that cut the Nicola Group basalts and are therefore younger. It is not uncommon to see augite porphyry clasts within intrusion-hydrothermal breccias themselves crosscut by augite porphyry dikes. These dikes probably represent feeders to Miocene or younger (Mathews 1989) alkaline plateau basalt flows known from west of the study area. However, these dikes bound mineralized zones (earning them the name 'Death Dikes') and are locally deformed (east wall of Cariboo pit ramp), suggesting that at least some of them are pre to syn-mineralization (unless they have intruded along post-mineral faults with significant offsets).

CHEMISTRY

Samples were steel milled at the British Columbia Geological Survey Branch Laboratory in Victoria. Splits were shipped for analysis to TeckCominco Laboratories, Vancouver for major element and trace element abundances (Ba, Rb, Sr, Nb, Zr and Y) by X-ray fluorescence (XRF); ACME Analytical, Vancouver for trace element analyses using inductively coupled plasma – emission spectrometry (ICP-ES); and Actlabs, Ancaster, Ontario for trace element analyses using instrumental neutron activation (INAA). A subset of these samples has also been sent to Memorial University, Newfoundland for trace element analyses using inductively coupled plasma – mass spectrometry (ICP-MS). Results are pending.

STRUCTURAL STYLE

Scattered exposures of well-bedded sediment and water-lain tuff are sources of reliable paleohorizontal orientation data that can be used to assess the effects of folding and faulting in the Polley area. Local excellent preservation of bedding tops indicators shows that, with the exception of a

single outcrop that may have slumped, all beds are upright. Bedding orientation data are sparse and potentially unreliable in the volcanic-intrusive Mount Polley complex but, on its northern flank, orientation data form a low variance (0.018) unimodal population with minor dispersion on a Pi girdle (Fig. 15A). A lack of measurements from the fold limbs limits reliability of the calculated beta axis, $35^\circ/300^\circ$ (Fig. 15A). In a single-phase cylindrical fold, the beta axis is parallel with the fold axis. When combined with all reliable bedding determinations, the calculated Pi girdle is more robust, indicating a shallowly north-northwest-plunging fold, with a beta axis of $21^\circ/353^\circ$ (Fig. 15B). Effects of this plunge, if regionally applicable, could be substantial. For example, in the absence of block fault adjustments to compensate, the tilting of the Bootjack stock may have resulted in a differential exhumation of 2.6 km from northwest to southeast. That is to say, the exposed southern part of the stock was emplaced 2.6 km deeper than the currently exposed northern end. A south to north variation from megacrystic orbicular syenite to hydrothermally altered fine to coarse-grained syenite is consistent with this magnitude of regional tilting. However, an invariant regional metamorphic grade in Nicola Group strata does not permit differential uplifts of tens of kilometres, so extensional block faulting must have accompanied tilting of blocks that extend more than 20 or 30 km in a direction parallel to the regional fold axes. Major discontinuities in the fabric of the regional aeromagnetic total field data occur between the Bootjack stock and Shiko Lake stock, and between Morehead Lake and Quesnel River, possibly related to northeast-trending normal faults. Along the southern discontinuity are relicts of Miocene plateau basalt, perhaps fed from dikes that invaded these proposed faults.

Existence of north-northwest-trending faults is firmly established. Dominant structures in the mine area are the Polley Fault and the unnamed fault that truncates mineralization in the Northeast zone. The Polley fault is a steep easterly-dipping brittle structure that separates the deposit into the Central zone (Cariboo and Bell pits) and the West zone (Springer pit), each with distinctive mineralization, alteration and style of brecciation. In the southwest corner of the Cariboo pit, the structure comprises a 50 m wide zone of sheared and fractured rocks containing fault breccias and clay gouge, but the fault zone narrows to the north and south (Wild, 1999). The fault does result in apparent horizontal displacement of the northern contact of the Bootjack stock, and therefore any motion along the structure must either 1) have a displacement vector that is approximately parallel to the dip of the intrusive contact; 2) be a rotational fault with an axis of rotation located near the location of the Bootjack stock; 3) predates intrusion of the Bootjack stock (200 Ma); or 4) record a tremendous amount of motion but with no net displacement, and therefore be of little regional significance. Layered strata on the northern flank of Mount Polley are apparently not offset by the fault, and we show a deflection in the trace of the fault from $\sim 350^\circ$ to $\sim 290^\circ$ in order to continue the fault west of exposures of well-layered rocks. In this area, only two reliable well-bedded exposures lie west of the fault and they have an average orientation of $219^\circ/42^\circ$, as compared to those east of the fault

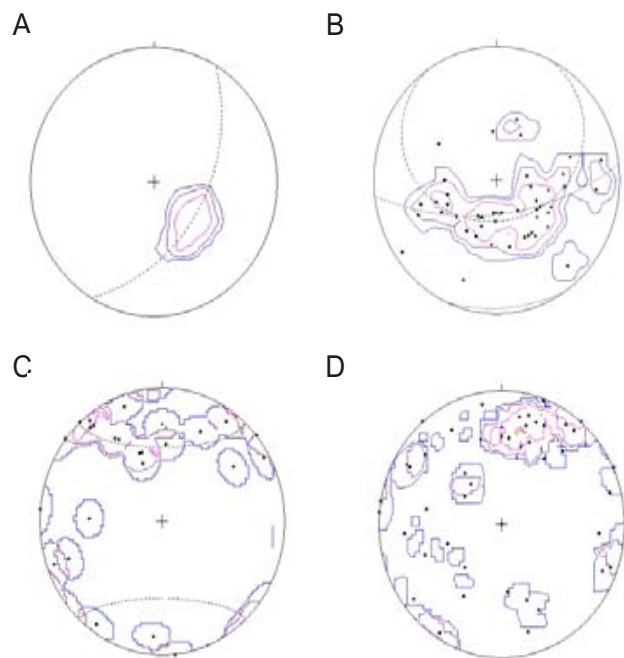


Figure 15. Equal area plots of **A**) reliable bedding measurements (N=14) from the northern flank of Mount Polley; contours are 8, 16, and 32% of data points per 1% of plot area; **B**) all reliable bedding measurements from the Polley area (N=51); contours are 2, 4, 8, and 16% of data points per 1% of plot area; **C**) all veins from the Polley area (N=25); contours are 4, 8, and 16% of data points per 1% area; and **D**) all dikes from the Polley area (N=51); contours are 2, 4, 8, and 16% of data points per 1% area.

($226^\circ/35^\circ$; N=11). The averaged bedding orientation from east of the fault falls within the 20% contour (points per 1% area) of the eastern population (Fig. 15A) and is therefore not statistically different. Consistent bedding orientation rules out significant rotational variation across the Polley fault.

A second north-northwest-trending fault corridor has been intersected by drilling in the Northeast zone, where it marks the northwestern limit of mineralization. These structures may be related to a major fault that is obscured by cover within the Polley Lake valley. Possible continuation of this fault beneath cover northwest of Polley Lake is suggested by truncation of regional magnetic fabric shown on the Polley multiparameter dataset (BC MapPlace). In particular, apparently folded vertical-gradient magnetic lineaments (Fig. 4) that are consistent with the broad fold on the north flank of Mount Polley (Fig. 2) are truncated at the presumed fault extension (Fig. 4). If this is truly the same structure, its trend is deflected by about 60° from 350° to 290° , similar to the proposed deflection on the Polley fault. One highly speculative interpretation is that both faults are folded about a near-vertical axis. If this is so, the Northeast zone is located in the outer (dilatant) part of the hinge zone.

Most veins in the Polley area are steep (Fig. 15C) except for a small subset that dips moderately south-southeast. The mode represents a set of veins that dips steeply toward $\sim 150^\circ$. Because paleohorizontal control is lacking for most of the Polley area, we have not attempted to unfold

and rotate the data based upon the apparent regional folding.

Dike orientations display a mode of approximately 120°/65° (Fig. 15D); a smaller population is oriented about 310°/85°. Dikes may be useful indicators of the paleostress field, but relative ages and effects of later tilting and rotation must first be established.

MINERALIZATION AND ALTERATION

Alkalic intrusion-related mineralization defines the centre or axis of the Quesnel arc (Panteleyev *et al.*, 1996, Fig. 8); fewer and more widely-spaced mineral occurrences associated with calcalkaline intrusions are located on the western margin of Quesnellia. In the area surrounding Mount Polley, there are a number of small, high-level composite intrusions with compositions ranging from diorite through monzonite to syenite. These are interpreted to have been emplaced into the upper levels of the arc and are often hosted by coarse extrusive facies equivalent volcanics that indicate individual eruptive centres (i.e., Mount Polley, Bailey and Hodgson, 1979; Shiko Lake, Panteleyev *et al.*, 1996).

INTRUSIVE CENTRES

Mount Polley (MINFILE 093A/008 and 164)

Mineralization at Mount Polley is hosted by a variety of hydrothermal breccias that cut a high-level multiphase dioritic intrusion. Alteration and mineralization are interpreted to be related to a single hydrothermal centre modified by faulting (Fraser, 1994). However, they display sufficient zonal variation to warrant subdivision into West, Central and Northeast zones (Fig. 16).

Central and West Zones (Cariboo-Bell-Springer)

Alteration studies by Hodgson *et al.* (1976) and Bailey and Hodgson (1979) identified three roughly concentric alteration assemblages associated with the copper-gold mineralization at Mount Polley: a central potassic core, an intermediate garnet-epidote zone and an outer propylitic zone. Work by Fraser (1994, 1995) on the mineral zonation in the Central (Cariboo and Bell) and West (Springer) zones resulted in the subdivision of the potassic core into three subzones defined on the basis of the dominant alteration mineral: biotite, actinolite and K-feldspar-albite. The biotite and actinolite subzones occupy the Central zone, east of the Mount Polley fault, the K-feldspar-albite zone occurs west of the fault (West zone), and east of the actinolite zone in a northwest-trending belt west of Mount Polley (this study). Alteration mineral zonation appears to have been controlled by the distribution of hydrothermal breccias and reflects the evolving permeability, fluid composition and temperature of the hydrothermal system (Fig. 16).

The biotite subzone is characterized by coarse secondary biotite developed interstitial to hydrothermal breccias in the core of the Central zone. Extending north from the biotite subzone is the 600 by 200 m north-trending actinolite

subzone (Fraser, 1995). It is characterized by abundant actinolite-chalcopyrite-pyroxene-magnetite veins that are enveloped by extensive K-feldspar alteration envelopes. Surrounding the actinolite and biotite subzones is a circular 0.8 km² zone of intense K-feldspar flooding. Where pervasive, potassic alteration has destroyed primary textures and fine-grained disseminated hematite imparts a salmon-pink colouration to the rocks. The eastern and western margins of the potassic core are marked by orange-weathering potassic hydrothermal breccias. In these zones, coarse granular white albite crystals fill veins and the spaces between the potassic-altered breccia fragments (West zone and west flank of Mount Polley).

Wild (1999) recognized that the relative abundance of main alteration minerals (K-feldspar, actinolite-biotite and magnetite) correlated well with copper grade. From this, an alteration scoring system was devised to estimate copper grades. Each of the constituents is scored from 0 to 5 based on intensity (low to high), with a total of 15. Grade or ~0.3% Cu corresponds to a 10–12 or higher score. From these criteria, it is necessary to have at least some of each of the main alteration constituents to reach grade. The alteration scoring system does not work at the Northeast zone (McAndless, personal communication, 2004).

The Mount Polley deposit (Cariboo-Bell-Springer) contains chalcopyrite, pyrite and bornite as primary sulphides that are associated with magnetite. Polished sections indicate rare tetrahedrite, galena, sphalerite and molybdenite. Oxide minerals include malachite, azurite, magnetite, hematite, and limonite. Native gold is present as 5 to 30 µm inclusions in chalcopyrite (Wild, 1999). Mineralization is hosted primarily in hydrothermal and intrusion breccias, with lesser amounts in fractured country rocks.

Northeast Zone

The Cu-Au-Ag mineralization at the Northeast zone occupies a 150 by 500 m, northwest-trending, steeply dipping tabular zone located close to the northern margin of the Polley stock. Hostrocks are interpreted as hydrothermally brecciated monzodiorite, monzonite and porphyritic monzonite phases of the stock that are cut by premineral K-feldspar megacrystic syenite and plagioclase porphyry dikes. Post-mineral plagioclase porphyry and augite porphyry dikes also cut the Northeast zone.

A comprehensive petrographic study, augmented by scanning electron microscope (SEM) work on the mineralogy at the Northeast zone was completed by Ross (2004) for Imperial Metals. Quick logs of six drillholes along sections 14, 18 and 22, discussions with Pat McAndless, Lee Ferreira and Chris Rees during the ongoing drilling, and examination of select drillcore form the basis of the following description of the Northeast zone.

Alteration at the Northeast zone is not dissimilar to that present at the Central and West zones (1.5 km southwest). The Northeast zone consists of an early pervasive and texturally destructive potassium metasomatic event that predated or coincided with brecciation. Pink veinlets consist of cloudy brown secondary K-feldspar, which overprints the

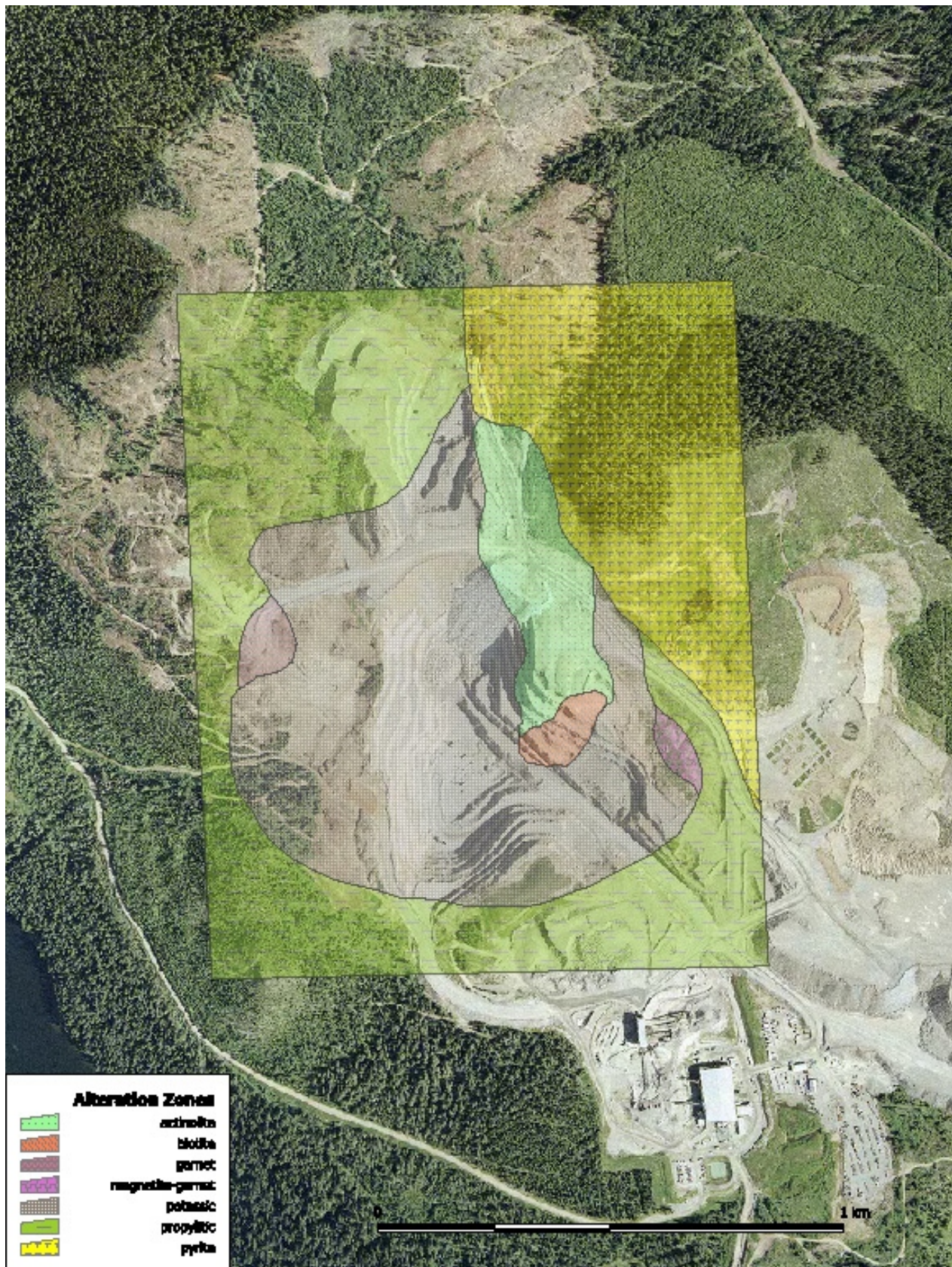


Figure 16. Distribution of alteration zones at Mount Polley (*from Fraser, 1994*). Biotite and actinolite subzones occupy the Central zone, east of the Mount Polley fault; the K-feldspar–albite zone occurs west of the fault (West zone) and east of the actinolite zone in a northwest-trending belt west of Mount Polley

groundmass plagioclase and locally destroys mafic minerals. Diffuse green veinlets consist of a very fine grained intergrowth of epidote-clinzoisite and calcite. (clinzoisite is an aluminum-rich epidote mineral). Fine-grained pyrite and chalcopyrite are associated with the green alteration. This was followed by a calcsilicate assemblage that Ross (2004) divided into two stages: an early magnetite-garnet-apatite stage; and a slightly younger clinzoisite-albite-calcite stage, which introduced most of the Cu sulphides. A late-stage, lower temperature alteration assemblage of calcite-albite-chlorite (retrograde continuum to the mineralizing stage; according to Ross, 2004) is separate from a propylitic assemblage of calcite-chlorite-pyrite that envelops the breccias but is more strongly developed in the volcanic rocks adjacent to the northeastern margin (Fig. 17). Late-stage calcite-gypsum veins occur deep in the section. They crosscut the peripheral propylitic zones as well as the intrusive breccias. Calcite and fibrous radiating zeolites are late and fill open spaces in the Central zone.

Garnet compositions from the Northeast zone are identical to those from Central and West zones (Ross, 2004; Fraser, 1994); both are nearly pure andradite with minor (10–15%) grossular (Ca) component in rims. Magnetite is inferred to be less important in the Northeast zone, although Ross (2004) reported that the highest grade min-

eralization is developed in magnetite-rich sections of the intrusive breccia. In drillhole WB-04-21, a post-mineral hydrothermal brecciation and albite-clinzoisite alteration overprints the mineralized breccia (Fig. 18). The zone is veined by coalescing white and pale green, banded or crustiform veinlets and a fine-grained sugary texture matrix containing tabular albite crystals. Breccia fragments of mineralization are surrounded by albite-altered matrix (Fig. 19).

The Northeast zone copper mineralization consists of chalcopyrite and bornite as primary sulphides that are sporadically intergrown with magnetite and lesser pyrite. Copper mineralization occurs as finely disseminated chalcopyrite and as coarse intergrown clots of chalcopyrite and bornite. Petrographic analysis shows bornite and chalcopyrite exsolution textures, one from the another. Copper mineralization appears to have pervaded the Northeast zone in two stages: first chalcopyrite, occurring within an interconnected network of fractures and veinlets; and later bornite, rimming and replacing chalcopyrite in veinlets (Fig. 19).

Gold and silver minerals occur with copper. Silver±selenium occur in tellurides, silver occurs in galena, and selenium occurs as inclusions in bornite and chalcopyrite (Ross, 2004). Mineralization at the Northeast zone is

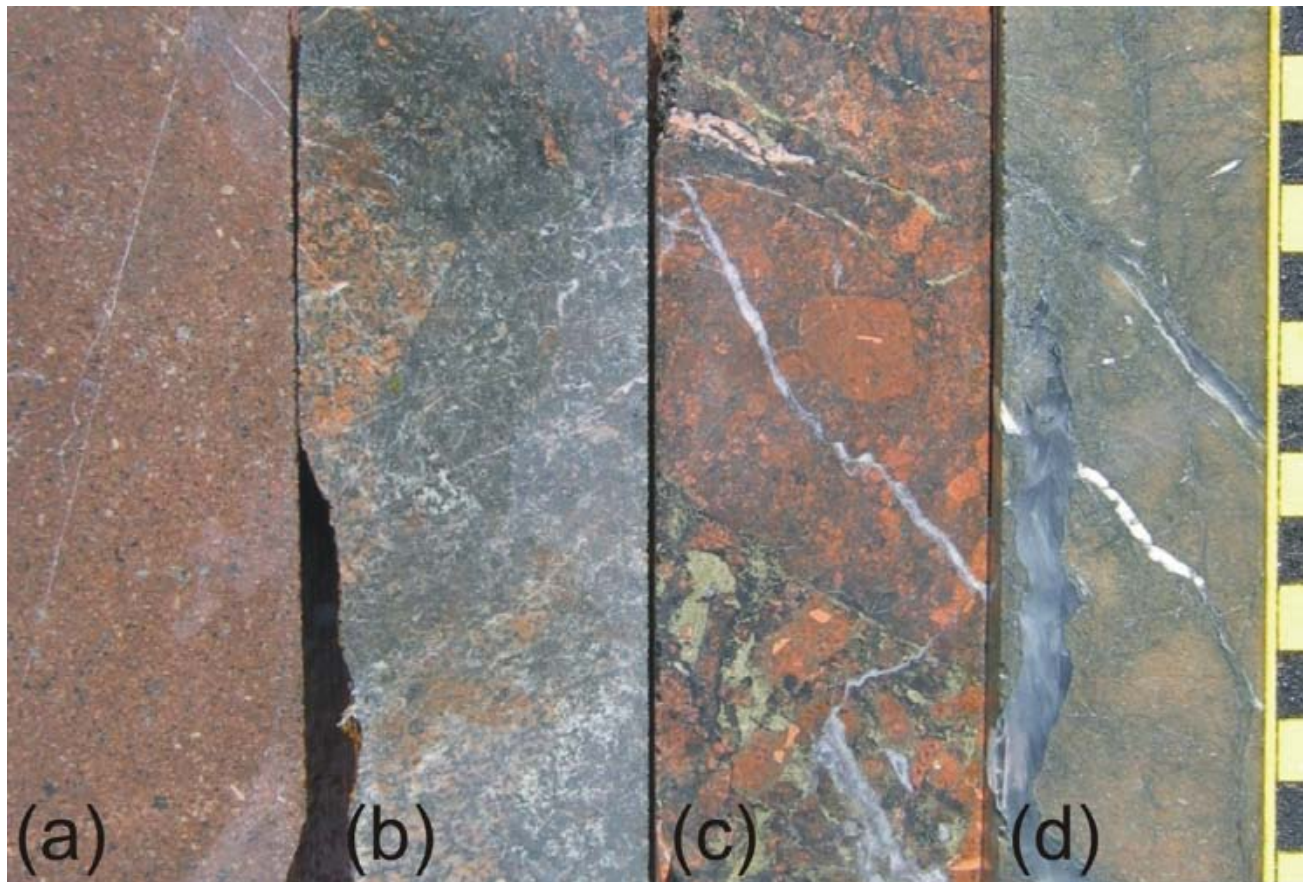


Figure 17. Four characteristic examples of Northeast zone lithology-alteration from DDH WB-03-27: **a)** postmineral plagioclase porphyry dike at 14.5 m; **b)** propylitic overprint weak potassic-altered monzonite in hanging wall at 19.0 m; **c)** potassic-altered, brecciated, brown calcsilicate overprint of matrix associated with chalcopyrite and magnetite at 202.2 m; and **d)** fine-grained, propylitic metavolcanic footwall rocks, disseminated pyrite cut by calcite and gypsum veinlets.



Figure 18. Post-mineral hydrothermal breccia with an albite-clinozoisite alteration overprint. Note clasts of mineralization within matrix.

characterized higher copper grades, higher bornite content, higher copper:gold ratios, higher silver content, and lower magnetite content than other breccias in the camp. Copper grades are consistent and up to three times higher than the historical copper grades from the Cariboo and Bell pits. In addition, the Northeast zone contains silver, which is not recoverable elsewhere.

Abrupt termination of Northeast zone mineralization and decrease in the intensity of alteration on its northeastern side corresponds with a brittle fault zone invaded by numerous augite porphyry dikes. Southwest of the Northeast zone, the tenor of mineralization diminishes, except at the Leak and Boundary zones; which both have a mineralogy that differs slightly from that of the Northeast zone. The Leak zone more closely resembles alteration (actinolite-K-feldspar-magnetite) and metal grades (0.30% Cu) in the Cariboo pit; and the Boundary zone is an auriferous magnetite-rich breccia. The northwestern contact relationships of the Northeast zone are poorly exposed and pervasive potassic alteration makes it difficult to distinguish between



Figure 19. Coarse intergrown clots of chalcopyrite and bornite in fractures cutting potassic altered monzonite breccia in the Northeast zone.

intrusive breccias and the Upper Triassic volcanic breccias, lahar and conglomerate units known to crop out in the area. The mineralized breccia is heterolithic and clast supported. Clast compositions include equigranular monzonite, megacrystic K-feldspar porphyry syenite, and early plagioclase porphyry. The matrix is dark, fine grained and invariably altered and mineralized.

Bullion Lode (MINFILE 093A/041)

A north-trending body of equigranular, pink to grey monzodiorite is exposed in the placer workings at the Bullion pit, approximately 5 km northwest of Likely. The monzodiorite intrudes alkaline pyroxene-olivine-phyric basalt breccias and volcanoclastic rocks correlative with the basal volcanic 'unit 2' of Panteleyev *et al.* (1996).

The Bullion monzodiorite is a fine to medium-grained, melanocratic rock composed of plagioclase, orthoclase and clinopyroxene with coarse poikilitic biotite crystals and accessory minerals that include magnetite, apatite and sphene. The monzodiorite is cut by closely spaced fractures and stockworks, and veined by pegmatitic syenite segregations of orthoclase and albite that coalesce to form irregular intrusive breccias. In addition, narrow (<1 m), east-trending pink dikes of medium-grained, equigranular hornblende-biotite syenite intrude the monzodiorite. The syenite is composed of 3–5 mm equant salmon pink orthoclase and white plagioclase phenocrysts, 1–2 mm interstitial hornblende, biotite and magnetite.

The syenite contains disseminated clots of 1–2% chalcopyrite. Locally pyrite, chalcopyrite and molybdenum mineralization is developed along dike contacts or late fractures, which are crosscut by younger narrow veinlets of albite with sericite alteration envelopes.

Shiko Lake (Redgold; MINFILE 093A/058)

A high-level multiphase alkalic complex occurs northeast of Shiko Lake. At its western end, three separate intrusive phases are well exposed within a (ca. 1994) quarry that supplied syenite to colour the exterior of the Vancouver Public Library. From oldest to youngest, these include a melanocratic, medium-grained equigranular, biotite-pyroxene monzodiorite; a pink, trachytic, medium to coarse-grained, K-feldspar-phyric syenite; and a leucocratic alkali feldspar quartz syenite. The quartz syenite truncates a well-developed, west-striking, 30° north-dipping trachytic fabric in the K-feldspar megacrystic syenite, which veins and engulfs the earlier diorite. All phases contain mafic xenoliths of olivine-pyroxene-phyric basalt, fine-grained metasedimentary rocks and subvolcanic dioritic to monzonitic compositions that increase in abundance as the contact is approached. Toward the centre of the stock, the dominant phase is a white, medium to coarse-grained, equigranular monzonite containing 0.7–1.0 mm grains of biotite and hornblende (biotite > hornblende) with trace amounts of magnetite, sphene and pyrite and abundant rounded, partially digested xenoliths of country rock. The monzonite is intruded by dikes and veins of fine-grained pink quartz syenite that co-

alesce to form zones of intrusive breccia. Rotation and incorporation of the monzonite blocks is evident from their random trachytic textures. Matrix to the breccia contains disseminated chalcopyrite and pyrite.

Country rock exposed adjacent to the stock includes fine-grained, hornfelsed metasedimentary and thin-bedded volcanoclastic rocks and a mixed volcanic package that includes stubby plagioclase, pyroxene-phyric massive basalt flows and crowded hornblende-plagioclase porphyritic dikes. Approximately 1 km southeast of the contact are coarse breccias and pillowed flows of olivine-pyroxene-phyric basalt with interclast limestone, fine-grained chert and limy lapilli tuff horizons. Heterolithic plagioclase, pyroxene-phyric breccias and chaotic volcanoclastic deposits are exposed in trenches on the Redgold mineral occurrence, located approximately 1.5 km east of the quarry.

Copper (chalcopyrite and bornite) and gold mineralization occurs as veins and disseminated clots within all three intrusive phases, but appears to be associated with the youngest quartz syenite phase. Vein assemblages cutting the intrusive rocks include intergrowths of actinolite, K-feldspar, sphene, magnetite, pyrite ± chalcopyrite. Potassic overgrowths on feldspars and replacement of hornblende by actinolite and biotite by chlorite are attributed to late deuteric alteration. The leucocratic quartz syenite hosts the majority of mineralization exposed in the quarry. It is characterized by quartz-filled miarolitic cavities and a low magnetic susceptibility response. A grab sample of the mineralized syenite (MMI04-22-1b; see Table 1) returned low copper and gold values. Additional mineralization-alteration has been recognized outside the stock in the volcanic cover rocks (Morton and Durfeld, 1998). Alteration and mineralization in the plagioclase-pyroxene-phyric volcanoclastic rocks is characterized by fracture-controlled, locally pervasive potassium flooding of the groundmass accompanied by epidote replacing either pyroxene ± plagioclase or the matrix, and introduction of magnetite and disseminated chalcopyrite. Late-stage white calcite veinlets crosscut earlier alteration minerals. Grab samples of alteration-mineralization from the trenches returned low copper (~0.2%) and gold (51 and 558 ppb) values (JLO04-21-90 and MMI04-22-6; see Table 1).

Potassium-argon dating carried out by J.E. Harakal at the University of British Columbia on samples from the monzonitic core zone gave ages of 192 ± 10 Ma and 182 ± 6 Ma and a slightly older age of 196 ± 7 Ma for a hornblende porphyry dike cutting the stock (Panteleyev *et al.*, 1996). A number of macrofossil identifications from the sedimentary rocks intruded by the Shiko stock are early Jurassic (GSC-C-118687, probable Sinemurian; GSC-C-118685, Lower Sinemurian or possibly Hettangian; GSC-C-118686, Lower Sinemurian, lower Pleinsbachian). Panteleyev *et al.* (1996) described volcanic and intrusive breccias along the southern contact of the stock that they interpreted to represent the vent zone of an intrusive centre. Field evidence could neither refute nor substantiate an age for the mineralization and emplacement of the Shiko stock or its enclosing rocks. A sample of leucocratic alkali feld-

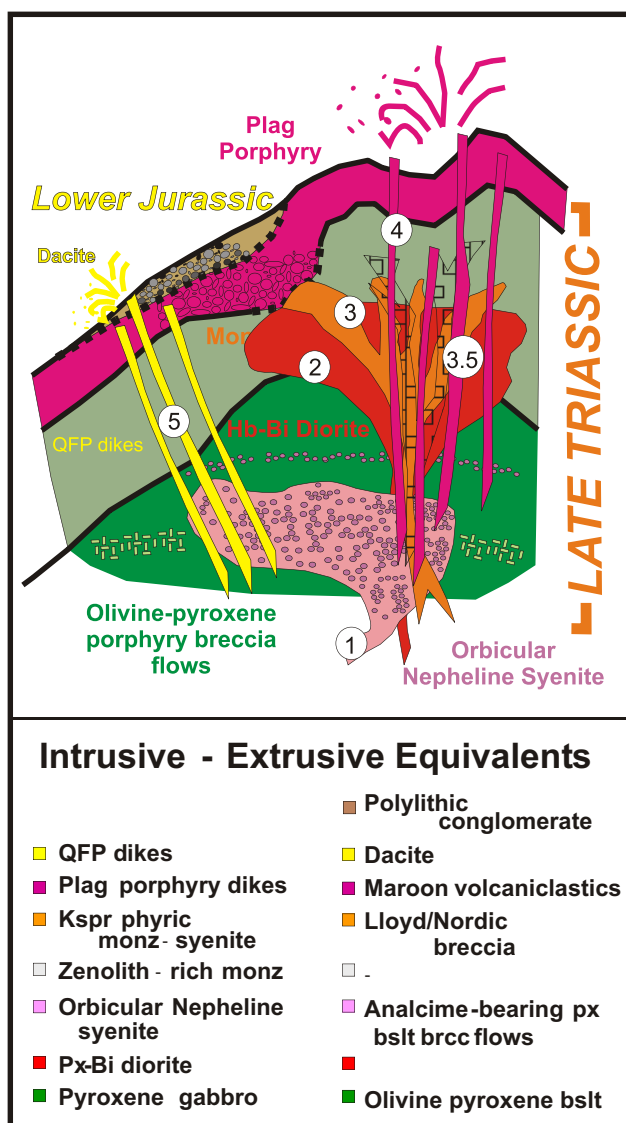


Figure 20. Schematic representation of Late Triassic volcanism and intrusion, showing relative age of events.

spar quartz syenite was collected for U-Pb geochronology; results are pending.

CONCLUSIONS

The spatial and temporal association of the Mount Polley intrusives with the thick pile of heterolithic, in part comagmatic volcanic breccias suggests that they were emplaced at shallow depths and proximal to a vent (Fig. 20; Bailey and Hodgson, 1979; Fraser, 1994;). Their northerly trend and position with respect to the Polley fault may also have exerted a structural control on emplacement, breccia development and hydrothermal flow of alteration and mineralizing fluids. The general evolution of the arc from early pyroxene-plagioclase-olivine to pyroxene-plagioclase± analcime and plagioclase-dominated basalt compositions is consistent with the successive emplacement of comag-

matic pyroxene diorite, monzonite, plagioclase porphyry and potassium megacrystic monzosyenites.

According to Fraser (1994), alteration-mineralization paragenesis for the Central zone (Cariboo-Bell pits) progresses outward from a higher temperature core of biotite to an intermediate actinolite zone and an outer zone of K-feldspar and albite. The degree of mineralization is directly related to secondary permeability developed by fracture and brecciation, which in many examples affects intrusives that have been pervasively potassium metasomatized prior to brecciation. The potassium-albite breccia zones that flank the Cariboo pit (i.e., West zone and Mount Polley) exhibit this early pervasive, generally barren potassium metasomatism, brecciation and what appears to be open space deposition of albite±biotite±actinolite and sulphides. In places, coalescing albite fractures produce pseudo-breccia textures, but hydrothermal breccia textures are recognized in the western zone. Alteration zonation is related to a migrating, cooling hydrothermal fluid, which evolved through a variety of fluid-wallrock interactions as it moved outward from the hydrothermal centre.

The relationship between the Polley and Bootjack stocks is equivocal.

ACKNOWLEDGMENTS

Pat McAndless and the Mount Polley geology team of Chris Reese, Leif Bjornson, Lee Ferreira, Chris Taylor, Jacquelline Blackwell and Sheila Jonnes contributed greatly to the success of this project through their efforts at introducing and educating us to the subtle relationships of alteration-mineralization at each of the Cariboo-Bell, Springer and Northeast mineral zones. We thank them all, whole heartedly. A special thanks to Pat McAndless for suggesting the project and to Imperial Metals Corporation for providing the financial support to carry out fieldwork and analyses.

We thank consulting geologist Rudi Durfeld for touring us around the Redgold (Shiko Lake stock) property together with BC Ministry of Mines Regional Geologists, Bob Lane (Northeast) and Mike Cathro (South Central).

REFERENCES

- Bailey, D.G. (1976): Geology of the Morehead Lake Area, central British Columbia; *BC Ministry of Energy, Mines and Petroleum Resources*, Preliminary Map 20 with notes, scale 1:31 680.
- Bailey, D.G. (1978): The geology of the Morehead Lake area; unpublished Ph.D. thesis, *Queen's University*, 198 pages.
- Bailey, D.G. (1988a): Geology of the Central Quesnel Belt, Hydraulic, south-central British Columbia (93A/12); in *Geological Fieldwork 1987, BC Ministry of Energy, Mines and Petroleum Resources*, Paper 1988-1, pages 147-153.
- Bailey, D.G. (1988b): Geology of the Hydraulic map area, NTS 93A/12; *BC Ministry of Energy, Mines and Petroleum Resources*, Preliminary Map 67, scale 1:50 000.
- Bailey, D.G. (1989): Geology of the Central Quesnel Belt, Swift River, south-central British Columbia (93B/16, 93A/12, 93G/1); in *Geological Fieldwork 1988, BC Ministry of En-*

- ergy, *Mines and Petroleum Resources*, Paper 1989-1, pages 167–172.
- Bailey, D.G. (1990): Geology of the Central Quesnel Belt, British Columbia; *BC Ministry of Energy, Mines and Petroleum Resources*, Open File 1990-31, 1:100 000-scale map with accompanying notes.
- Bailey, D.G. and Archibald, D.A. (1990): Age of the Bootjack Stock, Quesnel Terrane, south-central British Columbia (93A); in *Geological Fieldwork 1989*, *BC Ministry of Energy, Mines and Petroleum Resources*, Paper 1990-1, pages 79–82.
- Bailey, D.G. and Hodgson, C.J. (1979): Transported altered wall rock in laharc breccias at the Cariboo-Bell Cu-Au porphyry deposit, British Columbia; *Economic Geology*, Volume 74, pages 125–128.
- Barr, D.A., Fox, P.E., Northcote, K.E. and Preto, V.A. (1976): The alkaline suite porphyry deposits: a summary; in *Porphyry Deposits of the Canadian Cordillera*, Sutherland Brown, A., Editor, *Canadian Institute of Mining and Metallurgy*, Special Volume 15, pages 359–367.
- Barrie, C.T. (1993): Petrochemistry of shoshonitic rocks associated with porphyry copper-gold deposits of central Quesnellia, British Columbia, Canada; *Journal of Geochemical Exploration*, Volume 48, pages 225–258.
- Bloodgood, M.A. (1990): Geology of the Eureka Peak and Spanish Lake map area, British Columbia; *BC Ministry of Energy, Mines and Petroleum Resources*, Paper 1990-3, 36 pages.
- Campbell, K.V. and Campbell, R.B. (1970): Quesnel Lake map-area, British Columbia (93A); in *Report of Activities, Part A*, *Geological Survey of Canada*, Paper 70-1A, pages 32–35.
- Campbell, R.B. (1961): Geology of Quesnel Lake, Sheet 93A (West Half), British Columbia; *Geological Survey of Canada*, Map 3-1961.
- Campbell, R.B. (1963): Geology of Quesnel Lake, sheet 93A (east half), British Columbia; *Geological Survey of Canada*, Map 1-1963.
- Fox, P.E. (1975): Alkaline rocks and related mineral deposits of the Quesnel Trough, British Columbia (abstract); *Geological Association of Canada*, Symposium on Intrusive Rocks and Related Mineralization of the Canadian Cordillera, Program and Abstracts, page 12.
- Fox, P.E. (1991): A model for alkaline copper-gold porphyry deposits; abstract; *Geological Association of Canada – Mineralogical Association of Canada*, Joint Annual Meeting, Program with Abstracts, page A39.
- Fraser, T.M., (1993): Geology and alteration of the Mount Polley alkalic porphyry copper-gold deposit, British Columbia (93A/12); in *Geological Fieldwork 1992*, *BC Ministry of Energy, Mines and Petroleum Resources*, Paper 1993-1, pages 295–300.
- Fraser, T.M. (1994): Hydrothermal breccias and associated alteration of the Mount Polley copper-gold deposit; in *Geological Fieldwork 1993*, *BC Ministry of Energy, Mines and Petroleum Resources*, Paper 1994-1, pages 259–267.
- Fraser, T.M. (1995): Geology, alteration and the origin of hydrothermal breccias at the Mount Polley alkalic porphyry copper-gold deposit, south-central British Columbia; unpublished M.Sc. thesis, *University of British Columbia*, 259 pages.
- Fraser, T.M., Stanley, C.R., Nikic, Z.T., Pesalji, R., and Gorc, D. (1995): The Mount Polley copper-gold alkalic porphyry deposit, south-central British Columbia; in *Porphyry Deposits of the Northern Cordillera*, Schroeter, T.G., Editor, *Canadian Institute of Mining and Metallurgy*, Special Volume 46, pages 609–622.
- Hodgson, C.J., Bailes, R.J. and Versoza, R.S. (1976): Cariboo-Bell; in *Porphyry Deposits of the Canadian Cordillera*, Sutherland Brown, A., Editor, *Canadian Institute of Mining and Metallurgy*, Special Volume 15, pages 388–396.
- Karlsson, H.R. and Clayton, R.N. (1991): Analcime phenocrysts in igneous rocks: primary or secondary? *American Mineralogist*, Volume 76, pages 189–199.
- Mathews, W.H. (1989): Neogene Chilcotin basalts in south-central British Columbia: geology, ages, and geomorphic history; *Canadian Journal of Earth Sciences*, Volume 26, pages 969–982.
- McMullin, D.W.A. (1990): Thermobarometry of pelitic rocks using equilibria between quartz-garnet-aluminosilicate-muscovite-biotite, with application to rocks of the Quesnel Lake area, British Columbia; unpublished Ph.D. thesis, *University of British Columbia*, 291 pages.
- Mortensen, J.K., Ghosh, D.K. and Ferri, F. (1995): U-Pb geochronology of intrusive rocks associated with copper-gold porphyry deposits in the Canadian Cordillera; in *Porphyry Deposits of the Northwestern Cordillera of North America*, T. G. Schroeter, Editor, *Canadian Institute of Mining, Metallurgy and Petroleum*, Special Volume 46, pages 142–158.
- Mortimer, N. (1987): The Nicola Group: Late Triassic and Early Jurassic subduction-related volcanism in British Columbia; *Canadian Journal of Earth Sciences*, Volume 24, pages 2521–2536.
- Morton, J.W. and Durfeld, R.M. (1998): Summary report on the Redgold porphyry copper gold project; *BC Ministry of Energy, Mines and Petroleum Resources*, Assessment Report 25 867.
- Morton, R.L. (1976): Alkalic volcanism and copper deposits of the Horsefly area, central British Columbia; unpublished Ph.D. thesis, *Carleton University*, 196 pages.
- Nelson, J.L. and Mihalynuk, M. (1993): Cache Creek Ocean: closure or enclosure? *Geology*, Volume 21, Number 2, pages 173–176.
- Nixon, G.T., Archibald, D.A. and Heaman, L.M. (1993): ⁴⁰Ar-³⁹Ar and U-Pb geochronometry of the Polaris Alaskan-type complex, British Columbia; precise timing of Quesnellia – North America interaction; *Geological Association of Canada – Mineralogical Association of Canada – Canadian Geophysical Union*, Joint Annual Meeting, Program with Abstracts, page 76.
- Palfy, J., Smith, P.L. and Mortensen, J.K. (2000): A U-Pb and ⁴⁰Ar-³⁹Ar time scale for the Jurassic; *Canadian Journal of Earth Sciences*, Volume 37, pages 923–944.
- Panteleyev, A. (1987): Quesnel gold belt – alkalic volcanic terrane between Horsefly and Quesnel Lakes (93A/6); in *Geological Fieldwork 1986*, *BC Ministry of Energy, Mines and Petroleum Resources*, Paper 1987-1, pages 125–133.
- Panteleyev, A. (1988): Quesnel mineral belt – the central volcanic axis between Horsefly and Quesnel Lakes (93A/5E, 6W); in *Geological Fieldwork 1987*, *BC Ministry of Energy, Mines and Petroleum Resources*, Paper 1988-1, pages 131–137.
- Panteleyev, A. and Hancock, K.D. (1989): Quesnel mineral belt: summary of the geology of the Beaver Creek – Horsefly River map area; in *Geological Fieldwork 1988*, *BC Ministry of Energy, Mines and Petroleum Resources*, Paper 1989-1, pages 159–166.
- Panteleyev, A., Bailey, D.G., Bloodgood, M.A. and Hancock, K.D. (1996): Geology and mineral deposits of the Quesnel River – Horsefly map area, central Quesnel Trough, British Columbia (NTS 93A/5, 6, 7, 11, 12, 13; 93B/9, 16; 93G/1; 93H/4); *BC Ministry of Energy, Mines and Petroleum Resources*, Bulletin 97, 156 pages.
- Preto, V.A. (1977): The Nicola Group: Mesozoic volcanism related to the rifting in southern British Columbia; in *Volcanic Regimes in Canada*, Baragar, W.R.A., Coleman, L.C. and

- Hall, J.M., Editors, *Geological Association of Canada, Special Paper 16*, pages 39–57.
- Preto, V.A., Osatenko, M.J., McMillan, W.J. and Armstrong, R.L. (1979): Isotopic dates and strontium isotopic ratios for plutonic and volcanic rocks in the Quesnel Trough and Nicola Belt, south-central British Columbia; *Canadian Journal of Earth Sciences*, Volume 16, pages 1658–1672.
- Rees, C.J. (1987): The Intermontane – Omineca Belt boundary in the Quesnel Lake area, east-central British Columbia: tectonic implications based on geology, structure and paleomagnetism; unpublished Ph.D. thesis, *Carleton University*, 421 pages.
- Ross, J.V., Fillipone, J.A., Montgomery, J.R., Elsby, D.C. and Bloodgood, M.A. (1985): Geometry of a convergent zone, central British Columbia, Canada; *Tectonophysics*, Volume 119, pages 285–297.
- Ross, J.V., Garwin, S.L. and Lewis, P.D. (1989): Geology of the Quesnel Lake region, central British Columbia: geometry and implications; in *Proceedings, 7th International Conference on Basement Tectonics, D. Reidel*, Dordrecht, Netherlands, pages 1–23.
- Ross, K.V. (2004): Alteration study of the Northeast zone, Mount Polley Mine, British Columbia; unpublished report, *Imperial Metals Corporation*, 84 pages.
- Schink, A.E. (1974): Geology of the Shiko Lake stock, near Quesnel Lake, British Columbia, unpublished B.Sc. thesis, *University of British Columbia*, 64 pages.
- Shives, R.B.K., Carson, J.M., Ford, K.L., Holman, P.B. and Cathro, M. (2004): Imperial Metals Corp. Mt. Polley 2003 multisensor geophysical survey; *BC Ministry of Energy and Mines*, Open File 2004-10.
- Souther, J.G. (1977): Volcanism and tectonic environments in the Canadian Cordillera – a second look; in *Volcanic Regimes in Canada*, Baragar, W.R.A., Coleman L.C. and Hall, J.M., Editors, *Geological Association of Canada*, Special Paper 16, pages 3–24.
- Struik, L.C. (1986): Imbricated terranes of the Cariboo gold belt with correlations and implications for tectonics in southeastern British Columbia; *Canadian Journal of Earth Sciences*, Volume 23, pages 1047–1061.
- Struik, L.C. (1987): The ancient western North American margin: an alpine rift model for the east-central Canadian Cordillera; *Geological Survey of Canada*, Paper 87-15, 19 pages.
- Struik, L.C. (1988a): Regional imbrication within Quesnel Terrane, central British Columbia, as suggested by conodont ages; *Canadian Journal of Earth Sciences*, Volume 25, pages 1608–1617.
- Struik, L.C. (1988b): Structural geology of the Cariboo gold mining district, east-central British Columbia; *Geological Survey of Canada*, Memoir 421, 100 pages.
- Sutherland Brown, A. (1976): Morphology and classification; in *Porphyry Deposits of the Canadian Cordillera*, Sutherland Brown, A., Editor, *Canadian Institute of Mining and Metallurgy*, Special Volume 15, pages 44–51.
- Tennant, S.J. (1997): 1997 – diamond drilling assessment report on the Lloyd property; *BC Ministry of Energy, Mines and Petroleum Resources*, Assessment Report 25 300.
- Tennant, S.J. (1998): Diamond drilling report on the Lloyd and Nordik claim; *BC Ministry of Energy, Mines and Petroleum Resources*, Assessment Report 25 651.
- Tennant, S.J. (2000): 2000 drilling on the Lloyd property; *BC Ministry of Energy, Mines and Petroleum Resources*, Assessment Report 26 495.
- Tipper, H.W. (1959): Quesnel, British Columbia; *Geological Survey of Canada*, Map 12-1959.
- Tipper, H.W. (1978): Northeastern part of Quesnel (93B) map-area, British Columbia; in *Current Research, Part A*, *Geological Survey of Canada*, Paper 78-1A, pages 67–68.
- Travers, W.B. (1977): Overturned Nicola and Ashcroft strata and their relations to the Cache Creek Group, southwestern Intermontane Belt, British Columbia; *Canadian Journal of Earth Sciences*, Volume 15, pages 99–116.
- Wheeler, J.O. and McFeely, P. (1991): Tectonic assemblage map of the Canadian Cordillera and adjacent parts of the United States of America; *Geological Survey of Canada*, Map 1712A, scale 1:2 000 000.
- Wild, C. J. (1999): Diamond drilling report on the Mount Polley project; *BC Ministry of Energy, Mines and Petroleum Resources*, Assessment Report 25 906.

Porphyry Cu-Au Deposits of the Iron Mask Batholith, Southeastern British Columbia

By James M. Logan and Mitchell G. Mihalynuk

KEYWORDS: geology, mineralization, geochronology, alkaline, porphyry copper-gold, Nicola, picrite, Pothook, Cherry Creek, Sugarloaf, Afton, Ajax, Crescent, Audra, Rainbow, Kamloops

INTRODUCTION

The Iron Mask batholith is located 10 km southwest of Kamloops (Fig. 1). It is the source of Cu-Au-Ag produced from porphyry deposits such as Afton, Crescent, Pothook, Ajax West and Ajax East, as well as structurally controlled Cu-magnetite veins (Iron Mask, Makaoo, Grey Mask). Currently, it is the target of exploration for Cu-Au-Ag-Pd mineralization by DRC Resources at the Afton mine property and by Abacus Mining and Exploration Corp. at the Rainbow-Coquihalla East and DM-Audra occurrences.

The Iron Mask component of the Cu-Au Porphyry Project is a regional mapping and compilation study designed to produce an up-to-date geological map of the Cu-Au-enriched Iron Mask batholith. The study incorporates information from the MDRU-Porphyry Cu-Au study (ca. 1991) and company reports to update the last published re-

gional map of Kwong (1987). The compilation has utilized the detailed, low-level, airborne geophysical survey carried out over the Iron Mask batholith by the Geological Survey of Canada (Shives, 1994) to better define structures and the distribution of individual intrusive phases, alteration and mineralization in areas of little or no outcrop. Results of the study arise from collaborative partnerships between the British Columbia Ministry of Energy and Mines, Abacus Mining and Exploration Corporation, Imperial Metals Corporation and NovaGold Resources Inc.

PREVIOUS WORK

The geology of the Iron Mask batholith and its ore deposits have been described by Cockfield (1948), Carr (1957), Carr and Reed (1976), Preto (1967, 1972), Northcote (1974, 1976, 1977), Hoiles (1978), Kwong (1982, 1987) and Kwong *et al.* (1982). Recent work on porphyry Cu-Au deposits by the Mineral Deposit Research Unit of the University of British Columbia include studies by Ross (1993), Snyder and Russell (1993, 1995), Snyder (1994), Lang and Stanley (1995) and Ross *et al.* (1995). Nixon

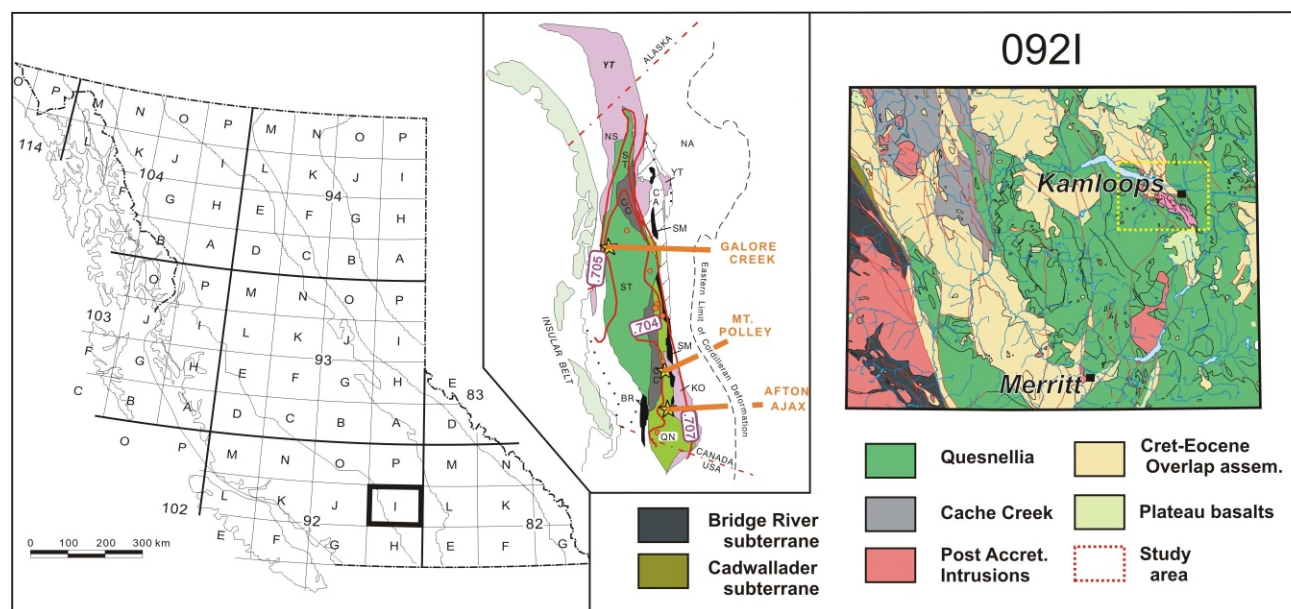


Figure 1. Location of the Iron Mask component of the Cu-Au Porphyry Project in south-central British Columbia (NTS 0921). Inset is terrane map of northern Cordillera (modified from Wheeler and McFeely, 1991), showing the tectonostratigraphic setting of the three study areas. Mesozoic initial strontium isopleths are from Armstrong (1988). Box on right shows detailed terrane relationships for NTS 0921 and the project area.

(2004) conducted petrographic and geochemical studies of the PGE distribution in the Afton deposit as part of a larger provincial study.

REGIONAL GEOLOGY

The study area lies along the eastern margin of the Intermontane Belt close to its tectonic boundary with the Omineca Belt, in south-central British Columbia. At this latitude, the Intermontane Belt is underlain mainly by unmetamorphosed Upper Paleozoic to Lower Paleozoic arc-volcanic, plutonic and sedimentary rocks of the Quesnel Terrane. Farther west are coeval rocks of the oceanic Cache Creek Terrane (Fig. 1). The Quesnel Terrane consists of a Late Triassic to Early Jurassic magmatic-arc complex that formed above an east-dipping subduction zone (Mortimer, 1987). The Cache Creek Terrane, with its blueschist-facies rocks, represents the remnants of this subduction-accretionary complex (Travers, 1977), which was active until the Middle Jurassic. To the east of the Quesnel Terrane are rocks of the Omineca Belt, which include Upper Paleozoic oceanic rocks of the Slide Mountain Terrane and Paleozoic and older metasedimentary, meta-volcanic and metaplutonic rocks of the pericratonic Kootenay Terrane. The Slide Mountain Terrane consists of basalt, chert and gabbro, but also clastic units that can be correlated with rocks of the Kootenay Terrane and has been interpreted to represent a marginal or back-arc basin that developed directly outboard of North America (Klepaki and Wheeler, 1985; Schiarizza, 1989; Ferri, 1997). Amalgamation of the Intermontane Belt (Cache Creek, Quesnel, Stikine and Slide Mountain terranes) began in the Late Paleozoic with initial closure of the Slide Mountain ocean basin and was complete by the Middle Jurassic. In the Early Jurassic (186 Ma), Quesnellia rocks were thrust eastward over the North American miogeocline. By the Middle Jurassic, Stikinia had collided with Quesnellia, resulting in the demise of the Cache Creek subduction zone (173 Ma) and stitching of the boundary by ~172 Ma plutons. The tectonic boundary between the Kootenay and Quesnel terranes is intruded by the Jura-Cretaceous Raft batholith north of Kamloops. Middle Eocene volcanic and sedimentary rocks of the Kamloops Group unconformably overlie the Nicola Group and Iron Mask rocks, and Miocene alkaline flood basalts are the youngest rocks in the region (Fig. 2).

MAP COMPILATION

Figure 2 is a compilation map of the Iron Mask batholith. Contact configuration is based upon seven weeks of fieldwork by the authors, with heavy reliance on previously published mapping. Principal compilation sources are Carr (1957), Northcote (1977) and compilations by Kwong (1987), and Stanley *et al.* (1994). Company reports and maps, as well as topical studies, contain many excellent observations, normally on a detailed scale, that have been incorporated into the works cited. Many of the compilation sources lack indication of outcrop distribution or other data sources that constrain the geological contacts shown, such

as drillholes, trenches, or underground workings. Carr (1957) is one exception, and we have applied a high weighting to this compilation source. In many instances, workings that were open to Carr, have now collapsed, or have been overgrown. We show the outcrops, workings and drillholes that helped to constrain his interpretations in areas where we lacked field data. Field stations shown by Northcote (1977), presumably indicating the presence of outcrop, are also given a high weighting. Where the near-subsurface geology is constrained by underground workings, we have shown the data projected to surface as if the geological relationships were visible in outcrop. In areas of no exposure or subsurface information, we have relied upon the aeromagnetic response of the buried bedrock to guide the interpretation of contacts shown in Figure 2.

AEROMAGNETIC LINEAMENTS

In 1993, a multiparameter airborne geophysical survey of the Iron Mask batholith area was flown by Sander Geophysics Limited, under contract to the Geological Survey of Canada. The survey collected quantitative gamma-ray spectrometric (K, U, Th), VLF-EM and aeromagnetic data. The data were processed and results presented on 1:150 000-scale colour maps and stacked profiles (Shives, 1994). Distinctive airborne geophysical signatures are apparent for all 20 of the known deposits (low eTh/K ratio with strong, flanking, high magnetic signature). Carmel Lowe of the Geological Survey of Canada, Sidney Subdivision reprocessed components of the 1993 data and converted them into image formats that could be registered with our current geological compilation.

A structural discontinuity that marks an abrupt transition from nonfoliated to strongly foliated rocks, situated southwest of the batholith, corresponds with an equally abrupt drop in the aeromagnetic response of the well-exposed rocks. This is presumably due to magnetite destruction during fabric development. A strong vertical gradient results, which roughly corresponds with the mapped trace of the Cherry Creek Fault (Fig. 3). Flexures within the trend of the vertical gradient anomaly (4 km due west of Jacko Lake), might be due to a folded deformation front.

Aeromagnetic response does not in all instances reflect the bedrock lithology. The Iron Mask Hybrid phase contains abundant coarse interstitial grains of magnetite and typically displays magnetic susceptibility an order of magnitude higher than most other rock types. However, extensive brittle faulting can destroy magnetite in the hybrid unit (such as the eastern contact near the Makaoo, or at the Galaxy deposit) and undeformed pegmatitic hybrid phases may also lack a high magnetic susceptibility. Intrusive units with a typically low magnetic susceptibility may show elevated values, particularly where adjacent to the hybrid unit. Such anomalies appear to have a strong association with copper mineralization (e.g., Joker).

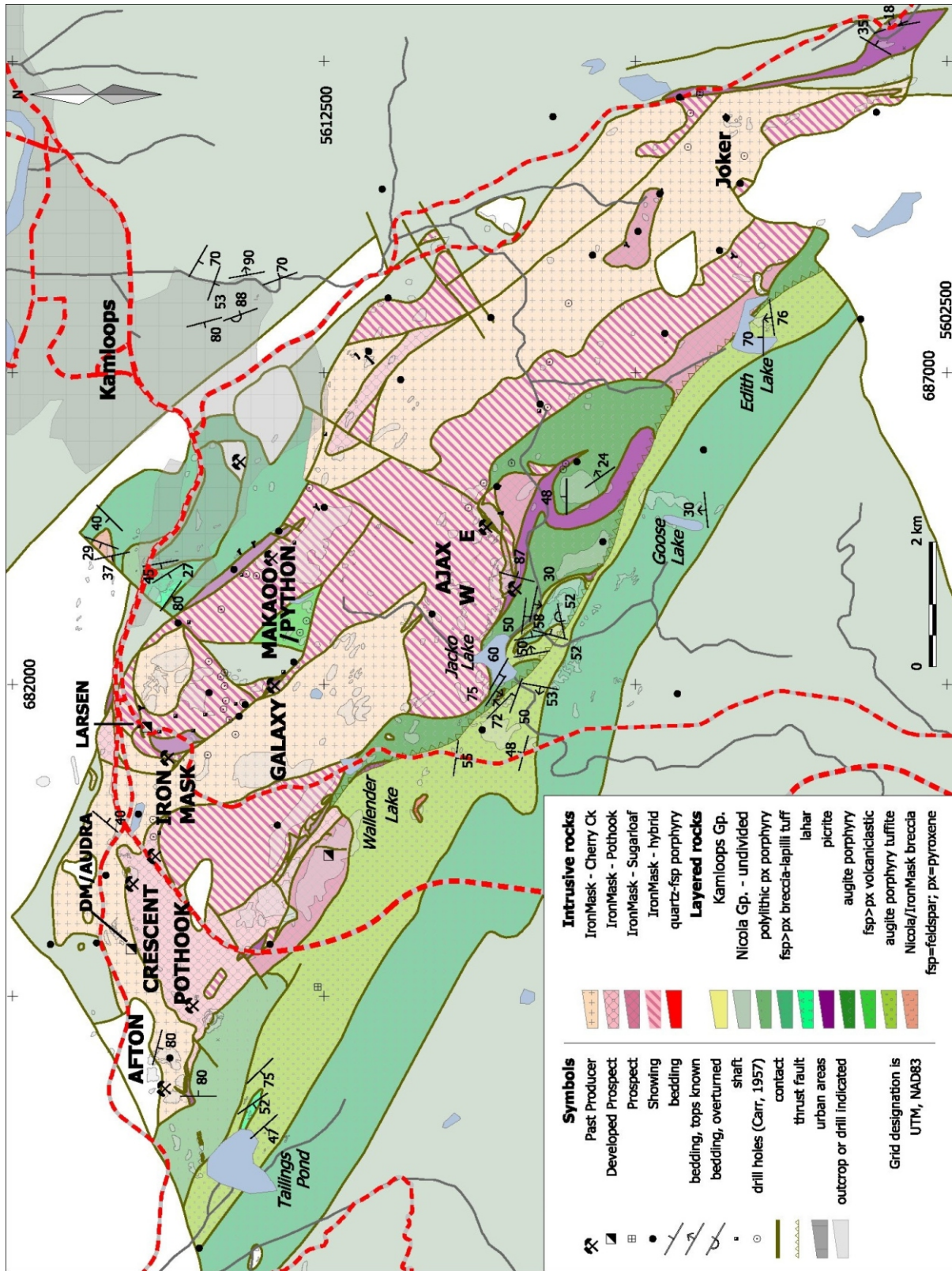


Figure 2. Compilation map of the Iron Mask batholith, incorporating unpublished assessment work and published work by Carr (1957), Kwong (1987), Preto (1967), Northcote (1976, 1977), Snyder and Russell (1994, 1995), Stanley et al. (1994) and Ross et al. (1995).

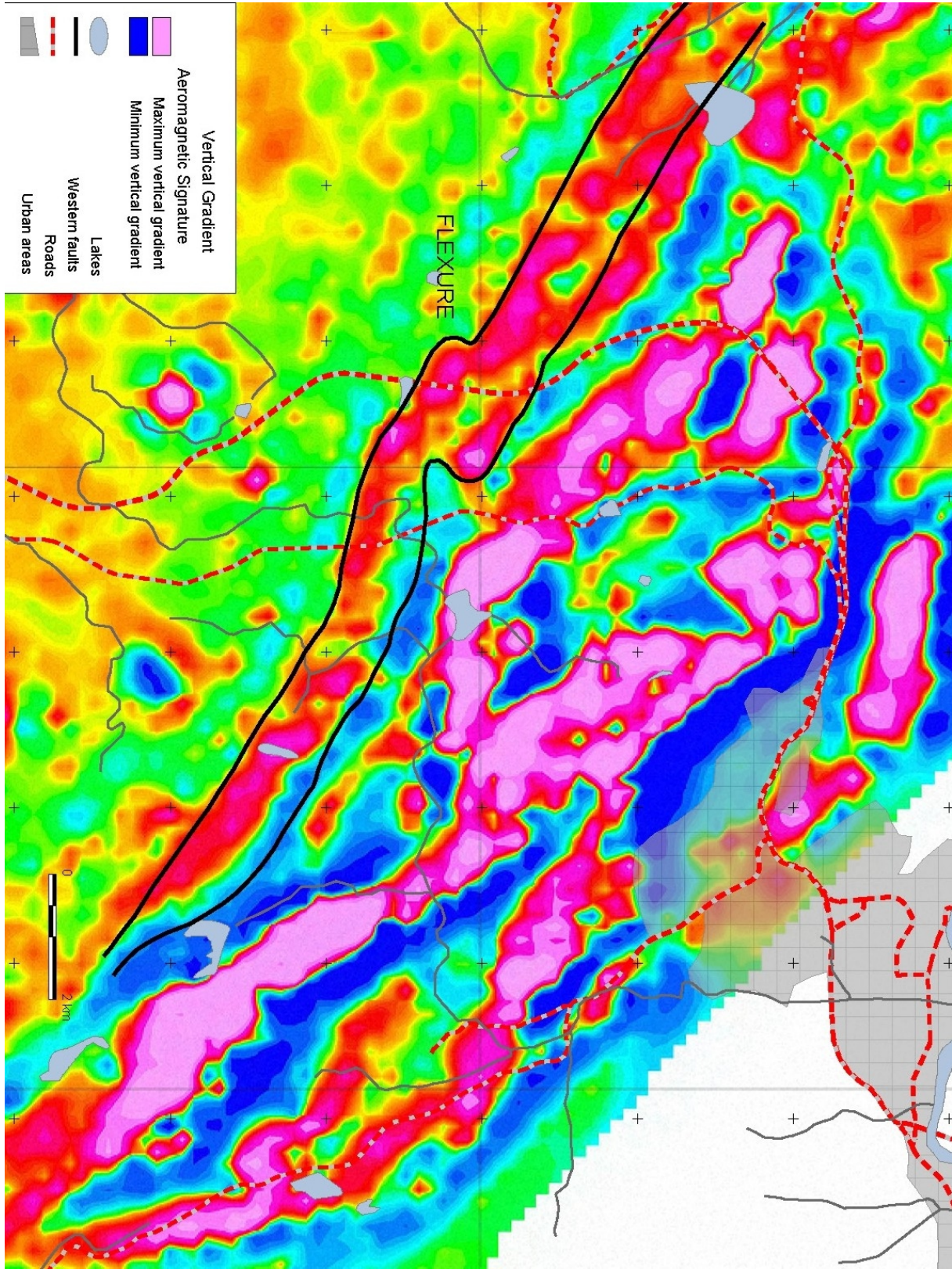


Figure 3. Vertical gradient aeromagnetic map of the Iron Mask batholith. See text for discussion.

NICOLA GROUP ROCKS

The Late Triassic Nicola Group of south-central British Columbia comprises Carnian to Norian, subaerial and submarine assemblages that include pyroxene and plagioclase-phyric basaltic and andesitic flows, breccias, lahars and conglomerate that have been intruded by Late Triassic to Early Jurassic alkalic and calcalkalic plutons and batholiths (Preto, 1977, 1979). They have been subdivided into three north-trending fault-bounded belts. The Iron Mask batholith intrudes volcanic and sedimentary rocks of the eastern belt of the Nicola Group (Preto, 1979; Mortimer, 1987).

Within the study area, the Nicola Group rocks situated southwest of the batholith can be divided into three main units: 1) picrite and pyroxene porphyritic breccias; 2) heterolithic pyroxene-dominant tuffs and volcanic wacke, siltstone and tuffite; and 3) tabular feldspar porphyry breccias and tuffs. North of the batholith in the Dufferin Hill area, the Nicola Group rocks comprise three main rock types: 1) heterolithic tuff, 2) monolithic monzonitic-latitude breccias, and 3) a mixed volcanoclastic and epiclastic lahar unit (Fig. 4).

The Nicola Group rocks are metamorphosed to a lower greenschist facies mineral assemblage that includes chlorite, epidote, actinolite and calcite. Adjacent to the batholith the Nicola rocks are hornfelsed.

Stratigraphy Southwest of the Batholith

PICRITE UNIT

Coarse olivine-augite-bearing porphyritic (picritic) basalt and augite porphyritic (absarokitic ankaramite) breccia is a common hostrock to the Iron Mask batholith. Excellent, bright blue-green exposures are seen at Jacko Lake, northwest of Shumway Lake, south of the Afton pit and north of Goose Lake. Unit thickness is difficult to assess, but distribution of outcrops suggests a thickness in excess of 200 m. It is clearly volcanosedimentary in nature, as indicated by sedimentary interbeds and lobes of picritic basalt breccia within tuffite (Fig. 2, 5). In all exposures, it displays a good breccia texture on clean, weathered surfaces. Weathering may reduce the unit to rubble, which can be disaggregated by hand except for dense clast interiors. In no location is it possible to demonstrate unequivocal intrusive relationships, although feeder dikes must exist locally. In hand specimen, picrite is characterized by serpentinized rounded olivine phenocrysts, prismatic relict clinopyroxene, and magnetite grains in a fine-grained groundmass of serpentine-tremolite. Where sheared, fractures are coated with serpentine.

Pyroxene-olivine breccia forms the lowest unit below well-indurated angular pyroxene lapilli tuff. The relationship of the picrite breccia to the main augite porphyry unit is not certain. Near the Iron Mask mine, a large xenolith of serpentinized picrite marks the contact zone between Iron Mask hybrid diorite and Cherry Creek monzonite. The picrite is hornfelsed/recrystallized by the intrusions and

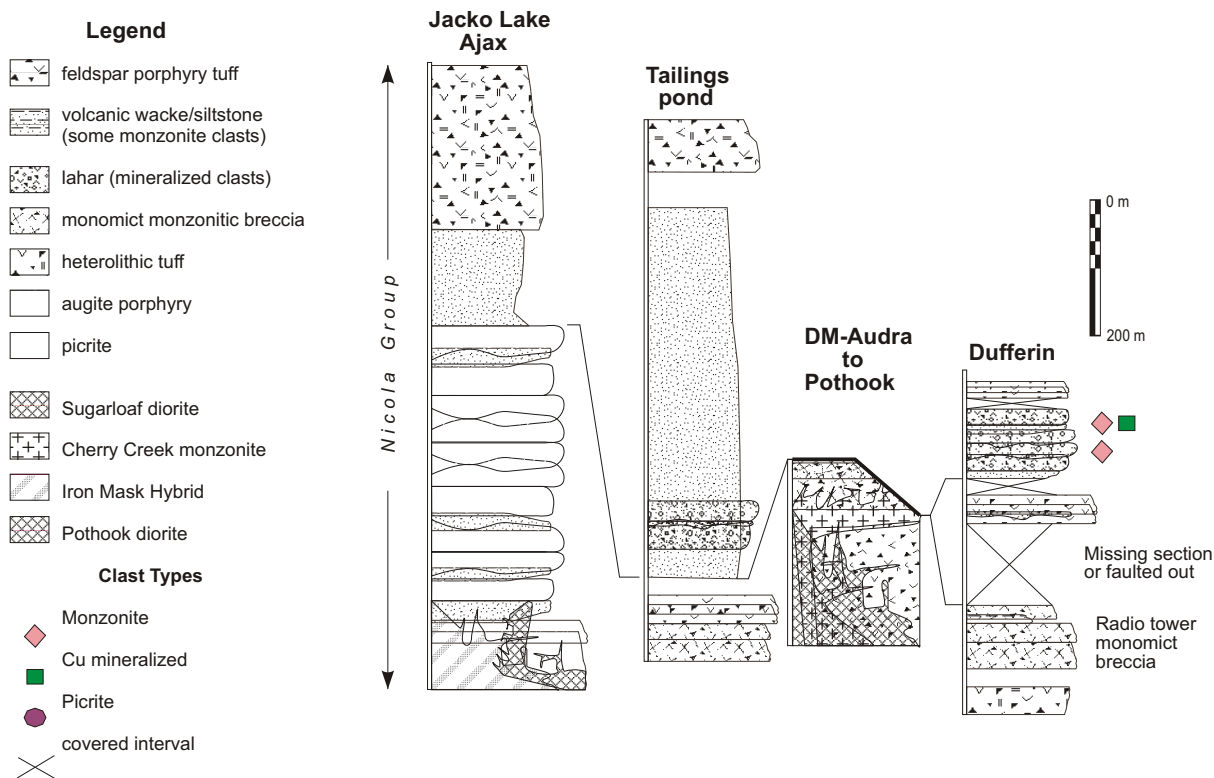


Figure 4. Stratigraphic sections for Nicola Group volcanic and sedimentary rocks at Jacko Lake, Afton tailings pond, DM-Audra to Pothook and Dufferin Hill areas.



Figure 5. Picritic basalt breccia interbedded with volcanoclastic units of the Nicola Group, southeast of Jacko Lake.

contains coarse crystals of tremolite and talc. In the south wall of the Ajax West pit, serpentinized picrite is intruded by hornblende-phyric Sugarloaf diorite dikes (Fig. 6). From these observations, the picrite must be older than the batholith. Evidence derived from sections studied outside of the batholith by Snyder and Russel (1993, 1994) favours a brecciated basalt flow origin. Our observations are in accord with the conclusions of Snyder and Russell (1993, 1994), but indicate that the picrite is part of the Nicola Group stratigraphy and not younger, because massive picrite bodies in the Jacko Lake – Edith Lake area can be traced along strike to where they are interbedded with sedimentary strata.

AUGITE PORPHYRY BRECCIA, MINOR FLOWS

Dark green, maroon and purple clinopyroxene porphyritic and clinopyroxene-plagioclase porphyritic basalt breccias and massive flows or dikes are spatially associated with the picrite unit and occupy the area adjacent to the southern contact of the batholith (Fig. 2). The breccias, which dominate the unit, are entirely composed of pyroxene porphyritic fragments. The fragments are typically angular to subrounded and unsorted. They are commonly up to 10 cm but can exceed 100 cm in size. The matrix to the breccias consists of juvenile pyroxene and plagioclase crystals and small pyroxene porphyritic lithic fragments. Along strike and up section, the breccias become finer grained and epiclastic in nature. South of Jacko Lake, the breccias contain interclast laminated ash and dust tuffs.

Their position adjacent to the batholith has resulted in hornfelsing, fracture-controlled potassic and/or albite alteration, and their incorporation as xenoliths and large screens.

AUGITE PORPHYRY TUFFITE, VOLCANIC SANDSTONE AND SILTSTONE

Green, grey and black interlayered pyroxene porphyritic breccias, crystal-rich tuffite and subordinate thin-laminated siltstone define a regionally mappable unit that ex-



Figure 6. Serpentinized picrite intruded by north-trending hornblende-phyric Sugarloaf diorite dike, south wall of the Ajax West pit. Inset shows detail of picrite breccia texture.

tends northwesterly from Edith Lake to the Afton tailings pond (Fig. 2–4). Local sections contain plagioclase greater than pyroxene, but overall pyroxene dominates. The unit consists primarily of thick-bedded or massive, well-sorted sandstone units comprising primarily pyroxene and plagioclase crystals and rare lithic grains. Intercalated with these massive sandstone units are crystal-lithic tuff (tuffite) that form distinct graded beds, between 10 and 50 cm thick, and thin-laminated, commonly graded, siltstone-sandstone couplets. Crystal-rich sandstone displays good crosslaminations, normal graded beds and load structures that give bedding top directions in the finer grained volcanoclastic and epiclastic sections south of Jacko Lake.

North of the Afton tailings pond, the tuffite is interlayered with coarse pyroxene porphyritic breccia, polyolithic tuff and polyolithic conglomerate. Sections of the tuffite are normal-graded, pale green siltstone and coarse granule sandstone containing pink clasts and feldspar crystals, but most of the outcrop is a chaotic mix of tuffite, pink plagioclase-phyric lapilli and green pyroxene-phyric lapilli. The rocks are irregularly fractured and veined by anastomosing, locally coalescing veins of specular hematite and rare disseminated chalcopyrite. Eastward, toward the open pit, are polyolithic tuff and conglomeratic horizons within a section that contains pyroxene porphyry and other igneous clasts with compositions similar to the main intrusive phases of the Iron Mask batholith: tabular plagioclase microporphyritic monzonite and hornblende-phyric diorite fragments. Overprinting by fine-grained pyrite or epidote-chlorite produces a bleaching or green colouration. Disrupted fabrics in the tuffite are pre-lithification; alteration and mineralization postdate intrusion of the Iron Mask batholith.

FELDSPAR PORPHYRITIC LAPILLI TUFF

A great thickness of fine tabular feldspar porphyritic lapilli tuff, lesser breccia and tuffite is exposed in the Iron Mask region. Resistant, blocky outcrops are well exposed on the mountain slopes north of Kamloops Lake near Fred-

erick, between Jacko and Goose Lakes, and on Dufferin Hill (Fig. 2). Probably more than 1 km thick, this unit displays wide textural variability from finely laminated to coarse, weakly stratified breccia, although the most abundant lithology is lapilli tuff, which is typically massive, with little indication of layering (Fig. 4).

Variiegated lapilli tuff constitutes most of the outcrops at the Maxine (MINFILE 0921/032) mineral occurrence, north of Kamloops Lake. The matrix contains specular hematite and, as a result, is a conspicuous mottled maroon and green colour. Tabular white plagioclase–phyric lapilli constitute the majority of the fragments, which are supported in a plagioclase crystal–rich ash matrix. Inflation of the section are hematitic, holocrystalline, crowded-plagioclase–phyric trachyte units. East of Frederick, the tuffs are finer grained and consist of more than 200 m of brown-weathering, fine plagioclase crystal tuff.

In the vicinity of Jacko Lake and Goose Lake, the tuffs are well indurated and consist of fine plagioclase laths and lesser pyroxene. Sections of light grey cherty tuff were noted, but most outcrops are dark green fine lapilli of feldspar porphyry.

Stratigraphy North of the Batholith

FELDSPAR PYROXENE BRECCIA, LAPILLI TUFF

Coarse breccia at Dufferin Hill has been mapped as Cherry Creek intrusive breccia. However, it is crudely stratified and interpreted here as a proximal, monomict flow breccia. The breccia is intermediate in composition, comprising 5 to 7 mm stubby plagioclase phenocrysts and slightly coarser pyroxene phenocrysts in an aphyric groundmass. Fragments are angular, poorly sorted and of highly variable size, from ash through lapilli to block, suggesting little reworking (Fig. 7). Massive centres, brecciated flow tops and intervening airfall tuffs indicate



Figure 7. Poorly sorted angular blocks of feldspar porphyritic breccia with lesser lapilli and ash fragments, forming the top of Dufferin Hill. Textures suggest little reworking.

meter-scale flow thicknesses at this location. Blocks of identical composition and size occur in lahar units to the south.

LAHAR

A mottled purplish-green to maroon polymictic volcanoclastic is well exposed south of Dufferin Hill and the Trans-Canada Highway. The unit consists of mainly subangular blocks and cobbles of volcanic and intrusive rocks in a hematitic ash matrix. It is interpreted as a lahar. The most abundant clast type is a flesh-coloured, fine-grained monzodiorite, as blocks commonly between 0.5 and 1.0 m across. Subordinate clast compositions include potassium-metasomatized subporphyritic monzodiorite, tabular felted plagioclase-pyroxene porphyry, and augite porphyry. Conspicuously, some of the clasts are strongly copper stained, epidote and K-feldspar altered, and mineralized with chalcopyrite (Fig. 8). In addition, subangular to rounded clasts of volcanic breccia are present within the unit. Crude clast imbrication and sorting are locally apparent.

This unit is interpreted as coeval with mineralization within the Afton-Ajax system. A lateral gradation with breccia on Dufferin Hill seems likely.

IRON MASK BATHOLITH

The Iron Mask batholith is a northwest-trending, silica-saturated alkalic intrusive complex (Lang *et al.*, 1995). It consists of two separate bodies: the 22 km long by 5 km wide Iron Mask batholith in the southeast, which was the focus of our study (Fig. 2), and the 5 km by 5 km Cherry Creek pluton in the northwest. The two are separated by an east-trending graben structure filled with Eocene Kamloops Group volcanic and sedimentary rocks. Snyder and Russell (1993, 1995) have described the various phases of the batholith and studied the petrogenetic relationships between them and the pirite unit (Snyder and Russell,



Figure 8. Maroon polymictic lahar consists of mainly subangular blocks and cobbles of volcanic and intrusive rocks in a hematitic ash matrix. Inset shows potassic altered, chalcopyrite mineralized clast. Exposure south of Dufferin Hill, and the Trans Canada Highway.

1994). We follow their revised sequence of major intrusions (i.e., from oldest to youngest: Pothook diorite, Cherry Creek monzonite and Sugarloaf diorite) and their conclusion that the Iron Mask hybrid was derived mainly from Pothook diorite and assimilated Nicola volcanic rocks, although xenolith-rich Sugarloaf diorite can also form a hybrid unit (e.g., East of Edith Lake).

The U-Pb ages for samples of the Pothook, Hybrid and Cherry Creek phases of the batholith (Mortensen *et al.*, 1995) are 204 ± 3 Ma, or Upper Triassic, using the time scale of Palfy (2000). The Sugarloaf diorite is the youngest phase but remains undated (results from samples collected for geochronology are pending).

Pothook Phase

Pothook diorite forms the northern part of the Iron Mask batholith (Fig. 2). Its distribution suggests that emplacement was controlled by northwest and northeast-trending faults. Contacts with the Hybrid unit are gradational, and contacts with Cherry Creek rocks are faulted and masked by strong potassic alteration. Contacts with the Sugarloaf phase are reportedly intrusive at the Pothook deposit (Stanley, 1994).

The Pothook unit is an equigranular, medium to coarse-grained biotite-pyroxene diorite, defined by the presence of poikilitic biotite (Northcote, 1974; Synder, 1994). The rock contains 40 to 60% subhedral plagioclase (An₄₃ to An₅₂; Synder, 1995), 10 to 25% clinopyroxene, 5 to 10% magnetite, 5 to 7% biotite and up to several percent K-feldspar, apatite and lesser accessories including sphene and zircon. Poikilitic biotite (up to 2 cm) encloses earlier formed plagioclase, clinopyroxene and magnetite grains. Widespread alteration minerals include K-feldspar, sericite, epidote and chlorite.

Hybrid Phase

The Iron Mask Hybrid phase is a xenolith-rich, heterogeneous unit that forms approximately 45% of the Iron Mask batholith (Fig. 2). Hybrid rocks mark the contact zones between individual phases (i.e., Pothook, Cherry Creek and Sugarloaf) within the batholith, as well as the contact zones between the margin of the batholith and the volcanic country rock. Snyder (1994) redefined the Hybrid phase to be a facies equivalent of the Pothook diorite, suggesting it represented the outer margins to the Pothook intrusion (i.e., top and sides), which interacted and incorporated country rock of the Nicola Group. The matrix to all Hybrid rocks is not necessarily Pothook diorite. Locally, xenolith-rich marginal phases of Cherry Creek and Sugarloaf are hybrid zones.

The Iron Mask Hybrid phase has been subdivided into three main types on the basis of texture and clast abundance (Synder and Russell, 1995). Type 1 is restricted to contact zones between the Iron Mask batholith and the volcanic and sedimentary rocks of the Nicola Group. It is an intrusive breccia, characterized by angular fragments of hornfelsed country rock, veined by a matrix of pyroxene-hornblende diorite. Type 2 hybrid occurs in the centre of the batholith,

enveloping a large body of Cherry Creek monzonite that is centred on Ironmask Hill. The unit is xenolith rich, characterized by abundant (15–80%) volcanic, plutonic and sedimentary rocks, some of which have reacted with the matrix. The matrix to Type 2 hybrid is variable: in places, it consists of medium to coarse-grained plagioclase, pyroxene, biotite, magnetite and rare hornblende that resembles Pothook diorite and, elsewhere, it consists of hornblende-plagioclase-rich trachytic phases. Type 3 hybrid occupies the northeastern margin of the batholith at Knutsford and a northerly-trending belt extending from the Ajax deposit to Coal Hill. This unit is a xenolith-poor intrusive breccia with textural and compositional variability that includes fine-grained to pegmatitic, and locally trachytic segregations of clinopyroxene, plagioclase, hornblende and magnetite.

The Iron Mask Hybrid phase contains abundant coarse interstitial grains of magnetite in a Pothook dioritic matrix and displays a magnetic susceptibility typically an order of magnitude higher than most other rock types.

Cherry Creek Phase

The Cherry Creek suite was defined by Livingston (1960 *in* Preto, 1967) and was originally restricted to a suite of felsic porphyritic intrusions, dikes and breccias found mostly along the northeastern margin of the Iron Mask batholith (e.g., Preto, 1967), and forming the satellite Cherry Creek pluton. Hoiles (1978), recognized four varieties of Cherry Creek rocks at the Afton deposit: breccias, porphyries, syenite to monzonite trachytes and non-porphyritic medium to fine-grained diorites. Work by Stanley *et al.* (1994), Lang (1994) and Snyder and Russel (1995) discussed the difficulty of separating the Cherry Creek from the Pothook phase and concluded that earlier maps may have overrepresented Cherry Creek due to the pervasive potassium metasomatism of Pothook and Cherry Creek rocks that is commonly developed adjacent to their contacts.

Cherry Creek rocks display textures that vary from plutonic to hypabyssal and locally volcanic. In the core of the batholith, near Ironmask Hill and south of Knutsford, Cherry Creek rocks are leucocratic, fine to medium-grained, equigranular biotite monzonite. Near the margins of the batholith, the rocks are characteristic orange to brown microporphyries speckled with fine-grained indistinct ferromagnesian minerals that range in composition from monzodiorite to monzonite. The pervasive pink to orange colouration results from the finely disseminated microcrystalline inclusions of red hematite in the secondary K-feldspar. In general, the rocks are fine-grained, holocrystalline subporphyritic units that exhibit crudely aligned tabular plagioclase crystals and minor chloritized mafic minerals. In thin section, relicts of mafic minerals can be identified as clinopyroxene and less commonly hornblende. Magnetite is disseminated throughout the groundmass in amounts up to 10%. The rocks contain sparse primary quartz. Accessory minerals include apatite, zircon and titanite.

Finer grained varieties of the Cherry Creek phase include trachyte and latite porphyries (Preto, 1967). The ma-

trix is commonly altered to a mixture of epidote, chlorite, sericite and carbonate. Commonly associated with these fine-grained porphyries are intrusive and hydrothermal breccias at the Crescent, DM and Kimberley mineral deposits (Preto, 1967). In addition, Snyder (1994) mapped a zone of Cherry Creek breccia east of the Iron Mask mine. Here, the intrusion breccia is characterized by angular metavolcanic fragments ranging in size from 10 to 100 cm and set in a fine to medium-grained biotite monzonite matrix. Snyder (1994) noted that the boundaries between clasts and matrix varied from diffuse to sharp, with the sharpest contacts (Fig. 9) at the shallowest intrusive levels. Surrounding the intrusive breccia are Iron Mask hybrid rocks that characteristically show a higher degree of assimilation, a greater variety of clast rocks types and a dioritic matrix to the breccia.

Northcote (1976) included outcrops of fine-grained, brecciated and ankeritic rocks east of Galaxy with the Cherry Creek phase. We have reassigned them, based on similarity with ankeritic rocks located between Wallender and Jacko lakes, to Nicola Group metavolcanic rocks (Fig. 2).



Figure 9. Cherry Creek intrusion breccia, consisting of angular metavolcanic fragments set in a fine to medium-grained biotite monzonite matrix, hilltop east of Iron Mask mine.

Sugarloaf Phase

The term ‘Sugarloaf porphyritic diorite’ was also introduced by E. Livingston in 1960 (*in* Preto, 1967) for a suite of hornblende porphyritic, trachytic rocks of dioritic composition. It primarily crops out along the western margin of the batholith (Fig. 2) as lenticular bodies (Sugarloaf Hill, Ajax East deposit) or as metre-wide dikes in the adjacent Nicola volcanic rocks (Coquihalla East zone, Pothook and Ajax West deposits). The distribution of the Sugarloaf rocks was apparently controlled by northwest-trending structures. Sugarloaf dikes are radially oriented around Sugarloaf Hill, which Snyder and Russell (1993) interpreted as a volcanic neck and intrusive centre. On the southwest flank of Sugarloaf Hill is a bleached, albite-altered, monomictic hornblende-phyric breccia. It is lithologically identical to the stock and represents either an extrusive equivalent or intrusive breccia. The unit possesses sub-horizontal jointing planes suggestive of bedding, which favours an extrusive origin and accumulation on the flank of the stock. Further work is needed to confirm this interpretation.

Sugarloaf rocks are characterized by 1–1.5 mm hornblende and plagioclase phenocrysts in a fine-grained groundmass of plagioclase, clinopyroxene, magnetite and K-feldspar. Accessory minerals include apatite, sphene, pyrite and rare quartz (Snyder, 1994). The unit displays considerable textural variation, ranging from fine-grained to medium-grained holocrystalline trachytic porphyries. Albite alteration affects Sugarloaf rocks and extends into the Nicola Group volcanic rocks at the Ajax deposit.

Quartz-Feldspar Porphyry Dike

Quartz-feldspar porphyry dikes have been mapped at the Ajax (Ross, 1993) and Afton (Kwong, 1987) deposits and south of the Rainbow property. These dikes range in thickness from less than 1 m to more than 10 m. The rock varies in grain size and texture from a uniform, fine-grained, pinkish brown rock containing acicular hornblende, lesser biotite, quartz and feldspar to a coarse quartz-feldspar porphyry. Some of these dikes contain sparse to abundant xenoliths, including coarse-grained quartz monzonite, metabasalt and medium-grained holocrystalline granite. Where thickest, the dikes may contain up to 10% coarse quartz eyes and 30% tabular, zoned feldspar.

They cut the picrite and Sugarloaf phase in the vicinity of the Ajax deposits and Cherry Creek rocks in the Afton pit. Ross (1993) suggested that they postdate alteration, mineralization and many of the faults. However, samples of lithologically similar rocks from the Ajax pit are albitized, and mineralized with chalcopyrite.

KAMLOOPS GROUP

Sedimentary and volcanic rocks of the Kamloops Group unconformably overlie the Nicola Group rocks and the Iron Mask batholith. The unconformity is typically flat-lying and postdates development of supergene ore at Afton.

The Kamloops Group includes tuffaceous sandstone, siltstone and shale with minor conglomerate, and alkali olivine basaltic to andesitic flows and agglomerates with minor dacite, latite and trachyte (Ewing, 1981).

STRATIGRAPHIC RELATIONSHIPS

The picrite unit is an olivine greater than pyroxene porphyritic basalt breccia. All exposures of picritic basalt display brecciated textures, and at most localities are either bordered by clastic rock types that contain clasts of picritic basalt or can be traced laterally into facies that interdigitate with tuffaceous sediment derived from either a picritic or feldspathic volcanic source. At two localities, picritic clasts occur within argillaceous strata. Picrite may occur as isolated units within augite porphyritic volcanic strata, but can be traced as a stratigraphic unit across the study area. We were unable to conclusively demonstrate that the picrite is intrusive at any locality; however, intrusive feeders to the picritic basalts are expected. The picritic basalt is intruded by acicular hornblende-phyric monzodiorite (Fig. 6) and is a locally important constituent of the hybrid unit.

The Sugarloaf phase becomes hybridized with increasing contamination by picritic basalt and other Nicola units. This relationship is well displayed in the Ajax West pit, at Edith Lake and the Goose Lake road (Fig. 2). At Edith Lake, the picritic basalt breccia is hornfelsed by the Sugarloaf phase (which is locally chilled against the picrite), and dykes of Sugarloaf within the picrite decrease in abundance away from the contact, while xenoliths of picrite occur within the Sugarloaf where it becomes hybridized.

The Hybrid rocks possess a consistent east-trending magmatic foliation that suggests a regional 200 Ma tectonic control during emplacement: the pegmatitic mineral growth direction is perpendicular to the regional foliation, in the direction of dilatancy (Fig. 10). Magmatic foliation in Cherry Creek monzonites at the Crescent deposit and mineral lineations in Sugarloaf dikes at the Ajax deposits are more northerly (010°–345°).

Northcote (1974, 1976) and Preto (personal communication, 2004) recognized intrusive rock fragments of Cherry Creek plagioclase porphyries within lahar and volcanic breccia units of the Nicola Group and concluded a close association in time between volcanism and intrusion. The polyolithic Nicola tuff, located north of the Afton tailings pond, contains pink monzonitic lapilli of Cherry Creek affinity. This tuff is weakly mineralized and overprinted by the disseminated pyrite halo associated with mineralization at the Afton deposit. These relationships suggest that Cherry Creek magma was erupted and deposited as pyroclastic units before the alteration-mineralization event at Afton was complete. The fine-grained, holocrystalline Cherry Creek porphyries suggest near-surface conditions of emplacement and the andesite and latite breccias and flows that characterize the northern margin of the batholith probably represent extrusive equivalent rocks to the microdiorite and micromonzonite. Cherry Creek intrusive and diatreme breccias crosscut the northern margin of the

batholith. Diatreme breccias within the Crescent pit contain a wide variety of angular to rounded clasts of syenite (potassium-metasomatized monzonite?), amphibolite, pyroxene porphyry, coarse magnetite and chalcopyrite mineralization. They postdate mineralization. Although we cannot prove conclusively that these vented to the surface, the presence of mineralized clasts within the lahar unit suggests that this may have been the case.

STRUCTURE

The structural setting of the Iron Mask intrusive complex is dominated by north to northwest-trending high and moderate-angle faults. Previous authors have considered these to be major deep-seated structures that were active as early as the mid-Triassic (Campbell and Tipper, 1970; Preto, 1977). As such, they were thought to have controlled deposition of the volcanic and sedimentary rocks of the Nicola Group (Preto, 1977) as well as the intrusion of various phases of the Iron Mask batholith.



Figure 10. East-west magmatic foliation in Iron Mask Hybrid phase, note, the pegmatitic mineral growth direction (hornblende) is perpendicular to the regional foliation, in the direction of dilatancy.

Schistosity

For the most part, rocks in the study area are not penetratively deformed. Exceptions occur 2 km south of Jacko Lake, where Nicola volcanic rocks display an abrupt change from nonfoliated to strongly schistose rocks over a strike-normal distance of ~100 m. Two schistosity are developed. A primary, pervasive (S1) schistosity envelops pyroxene and feldspar porphyroclasts and flattened pyroclasts. It generally displays relatively steep northeast dips, suggesting a strain field orientation like that which produced the folds at Jacko Lake. Typical biaxial strain is about 4:1. This same fabric can be traced at least 12 km to the northwest to near the Afton tailings pond. The S1 schistosity is locally folded by southeast-verging chevron folds, with development of a second axial-planar crenulation cleavage (S2) that dips moderately northwest (Fig. 11).

Schistose rocks also occur locally within the batholith, at the Ajax East and West pits, and it is reported in drillcore from the Galaxy (Preto, 1967). Schistosity is well developed within carbonate porphyroblastic augite tuff and sericitic metasediment near the south rim of the Ajax West pit. There, Sugarloaf dike rocks are also foliated, but less intensely.

Folds

Previous authors have noted three zones of recurring near-vertical faulting: along the northeast and southwest margins of the batholith, and an arcuate zone just east of the batholith axis (best developed between the Evening Star and Iron Mask occurrences; e.g., Carr, 1957). These 'active zones' were thought to be the main locus of intrusion, beginning with the main Iron Mask phase (Pothook and Hybrid units), followed by picrite intrusions, and lastly the finer grained intrusions. However, if a volcanostratigraphic origin for the picrite is correct, the Makaoo–Larsen–Iron Mask picrite bodies could be parts of the same picrite horizon, now folded into a kilometre-scale synform. In this interpretation, the sheared limbs of the fold form the arcuate and northeastern zones of faulting. Picrite at the western



Figure 11. Folded schistosity Cherry Creek Fault zone.

contact of the batholith can likewise be interpreted as a volcanostratigraphic horizon, as noted for the section at Jacko Lake. In all cases, sheared mafic volcanic rocks occur with or near the picrite, further supporting a stratigraphic linkage. Orientations of mineralized veins between the Iron Mask and Larsen are consistent with dilational veins in a fold closure (Fig. 12) and, if related to the fold, suggest that folding and mineralization were synchronous. Subsequent strain has tended to concentrate in the relatively ductile, serpentinized picrite. This fold may have been decapitated by low-angle faults translating coarse, deep-level hybrid rocks in the fold core over microdiorite and hypabyssal or extrusive Cherry Creek phase (cf. 'Low-Angle Faults' section).

On the ridge east of Jacko Lake (Fig. 2), a crude stratigraphy (pyroxene porphyritic breccias, crystal-rich tuffite and thin-laminated siltstone) can be traced in a discontinu-

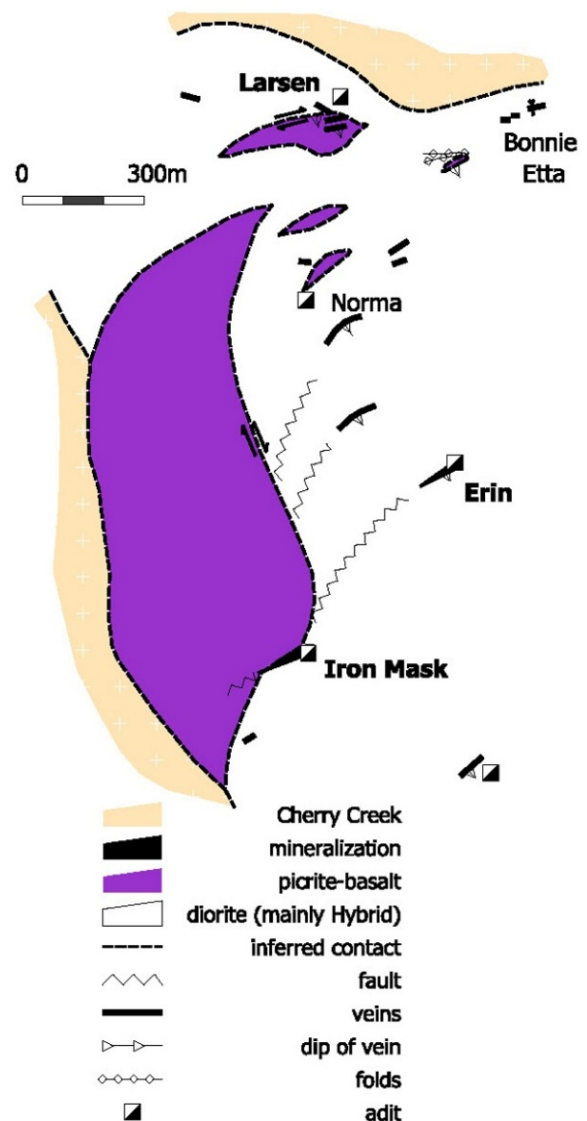


Figure 12. Dilational vein orientations, adapted from Figure 6 of Carr (1956): "Hypothetical structural interpretation in the area of the Iron Mask mine".

ous fashion through a fold closure. Confirmation of the fold is shown by reversal of facing direction in bedding.

On the south side of the Ajax West pit decline, foliated, carbonate-altered pyroxene porphyry is intruded by a 1.2 m thick Sugarloaf dike. Both foliation and dike are warped by a gentle upright fold. Foliation and the fold-axial plane average $120^{\circ}/60^{\circ}\text{S}$; mineral elongation lineation developed around magnetite porphyroblasts in the adjacent picrite trends $10^{\circ}/115^{\circ}\text{E}$.

Low-Angle Faults

Low-angle fault zones are sporadically observed in the batholith. Good examples are exposed in the Pothook and Ajax West pits. However, the best documented evidence is from Preto (1967) at the Galaxy deposit. At least 20 drill-holes intersect a moderate to shallowly west-dipping mylonite zone that separates Nicola volcanic rocks, picrite and hybrid phase from fine-grained ‘albitized microdiorite’, considered to be part of the Cherry Creek intrusive suite. According to Preto (1967), copper mineralization is focused both within the hangingwall volcanic rocks and in the mylonite zone. Structural juxtaposition of the mineralized and nonmineralized rocks, as well as development of copper mineralization within the mylonite zone, suggest that deformation and mineralization were at least partly synchronous (Fig. 13). Kinematic analysis of the mylonite zone is lacking, and a compressional versus extensional origin cannot be determined from the available information. In both the Ajax and Pothook pits, low-angle faults also exert some control on mineralization.

In the Ajax West pit, a low to moderately west-dipping fault (average orientation $166^{\circ}/42^{\circ}\text{W}$) juxtaposes albitized gabbroic rocks with diorite. Epidote and chalcopyrite-calcite veins parallel the fault. Some fault-parallel veins display fist-sized knots of chalcopyrite. Subsidiary, parallel faults in the hangingwall cut and offset a series of epidote-calcite veins. Apparent sense of offset on the subsidiary faults is consistent with gash veins ($055^{\circ}/68^{\circ}\text{S}$; Fig. 14, inset), indicating top-to-the-southeast sense of motion. Late open-space veins with vein-perpendicular quartz fibres and intergrown chalcopyrite also indicate extension in a north-east direction. Similar top-to-the-east apparent offset is displayed in the south wall of the Ajax West pit across a subhorizontal fault trace that truncates a north-trending dike of Sugarloaf hornblende porphyry (Fig. 6).

At the southwest margin of the Ajax East pit, a strong phyllitic fabric is cut by Sugarloaf intrusive upon which a less intense tectonic foliation has been imparted. A mineral elongation fabric developed within the foliation has undulating northeast and southwest plunges, averaging $004^{\circ}/43^{\circ}\text{E}$ on foliation planes that average $220^{\circ}/44^{\circ}\text{W}$. Sense of rotation on foliation-parallel brittle shear zones indicates a top-to-the-northeast sense of motion, parallel with the mineral elongation direction. Millimetre-thick intra-folial chalcopyrite-quartz (or albite?) veinlets are oriented perpendicular to the extension direction. All fabrics are cut by a 3 m thick microdiorite dike ($250^{\circ}/80^{\circ}\text{N}$) that contains

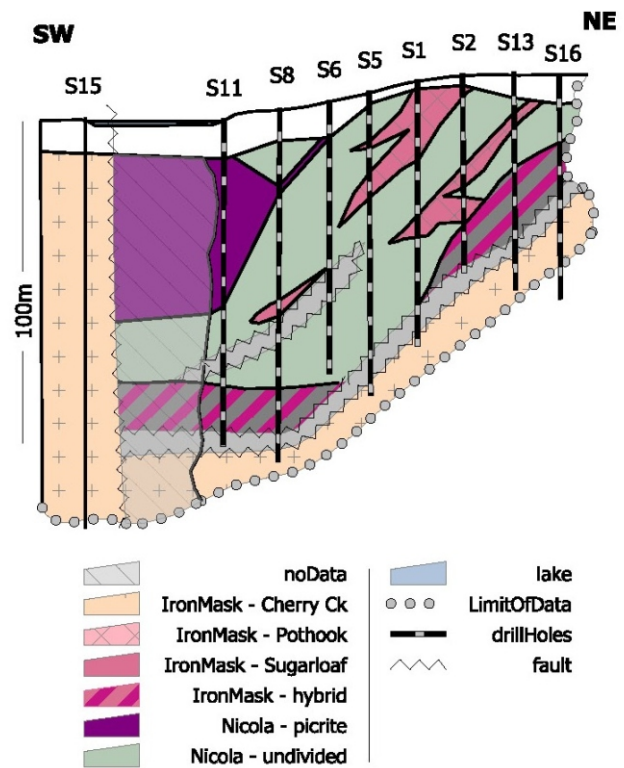


Figure 13. Section 1100 N from Galaxy Copper Ltd. plan showing surface cuts and diamond-drill holes (Preto, 1967, Fig. 14).

xenoliths of feldspar porphyry and medium-grained granite.

Cursory examination of the Pothook pit also reveals low-angle brittle shear zones. Near the base of the southern pit wall, banded shear veins dip shallowly to moderately southeast (Fig. 15; looking toward 200°). These 20 cm thick veins comprise brecciated quartz cemented by chalcopyrite (up to 60%) and pyrite. They bound panels that are cut by extensional vein sets dipping moderately southwest, indicating a top-to-the-southwest sense of motion across the



Figure 14. Low angle west dipping fault, juxtaposes albitized gabbroic rocks with diorite. Inset shows offset epidote-calcite veins with apparent tops to the southeast sense of motion.

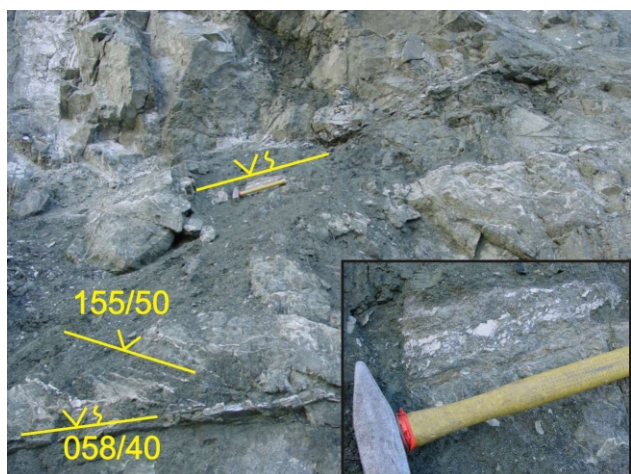


Figure 15. Banded, shear veins dipping moderately southeast and mineralized with quartz-chalcopyrite-pyrite, Pothook pit.

zone. A chaotic assemblage of rock types within this structural zone, including picrite breccia, lamprophyre, fresh hornblende porphyry and K-feldspar-epidote-flooded rock. This diversity of rock types suggests that motion on the zone could be substantial.

To what degree the low-angle shear zones contribute to economic mineralization within the Iron Mask batholith is unknown. It is, however, clear that such faults can be the loci of enhanced copper mineralization (e.g., Galaxy, Pothook), commonly with addition of quartz. Our preliminary observations indicate both top-to-the east and top-to-the-southwest sense of motion. If offset on such zones is substantial, they may decapitate vertically developed zones of porphyry mineralization, translating them to deeper or shallower crustal levels.

MINERALIZATION AND ALTERATION

At least 10 copper-gold deposits are hosted by the Late Triassic polyphase Iron Mask batholith (Fig. 2). Five of the deposits are past producers: Afton, Ajax East, Ajax West, Crescent and Pothook. The Big Onion, DM, Python-

Makao and Rainbow have published reserves but no production (Lang and Stanley, 1995). Mineralization consists primarily of fracture-controlled chalcopyrite and bornite associated with magnetite, while pyrite or pyrrhotite occur peripherally. Mineralization is hosted in all of the different phases of the batholith (Table 1). To date, no significant mineralization has been delineated outside the batholith in the Nicola volcanic rocks (although Nicola strata do host much of the mineralization at Copper Mountain, 140 km to the south). Lang *et al.* (1994) showed that distinct alteration assemblages affected different intrusive phases. Magnetite-apatite±actinolite are dominant alteration minerals in the Pothook and hybrid units; potassic alteration affects the Cherry Creek monzonite; and sodic alteration affects the Sugarloaf diorite (Fig. 16). In each case, alteration accompanies mineralization, but not all altered zones are mineralized. Mineral occurrences visited during the course of this study are grouped according to their host/causative intrusive phase and described below.

Pothook and Hybrid Phases

MAGNET MINE (MINFILE 0921/022)

The Magnet showing is located east of the Afton pit (Fig. 2). It consists of a zone of northwest-trending, steeply dipping veins of massive magnetite containing euhedral white crystals of apatite and green amphibole. The apatite is coarsely crystalline (up to 3 cm) and has grown perpendicular to the vein walls into the centre of the veins. The magnetite displays fine-grained exsolution of ilmenite (Cann, 1979). Magnetite veins trend 120–140°, and dip vertically and locally show well-developed dilatant zone splays filled with magnetite. The geometry indicates sinistral shear at the time of magnetite deposition (Fig. 17). The shear veins are crosscut and offset by specular hematite±chlorite veins with K-feldspar alteration envelopes, and crosscut but not offset by a younger set of pyrite-epidote-calcite and calcite veins.

PYTHON (MINFILE 0921/002)

The Python property straddles the northeastern margin of the Iron Mask batholith, about 7 km east of the Afton de-

TABLE 1. MINERALIZATION HOSTED IN PHASES OF BATHOLITH

Intrusive Host	Deposit	MTonnes	Cu%	Au ppm	Source
Sugarloaf-Hybrid Contact zone	Ajax (mineable+prod)	20.7	0.45	0.34	Ross et al. (1995)
	Pothook (prod)	2.36	0.35	0.77	Lang and Stanley (1995)
	Rainbow (indicated)	0.015	0.52		GCNL, 1997; BC MINFILE
Cherry Creek	Afton (mineable+prod)	30.8	1	0.58	Kwong (1987)
	Afton (meas+Indicated)	68.7	1.08	0.85	DRC Res. (2004)
Pothook-Cherry Creek Contact Zone	Crescent (prod)	1.448	0.44	0.18	Lang and Stanley (1995)
	DM/Audra (geologic)	2.68	0.38	0.27	Lang and Stanley (1995)
	Big Onion (mineable)	2.4	0.84	0.4	Vollo (1985)
Pothook/Hybrid	Magnet Mine (prod)	0.005	magnetite		1960-1961, BC MINFILE
Nicola-Hybrid Contact Zone	Python/Makao (indicated)	0.19	1.11	-	Seraphim, 1972; MINFILE
Nicola Group	Galaxy (indicated)	0.003	0.65	0.34	BC MINFILE



Figure 16. Hydrothermal alteration assemblages: **a)** magnetite-actinolite-apatite dilated veins, Afton; **b)** K-feldspar alteration of Pothook diorite, Audra area; **c)** pervasive zone of white albite alteration in metavolcanic Nicola rocks, north of Jacko Lake.

posit (Fig. 2). Three mineralized zones are known to occur on the property: the Python, Copper Head and Noonday. These are localized along the northwest-trending sheared contact between serpentinized picrite of the Nicola Group and coarse-grained diorite agmatite of the Iron Mask hybrid unit. Alteration assemblages consist of epidote-actinolite-magnetite-calcite±chalcopyrite with pink K-feldspar alteration envelopes that replace the matrix to the breccia and fill fractures and veins that vary in width from 1–20 cm. Copper minerals include chalcopyrite and lesser malachite and azurite. Alteration and mineralization are primarily focused in the shear zone and hangingwall hybrid intrusive unit.

The Python showing is hosted in a breccia pipe that cuts the northern margin of the Iron Mask batholith. The breccia has ill-defined margins and grades into less altered diorite. It is reported to be elongate east-west, and thought to form a steeply dipping tabular pipe (MINFILE). Chalcopyrite and magnetite occur as disseminated blebs, stringers and thick lenses, intergrown with epidote, albite, calcite and K-feldspar. The faults and mineralized fractures trend 145°. These are cut by K-feldspar-epidote±chalcopyrite veins that contain hematite (specular) and lesser magnetite. The veins trend 075° with little or no offset. Mineralization displays the same sinistral shear/dilated relationships that were observed at the Magnet mine.

Cherry Creek Phase

AFTON (MINFILE 0921/023)

The Afton deposit is the largest of the porphyry deposits located in the Iron Mask batholith (Fig. 2). It is situated at the intersection of an easterly-trending corridor of potassic alteration, brittle shearing, hydrothermal breccias

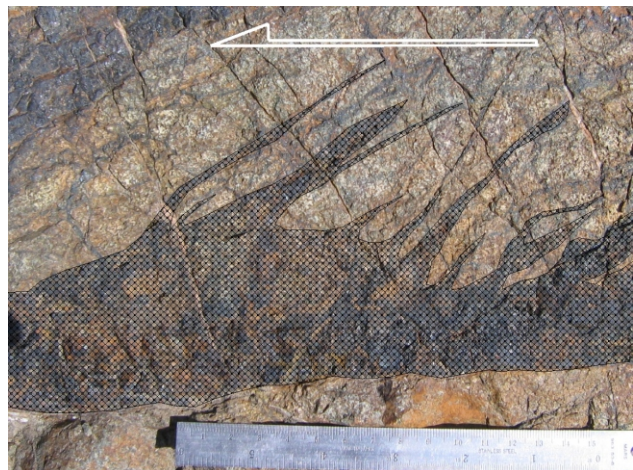


Figure 17. Magnetite-apatite±actinolite vein at the Magnet mine, viewed toward southwest. Vein trends 140°/90°W; dilatent vein splays indicate a sinistral shear sense.

and copper mineralization, which extends for more than 5 km and includes the DM, Audra, and Big Onion mineral occurrences, with a northwesterly-trending corridor of albite alteration, brittle shearing and copper-mineralized hydrothermal breccias that includes the Pothook, Rainbow, Ajax East and Ajax West mineral occurrences. It is located 10 km west of Kamloops and produced 23.0 million tonnes of ore with an average grade of 0.85% Cu and 0.52 g/t Au between 1977 and 1987 (BC Ministry of Energy and Mines, MINFILE). Start-up reserves were 30.8 million tonnes of ore grading 1.0% Cu, 0.58 g/t Au and 4.19 g/t Ag at 0.25% Cu cutoff grade (Kwong, 1987).

The Afton orebody is a west-striking (290°) tabular body that plunges 30–50° to the south. Alteration at the Afton deposit was divided by Kwong (1987) into a potassic alteration assemblage comprising K-feldspar, epidote, magnetite and hematite in the northeastern part and an assemblage dominated by ankeritic alteration and/or amphibole and pyrite in the southwestern part of the pit. A pyritic (up to 10%) propylitic alteration zone surrounds the orebody and occupies much of the hangingwall Nicola Group volcanic rocks to the deposit. The eastern portion of the deposit is superposed by a southeast-trending magnetite-apatite-hematite alteration zone (800 by 300 m) that extends to the Magnet mine. This iron oxide zone is flanked on either side by a pyrite-enriched propylitic alteration zone with epidote, chlorite and calcite. A narrow zone of quartz-sericite (phyllitic) alteration was recognized by Preto (1972). It is situated peripheral to the main orebody and grades outwards into the propylitic zone. In addition, albite, sericite, kaolin, montmorillonite, talc, pyrophyllite, titanite, zoisite and less commonly prehnite, zeolite, quartz, barite, dolomite, ankerite gypsum and chalcedony have been identified (Hoiles, 1978). Plagioclase is replaced by epidote and a fine-grained mixture of sericite, carbonate and chlorite, while ferromagnesian minerals are replaced by chlorite, calcite, epidote and pyrite. Vein calcite deposition appears to have accompanied several stages of alteration and mineralization, but most prominently occurs as late, crosscutting features.

Easterly and northeasterly-trending faults are thought to have controlled the emplacement of the Afton intrusion (Preto, 1972; Northcote, 1974). Steep to vertical magnetite veins in the Afton pit trend mainly 110° but also 310° and 170°. The easterly-trending, steep southerly dipping magnetite veins are thought to predate and accompany copper mineralization and may be part of the same event that results in dilational veins at the Magnet mine.

Hypogene mineralization consists of bornite, chalcopyrite, lesser chalcocite, tetrahedrite and tennantite, and traces of molybdenite. Supergene alteration extends to depths of up to 400 m and consists of native copper and chalcocite, with minor amounts of cuprite, malachite and azurite (Hoiles, 1978; Kwong, 1987; Nixon, 2003).

CRESCENT (MINFILE 0921/026)

The Crescent deposit is located along the northern margin of the Iron Mask batholith, within an easterly-trending corridor of potassic alteration, brittle shearing, hy-

drothermal breccias and copper mineralization that extends for over 5 km and includes the Afton, DM, Audra, and Big Onion mineral occurrences. It is located 3 km east of the Afton pit (Fig. 2) and produced 1.36 million tonnes of ore with an average grade of 0.46% Cu and 0.2 g/t Au during production between 1989 and 1990.

Crescent pit geology was mapped by Lang *et al.* (1994). The pit straddles the northeast-trending contact between Pothook diorite (on the south) and Cherry Creek porphyritic monzodiorite (on the north). North-trending, metre-scale, intermediate and plagioclase porphyritic dikes cut the Cherry Creek monzodiorite in the pit and in outcrop exposures on Highway 1. Unaltered, Pothook diorite is typically a green-grey, medium-grained, equigranular pyroxene diorite that contains large poikilitic biotite crystals, abundant magnetite and apatite. Most of the Pothook diorite in the vicinity of the Crescent deposit has been overprinted by potassium metasomatism, which increases in intensity as the contact is approached. The Cherry Creek rocks are fine-grained plagioclase porphyritic monzodiorite with trachytic to magmatic foliated fabrics (010–015°) that are pervasively potassium metasomatized near the contact.

The deposit is a tabular zone that trends 050° and dips 60° southeast. It is centred on an intrusion breccia that developed at the contact between the Pothook and Cherry Creek phases. The zone is characterized by the pervasive potassium metasomatism, intrusive breccias, hydrothermal stockwork veining and phreatomagmatic breccias. The breccias are heterolithic with clast compositions dominated by Pothook diorite, pyroxene porphyritic Nicola Group metavolcanic rocks, and magnetite. Mineralization occupies the matrix to the clasts. Younger, phreatomagmatic breccias are characterized by the addition of rounded mineralized clasts in addition to a wide variety of the volcanic and intrusive rock types of the area.

Three major east-trending faults, as well as several sets of prominent spaced fractures, are exposed in the pit walls. Lang (1994) measured three dominant fracture orientations, 350°, 060° and 120°, all with dips greater than 60°. Vein fillings comprise calcite-chlorite-quartz±pyrite±epidote±chalcopyrite assemblages, invariably with K-feldspar alteration envelopes. The North and Central faults trend east and dip north; the South fault trends 070° (*see* Lang, 1994, Fig. 2). They are 1–5 m wide brittle features, characterized by gouge and shattered rock, that contain white calcite, chlorite and minor quartz-calcite±pyrite veins.

Chalcopyrite is the dominant ore mineral; bornite and molybdenum are present in trace amounts. Chalcopyrite occurs as blebs and fine disseminations in fractures, veins and filling the matrix to the breccias. Constant copper-gold ratios suggest that gold and copper were deposited together in a single hydrothermal event (Lang, 1994).

Sugarloaf Phase

AJAX (MINFILE 0921/012 AND 013)

The Ajax West and Ajax East deposits are located on the southwest side of the Iron Mask batholith, approximately 12 km southwest of Kamloops (Figure 2) and produced 7.9 million tonnes of ore with an average grade of 0.37% Cu and 0.27 g/t Au during production between 1989 and August of 1991. The pits were mapped by Ross *et al.* (1992, 1993 and 1995).

The deposits are localized at the contact between medium to coarse-grained Iron Mask hybrid diorite and Sugarloaf diorite. The contact trends easterly in the West pit and more northeasterly in the East pit. The main alteration stages include propylitic, albitic and potassic assemblages, with scapolite veins developed only locally in the Ajax East (Ross *et al.*, 1995). Alteration in the West deposit consists of a core of pervasive albite alteration that passes outwards to less pervasive albite alteration and into a peripheral zone of propylitic alteration characterized by chlorite, epidote, calcite±pyrite. The ore zones are spatially distributed along the contact between the intermediate albite alteration and the propylitic zone (Ross *et al.*, 1995, Fig. 9). Areas of intense albitization, carbonatization and brecciation mark the location of breccia pipes, and the centre of the hydrothermal system. The alteration-mineralization system in the East pit is essentially identical, but hosted primarily within the Sugarloaf diorite.

Chalcopyrite is the predominant copper mineral in both West and East deposits. It occurs as disseminations and blebs in fracture fillings and breccias associated with calcite. Pyrite is equally abundant and occurs in concentrations up to 2%, together with chalcopyrite or alone in the propylitic zone. Magnetite occurs as disseminations associated with potassic alteration. Low values of molybdenum are reportedly widespread throughout.

An en echelon set of salmon pink K-feldspar veins cuts Iron Mask Hybrid rocks in the north wall of the West pit. The bounding surface veins (10–50 cm wide) trend 300°/62°N and the en echelon tension gash veins (5–10 cm wide) trend 160°/72°W, consistent with tops-to-the-southeast sense of motion. The vein assemblage from wall to core consists of magnetite intergrown with biotite±chlorite, and a vuggy intergrown aphyric matrix of K-feldspar and albite with calcite, chalcopyrite, pyrite and coarse euhedral crystals of titanite filling fractures and interconnected vugs (Fig. 18). The titanite was submitted for U-Pb age dating; results are pending.

POTHOOK (MINFILE 0921/023)

The Pothook deposit is located on the southwest edge of the Iron Mask batholith, approximately 10 km west of Kamloops (Fig. 2) and less than 1 km southeast of the Afton pit, which produced 2.60 million tonnes of ore with an average grade of 0.35% Cu and 0.21 g/t Au between 1986 and 1988 (L. Tsang, personal communication, 1993, in Stanley, 1994). The deposit is centred on an intrusion breccia that developed close to the southwestern margin of the batholith. Pyrite is dominant over chalcopyrite, and bornite



Figure 18. Vuggy intergrown matrix of K-feldspar and albite with calcite, chalcopyrite, pyrite and coarse euhedral crystals of sphene filling open spaces.

is present in trace amounts. Chalcopyrite occurs as disseminations and veinlets and filling matrix to breccias. Supergene minerals consist of chalcocite, native copper and remnant bornite and chalcopyrite. Copper-gold ratios show considerable variation and suggest that gold and copper have been deposited separately (Stanley, 1994).

The Pothook pit exposes the complex southwestern contact zone between the Iron Mask batholith and mafic volcanic rocks of the Nicola Group. The geology of the pit was mapped by Stanley (1994). He documented three episodes of steep faulting that followed the intrusion and cooling of successively younger phases of the batholith (i.e., post-Pothook, post-Cherry Creek and post-Sugarloaf). The faults are oriented north-northwest and east-northeast, and have disrupted the northwest-trending contact and have interleaved the Pothook diorite with picrite, pyroxene porphyritic flows and volcaniclastic units of the Nicola Group. Cherry Creek monzonite intruded and caused potassic alteration of the Pothook diorite exposed in the north wall of the pit. Intrusion of fine-grained hornblende porphyritic dikes of Sugarloaf diorite was focused near the batholith contact, primarily in volcanic rocks and locally in the Pothook diorite but not in the Cherry Creek monzonite. Pervasive albite alteration is developed on the east wall of the pit in Pothook diorite and less pervasive alteration affects dikes of Sugarloaf diorite. A younger fracture-con-

trolled potassic alteration overprints the albite alteration (Stanley, 1994). Veins of K-feldspar-biotite-epidote dip steeply and strike north-northwest. These veins contain pyrite, copper (chalcopyrite, bornite) and gold, but they are not the major source of economic mineralization.

The main copper-gold mineralizing event was associated with iron-oxide and iron-sulphide vein deposition. "On the southwest side of the open-pit, these veins are characterized by a chlorite-pyrite-chalcopyrite-magnetite-(specular) hematite mineral assemblage, whereas on the northeast side they contain chalcopyrite, bornite and magnetite.... They have a preferred orientation approximately perpendicular to the orientation of the potassium feldspar-epidote veins, ranging from west-southwest to northwest with dips generally greater than 45°." (Stanley, 1994, page 280). A heterolithic, hydrothermal breccia comprising clasts of Nicola volcanic rocks and all phases of the batholith was intersected in drilling below the centre of the pit. The breccia contains subordinate magnetite, chalcopyrite and bornite mineralization, and is interpreted to be a deeper manifestation and hydrothermal link to the vein mineralization (Stanley, 1994). Evolution or collapse of this system produced the propylitic overprint of chlorite±pyrite veining that pervades all but the albitite rocks in the open pit. White calcite veins crosscut the chlorite veins. The youngest events are low-angle southwest-dipping faults, mafic dike emplacement and late chalcidonic quartz veins that reflect the Eocene extension that affected the area (Souther, 1992; Stanley, 1994; this study).

RAINBOW (MINFILE 0921/028)

The Rainbow deposit is located on the southwest margin of the Iron Mask batholith, approximately 7 km southwest of Kamloops (Fig. 2). It is located on the eastern slopes of Sugarloaf Hill, less than 4 km southeast of the Afton pit. The property has been mapped and drill tested (Oliver, 1995), and is one focus of active exploration by Abacus Mining and Exploration Corp. Drill-indicated resources on the combined #2 and #22 zones is 15 860 tonnes of ore with an average grade of 0.528% Cu (BC Ministry of Energy and Mines, MINFILE). Subsequent drilling (2002 and 2004) indicated that the #2 and #22 zones form a north-west-trending zone of steeply dipping copper-gold mineralization, 700 m long and up to 500 m deep, that is open along strike and at depth. A new drill-indicated resource is currently being calculated.

The area of interest straddles the northwestern contact zone of the batholith. The contact is a complex northwest-trending fault zone, referred to as the Leemac Fault, which separates the main batholith, comprising the Pothook and Hybrid phases, from picrite, metavolcanic and metavolcaniclastic rocks of the Nicola Group. The fault is a brittle shear zone up to 300 m wide that parallels the intrusive-volcanic contact. Directly southwest of the fault is a northwesterly-elongated intrusion of Sugarloaf diorite that intrudes the Nicola country rock and underlies most of Sugarloaf Hill. Oliver (1995) has shown Sugarloaf Hill to comprise three contemporaneous but mappable stocks of hornblende diorite, albite-pyritic monzodiorite and

microphyric hornblende diorite. Northeast-trending apophyses of porphyritic hornblende diorite crosscut the main Leemac Fault structure, intrude older phases of the batholith (Pothook and Hybrid), and host copper-gold mineralization. Younger (?) northeast-trending faults crosscut hornblende diorite on Sugarloaf Hill.

Mineralization on the Rainbow property is focused close to the Leemac Fault. The #1 and #17 zones are hosted in Sugarloaf hornblende porphyry; the #2 and #22 zones in Pothook/Sugarloaf hybrid and metavolcanic rocks, respectively. All mineralization is fracture or breccia controlled and consists of chalcopyrite±magnetite accompanied by pyrite and alteration mineralogy. Crosscutting veins in drillcore give the following paragenesis: 1) pale creamy green to white albite zones, accompanied by narrow K-feldspar envelopes and commonly mantled by epidote; 2) the first set of veins, fractured and cut by flat zones of massive pyrite replacement ± chalcopyrite; 3) final veining, comprising tight 1–3 mm, white, crustiform calcite veinlets with brown iron-carbonate selvages and narrow black chlorite envelopes. Selective zones of early andradite alteration of Sugarloaf rocks occurs along the Leemac Fault and in the #17 zone (Oliver, 1995). The fault zone is characterized by carbonate, silica and less often sulphide-healed breccias and open-space fillings.

Several types of mineralization that are under-documented for the Iron Mask camp are present on the Rainbow property. These include a single occurrence of visible gold (DDH R-04-44) and massive pyrite replacements containing elevated cobalt values (0.21% cobalt over 37.80 m; DDH R-04-023). The gold grain (0.5 by 2.0 mm) occupies a narrow white calcite veinlet cutting albitized Sugarloaf diorite in the #2 zone. The cobalt enrichment was intersected in drilling on the #1 zone in an interval of massive pyrite replacement of Sugarloaf diorite.

COQUIHALLA EAST (MINFILE 0921/120)

The Coquihalla East zone is gold-rich, copper-poor mineralization that was first recognized by TeckCominco in the 1990s. It comprises two northwest-trending zones that are located immediately southwest of the Pothook pit (Fig. 2) in the structurally complicated contact zone between the Pothook/Cherry Creek phases of the batholith and Nicola country rocks, where a number of Sugarloaf diorite dikes intrude the package. Alteration styles include pervasive and patchy albite, fracture-controlled potassium±epidote, and pyrite-chlorite-calcite propylitic overprint. The Coquihalla east zone lies within the broader propylitic alteration zone that encompasses the Afton alteration-mineralization system. The relationship between the Coquihalla East, and the Afton or the Pothook mineralizing systems remains to be established. It may be a younger event that locally overprints earlier mineralization. The poor correlation between Cu: Au ratios in the Pothook may reflect an overprint from a gold-only copper-poor mineralization.

DISCUSSION

Mineralized intrusions display high-level textures/features, such as aphanitic to microporphyritic textures, magmatic flow banding, miarolitic cavities and numerous open spaces filled with alteration (sphene, calcite, K-feldspar) and hypogene (chalcopyrite, magnetite, chalcocite, pyrite) minerals.

The Iron Mask batholith is characterized by three distinct hydrothermal events that accompanied the intrusion and fractionation of its three main phases, the Pothook, Cherry Creek and Sugarloaf. Within the Pothook diorite, hydrothermal magnetite-apatite-actinolite-epidote veins are common and form large dilatent veins at Afton, the Magnet mine and the Rainbow property (Figure 16a). No significant amount of copper or gold was introduced with this early hydrothermal event. Potassic metasomatism has a close spatial association with Cherry Creek monzonite and those deposits it hosts (Afton, Crescent, DM and Big Onion), suggesting that the potassic fluids originated as a deuteric product during cooling of the Cherry Creek monzonite (Stanley *et al.*, 1994). Potassic alteration weathers a characteristic pink to orange colour due to the finely disseminated hematite that accompanied introduction of secondary K-feldspar and biotite±magnetite that makes up this assemblage (Figure 16b). Disseminated copper sulphides accompanied potassic alteration in the Crescent, DM and Afton deposits, but similar sulphide-barren zones are present along the margins of the Cherry Creek phase throughout the northern margins of the batholith (Lang *et al.*, 1995). Sodium alteration is spatially associated with and genetically related to the youngest, Sugarloaf diorite phase. Alteration is characterized by features ranging from individual albite fractures to wide zones of pervasive white albitic alteration (Figure 16c), specifically at the Pothook, Ajax West and East deposits. Copper and gold mineralization is fracture hosted in zones of intermediate albitic alteration, located peripheral to the hydrothermal centre, which is characterized by pervasive albitic alteration and weak mineralization (Ajax West and East; Ross *et al.*, 1995).

Due to the spatial distribution of Cherry Creek monzonite along the northern margin of the batholith and the Sugarloaf diorite along the southern margin, Na-rich and K-rich alterations are rarely present together. A caveat to this generalization occurs at the Pothook deposit, where both alteration assemblages are present and define the following paragenesis: a pervasive potassic metasomatism related to the Cherry Creek phase; pervasive albitic alteration zones related to Sugarloaf dike emplacement; and late crosscutting K-feldspar-biotite-epidote veins and later mineralization related to an Fe-oxide–Cu-sulphide stage of veining associated (?) with chlorite (Stanley, 1994). Late-stage banded shear veins of quartz-chalcopyrite and pyrite related to low-angle shear zones are the youngest episode of mineralization. The relationships in the Pothook pit suggest that the bulk of copper-gold mineralization postdates albitic alteration and Sugarloaf diorite. Mineralization at Afton is related to potassic alteration; at Crescent and DM/Audra, fracture-controlled mineralization closely follows an early pervasive barren potassic event; and, at Ajax,

mineralization is directly associated with albitization related to Sugarloaf diorite. Copper-gold mineralization apparently is not restricted to one or even two hydrothermal events.

The temporal relations between various mineralized and unmineralized structures also infers that mineralization continued over a protracted period of time. Mineralized vein arrays at the Magnet and Python mines indicate a northwesterly-oriented sinistral shear sense at the time of mineralization. East-trending dilatent structures or 'alteration and mineralization corridors' host intrusive breccias (Crescent) and preferred vein sets (DM/Audra). Potassium-metasomatized Cherry Creek rocks in the west wall of the Crescent pit display a well-developed, north-trending vertical magmatic foliation, defined by hornblende and plagioclase phenocrysts and xenoliths.

Restoration of alteration asymmetries in the footwall and hangingwall contacts to the #17 mineralized zone on the Rainbow property suggests that the Leemac fault may have 350 m of dextral movement, interpreted by Oliver (1995) to be synchronous with mineralization.

CONCLUSIONS

Magmatic, stratigraphic and tectonic features of the Iron Mask area support the following conclusions. Intrusion of the main phases of the batholith occurred over a short time span in the Late Triassic (204 ± 3 Ma), probably in a shallow or subvolcanic environment with rapid vertical and horizontal facies transitions from mineralized intrusion breccias to monolithic layered volcanic breccias to lahar deposits that contain mineralized clasts. An apparent regionally consistent magmatic foliation in the Hybrid phase, trending $\sim 280^\circ$, indicates a Late Triassic tectonic control. Chemically distinctive hydrothermal systems accompanied each intrusive phase of the batholith. Copper and gold mineralization are associated with at least two of these: the potassic alteration associated with the Cherry Creek monzonite, and the sodic alteration associated with the Sugarloaf diorite. Alteration and mineralization are localized along intrusive contacts between the older Pothook/Hybrid phases and the younger feldspar and hornblende-phyric phases. Mineralized vein arrays at the Magnet and Python mines indicate a northwesterly-oriented sinistral shear sense at the time of mineralization. East-trending dilatent zones may have accommodated the ore zones at the Afton deposit, the intrusive breccias and veins at Crescent, and the preferred vein sets noted on the DM/Audra zones. Structures in the batholith and Nicola Group along the southwest margin of the batholith post-date the bulk of copper-gold mineralization and show consistent southwest-trending ductile mineral lineations.

ACKNOWLEDGMENTS

The Iron Mask component of the Cu-Au Porphyry Project was conceived through discussions between Doug Fulcher of Abacus Mining and Exploration Corp. and the British Columbia Ministry of Energy and Mines. It was

jointly funded and supplemented by funding from a BC & Yukon Chamber of Mines *Rocks to Riches* grant. Bob Darney is thanked for sharing his in-depth knowledge of the exploration history of the area, the location of most mineral showings and his kind logistical support. Discussions in the field with the three Bobs, Robert Darney, Robert Friesen and Robert Falls, were helpful and much appreciated. Colin Russell shared his knowledge of the Rainbow deposit.

The raw geophysical data from the 1994 low-level airborne survey were acquired from the Geological Survey of Canada, Mineral Deposits and Applied Geophysics Subdivision, Ottawa. Carmel Lowe, GSC-Sidney Subdivision helped with acquisition and kindly spent time reprocessing and formatting the data into usable digital images.

Ongoing discussions with Vic Preto about the geology of the Iron Mask batholith and the regional characteristics of the Nicola Group are gratefully acknowledged. Mike Cathro, Regional Geologist, South-Central District introduced us to the local geology of the Kamloops area by way of a fieldtrip in May. Marek Mroczek escorted us into the Afton pit and described the deposit geology. Brian Grant is thanked for providing editorial comments and ensuring that this paper saw the light of day.

REFERENCES

- Campbell, R.B. and Tipper, H.W. (1970): Geology and mineral exploration potential of the Quesnel Trough, British Columbia; *Canadian Institute of Mining and Metallurgy Bulletin*, Volume 63, Number 699, pages 785–790.
- Cann, R.M. (1979): Geochemistry of magnetite and the genesis of magnetite-apatite lodes in the Iron Mask batholith, British Columbia; unpublished M.Sc. thesis, *University of British Columbia*, 196 pages.
- Carr, J.M. (1957): Copper deposits associated with the eastern part of the Iron Mask Batholith near Kamloops; *BC Minister of Mines*, Annual Report, 1956, pages 47–69.
- Carr, J.M. and Reed, A.J. (1976): Afton: a supergene copper deposit; in *Porphyry Deposits of the Canadian Cordillera*, Sutherland Brown, A., Editor, *Canadian Institute of Mining and Metallurgy*, Special Volume 15, pages 376–387.
- Cockfield, W.E. (1948): Geology and mineral deposits of Nicola map area, British Columbia; *Geological Survey of Canada*, Memoir 249, 164 pages.
- Ewing, T.E. (1981): Regional stratigraphy and structural setting of the Kamloops Group, south-central British Columbia; *Canadian Journal of Earth Sciences*, Volume 18, pages 1464–1477.
- Ferri, F. (1997): Nina Creek Group and Lay Range Assemblage, north-central British Columbia: remnants of Late Paleozoic oceanic and arc terranes; *Canadian Journal of Earth Sciences*, Volume 34, pages 854–874.
- Hoiles, H.H.K. (1978): Nature and genesis of the Afton copper deposit, Kamloops, British Columbia; unpublished M.Sc. thesis, *University of Alberta*, Edmonton, Alberta, 186 pages.
- Klepaki, D.W. and Wheeler, J.O. (1985): Stratigraphic and structural relations of the Milford, Kaslo and Slocan groups, Goat Range, Lardeau and Nelson map areas, British Columbia; in Report of Activities, Part A, *Geological Survey of Canada*, Paper 85-1A, pages 277–286.
- Kwong, Y.T.J. (1982): A new look at the Afton copper mine in the light of mineral distributions, host rock geochemistry and irreversible mineral-solution interactions; unpublished Ph.D. thesis, *University of British Columbia*, 121 pages.
- Kwong, Y.T.J. (1987): Evolution of the Iron Mask Batholith and its associated copper mineralization; *BC Ministry of Energy, Mines and Petroleum Resources*, Bulletin 77, 55 pages.
- Kwong, Y.T.J., Greenwood, H.J. and Brown, T.H. (1982): A thermodynamic approach to the understanding of the supergene alteration at the Afton copper mine, south-central British Columbia; *Canadian Journal of Earth Sciences*, Volume 19, pages 2378–2386.
- Lang, J.R. (1994): Geology of the Crescent alkalic Cu-Au porphyry deposit, Afton Mining Camp, British Columbia (92I/9), in *Geological Fieldwork 1993*, *BC Ministry of Energy, Mines and Petroleum Resources*, Paper 1994-1, pages 285–293.
- Lang, J.R. and Stanley, C.R. (1995): Contrasting styles of alkalic porphyry copper-gold deposits in the northern Iron Mask Batholith, Kamloops, British Columbia; in *Porphyry Deposits of the Northwestern Cordillera of North America*, T. G. Schroeter, Editor, *Canadian Institute of Mining, Metallurgy and Petroleum*, Special Volume 46, pages 581–592.
- Lang, J.R., Stanley, C.R. and Thompson, J.F.H. (1994): Porphyry copper deposits related to alkalic igneous rocks in the Triassic-Jurassic arc terranes of British Columbia; in *Bootprints Along the Cordillera*, Bolm, J.G. and Pierce, F. W., Editors, *Arizona Geological Society Digest*, Volume 20, pages 219–236.
- Lang, J.R., Lueck, B., Mortensen, J.K., Russell, J.K., Stanley, C.R. and Thompson, J.F.H. (1995): Triassic-Jurassic silica-undersaturated and silica-saturated intrusions in the Cordillera of British Columbia: implications for arc magmatism; *Geology*, Volume 23, pages 451–454.
- Mortensen, J.K., Ghosh, D.K. and Ferri, F. (1995): U-Pb geochronology of intrusive rocks associated with copper-gold porphyry deposits in the Canadian Cordillera; in *Porphyry Deposits of the Northwestern Cordillera of North America*, Schroeter, T.G., Editor, *Canadian Institute of Mining, Metallurgy and Petroleum*, Special Volume 46, pages 142–158.
- Mortimer, N. (1987): The Nicola Group: Late Triassic and Early Jurassic subduction-related volcanism in British Columbia; *Canadian Journal of Earth Sciences*, Volume 24, pages 2521–2536.
- Nixon, G.T. (2004): Platinum group elements in the Afton Cu-Au porphyry deposit, southern British Columbia; in *Geological Fieldwork 2003*, *BC Ministry of Energy and Mines*, Paper 2004-1, pages 263–289.
- Nixon, G.T., Archibald, D.A. and Heaman, L.M. (1993): ⁴⁰Ar-³⁹Ar and U-Pb geochronometry of the Polaris Alaskan-type complex, British Columbia: precise timing of Quesnellia – North America interaction; *Geological Association of Canada – Mineralogical Association of Canada*, Joint Annual Meeting, Program with Abstracts, p. 76.
- Northcote, K.E. (1974): Geology of the northwest half of the Iron Mask Batholith; in *Geological Fieldwork 1974*, *BC Ministry of Energy, Mines and Petroleum Resources*, Paper 1975-1, pages 22–26.
- Northcote, K.E. (1976): Geology of the southeast half of the Iron Mask Batholith; in *Geological Fieldwork 1976*, *BC Ministry of Energy, Mines and Petroleum Resources*, Paper 1977-1, pages 41–46.

- Northcote, K.E. (1977): Iron Mask Batholith; *BC Ministry of Energy, Mines and Petroleum Resources*, Preliminary Map 26, with accompanying notes.
- Oliver, J.L. (1995): Report on the 1994 exploration program, Rainbow property; *BC Ministry of Energy, Mines and Petroleum Resources*, Assessment Report 23 917.
- Palfy, J., Smith, P.L. and Mortensen, J.K. (2000): A U-Pb and ^{40}Ar - ^{39}Ar time scale for the Jurassic; *Canadian Journal of Earth Sciences*, Volume 37, pages 923–944.
- Preto, V.A. (1967): Geology of the eastern part of the Iron Mask Batholith; *BC Ministry of Mines*, Annual Report, 1967, pages 137–147.
- Preto, V.A. (1972): Report on Afton, Pothook; *BC Ministry of Energy, Mines and Petroleum Resources*, Geology, Exploration and Mining 1972, pages 209–220.
- Preto, V.A. (1977): The Nicola Group: Mesozoic volcanism related to the rifting in southern British Columbia; in *Volcanic Regimes in Canada*, Baragar, W.R.A., Coleman, L.C. and Hall, J.M., Editors, *Geological Association of Canada*, Special Paper 16, pages 39–57.
- Preto, V.A. (1979): Geology of the Nicola Group between Merritt and Princeton, British Columbia; *BC Ministry of Mines*, Bulletin 69, 90 pages.
- Ross, K.V. (1993): Geology of the Ajax East and West, silica-saturated, alkali copper-gold porphyry deposits, Kamloops, south-central British Columbia; unpublished M.Sc. thesis, *University of British Columbia*, 210 pages.
- Ross, K.V., Dawson, K.M., Godwin, C.I. and Bond, L. (1992): Major lithologies of the Ajax West pit, an alkali copper-gold porphyry deposit, Kamloops, British Columbia; in *Current Research, Part A*, *Geological Survey of Canada*, Paper 92-1A, pages 179–183.
- Ross, K.V., Dawson, K.M., Godwin, C.I. and Bond, L. (1993): Lithologies and alteration of the Ajax East zone, an alkali copper-gold porphyry deposit, Kamloops, British Columbia; in *Current Research, Part A*, *Geological Survey of Canada*, Paper 93-1A, pages 87–95.
- Ross, K.V., Godwin, C.I., Bond, L. and Dawson, K.M. (1995): Geology, alteration and mineralization in the Ajax East and Ajax West deposits, southern Iron Mask Batholith, Kamloops, British Columbia; in *Porphyry Deposits of the Northwestern Cordillera of North America*, Schroeter, T.G., Editor, *Canadian Institute of Mining, Metallurgy and Petroleum*, Special Volume 46, pages 565–580.
- Schiarizza, P. (1989): Structural and stratigraphic relationships between the Fennell Formation and Eagle Bay Assemblage, western Omineca Belt, south-central British Columbia; implications for Paleozoic tectonics along the paleocontinental margin of western North America; unpublished M.Sc. thesis, *University of Calgary*, 343 pages.
- Souther, J.G. (1992): Volcanic regimes; in Chapter 14, *Geology of the Cordilleran Orogen in Canada*, Gabrielse, H. and Yorath, C.J., Editors, *Geological Survey of Canada*, Geology of Canada, Number 4, pages 457–490.
- Shives, R.B.K. (1994): Airborne geophysical survey, Iron Mask batholith, British Columbia, *Geological Survey of Canada*, Open File 2817, 1:150 000 scale.
- Snyder, L.D. (1994): Petrological studies within the Iron Mask Batholith, south-central British Columbia; unpublished M.Sc. thesis, *University of British Columbia*, 192 pages.
- Snyder, L.D. and Russell, J.K. (1993): Field constraints on diverse igneous processes in the Iron Mask Batholith (92L/9); in *Geological Fieldwork 1992*, *BC Ministry of Energy, Mines and Petroleum Resources*, Paper 1993-1, pages 281–286.
- Snyder, L.D. and Russell, J.K. (1994): Petrology and stratigraphic setting of the Kamloops Lake picrite basalts, Quesnellia Terrane, south-central B.C. (92I/9, 15 and 16); in *Geological Fieldwork 1993*, *BC Ministry of Energy, Mines and Petroleum Resources*, Paper 1994-1, pages 297–311.
- Snyder, L.D. and Russell, J.K. (1995): Petrogenetic relationships and assimilation processes in the alkalic Iron Mask batholith, south-central British Columbia; in *Porphyry Deposits of the Northwestern Cordillera of North America*, Schroeter, T.G., Editor, *Canadian Institute of Mining, Metallurgy and Petroleum*, Special Volume 46, pages 593–608.
- Stanley, C.R. (1994): Geology of the Pothook alkalic copper-gold porphyry deposit, Afton Mining Camp, British Columbia (92I/9, 10); in *Geological Fieldwork 1993*, *BC Ministry of Energy, Mines and Petroleum Resources*, Paper 1994-1, pages 275–284.
- Stanley, C.R., Lang, J.R. and Snyder, L.D. (1994): Geology and mineralization in the northern part of the Iron Mask batholith, British Columbia (92I/9, 10); in *Geological Fieldwork 1993*, *BC Ministry of Energy, Mines and Petroleum Resources*, Paper 1994-1, pages 269–274.
- Travers, W.B. (1977): Overtaken Nicola and Ashcroft strata and their relations to the Cache Creek Group, southwestern Intermontane Belt, British Columbia; *Canadian Journal of Earth Sciences*, Volume 15, pages 99–116.
- Vollo, N.B. (1985): Report on the CID claim Group, Iron Mask area, Kamloops, BC; unpublished report for Comet Industries Ltd., Initial Developers Ltd., and Davenport Industries Ltd., 7 pages.
- Wheeler, J.O. and McFeely, P. (1991): Tectonic assemblage map of the Canadian Cordillera and adjacent parts of the United States of America; *Geological Survey of Canada*, Map 1712A, scale 1:2 000 000.

Initial Evaluation of Bedrock Geology and Economic Mineralization Potential of Southern Whitesail Lake Map Area (NTS 093E/02, 03), West-Central British Columbia

By J.B. Mahoney¹, R.L. Hooper¹, S.M. Gordee², J.W. Haggart³ and J.K. Mortensen²

KEYWORDS: Whitesail map area, Bella Coola map area, economic mineralization, Hazelton Group, Monarch assemblage, Coast Plutonic Complex, layered mafic intrusion, volcanogenic massive sulphide deposits, Eskay Creek, Rocks to Riches program

INTRODUCTION

Regional Geological Setting

The eastern Bella Coola (NTS 093D) and southern Whitesail Lake (NTS 093E) 1:250 000 map areas comprise a region of rugged mountainous topography and limited access on the eastern margin of the Coast Mountains. These map areas straddle the transition zone between the Coast and Intermontane morphogeological belts, and encompass the boundary between igneous and metamorphic rocks of the Coast Plutonic Complex on the west and Jurassic and Cretaceous volcanic-sedimentary successions of southwestern Stikinia on the east (Fig. 1, 2). Bedrock geological mapping and economic mineral assessment in the eastern Bella Coola (NTS 093D) map area have been the primary focus of the 2001–2004 Bella Coola Targeted Geoscience Initiative (TGI), a coordinated federal-provincial project designed to improve understanding of the geological evolution for this part of the central coast region and assess the economic potential of little-known Mesozoic volcanic assemblages in the region (Haggart *et al.*, 2004, and references therein). During the 2004 field season, the geological framework established by the Bella Coola TGI was extended to the north, into the southern Whitesail Lake map area (NTS 093E/02, 03), under the auspices of the Rocks To Riches Program, by a combined research team from the University of Wisconsin – Eau Claire, the University of British Columbia and the Geological Survey of Canada.

The primary area of interest includes the Foresight Mountain (NTS 093E/03) and Tesla Lake (NTS 093E/02) 1:50 000 map sheets in the south-central Whitesail Lake map area, on the eastern side of the Coast Mountains west

of Tweedsmuir North Provincial Park (Fig. 1). This area contains Jurassic and Cretaceous volcanic successions on the western edge of Stikinia that are known to host volcanogenic massive sulphide (VMS) mineralization elsewhere in the Cordillera, as well as Jurassic to Eocene plutonic bodies along the eastern margin of the Coast Plutonic Complex that are known hosts for a variety of porphyry deposits (Woodsworth, 1980; Dawson *et al.*, 1991; Diakow *et al.*, 2001). Stream sediment geochemistry (Regional Geochemical Survey data; Lett *et al.*, 2002), associated MineMatch anomaly clusters and MINFILE occurrences suggest the potential for economic mineralization in both Mesozoic volcanogenic successions of western Stikinia and plutonic bodies along the eastern margin of the Coast Plutonic Complex (Fig. 1). This investigation integrates regional bedrock mapping, stratigraphic and structural analyses, geochronology, plutonic and volcanic geochemistry, and isotopic analyses to document the regional geological framework and to provide a first-order assessment of the economic mineral potential in the area.

This report briefly describes the geology of the south-central Whitesail Lake 1:250 000 map area (NTS 093E/02, 03), documented by detailed bedrock mapping during the 2004 field season (Fig. 2). This bedrock mapping is a continuation of regional mapping conducted to the south by the Bella Coola TGI project (Haggart *et al.*, 2004, and references therein). The preliminary results from this investigation are integrated with a detailed analysis of Hazelton Group volcanic stratigraphy in the eastern half of the Tesla Lake 1:50 000 map area by Gordee *et al.* (this volume).

GEOLOGICAL SETTING

Volcanic Assemblages

Hazelton Group

Volcanic rocks of the Early and Middle Jurassic Hazelton Group form a thick (>4 km), broadly bimodal volcanic succession consisting of basaltic and basaltic andesite flows interbedded with and overlain by dacitic to rhyolitic tuff, lapilli tuff, tuff-breccia, tuffaceous sedimentary rocks and associated rhyolitic domes and flows. These rocks are widespread and well preserved in the eastern third of the map area and occur in well-exposed, generally eastward-younging, gently dipping structural panels along the eastern margin of the Coast Plutonic Complex. Preliminary

¹Department of Geology, University of Wisconsin – Eau Claire, Wisconsin, USA

²Mineral Deposit Research Unit, Department of Earth and Ocean Sciences, University of British Columbia, Vancouver, BC

³Geological Survey of Canada, Vancouver, BC

stratigraphic analyses suggest that the stratigraphy, composition, age and facies architecture of the Hazelton Group in this region strongly resemble strata that host the Eskay Creek VMS deposit in the northwestern portion of Stikinia (Diakow et al., 2001; Gordee et al., this volume). Hazelton Group strata in this area are the focus of an ongoing stratigraphic, geochemical and geochronological investigation by S.M. Gordee at the University of British Columbia. The

following description is a synopsis, and detailed volcanostratigraphic descriptions of Hazelton Group strata in the region are provided by Gordee et al. (this volume).

One of the most significant results of the 2004 field season was the recognition that Hazelton Group strata are substantially more widespread in the area than suggested by earlier reconnaissance mapping (i.e., Woodsworth, 1980). Regionally, the Hazelton Group forms a gently east-

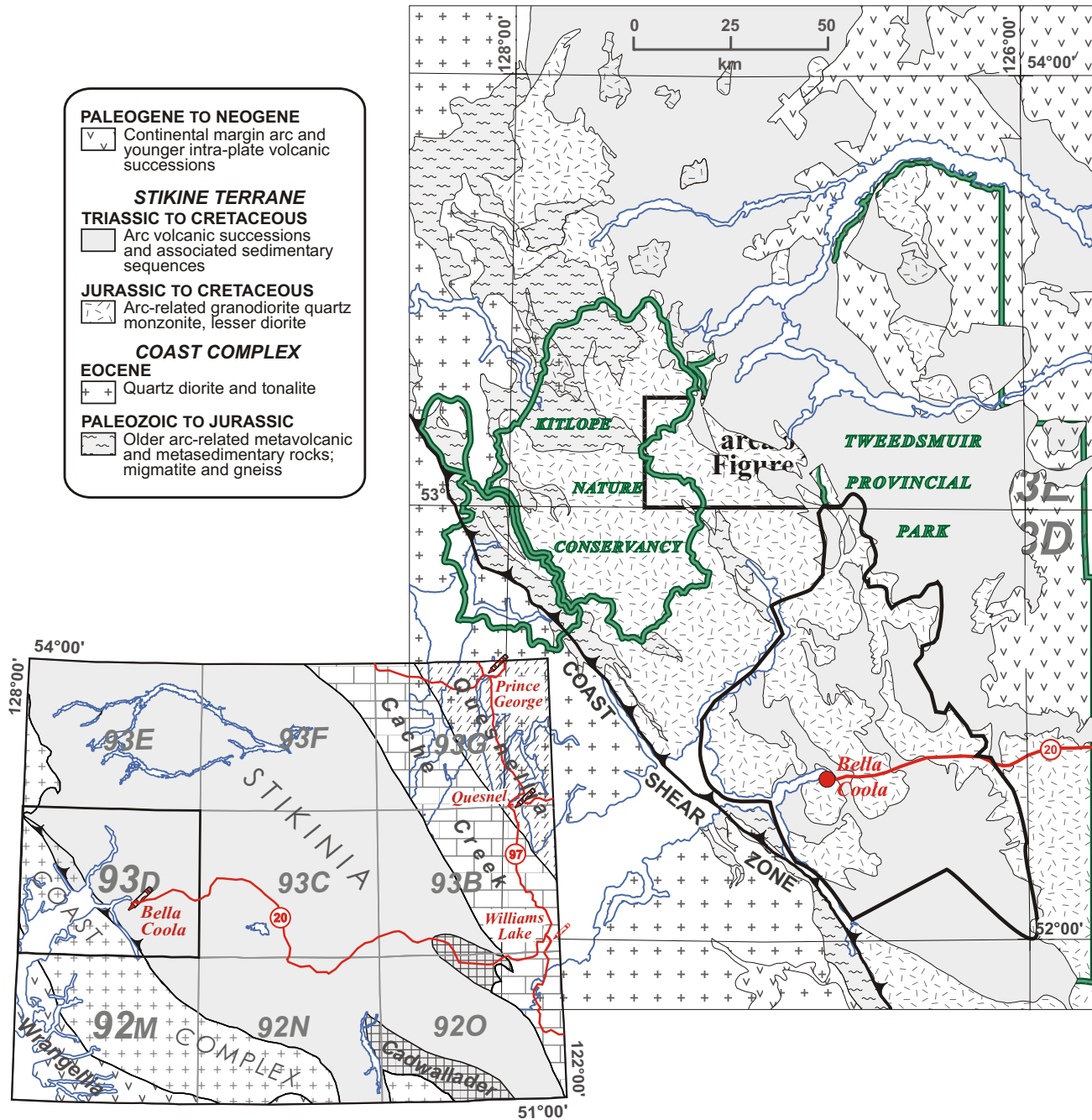


Figure 1. Schematic regional geological map of Bella Coola (NTS 093D), Whitesail Lake (NTS 093E) and adjoining map areas. The irregular polygon represents the area mapped during the TGI project (Haggart et al., 2004). Inset box shows current study area, including NTS 093E/02 and 03. Diagram modified from Diakow et al. (2003). Inset map shows morphogeological belts and tectonic terranes for the west-central Canadian Cordillera.

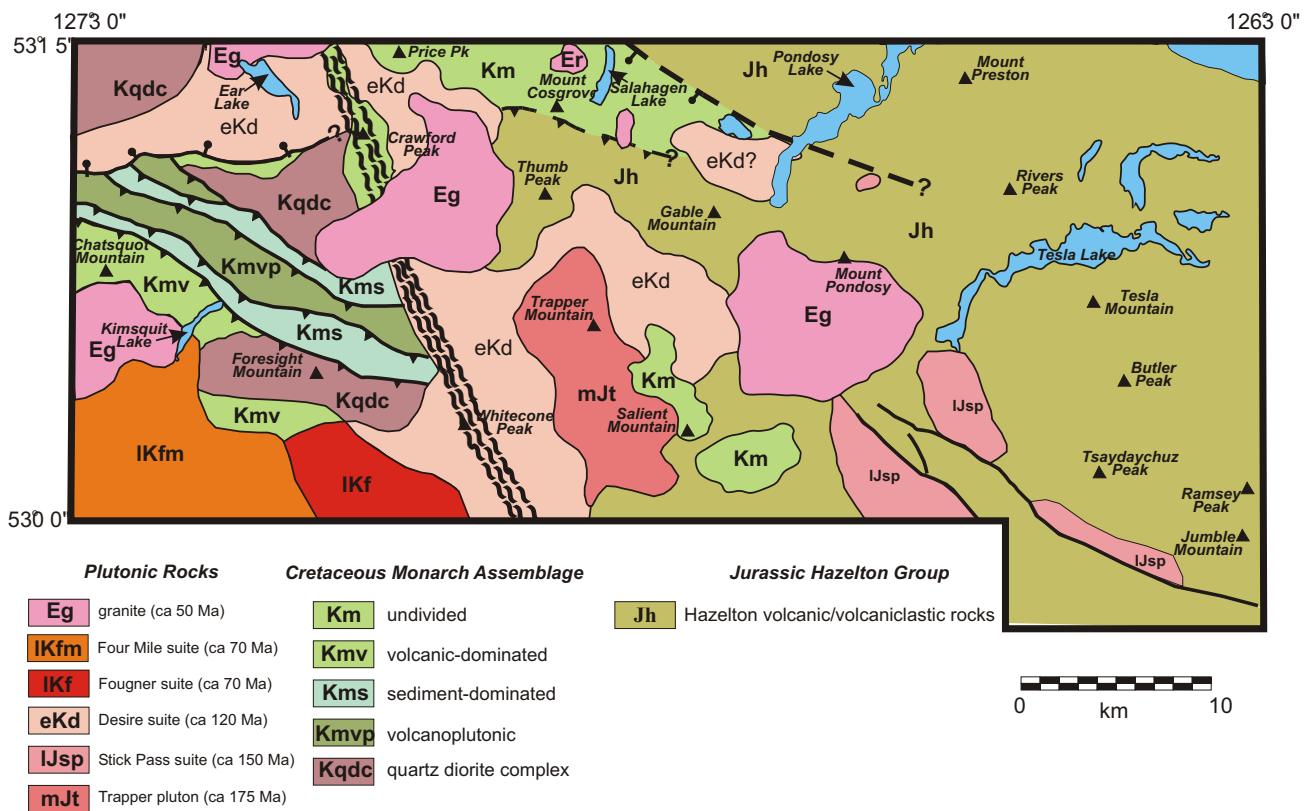


Figure 2. Generalized geology of the northeastern Bella Coola – southeastern Whitesail Lake map area, showing major lithological units, structures and physiographic features referred to in the text.

northeast-dipping homocline that can be crudely subdivided into two stratigraphic packages. The basal package consists of a thick succession (>2000 m) of intermediate to mafic volcanic flows, tuff-breccias, lapilli tuffs and associated medium to coarse-grained volcanoclastic sedimentary rocks that form the jagged massifs of the Tsaydaychuz Peak – western Jumble Mountain area (Fig. 2). Hypabyssal intrusions are common, and much of the area consists of complexly intercalated basalt and basaltic andesite flows, dikes and sills, and associated tuffaceous strata intruded by abundant gabbroic to dioritic hypabyssal intrusions.

The ‘lower’ mafic assemblage is gradationally overlain by a very thick succession (>3000 m) of laterally extensive dacitic to rhyolitic tuff, lapilli tuff, tuff-breccia and associated volcanoclastic sediments (Fig. 3). This ‘upper’ felsic package makes up over 80% of the Hazelton Group in the area. The rocks are very well bedded, and individual beds can be traced for hundreds of metres along strike. The package is dominated by maroon to red, thin to medium-bedded, rhyolitic welded to unwelded tuff and lapilli tuff, pebble to cobble conglomerate, volcanic lithic arenite and wacke; and mudstone interbedded with medium to thick-bedded lapilli tuff, tuff-breccia and conglomerate. The entire sequence fines upward, with thin-bedded mudstone, siltstone and sandstone dominating in the northern and eastern portions of the map area.

In the Rivers Peak – Mount Preston area, an impressive sequence of aphanitic rhyolite flow domes intrudes thin to

medium-bedded volcanoclastic strata, and follows the trace of a down-to-the-south, apparently synvolcanic extensional fault. Both the fault zone and rhyolite domes are extensively sericitized and oxidized, forming a very distinct red-stained gossan zone immediately south of Mount Preston.

The age of the Hazelton Group in the southern Whitesail Lake area is constrained by a combination of fossil ages and U-Pb geochronology. The age of the base of the Hazelton Group section to the west of Tsaydaychuz Peak is poorly constrained by the combination of a 191 ± 12 Ma U-Pb age from dacitic tuff underlying the major mafic interval, and by an intrusive contact between Hazelton Group strata and the ca. 177 Ma Trapper Peak pluton (P. van der Heyden and G. Woodsworth, unpublished data). Up section, in the Jumble Mountain area, fine to coarse-grained feldspathic lithic arenite and wacke have yielded a diverse assemblage of bilvalves, gastropods, belemnoids and ammonites that constrain the strata to Late Toarcian to Early Aalenian age (T.P. Poulton, personal communication, 2003). This age designation is supported by a U-Pb zircon age of 176.6 ± 0.7 Ma, derived from overlying rhyolitic lapilli tuff (R.M. Friedman, personal communication, 2003). The Jumble Mountain area straddles the contact between the ‘lower’ mafic and ‘upper’ felsic stratigraphic packages, suggesting that the transition from effusive basaltic volcanism to explosive rhyolitic volcanism is roughly Aalenian in age. The correlation between rhyolitic strata in

the Jumble Mountain area and those of the Mount Preston area is provided by U-Pb ages of 176.3 ± 3.3 Ma and 175.4

0.9 Ma, derived from rhyolitic lapilli tuff from the base and top of the Mount Preston section, respectively (S.M. Gordee, work in progress). The youngest Hazelton Group strata in the region are found to the east of the map area, where a Late Bathonian to Early Callovian fauna has been identified near Oppy Lake (H. Fربول, unpublished data).

Monarch Assemblage

The Lower Cretaceous Monarch assemblage is exposed in a series of northwest-trending structural panels in the western and northern portions of the map area, and as erosional remnants near Salient Mountain in the southern portion of the map area (Fig. 2). These exposures represent a continuation of the outcrop pattern in the Bella Coola area to the south, where volcanic strata of the Monarch assemblage are exposed in a series of imbricate structural panels developed to the west of the main Hazelton Group outcrop belt.

The base of the Monarch assemblage in the southern Whitesail Lake map area is represented by a prominent angular unconformity between rocks of the Hazelton Group and basaltic andesite and andesite of the Monarch assemblage. The contact is visible on the south and east flanks of Salient Mountain, where volcanic rocks of the Monarch assemblage forming the steep massif of Salient Mountain overlie steeply dipping felsic strata typical of the upper Hazelton Group. The underlying felsic strata are intruded by the ca. 177 Ma Trapper Mountain pluton on the south side of Salient Mountain, thus verifying assignment to the Hazelton Group. This is the first locality where an unconformable contact has been identified between the Monarch assemblage and the Hazelton Group. To the south, the Monarch assemblage erosionally overlies both ca. 155 Ma and ca. 134 Ma plutonic rocks, but the contact between the Monarch assemblage and older volcanic rocks in the eastern Bella Coola map area is equivocal (Haggart *et al.*, 2004).

The Monarch assemblage is dominated by olive green, locally amygdaloidal basalt, basaltic andesite and dacite flows and associated breccias and tuff-breccias, intercalated with distinctive intervals of argillite, siltstone and volcanic lithic arenite to wacke. The sedimentary intervals locally amalgamate to sections hundreds of metres thick, and contain thin to medium-bedded lapilli tuff, volcanic pebble conglomerate, medium to coarse-grained

feldspathic lithic sandstone, and thin-bedded tuff, siltstone and rare limestone interbeds. Sedimentary interbeds are tabular and laterally continuous, and locally may represent amalgamated partial bottom-cut-out turbidite beds. The lateral continuity, partial turbidite sequences and presence of limestone and fossiliferous intervals indicate, at least in part, a sub-wavebase marine depositional environment. Stratigraphy within the assemblage is complex, however, a result of abrupt lateral facies changes complicated by structural deformation. The Monarch assemblage is differentiated from the Hazelton Group by its higher percentage of mafic amygdaloidal flows, lower amount of rhyolite, overall green chloritic color (contrasting with the predominantly reddish-purple cast of the Hazelton) and the presence of laterally continuous thin-bedded argillite, siltstone and sandstone intervals that form distinct marker horizons between massive mafic flow packages.

In the western portion of the map area, the Monarch assemblage is exposed within a series of structural panels that are interpreted to represent an imbrication of several different stratigraphic-structural levels within a single volcanoplutonic arc assemblage (Fig. 4). From the lowest structural level upward, these panels include 1) a foliated to nonfoliated hornblende quartz diorite complex with meta-volcanic xenoliths (10–20%) and abundant mafic dikes trending roughly east-west; 2) metavolcanic and metasedimentary screens (40–50%) within a ‘matrix’ of texturally and compositionally complex, locally magmatically foliated biotite-hornblende, pyroxene-hornblende and hornblende diorite to quartz diorite (Fig. 5); 3) massive basalt, basaltic andesite and andesite flows, associated tuff-breccia and other fragmental rocks; and 4) volcanoclastic sedimentary strata and associated pyroclastic rocks. These structural panels are interpreted to



Figure 3. Thick succession of rhyolitic tuff, lapilli tuff, and associated volcanoclastic sedimentary rocks on the south end of Gable Mountain. Note abundant gossan associated with strata and associated structures.

represent ‘slices’ of a single volcanoplutonic-arc assemblage, from the subvolcanic plutonic roots, through the plutonic-volcanic intrusive contact, to the surficial volcanic flows and associated volcanogenic sedimentary rocks (Fig. 2). In this succession, the rheologically weak sedimentary intervals tend to form décollement surfaces, whereas the massive flow units tend to be structurally resistant.

One of the structurally resistant structural panels is exposed on Chatsquot Mountain and the ridges immediately to the southeast and northwest of the main massif, which harbour spectacular exposures of a mineralized layered mafic intrusion (LMI; Fig. 2). Compositional banding in the LMI is typically defined by variable proportions of olivine, pyroxene, plagioclase and magnetite, and ranges in composition from ultramafic magnetite-olivine websterite to anorthositic gabbro. The prominent foliation in the rock parallels the compositional layering and results in a distinctly layered appearance visible from several kilometres away. Typical compositional layers are less than 1 m thick, with clinopyroxene (cpx)-rich gabbro (80% cpx) alternating with more plagioclase-rich layers that distinctly weather to a lighter colour (Fig. 6). Subordinate ultramafic layers include magnetite and olivine-rich rocks (apparent cumulate layers), which weather to a distinctive rusty brown, knobby surface. Along the ridge northeast of Chatsquot Mountain, the LMI is cut by numerous mafic and intermediate porphyry dikes, which occasionally exceed the LMI in volume and form intrusion breccias.

In the Bella Coola map area (NTS 093D), the Monarch assemblage is interpreted to be Valanginian in age, based on sparse ammonite collections from several localities (Struik *et al.*, 2002). In the Whitesail Lake map area, this interpretation is supported by a 124 ± 4 Ma K-Ar age on hornblende from the top of George Peak, and by an imprecise 128–136 Ma U-Pb age from the summit of Salient Mountain (P. van der Heyden and G. Woodsworth, unpublished data; Fig. 2). However, Albian ages have been reported from strata lithologically identical to the Monarch assemblage from the Bella



Figure 4. Imbricate thrust stack within Monarch assemblage and subjacent intrusive rocks, northeast of Chatsquot Mountain.

Coola area (Haggart *et al.*, 2004). Fieldwork in the type area of the Monarch assemblage on the south side of the Monarch Icefield, south of the Bella Coola (NTS 093D) map area, during 2004 yielded fossils of Albian age, indicating that the Monarch assemblage most likely ranges from Valanginian to Albian in age. It is unclear if this age range encompasses a single stratigraphic succession or two (or more?) unconformity-bound successions. Fossils collected east of Price Peak have been submitted for identification, and U-Pb geochronology samples from rhyolitic lapilli tuff within the Monarch assemblage east of Chatsquot Peak are being analyzed.



Figure 5. Clasts of metavolcanic rocks from the basal Monarch assemblage within hornblende diorite to quartz diorite. Intrusive rocks are presumed to be subvolcanic equivalent of Monarch assemblage. Rock hammer for scale.

PLUTONIC ASSEMBLAGES

The central portion of the southern Whitesail Lake map area (NTS 093E/02, 03) is characterized by a westerly-increasing volume of plutonic rocks of Middle Jurassic to Eocene age. The spatial and temporal magmatic pattern in the southern Whitesail Lake map area mimics that of the Bella Coola area to the south, which is characterized by a northwest-trending belt of plutonic rocks that is subdivided into intrusive suites on the basis of lithological characteristics, crosscutting field relationships, mineralogy, alteration assemblages, geochemical attributes and age (Gordee *et al.*, 2003). Plutonic rocks in the study area have been subdivided on the basis of crosscutting relations and lithology, with limited geochronology. Geochemical, geochronological and isotopic analyses are in progress.

Early Jurassic(?) Plutons

Crosscutting relations along the margins of the Middle Jurassic Trapper Peak pluton (*see below*) indicate that the oldest plutonic rocks in the southern Whitesail Lake map area consist of a texturally and compositionally complex suite of hornblende diorite and quartz diorite. The unit displays a wide textural variation from fine grained holocrystalline to locally pegmatitic. It is variably foliated, ranging from unfoliated to complexly magmatically foliated, and displays a strong tectonic foliation adjacent to the shear zone west of Whitecone Peak. Metavolcanic mafic xenoliths are common, ranging from pebble to boulder size, but generally constitute less than 20% of the unit. To the south, in the Bella Coola map area, rocks lithologically similar to those intruded by the Trapper Peak pluton are referred to as the Howe Lake suite, and yield U-Pb crystallization ages of ca. 180–185 Ma.

Middle Jurassic Plutons

The oldest dated plutonic rock in the southern Whitesail Lake map area is the Trapper Peak pluton, which is a medium to coarse-grained, locally K-feldspar porphyritic hornblende-biotite granite. The rock is relatively fresh, with weak chloritization of hornblende and weak sericitization of plagioclase feldspar. The unit is unfoliated, and appears relatively homogeneous on a regional scale. The Trapper Peak pluton clearly intrudes andesitic volcanic rocks of the Hazelton Group along its southeast margin, and intrudes texturally complex, locally foliated hornblende diorite along its southern and northeastern margins. Contact relations with plutons on the northwestern and western sides are ambiguous. The Trapper Peak pluton yielded a 177.4 ± 0.7 Ma U-Pb zircon age (P. van der Heyden and G.

Woodsworth, unpublished data). This age is only slightly younger than U-Pb ages obtained from rhyolitic tuffs in the Hazelton Group, and overlaps paleontological ages from the upper portion of the Hazelton Group stratigraphy. The coeval nature of the pluton and its spatial association with thousands of metres of rhyolitic pyroclastic rocks and associated rhyolite domes strongly suggest this pluton may represent the source magma chamber for rhyolitic volcanism in the upper Hazelton Group.

Late Jurassic (?) Plutons

Plutonic rocks of apparent Late Jurassic age form a northwest-trending belt between Tsaydaychuz Peak and Salient Mountain. These rocks are characterized by fine to medium-grained biotite hornblende granodiorite to quartz diorite. Aplite dikes are common, and small (<4–5 cm), strongly recrystallized mafic xenoliths are locally abundant. The unit is heavily fractured. Hornblende is commonly glomerocrystic and chloritized, and with widespread interstitial pink K-feldspar imparts a distinct green and pink tint to the rock. The unit clearly intrudes mafic volcanic rocks of the Hazelton Group, and is intruded on its northern end by rhyolite porphyry associated with the Eocene (?) Mount Podosy pluton. These rocks form the northern continuation of a northwest-trending belt of lithologically similar rocks in the Bella Coola map area assigned to the Stick Pass suite, which is constrained to be 148–156 Ma (Gordee *et al.*, 2003; Haggart *et al.*, 2004).

Early Cretaceous (?) Plutons

One of the most abundant plutonic suites in the southern Whitesail Lake map area is a texturally and compositionally complex assemblage of fine to medium-grained, hornblende to biotite hornblende granodiorite, quartz diorite and tonalite that is primarily exposed in the



Figure 6. Typical compositional layering of plagioclase-rich (lighter) bands and pyroxene-rich (darker) bands within the layered mafic intrusion on Chatsquot Mountain. Rock hammer for scale

northwestern portion of the map area (Fig. 2). Compositional variations are complex, with abundant gradational variations in the percentage of hornblende, biotite, plagioclase and quartz. The alteration character also varies, ranging from fresh and unaltered mineral assemblages to rocks containing pervasively chloritized hornblende and sericitized plagioclase. The unit is variably foliated, with a locally strong magmatic foliation, particularly in xenolith-rich phases, and a distinct tectonic foliation associated with crosscutting shear zones, particularly east of Crawford Peak. Metavolcanic xenoliths are abundant, particularly near the contact with adjacent Monarch assemblage volcanic rocks. The xenolith density varies considerably, from relatively uncommon to locally dense enough to form an intrusion breccia (Fig. 5). Crosscutting andesite dikes are common.

These plutonic rocks are spatially associated with exposures of the Monarch assemblage, and clearly intrude the Monarch assemblage on Crawford Peak and south of Price Peak (Fig. 2). Lithologically similar rocks are incorporated into an imbricate stack of thrust panels exposed northeast of Chatsquot Mountain, where they are interpreted to form the subvolcanic plutonic root of the Monarch assemblage. Similar rock types and crosscutting relations exist to the south, along the western side of the eastern Bella Coola map area (Gordec *et al.*, 2003; Haggart *et al.*, 2004), where these rocks are assigned to the Desire suite. The Desire suite is assumed to be comagmatic with the Monarch assemblage, and is constrained to be ca. 118–122 Ma.

Late Cretaceous to Paleocene(?) Plutons

Rocks of presumed Late Cretaceous to Paleocene age are restricted to the southwestern portion of the Foresight Mountain map area (NTS 093E/03). The plutons form distinct, massive, homogeneous intrusive bodies that display steep vertical walls and well-developed exfoliation joint patterns. Mineral assemblages are very fresh, xenoliths are rare, and crosscutting dikes are relatively uncommon. These plutons can be compositionally subdivided into two distinct intrusive rock types. The first is a medium-grained, equigranular to plagioclase porphyritic, hornblende-biotite tonalite to granodiorite with fine-grained, conspicuous honey brown sphene (1–3%). Fresh books of euhedral biotite and elongate hornblende crystals, together with fresh euhedral to subhedral plagioclase and anhedral vitreous quartz give the unit a distinctive ‘salt and pepper’ appearance. This rock is compositionally and texturally similar to the Fougner suite of the Bella Coola map area, which is constrained to be approximately 70 Ma (Gordec *et al.*, 2003; Haggart *et al.*, 2004).

The second rock type is a yellow-weathering, medium to coarse-grained, crudely equigranular two-mica granite characterized by large (0.5–1 cm) euhedral books of muscovite and biotite and large (0.25–0.5 cm) anhedral blebs of quartz that locally displays a grey or bluish tint. The muscovite:biotite ratio varies throughout the unit, but its low, rounded weathering profile, pervasive yellow weathering and presence of well-developed exfoliation joints makes the unit distinctive in the field. This two-mica granite is

lithologically similar to the two-mica granite of the Four Mile suite to the south, which yields U-Pb ages of 62–73 Ma. The close spatial association between the ‘salt and pepper’ hornblende-biotite tonalite to granodiorite and the two-mica granite in the southern Whitesail Lake map area mimics the close spatial association of the lithologically similar Fougner and Four Mile suites in the Bella Coola map area to the south (Gordec *et al.*, 2003; Haggart *et al.*, 2004).

Eocene (?) plutons

The map area contains several large, roughly circular bodies of biotite granite, K-feldspar porphyritic granite and rhyolite porphyry that extend in a crudely northwest direction from Mount Pondosy. Similar bodies were reported by Woodsworth (1980) to the east and northeast of Tesla Lake, but these bodies were not examined during this investigation. These rocks are characteristically medium to coarse-grained, equigranular, locally K-feldspar porphyritic biotite granite with clean, fresh books of biotite, white to pink K-feldspar, euhedral white plagioclase and large, anhedral quartz blebs. Associated rhyolite porphyry is generally pink, with distinct coarse-grained plagioclase phenocrysts and finer grained phenocrysts of biotite and quartz. Xenoliths are present but rare, and crosscutting andesite dikes are locally evident. The plutons are relatively homogeneous, and tend to have sharp, unaltered contacts with adjacent country rocks. These bodies are the source of abundant white, locally quartz-phyric rhyolite dikes that cut a variety of rock units in the vicinity of the plutons.

STRUCTURAL GEOLOGY

The southern Whitesail Lake map area displays three distinct types of structural deformation, each indicative of a specific stress regime operating at different times in the geological evolution of the region. These deformational regimes are discussed sequentially, from oldest to youngest:

Mt. Waddington Fold and Thrust System

The western portion of the map area is underlain by an imbricate stack of northeast-vergent thrust sheets that complexly interdigitates various structural levels within the Monarch volcanoplutonic assemblage (Fig. 4). The primary décollement horizons are within sediment-dominated intervals, with the massive mafic volcanic units acting as structural buttresses. The northern edge of the thrust system appears to juxtapose Monarch assemblage volcanic rocks over Hazelton Group stratigraphy, similar to inferred structural relations to the south. The maximum age of the system is constrained by the age of the deformed Monarch assemblage, which is believed to be Valanginian to Albian. The system is truncated on its eastern side by a high-angle dextral shear zone (discussed below) that runs between Whitecone Peak and Crawford Peak. This shear zone is cut by a biotite granite of presumed Eocene age, providing a minimum age for the contractional deformation. Regional analysis suggests this thrust system is continuous with the

Late Cretaceous Mt. Waddington fold and thrust system, exposed in the Bella Coola map area to the south (Haggart *et al.*, 2003, 2004).

High-Angle Dextral Shear System

A prominent north-northwest-trending, high-angle shear zone extends through the western side of the map area. It extends north from the northern end of Dean Channel, through Whitcone Peak and the eastern flank of Crawford Peak and continues north out of the area. This shear zone continues south into the Bella Coola map area, where it connects into the Pootlass shear zone (Haggart *et al.*, 2004). The shear zone is recognized in plutonic rocks by the presence of pervasive near-vertical fracture planes and locally intense foliation development, manifested by mineral realignment and the stretching and reorientation of xenoliths and metamorphic screens. On the eastern flank of Crawford Peak, graphitic phyllite, chloritic schist, clastic metasedimentary rocks and metavolcanic rocks are incorporated in the shear zone. Well-developed kink bands, isoclinal folds with moderately plunging (30–35°) fold axes clearly indicate dextral transpression. Offset of the previously described Mt. Waddington fold and thrust system, which reappears on the east side of the shear zone south of the Dean River, suggests an offset of approximately 20–25 km. The southern continuation of this shear zone, the Pootlass shear zone, is truncated by the ca. 70 Ma Four Mile plutonic suite, providing a maximum age of transpressional deformation (Haggart *et al.*, 2004).

High-Angle Normal Faults

Several major northwest to west-trending normal faults juxtapose rocks of all ages in the southern Whitesail Lake map area. The most prominent high-angle fault in the area trends northwest from Tesla Mountain toward Salahagen Lake (Fig. 2). At its north end, this structure clearly drops Monarch assemblage volcanic rocks down to the south relative to Hazelton Group strata to the north (Fig. 2). This offset changes to the southeast, where it places Hazelton Group on Hazelton Group in the vicinity of Tesla Mountain. In the Tesla Mountain area, the type and magnitude of offset are not constrained, although there appears to be a significant counterclockwise rotation across the structure (Gordee *et al.*, this volume).

A second major normal fault occurs on the west side of the previously discussed shear zone, where a west-trending normal fault truncates the northern end of the Mt. Waddington fold and thrust belt. The age of normal faulting in the region is poorly constrained, but must be Late Cretaceous or younger, based on the presumed age of truncated structures.

ECONOMIC POTENTIAL

The primary focus of this investigation was to assess the economic mineral potential of Mesozoic volcanogenic assemblages and Jurassic to Tertiary plutonic rocks in the southern Whitesail Lake map area. Preliminary analysis of

bedrock geological mapping suggests that there are three potential targets of economic importance:

Volcanogenic Massive Sulphide Deposits within the Hazelton Group

Mapping described herein has substantially expanded the known areal extent of Hazelton Group stratigraphy in this region. Rocks previously mapped as Cretaceous Kasalka or Gambier groups by Woodsworth (1980) have been reassigned to the Middle Jurassic Hazelton Group. Preliminary facies analysis, geochronology and geochemistry from this area and the Bella Coola area to the south (Diakow *et al.*, 2003) indicate that these rocks are age equivalent to hostrocks for the Eskay Creek VMS deposit, and are characterized by predominantly shallow-water deposition, probably in a rifted arc setting. The similarities between these strata and those in the Eskay Creek area suggest that the Hazelton Group in the southern Whitesail Lake area is highly prospective for VMS mineralization. Volcanogenic massive sulphide mineralization has been documented at the Nifty property to the south, and the occurrence of extensive rhyolitic stratigraphy, rhyolite domes, and potentially synvolcanic extensional faults suggest that Hazelton Group stratigraphy in the southern Whitesail Lake map area may represent an important new economic target. Details of this stratigraphy and economic potential are provided in a companion paper (Gordee *et al.*, this volume)

Monarch assemblage mineralization

Rocks of the Early Cretaceous Monarch assemblage are widespread to the south of the Whitesail Lake map area, where they are clearly imbricated within the Late Cretaceous Mt. Waddington fold and thrust system. These strata are apparently offset to the north into NTS 093E/03 by dextral translation associated with the Pootlass shear zone, a strand of the Coast Shear Zone. In this area, imbricate thrust panels of the Monarch assemblage host the Smaby deposit, which is interpreted to be a Noranda/Kuroko-type VMS deposit (Massey *et al.*, 1999). Paleontological, geochronological and geochemical analyses will test this correlation. If correct, this would represent the first significant mineralization within the Monarch assemblage, suggesting that economic potential may exist within large areas to the northwest and southeast that are underlain by coeval strata.

Layered mafic intrusions

The large layered mafic intrusion (LMI; described above) within the Monarch assemblage appears to have strong potential for significant Cu-Ni sulphide and PGE mineralization. Some pyroxene-rich compositional layers (clinopyroxene gabbro) near the southwestern contact have substantial chalcopyrite (or Cu-Ni sulphide) mineralization, both as disseminated sulphides and as sulphide veins. In addition, the southwestern margin of the LMI is intruded by a K-feldspar megacrystic biotite granite of Paleogene (Eocene?) age, and the LMI near the contact displays weak

hydrothermal alteration and significant Cu-Ni sulphide mineralization. Conversely, the granite has very little hydrothermal alteration, although there is minor sericitization of feldspars, and it displays only weak Cu mineralization, primarily as malachite and azurite coating fracture surfaces within a few tens of metres of contact. The contact zone between the LMI and the granite is well exposed in a zone of glacial scour in the saddle between Chatsquot Mountain and the ridge to the southeast, where the contact is a breccia zone 50–100 m wide with clasts of both LMI and granite in a matrix of open stockwork quartz veins. The stockwork in the LMI consists of quartz, pyrite and molybdenite veins with substantial molybdenite mineralization ($\text{MoS} > \text{FeS}_2$). The LMI and the associated rocks along its contact may prove to be an interesting target for more detailed study.

ACKNOWLEDGMENTS

Danny Hodson of Rainbow West Helicopters provided excellent helicopter support during this investigation. Christopher Kohel, Emily Hauser and Joe Nawikas provided expert field assistance. Funding for this investigation was provided by the Rocks to Riches Program, the Geological Survey of Canada, the University of British Columbia and the University of Wisconsin – Eau Claire.

REFERENCES

- Dawson, K.M., Panteleyev, A., Sutherland Brown, A. and Woodsworth, G.J. (1991): Regional metallogeny; Chapter 19 in *Geology of the Cordilleran Orogen in Canada*, Gabrielse, H. and Yorath, C.J., Editors, *Geological Survey of Canada*, Geology of Canada, number 4, pages 707–768.
- Diakow, L.J., Mahoney, J.B., Haggart, J.W., Woodsworth, S.M., Gordee, S.M., Snyder L.D., Poulton, T.P., Friedman, R.M. and Villeneuve, M. (2003): Geology of the eastern Bella Coola map area, west-central British Columbia; in *Geological Fieldwork 2003, BC Ministry of Energy and Mines*, Paper 2003-1, pages 65–76.
- Diakow, L.J., Mahoney, J.B., Johnson, A.D., Gleason, T.G., Hrudey, M.G. and Struik, L.C. (2002): Middle Jurassic stratigraphy hosting volcanogenic massive sulphide mineralization in eastern Bella Coola map area (NTS 093/D), southwest British Columbia; in *Geological Fieldwork 2001, BC Ministry of Energy and Mines*, Paper 2002-1, pages 119–134.
- Gordec, S.M., Mahoney, J.B., Diakow, L.J., Friedman, R.M., Haggart, J.W., Woodsworth, G.M. and Villeneuve, M. (2003): Magmatic episodocity in the eastern Coast Plutonic Complex, Bella Coola, British Columbia; *Geological Society of America*, Abstracts with Programs, Volume 34, number 7, page 390.
- Haggart, J.W., Diakow, L.J., Mahoney, J.B., Struik, L.C., Woodsworth, G.J. and Gordec, S.M. (2004): Geology, Bella Coola area (parts of 93D/01, D/02, D/06, D/07, D/08, D/09, D/10, D/11, D/15 and D/16), British Columbia; *Geological Survey of Canada*, Open File 4639; *British Columbia Geological Survey and Development Branch*, Open File 2004-13, scale 1:150 000.
- Haggart, J.W., Mahoney, J.B., Diakow, L.J., Woodsworth, G.J., Gordec, S.M., Snyder, L.D., Poulton, T.P., Friedman, R.M. and Villeneuve, M. (2003): Geological setting of eastern Bella Coola map area (93 D), west-central British Columbia; *Geological Survey of Canada*, Current Research 2003-A04, 9 pages.
- Lett, R., Jackaman, W. and Friske, P. (2002): Regional geochemistry sampling program – NTS 93C, 93D 103A / Bella Coola; *Geological Survey of Canada*, Open File 4414; *BC Ministry of Energy and Mines*, RGS 56.
- MacIntyre, D.G., McMillian, R.H. and Villeneuve, M.E. (2004): The mid-Cretaceous Rocky Ridge Formation – important host rocks for VMS and related deposits in central British Columbia, in *Geological Fieldwork 2003, BC Ministry of Energy and Mines*, Paper 2004-1, pages 231–246.
- Massey, N.W.D., compiler (1999): Volcanogenic massive sulphide deposits of British Columbia; *BC Ministry of Energy and Mines*, Open File Report 1999-2, 1 sheet.
- Woodsworth, G.J. (1980): Geology of the Whitesail Lake map area, BC; *Geological Survey of Canada*, Open File 708, 1 sheet.

Gold Mineralization and Geology in the Zeballos Area, Nootka Sound, Southwestern British Columbia

By Dan Marshall, Scott Close, Nataalka Podstawskyj and Adolf Aichmeier

KEYWORDS: Zeballos, Nootka, gold veins, fluids, thermobarometry, mineralization, Eocene, sulphur isotopes

INTRODUCTION

The Zeballos mining camp, located in the Nootka Sound map area (NTS 92E), was an important gold producer in the 1930s and 1940s. Although not the largest gold camp in British Columbia (Schroeter and Pinsent, 2000), it is in all likelihood significantly underexplored due to its poor access, heavy vegetation, mountainous rugged terrain and relative lack of geological research. The region has not been studied in any detail since the regional geological investigations of Muller *et al.* (1981) and, with the exception of two preliminary reports published in the early 1980s (Sinclair and Hansen, 1983; Hansen and Sinclair, 1984), the majority of the geological work on the Zeballos camp was done by Stephenson (1938, 1939, 1950) in the 1930s and 1940s, during the height of mining activity.

A project to investigate the metallogeny of the Zeballos camp and to put the geology and mineral deposits of the area into a modern geological-tectonic context was initiated in August 2004. Work undertaken this summer included:

- regional mapping in the area, including verification of previous work and remapping of Nootka Island in light of our new interpretations of the rock types and tectonic setting of the area;

- sampling of the representative units; intrusive, volcanic, sedimentary and mineralized veins, for lithogeochemistry;

- mapping and sampling underground at the Privateer mine to develop a detailed paragenetic and geochronological framework for gold mineralization at the main producer within the camp; sampling for geochronology included mafic dykes, rhyolite dykes and the Zeballos stock; and

- developing pressure and temperature depositional constraints for gold mineralization at the Privateer mine (as a proxy for the region) from stable isotopes, fluid inclusions and geothermobarometric studies.

GENERAL GEOLOGY

The Nootka Sound area is underlain by the Wrangellia tectonostratigraphic terrane, which extends from southern Vancouver Island through the Queen Charlotte Islands and

into southeastern Alaska and the Yukon. (Jones *et al.*, 1977; Wheeler *et al.*, 1991). Wrangellia is a large, complex oceanic terrane dominated by extensive accumulations of flood basalt. This terrane was accreted onto the western margin of the North American plate by the Late Jurassic to Early Cretaceous.

The general geology of the study area is complex (*see* Fig. 1, 2) and consists of periods of volcanism punctuated by periods of sedimentation, deformation, metamorphism and hydrothermal activity. The relative timing of volcanism, sedimentation, plutonism, regional fabrics, deformation, metamorphism and mineralization is depicted in Figure 3.

Within the Nootka Sound area around Zeballos and on Nootka Island, the bedrock includes Triassic Karmutsen volcanic rocks and Quatsino limestone (and possibly the Parson Bay formation), collectively known as the Vancouver Group; mid-Jurassic granodiorite, diorite, hornblende diorite and gabbro of the Island Intrusive Suite; and the coeval mid-Jurassic Bonanza volcanic rocks, consisting of andesite pyroclastics and flows, dacite tuffs and flows, and some calcsilicate rocks. All of these rocks are cut by Mount Washington intrusions of the Tertiary Catface intrusive suite. Outcrops of the Carmanah Group conglomerate and sandstone are exposed on the southwest coast of Nootka Island.

The Karmutsen formation is over 3000 m thick and comprises tholeiitic pillow basalt, massive basaltic lavas and comagmatic dykes and sills, with minor sedimentary and volcanoclastic rocks. The origin of the Karmutsen formation is enigmatic but is presently thought to represent oceanic flood basalts associated with a back-arc rift or a primitive marine volcanic arc (Yorath *et al.*, 1999). The Quatsino limestone lies conformably on the Karmutsen formation but may be interfolded and interfaulted with the Karmutsen. A gradational contact separates the Quatsino formation from the overlying Parson Bay formation; however, in this study, these two units are mapped together as Quatsino.

The Jurassic calcalkaline rocks of the Bonanza Group unconformably overlie the Triassic rocks of the Vancouver Group. The Bonanza Group is interpreted to be an Early to Middle Jurassic island arc (Debari *et al.*, 1999), intruded by the comagmatic Island Intrusive Suite. Emplacement of the Island intrusions at mid-crustal levels produced partial melts and amphibolite-grade metamorphic rocks (Muller *et al.*, 1981). These partial-melt metamorphic rocks were

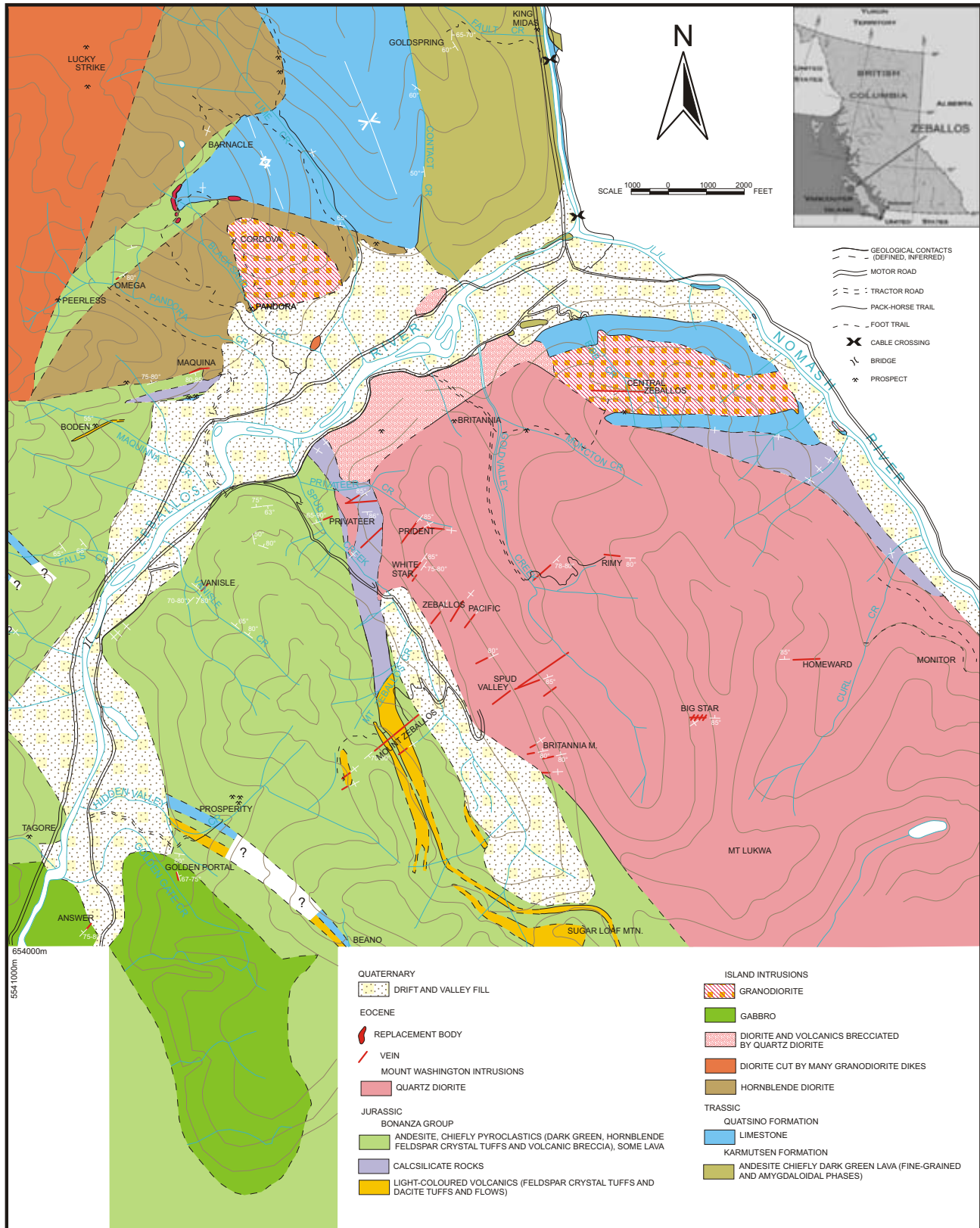


Figure 1. Geology of the Zeballos region (*modified from Stevenson, 1950*).

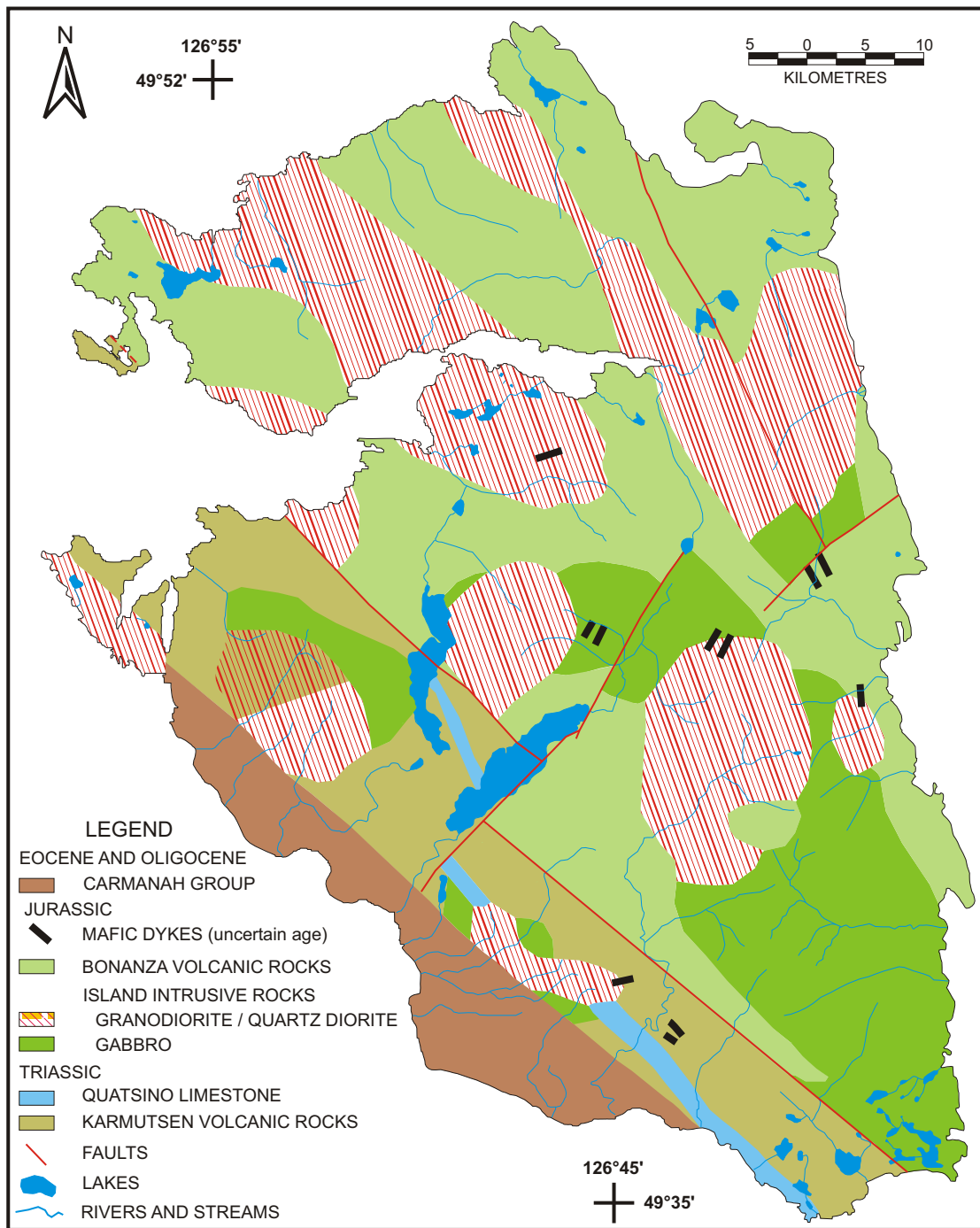


Figure 2. Geology of Nootka Island.

named the Westcoast Crystalline Complex (WCC) by Muller and Carson (1969).

Accretion of Wrangellia to the continental margin occurred between the Late Jurassic and Middle Cretaceous. The Cretaceous Nanaimo Group sediments overlie all the aforementioned rocks just to the east and north of the study area, although there are no outcrops of this formation within the study area.

Tertiary Catface intrusions and succeeding Eocene to Oligocene Carmanah Group sediments are the youngest rocks in the study area. The Carmanah is thought to be age equivalent to the Catface Suite, but contact and timing relationships are still unclear. The Catface intrusions have been subdivided into the older (60–45 Ma) Clayoquot and younger (38–47 Ma) Mount Washington intrusions (Massey, 1995). The Zeballos Stock, which hosts to most of the gold mineralization in the study area, is part of the Mount Washington suite.

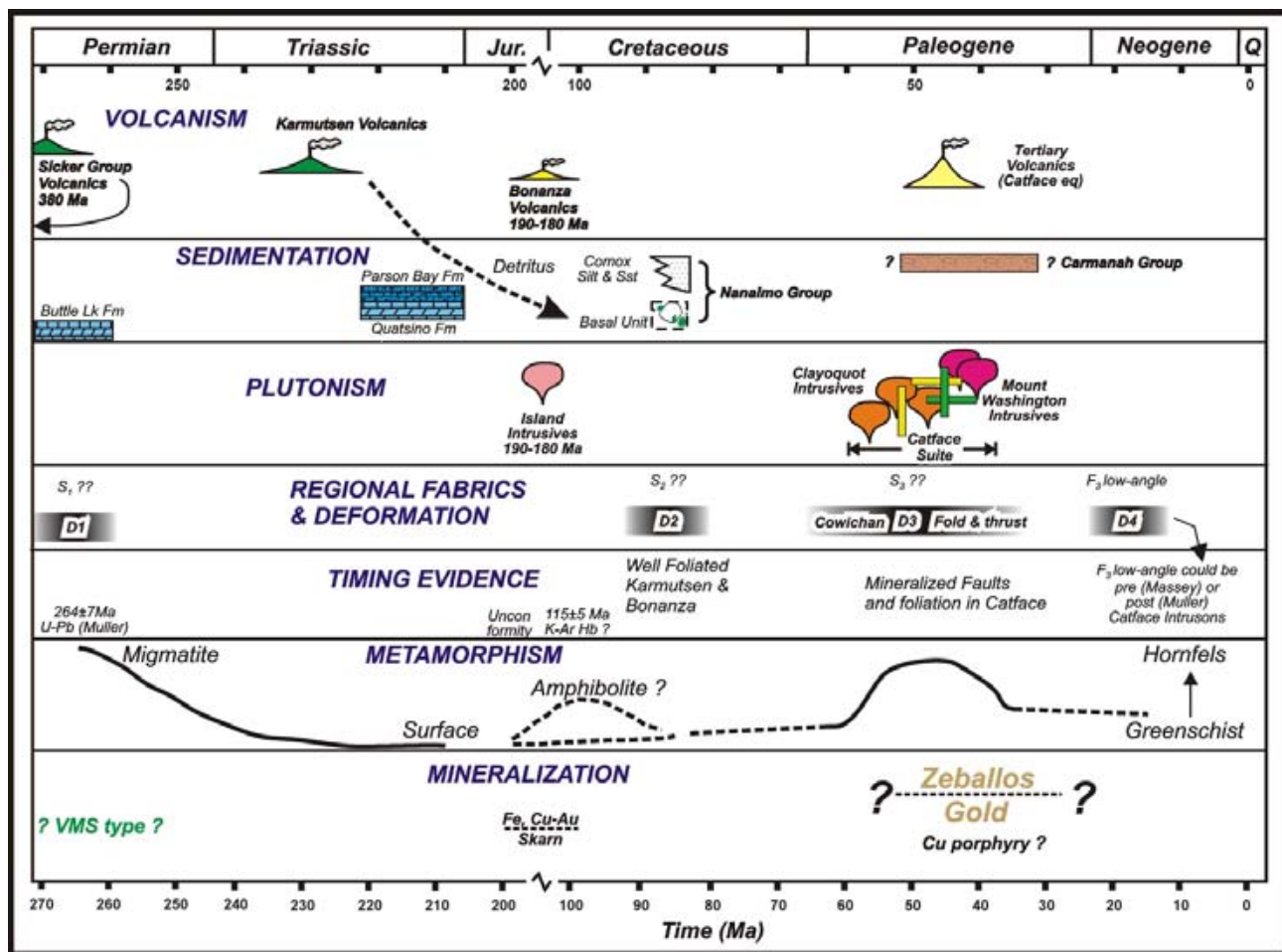


Figure 3. Schematic diagram illustrating the timing of principal geological events in the Nootka Sound region.

REGIONAL GEOLOGY: REVISIONS TO NOOTKA SOUND MAP UNITS

Large areas of Nootka Island were mapped as the Westcoast Crystalline Complex (WCC) by Muller *et al.* (1981). The WCC was originally identified by Muller and Carson (1969) and described as “a heterogeneous assemblage of amphibolite and basic migmatite with minor metasedimentary and metavolcanic rocks of greenschist metamorphic grade.” It was subsequently subdivided into two mappable units; migmatite and amphibolite, by Muller *et al.* (1981), which they considered to be migmatized pre-existing volcanic and sedimentary rocks. Muller *et al.* (1981) suggested that, during Early to Middle Jurassic time, the pre-Jurassic rocks were subjected to very high grade metamorphic conditions, ranging up to migmatitic, and that the highest grade metamorphism yielded the WCC and the Island Intrusive Suite.

Our field observations have not yielded any evidence of an extensive high-grade metamorphic or migmatization event in the area. Rather, exposures of migmatized rock are restricted to what appear to be clasts of country rock stowed into the magma chambers of the Island Intrusive Suite.

Metamorphic grade at the time of intrusion of the Island Intrusive Suite appears to have been greenschist.

Mapping and the results from an ongoing geochemical study indicate that the majority of what was mapped as WCC is in fact Island Intrusion, Karmutsen and/or Bonanza volcanic rocks. As the volcanic rocks can generally be identified, we suggest that the Triassic and Jurassic Nootka Island rocks be mapped as meta-Bonanza, meta-Karmutsen or Island Intrusives and thus the term Westcoast Crystalline Complex is superfluous to the list of rock units for Nootka Island (Fig. 2).

The implication of this reinterpretation of the WCC on Nootka Island is two-fold. Firstly, Muller *et al.* (1981) identified extensive areas of WCC elsewhere on the west coast of Vancouver Island and these units should be re-examined. Secondly, the recognition of additional areas of Triassic and Jurassic volcanic and related intrusive rock may increase the prospectivity of parts of the Nootka Sound area for VMS and/or Cu-Ni-PGE mineralization.

LITHOGEOCHEMISTRY

Thirty-five samples representative of the main rock units in the Zeballos area have been collected for

lithochemical study. As part of this ongoing geochemical study, these samples will be analyzed for whole-rock major and trace element chemistry and then compared to existing geochemical data sets from similar rocks on Vancouver Island (Massey 1991; 1995; Debari *et al.*, 1999; Yorath *et al.*, 1999) as an aid to mapping and interpreting tectonic provenance.

GOLD VEIN MINERALOGY, PETROGRAPHY AND STRUCTURE (PRIVATEER MINE)

The gold veins at the Privateer mine vary in width up to approximately 30 cm. The veins are hosted within the Zeballos Stock and surrounding calcsilicate (skarn) rocks. The veins comprise, in order of abundance, quartz, calcite, arsenopyrite, pyrite, sphalerite, pyrrhotite, galena, chlorite and gold. The modal mineralogy of the veins is not consistent, but quartz (or quartz-vein breccia fragments) generally constitute some 70% of the vein material. The quartz varies from idiomorphic, clear crystalline quartz displaying cockscomb textures to anhedral, white massive quartz. There is a tendency for the brecciated quartz fragments to have a milky colour. This is probably attributable to the degree of deformation. Euhedral quartz crystals range in size up to 2 cm, while the milky brecciated polycrystalline quartz clasts range up to 10 cm. Calcite and arsenopyrite are generally the second and third most abundant minerals within the veins. Both of these minerals have habits that range from euhedral to anhedral, and grain sizes that vary up to 2 cm. The other vein minerals tend to have smaller grain sizes (rarely achieve sizes of more than a few millimetres) and range from euhedral to anhedral. In some cases, the veins are rich in very fine grained fault gouge, which ranges in colour from silvery-white and grey to dark brown.

Gold concentrations within the veins are sporadic. Visible gold accompanies good gold grades, so a good portion of the gold is deemed to be free gold and not (refractory gold) existing as solid solutions in the arsenopyrite and sulphides. Typical visible gold hosted within an arsenopyrite-rich quartz vein is shown in Figure 4. In more detail (Fig. 5), the timing relationships between gold, arsenopyrite, galena and quartz indicate that quartz is early in the paragenesis, followed by or in some cases contemporaneous with arsenopyrite. Galena replaces arsenopyrite and gold replaces both arsenopyrite and galena. Thus, gold is one of the latest minerals in the paragenetic sequence. Calcite precipitates throughout the paragenesis of the veins, and the other sulphides (pyrite, sphalerite and pyrrhotite) appear to be contemporaneous with galena.

In general, the gold-bearing veins trend northeast and dip steeply. The veins are concentrated on the southwest flank of the Zeballos Stock, suggesting that they formed as



Figure 4. Quartz vein from the Privateer mine. Native gold is visible in association with arsenopyrite at the tip of the finger.



Figure 5. Slab of gold-bearing quartz (qtz) vein from the Privateer mine. Slab length is approximately 15 cm. Note the relationship between the galena (gn), which replaces arsenopyrite (apy), and the gold (au), which cuts both arsenopyrite and galena.

a result of heat from the stock and structures developed during emplacement or related to continuing tectonic forces during cooling. Underground observations at the Privateer mine indicate that the veins formed near the brittle-ductile transition, as both types of structures are observed (Fig. 6) in the veins. The majority of offsets along structures in the mine are sinistral, but there are numerous examples of dextral offsets as well.

Wallrock alteration surrounding the veins is cryptic. In most cases, the granitic wallrock appears to have no alteration halo. Closer inspection reveals that all of the mafic minerals within the Zeballos Stock have been altered to chlorite. The feldspars appear to be unaffected in hand specimen. If the wallrock to the veins is the calcsilicate rocks, there is no wallrock alteration visible. This lack of wallrock alteration is consistent with focused fluid flow along the vein structures and also consistent with the lack of gold or sulphides within the wallrock.

PRESSURE AND TEMPERATURE CONSTRAINTS ON GOLD MINERALIZATION

Fluid Inclusions

Preliminary fluid inclusion work indicates the presence of at least two fluid inclusion assemblages (FIAs) within the quartz-carbonate gold-bearing veins. Both FIAs occur within the vein carbonate and quartz, but we have limited the microthermometric measurements to inclusions within euhedral quartz crystals (Fig. 7). Both FIAs consist of a liquid and vapour component at room temperature. However, what we interpret to be the early FIA is a CO₂-bearing (carbonic) fluid with an aqueous saline liquid, whereas the later FIA consists of only aqueous saline liquid and vapour (i.e., no CO₂).

The vapour bubble within the carbonic FIA occupies approximately 20% of the fluid inclusion volume, while the vapour phase in the aqueous inclusions occupies approximately 10% of the inclusion volume. Preliminary petrographic and microthermometric measurements suggest the two FIAs are independent of each other and do not represent conjugates of a boiling system, as both inclusion types homogenize into the liquid phase. Additionally, the smaller bubble size and lower total homogenization temperatures for the aqueous inclusions are consistent with this FIA being later. We interpret this to mean that the carbonic fluid inclusions are responsible for the majority of the minerals precipitated within the gold-bearing quartz-carbonate veins. Moreover, the carbonic fluid inclusions are consistent with the typical gold-bearing quartz veins elsewhere (Ridley and Diamond, 2000).

The microthermometric behaviour of the carbonic inclusions upon cooling from room tempera-

ture is as follows. A clathrate phase nucleates at approximately -28°C and continued cooling results in the nucleation of ice at approximately -37°C and the nucleation of solid CO₂ at approximately -98°C. Upon heating, the solid CO₂ is observed to melt at approximately -58°C. This depression of the freezing point from the triple point of pure CO₂ (at -56.6°C) is due to the presence of some other dissolved gas phase within the vapour phase of the inclusions, most likely N₂ or CH₄. Continued heating results in ice melting at approximately -4°C, followed by clathrate melting at various temperatures in the +8 to +12°C range. The elevation of the clathrate melting temperature above 10°C is consistent with the dissolved gas being dominantly CH₄ rather than N₂, but some N₂ may also be present. Further heating results in the total homogenization of the fluid inclusion into the liquid phase.

The microthermometric data are consistent with an average fluid composition of X_{H₂O} equal to 0.974, an X_{CO₂} of 0.020 and X_{NaCl} of 0.006 (2.0 wt % NaCl equivalent). Isochoric data have been derived using the equation of state for H₂O-CO₂-NaCl of Bowers and Helgeson (1983) and the average composition. The isochores have been used (*see*



Figure 6. Back of the 2-3A vein, Privateer mine. Some deformation is accommodated in a brittle manner, as evidenced by the splays coming off the main vein, while some structures within the vein show ductile deformation textures (*see* arrow). Hammer for scale.

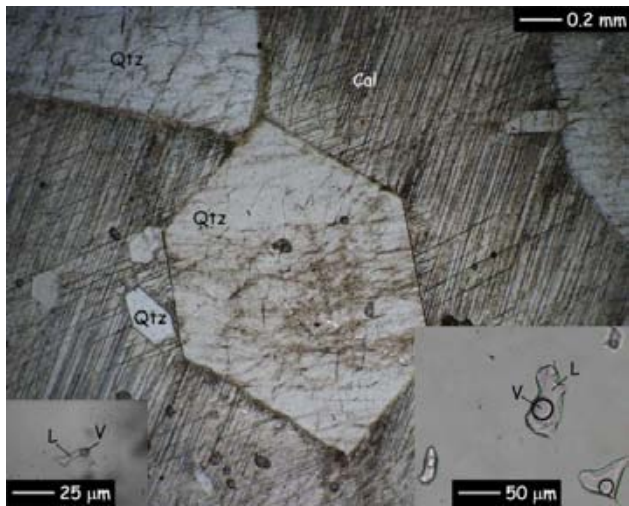


Figure 7. Photomicrograph of euhedral quartz (Qtz) and calcite (Cal) from the gold-bearing quartz-carbonate veins of the Privateer mine. The inset photomicrographs show typical examples of the CO₂-bearing fluid inclusions (right) and aqueous fluid inclusions (left). Both FIAs are two-phase inclusions consisting of an aqueous saline liquid (L) and vapour (V). Photos taken in plane polarized transmitted light.

below) to constrain pressure and temperatures of quartz-carbonate vein formation.

Sphalerite Geobarometry

Petrology of the gold-bearing quartz-carbonate veins has shown more paragenetic relationships between sulphides. Most notably, in this case, is sphalerite, pyrite and pyrrhotite in textural equilibrium (Fig. 8). The presence of this assemblage provides the necessary mineralogical constraints to apply the sphalerite geobarometry, as initially developed by Scott and Barnes (1971) and subsequent improvements (Toulmin, 1991 and references within). The sphalerite geobarometer can be used to complement the fluid inclusion work and establish some unique pressure-temperature constraints of vein formation. The sphalerite geobarometer is based on the Fe content of sphalerite in equilibrium with pyrite and pyrrhotite. The electron microprobe analyses of the sphalerite (Fig. 8) are shown in Table 1. The sphalerite Fe compositions were combined with fluid inclusion homogenization temperatures and stable vein assemblages, then plotted on a pressure-temperature diagram (Fig. 9).

Sulphur Isotopes

A sulphur isotope study of coexisting pyrite and sphalerite was carried out to provide an additional constraint on the temperature of vein formation. Sphalerite and pyrite can be seen rimming quartz breccia clasts within vein samples (Fig. 10). Small aliquots of both minerals were extracted from specific locations where there was clear indication of textural equilibrium between sphalerite and pyrite. The sulphur isotope data (Table 2) are consistent with disequilibrium precipitation, using the calibrations of

Kajiwara and Krouse (1971) and Ohmoto and Rye (1979). Due to the interpretation of disequilibrium, no temperature data can be derived.

CONCLUSIONS

The mapping and preliminary lithogeochemistry of Nootka Island indicates the presence of Karmutsen volcanic rocks and Quatsino limestone on the southern portion of the island. These observations and the removal of the West Coast Crystalline Complex from the local stratigraphy means that there is a little more fertile ground for VMS and Ni±PGE mineralization associated with mafic intrusions related to flood basalts, and skarn-type mineralization on Nootka Island. Additionally, these revisions to the bedrock mapping have implications concerning mapping, stratigraphy and tectonic interpretation for the region surrounding Nootka Island.

Preliminary pressure-temperature constraints derived from fluid inclusion studies and combined sphalerite geobarometry of vein material from the Privateer mine are consistent with vein formation temperatures ranging from 300 to 500°C, pressures on the order of 1.5 to 4 kb (Fig. 11) and deposition from a fluid with an average composition of $X_{H_2O} = 0.974$, $X_{CO_2} = 0.020$ and $X_{NaCl} = 0.006$ (2.0 wt % NaCl equivalent).

ACKNOWLEDGMENTS

Nick Massey is gratefully acknowledged for many fruitful discussions on the geology, geochemistry and tectonics of the Nootka Sound region. This study was undertaken as part of the Rocks to Riches program, and the authors would like to thank the British Columbia and Yukon Chamber of Mines for partial funding for this study. Additional funding for the study was from an NSERC grant to the senior author and a small grant from NewMex Mining.

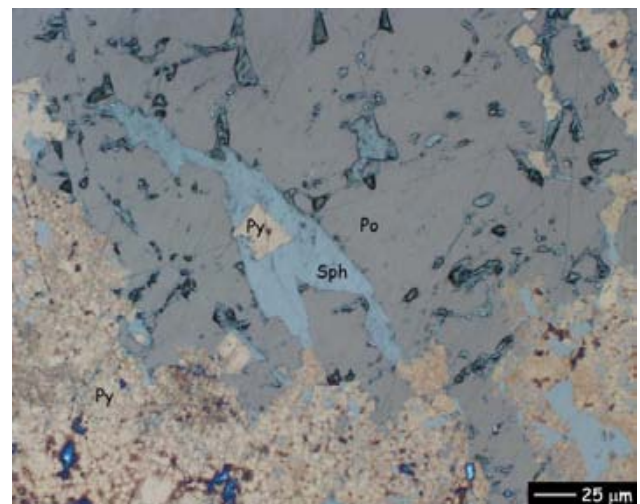


Figure 8. Photomicrograph of intergrown sulphides from the Privateer Mine showing textural equilibrium between pyrite (Py), pyrrhotite (Po) and sphalerite (Sph). Photograph taken in plane polarized reflected light.

TABLE 1. ELECTRON MICROPROBE ANALYSES OF SPHALERITE IN TEXTURAL EQUILIBRIUM WITH PYRITE AND PYRRHOTITE.

Sample	Zn (wt%)	Fe (wt%)	Mn (wt%)	Cd (wt%)	S (wt%)	Total	Zn (mol)	Fe (mol)	Mn (mol)	Cd (mol)	S (mol)	Total (mol)
ZEB1-C-1	57.32	8.92	0.13	0.52	33.84	100.73	0.42	0.08	0	0	0.5	1
ZEB1-C-2	55.97	9.77	0.15	0.54	33.82	100.25	0.41	0.08	0	0	0.5	1
ZEB1-C-3	55.54	10.2	0.27	0.55	33.79	100.35	0.41	0.09	0	0	0.5	0.999
ZEB1-C-4	55.63	10	0.22	0.41	33.62	99.88	0.41	0.09	0	0	0.5	1.001
ZEB1-C-5	55.05	10.41	0.25	0.54	33.95	100.2	0.4	0.09	0	0	0.51	1
ZEB1-B16	57.13	8.82	0.17	0.57	32.87	99.56	0.42	0.08	0	0	0.5	0.999
ZEB1-B17	55.99	8.99	0.15	0.54	33.42	99.09	0.41	0.08	0	0	0.5	0.999
ZEB1-B18	56.1	9.91	0.18	0.6	33.51	100.3	0.41	0.09	0	0	0.5	1.001
ZEB1-B19	56.53	10.23	0.21	0.57	33.37	100.91	0.41	0.09	0	0	0.5	0.999
ZEB1-B20	56.46	10.63	0.21	0.58	33.5	101.38	0.41	0.09	0	0	0.5	1
ZEB1-B21	53.94	10.59	0.22	0.55	33.79	99.09	0.4	0.09	0	0	0.51	0.999
ZEB1-B22	56.36	10.48	0.22	0.51	33.59	101.16	0.41	0.09	0	0	0.5	0.999
ZEB1-B23	56.44	10.22	0.16	0.66	33.78	101.26	0.41	0.09	0	0	0.5	1
ZEB1-B24	57.4	9.72	0.11	0.56	33.56	101.35	0.42	0.08	0	0	0.5	1
ZEB1-B25	56	9.07	0.1	0.53	32.81	98.51	0.42	0.08	0	0	0.5	0.999

Abbreviations: wt%, weight percent; mol, molecular proportion.

Support of the local road builders, forestry workers and residents of the area is greatly appreciated. Their interest in basic prospecting and their generous provision of logistical assistance was of significant benefit to this study.

REFERENCES

- Bowers, T.S. and Helgeson, H.C. (1983): Calculation of the thermodynamic and geochemical consequences of nonideal mixing in the system H_2O-CO_2-NaCl on phase relations in geologic systems: equation of state for H_2O-CO_2-NaCl fluids at high pressures and temperatures; *Geochimica Cosmochimica Acta*, Volume 47, pages 1247–1275.
- DeBari, S.M., Anderson, R.G. and Mortensen, J.K. (1999): Correlation among lower to upper crustal components in an island arc: the Jurassic Bonanza arc, Vancouver Island, Canada; *Canadian Journal of Earth Sciences*, Volume 36, pages 1371–1413.
- Hansen, M.C. and Sinclair, A.J. (1984): A preliminary assessment of Zeballos mining camp (92L); in Geological Fieldwork, 1983, *BC Ministry of Energy, Mines and Petroleum Resources*, pages 219–232.
- Jones, D.L., Silberling, N.J. and Hillhouse, J. (1977): Wrangellia – a displaced terrane in northwestern North America; *Canadian Journal of Earth Sciences*, Volume 14, pages 2565–2577.
- Kajiwaru, Y. and Krouse, H.R. (1971): Sulphur isotope partitioning in the metallic sulfide systems; *Canadian Journal of Earth Sciences*, Volume 8, pages 1397–1408.
- Massey, N.W.D. (1991): The geology of the Port Alberni – Nanaimo Lakes area; *BC Ministry of Energy, Mines and Petroleum Resources*, Geoscience Map 1991-1.
- Massey, N.W.D. (1995): Geology and mineral resources of the Alberni – Nanaimo Lakes sheet, Vancouver Island, 92 F/1W, 92 F/2E and part of 92 F/7E; *BC Ministry of Energy, Mines and Petroleum Resources*, Paper 1992-2, 132 pages.
- Muller, J.E. and Carson, D.J. (1969): Geology and mineral deposits of Alberni map-area, British Columbia, (92F); *Geological Survey of Canada*, Paper 68-50, 52 pages.
- Ohmoto, H. and Rye, R.O. (1979): Isotopes of sulfur and carbon; in *Geochemistry of Hydrothermal Ore Deposits* (2nd edition, Barnes, H.L., Editor, John Wiley and Sons, New York, pages 509–567.
- Ridley, J.R. and Diamond, L.W. (2000): Fluid chemistry of orogenic lode gold deposits and implications for genetic models; in *Gold in 2000*, Hagemann S. and Brown, P., Editors, *Reviews in Economic Geology*, Volume 13, pages 141–162.

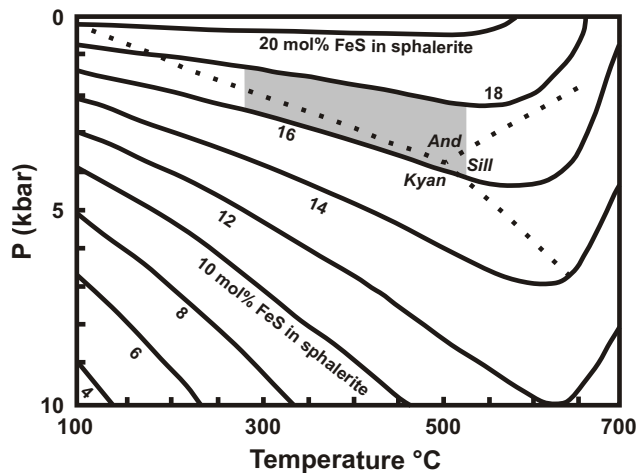


Figure 9. Sphalerite geobarometry diagram showing the isocompositional contours for mole % FeS for sphalerite in equilibrium with pyrite and pyrrhotite (Toulmin, 1991). The position of the aluminosilicate triple point is shown for reference in a dashed pattern. The range of compositions reported from electron microprobe analyses is shown in grey, with the lower temperature constraint defined by fluid inclusion total homogenization temperatures and the upper temperature constraint based on stable mineral assemblage within the veins. Abbreviations: And, andalusite; Kyan, kyanite; Sill, sillimanite.

- Schroeter, T. and Pinsent, R.H. (2000): Gold production and resources in BC (1858–1998); *BC Ministry of Energy and Mines*, Open File 2000-2.
- Scott, S.D. and Barnes, H.J. (1971): Sphalerite geothermometry and geobarometry; *Economic Geology*, Volume 66, pages 653–669.
- Sinclair, A.J. and Hansen, M.C. (1983): Resource assessment of gold-quartz veins, Zeballos mining camp, Vancouver Island: a preliminary report (92L); in *Geological Fieldwork 1982, BC Ministry of Energy, Mines and Petroleum Resources*, pages 290–303.
- Stephenson, J.S. (1938): Lode-gold deposits of the Zeballos area, west coast of Vancouver Island, British Columbia; *BC Department of Mines*, Bulletin 20.
- Stephenson, J.S. (1939): Geology and ore deposits of the Zeballos area, British Columbia; *Transactions of the Canadian Institute of Mining and Metallurgy and of the Mining Society of Nova Scotia*, Volume 42.
- Stephenson, J.S. (1950): Geology and mineral deposits of the Zeballos mining camp; *BC Department of Mines*, Bulletin 27, 145 pages.
- Toulmin, P. (1991): Commentary on the sphalerite geobarometer; *American Mineralogist*, Volume 76, Numbers 5–6, pages 1038–1051
- Wheeler, J.O., Brookfield, A.J., Gabrielese, H., Monger, J.W.H., Tipper, H.W. and Woodsworth, G.J. (1991): Terrane map of the Canadian Cordillera; *Geological Survey of Canada*, Map 1713.
- Yorath, C.J., Sutherland Brown, A. and Massey, N.W.D. (1999): Lithoprobe, Southern Vancouver Island, British Columbia: geology; *Geological Survey of Canada*, Bulletin 498, 145 pages.



Figure 10. Slab of quartz carbonate vein containing brecciated vein material rimmed by sphalerite (Sph) and pyrite (Py). The circles indicate the areas where coexisting pyrite and sphalerite were sampled for sulphur isotopes. Pen for scale.

TABLE 2. SULPHUR ISOTOPE DATA FROM PYRITE-SPHALERITE MINERAL PAIRS.

Sample	Mineral	$\delta^{34}\text{S}_{\text{CDT}}$	$\Delta^{34}\text{S}_{\text{py-sph}}$	Temperature ¹ (°C)
04-666-01	pyrite	-0.5	-1	disequilibrium
04-66601	sphalerite	0.5		
04-66602	pyrite	0.3	-0.6	disequilibrium
04-66602	sphalerite	0.9		
04-66603	pyrite	-0.3	-0.3	disequilibrium
04-66603	sphalerite	0		

¹ Temperatures calculated using calibration of Kajiwara and Krouse (1971)

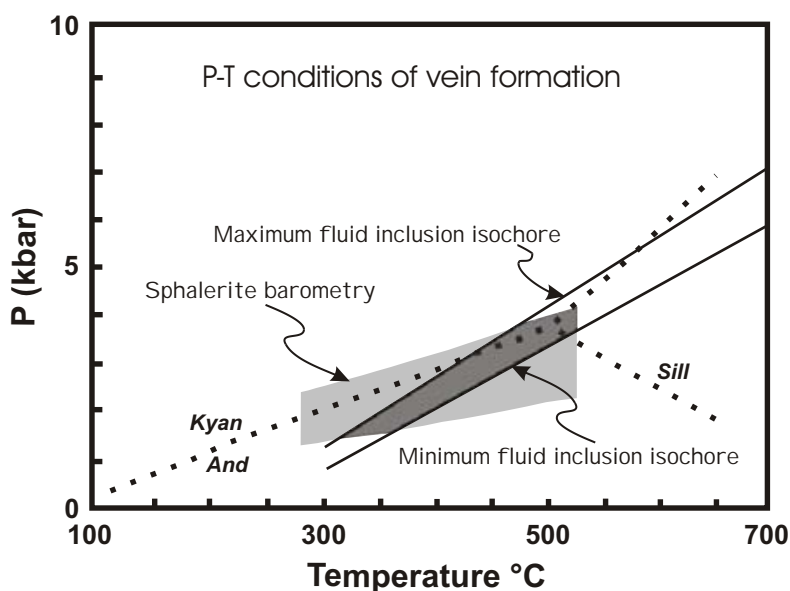


Figure 11. Pressure temperature diagram showing the range of conditions for quartz-carbonate vein formation (dark grey) from the combined constraints of sphalerite geobarometry and the fluid inclusion isochores.

Volcanostratigraphy, Lithochemochemistry and U-Pb Geochronology of the Upper Hazelton Group, West-Central British Columbia: Implications for Eskay Creek–Type VMS Mineralization in Southwest Stikinia

By S.M. Gordee¹, J.K. Mortensen¹, J.B. Mahoney² and R.L. Hooper²

KEYWORDS: volcanostratigraphy, volcanogenic massive sulphide deposits, Eskay Creek, Stikinia, Early to Middle Jurassic, Hazelton Group, Bella Coola area, Whitesail Lake area, Rocks to Riches program

INTRODUCTION

The Hazelton Group is one of the most widely exposed Mesozoic volcanic-arc successions in the Canadian Cordillera, occurring along nearly the entire length and breadth of the Stikine Terrane (Fig. 1). Despite hosting a number of significant mineral deposits (e.g., Eskay Creek–type volcanogenic massive sulphide [ECT-VMS] deposits, epithermal gold and associated copper-gold porphyry deposits in subvolcanic intrusions; Diakow *et al.*, 2002), there have been relatively few regional studies of the nature of Hazelton Group arc magmatism outside of the immediate vicinity of known deposits (e.g., Tipper and Richards, 1976; Marsden and Thorkelson, 1992; Thorkelson *et al.*, 1995).

This study investigates Hazelton Group successions in the Bella Coola and Whitesail Lake map areas of west-central British Columbia in order to constrain the evolution of the volcanic package and assess its potential for economic mineralization. This study builds upon the framework established through a joint federal-provincial Targeted Geoscience Initiative (TGI) that operated in the area from 2001 to 2004 (e.g., Haggart *et al.*, 2004 and references therein), and aims to refine our understanding of the tectonic setting and specific depositional environment(s) of rocks emplaced during Hazelton arc volcanism and sedimentation. This could provide controls on the existence and/or nature of syngenetic mineralization within the Hazelton Group in this area.

Bella Coola is located within a rugged part of the Coast Mountains, and includes the topographic divide and transition zone between the Coast and Intermontane morphogeological belts (Fig. 1, inset). Specifically, the northeastern Bella Coola (NTS 093D) – southeastern

Whitesail Lake (NTS 093E) map area is situated in southwestern Stikinia of the Intermontane Superterrane (Fig. 1). In this area (predominantly the eastern half of NTS 093D/15 and 093E/02), thick, laterally continuous, dominantly eastward-younging successions of Early to Middle Jurassic Hazelton Group form the high jagged massifs along the western boundary of Tweedsmuir Provincial Park. To the east of this area, exposures of the Hazelton Group are unconformably overlain by remnants of a moderately dissected Miocene peralkaline shield volcano that form the Rainbow Range (Diakow *et al.*, 2002 and references therein). Exposures of Hazelton Group decrease progressively to the west, where they are unconformably overlain by the Cretaceous Monarch Assemblage and intruded by numerous Jurassic to Eocene plutons of the Coast Plutonic Complex. Volcanogenic strata within the study area are relatively structurally intact, in contrast to Hazelton Group and Monarch Assemblage exposures further to the west, which are variably deformed within the Waddington Fold and Thrust belt (Mahoney *et al.*, this volume).

PRELIMINARY RESULTS FROM GEOLOGICAL MAPPING

Two summers of field mapping (2003–2004) in the northeastern Bella Coola – southeastern Whitesail Lake map area focused on the area between Jumble Mountain in the south and Mount Preston in the north (Fig. 2). Hazelton Group volcanosedimentary successions in this area represent a northwestern continuation of the package of mainly felsic volcanic strata that hosts the Nifty VMS occurrence in the east-central Bella Coola map area (e.g., Ray *et al.*, 1998; Diakow *et al.*, 2002; Haggart *et al.*, 2004). Uranium-lead dating of a dacite breccia that hosts mineralization at Nifty indicates an age of 163.7 ± 0.4 Ma (M. Villeneuve, unpublished data), and this, together with several ca. 176 Ma dates and Early-Middle Jurassic fossil collections from the northeastern Bella Coola map area, demonstrates that Hazelton Group rocks in this area are roughly age equivalent to hostrocks of the Eskay Creek deposit.

This study targeted four main areas in the 30 km transect between Jumble Mountain and Mount Preston, including (from south to north): the Jumble Mountain – Ramsey Peak area, the Tsaydaychuz Peak – Butler Peak area, Tesla Mountain and the Rivers Peak – Mount Preston

¹Mineral Deposit Research Unit, Department of Earth and Ocean Sciences, The University of British Columbia, Vancouver, B.C.

²Department of Geology, University of Wisconsin at Eau Claire, Wisconsin, U.S.A.

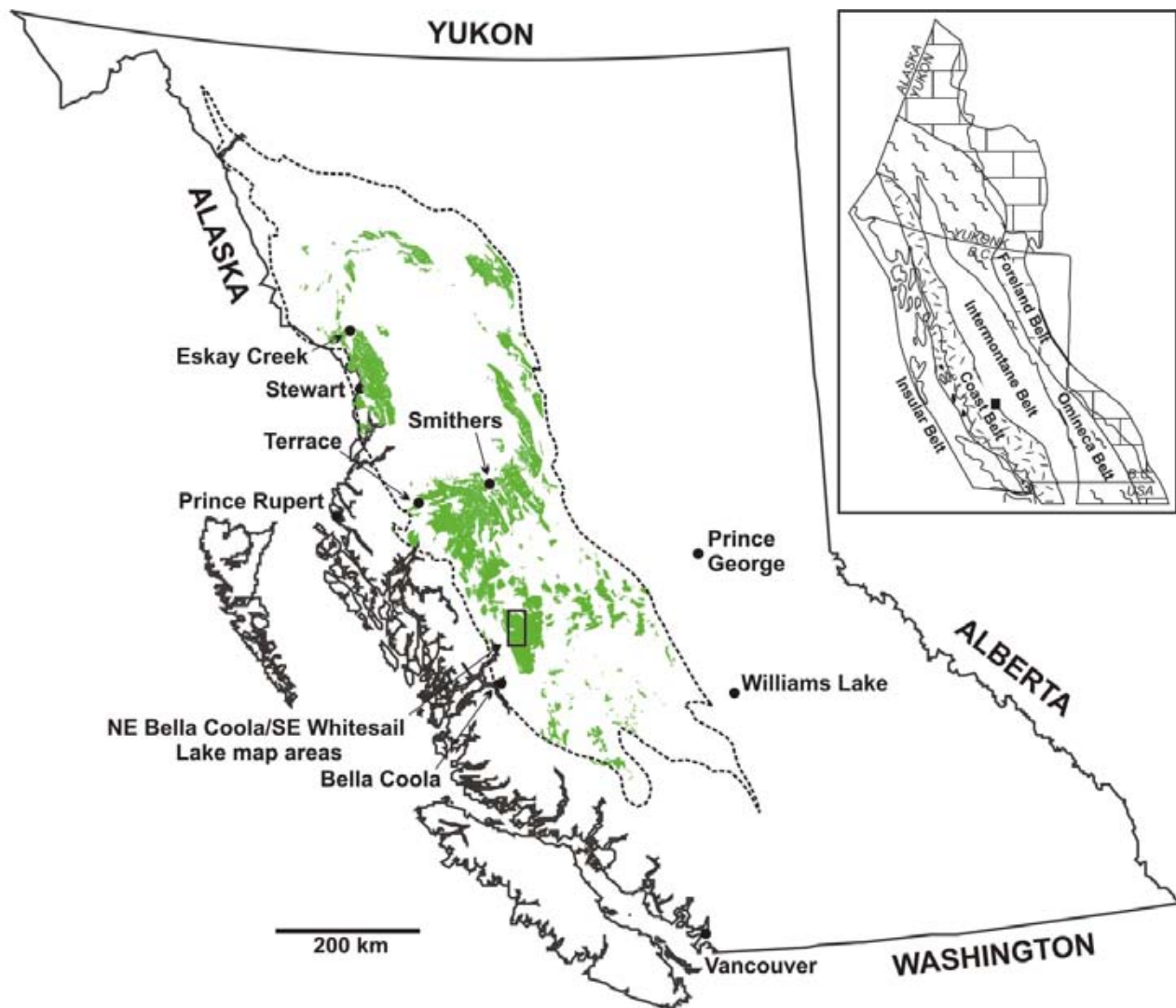


Figure 1. Distribution of Early-Middle Jurassic volcanosedimentary strata of the Hazelton Group (shown in green) within the Stikine Terrane of British Columbia (outlined with dashed boundary), showing specific localities referred to in the text, and the location of the northeast Bella Coola – southeast Whitesail Lake map area (black box). The inset map illustrates the morphogeological belts of the Canadian Cordillera (*modified after* Wheeler and McFeely, 1991).

area (Fig. 2). Fly camps were placed in central locations within these areas, and traverses were completed in accessible subalpine regions, where outcrop is continuous among snow and ice fields. Inaccessible areas were spot-checked with helicopter support.

Field investigations focused on the identification and development of large-scale lithological subdivisions; detailing and measuring volcanostratigraphic sections; defining large-scale structures; geochemical, isotopic and geochronologic sampling; and characterization of mineral occurrences recognized within the study area.

VOLCANOSTRATIGRAPHY

Geological mapping and analysis of numerous volcanostratigraphic sections in studied areas throughout the 2003 and 2004 field seasons permits a number of key

observations to be made, based on interpretation of large-scale lithological subdivisions across the map area. Figure 3 shows a schematic volcanostratigraphic fence diagram of measured sections within the field area (section lines drawn in Fig. 2), and can be referred to throughout this section. Horizontal and vertical distances are scaled accordingly; U-Pb dates, fossil ages and lithological associations are used to correlate between the sections.

TSAYDAYCHUZ PEAK AND BUTLER PEAK AREAS

Map patterns and crosscutting relationships suggest that the Tsaydaychuz Peak – Butler Peak area forms the base of the volcanosedimentary sequence in the map area. Rocks of this area overlie mafic to intermediate, dominantly fragmental successions west of the East Sakumtha River, where a U-Pb date from a quartz-phyric dacite breccia

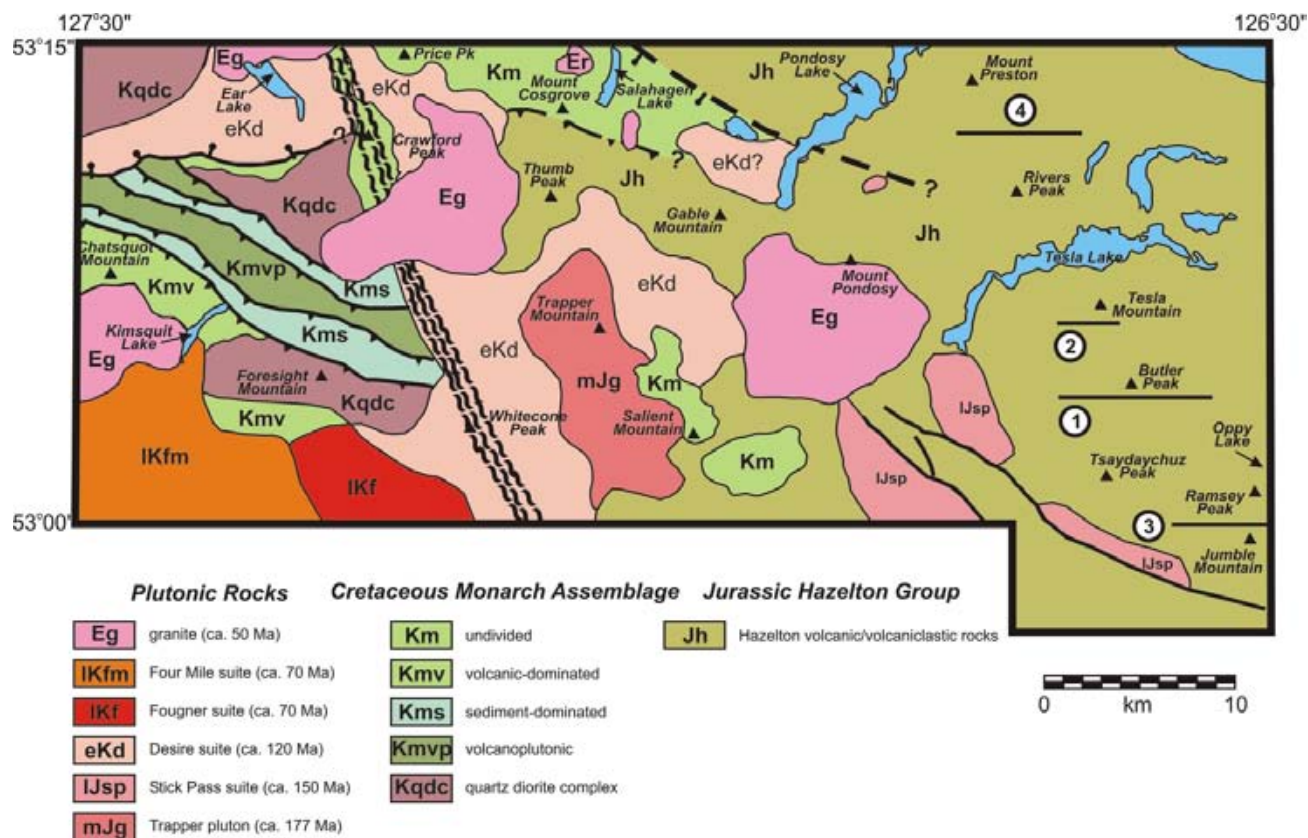


Figure 2. Generalized geologic map of the northeast Bella Coola/southeast Whitesail Lake map area, showing major lithologic subdivisions, structures and physiographic features referred to in the text (modified after Mahoney *et al.*, 2005, this volume). Location of measured sections is indicated by bold lines adjacent to encircled numbers.

cia indicates an age of 191 ± 12 Ma (R.M. Friedman, unpublished data). Separating the two sections is a broad, northwest-trending belt of complexly interfingering aphanitic basalt, and very fine to medium-grained diorite and lesser quartz diorite ('microdiorite'); the latter may represent recrystallized mafic flows and/or small pyroxene diorite plug-like intrusions (Haggart *et al.*, 2004). Importantly, this belt of mafic-intermediate rocks may record the early stages of the widespread basaltic-andesitic volcanism that characterizes the Tsaydaychuz Peak – Butler Peak region.

Tsaydaychuz Peak is the highest massif within the Whitesail Lake map sheet. At 9085 feet (2769 m) in elevation, its vertical walls and extensive ice cover render the mountain completely inaccessible, and has limited us to numerous spot checks along its flanks. Extensive traversing has been completed in the Butler Peak area and, assuming that no major structure exists between the two peaks, volcanogenic strata and field relationships observed at Butler Peak are presumed to extend to its sister mountain to the south. Traverses completed in the Butler Peak area encompass the subalpine region between north Tsaydaychuz Peak and north Butler Peak (Fig. 2). Strata in the area generally strike north-northwesterly and dip gently to moderately to the east; exposures west of Butler Peak are dominated by volcaniclastic rocks, while rock types farther upsection to

the east are dominated by intermediate and lesser mafic flows and subvolcanic intrusions.

Volcanostratigraphy west of Butler Peak is dominated by orange-purple, massive, coarse-grained tuff-breccia, lapilli tuff and lesser tuff. Tuff-breccia and lapilli tuff units range from 1 to 25 m in thickness and are dominantly very lithic and crystal-rich; modal phenocryst assemblages (plagioclase and rare quartz) suggest an intermediate to felsic composition for these fragmental rocks. Tuffs rare throughout this area; these units, which range from <1 to 5 m in thickness, are typically very light grey to tan in colour, and plagioclase is locally observed as the only phenocryst phase. Pyroclastic rocks constitute about 45 vol % of exposed bedrock in the west Butler Peak region, and are intercalated with lesser (~15%) sandstone and mudstone beds. Ignimbrite units commonly display a gradational upper contact with overlying sedimentary beds, which are sharply overlain by subsequent ignimbrite units. Volcaniclastic rocks are typically either a deep purple-maroon and dark green (more typical of Hazelton Group sediments throughout the Bella Coola and Whitesail Lake map areas) or white to tan to grey in colour. They generally consist of interbedded, thin to medium-bedded, dominantly parallel, wavy and locally ripple crosslaminated, \pm granule \pm pebble mudstone and lesser conglomerate, sandstone and siltstone. Sedimentary rocks are typically immature, ranging from poorly to moderately well sorted, with

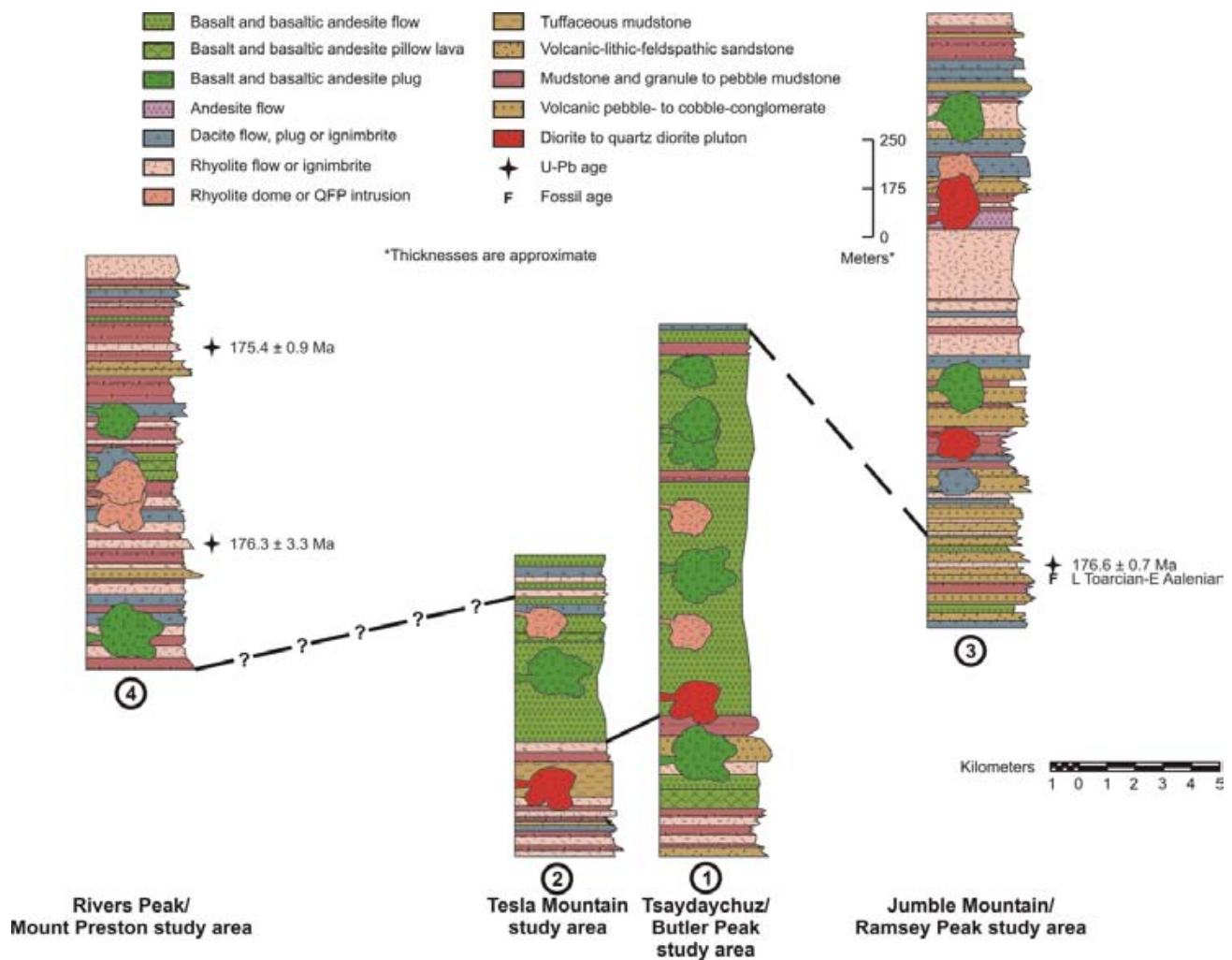


Figure 3. Measured volcanostratigraphic sections of the Hazelton Group within the northeast Bella Coola – southeast Whitesail Lake map area.

angular to subangular clasts of aphanitic to plagioclase±hornblende–phyric basalt, andesite, dacite and rhyolite. Fossils have not been found in this area.

The remaining 40% of outcrop in the west Butler Peak region consists of mafic lava flows, which occur in two broad, north-trending belts across the map area. The bases and tops of these flows are commonly not exposed but, where present, occur as metre-scale brecciated zones. Flows range from dark grey-purple to dark grey-green, are aphyric to plagioclase±pyroxene phyric, variably amygdaloidal (epidote and quartz-filled) and remarkably poorly layered. Crude compositional and/or textural boundaries (on a scale of tens of metres) within flow(s) that are approximately concordant with local strike trends may represent differences between individual flows, or may simply be variations within a single flow. One spectacular exposure of radiating cooling joints within the sequence (approximately 25 m high) may represent a cross-section through a lava feeder tube. Part of the volcanosedimentary sequence in this region is assumed to be subaqueous on the basis of an outcrop of orthogonally dissected, pillowed basaltic ande-

site, which is exposed along a vertical cleft on the southwestern margin of the field area (Fig. 4). A number of small, bladed-plagioclase, andesite porphyry plugs and associated dikes cut the volcanic successions in the area, and are interpreted to represent hypabyssal subvolcanic intrusions.

Geological mapping suggests that the Tsaydaychuz Peak region, which lies directly along strike to the south, likely represents the southern continuation of the volcanostratigraphic section documented in the Butler Peak region. Numerous spot checks and sample collections completed along the flanks of the massif yielded similar rock types and lithological associations, which supports this generalization.

The size and abundance of basalt to basaltic andesite lava flows and bladed-plagioclase porphyry plugs increases dramatically east of Butler Peak. The area is being collectively described as the Butler Peak andesitic complex, and is characterized by a complexly interfingering assemblage of basalt to basaltic andesite lava flows, dikes and hypabyssal intrusions, gabbroic to dioritic plugs, widespread microdiorite and <10% welded lapilli tuff and inter-

calated volcanogenic sediments; the latter are commonly locally folded around intrusive units. As in the lower portion of the section, individual lava flows in this area are commonly difficult to subdivide; lava flow margins, where observed, are highly brecciated over a thickness of 3–5 m. Intrusive relationships are complex and the relative timing between units is often ambiguous; this, coupled with the compositional similarities shared between rock types, leads to the interpretation that this area comprises a mafic eruptive centre. Geochemical comparisons and U-Pb dating studies are currently underway to test this hypothesis and potentially confirm the coeval nature of rocks in this area.

At least four rhyolite domes have been identified that intrude the volcanic sequences in the Tsaydaychuz Peak – Butler Peak area. Domes are pink to white in colour, aphanitic to plagioclase±quartz -phyric, massive to flow-banded, rarely fragmental, and associated with gossans characterized by disseminated pyrite west of Butler Peak. It is uncertain whether these units represent intrusive and/or extrusive domes.

TESLA MOUNTAIN AREA

The Tesla Mountain area comprises a low, east-trending ridge immediately south of Tesla Lake, approximately 4 km north of Butler Peak (Fig. 2). Structural trends suggest that this area should represent the northern continuation of the east-dipping outcrop belt in the Tsaydaychuz Peak – Butler Peak region; although this can be assumed based upon lithological and structural similarities between the two areas, a number of differences were noted. Important differences include a) a decrease in mafic volcanic rocks; b) a subsequent increase in the proportion of volcanoclastic material, including a thick section of pyritiferous tuffaceous mudstones; c) the existence of several mineral showings; and d) a pervasive, well-developed deformation fabric throughout the area.



Figure 4. Cross-section through a stack of basaltic andesite pillow lavas in the west Butler Peak region. Note the large pillow in the upper left corner. Ice axe (~60 cm) for scale.

The widespread mafic volcanic rocks that characterize the Tsaydaychuz Peak – Butler Peak region extend northward into the Tesla Mountain area, but decrease in volume significantly across the 4 km distance; mafic flows and subvolcanic intrusions are subordinate to volcanoclastic rocks and fine-grained volcanogenic sediments in this area. In general, the western half of this mountain consists of volcanogenic sedimentary rocks and lesser welded ignimbrite sequences with interbedded mafic lava flows that increase in thickness and number to the east across the summit of Tesla Mountain. Complex, outcrop-scale folding is developed west of Tesla Mountain, where mafic plugs intrude volcanoclastic sequences, a lithological association that is consistent with observations made in the west Butler Peak region. Possible pillows in flow-banded basaltic flows northwest of Tesla Mountain suggest that part of this section may represent a submarine sequence.

A thick section of tuffaceous mudstone exposed west of Tesla Mountain is unique to the field area. This sequence is approximately 100 m thick and consists of interbedded, thin to medium-bedded, parallel-laminated mudstone and rhyolitic tuffaceous mudstone, and lesser siltstone and sandstone (Fig. 5). Outcrops weather rusty orange in part, and upon initial examination appear to be devoid of sulphides; however, cut slabs reveal thin conformable layers of disseminated to semimassive pyrite. Petrographic studies are in progress to determine whether this represents syngenetic or epigenetic mineralization.

Several small rhyolite plugs and associated dikes similar to those described near Butler Peak cut the volcanic sequence near the summit of Tesla Mountain. These rhyolites are highly silicified and are responsible for wide alteration haloes and minor disseminated pyrite in the surrounding country rock. At least one claim has been staked and several prospecting pits excavated on or near the margins of these intrusions. Mineralization, in the form of narrow veins of hematite, pyrite, chalcocopyrite and malachite, has been observed within mafic dikes at two locations in the west Tesla Mountain area. A zone of fracture-controlled, comb-textured quartz veins occurs near the top of Tesla Mountain; these veins are devoid of mineralization, but may be related to “rather disappointing”, narrow and low-grade Cu and Au-bearing veins described in this area by Duffell (1959).

The Tesla Mountain region displays a very well developed, pervasive, east-trending closely spaced cleavage. This fabric extends to the south into the northwest Butler Peak region, where it is locally well developed, but does not extend across Tesla Lake into the Rivers Peak region to the north. The nature and localization of this fabric suggests that Tesla Mountain represents a zone of localized strain associated with regional deformation. Much of the vein and dike-hosted mineralization observed in the Tesla Mountain area ap-

pears to be concentrated along these zones of structural weakness.

It has been hypothesized that the large linear lakes and valleys in the Tesla Lake area may represent major faults bounding large structural blocks (e.g., Duffell, 1959). South of Tesla Mountain, Lower to Middle Jurassic volcanic stratigraphy forms an east-dipping, eastward-younging homocline, based on geological mapping, paleontology and U-Pb ages. Conversely, north of Tesla Lake between Rivers Peak and Mount Preston, strata dip and young to the west and northwest, demonstrating the existence of an east-trending structure that lies within the Tesla Lake basin.

UPPERMOST VOLCANOSTRATIGRAPHY

Uranium-lead dating of tuffs within the Rivers Peak – Mount Preston and Jumble Mountain – Ramsey Peak areas has established that the two homoclines are of similar age, and geological mapping suggests that they represent the youngest Hazelton Group strata in the study area. Individual units cannot be traced between the two areas; however, broadly similar rock types on a scale of hundreds of metres, together with U-Pb dating, demonstrate that these areas represent similar volcanic and sedimentary depositional environments.

JUMBLE MOUNTAIN AND RAMSEY PEAK AREAS

Detailed geological mapping carried out during the 2004 field season in the Jumble Mountain – Ramsey Peak area has significantly expanded the area covered during the 2003 field season. Previous work concentrated on the area between northeast Jumble Mountain and Ramsey Peak, whereas work during the 2004 field season focused on the area further to the north, between Ramsey Peak and Oppy Lake. Results from work completed in this area during the 2003 field season are detailed in Mortensen *et al.* (2004).

In general, the area between Jumble Mountain and Oppy Lake consists of an eastward-younging succession of thick ignimbrites, intercalated with lesser marine sandstone and siltstone, mudstone, conglomerate and mafic lava flows near the base. Near Jumble Mountain, the section is cut by numerous mafic plugs, sills and dikes, which may be the source of these minor basaltic lava flows. Mafic flows are generally dark green to red, aphanitic and variably flow banded and brecciated, whereas the intrusive equivalents are dark green to grey and range from aphanitic to plagioclase±pyroxene±hornblende phyric basalt to andesite to microdiorite plugs. Mafic rocks in this area presumably represent the southern extent of the mafic eruptive centre in the Tsaydaychuz Peak – Butler Peak area, which lies directly along strike to the north.

Ignimbrites in this area are pink to purple to grey, massive, unstructured, poorly to mod-

erately welded, lithic and crystal rich, and range from tuff to lapilli tuff to tuff-breccia.

Sedimentary rocks are variably fossiliferous and consist of fine to coarse-grained feldspathic lithic wacke and calcareous lag deposits. Fossils present in the coquinas include a diverse assemblage of bivalve taxa, high-spined gastropods, rare belemnoids, and possibly mollusc fragments, most of which are thick-shelled and robust, and of shallow-marine forms that characterize the sublittoral region. Many shells have been abraded due to high-energy postmortem processes; this, coupled with a distinct grading and lateral continuity of shell beds, suggests that these beds represent storm deposits. The articulated nature of shells in some beds implies a rapid sedimentation rate. Ammonites recovered from this section during previous field seasons have been identified as probable Early Aalenian taxa (T.P. Poulton, personal communication, 2003), and a U-Pb zircon age of 176.6 ± 0.7 Ma was obtained from an overlying rhyolitic crystal-lithic tuff (R.M. Friedman, unpublished data; Mortensen *et al.*, 2004).

Volcanic composition changes to a more intermediate to felsic-dominated system farther upsection between Ramsey Peak and Oppy Lake, as evidenced by a decrease in mafic lavas and subvolcanic intrusions and a subsequent increase in intermediate to felsic ignimbrites and associated plugs and dikes. Ignimbrites range from tuff to lapilli tuff to tuff-breccia and are purple to pink to dark grey, massive, poorly to moderately welded, crystal- and lithic-rich, and typically 5–20 m thick. Several very coarse grained volcanic units within this section may represent vent-proximal and/or intracaldera facies. These coarse facies range from lapillistone to tuff-breccia to block tuff, and commonly include lapilli to block-size, chloritized pumice/fiamme. At least two anomalously thick tuffaceous units exist within this section, each of which includes a very thick, very densely welded facies. These units are homogeneous throughout their observed lateral extent, and are purple,



Figure 5. Tuffaceous mudstone sequence with possible syngenetic sulphide mineralization at Tesla Mountain. Rock hammer (~40 cm) for scale.

massive, very densely welded, rhyolitic±lithic crystal-vitric tuff to lapilli tuff, with unwelded and lithic and crystal-rich basal and upper contacts (Fig. 6). The calculated thickness of one of these units exceeds 400 m, a thickness that may also support an intracaldera or near-vent setting for rocks in this area.

As in the Tsaydaychuz Peak – Butler Peak region, primary volcanic units in this area commonly display a gradational upper contact, transitioning into lithic and crystal-rich wacke and mudstone units that, in turn, are sharply overlain by succeeding ignimbrite units. Sedimentary rocks in this package are dark maroon, thin to medium-bedded to massive, parallel-laminated to structureless mudstone to granule to pebble mudstone. Individual mudstone beds commonly contain up to 10% articulate to inarticulate armored accretionary lapilli up to 1 cm in diameter, which are interpreted to represent the erosional remains of a phreatoplinian eruption (Fig. 7). This section also contains several thick exposures of massive, matrix-supported, polymict, pebble to cobble conglomerate. Clasts are subangular to rounded and comprise a variety of rock types, including mafic to felsic lavas, hypabyssal intrusions and rare intermediate plutons. These conglomerate beds are massive and homogeneous, containing very few sedimentary structures. Rare parallel and locally cross-laminated sandstone lenses have been observed within these conglomerate sequences. Rocks within this volcanostratigraphic section are remarkably devoid of fossils and, where observed, fossil fragments are always associated with very coarse grained facies.

Field mapping for this study terminated at the ridgeline 3.5 km north of Ramsey Peak, approximately 4 km southwest of Oppy Lake; however, this homoclinal volcanosedimentary succession extends at least as far as Oppy Lake, where Late Bathonian or Early Callovian fossils have been recovered (H. Frebald, unpublished data).



Figure 6. Densely welded rhyolitic ignimbrite unit within the upper Ramsey Peak section. This ~400 m thick unit may represent an intracaldera facies. Pencil (~8 cm) for scale.

RIVERS PEAK AND MOUNT PRESTON AREAS

The Rivers Peak – Mount Preston area consists of an isolated west-dipping block that is presumably separated from the Tesla Mountain block to the south by a fault beneath Tesla Lake, and from the Mount Pondosey massif to the west by a north-trending structure that forms the Pondosey Pass and South Creek topographic low (Fig. 2). A U-Pb zircon age of 176.3 ± 3.3 Ma from a rhyolite lapilli tuff near the base of the section southeast of Mount Preston, together with a U-Pb zircon age of 175.4 ± 0.9 Ma from the top of the section immediately south of Mount Preston, indicates that volcanogenic strata in this area are coeval with strata in the Jumble Mountain region. Broad-scale volcanostratigraphic similarities between the two areas reinforce this correlation. Specifically, rock types in the Rivers Peak – Mount Preston area are consistent with those documented in the north Ramsey Peak area, which lies along strike 30 km to the south.

Rocks in this area are characterized by coarse-grained, intermediate to felsic volcanic facies and minor intercalated sedimentary rocks, which increase in abundance and eventually predominate over ignimbrite units near the top of the section south of Mount Preston. Primary volcanic units in this area include andesitic to rhyolitic lapilli tuff to tuff-breccia units that are pink to purple to maroon in colour, thick and massive, poorly to moderately welded, and notably lithic and crystal-rich. Sedimentary rocks consist of maroon mudstone to granule to pebble mudstone and lesser feldspathic lithic wacke intercalated with thin (10–30 cm thick) lithic- and crystal-rich chloritic lapilli tuff sequences. These intermediate composition tuff units are spatially and temporally associated with, and may be the eruptive source of, ballistic blocks that produce block sag structures within several mudstone horizons in this area. Northeast of Rivers Peak, a thin, thinly bedded limestone

unit is immediately overlain by a 25 m thick section of massive, unstructured, very coarse grained, quartz-eye feldspathic sandstone (Fig. 8). Quartz and plagioclase grains are euhedral to subrounded and broken, respectively, and are assumed to represent detritus shedding off a proximal rhyolite flow or granitic pluton. Rare (<1%), subangular to rounded, aphanitic mafic to intermediate and quartz-phyric rhyolite clasts occur along the base of this unit. This anomalous sandstone unit is laterally discontinuous, and may be infilling a paleovalley or channel. A collection of marine fossils recovered from a calcareous sandstone unit near the summit of Rivers Peak is currently being examined to provide additional age constraints for this section and to assist in determining the environment of deposition.

Sedimentary rocks dominate in the Mount Preston area, where they are characterized by maroon mudstones intercalated with lesser rhyolitic lapilli tuff and mafic to intermediate flows and sills. The top of the section in this

area is marked by a thick, purple, massive, very densely welded rhyolite lapilli tuff unit, which may correlate regionally with one of the aforementioned units observed in the Ramsey Peak area.

Southeast of Mount Preston, near the base of the measured section in the area, mudstones and lesser rhyolitic tuffs are intercalated with a series of plagioclase-phyric to aphyric, variably amygdaloidal basalt to basaltic andesite flows, pillow lavas and broken pillow breccia, which are intruded by an aphanitic basaltic plug. These basaltic pillow lavas are intruded by a dacitic to rhyodacitic flow-dome complex with a well-developed carapace breccia (refer to Mortensen *et al.*, 2004 for photograph). Geological mapping in this area during the 2004 field season has demonstrated the existence of numerous other extrusive felsic (dacitic to rhyolitic) domes in this area. The domes are highly fractured and silicified, with well-developed carapace breccias, and are aphanitic to sparsely quartz phyric. Geochemical analysis of several dome samples yielded 68–98% silica; this high degree of silicification makes the domes more resistant to weathering than local country rock, and they subsequently form round knobs along a linear outcrop belt. The linear distribution of these domes follows the trace of an east-trending extensional fault south of Mount Preston. This fault is characterized by zones of intense fracturing with abundant slip surfaces, and well-developed ferricrete overlying fault breccia. It may represent a synvolcanic extensional structure — a zone of weakness through which the spatially and potentially temporally associated rhyolite domes were intruded. A small granite stock intrudes the fault-dome sequence; this intrusion is lithologically similar to a suite of ca. 148–149 Ma plutons mapped to the south in the northeastern Bella Coola map sheet (Fig. 9). Uranium-lead dating studies of felsic dome samples and this granite stock are currently underway, and will assist in constraining the age of this extensional structure.

The Pond – Rivers Peak mineral occurrence in this area (BC MINFILE 093E 058) and impressive gossans developed south of Mount Preston are characterized by finely disseminated pyrite, and occur in wallrocks immediately adjacent to this structure. Small (centimetre-scale) bodies of chalcopyrite±bornite-bearing vein breccia were observed in several areas in the Mount Preston – Rivers Peak area.

YOUNGER MAGMATISM

The upper Ramsey Peak section is cut by a small pyroxene-hornblende quartz diorite stock, which is texturally and compositionally similar to other small dioritic stocks documented throughout the field area. Argon-argon (hornblende) dating of this pluton indicates an age of 136.4 ± 1.5 Ma, which is temporally consistent with a ca. 139–132 Ma intrusive suite documented immedi-

ately to the south in the Bella Coola area (T.D. Ullrich, unpublished data; Haggart *et al.*, 2004).

The entire field area is cut by numerous grey-green, centimetre- to metre-scale (up to 10 m in width), aphanitic to plagioclase±pyroxene±hornblende-phyric basalt to andesite dikes. These dikes are typically randomly oriented but are locally consistently oriented where they intrude local fracture sets and faults; one such dike swarm has been observed at Butler Peak. The aforementioned quartz diorite pluton at Ramsey Peak is cut by these dikes, suggesting that these dikes are at least partly post-ca. 136 Ma, and therefore represent a younger magmatic event in the area.

The upper Mount Preston volcanostratigraphic section is cut by a biotite-quartz-phyric rhyolite porphyry dike, which has been dated (Ar-Ar biotite) at 51.87 ± 0.79 Ma (T.D. Ullrich, unpublished data). This Early Eocene age is interpreted to represent the youngest magmatic event within the study area, and suggests correlation with the Ootsa Lake Group, which is diffusely exposed throughout the eastern half of the Whitesail Lake map sheet.

GEOCHRONOLOGY

In addition to the four U-Pb and Ar-Ar dates completed from samples collected during the 2003 field season (several samples yielded insufficient zircon for dating), 15 samples collected throughout the study area in the 2004 field season are currently in the mineral-separation stage for U-Pb zircon dating.

Several rhyolite tuff samples from the study area are being dated, which will assist in constraining the age range for each measured volcanostratigraphic section. A number of rhyolitic intrusive (?) and extrusive dome samples from the Rivers Peak and Butler Peak areas are being dated to de-



Figure 7. Articate armored accretionary lapilli in rhyolitic vitric-lithic crystal tuff in the Ramsey Peak area. Accretionary lapilli are quite common throughout the entire field area, and occur as primary and reworked fragments within maroon mudstone and fine-grained tuffaceous units. Rock hammer for scale. Field of view is approximately 30 cm.

termine if the domes represent synvolcanic intrusions. A sample of microdiorite from the Butler Peak andesitic complex may help constrain the age of the thick pile of mafic lavas and subvolcanic intrusions in this area. Detrital zircons studies from one or more sandstones throughout the field area, including the quartz-eye feldspathic sandstone from the Rivers Peak section, may provide controls on the source regions that were eroding during the Middle Jurassic.

LITHOGEOCHEMISTRY

Geochemical studies of volcanic rock units from the northeastern Bella Coola – southeastern Whitesail Lake map area are underway to characterize the geochemical affinity of Middle Jurassic Hazelton Group volcanic rocks in this area and place constraints on the paleotectonic setting in which they were emplaced.

Complete major, trace and rare earth element analyses have been obtained from 64 representative samples of lava flows, ignimbrites, intrusive and extrusive domes, sills, dikes and hypabyssal intrusions from the study area. Geochemical analyses from samples collected in the 2004 field season have only recently been obtained, and have not yet been examined in detail. These new data and the analyses from the study area completed in 2003, together with reconnaissance data from host volcanic rocks at the Nifty VMS occurrence in the east-central Bella Coola map area (e.g., Ray *et al.*, 1998) are shown on several geochemical discriminant plots in Figure 10. Mafic dike samples are not included on these discriminant plots.

Volcanic and subvolcanic rock units in the northeastern Bella Coola – southeastern Whitesail Lake map area geochemically resemble the broadly age equivalent Middle Jurassic host volcanic rocks at the Nifty VMS occurrence, which is on strike to the southeast. When plotted on a TAS diagram, samples from the study area are moderately bimodal in composition (mainly basaltic to basaltic andesitic and dacitic to rhyolitic); however, on a discriminant plot of immobile trace element ratios (Nb/Y vs. Zr/TiO₂), the samples span the basaltic to rhyolitic compositional range, and the Nifty samples show a distinctly higher Nb/Y ratio than do samples from the current study area. The felsic units are all subalkaline, but the mafic units include both subalkaline and alkaline compositions. On an AFM diagram, the Nifty samples and the felsic intrusive and extrusive samples from the study area are calcalkaline to transitional in composition, whereas mafic intrusive and extrusive samples from the study area fall almost exclusively into the tholeiitic field. A plot of Rb vs. Y+Nb suggests that all of the volcanic rocks formed in a volcanic-arc setting; however, immobile trace element plots such as V vs. TiO₂ indicate that the mafic volcanic and subvolcanic units from the study area include both island-arc tholeiites and back-arc tholeiites.



Figure 8. Very coarse-grained quartz-eye feldspathic sandstone in the Rivers Peak area. Gritty-looking regions comprise euhedral to subrounded and broken quartz and plagioclase. Rusty orange and green, more coherent splotches comprise aphanitic, mafic to intermediate volcanic clasts that occur near the base of this unit. Pencil (~8 cm) for scale.

These mixed volcanic-arc–back-arc geochemical signatures are very similar to those described by Barrett and Sherlock (1996) at Eskay Creek, and are consistent with an overall rifted arc (intra-arc or back-arc) setting.

ALTERATION AND IMPLICATIONS FOR VMS POTENTIAL

Mafic rocks throughout the entire study area have undergone a high degree of alteration, which is characterized by pervasive epidotization in basaltic and basaltic andesitic flows, plugs, dikes and sills. The resulting epidosite occurs as large (up to 1 m in diameter) clots, and is commonly spatially associated with intense quartz and epidote-veining and large jasperite clots, and may reflect semiconformable, synvolcanic alteration above a subvolcanic intrusion. Although no Middle Jurassic intrusions have been recognized within the study area, at least one Middle Jurassic pluton has been identified, ~30 km to the west-southwest: the Trapper Pluton is a large (exposed over 200 km³), coarse-grained granite pluton with a U-Pb zircon age of 177.4 ± 0.7 Ma (P. van der Heyden, unpublished data; Fig. 2; for more details, see Mahoney *et al.*, this volume). We speculate that the Trapper and possibly other coeval intrusions that are not exposed at the present level of erosion may have been subvolcanic equivalents of the locally abundant rhyolitic ignimbrite units that have been recognized throughout the study area and yielded similar U-Pb zircon ages. These intrusions may have driven hydrothermal circulation that produced widespread, semiconformable alteration (characterized by development of epidosite and jasperoid) in more permeable portions of the sequence.

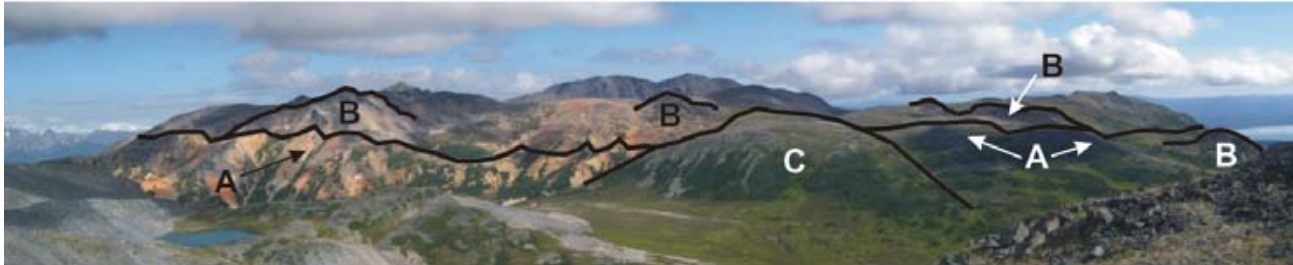


Figure 9. View to the north toward Mount Preston (not visible) from the north Rivers Peak region. The trace of an east-trending extensional fault is indicated by (A), which may represent a synvolcanic extensional structure along which Jurassic (?) rhyolite domes (B) intruded. (C) represents a small biotite-hornblende granite stock that intrudes Jurassic volcanogenic strata in the area. Width of image is ~5 km.

Specific results of our study that emphasize the high potential for VMS mineralization in Hazelton Group volcanogenic strata in the Bella Coola – Whitesail Lake map areas include 1) the linear arrangement of extrusive felsic domes; together with 2) indications of a synvolcanic extensional structure in the Rivers Peak – Mount Preston area; 3) evidence for shallow water, submarine deposition, as indicated by specific fossil assemblages, sedimentary structures and pillow lavas; 4) the presence of known Middle Jurassic syngenetic (e.g., Nifty) and epigenetic mineral occurrences (e.g., Mortensen, this volume); 5) stratiform pyrite occurring locally within tuffaceous mudstones at Tesla Mountain; and 6) widespread epidosite clots that may reflect semiconformable alteration above a buried subvolcanic intrusion.

ONGOING RESEARCH

Ongoing research for this study includes: (1) compilation of detailed measured volcanostratigraphic sections; (2) petrographic studies of volcanic and sedimentary rocks from the study area; (3) processing of U-Pb samples collected during the 2004 field season; (4) detailed lithochemical comparisons with other Hazelton Group suites available from throughout Stikinia and volcanic hostrocks for the Eskay Creek deposit; and (5) studies of the specific volcanologic, sedimentologic, and large scale tectonic processes operating during deposition of Middle Jurassic Hazelton Group rocks in this area.

ACKNOWLEDGMENTS

Danny Hodson of Rainbow West Helicopters provided outstanding helicopter support during the 2004 field season. We thank Jim Haggart and the Geological Survey of Canada for providing mapping expertise and logistical sup-

port for the mapping project. David Gale of the Barrick Gold Corporation provided an excellent and informative tour of the Eskay Creek mine and vicinity. We thank Jim Haggart, Larry Diakow, Lori Snyder, Glenn Woodsworth, Margi Rusmore, Bob Anderson and Kirstie Simpson for valuable ongoing discussions about Hazelton Group volcanostratigraphy and volcanological and sedimentological processes. Chris Kohel, Emily Hauser and Joe Nawikas provided excellent assistance in the field. Funding for this project was provided by the Rocks to Riches Program, which is administered through the British Columbia and Yukon Chamber of Mines, as well as four mining companies (Barrick Gold Corp., Heritage Exploration Inc., Kenrich-Eskay Mining Corp. and Placer Dome Inc.). Rich Friedman provided a helpful review of the manuscript and assistance with U-Pb dating. Argon-argon dating was carried out by Tom Ullrich of the Pacific Centre for Isotopic and Geochemistry Research (PCIGR).

REFERENCES

- Barrett, T.J. and Sherlock, R.L. (1996): Geology, lithochemistry and volcanic setting of the Eskay Creek Au-Ag-Cu-Zn deposit, northwestern British Columbia; *Exploration and Mining Geology*, Volume 5, pages 339–368.
- Diakow, L.J., Mahoney, J.B., Gleeson, T.G., Hruddy, M.G., Struik, L.C. and Johnson, A.D. (2002): Middle Jurassic stratigraphy hosting volcanogenic massive sulphide mineralization in eastern Bella Coola map area (NTS 093/D), southwest British Columbia; in Geological Fieldwork 2001, *BC Ministry of Energy, Mines and Petroleum Resources*, Paper 2002-1, pages 119–134.
- Diakow, L.J., Mahoney, J.B., Haggart, J.W., Woodsworth, G.J., Gordee, S.M., Snyder, L.D., Poulton, T.P., Friedman, R.M. and Villeneuve, M. (2003): Geology of the eastern Bella Coola map area (93D), west-central British Columbia; in Geological Fieldwork 2002, *BC Ministry of En-*

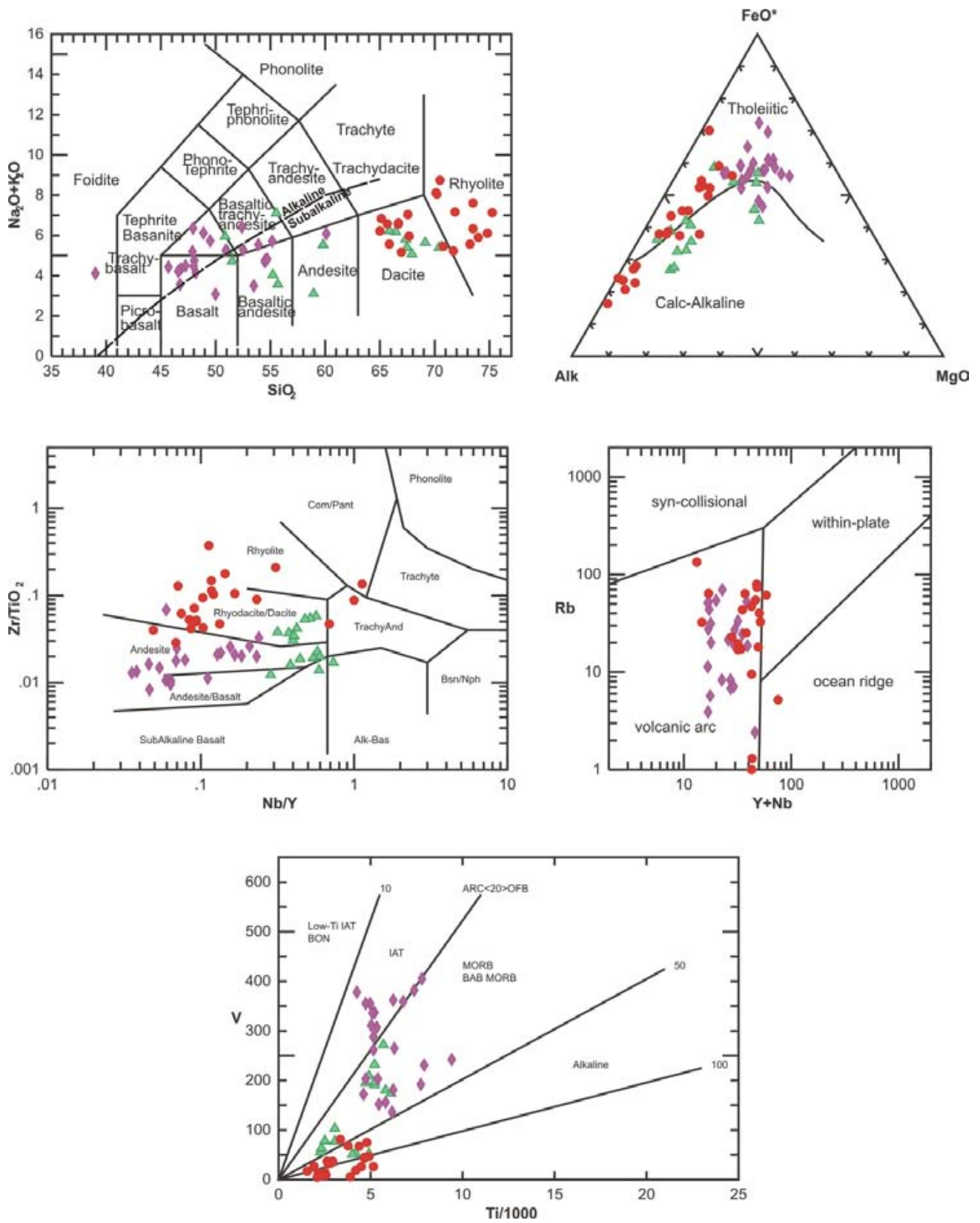


Figure 10. Geochemical discriminant diagrams for volcanic and hypabyssal rocks in the northeastern Bella Coola – southeastern Whitesail Lake map area. Diamonds indicate mafic to intermediate lava flows and plugs, and circles indicate intermediate to felsic lava flows, ignimbrites and plugs. Triangles represent analyses of mafic to felsic samples from the vicinity of the Nifty prospect (data from Ray *et al.*, 1998).

- ergy, *Mines and Petroleum Resources*, Paper 2003-1, pages 65–75.
- Duffell, S. (1959): Whitesail Lake map-area, British Columbia; *Geological Survey of Canada*, Memoir 299, 119 pages.
- Haggart, J.W., Diakow, L.J., Mahoney, J.B., Struik, L.C., Woodsworth, G.J. and Gordee, S.M. (2004): Geology, Bella Coola area (parts of 93D/01, 93D/02, 93D/06, 93D/07, 93D/08, 93D/09, 93D/10, 93D/11, 93D/15 and 93D/16), British Columbia; *Geological Survey of Canada*, Open File 4639; *BC Ministry of Energy and Mines*, Open File 2004-13, scale 1:150 000.
- Haggart, J.W., Mahoney, J.B., Diakow, L.J., Woodsworth, G.J., Gordee, S.M., Snyder, L.D., Poulton, T.P., Friedman, R.M. and Villeneuve, M.E. (2003): Geological setting of the eastern Bella Coola map area, west-central British Columbia; *Geological Survey of Canada*, Current Research 2003-A4, 9 pages.
- Marsden, H. and Thorkelson, D.J. (1992): Geology of the Hazelton volcanic belt in British Columbia; implications for the Early to Middle Jurassic evolution of Stikinia; *Tectonics*, Volume 11, pages 1266–1287.
- Mortensen, J.K., Gordee, S.M., Mahoney, J.B. and Tosdal, R.M. (2004): Regional studies of Eskay Creek-type and other volcanogenic massive sulphide mineralization in the upper Hazelton Group in Stikinia: preliminary results; in *Geological Fieldwork 2003*, *BC Ministry of Energy and Mines*, Paper 2004-24, pages 249–262.
- Ray, G.E., Brown, J.A., Friedman, R.M. and Cornelius, S.B. (1998): Geology of the Nifty Zn-Pb-Ba prospect, Bella Coola district, British Columbia; in *Geological Fieldwork 1997*, *BC Ministry of Energy, Mines and Petroleum Resources*, Paper 1998-1, pages 20-1–20-28.
- Thorkelson, D.J., Mortensen, J.K., Marsden, H. and Taylor, R.P. (1995): Age and tectonic setting of Early Jurassic episodic volcanism along the northeastern margin of the Hazelton Trough, northern British Columbia; in *Jurassic Magmatism and Tectonics of the North American Cordillera*; Miller, D.M. and Busby, C., Editors, *Geological Society of America*, Special Paper 299, pages 83–94.
- Tipper, H.W. (1979): Jurassic stratigraphy of the Whitesail Lake map area, British Columbia; in *Current Research, Part A*, *Geological Survey of Canada*, Paper 79-1A, pages 31–32.
- Tipper, H.W. and Richards, T.A. (1976): Jurassic stratigraphy and history of north-central British Columbia; *Geological Survey of Canada*, Bulletin 270, 73 pages.
- Wheeler, J.O. and McFeely, P. (1991): Tectonic assemblage map of the Canadian Cordillera and adjacent parts of the United States of America; *Geological Survey of Canada*, Map 1712A, scale 1:2 000 000.
- Woodsworth, G.J. (1980): Geology of Whitesail Lake (93E) map area, British Columbia; *Geological Survey of Canada*, Open File 708, scale 1:250 000.

Helicopter-borne Gamma-Ray Spectrometric and Magnetic Surveys, Central British Columbia, 2004: Status Report

By R.B.K. Shives¹

KEYWORDS: Quesnel mineral belt, Quesnel trough, Horsefly, Mount Milligan, airborne multisensor geophysical survey, radiometric, gamma-ray, magnetic

INTRODUCTION

Helicopter-borne multisensor (gamma-ray spectrometer, magnetometer) geophysical surveying continued in central British Columbia in 2004, funded by the Rocks to Riches Program and a consortium of industry partners. Surveys were completed in the Mount Milligan (Area 1 in Figure 1) and Horsefly – Little Fort areas of the Quesnel mineral belt. Results of these surveys will be released to the public in the late spring of 2004. Additional surveying was planned but was not completed, and has been rescheduled for completion in summer 2005. The industry-funded survey locations are also indicated in Figure 1, generalized to respect confidentiality.

Fugro Airborne Surveys carried out the work under contract to the Geological Survey of Canada. The overall purpose of the surveys is to provide modern, high-definition radiometric and magnetic data that can be used in the assessment and development of targets for mineral exploration, and to assist future bedrock and surficial mapping.

RATIONALE

These areas lie within the Quesnel Terrane and are highly prospective for discovery of alkalic porphyry copper-gold and related deposits, but exploration and mapping have been inhibited by subdued topography, tree cover and extensive glaciofluvial deposits. The surveys will provide new geochemical-geophysical information to support improved geological knowledge and mineral exploration, by fingerprinting geological units and defining new targets within and beneath the locally thick cover. A summary of the regional geology, exploration history and mineral potential of the central Quesnel trough is provided by Cathro *et al.* (2004).

The combined radiometric and magnetic data are useful in identifying potassic alteration and magnetite enrichment

or depletion zones, which commonly accompany copper-gold porphyry systems. The same geophysical information can be a valuable tool in geological mapping and identifying rock types and structures. The overall goal is to provide new, high-quality geophysical data that will stimulate exploration investment.

METHODS

The surveys are flown using an Aerospatiale AS350 helicopter. Flight-path information is recovered using a postflight differential Global Positioning System. A vertically mounted video camera is used for verification of the flight path. Traverse lines are flown at various line spacings, from 150 to 500 m, with magnetic control lines every 1500 to 4000 m. Helicopter altitude is maintained at an average ground clearance of 135 m. The gamma-ray spectrometry data are recorded at a 1.0 second sample rate using a 256-channel Exploranium GR820 spectrometry system with 33.6 litres of downward-looking and 4.2 litres of upward-looking sodium-iodide detectors. The aeromagnetic data are recorded at a 0.1 second sample rate using a 0.01 nT split beam line cesium-vapour magnetometer housed in a forward mounted stinger.

Measured and computed data include eight radiometric parameters (ternary, total count, K, eU, eTh, and ratios eU/eTh, eU/K, eTh/K) and two magnetic parameters (total field and calculated magnetic vertical gradient). The contractor will process the data and prepare final maps and digital data to NATGAM standards. Where appropriate, the new data will be merged with the existing NATGAM surveys in the Mount Polley, Horsefly and Mount Milligan areas.

RESULTS TO DATE

The airborne survey contract was awarded to Fugro Airborne Surveys, Mississauga, Ontario, following a competitive bidding process through Public Works and Government Services Canada (PWGSC). The Radiation Geophysics Section (RGS), Geological Survey of Canada, is providing the technical expertise and contract supervision for this project.

A total of 14 090 line km of surveying have been planned, based on a total of \$786 000 (\$280 000 Rocks to Riches and \$506 000 combined industry funding). Approx-

¹Radiation Geophysics Section, Geological Survey of Canada, Ottawa

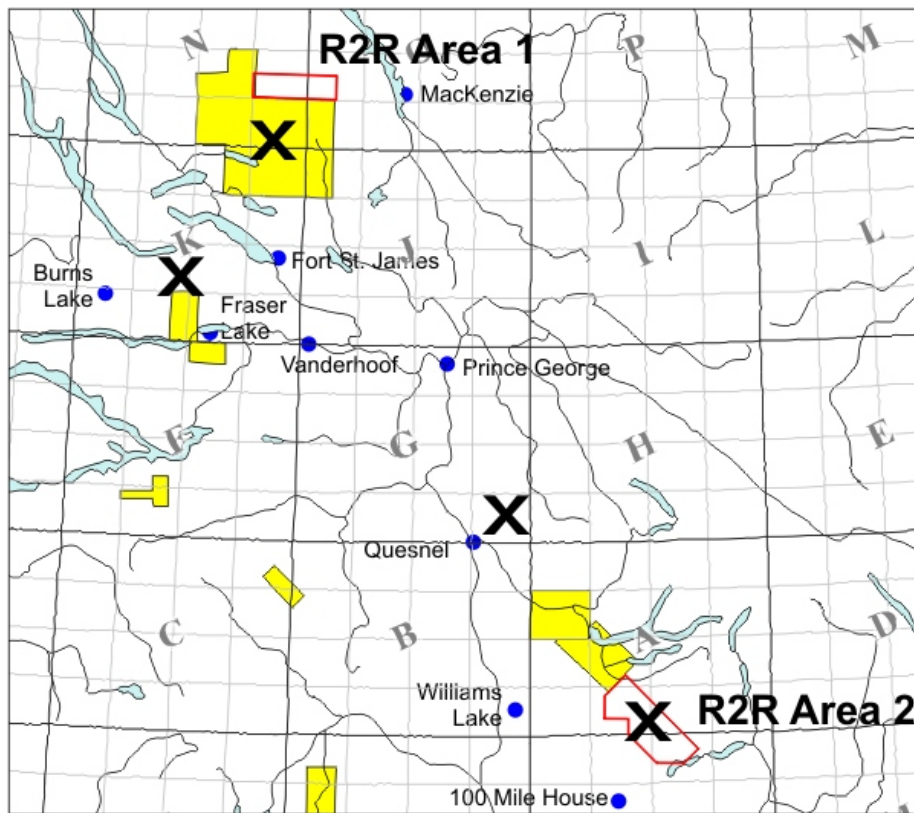


Figure 1: Location of Rocks to Riches funded survey blocks (open polygons in R2R Areas 1 and 2). The black “x”s indicate only generalized locations of industry partner surveys.

imately one-third of the total surveying was completed in the 2004 field season, in three of several survey blocks. The data collected will be released in various formats, similar to the Toadogone and Horsefly surveys flown in 2003: a) on MapPlace on April 1, 2005, as grid images; b) as paper map Open Files in spring or early summer of 2005; c) as digital images of those maps in PDF format, in spring or summer of 2005.

Surveying will recommence under the same Fugro contract in late June or early July 2005, depending on field conditions. This startup period will support completion of all flying before the end of the summer. These results from

this portion of the survey program will follow a similar publication schedule and format as above, in 2006.

REFERENCES

- Cathro, M.S., Lane, R.A., Shives, R.B.K. and McCandless, P.M. (2004): Airborne multisensor geophysical surveys in the central Quesnel mineral belt; in *Geological Fieldwork 2003, BC Ministry of Energy and Mines*, Paper 2004-1, pages 185–188.

Kimberlite Indicator Minerals in the Fort Nelson Area, Northeastern British Columbia

By G.J. Simandl¹, T. Ferbey², V.M. Levson², T.E. Demchuk², S. Mallory¹, I.R. Smith³ and I. Kjarsgaard⁴

ABSTRACT

Parts of northeastern British Columbia are underlain by Precambrian basement that belongs to the North American craton. These areas have a moderate exploration potential for diamonds in terms of the traditional 'diamondiferous mantle root model'. The potential of any area to host kimberlite or lamproite-hosted diamond deposits may be assessed based on the thickness and age of basement rocks, geophysical anomalies and other data sets including the presence of kimberlite indicator minerals (KIMs) in Quaternary sediments. This study concentrates mainly on KIMs presence in Late Pleistocene glaciofluvial sands and gravels. Of the 20 samples collected and processed, 14 contain KIMs such as purple pyrope, yellowish eclogitic garnet, Cr-diopside, olivine, ilmenite or spinel. It is probable that some of these KIMs were derived from primary and secondary sources within the Fort Nelson area, however others may have been transported to the Fort Nelson area from the Northwest Territories and Alberta by Late Pleistocene glacial and/or glaciofluvial systems. Corundum and diaspore were also recovered from collected samples. At this stage, semiquantitative data do not allow for a definitive interpretation as to whether this corundum is kimberlite-related.

INTRODUCTION

Rich deposits of high-quality diamonds have been documented within the Slave Craton of Northwest Territories (Carlson *et al.*, 1999; Lockhard *et al.*, 2004), approximately 600 km northeast of the Fort Nelson area. Several of these deposits are currently being mined or are under development. Primary diamond deposits have been discovered in the Buffalo Head Terrane in neighbouring Alberta (Eccles, 2002; Hood and McCandless, 2004), approximately 400 km southeast of the Fort Nelson area. Several alluvial diamond occurrences have been also reported in the literature (Fig. 1). Recently, indicator minerals and diamonds, in association with gem-like corundum, were reported in

surficial material of the Blackwater Lake area, located in the western sector of the Northwest Territories, some 600 km north of the Fort Nelson area (Dow, 2003, 2004).

Diamond occurrences have been reported in British Columbia's Alkaline province, as shown in Figure 1. (Northcote, 1983a, b; Pell 1994; Anonymous, 1994; McCallum, 1994; Allan, 1999, 2002; Roberts, 2002). The similarities between the geological settings of northern Alberta and northeastern British Columbia, and the findings in past research indicate that there is potential for primary (kimberlite, lamproite, or lamprophyres-hosted) and/or secondary (placer or paleoplacer in the Paleozoic sedimentary sequence) diamond occurrences in British Columbia. Documented diamond occurrences in British Columbia have been summarized by Simandl (2004).

The main objective of this study is to examine glaciofluvial sands and gravels for the presence of kimberlite indicator minerals (KIMs) in the Fort Nelson area. A second paper, to be released later this year will contain results of 50 additional samples collected as far as 200 km west and 350 km south of the Fort Nelson area, from Muncho Lake Park to Dawson Creek.

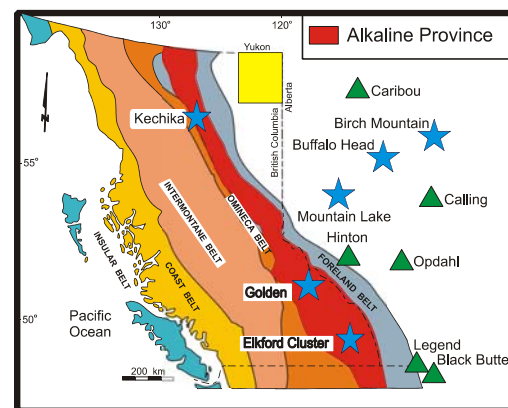


Figure 1. Location of study area (in yellow). Known primary (star) and secondary (triangle) diamond occurrences in British Columbia and Alberta are also provided. Crossing Creek diatreme, within the Elkford cluster, is the only confirmed kimberlite in British Columbia (modified from Simandl, 2004).

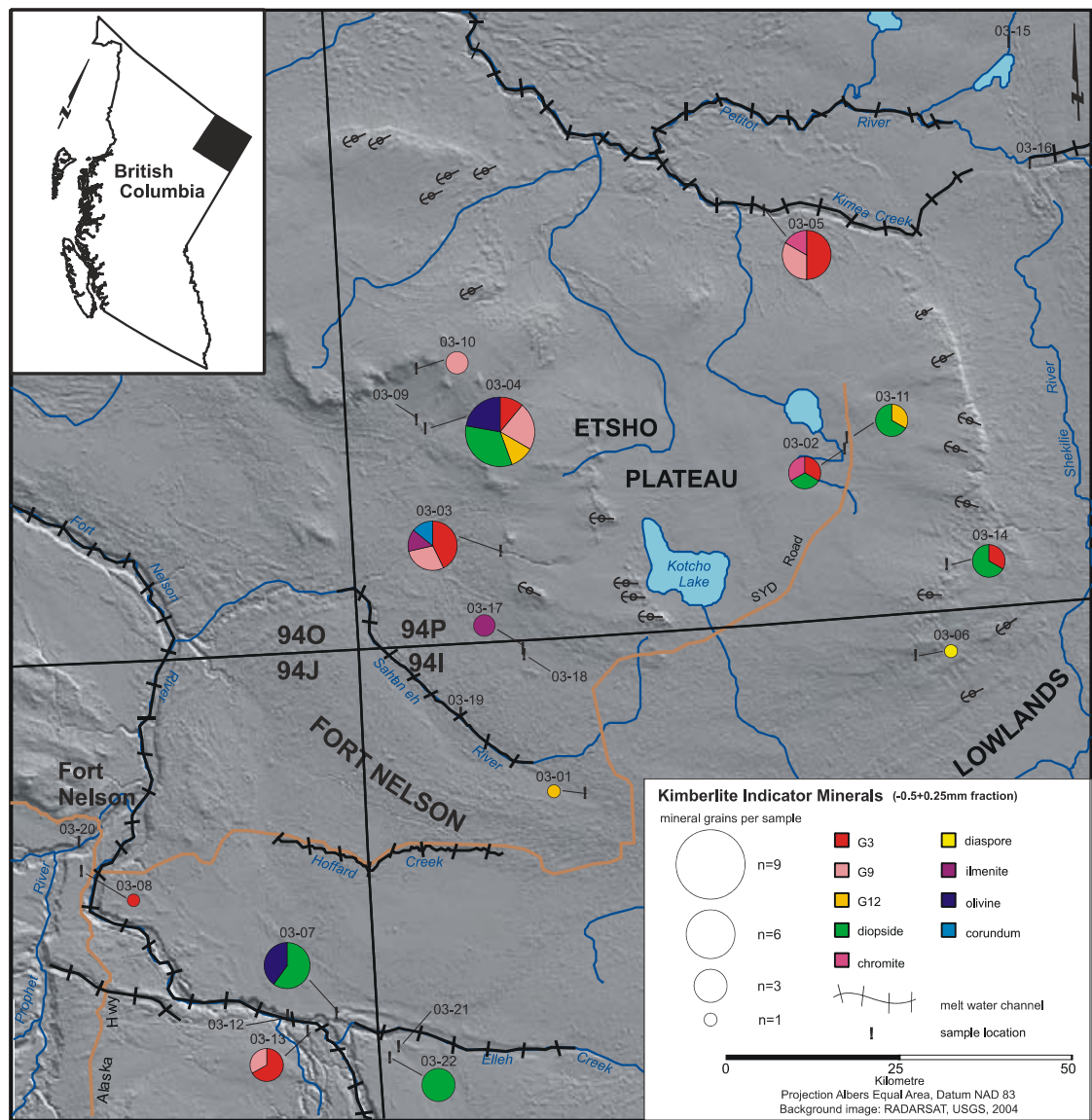


Figure 2. Location of glaciofluvial samples. Samples with kimberlite indicator minerals (KIMs) are shown; grain counts for each mineral type in brackets. Regional ice-flow directions, and orientations of major meltwater channel systems are provided.

LOCATION AND PHYSIOGRAPHY

The study area is located northeast of Fort Nelson, and is included in portions of NTS map areas of 094I/north, 094P and 094J/northeast (Fig. 2). The majority of the study area occurs within the Fort Nelson Lowlands physiographic region which is a subdivision of the Interior Plains (Holland, 1976).

This area is characterized by flat to subdued topography, which is an expression of the horizontally to subhorizontally bedded

sedimentary rocks that underlie the region. The combination of low-relief topography and clay-rich soils results in poor drainage, and a shallow water table is present in most areas. Small shallow lakes and narrow, often meandering, low-gradient streams are common. However, larger river systems, such as the Fort Nelson, Prophet, and Petitot rivers, occur in the region.

In contrast to the lowlands, the Etsho Plateau stands approximately 700 m above sea level (Fig. 2). This feature forms a broad topographic high, 140 km long by 80 km wide,

that trends roughly northwest. The plateau rises up to 300 m above the surrounding Fort Nelson Lowlands and is thought to be an outlier of the Alberta Plateau (Holland, 1976).

BEDROCK GEOLOGY

Precambrian Basement

Parts of British Columbia east of the Rocky Mountain Trench system and the alkaline province, including the Fort Nelson area, are underlain by a Precambrian basement that belongs to the North American craton (Hoffman, 1988, 1989, 1991; Ross *et al.*, 1991, 1995; Villeneuve *et al.*, 1993). This basement may contain kimberlite or lamproite-hosted diamond occurrences (Simandl, 2004). The boundaries of individual basement terranes are based largely on geophysical interpretation, geological extrapolation and isolated radiometric ages (Pilkington *et al.*, 2000). One of these basement terranes, commonly referred to as Archean Nova Terrane, is located south and southeast of the Fort Nelson study area and is believed to be of Archean age.

There are not enough isotopic dates to confirm the prevailing hypothesis that the Nova Terrane is a slice of Archean Slave craton. Zircons recovered from Penn West's borehole Numac Septimus 7-27-81-18 suggest that the Nova Terrane may be related to Buffalo Head Hill Terrane (Simandl and Davis, 2005), indicating that the current basement subdivision is unreliable at best. It is possible that some of the basement terranes currently located in northeastern British Columbia were previously associated with a deep crustal keel (Simandl, 2004). Such keels are characterized by old, thick and stable cratons, as illustrated by the 'Diamondiferous Mantle Root' model, described by Haggerty (1986), Mitchell (1991), Kirkley *et al.* (1991), and Helmstaedt and Gurney (1995), and commonly used to explain Clifford's rule (Janse, 1994). Such roots however, may have since been destroyed.

Most kimberlite pipes in the Northwest Territories were emplaced between 45 and 75 Ma (Lockhart *et al.*, 2004). Within the Lac de Gras area, pipes with the highest diamond potential seem to be restricted to periods of emplacement of 51 to 53 Ma and 55 to 56 Ma (Creaser *et al.*, 2004). In northern Alberta,

radiometric ages of kimberlite emplacement range from 70.3 ± 1.6 Ma to 88 ± 5 Ma (Eccles *et al.* 2004). The radiometric ages of lamprophyres, lamproites and kimberlites within the British Columbia alkaline province vary from 391 ± 12 Ma for HP pipe to approximately 240 Ma (Smith *et al.*, 1988; Pell, 1994). It is possible that pipes of similar age to those listed above cut comparable or older stratigraphic levels in northeastern British Columbia.

Mesozoic Rocks

Bedrock outcrops in the study area are rare except along stream cuts and in some excavations on the Etsho Plateau. The Fort Nelson Lowlands are predominantly underlain by marine shales of the Shaftsbury Formation, part of the Lower Cretaceous Fort St. John Group. These shales are dark grey and flaky to fissile, and are interpreted to have been deposited in a prodelta or shelf environment during a transgression of an embayment in Early Cretaceous time (Thompson, 1977). These rocks are part of the Blaimore foredeep clastic wedge tectonic assemblage (Journeay *et al.*, 2000).

Directly overlying the Fort St. John Group, and forming the resistive cap of the Etsho Plateau, are sandstones of the Duvegan Formation, of the Upper Cretaceous Smoky Group. On the Etsho Plateau these sandstones are mainly fine grained; however elsewhere in northeastern British Columbia, the Duvegan Formation ranges from clay-rich shales and mudstones to boulder conglomerates. This variability is attributable to the contrasting deltaic and prodeltaic depositional environments in which these rocks are interpreted to have been deposited during a regressive cycle. The contact between the Dunvegan and Shaftsbury formations is gradational and consists of sandy siltstones and fine-grained sandstones interbedded with silty shales (Thompson, 1977; Stott, 1982). The stratigraphy and sedimentology of the Dunvegan Formation have recently been discussed in detail by Plint *et al.* (2001), Plint (2002), and Plint and Wadsworth (2003). These rocks are part of the Trevor wedge tectonic assemblage (Journeay *et al.*, 2000).

SURFICIAL GEOLOGY

The dominant surficial materials in the study area are silt and clay-rich morainal deposits. They typically occur at the surface in better-

drained forested areas, and are overlain by organic materials and/or glaciolacustrine sediments in poorly drained areas. Moraine landforms include low-relief plains, crevasse-squeeze ridges, flutes and rolling, recessional and interlobate moraines (Levson *et al.*, 2004). Quaternary studies on the Alberta side of the border have described similar surficial materials and glacial features (e.g., Plouffe *et al.*, 2004; Paulen *et al.*, in press; Smith *et al.*, in press).

Glaciofluvial landforms are relatively uncommon in the region, although eskers, kames, fans, deltas and terraces can occasionally be observed. Most of the larger terrace features occur within the Kimea Creek – Petitot River meltwater channel system (Fig. 2). Other large meltwater channel systems occur in the study area (e.g., Fort Nelson River, Elleh Creek) and contain elevated glaciofluvial landforms that are thought to be ice proximal and/or subglacial in origin. Glaciofluvial sands and gravels were locally deposited in smaller meltwater channel systems (e.g., Hoffard Creek), although many of these systems appear to be almost entirely erosional and may have formed subglacially (Levson *et al.*, 2004). Irrespective of type and size of glaciofluvial landform, the presence of clast rock types from the Precambrian Shield (red and pink granites and gneisses) indicate that these glaciofluvial sands and gravels have an eastern provenance, or are derived from tills with an eastern provenance.

Quaternary History

During the Late Pleistocene (after 25 000 years BP), the Laurentide ice sheet advanced westward up the regional slope into northeastern British Columbia. The region was covered by ice during the glacial maximum. The configuration of advancing and retreating ice fronts was complex, as indicated by crosscutting relationships observed in large-scale landforms (e.g., flutes, crag and tail landforms and recessional moraines).

The regional ice-flow record is preserved almost exclusively in flutes and crag-and-tail ridges that occur on, and along, the periphery of the Etsho Plateau (Fig. 2). Although, in general terms, the Laurentide ice sheet moved into the region from the east and northeast, there is variability in the details of this glacial advance. As seen in Figure 2, differing orientations of large-scale landforms suggest that multiple ice-

flow events occurred in the region during the Late Wisconsinan and that ice lobes were active during the later stages of glaciation. While the orientations of some features likely indicate divergent flow around topographic barriers (e.g., southeast portions of the Etsho Escarpment), the orientations of other features located in the northeastern and east-central portions of the Etsho Escarpment suggest that topography had less influence in these areas.

During retreat of the Laurentide ice sheet, numerous meltwater channels were incised by streams generally flowing west, away from the retreating ice sheet. Glacial lakes commonly developed along the ice margin as drainage down the regional slope to the east was blocked by the ice (Mathews, 1980). For example, Glacial Lake Hay formed in the lowlands southeast of Kotcho Lake and extended east into Alberta, as a result of damming by the eastward retreating Laurentide ice sheet. This resulted in the widespread deposition of clay-rich glaciolacustrine sediments over pre-existing Quaternary deposits. These fine-grained deposits are common and are one reason why glaciofluvial deposits occur only rarely at surface in the region.

SAMPLE COLLECTION, PROCESSING AND ANALYSIS

During the 2003 field season, 20 samples of glaciofluvial sands and gravels were collected (Fig. 2). Sample weights typically ranged from 20 to 30 kg but were occasionally up to 40 kg. Although not sieved in the field, an effort was made while collecting samples to exclude clasts >4 mm in size and to include as much sand-sized material as possible. Vertical exposures in operating gravel pits or roadcuts and rare test pits dug by a tracked excavator were sampled. The spatial coverage of samples was limited by the scarcity of glaciofluvial surface material and poor access. Sample depth was typically 1 to 4 m below surface in undisturbed material.

Descriptions were made for each sample collected, and included sedimentological data such as clast sizes, matrix texture, degree of sorting and rounding, petrological data, primary structures, within-unit variability, and type and orientation of contacts. Also at each sample site, notes were made on type of exposure, terrain map unit, geomorphology (e.g., topographic

position, aspect, slope, drainage), and local stratigraphy.

Heavy mineral concentrates were produced by Vancouver Indicator Processors Inc. A +4.75 mm fraction was produced first by dry screening deslimed samples, with the undersize from this fraction screened on two single-deck, 30-inch, vibrating, self-cleaning wet screens. These screens were operated in tandem with the underflow from the coarser screen cascading

onto the finer screen. The -4.75+2 mm, -0.0+1.11 mm, -1.11+0.5 mm and -0.5+0.25 mm fractions were produced using this wet method.

The -0.5+0.25 mm fraction was dried and a magnetic concentrate produced from it using a permanent-type, dry magnetic separator operating at 2.1 T. Heavy liquid processing on up to 1.0 kg of the strong and weakly magnetic fractions was carried out at the Global Discovery Laboratories of TeckCominco Ltd., a partner of

Sample ID	Glaciofluvial System	Glaciofluvial Feature Sampled	Depositional Environment
03-01	Sahtenah River	meltwater channel terrace	subaerial
03-02	unnamed	esker	subglacial
03-03	Courvoisier Creek	meltwater channel terrace	subaerial
03-04	unnamed	delta	subaerial
03-05	Kimea Creek - Petitot River	meltwater channel terrace	subaerial
03-06	unnamed	buried sands and gravels	?
03-07	Elleh Creek	kame?	subglacial, ice-proximal
03-08	Fort Nelson River	meltwater channel	subaerial
03-10	unnamed	outwash	subaerial
03-11	unnamed	esker	subglacial
03-13	Klua Creek	fan-delta	subaerial
03-14	unnamed	buried sands and gravels	?
03-17	unnamed	esker	subglacial
03-22	Elleh Creek?	buried channel	subglacial?

Table 1. Details of glaciofluvial systems, features, and depositional environments sampled.

Vancouver Indicator Processors Inc. Here, a two-stage process was used in which the heavy sink from tetrabromoethane (2.96 g/cm³) was further concentrated in methylene iodide to produce a heavy mineral concentrate of >3.33 g/cm³.

The -0.5+0.25 mm heavy mineral concentrates were sent to I. & M. Morrison Geological Services Ltd., Delta, BC, for visual picking and characterization of minerals that are thought to have a kimberlitic source or mantle source. A representative sample-split was produced from the concentrate, and kimberlite indicator minerals (KIMs) were picked and described in terms of their size, shape, surface morphology, colour, and where applicable, alteration.

One hundred ninety-seven hand-picked mineral grains were sent to SGS Lakefield Research Ltd., Lakefield, ON, to be set in a circular epoxy mount for microprobe analysis. This analysis was conducted by I. Kjarsgaard (Consulting Mineralogist) at Carleton University's microprobe facility.

Out of 197 analyzed mineral grains, 46 grains were confirmed as KIMs using discriminative data analysis. The locations of the samples containing these grains are provided in Figure 2.

DEPOSITIONAL SETTINGS OF SELECTED SAMPLES

Glaciofluvial environments vary in terms of flow regimes, depositional settings, the length of time a system is active and sediment transport distances. Table 1. summarizes the glaciofluvial systems and features sampled. Larger meltwater channel systems (i.e., widths from 1 to >2.5 km, 10 to 30 m deep and >40 km long), such as Kimea Creek, Petitot River and Elleh Creek with westerly paleoflows; and Fort Nelson River and possibly Sahtaneh River with northerly paleoflows, were high-energy systems that would have transported some sediment particles long distances (tens to hundreds of kilometres). The size of these systems, their orientation and the presence of red and pink granitic and gneissic clasts (i.e., Precambrian Shield rock types)

suggest that sediments occurring in these meltwater channel systems (i.e., samples 03-01, 03-05, 03-07, 03-08) have sources as far east and northeast as Alberta and the Northwest Territories. However, some sedimentary clasts in these systems are also locally derived (less than 10 km from the source). Subaerial depositional settings dominate in these systems however, some sediments in the region were deposited in an ice-proximal and/or subglacial environment.

Sample 03-13 was collected from boulder-size gravels deposited in a fan delta on the Klua Creek meltwater channel system. These gravels occur near the confluence of the Elleh Creek and Fort Nelson River systems, with a northward paleoflow. The difference between the Klua Creek gravels compared to the Elleh Creek and Fort Nelson River gravels, is an abundance of local cobble to boulder-size shale clasts. The Klua Creek gravels probably were deposited in an aggradational and less mature system. The relative abundance of soft local bedrock types suggests shorter transport distances for a greater proportion of sedimentary clasts.

In contrast to the large glaciofluvial systems, there are smaller scale systems situated along the periphery of the Etsho Plateau. These meltwater channel systems (e.g., in the vicinity of samples 03-03, 03-04, and 03-10), are typically 10 to 30 m wide, 5 to 10 m deep and up to 10 km long. These systems head on the top of the plateau and paleoflow data indicate westerly flow. Transport distances, relative to the systems discussed above, are probably much shorter. These systems probably also had a lower energy flow regime, as suggested by the dominance of sand-size material. Sources for these sediments, including KIMs could be on the plateau itself, and could be primary (kimberlitic), secondary (paleoplacer), or tertiary (eroded from till, transported and redeposited in a glaciofluvial system). Although likely deposited in a different environment, sediments collected in samples 03-06 and 03-14 could also have a source on the plateau. As these sediments are buried, it is difficult to assess the length of the transport and characteristics of these depositional systems. The cobble to boulder-size gravels that occur at sample site 03-06 suggest deposition in a higher energy system. Conversely, the finer-textured sands and gravels occurring at sample site 03-14 suggest deposition in a lower energy system. Sample 03-22 was also collected from buried sands and gravels, and similarly, little is known

about the system of transport and deposition.

Two esker systems with southwesterly paleoflow directions, located in the vicinity of the Etsho Plateau, were sampled (samples 03-02, 03-11, and 03-17). These features are also relatively small in scale (5 to 10 m wide, up to 5 m high and >1 km long), and dominated by sand-size material that was deposited subglacially. Esker systems are typically fed by a complex network of meltwater channels within the ice sheet and could have long transport distances. This is particularly true of the esker system that occurs northeast of Kotcho Lake. The esker segment sampled (samples 03-02 and 03-11) is part of a larger segmented esker system that trends northeast and continues for >20 km. The dominance of sand-size material in these eskers suggests that they were relatively low-energy systems.

INTERPRETATION OF INDICATOR MINERALS

Of the 22 samples collected for this study, 14 contain KIMs. Of these, eight contain more than one indicator mineral and often more than one grain of each (Fig. 2). This section presents identification and interpretation of KIMs based largely on microprobe analysis.

Garnet

Mantle-derived garnets are considered the most important kimberlite and diamond indicator minerals. The pioneering work of Dawson and Stephens (1975) and Gurney (1984) formed the base for the use of garnet as an indicator mineral, and many researchers have followed and refined these original studies. The two most current studies on garnet classification and interpretation are those of Schulze (2003) and Grütter *et al.* (2004). Both of these classifications are very effective in distinguishing pyropes, eclogitic and crustal garnets. The main elements used to identify and interpret mantle-derived garnets, and to estimate a diamond potential of an area or individual pipe, are Cr, Ca, Mg, Fe, Ti and Na.

In this paper, the scheme described by Grütter *et al.* (2004) is used to classify different garnet species. Although this approach introduces concepts that may not be familiar to some geologists, such as Ca-intercepts, it is a comprehensive, straightforward and well suited

for diamond exploration. In this classification scheme, garnets are divided into 12 categories (G1 to G12). Of these, harzburgitic (G10), pyroxenitic, websteritic and eclogitic garnets (G4, G5 and G3) are commonly associated with diamonds. Wehrlitic garnets are referred to as G12, low-Cr megacrysts as G1, and Ti-rich peridotitic varieties as G11. The garnets that do not fit into any of the twelve categories, including crustal garnets, are referred to as G0. The scheme is at least in part empirical; it was tested on a large data set and appears quite robust.

Of the 46 garnets that were visually picked and analyzed, at least 23 can be considered as KIMs. Microprobe analyses of selected garnets, and results of classification using the method outlined by Grütter *et al.* (2004), are provided in (Table 2.) and G9, G12 and G3 garnets are shown on Figure 3. Although there are no G10 garnets present, one of the G9 garnets plots very close to the G9-G10 boundary (Fig. 3). Eight of the mantle-derived garnets are lherzolitic (G9), three are wehrlitic (G12) and twelve can be considered as eclogitic (G3). The remaining garnets are classified as G0. The garnets with significant chrome content (G9) follow a well-defined trend from the G10-G9 to G9-G12 boundaries, forming an acute angle with the lherzolite field (Fig. 3). High Na₂O content (>0.07 wt %) in eclogitic garnets is considered as a positive indication of diamond potential (Gurney, 1984; Grütter *et al.*, 2004). However, no G3 grains recovered in this study have sufficiently high Na₂O content to merit the suffix 'D'.

With one possible exception, kelyphitic rims were not observed on any of the visually picked garnets. In this specific case, the dark substance covering less than 1% of the grain's surface was tentatively identified as a kelyphitic rim. Several of the garnets have orange-peel texture. The overall absence of kelyphitic rims and presence of orange-peel textures suggest that these garnets were probably subjected at least to limited transport or local reworking after being liberated from their host rock. The spatial distribution of G3, G9 and G12 garnets is presented in Figure 2.

Clinopyroxene

Chrome-bearing, green to bright green clinopyroxenes are easily identifiable in heavy mineral concentrates. For these reasons, clinopyroxenes are considered effective KIMs.

Unfortunately, clinopyroxenes with characteristics similar to those present in kimberlitic rocks are also found in a variety of other rock types. Consequently, microprobe analyses are required to differentiate kimberlite-related clinopyroxenes from those associated with other rock types. Twenty clinopyroxene grains were visually picked from concentrates. Their chemical composition is provided in Table 3.

As seen in Table 3, the Mg numbers (100Mg/[Mg+Fe]) of these clinopyroxenes vary from 77.52 to 93.52. Chrome diopside grains with an Mg number >88 are likely to be from mantle peridotite, particularly if they have elevated Cr₂O₃ (>0.5 wt.%). Based on Mg number, there appear to be 10 clinopyroxenes that could be considered as kimberlitic indicators.

The discrimination plot Cr₂O₃-Al₂O₃ of Ramsey and Tompkins (1994) was used to further refine this interpretation. Worldwide, most of the clinopyroxenes found as solid inclusions or intergrowths, in and/or with diamonds, plot in the 'on craton' garnet-peridotite field (Fig. 4). Of the 20 clinopyroxenes analyzed, 8 plot in this field. Of the 10 clinopyroxenes identified as being peridotitic or kimberlite indicators, based simply on the Mg number, 4 plot in the 'on craton' and 3 within the "off craton" fields (Fig. 4). Four additional clinopyroxenes plot within this field, although they have Mg numbers <88. Of the 20 clinopyroxenes identified during this study, 14 are considered to be KIMs (other considerations are involved as well). The spatial distribution of clinopyroxene is presented in Figure 2.

Spinel

Based on microprobe analyses, only one visually picked mineral grain is chromite (sample 03-05; Fig. 2). This black chromite grain consists mainly of Al₂O₃ (30.56%), Cr₂O₃ (33.22%), FeO (21.01%), MgO (12.67%) and smaller concentrations of TiO₂ (0.43%), ZnO (0.27%), MnO (0.21%), NiO (0.14%), SiO₂ (0.09 %); V₂O₅ and CaO were not detected. The grain has an MgO value comparable to chromites reported as inclusions or intergrowths in and/or with diamonds. Its Cr₂O₃ content (33.22%), however, is too low relative to compositional fields of diamond-associated chromites, which commonly contain >60% Cr₂O₃.

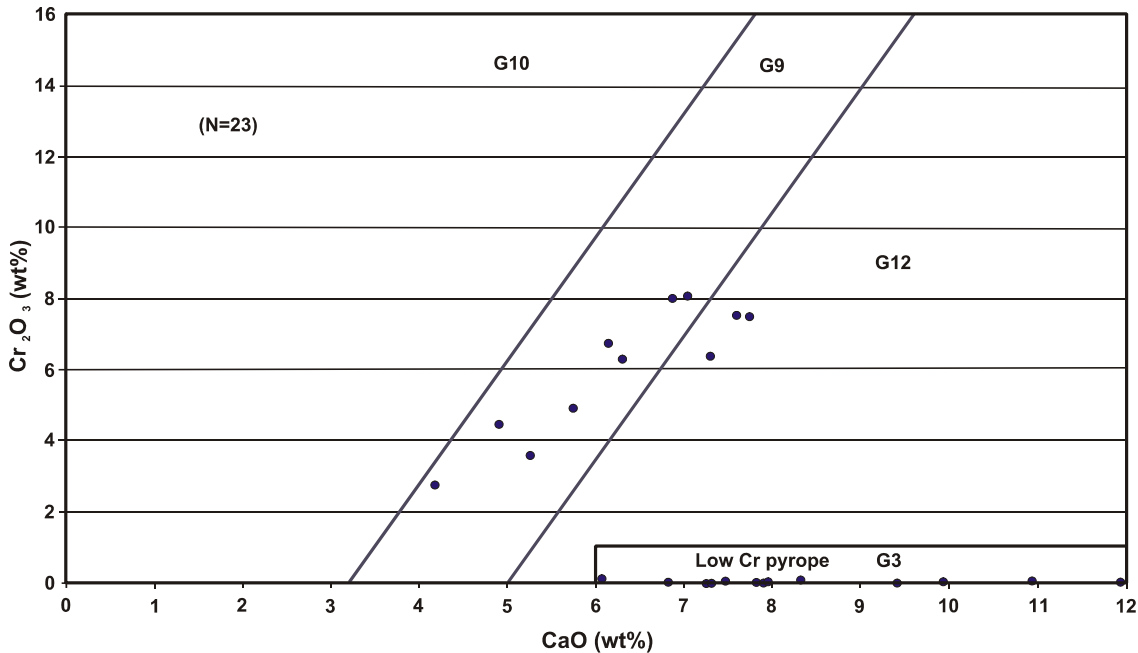


Figure 3. Garnet Cr₂O₃-CaO diagram showing composition of G9, G6 and G3 garnets. G0 garnets are not shown. Compositional fields from (Grütter et al., 2004).

This chromite grain may fit into the compositional fields of the spinels observed at the Prairie Creek, Kirkland Lake, Joff, Ile Bizard, Mountain and Blackfoot-type diatremes (Fipke *et al.*, 1995), but may also fit into compositional fields of spinels from a wide variety of other ultramafic rocks. Due to its association with other indicator minerals, however, this grain was retained as a potential KIM.

Ilmenite

Ilmenite is one of the most widely used kimberlite indicator minerals. It is a common member of the megacryst suite, and the major elements TiO₂, MgO, CrO₂, MnO₂ and Fe₂O₃ are used to distinguish kimberlitic ilmenites from those that are non-kimberlitic (Wyatt *et al.*, 2004). Microprobe analyses of ilmenite grains from the Fort Nelson area are given in Table 4. Based on the TiO₂ and MgO plot (Fig. 5), there are three analyses that plot in the kimberlite field (i.e., on the right of the curve marked 'A').

As shown in Figure 6, the Cr₂O₃ and MgO plot also suggests that the same three grains identified in Figure 5 are kimberlite related.

They have higher MgO values, and two of them have higher Cr₂O₃ content than their non-kimberlitic counterparts. The fields of typical North American, South African (on and off craton) and Australian kimberlitic ilmenites are provided in Figure 6 for reference (based on data from Wyatt *et al.*, 2004).

Most of the non-kimberlitic (crustal) ilmenites have low MgO values and probably originated from the same, non-kimberlitic, crustal protolith (Fig. 5, 6). One of these grains plots above the 0% Fe₂O₃ contour. That analysis is either incorrect and the mineral is not ilmenite, or the probe encountered a rutile inclusion. It is worth noting that the crustal ilmenite cluster shown in Figure 6 coincides with the crustal ilmenite clusters seen from the Slave Craton. Three kimberlitic ilmenites with low Fe³⁺/Fe²⁺ ratio were identified during this study. Two of them come from samples collected in the Etsho Plateau area and one of them occurs with G3 and G9 garnets and corundum (Fig. 2). Ilmenites with low Fe³⁺/Fe²⁺ ratios indicate favourable oxidation-reduction conditions for diamond preservation and therefore provide additional information for evaluation of individual pipes (Gurney and Moore, 1994). Such an exercise, however, is beyond the scope of this reconnaissance study.

Olivine

In cold climates, such as in northeastern British Columbia, olivine is more resistant to serpentinization and is considered a useful KIM. Although olivine is a common rock-forming mineral in kimberlites, it is also present in a variety of other ultramafic rocks in British Columbia (Voormeij and Simandl, 2004a, b) and therefore does not provide as much diamond potential information as garnet, clinopyroxene, chromite or ilmenite.

The Mg-rich variety of olivine identified in samples from Fort Nelson area is commonly pale yellow-green, equidimensional and subrounded to rounded, and has a fresh appearance. Olivine provenance cannot be established solely by visual examination, so microprobe analyses are required. Microprobe data on 28 olivine grains recovered from collected samples are presented in Table 5, while a NiO-Fo diagram using the same data is presented in Figure 7.

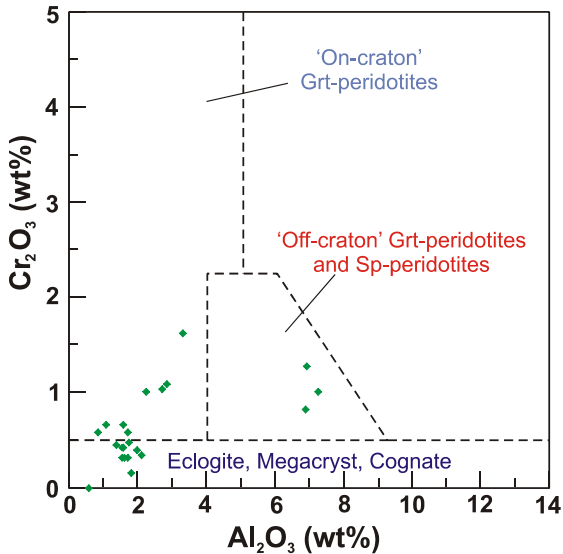


Figure 4. Clinopyroxenes Cr_2O_3 - Al_2O_3 discrimination plot (after Ramsey and omkins, 1994). Eight of the clinopyroxenes plot within the 'On-craton' garnet peridotite field and three plot within 'Off-craton' garnet peridotite and spinel peridotites field. Clinopyroxenes plot within the 'On-craton' garnet peridotite field.

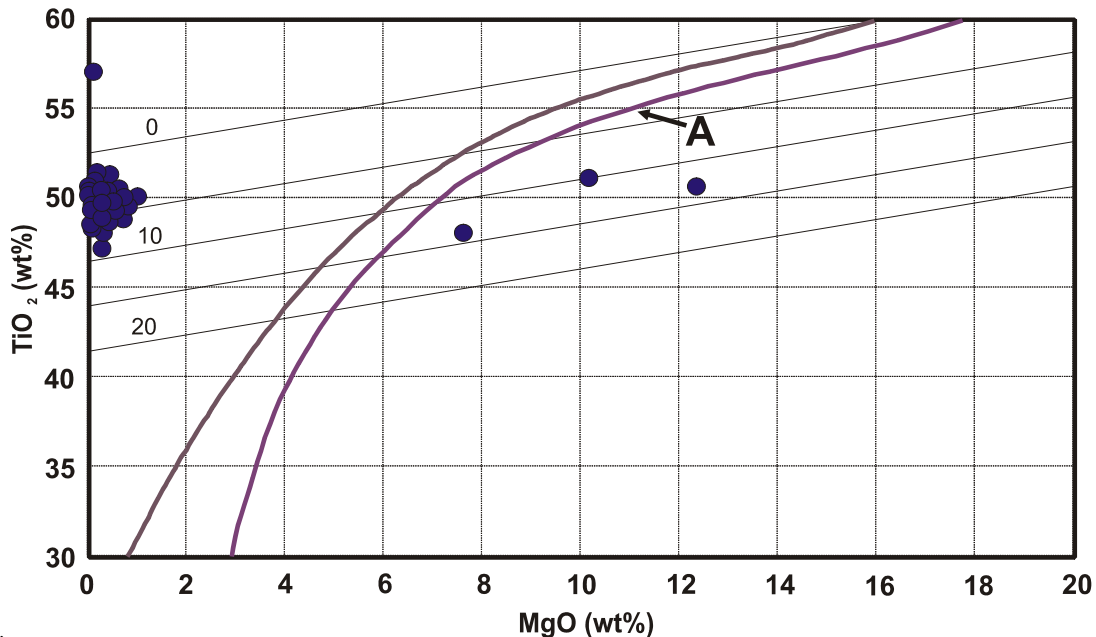


Figure 5. Ilmenite- TiO_2 and MgO discrimination plot (after Wyatt *et al.*, 2004). Three grains plot within the kimberlite field, which is located to the right of the curve marked 'A'.

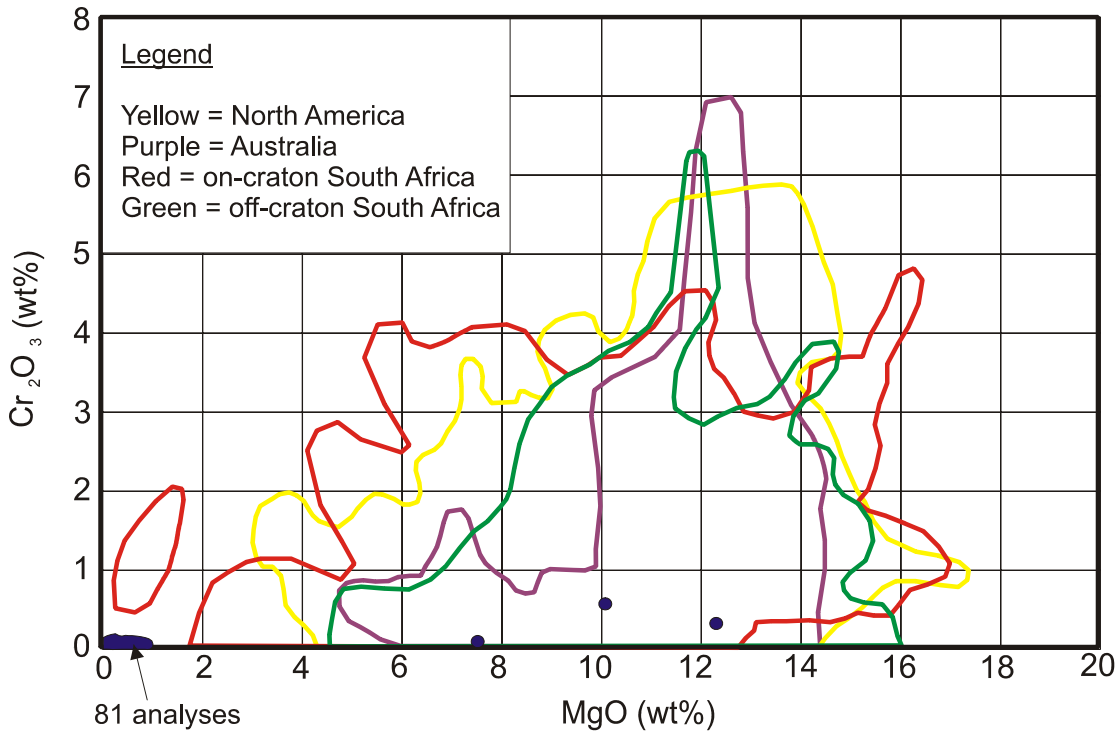


Figure 6. Ilmenite Cr_2O_3 and MgO discrimination plot (after Haggerty, 1991). Simplified fields representing North American, Australian and South African (on and off-craton) kimberlitic ilmenites are derived from plots by Wyatt *et al.*, (2004). Three out of 84 grains from the Fort Nelson area can be considered as KIMs.

The MgO content of these olivine grains ranges from ~41 to 50 wt % and that of FeO from ~8 to 19 wt %. Olivines derived from kimberlite rocks typically plot within the green field delineated by a curve (Fig. 7; Eccles *et al.*, 2004). Six olivine grains from the Fort Nelson area fall within this compositional field and three other grains are located on the periphery of the kimberlite field. Based on data from Eccles *et al.* (2004), orange field (Fig. 7) delineates a more restricted field, which represents the most common composition of olivine grains from the northern Alberta kimberlite province. Four of the most Mg-rich grains from this study fall within this field.

Of these four of the grains are KIMs and may have been derived from kimberlites in northern Alberta, from the local Mesozoic to Paleozoic sedimentary cover, or from undiscovered kimberlites within northeastern British Columbia. Locations of identified olivine grains are presented in Figure 2.

Corundum

Corundum and in rare circumstances, its gem quality equivalents; sapphire and ruby, are

found in silica-under-saturated rocks such as high-grade alumina-rich gneisses. They are also found in a variety of alkali basalts, lamprophyres, and other alkaline rocks from contact metamorphic settings (Simandl and Paradis, 1999a, b, c). It is also reported in association with placer diamond deposits in New South Wales (Coenraads, 1990). A direct but not exclusive corundum-diamond link was established through study of corundum inclusions in diamonds (Hutchinson *et al.*, 2001; Hutchinson *et al.*, 2004). Preliminary data indicate that these inclusions, interpreted as being syngenetic with the growth of diamond, have a higher Ni content and higher Mg/Fe ratio than corundum from any other temperature-pressure settings (Hutchison *et al.*, 2004). Corundum with 1.1–1.7 wt % Cr_2O_3 was also described in garnetite within the ultrahigh-pressure zone of Sulu Terrane, China (Zhang *et al.*, 2004), and in variety of eclogite-grade rocks (Morishita and Arrai, 2001; Qi *et al.*, 1997).

A single purple corundum grain was recovered during this study. Both its colour and high Cr content indicate that it is very similar to ruby. This grain is composed almost entirely of Al_2O_3 , with minor components of Cr_2O_3 (0.54%)

and FeO (0.19%), and even less NiO (0.03%) and MnO (0.01%). Laser-ablation ICP-MS, or energy dispersive spectrometry, would be necessary if further interpretation of the data based on chemical composition is required.

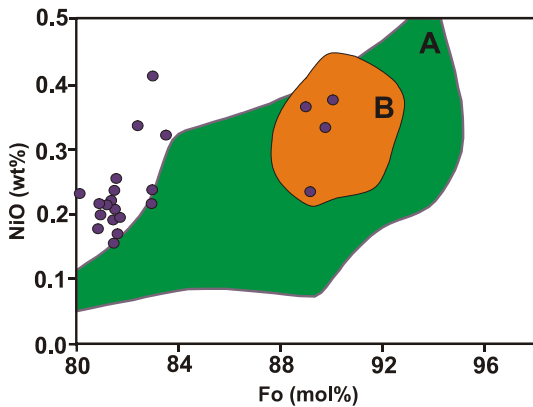


Figure 7. Olivine NiO-Fo discrimination plot. Olivines derived from kimberlite rocks plot in field A (Eccles *et al.*, 2004). Six olivine grains from the Fort Nelson area fall within this compositional field; three additional grains plot on the periphery. Field B, a more restricted field that represents typical compositions of olivine indicator grains from the northern Alberta kimberlite province, is based from Eccles *et al.*, (2004).

Chromium-bearing corundum similar in colour to the one described above is reported in association with spinel in barren and diamondiferous pipes in the Buffalo Head Hills, Alberta (Hood and McCandless, 2004), in the Fort-à-la-Corne area, Saskatchewan (Hutchison *et al.* 2004), and in the Northwest Territories. Although corundum (sapphire) grains are also reported in small quantities in some pipes and alkaline complexes within the British Columbia alkaline province, west to east transport in the study area is unlikely.

Corundum came from sample 03-03, which also contained several kimberlite indicators, including mantle-derived garnets and ilmenite. The sample, located in Figure 2, may be worth following-up both from diamond and gem corundum perspectives.

Diaspore

Diaspore, a hydrated alumina (AlOOH), is not typically considered a KIM. It is known to coexist with corundum in altered silica-undersaturated rock types, especially as a retrograde product in regionally metamorphosed

corundum-bearing alumina-rich sedimentary rocks (Simandl and Paradis, 1999a). Although it is not commonly reported as an accessory mineral in ultramafic rocks, it could be present in ultramafic-related corundum-bearing contact metamorphic rocks, such as those described by Simandl and Paradis (1999b), and in most corundum-bearing alkaline volcanics such as alkali basalts, kimberlites, and lamprophyres described by Simandl and Paradis (1999c). In its fine-grained and massive form, diasporite is also found as an important constituent in aluminous clay and bauxite deposits (Hill, 1994).

Two yellow grains from samples 03-06 and 03-02 were identified, based on their Al₂O₃ content, as diasporite. These grains have similar NiO values to those of the previously described corundum grains. The diasporite grains differ from the corundum grains in that they have lower Cr₂O₃ values, higher FeO values and detectable TiO₂ (Table 6). Little is known about the mobility of Cr, Ti and Fe during corundum-diasporite transition. Based strictly on the microprobe analyses, these diasporite grains do not appear to be genetically related to the Cr-rich corundum grain described above. The shape of diasporite grains does not provide clues to distance traveled, and their geographic distribution and chemical composition does not suggest strong association with kimberlite indicators or with the purple corundum grain.

DISCUSSION AND HIGHLIGHTS

The KIMs recovered in the Fort Nelson area likely originated from more than one source. Possible sources are known diatremes located east of the study area in the Buffalo Head Terrane and in the Slave Craton, undiscovered pipes cutting Mesozoic to Paleozoic sedimentary rocks in the Fort Nelson area, British Columbia's alkaline province, high-pressure zones such as those described by Canil *et al.* (2003) and, in the case of olivine, a variety of accreted terranes. The geology of the Precambrian basement in northeastern British Columbia is poorly understood, but there are indications that it could be more favourable for diamond exploration than previously reported (Simandl, 2004; Simandl and Davis, 2005). Therefore, the results of this study are important, particularly given alternative interpretations of the character of the Precambrian basement terranes.

Interpretations of the local surficial geology

(material types sampled as part of this study) and Late Pleistocene glacial history help constrain some of these options and suggest that some indicators may have been locally derived, while others may have been transported west and southwest from Northwest Territories or Alberta. Based on a combination of parameters such as indicator mineral grain count, coexistence of more than one KIM in the same sample, results of microprobe analyses and interpretation of transport distances based on surficial geology, it is possible that samples 03-03, 03-09, 03-10 and 03-17, and potentially samples 03-02 and 03-11, may contain indicators derived from proximal sources, possibly within the Etsho Plateau. Sample 03-04 is particularly encouraging as it contains a relatively high mineral indicator count and a combination of G3, G9 and G12 garnets, olivine and Cr-diopside (Figure 2).

The provenance of KIMs in samples collected within large-scale, high energy meltwater channels, such as the Kimea Creek – Petitot River, Elleh, and Fort Nelson River systems (Fig. 2), is more difficult to establish. Analysis of coarse fractions from selected samples and follow-up sampling may provide additional information that could be used to better constrain the sources of the indicator minerals and provide an estimate of transportation distance.

Existing geophysical surveys carried out by the oil and gas industry may help to further focus diamond exploration in this area, as diatremes may have an electromagnetic, magnetic, gravity or seismic expression.

SUMMARY

Kimberlite indicator minerals, including peridotitic and eclogitic garnets, ilmenite, Cr-diopside, olivine and corundum, were recovered from -0.5+0.25 mm heavy mineral concentrates from the Fort Nelson area. These concentrates were produced from glaciofluvial sands and gravels. Fourteen of the 20 samples collected contained KIMs, many with more than one mineral type. Most of the indicator grains appear fresh and subrounded to subangular, but several have sharp edges. Garnets do not appear to have kelyphitic rims, but a few do have an orange-peel texture, suggesting that they were subject to small degree of transportation or local reworking.

Indicator minerals present in samples proximal to or on the Etsho Plateau occur in small-scale, low-energy glaciofluvial systems and may have a local source, perhaps somewhere on the plateau itself. Others, particularly those occurring in large-scale, high-energy glaciofluvial systems, were more likely transported into the area by glaciofluvial processes from Alberta (Buffalo Head Terrane), the Northwest Territories (Slave Craton) and undiscovered pipes cutting sedimentary rocks of Mesozoic to Paleozoic age in other parts of northeastern British Columbia. The geology of the Precambrian basement in northeastern British Columbia is poorly understood, and this part of the province should not be ignored in diamond exploration.

During the 2004 field season, 50 additional samples were collected over an area extending 200 km west and 300 km south of Fort Nelson. These samples are currently being processed and may provide additional information on possible sources of KIMs identified here, and help to establish what is the background concentration of KIMs in the region.

ACKNOWLEDGMENTS

The document benefited from constructive comments by Suzanne Paradis (Pacific Geoscience Centre, Geological Survey of Canada) and Brian Grant. Enriching discussions with Herman Grütter (Mineral Services Canada) and Dan Schulze (University of Toronto) are gratefully acknowledged. Jan Bednarski (Pacific Geoscience Centre, Geological Survey of Canada) is thanked for his insights into the Quaternary history of the region. Adrian Hickin is thanked for discussions on relevant topics.

REFERENCES

- Allan, R.J. (1999): Micro-diamond results from Ice Claim project, BC; *Skeena Resources Limited*, news release, August 20, 1999.
- Allan, R.J. (2002): Diamond exploration corporate update; *Skeena Resources Limited*, news release, March 22, 2002.
- Anonymous (1994): BC diamonds discovered; in George Cross News Letter, *Consolidated Ramrod Gold Corporation*, No. 225.

- Canil, D., Schulze, D.J., Hall, D., Hearn, B.C. Jr., and Milliken, S.M. (2003): Lithospheric roots beneath western Laurentia: the geochemical signal in mantle garnets; *Canadian Journal of Earth Sciences*, Volume 40, pages 1027–1051
- Carlson, S.M., Hillier, W.D., Hood, C.T., Pryde, R.P. and Skelton, D.N. (1999): The Buffalo Hills kimberlites: a newly-discovered diamondiferous kimberlite province in north-central Alberta, Canada; in Proceedings of the VIIIth International Kimberlite Conference, Gurney, J.J., Gurney J.L., Pascoe, M.D. and Richardson, S.H., Editors, Volume 1, pages 109–116.
- Coenraads, R.R. (1990): Key areas for alluvial diamond, sapphire exploration in the New England gem fields, New South Wales, Australia; *Economic Geology*, Volume 85, pages 1186–1207.
- Creaser, R.A., Grütter, H., Carlson, J. and Crawford, B. (2004): Macrocystal phlogopite Rb-Sr dates for the Ekati property kimberlites, Slave Province, Canada: evidence for multiple intrusive episodes in the Paleocene and Eocene; *Lithos*, Volume 76, pages 399–414.
- Dawson, J.B. and Stephens, W.E. (1975): Statistical classification of garnets from kimberlite and associated xenoliths; *Journal of Geology*, Volume 83, pages 589–607.
- Dow, R.B. (2004): Patrician recovers another diamond; *Patrician Diamonds Inc.*, press release 04-04, February 11, 2003.
- Dow, R.B. (2003): Patrician recovers diamonds, sapphires and kimberlitic indicators in the Yukon; *Patrician Diamonds Inc.*, press release 03-08, November 10, 2003.
- Eccles, D.R. (2002): Enzyme leach-based soil geochemistry of the Mountain Lake diatreme, Alberta; in *Industrial Minerals in Canada*, Dunlop, S. and Simandl, G.J., Editors, *Canadian Institute of Mining and Metallurgy and Petroleum*, Volume 53, pages 355–360.
- Eccles, D.R., Heaman, L.M., Luth, R.W. and Creaser, R.A. (2004): Petrogenesis of the Late Cretaceous northern Alberta kimberlite province; *Lithos*, Volume 76, pages 435–459.
- Fipke, C.E., Gurney, J.J. and Moore, K.O. (1995): Diamond exploration techniques emphasizing indicator mineral geochemistry and Canadian examples; *Geological Survey of Canada*, Bulletin 423, 85 pages.
- Grütter, H.S., Gurney, J.J., Menzies, A.H. and Winter, F. (2004): An updated classification scheme for mantle-derived garnet, for use by diamond explorers; *Lithos*, Volume 77, pages 841–857.
- Gurney, J. J. (1984): A correlation between garnets and diamonds in kimberlites; in *Kimberlite Occurrence and Origin: A Basis for Conceptual Models in Exploration*, J.E. Glover and P.G. Harris, Editors, *University of Western Australia*, Geology Department and University Extension, Publication 8, pages 143–166.
- Gurney, J.J. and Moore R.O. (1994): Geochemical correlation between kimberlitic indicator minerals and diamonds as applied to exploration; in *Kimberlites, Related Rocks and Mantle Xenoliths*, 5th International Kimberlite Conference, Araxa, Brazil, *Companhia de Pesquisa de Recursos Minerais (CPRM)*, Volume 1, page 125.
- Haggerty, S.E. (1986): Diamond genesis in a multiply constrained model; *Nature*, Volume 320, pages 34–38.
- Helmstaedt, H.H. and Gurney, J.J. (1995): Geotectonic controls of primary diamond deposits: implications for area selection; *Journal of Geochemical Exploration*, Volume 53, pages 125–144.
- Hill, V.G. (1994): Bauxite; in *Industrial Minerals and Rocks* (6th Edition), Carr, D.D., Editor, *Society for Mining, Metallurgy, and Exploration Inc.*, pages 135–147.
- Hoffman, P.F. (1988): United plates of America: the birth of a craton; *Annual Reviews in Earth and Planetary Sciences*, Volume 16, pages 543–603.
- Hoffman, P.F. (1989): Speculations on Laurentia's first gigayear (2.0–1.0 Ga); *Geology*, Volume 17, pages 135–138.
- Hoffman, P.F. (1991): Did the breakout of Laurentia turn Gondwanaland inside-out? *Science*, Volume 252, pages 1409–1412.
- Holland, S.S. (1976): Landforms of British Columbia: a physiographic outline; *BC Ministry of Energy, Mines and Petroleum Resources*, Bulletin 48, 138 pages.
- Hood, C.T.S. and McCandless, T.E. (2004): Systematic variations in xenocryst mineral composition at the province scale, Buffalo Hills kimberlites, Alberta, Canada; *Lithos*, Volume 77, pages 733–747.
- Hutchinson, M.T., Husthouse, M.B. and Light, M.E. (2001): Mineral inclusions in diamonds: associations and chemical distinctions around the 670 km discontinuity; *Contributions to Mineralogy and Petrology*, Volume 142, pages 119–126.
- Hutchinson, M.T., Nixon, P.H. and Harley, S.L. (2004): Corundum inclusions in diamonds – discriminatory criteria and corundum compositional dataset; *Lithos*, Volume 77, pages 273–286.
- Janse, A.J.A. (1994): Is Clifford's Rule still valid? in

- Kimberlites, Related Rocks and Mantle Xenoliths, Proceedings of the 5th International Kimberlite Conference, Araxa, Brazil, *Companhia de Pesquisa de Recursos Minerais (CPRM)*, Volume 2, pages 215–235.
- Journeay, J.M., Williams, S.P. and Wheeler, J.O. (2000): Tectonic assemblage map, Fort Nelson, British Columbia; *Geological Survey of Canada*, Open File 2948, scale 1:1 000 000.
- Kirkley, M.B., Gurney, J.J. and Levinson, A.A. (1991): Age, origin and emplacement of diamonds: scientific advances in the last decade; *Gems and Gemology*, Spring 1991, pages 2–25.
- Levson, V.M., Ferbey, T., Kerr, B., Johnsen, T., Bednarski, J., Smith, I.R., Blackwell, J. and Jonnes, S. (2004): Quaternary geology and aggregate mapping in northeast British Columbia: applications for oil and gas exploration and development; in *Geological Fieldwork 2004, BC Ministry of Energy and Mines*, Paper 2004-1, pages 29–40.
- Lockhart, G., Grütter, H. and Carlson, J. (2004): Temporal, geomagnetic and related attributes of kimberlite magmatism at Ekati, Northwest Territories, Canada; *Lithos*, Volume 77, pages 665–682.
- McCallum, M.E. (1994): Lamproitic (?) diatremes in the Golden area of the Rocky Mountain Fold and Thrust Belt, British Columbia, Canada; in *Kimberlites, Related Rocks and Mantle Xenoliths, Proceedings of the 5th International Kimberlite Conference*, Araxa, Brazil, *Companhia de Pesquisa de Recursos Minerais (CPRM)*, Volume 1, pages 195–209.
- Mathews, W.H. (1980): Retreat of the last ice sheets in northeastern British Columbia and adjacent Alberta; *Geological Survey*, Bulletin 331, 22 pages.
- Mitchell, R.H. (1991): Kimberlites and lamproites: primary sources of diamonds; *Geoscience Canada*, Volume 18, pages 1–16.
- Morishita, T. and Arrai, S. (2001): Petrogenesis of corundum-bearing mafic rock in the Horoman Peridotite Complex, Japan; *Journal of Petrology*, Volume 42, pages 1279–1299.
- Northcote, K.E., (1983a): Report on Mark property, Pangman Peak (82N/15W); *BC Ministry of Energy, Mines and Petroleum Resources*, Assessment Report 13 596.
- Northcote, K.E. (1983b): Report on Jack Claims Lens Mountain (82N/14E); *BC Ministry of Energy, Mines and Petroleum Resources*, Assessment Report 13 597.
- Okulitch, A.V., MacIntyre, D.G., Taylor, G.C., Gabrielse, H., Cullen, B., Massey, N. and Bellefontaine, K., Compilers (2002): Bedrock geology, central Foreland, British Columbia, Yukon Territory, Northwest Territories: maps NO-10, NP 9-10; *Geological Survey of Canada*, Open File 3604 (revised), scale 1:500 000.
- Paulen, R.C., Fenton, M.M., Pawlowicz, J.G., Smith, I.R. and Plouffe, A. (in press): Surficial geology of the Zama Lake area (NTS 84L/NW); *Alberta Energy and Utilities Board*, EUB/AGS Map 315, scale 1:100 000.
- Pell, J., (1994): Carbonatites, nepheline syenites, kimberlites and related rocks in British Columbia; *BC Ministry of Energy and Mines*, Bulletin 88, 136 pages.
- Plint, A.G., McCarthy, P.J. and Faccini, U.F. (2001): Nonmarine sequence stratigraphy: updip expression of sequence boundaries and systems tracts in a high-resolution framework, Cenomanian Dunvegan Formation, Alberta foreland basin, Canada; *AAPG Bulletin*, Volume 85, pages 1967–2001.
- Plint, A.G. (2002): Paleovalley systems in the Upper Cretaceous Dunvegan Formation, Alberta and British Columbia; *Bulletin of Canadian Petroleum Geology*, Volume 50, pages 277–296.
- Plint, A.G. and Wadsworth, J.A. (2003): Sedimentology and palaeogeomorphology of four large valley systems incising delta plains, Western Canada foreland basin; implications for Mid-Cretaceous sea-level changes; *Sedimentology*, Volume 50, pages 1147–1186.
- Plouffe, A., Smith, I.R., Paulen, R.C., Fenton, M.M. and Pawlowicz, J.G. (2004): Surficial geology, Bassett Lake, Alberta (NTS 84L/SE); *Geological Survey of Canada*, Open File 4637, scale 1:100 000.
- Pilkington, M., Milles, W.F., Ross, G.M. and Roest, W.R. (2000): Potential-field signatures of buried Precambrian basement in Western Canada Sedimentary Basin; *Canadian Journal of Earth Sciences*, Volume 37, pages 1453–1471.
- Qi, Q., Taylor, L.A., Snyder, G.A., Clayton, R.N., Mayeda, T.K. and Sobolev, N.V. (1997): Detailed petrology and geochemistry of a rare corundum eclogite xenolith from Obzhennaya, Yakutia; *Russian Geology and Geophysics*, Volume 38, pages 247–260.
- Ramsey, R.R. and Tompkins, L.A. (1994): The geology, heavy mineral concentrate mineralogy, and diamond prospectivity of Boa Esperanca and Cana Verde pipes, Corrego D'anta, Minas Gerais, Brazil; in *Kimberlites, Related Rocks and Mantle Xenoliths, Proceedings of the 5th International Kimberlite Conference*, *Companhia de Pesquisa de Recursos Minerais (CPRM)*, Volume 2, pages 329–345.
- Roberts, W.J. (2002): Diamond discovery at Xeno; *Pacific Ridge Exploration Limited*, news Release,

March 13, 2002.

Ross, G.M., Parish, R.R., Villeneuve, M.E. and Bowring, S.A. (1991): Geophysics and geochronology of the crystalline basement of the Alberta Basin, Western Canada; *Canadian Journal of Earth Sciences*, Volume 28, pages 512–522.

Ross, G.M., Milkerreit, B., Eaton, D., White, D. Kanasewich, E.R. and Buryanyk, M.J.A. (1995): Paleoproterozoic collisional orogen beneath Western Canada Sedimentary Basin imaged by Lithoprobe crustal seismic reflection data; *Geology*, Volume 23, pages 195–199.

Schulze, D.J. (2003): A classification scheme for mantle-derived garnets in kimberlite: a tool for investigating the mantle and exploring for diamonds; *Lithos*, Volume 71, pages 195–213.

Simandl, G.J. (2004): Concepts for diamond exploration in “on/off craton” areas - British Columbia, Canada; *Lithos*, Volume 77, pages 749–764.

Simandl, G.J. and Paradis, S. (1999a): Ultramafic-related corundum; in Selected British Columbia Mineral Deposit Profiles, Volume 3, Industrial Minerals and Gemstones, Simandl, G.J., Hora, Z.D. and Lefebure, D.V., Editors, *BC Ministry of Energy and Mines*, pages 123–127.

Simandl, G.J. and Paradis, S. (1999b): Corundum in alumina-rich metasediments; in Selected British Columbia Mineral Deposit Profiles, Volume 3, Industrial Minerals and Gemstones, Simandl, G.J., Hora, Z.D. and Lefebure, D.V., Editors, *BC Ministry of Energy and Mines*, pages 105–108.

Simandl, G.J. and Paradis, S. (1999c): Alkali basalt and lamprophyre-hosted sapphire and ruby; in Selected British Columbia Mineral Deposit Profiles, Volume 3, Industrial Minerals and Gemstones, G.J., Hora, Z.D. and Lefebure, D.V., Editors, *BC Ministry of Energy and Mines*, pages 129–132.

Smith, C.B., Colgan, E.A., Hawthorne, J.B. and Hutchinson G. (1988): Emplacement age of the Cross kimberlite, southeastern British Columbia, by Rb-Sr

phlogopite method; *Canadian Journal of Earth Sciences*, Volume 25, pages 790–792.

Smith, I.R., Plouffe, A., Paulen, R.C., Fenton, M. and Pawlowicz, J.G. (in press): Surficial geology, southwest Zama Lake, Alberta (NTS 84L/SW); *Geological Survey of Canada*, Open File 4754, scale 1:100 000.

Stott, D.F. (1982): Lower Cretaceous Fort St. John group and upper Cretaceous Dunvegan formation of the foothills and plains of Alberta, British Columbia, District of MacKenzie and Yukon Territory; *Geological Survey of Canada*, Bulletin 328, 124 pages.

Thompson, R.I. (1977): Geology of Beaton River, Fontas River and Petitot River map-areas, northeastern British Columbia; *Geological Survey of Canada*, Paper 75-11, 8 pages.

Villeneuve, M.E., Ross, G.M., Thériault, R.J., Miles, W., Parrish, R.R. and Broome, J. (1993): Tectonic subdivision and U-Pb geochronology of the crystalline basement of the Alberta basin, Western Canada; *Geological Survey of Canada*, Bulletin 447, 93 pages.

Voormeij, D.A. and Simandl, G.J. (2004a): A Map of ultramafic rocks in British Columbia: applications in CO₂ sequestration and mineral exploration, *BC Ministry of Energy and Mines*, GeoFile 2004-1.

Voormeij, D.A. and Simandl, G.J. (2004b): Ultramafic rocks in British Columbia: delineating targets for mineral sequestration of CO₂; in Summary of Activities, *BC Ministry of Energy and Mines*, pages 157–167.

Wyatt, B.A., Baumgartner, M., Ancar, E. and Grütter, H. (2004): Compositional classification of “kimberlitic” and “non-kimberlitic” ilmenite; *Lithos*, Volume 77, pages 819–840.

Zhang, R.Y., Liou, J.G. and Zheng J.P. (2004): Ultrahigh-pressure corundum-rich garnetite in garnet peridotite, Sulu Terrane, China; *Contributions to Mineralogy and Petrology*, Volume 147, pages 21–31.

Table 2. Microprobe analysis of garnets (%).

Sample ID	UTM Easting	UTM Northing	SiO ₂	TiO ₂	Al ₂ O ₃	Cr ₂ O ₃	FeO	MnO	NiO	MgO	CaO	Na ₂ O	K ₂ O	Total	Garnet Type
03-01	589380	6518892	40.65	0.06	19.33	6.40	8.59	0.56	0.04	17.18	7.30	0.03	0.00	100.15	G12
03-02	628743	6566536	36.37	0.00	20.73	0.00	32.79	9.15	0.00	1.04	0.31	0.04	0.02	100.46	G0
03-02	628743	6566536	39.20	0.10	22.05	0.04	22.36	0.42	0.00	6.74	9.93	0.00	0.00	100.85	G3
03-02	628743	6566536	36.25	0.08	17.53	0.00	3.23	0.04	0.00	2.18	37.37	0.01	0.00	96.68	G0
03-03	578801	6554264	41.68	0.03	21.91	3.61	7.96	0.53	0.00	19.76	5.26	0.03	0.00	100.77	G9
03-03	578801	6554264	38.34	0.08	21.05	0.05	26.72	0.95	0.00	4.67	7.95	0.02	0.00	99.82	G3
03-03	578801	6554264	39.52	0.07	22.08	0.13	22.27	0.88	0.00	9.26	6.08	0.01	0.00	100.30	G3
03-03	578801	6554264	38.93	0.13	21.45	0.00	24.10	0.75	0.00	7.36	7.25	0.03	0.01	100.01	G3
03-04	568767	6571934	40.67	0.02	18.43	7.56	8.32	0.52	0.00	17.29	7.59	0.00	0.00	100.40	G12
03-04	568767	6571934	41.14	0.05	19.46	6.33	7.66	0.43	0.00	18.85	6.30	0.04	0.00	100.27	G9
03-04	568767	6571934	41.12	0.12	19.10	6.77	8.86	0.54	0.00	18.27	6.14	0.03	0.03	100.97	G9
03-04	568767	6571934	37.17	0.00	21.08	0.00	33.59	3.78	0.00	3.62	1.05	0.01	0.03	100.34	G0
03-04	568767	6571934	38.66	0.06	21.18	0.11	24.41	0.69	0.00	6.37	8.32	0.00	0.01	99.81	G3
03-05	618460	6601324	41.68	0.06	19.84	4.96	8.14	0.44	0.06	18.71	5.74	0.01	0.00	99.65	G9
03-05	618460	6601324	41.96	0.28	21.39	2.79	8.81	0.42	0.02	19.85	4.18	0.07	0.00	99.77	G9
03-05	618460	6601324	40.30	0.03	22.63	0.02	19.37	0.48	0.03	10.16	7.82	0.00	0.00	100.83	G3
03-05	618460	6601324	37.75	0.04	21.28	0.00	30.21	0.48	0.00	3.81	7.31	0.01	0.01	100.92	G3
03-05	618460	6601324	39.15	0.17	21.62	0.07	24.34	0.63	0.01	6.63	7.47	0.03	0.00	100.11	G3
03-06	637217	6536614	37.76	0.11	20.43	0.00	27.37	2.53	0.00	1.93	9.94	0.03	0.00	100.11	G0
03-06	637217	6536614	37.82	0.15	20.97	0.03	28.57	1.92	0.01	2.97	8.09	0.03	0.01	100.58	G0
03-06	637217	6536614	36.64	0.09	20.10	0.00	16.01	22.27	0.01	0.71	3.79	0.04	0.01	99.65	G0
03-07	552529	6488984	36.68	0.02	20.34	0.00	28.92	13.48	0.05	0.49	0.10	0.00	0.00	100.08	G0
03-08	517999	6510824	39.02	0.08	21.91	0.00	21.97	0.60	0.05	5.09	11.87	0.00	0.01	100.59	G3
03-10	567804	6580616	41.10	0.14	17.38	8.11	8.34	0.45	0.06	17.20	7.04	0.03	0.02	99.87	G9
03-10	567804	6580616	42.02	0.27	19.89	4.49	7.83	0.42	0.00	19.90	4.90	0.05	0.00	99.78	G9
03-10	567804	6580616	38.43	0.01	21.69	0.02	30.58	0.91	0.07	6.61	2.39	0.01	0.00	100.72	G0
03-10	567804	6580616	37.50	0.03	20.93	0.02	33.80	0.18	0.04	2.40	5.88	0.01	0.00	100.80	G0
03-10	567804	6580616	36.84	0.05	21.15	0.00	36.35	2.67	0.02	2.76	0.54	0.03	0.00	100.41	G0
03-11	628357	6566434	41.52	0.00	18.13	7.53	8.73	0.45	0.00	16.56	7.74	0.02	0.03	100.69	G12
03-12	545700	6489131	37.87	0.03	21.17	0.00	31.97	2.91	0.04	4.17	2.29	0.01	0.03	100.48	G0
03-13	548386	6486636	40.78	0.09	17.32	8.04	7.58	0.50	0.00	17.73	6.87	0.02	0.01	98.94	G9
03-13	548386	6486636	37.24	0.00	21.04	0.00	35.38	1.01	0.00	3.03	2.64	0.01	0.00	100.37	G0
03-13	548386	6486636	38.88	0.11	21.72	0.00	25.19	0.61	0.03	6.17	7.91	0.02	0.00	100.64	G3
03-13	548386	6486636	39.35	0.07	22.15	0.05	23.76	0.60	0.04	7.57	6.82	0.02	0.00	100.42	G3
03-14	642386	6549584	36.29	0.00	20.90	0.02	38.17	3.01	0.00	1.62	0.60	0.03	0.00	100.63	G0
03-14	642386	6549584	36.92	0.11	21.27	0.02	37.14	0.32	0.05	4.14	0.66	0.02	0.01	100.66	G0
03-14	642386	6549584	37.31	0.06	20.46	0.00	31.91	1.07	0.06	2.45	6.85	0.00	0.02	100.17	G0
03-14	642386	6549584	39.14	0.11	21.78	0.00	21.97	0.44	0.01	6.56	9.42	0.03	0.00	99.45	G3
03-16	656803	6606763	37.84	0.09	21.10	0.01	32.67	0.81	0.00	3.33	4.92	0.00	0.01	100.78	G0
03-16	656803	6606763	36.86	0.03	21.00	0.00	36.42	2.72	0.01	2.71	0.79	0.01	0.00	100.53	G0
03-16	656803	6606763	38.49	0.03	21.01	0.04	26.38	1.10	0.00	2.89	10.83	0.02	0.00	100.77	G0
03-16	656803	6606763	37.21	0.00	21.07	0.01	36.78	1.65	0.00	2.56	0.80	0.02	0.01	100.12	G0
03-17	581298	6540066	38.88	0.05	21.51	0.07	29.63	0.31	0.06	5.42	4.90	0.01	0.00	100.83	G0
03-17	581298	6540066	36.68	0.25	18.29	0.02	2.97	0.46	0.00	1.81	36.41	0.03	0.01	96.93	G0
03-20	516911	6515041	36.64	0.00	21.13	0.01	34.91	3.23	0.04	2.30	1.02	0.01	0.00	99.28	G0
03-20	516911	6515041	37.39	0.12	21.12	0.02	23.48	8.19	0.00	0.74	9.11	0.01	0.03	100.21	G0

Table 3. Microprobe analysis of diopside (%).

Sample ID	UTM Easting	UTM Northing	SiO ₂	TiO ₂	Al ₂ O ₃	Cr ₂ O ₃	FeO	MnO	NiO	MgO	CaO	Na ₂ O	K ₂ O	Total	100Mg/(Mg+Fe)
03-02	628743	6566536	53.40	0.08	3.08	1.61	3.01	0.04	0.08	14.74	22.18	1.19	0.00	99.42	89.72
03-02	628743	6566536	52.34	0.36	6.77	1.28	2.25	0.04	0.10	14.40	21.24	1.55	0.03	100.37	91.95
03-04	568767	6571934	53.10	0.17	1.26	0.44	3.30	0.10	0.00	16.42	24.60	0.24	0.00	99.64	89.87
03-04	568767	6571934	53.78	0.19	2.61	1.08	4.52	0.15	0.10	14.49	22.95	0.78	0.02	100.66	85.11
03-04	568767	6571934	54.49	0.10	0.77	0.65	2.15	0.04	0.07	17.42	24.08	0.16	0.00	99.94	93.52
03-07	552529	6488984	55.14	0.08	1.44	0.32	3.59	0.15	0.09	16.31	23.25	0.46	0.01	100.83	89.02
03-07	552529	6488984	55.18	0.12	2.00	1.02	5.16	0.11	0.12	13.97	20.70	2.00	0.01	100.39	82.85
03-07	552529	6488984	55.42	0.03	0.55	0.59	2.60	0.11	0.03	17.61	23.30	0.20	0.00	100.43	92.35
03-11	628357	6566434	54.31	0.07	1.43	0.59	3.58	0.04	0.14	15.76	23.71	0.56	0.00	100.18	88.71
03-14	642386	6549584	55.18	0.13	1.29	0.67	4.02	0.13	0.19	15.73	23.10	0.50	0.00	100.94	87.46
03-14	642386	6549584	53.98	0.14	1.29	0.43	5.37	0.17	0.12	16.06	21.38	0.63	0.00	99.56	84.21
03-14	642386	6549584	53.95	0.15	2.47	1.03	5.26	0.07	0.06	18.50	18.13	0.27	0.00	99.90	86.24
03-14	642386	6549584	54.27	0.07	1.86	0.35	5.37	0.18	0.00	14.97	22.66	0.86	0.00	100.59	83.26
03-16	656803	6606763	54.48	0.00	1.49	0.48	4.50	0.17	0.11	15.12	23.37	0.47	0.00	100.19	85.68
03-16	656803	6606763	54.18	0.06	1.53	0.17	5.18	0.33	0.04	14.26	23.57	0.64	0.03	99.99	83.08
03-16	656803	6606763	53.01	0.00	0.29	0.01	6.49	1.85	0.00	12.56	25.61	0.06	0.00	99.87	77.52
03-20	516911	6515041	53.74	0.06	1.71	0.40	6.14	0.19	0.06	14.18	22.35	0.77	0.00	99.62	80.46
03-22	560045	6482451	52.23	0.48	7.13	1.00	3.03	0.12	0.03	14.75	19.71	1.66	0.00	100.14	89.68
03-22	560045	6482451	52.71	0.29	6.75	0.82	3.04	0.09	0.01	15.07	20.46	1.33	0.00	100.56	89.83
03-22	560045	6482451	55.17	0.19	1.09	0.45	2.93	0.14	0.00	17.35	23.73	0.10	0.00	101.16	91.35

Table 4. Microprobe analysis of ilmenite (%).

Sample ID	UTM Easting	UTM Northing	TiO ₂	Al ₂ O ₃	Cr ₂ O ₃	FeO	MnO	MgO	CaO	ZnO	SiO ₂	V ₂ O ₃	NiO	Total
03-17	581298	6540066	48.13	0.37	0.06	41.09	0.25	7.55	0.01	0.00	0.03	0.23	0.01	97.95
03-17	581298	6540066	51.07	0.43	0.54	35.67	0.24	10.11	0.02	0.05	0.03	0.21	0.08	98.72
03-03	578801	6554264	50.75	0.66	0.31	33.64	0.30	12.30	0.02	0.00	0.02	0.17	0.13	98.55

Table 5. Microprobe analysis of olivine (%).

Sample ID	UTM Easting	UTM Northing	SiO ₂	TiO ₂	Al ₂ O ₃	Cr ₂ O ₃	FeO	MnO	NiO	MgO	CaO	Na ₂ O	K ₂ O	Total	100Mg/(Mg+Fe)
03-01	589380	6518892	38.96	0.04	0.05	0.05	17.68	0.23	0.22	41.80	0.20	0.04	0.00	99.25	80.82
03-01	589380	6518892	39.31	0.00	0.04	0.04	16.04	0.18	0.22	43.59	0.23	0.03	0.00	99.67	82.89
03-01	589380	6518892	39.23	0.02	0.03	0.04	17.26	0.20	0.19	42.24	0.26	0.02	0.00	99.51	81.35
03-02	628743	6566536	39.08	0.01	0.06	0.03	17.21	0.23	0.22	42.94	0.30	0.00	0.00	100.08	81.64
03-02	628743	6566536	38.93	0.01	0.05	0.02	17.57	0.21	0.19	42.42	0.22	0.02	0.01	99.65	81.14
03-02	628743	6566536	38.86	0.00	0.01	0.02	17.17	0.22	0.17	42.34	0.21	0.01	0.00	99.02	81.47
03-02	628743	6566536	39.14	0.03	0.06	0.06	17.14	0.23	0.24	42.56	0.20	0.00	0.00	99.66	81.57
03-02	628743	6566536	39.55	0.00	0.04	0.04	15.90	0.22	0.23	43.45	0.23	0.02	0.00	99.68	82.97
03-02	628743	6566536	38.86	0.02	0.05	0.06	18.38	0.25	0.21	41.45	0.24	0.02	0.03	99.56	80.08
03-02	628743	6566536	39.23	0.01	0.03	0.04	17.10	0.22	0.16	42.21	0.26	0.00	0.00	99.26	81.48
03-02	628743	6566536	38.63	0.01	0.07	0.06	17.18	0.19	0.20	42.29	0.22	0.01	0.01	98.87	81.44
03-04	568767	6571934	39.20	0.01	0.04	0.03	16.90	0.19	0.34	42.46	0.24	0.00	0.01	99.42	81.75
03-04	568767	6571934	39.04	0.02	0.04	0.05	16.33	0.20	0.31	42.80	0.22	0.02	0.00	99.02	82.37
03-04	568767	6571934	38.67	0.02	0.02	0.02	19.43	0.21	0.15	40.78	0.26	0.03	0.02	99.61	78.91
03-04	568767	6571934	38.81	0.05	0.04	0.05	18.87	0.18	0.24	41.15	0.22	0.00	0.00	99.60	79.54
03-04	568767	6571934	40.25	0.06	0.02	0.00	10.48	0.14	0.39	48.35	0.04	0.00	0.01	99.75	89.16
03-04	568767	6571934	38.36	0.02	0.03	0.06	19.55	0.26	0.24	40.68	0.22	0.00	0.02	99.42	78.77
03-04	568767	6571934	39.31	0.01	0.04	0.04	17.30	0.19	0.37	42.64	0.20	0.00	0.00	100.09	81.46
03-04	568767	6571934	40.20	0.03	0.02	0.00	10.54	0.18	0.38	47.82	0.05	0.00	0.00	99.21	89.00
03-05	618460	6601324	38.74	0.01	0.04	0.04	17.73	0.16	0.32	42.20	0.22	0.02	0.00	99.48	80.93
03-05	618460	6601324	39.45	0.00	0.04	0.07	15.30	0.16	0.25	43.38	0.23	0.00	0.02	98.90	83.48
03-05	618460	6601324	38.85	0.00	0.08	0.04	17.25	0.18	0.25	42.63	0.23	0.02	0.00	99.54	81.50
03-05	618460	6601324	38.61	0.01	0.05	0.04	18.64	0.27	0.22	41.37	0.22	0.02	0.00	99.45	79.82
03-06	637217	6536614	38.06	0.06	26.12	0.00	9.98	0.11	0.00	0.00	24.07	0.00	0.00	98.41	0.00
03-07	552529	6488984	40.68	0.00	0.00	0.02	9.60	0.19	0.33	48.77	0.03	0.00	0.00	99.65	90.06
03-07	552529	6488984	40.75	0.04	0.02	0.01	9.91	0.18	0.41	48.74	0.02	0.00	0.01	100.09	89.76
03-07	552529	6488984	39.69	0.05	0.05	0.02	16.06	0.23	0.18	43.76	0.22	0.01	0.01	100.27	82.93
03-17	581298	6540066	38.93	0.01	0.06	0.02	17.65	0.24	0.24	41.89	0.22	0.02	0.00	99.28	80.88

Table 6. Microprobe analysis of diaspore (%).

Sample ID	UTM Easting	UTM Northing	SiO ₂	TiO ₂	Al ₂ O ₃	Cr ₂ O ₃	FeO	MnO	NiO	MgO	K ₂ O	Total
03-06	637217	6536614	0.00	0.04	81.28	0.00	3.95	0.03	0.02	0.02	0.00	85.32
03-02	628743	6566536	0.00	0.01	81.92	0.00	2.83	0.00	0.03	0.00	0.01	84.81

Cratonic Basement in Northeastern British Columbia: New U-Pb Geochronological Results and their Significance for Diamond Exploration

By G. J. Simandl¹ and W. Davis²

ABSTRACT

This study was proposed to enhance our understanding of crystalline basement in northeastern British Columbia. Seven new U-Pb zircon ages for this area are reported from samples of drill cuttings. Samples B5 (1854 ± 6 Ma) and B25 (minimum age 1.75 Ga; inherited zircon 1.89–2.23 Ga) are located within but near the edge of the Nova Terrane, as it is currently defined. Sample B2 plots within the Kiskatinaw Terrane and samples B11 (1994 ± 7 Ma), B12 (1993 ± 7 Ma) and B14 (1993 ± 7 Ma) plot within the Ksituan Terrane. Sample B34 (1859 ± 10 Ma) is located near the British Columbia – Yukon Border, and occurs within the Fort Simpson Terrane. The samples from the Nova Terrane returned Paleoproterozoic ages and thus did not confirm the popular interpretation that assigns an Archean age to the Nova Terrane. The age indicated by the inherited zircon from sample B25 is similar to the 2.0 and 2.3 Ga ages previously reported for the Buffalo Head Terrane, which is believed to be reworked Archean basement. This finding is important from an exploration point of view, since the Buffalo Head Terrane in neighbouring Alberta hosts diamondiferous kimberlites.

INTRODUCTION

Major diamond-producing areas, such as the Diavik and Ekati mines in the Northwest Territories, are located within old stable cratons and conform to Clifford's rule, as considered by Janse (1994). Such areas host most of the known, large, primary diamond orebodies (Helmstaed, 1993). The Argyle mine (Australia), which is located within a mobile zone near the edge of the craton, is the only major exception (O'Neill *et al.*, 2003). Northeastern British Columbia (Fig. 1) is underlain by the Laurentian craton and is located east of the Foreland Belt (Gabrielse *et al.*, 1991; Monger and Price, 2002). It has been located near the edge of the Laurentian craton since the break-up of the Rodinia supercontinent more than 530 m.y. ago (Monger and Price, 2002).

All diamond occurrences reported in British Columbia (Northcote, 1983a, b; Anonymous, 1994; McCallum

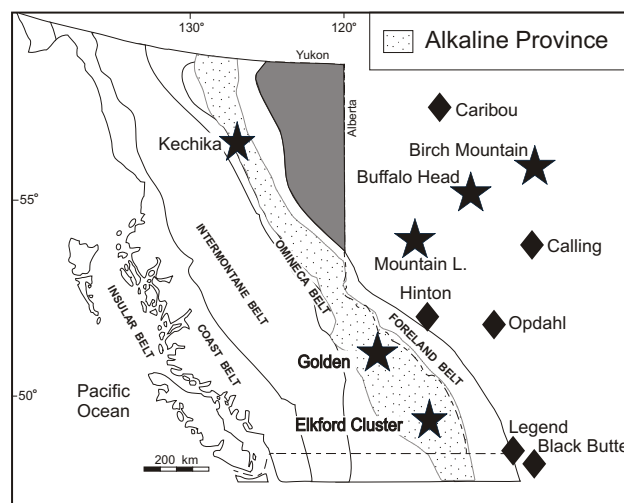


Figure 1: Morphogeological belts of the Canadian Cordillera; British Columbia's alkaline province shown in stipple; stars indicate primary diamond occurrences and lozenges represent alluvial diamond occurrences reported in the literature (*modified from Simandl, 2004*). Shaded area indicates British Columbia's portion of the Western Canada Sedimentary Basin, located northeast of the Foreland Belt. Basement underlying this and the adjacent area in Alberta is shown in more detail in the Figure 2. Location of belts according to Gabrielse *et al.* (1991).

(1994); Allan, 1999, 2002; Roberts, 2002) are located within the British Columbia alkaline province (Fig. 1). This belt-shaped province follows the Omineca-Foreland belt boundary and the Rocky Mountain Trench, and is characterized by a variety of alkaline rocks, including carbonates, nepheline syenites and kimberlites (Pell, 1994; Simandl, 2004). It is reported to coincide with an abrupt thickening of the crust and continental lithosphere, which persists and thickens eastward (Hyndman and Lewis, 1999). The rocks east and west of the British Columbia alkaline province (Fig. 1) have received very little attention from the diamond exploration industry, with the exception of a few isolated projects in the Peace River area, as exemplified by Stapleton (1997).

This paper concentrates on the Precambrian basement terranes in northeastern British Columbia (Fig. 2), situated between the British Columbia alkaline province and diamond discoveries within the Buffalo Head Terrane, Alberta. Current continental masses are a mosaic of welded

¹British Columbia Ministry of Energy and Mines, Victoria

²Geological Survey of Canada, Ottawa

fragments of ancient continents and accreted terrains, and it is possible that a portion of the Precambrian crystalline basement in eastern British Columbia was previously associated with a deep cratonic keel similar to that described by Haggerty (1986), Mitchell (1991), Kirkley *et al.* (1991) and Helmstaedt and Gurney (1995). It is possible that diamonds formed in Paleoproterozoic time or that the old basement fragments were displaced relative to their position of origin

and dissociated from their keel, but they may still host potential diamond transporters, such as kimberlites, lamproites and lamprophyres (Simandl, 2004). Any information about the tectonic history, structure, petrological, geophysical and geochemical characteristics, including age, are important for understanding the basement terranes and are of interest in diamond exploration.

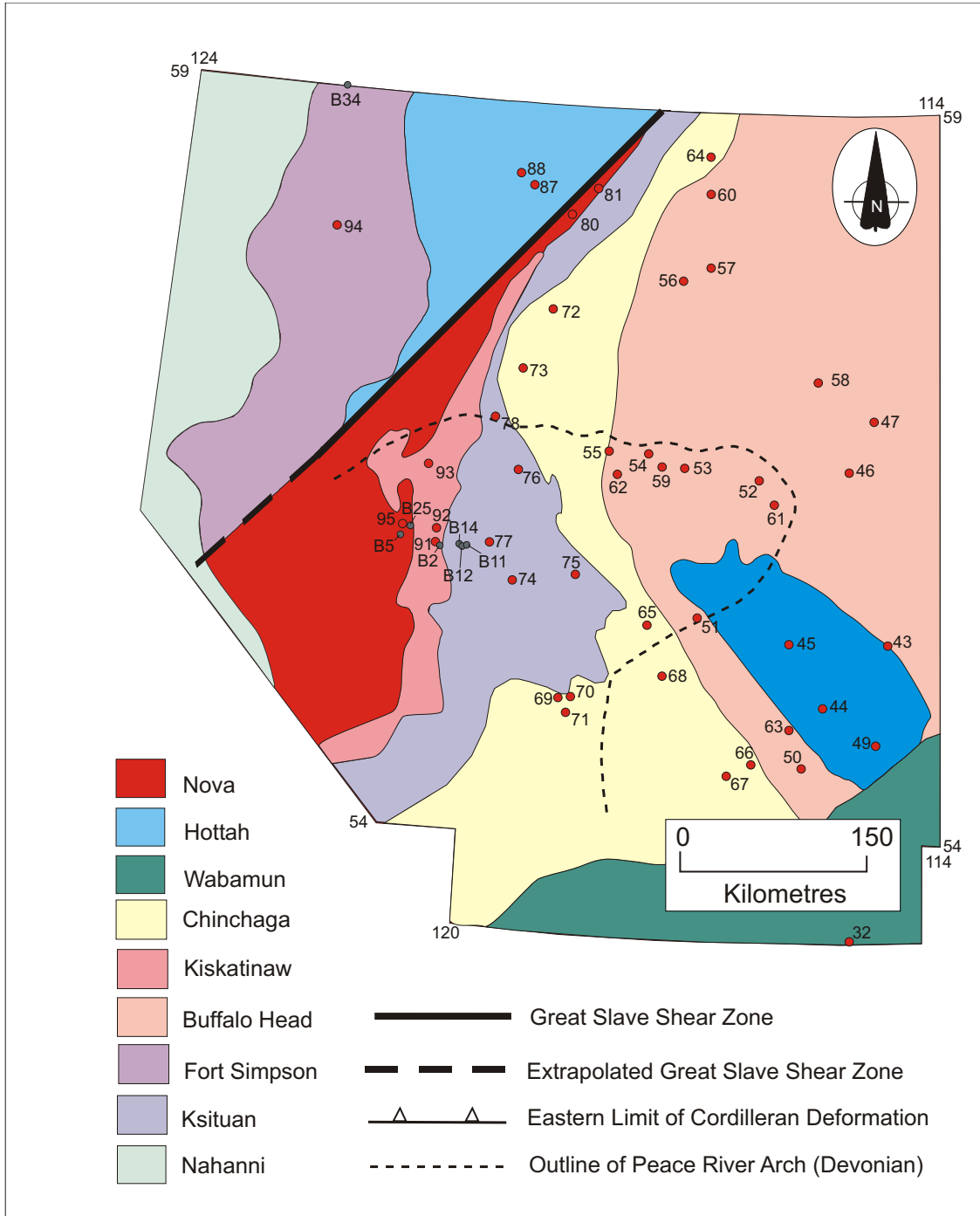


Figure 2: Generalized tectonic map of basement in northeast British Columbia and adjacent Alberta. The Nova Terrane is commonly interpreted as a sliver of Archean Slave craton (Villeneuve *et al.*, 1993). Samples that were submitted for radiometric dating and are discussed in the text are identified by numbers B2, B5, B11, B12, B14, B25 and B34. Dates for the remaining samples and their locations are provided by Villeneuve *et al.* (1993).

PRECAMBRIAN BASEMENT IN NORTHEASTERN BRITISH COLUMBIA

Along the Alberta border (Fig. 2), the basement terranes hidden beneath the cover sequence are defined and extrapolated based on a combination of potential-field geophysics combined with limited radiometric dating and petrological studies of oil and gas well cuttings from northern Alberta. These wells are unevenly distributed, forming tight clusters in areas of highest oil and gas potential. Consequently, the interpretation based on the work of Hoffman (1988, 1989) and Ross *et al.* (1991, 1995), with minor subsequent modification, is still in use (Gehrels and Ross, 1998; McNicoll *et al.*, 2000; Pilkington *et al.*, 2000).

The terranes in northeastern British Columbia are, from southwest to northeast, the Wabamun High (accreted terrane), Buffalo Head (accreted terrane), Chinchaga Low (accreted terrane), Ksituan High (magmatic arc), Kiscatinaw Low (accreted terrane), Nova (possible Archean basement?), Hottah (accreted terrane), Fort Simpson (magmatic arc) and Nahanni (uncertain age and origin). The characteristics of the key terranes (including their ages) are summarized below.

The most intriguing and controversial aspect of the prevailing interpretation (Fig. 2) is that the Nova Terrane, which is assigned an Archean age, is interpreted as a possible sliver of the Slave Craton, based on mylonites from Imperial Rainbow Lake (Alberta), which are dated at 2808 ± 30 Ma.

BUFFALO HEAD TERRANE

The Buffalo Head Terrane (BHT) consists mainly of metaplutonic and, to a lesser extent, metavolcanic and metasedimentary rocks. The U–Pb zircon ages for the magmatic rocks range from 2324 to 1990 Ma (Villeneuve *et al.*, 1993). Dioritic to granitic rocks are dated at 2324 to 2072 Ma. Monazite and zircon ages from granulite in the Chinchaga Domain and BHT suggest that a metamorphic event occurred at 2017 Ma, followed by the intrusion of granitic rocks from 1990 to 1998 Ma. The younger magmatism is interpreted to be penecontemporaneous with collision of the Buffalo Head and Chinchaga terranes (Ross and Eaton, 2002). Neodymium isotope data suggest that the Buffalo Head Terrane formed as a result of reworking of Archean crust (McNicoll *et al.*, 2000). This terrane hosts a number of barren and diamondiferous kimberlites (Carlson *et al.*, 1999).

CHINCHAGA TERRANE

The Chinchaga Terrane is an aeromagnetic low, separating the Buffalo Head Terrane from the Ksituan Terrane. It consists of metaplutonic rocks that recrystallized at 2.19 to 2.08 Ga, overlapping with ages reported from the Buffalo Head Terrane (Ross and Eaton, 2002). Argon-argon ages suggest that this terrane has a similar cooling history to that of the BHT. Neodymium isotope data from the Chinchaga indicate a recycling of Archean crust, similar to

that observed in the BHT (Theriault and Ross 1991; McNicoll *et al.*, 2000).

KSITUAN TERRANE

This terrane is characterized by an aeromagnetic high and consists mainly of metaplutonic rocks dated at 1986 to 1900 Ma (U–Pb zircon), younger than rocks within the Buffalo Head and Chinchaga terranes. Uranium-lead geochronology of titanite suggests that these rocks cooled to 600°C by 1885 Ma (Ross *et al.*, 2002).

KISKATINAW TERRANE

This terrane has an aeromagnetic low signature, with U–Pb ages that are similar to those of the Ksituan Terrane. The terrane is interpreted as a shear zone separating the Ksituan from the Nova Terrane (Ross *et al.*, 2002). Loss of magnetization may be deformation or alteration induced.

NOVA TERRANE

The Nova Terrane is an aeromagnetic high bounded by the Hay River Fault and the Liskatinaw Terrane. In Alberta, mafic gneiss and metarhyolite within this terrane give late Archean U–Pb ages of 2808 and 1990 Ma, respectively (Ross and Eaton, 2002).

HOTTAH TERRANE

This terrane coincides with an aeromagnetic low that grades eastward into the Great Bear Arc aeromagnetic high in northern Alberta. Rock types intercepted by drillholes are plutonic rocks and calcisilicate gneiss (Villeneuve *et al.*, 1993). The same authors stated that 1.92 Ga is a typical date from this terrane.

WABAMUN TERRANE

The Wabamun Terrane is characterized by a positive aeromagnetic signature with an internal fabric that consists of oval-shaped positive domains surrounded by magnetic lows. It is believed to consist largely of undeformed magmatic rocks. Villeneuve *et al.* (1993) reported a single age of 2.32 Ga.

FORT SIMPSON TERRANE

This terrane forms a magnetic high with ovoid internal structures. It is interpreted as a calcalkaline plutonic complex. The three dates available, all from biotite granites, range from 1.84 to 1.85 Ga. (Villeneuve *et al.*, 1991; Ross *et al.*, 2000).

NAHANNI TERRANE

The Nahanni magnetic low is interpreted as thinned Fort Simpson basement (Cook *et al.*, 1999); however, granite clasts from the Coates Lake diatreme indicate a crystallization age of 1100 to 1175 Ma (Jefferson and Parrish, 1989).

SAMPLE SELECTION, SAMPLE PREPARATION AND ANALYTICAL PROCEDURES

There are no outcrops of Precambrian basement within the study area, and less than 100 boreholes drilled for oil and gas in the area are reported to have reached the basement. Most of these boreholes are clustered in areas that were subject to the most intense oil and gas exploration. Cuttings from basement are available from a limited number of holes. Basement cuttings were collected, carefully handpicked to avoid cavings (contamination) from overlying shale and limestone units, crushed, and the heavy mineral fraction was separated using both heavy liquids and magnetic separation with a Frantz™ isodynamic separator. Zircons were recovered from seven of the nine samples processed.

The U-Pb ages of the zircons were determined using the sensitive high-resolution ion microprobe (SHRIMP) at the J.C. Roddick Ion Microprobe Laboratory, Geological Survey of Canada. Analytical procedures followed those described by Stern (1997), with standards and U-Pb calibration methods following Stern and Amelin (2003). Briefly, zircons were cast in 2.5 cm diameter epoxy mounts (GSC #333) along with fragments of the GSC laboratory standard zircon (z6266, with $^{206}\text{Pb}/^{238}\text{U}$ age = 559 Ma). The midsections of the zircons were exposed using 9, 6, and 1 μm diamond compound, and the internal features of the zircons (such as zoning, structures, alteration, etc.) were characterized with cathodoluminescence (CL) and back-scattered electrons (BSE) using a Cambridge Instruments scanning electron microscope. Mount surfaces were evaporatively coated with 10 nm of high purity Au. Analyses were conducted using an $^{16}\text{O}^-$ primary beam, projected onto the zircons at 10 kV. Two different sized spots were used for analysis, one $\sim 25 \mu\text{m}$ in diameter and another $\sim 16 \mu\text{m}$ in diameter, with a beam currents of ~ 9 and ~ 1.6 nA, respectively. The count rates of ten isotopes of Zr^+ , U^+ , Th^+ , and Pb^+ in zircon were sequentially measured over seven scans with a single electron multiplier and a pulse counting system with deadtime of 35 ns. Offline data processing was accomplished using customized in-house software. The 1 σ external errors of $^{206}\text{Pb}/^{238}\text{U}$ ratios reported in the accompanying data table incorporate a 1.4 to 2.0% (for larger spot and smaller spot, respectively) error in calibrating the standard zircon (see Stern and Amelin, 2003). No fractionation correction was applied to the Pb-isotope data; common Pb correction utilized the measured ^{204}Pb and composition of the surface gold coating (Stern, 1997). Isoplot v. 3.00 (Ludwig, 2003) was used to generate concordia plots and calculate weighted means.

SAMPLE LOCATIONS AND U-PB DATING RESULTS

Zircons were recovered from seven samples: B2, B5, B11, B12, B14, B25 and B34. Sample locations are indicated on Figure 2 and the sample descriptions are summarized in Table 1. Samples B5 and B25 are located within but

near the edge of Nova Terrane, as currently defined. Sample B2 plots within the Kiskatinaw Terrane and samples B11, B12 and B14 plot within the Ksituan Terrane. Sample B34, which is located near the British Columbia–Yukon boundary, occurs within the Fort Simpson Terrane. The results of U-Pb analyses are systematically described below and displayed on Figures 3 to 9.

U-PB AGE RESULTS

Sample B2: Kiskatinaw Terrane; cuttings of granitic basement. Zircons comprise a homogeneous population of euhedral to subhedral prismatic grains with broad oscillatory zoning typical of igneous crystals. Analyses of 13 individual zircon grains yielded a single age population with a weighted mean $^{207}\text{Pb}/^{206}\text{Pb}$ age of 1903 ± 7 Ma (Fig. 3), interpreted as the crystallization age of the sample. Evidence for older zircon in the form of inherited cores was not observed using BSE imaging.

Sample B11: Ksituan Terrane; cuttings of granitic basement. Zircons in this sample are euhedral to subhedral, equant to short prisms with well-developed oscillatory zoning. Some zones of presumably higher U content are altered

TABLE 1. DESCRIPTIONS OF SAMPLES DATED USING SENSITIVE HIGH-RESOLUTION ION MICROPROBE (SHRIMP).

Sample	Description of drillhole cuttings
B2	Crystalline basement (granitic composition) <i>Mineralogy: biotite, quartz, slight chloritization, feldspars (some altered)</i> <i>cavings: limestone/shale < 15% of the vial</i>
B5	Crystalline basement (granite) <i>Mineralogy: biotite, quartz, phlogopite, feldspar, sulphides, trace green mineral (epidote or amphibole, less likely pyroxene)</i> <i>cavings: < 15%</i>
B11	Crystalline basement (granite) <i>Mineralogy: chloritized biotite, quartz, feldspar, chlorite</i> <i>cavings: < 10%</i>
B12	Crystalline basement (granitic composition, possibly orthogneiss) <i>Mineralogy: quartz, feldspar, biotite, zircon, titanite, trace of phlogopite (~90-95%)</i> <i>cavings: < 5% limestone</i>
B14	Crystalline basement (granite) <i>Mineralogy: quartz, altered feldspar, epidote, biotite, chlorite, unknown brown mineral, sediment, some grains look like quartzite</i> <i>cavings: limestone/shale < 10%</i>
B25	Crystalline basement (granite/gneiss, possibly quartzite fragments) <i>Mineralogy: feldspar, quartz, mica is aligned in some grains</i> <i>cavings: 15%</i>
B34	Crystalline basement (granite) <i>Mineralogy: biotite, lots of quartz, some feldspar, trace muscovite</i> <i>cavings: < 10%</i>

and these areas were avoided during the analyses. A total of twelve analyses yielded variably discordant data that define a discordia line with an upper intercept age of 1994 ± 7 Ma (Fig. 4). This is interpreted as the igneous age of the sample. The discordance in the data may in part reflect the poor quality of many of the zircon crystals. No inherited component was recognized.

Sample B12: Ksituan Terrane; cuttings of granitic basement. Zircons recovered from this sample are dominantly prismatic with moderate terminations and concentric growth zoning in BSE images. The igneous age of 1993 ± 7 Ma is interpreted from the weighted mean $^{207}\text{Pb}/^{206}\text{Pb}$ age of the twelve least discordant analyses (Fig. 5), with the most discordant fraction excluded from the calculation.

Sample B14: Ksituan Terrane; cuttings of granitic basement. This sample yielded only a small number of zircons (~25). The grains are prismatic with fine to broad oscillatory zoning. No evidence for inherited cores was observed. Many of the crystals are altered and heavily fractured. Analyses were selectively located on unaltered domains and a weighted mean $^{207}\text{Pb}/^{206}\text{Pb}$ age of 1993 ± 5 Ma is interpreted as the igneous crystallization age (Fig. 6). The most discordant analysis was excluded from the calculation.

Sample B5: Nova Terrane; cuttings of granitic rock. Zircons recovered from this sample define a homogeneous population of prismatic zircons with broad diffuse zoning observed in BSE images. No evidence of inherited cores was noted in the approximately 47 grains imaged. An igneous crystallization age of 1855 ± 6 Ma was calculated from the weighted mean of 12 $^{207}\text{Pb}/^{206}\text{Pb}$ age determinations (Fig. 7).

Sample B25: Nova Terrane; cuttings of granitic basement. Zircons in this sample are dominantly prismatic with fine to diffuse oscillatory growth zoning. The analyses

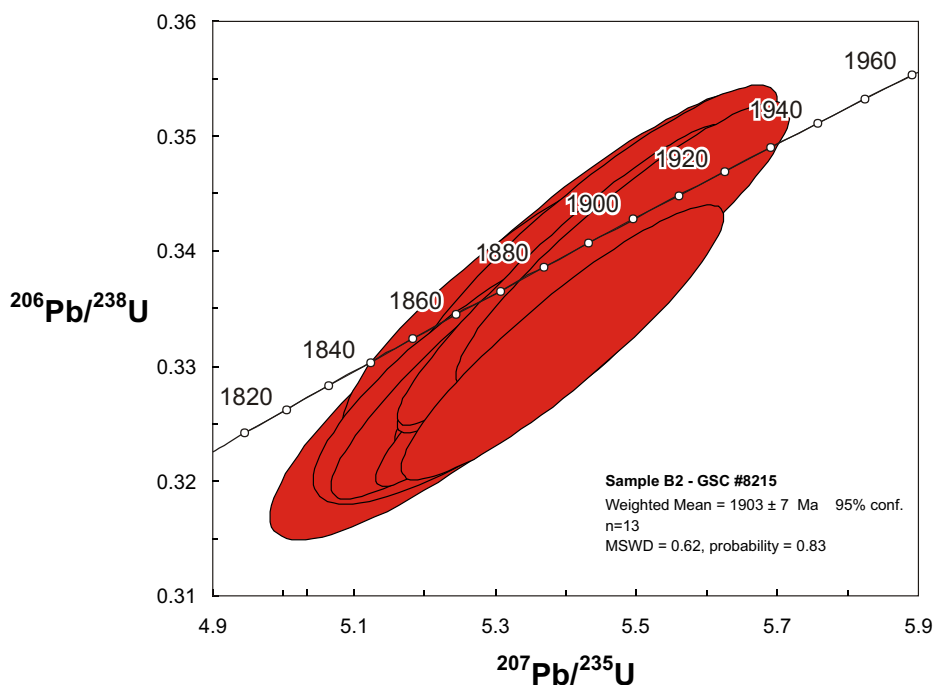


Figure 3. Interpretation of SHRIMP analytical data, sample B2; see text for explanations

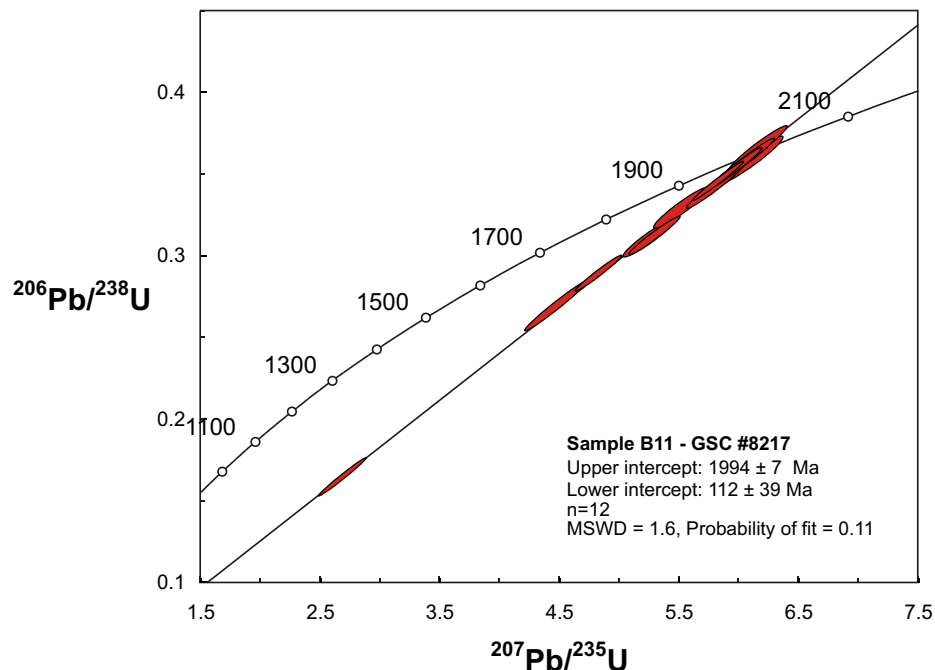


Figure 4. Interpretation of SHRIMP analytical data, sample B11; see text for explanations.

show a very large range in U and Th content, with individual analyses ranging from concordant to almost 70% discordant (Fig. 8), the more discordant grains containing higher U contents of up to 3400 ppm. It is likely that the Pb/U calibration for these analyses is unreliable due to the high U contents and variable matrix effects. The age results did not yield a definitive interpretation. Ages for the less

discordant analyses range from 1.89 to 2.23 Ga, an age range that is interpreted to indicate a significant inherited component in the sample. Three analyses yielded similar $^{207}\text{Pb}/^{206}\text{Pb}$ ages of ~ 1.75 Ga, but these ages are extremely discordant and therefore provide only a minimum age for the sample. A maximum age is estimated for the cluster of analyses at ~ 1.9 Ga. The pre-2.0 Ga zircons are interpreted as inherited.

Sample: B34: Fort Simpson Terrane; cuttings of granitic basement. Zircons from this sample are dominated by prismatic morphologies with prominent oscillatory growth zoning evident in BSE images. A total of 13 analyses define a simple discordia line with the upper intercept age of 1859 ± 10 Ma interpreted as the crystallization age of the rock (Fig. 9). No evidence for an older inherited component is noted in this sample.

DISCUSSION

Six of the seven samples yielded reliable age information, with Paleoproterozoic ages that fall within three age groupings: ~ 1990 , ~ 1900 and ~ 1850 Ma. Although sample B25 did not yield a reliable age estimate, it is most likely Paleoproterozoic and, perhaps most significantly, contains zircon that indicates interaction with ~ 2.0 – 2.3 Ga crust.

Sample B34 is from within the area of the Fort Simpson Terrane (Fig. 2), which is defined mainly as a magnetic high and interpreted as a calcalkaline plutonic complex. The 1859 ± 10 Ma age of the sample is older than a previously published age of 1845 ± 1 Ma for the Fort Simpson Terrane in British Columbia (locality 94; Villeneuve *et al.*, 1993). Two ages from the Fort Simpson Terrane in the Northwest Territories are 1.84 and 1.85 Ga (Villeneuve *et al.*, 1991; Ross *et al.*, 2000). The results for sample B34 support previous geophysical interpretations that extend the Fort Simpson Terrane from north-eastern British Columbia all the way to the Northwest Territories (e.g., Aspler *et al.* 2003).

Samples B11, B12 and B14 occur within the Ksituan Terrane. The three samples give consistent ages of 1994 ± 7 , 1993 ± 7 and 1993 ± 5 Ma. These ages are slightly older than the results of Ross and Eaton (1900 to 1986 Ma, 2004) but still within the proposed range because of associated uncertainties. Dates in the Ksituan Terrane are in the same range as the Kiskatinaw dates reported by Villeneuve *et al.* (1993), and there is no

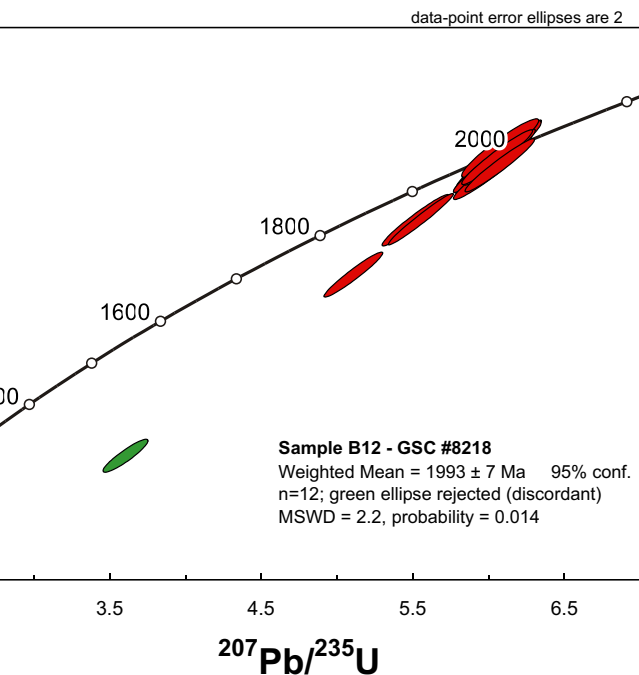


Figure 5 Interpretation of SHRIMP analytical data, sample B12; see text for explanations.

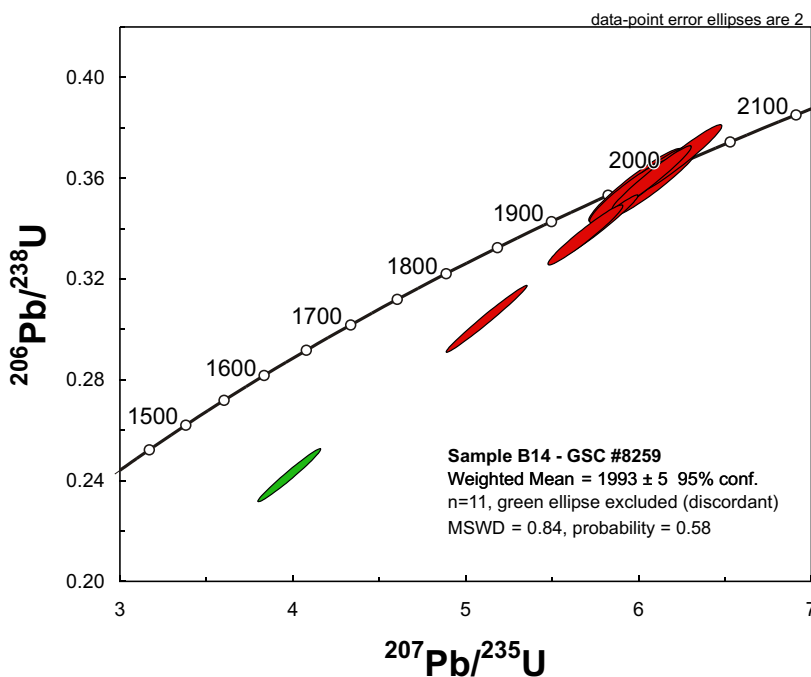


Figure 6 Interpretation of SHRIMP analytical data, sample B14; see text for explanations.

distinction in age between these terranes. Samples B5 and B25 are located within the Nova Terrane (Fig. 2) near its boundary with the Kiskatinaw Terrane. The 1854 ± 6 Ma age for sample B5 is similar to Kiskatinaw ages previously reported by Villeneuve *et al.* (1993).

Sample B25 provided an unexpected result and is extremely important. Three highly discordant analyses yield similar $^{207}\text{Pb}/^{206}\text{Pb}$ ages of ~ 1.75 Ga, and constrain the minimum age for this sample. The most concordant analyses range in age from 1.89 to 2.23 Ga, indicating a significant inherited component in the sample. A maximum age is estimated for the cluster of analyses at ~ 1.9 Ga. This result suggests that rocks within at least a portion of the Nova Terrane contain zircons with characteristics similar to those of the Buffalo Head and Chinchaga terranes. The Buffalo Head Terrane is believed to consist mainly of Paleoproterozoic rocks (2.0 to 2.3 Ga) intruded by a magmatic event at ~ 1.96 Ga (Villeneuve *et al.*, 1993). Archean magmatic ages are not documented in the diamondiferous kimberlite-bearing Buffalo Head Terrane as they have been in the Nova Terrane in Alberta (Ross and Eaton, 2002). However, U-Pb upper intercept ages in some Buffalo Head rocks and Nd isotopic data are interpreted to indicate Archean inheritance (Villeneuve *et al.*, 1993).

The difference between samples B25 and B5 is striking and requires additional consideration. Our results do not support the hypothesis that the Nova Terrane is a sliver of the Archean Slave craton (Fig. 2). Basement samples located centrally within the Nova Terrane are lacking, so some caution should be exercised.

Other approaches, such as Nd isotopic analyses, could be used to further compare sample B25 with existing data from the Buffalo Head and Chinchaga terranes in Alberta, where Nd data suggest that these terranes formed on a foundation consisting of Archean crust

CONCLUSION

This study confirms the presence of Precambrian basement throughout the northeastern British Columbia study area. The dates of 1993 ± 5 , 1993 ± 7 and 1994 ± 7 Ma within the Ksituan Terrane represent the timing of igneous activity, and these rocks must have intruded older basement, the age of which remains undetermined. Interpretation of $^{207}\text{Pb}/^{206}\text{Pb}$ zircon ages for the samples studied does not confirm the presence of Archean basement within the projected area of the Nova Terrane. Sample B25, located within but near the edge of the Nova Terrane, contains inherited zircon of ~ 2.0 to 2.2 Ga age, similar to rocks from the Buffalo Head and Chinchaga ter-

ranes. This is significant, because the Buffalo Head Terrane hosts diamond-bearing kimberlites in neighbouring Alberta. This indicates that basement of BHT age is present much farther west than previously proposed.

Future work, including Nd isotope analysis, could establish additional similarities or differences between the

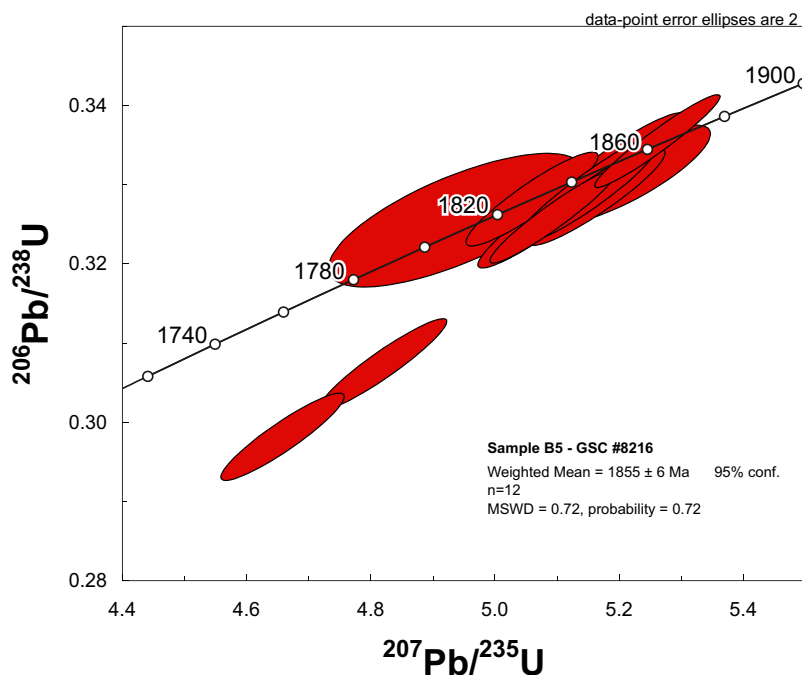


Figure 7. Interpretation of SHRIMP analytical data, sample B5; see text for explanations

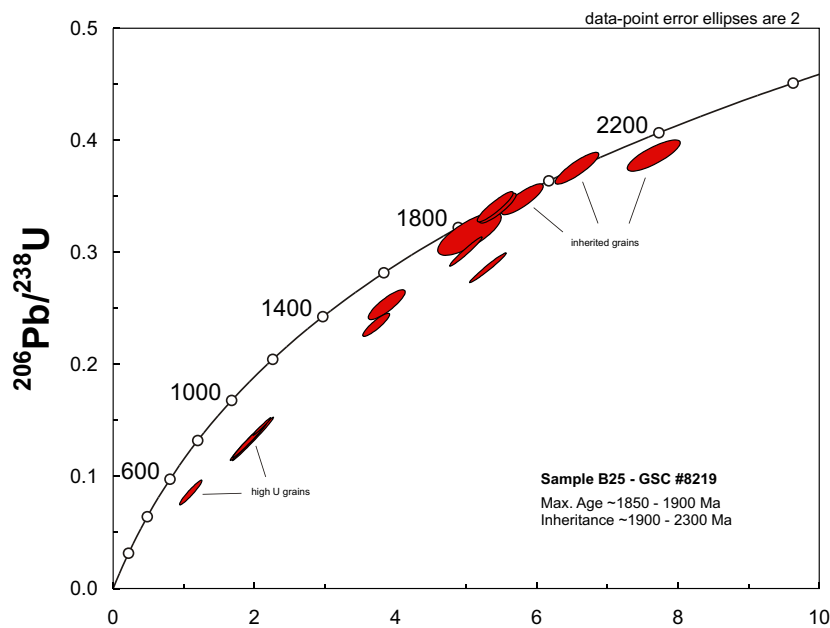


Figure 8. Interpretation of SHRIMP analytical data, sample B25; see text for explanations.

Buffalo Head Terrane in Alberta and the Nova Terrane in British Columbia. A key question is whether Nova Terrane rocks were derived through recycling of Archean material. Additional dating and detailed geophysical interpretation are required to reconcile existing data. Based on similarities with the diamondiferous kimberlite-hosting BHT Terrane in Alberta, portions of northeastern British Columbia should be considered as legitimate but speculative diamond exploration areas.

ACKNOWLEDGMENTS

The document benefited from the constructive comments by Warren Walsh and Mark Hayes from the Oil and Gas Division and Brian Grant from the Geological Survey and Development Branch of the British Columbia Ministry of Energy and Mines. Nicole Robinson from the University of Victoria helped with sample selection, and Tom Pestaj and Nicole Rayner from Geological Survey of Canada in Ottawa are thanked for their help in data acquisition and processing.

REFERENCES

- Allan, R.J. (1999): Micro-diamond results from Ice Claim Project, BC; *Skeena Resources Ltd.*, news release, August 20, 1999.
- Allan, R.J. (2002): Diamond exploration corporate up-date; *Skeena Resources Limited*, news release, March 22, 2002.
- Anonymous (1994): BC Diamonds discovered – Consolidated Ramrod Gold Corporation; *George Cross News Letter*, No. 225.
- Aspler, L.B., Pilkington, M. and Miles, W.F. (2003): Interpretations of Precambrian basement based on recent aeromagnetic data, Mackenzie Valley, Northwest Territories; *Geological Survey of Canada*, Current Research, 2003-2, 13 pages.
- Carlson, S.M., Hillier, W.D., Hood, C.T., Pryde, R.P. and Skelton, D.N. (1999): The Buffalo Hills kimberlites: A newly-discovered diamondiferous kimberlite province in north-central Alberta, Canada; in *Proceedings of the 7th International Kimberlite Conference*, Gurney, J.J., Gurney J.L., Pascoe, M.D. Richardson, S.H., Editors, Volume 1, pages 109–116.
- Gabrielse, H., Monger, J.W.R., Wheeler, J.O. and Yorath, C.J. (1991): Part A. Morphogeological belts, tectonic assemblages and terranes; Chapter 2 in *Geology of the Cordilleran Orogen in Canada*, Gabrielse H. and Yorath C.J., Editors, *Geological Survey of Canada*, Geology of Canada, Number 4, pages 15–28.
- Gehrels, G.E. and Ross, G.M. (1998): Detrital zircon geochronology of Neoproterozoic to Permian miogeoclinal strata in British Columbia and Alberta; *Canadian Journal of Earth Sciences*, Volume 35, pages 1380–1402.

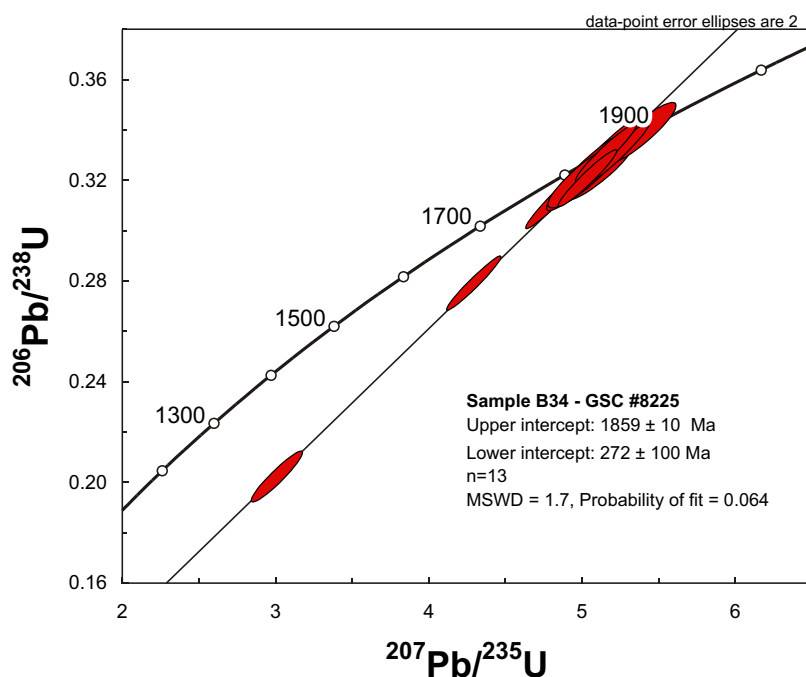


Figure 9 Interpretation of SHRIMP analytical data, Sample B34; see text for explanations.

- Haggerty, S.E. (1986): Diamond genesis in a multiply constrained model; *Nature*, Volume 320, pages 34–38.
- Helmstaedt, H.H. (1993): ‘Primary’ diamond deposits – what controls their size, grade, and location? in *Giant Ore Deposits*, Whiting, B.H., Mason, R. and Hodgson, C.J., Editors, *Society of Economic Geologists*, Special Publication 2, pages 13–80.
- Helmstaedt, H.H. and Gurney, J.J. (1995): Geotectonic controls of primary diamond deposits: implications for area selection; *Journal of Geochemical Exploration*, Volume 53, pages 125–144.
- Hoffman, P.F. (1988): United plates of America: the birth of a craton; *Annual Reviews in Earth and Planetary Sciences*, Volume 16, pages 543–603.
- Hoffman, P.F. (1989): Precambrian geology and tectonic history of North America; in *Geology of North America – an Overview*; Bally, A.W. and Palmer, A.R., Editors, *Geological Society of America*, Volume A, pages 447–512.
- Hyndman, R.D. and Lewis, T. J. (1999): Geophysical consequences of the Cordillera-craton thermal transition in southwestern Canada; *Tectonophysics*, Volume 306, pages 397–342.
- Janse, A.J.A. (1994): Is Clifford’s Rule still valid? in *Kimberlites, Related Rocks and Mantle Xenoliths*, Meyer, H.O.A. and Leonardos, O.H., Editors, *Proceedings of the 5th International Kimberlite Conference*, *Companhia de Pesquisa de Recursos Minerais (CPRM)*, Special Publication 1/A, Jan. 94, Volume 2, pages 215–235.
- Jefferson, C.V. and Parrish, R.R. (1989): Late Proterozoic stratigraphy, U-Pb zircon ages, and rift tectonics Mackenzie Mountains, northwestern Canada; *Canadian Journal of Earth Sciences*, Volume 26, pages 1784–1801.
- Kirkley, M.B., Gurney, J.J. and Levinson, A.A. (1991): Age, origin and emplacement of diamonds: scientific advances in the last decade; *Gems and Gemology*, Spring 1991, pages 2–25.

- Ludwig, K.R. (2003): User's manual for Isoplot/Ex rev. 3.00: a geochronological toolkit for Microsoft Excel; *Berkeley Geochronology Center*, Berkeley, CA, Special Publication, 4, 70 pages.
- McCallum, M.E. (1994): Lamproitic (?) diatremes in the Golden area of the Rocky Mountain Fold and Thrust Belt, British Columbia, Canada; *in* Kimberlites, Related Rocks and Mantle Xenoliths, Meyer, H.O.A. and Leonardos, O.H., Editors, Proceedings of the 5th International Kimberlite Conference, *Companhia de Pesquisa de Recursos Minerais (CPRM)*, Special Publication 1/A, Jan. 94, Volume 2, pages 195–209.
- McNicoll, V.J., Theriault, R.J. and McDonough, M.R. (2000): Taltson basement gneissic rocks: U-Pb and Nd isotopic constraints on the basement to the Paleoproterozoic Taltson magmatic zone, northeastern Alberta; *Canadian Journal of Earth Sciences*, Volume 37, pages 1575–1594.
- Mitchell, R.H. (1991): Kimberlites and lamproites: primary sources of diamonds; *Geoscience Canada*, Volume 18, pages 1–16.
- Monger, J.W.H. and Price, R. (2002): The Canadian Cordillera: geology and tectonic evolution, *CSEG Recorder*, February 2002, pages 17–36.
- Northcote, K.E. (1983a): Report on Mark property, Pangman Peak (82N/15W); *BC Ministry of Energy, Mines and Petroleum Resources*, Assessment Report 13 596.
- Northcote, K.E. (1983b): Report on Jack Claims Lens Mountain (82N/14E); *BC Ministry of Energy, Mines and Petroleum Resources*, Assessment Report 13 597.
- O'Neill, C., Moresi, L., Lenardic, A. and Cooper, C.M. (2003): Inferences on Australia's heat flow and thermal structure from mantle convection modelling results; *in* Evolution and Dynamics of the Australian Plate, Hillis R.R. and Müller, R.D., Editors, *Geological Society of Australia*, Special Publication 22, pages 163–178.
- Pell, J., (1994): Carbonatites, nepheline syenites, kimberlites and related rocks in British Columbia; *BC Ministry of Energy and Mines*, Bulletin 88.
- Pilkington, M., Milles, W.F., Ross, G.M. and Roest, W.R. (2000): Potential-field signatures of buried Precambrian basement in Western Canada Sedimentary Basin; *Canadian Journal of Earth Sciences*, Volume 37, pages 1453–1471.
- Roberts, W.J. (2002): Diamond discovery at Xeno; Pacific Ridge Exploration Limited, news release, March 13, 2002.
- Ross, G.M., Parish, R.R., Villeneuve, M.E. and Bowring, S.A. (1991): Geophysics and geochronology of the crystalline basement of the Alberta Basin, western Canada; *Canadian Journal of Earth Sciences*, Volume 28, pages 512–522.
- Ross, G.M., Milkerreit, B., Eaton, D., White, D., Kanasewich, E.R. and Buryanyk, M.J.A. (1995): Paleoproterozoic collisional orogen beneath Western Canada Sedimentary Basin imaged by LITHOPROBE crustal seismic reflection data; *Geology*, Volume 23, pages 195–199.
- Ross, G.M., Annel, H.C. and Hamilton, M.A. (2000): Lithology and U-Pb geochronology of shallow basement along the SNORCLE line, southwest Northwest Territories: a preliminary report; *in* Slave-Northern Cordillera Lithospheric Evolution (SNORCLE) Transect and Cordillera Tectonic Workshop Meeting, Cook, F.A. and Erdmer, P., Editors, LITHOPROBE Secretariat, University of British Columbia, LITHOPROBE Report 72, pages 76–80.
- Ross, G.M. and Eaton, D.W. (2002): Proterozoic tectonic accretion and growth of western Laurentia: results from LITHOPROBE studies in northern Alberta; *Canadian Journal of Earth Sciences*, Volume 39, pages 313–329.
- Simandl, G.J. (2004): Concepts for diamond exploration in "on/off craton" areas, British Columbia, Canada; *Lithos*, Volume 77, pages 749–764.
- Stapleton, B.A. (1997): Moose Creek and neighbouring claims, Peace Diamond Project; *BC Ministry of Energy and Mines*, Assessment Report 25 081.
- Stern, R.A., (1997): The GSC sensitive high-resolution ion microprobe (SHRIMP): analytical techniques of zircon U-Th-Pb age determinations and performance evaluation; *in* Radiogenic Age and Isotopic Studies, Report 10, *Geological Survey of Canada*, Current Research 1997-F, pages 1–31.
- Stern, R.A. and Amelin, Y. (2003): Assessment of errors in SIMS zircon U-Pb geochronology using a natural zircon standard and NIST SRM 610 glass; *Chemical Geology*, Volume 197, pages 111–146.
- Theriault, R.J. and Ross, G.M. (1991): Nd isotopic evidence for crustal recycling in the 2.0 Ga subsurface of western Canada; *Canadian Journal of Earth Sciences*, Volume 28, pages 1149–1157.
- Villeneuve, M.E., Theriault, R.J. and Ross, G.M. (1991): U-Pb ages and Sm-Nd signature of two subsurface granites from the Fort Simpson magnetic high, northwest Canada; *Canadian Journal of Earth Sciences*, Volume 28, pages 1003–1008.
- Villeneuve, M.E., Ross, G.M., Theriault, R.J., Miles, W., Parrish, R.R. and Broome, J. (1993): Tectonic subdivision and U-Pb geochronology of the crystalline basement of the Alberta basin, western Canada; *Geological Survey of Canada*, Bulletin 447.

Late Cretaceous Volcanoplutonic Arcs in Northwestern British Columbia: Implications for Porphyry and Epithermal Deposits

By A.T. Simmons¹, R.M. Tosdal¹, D.E.L. Baker², R.M. Friedman¹ and T.D. Ullrich¹

KEYWORDS: epithermal deposits, volcanic rocks, plutonic rocks, Late Cretaceous, Tulsequah area, Thorn property area, regional geology, Windy Table Suite magmatic rocks, Rocks to Riches Program

INTRODUCTION

Porphyry Cu and epithermal deposits are spatially and temporally related to specific volcanic and plutonic rocks emplaced during the formation of long-lived magmatic arcs formed along convergent plate boundaries (*e.g.*, Sillitoe, 1972; Sutherland Brown, 1976; Titley, 1982; Sawkins, 1990; Bissig *et al.*, 2003). Recognizing the presence, types of deposits, and age of the mineralized volcanoplutonic complexes in under-explored terranes is an important step toward identifying the metallogenic potential of a terrane as a means to aid exploration. Historically in British Columbia (BC), porphyry Cu deposits have dominated exploration and mining activity (*e.g.*, Highland Valley, Gibraltar, Afton, Copper Mountain, Galore Creek). In contrast, epithermal deposits have until recently (*e.g.*, Toodoggone district deposits) remained largely underexplored because of their low preservation potential coupled with the Mesozoic age of most of the convergent margin arcs in the western Canadian Cordillera. For example, the known porphyry Cu and several epithermal deposits in British Columbia are associated with Jurassic arcs, with the Cretaceous arc seemingly of less interest from a metallogenic viewpoint.

The Cretaceous arc in British Columbia is represented principally by the Coast Plutonic belt located along the west coast of BC and in adjacent Alaska. It can be divided into a series of magmatic belts with no obvious time-space distribution based on current data (Brew and Morell, 1983; Barker *et al.*, 1986). In northern BC in the Taku River area, however,

work by the British Columbia Geological Survey identified a series of Late Cretaceous volcanic and subvolcanic plutonic rocks that form a belt on the eastern margin of the Coast Plutonic Belt where it intrudes the Stikine Terrane (*e.g.*, Mihalynuk, 1999). This belt extends from at least the Golden Bear Mine (Oliver, 1996) in the southeast to the Surprise Lake Batholith in the northwest (Mihalynuk, 1999). The known or inferred Late Cretaceous volcanoplutonic complexes are varyingly eroded, are spaced 10 to 20 km apart, and have associated hydrothermally altered rocks (Souther, 1971; Mihalynuk, 1999; Simmons *et al.*, 2003). Porphyry Cu-Mo, Au-Ag-Cu veins, breccia-hosted Ag-Au-Pb-Zn, Zn skarn, and sedimentary hosted Carlin-like Au are recognized.

In 2003, a research project was initiated by the Mineral Deposit Research Unit (MDRU) at the University of British Columbia (UBC) to investigate Late Cretaceous volcanoplutonic complexes in the Taku River area of the Stikine Terrane, northwestern BC. A goal of the project sought to evaluate the mineralization potential along the belt, with emphasis placed upon epithermal types of deposit because of their high value and low tonnage. Work reported herein is drawn on fieldwork in 2004 and data from a MSc thesis at UBC by Adam Simmons on the Thorn property, which is situated within the Late Cretaceous volcanoplutonic belt. Particular emphasis is placed on presenting the timing and known or inferred relationships between mineralizing types and magmatic rocks. The goal is to establish a framework from which better exploration strategies in northern BC can be developed. Funding for the project derives in part from the Rocks to Riches program, which is administered by the BC and Yukon Chamber of Mines, and from the Natural Sciences and Engineering Research Council of Canada (NSERC) through an Industrial Post-Graduate Fellowship to Adam Simmons and a Discovery Grant to Richard Tosdal.

Fieldwork in the 2004 field season had two main goals. Firstly, regional mapping was carried out in the Taku River area aimed at refining the current understanding of Late Cretaceous magmatic rocks in this region, defining the magmatic evolution and investigating the geological setting of mineralization as-

¹Mineral Deposit Research Unit (MDRU), Department of Earth and Ocean Sciences, The University of British Columbia, Vancouver, B.C.

²Equity Engineering Ltd., Vancouver, B.C.

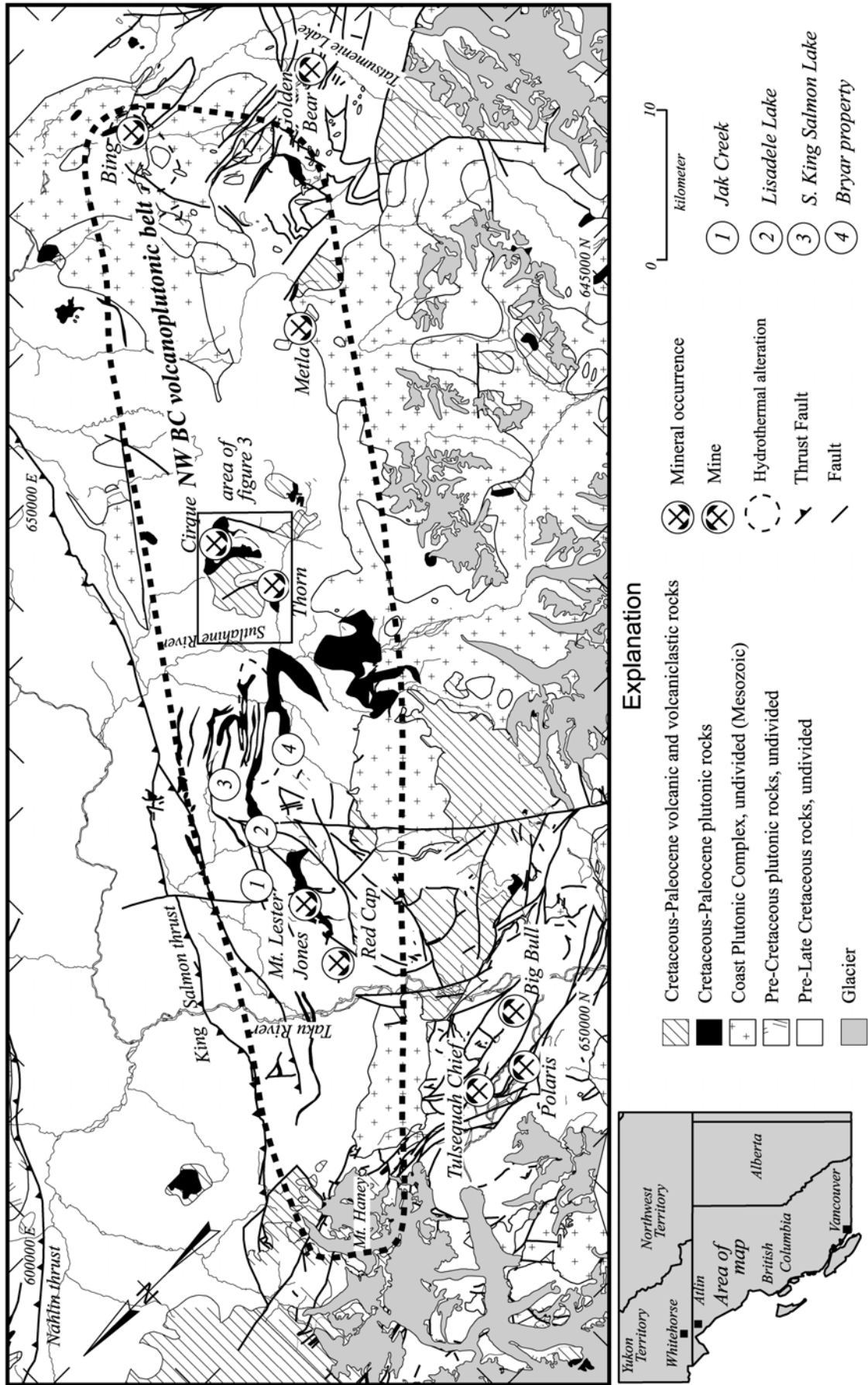


Figure 1. Simplified geologic map of Cretaceous belt of volcanic-plutonic complexes and associated hydrothermal systems. Belt stretches from Mount Haney in the northwest to perhaps the Golden Bear mine in the southeast. Note that map is tilted 45° to northwest. Base geology from the British Columbia Department of Energy and Mines (<http://www.em.gov.bc.ca/Mining/Geology/Publications/catalog/bcgeomap.htm#2003-17>) with location of mines and prospects from Souther (1971) and Minfile.

sociated with these magmatic rocks. Approximately seven weeks of mapping and sampling was carried out over an area from the Thorn property in the southeast to Mt. Lester Jones in the northeast. Secondly, a regional investigation of mineralized occurrences along this belt aimed to define their petrogenesis, timing history and fluid chemistry. The goals are to establish source of fluids for the mineralizing types and linking them to particular magmatic events along the belt. Effort was devoted to determining their relative timing in the field, and collecting samples for absolute timing relationships using U-Pb and $^{40}\text{Ar}/^{39}\text{Ar}$ geochronology. Twelve days was devoted to the regional reconnaissance study. Preliminary results of this study are presented herein.

2004 FIELD MAPPING STUDIES IN THE TAKU RIVER AREA

During the 2004 field season, mapping in the Taku River area was concentrated on five areas between the Thorn property and the Taku River (Fig. 1). These areas were selected based on mineral potential as inferred from Regional Geochemical Survey data and favourable geology interpreted from the geologic map of Souther (1971) and publicly available assessment reports. Rocks in the study area are variably deformed Triassic and Jurassic volcanic and clastic sedimentary rocks, which have been intruded by granitic rocks and overlain by dacitic rocks. The igneous rocks range in age from 168 to 55 Ma (Table 1). The spatial and temporal distribution of the magmatic rocks are not well understood, however the majority of the magmatic rocks located in the volcanoplutonic belt are constrained between the ages of 93 and 81 Ma (Mihalynuk, *et al.*, 2003; this study).

Pre-Cretaceous Stikine Terrane Supracrustal Rocks

Mapping during the 2004 field season identified three dominant rock units of the Stikine volcanic arc in the Taku River area. These are the Upper Triassic Stuhini Group volcanic and sedimentary rocks including the Upper Triassic Sinwa Formation sedimentary rocks. The Lower to Middle Jurassic clastic sedimentary rocks of Laberge Group unconformably overlie the Triassic rocks (Fig. 2). All sedimentary rocks are weakly to strongly altered and variably deformed. Alteration is limited to rocks adjacent to younger magmatic rocks. North-northwest verging, open to close folds and post-accretionary normal faults deform the sedimentary rocks. These rocks are only briefly described below.

STUHINI GROUP

Stuhini Group strata form a northwesterly trending belt from the Golden Bear mine area to the Tulsequah

area where the strata were named by Kerr (1948) after Stuhini Creek. These strata continue to the north through the Tagish Lake area (Mihalynuk, 1999) and are correlative to the Lewis River Group farther north (Wheeler, 1961; Hart *et al.*, 1989).

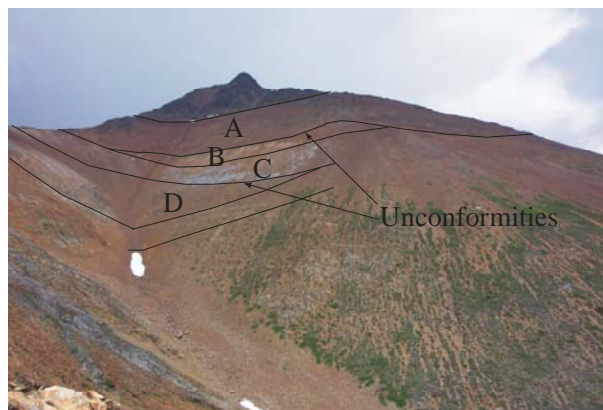


Figure 2. Lower to Middle Jurassic Laberge Group clastic sedimentary rocks (A) unconformably overlie Upper Triassic Sinwa Formation clastic sedimentary rocks (B) and limestone (C), which unconformably overlie Stuhini Group clastic sedimentary rocks at the Thorn property.

A wide range of rock types including basic to intermediate subalkaline flows, pyroclastic rocks and related sedimentary rocks characterize the Stuhini Group (Mihalynuk, 1999). The Stuhini Group may be divided in the study area into a sequence dominated by submarine volcanic rocks and a sequence dominated by clastic sedimentary rocks and lesser carbonate rocks. Near the Thorn property (Fig. 3), submarine mafic volcanic strata are overlain by sedimentary strata (Simmons, 2003; Baker, 2004) and are similar to the section described by Mihalynuk (1999) at Willison Bay. However, north of the Thorn property, in the Mt. Lester Jones area, this subdivision is not evident. Mihalynuk (1999) attributes the lack of stratigraphic continuity to major lateral facies variations, deposition on surfaces with major paleotopographic relief, and disruption by later faults.

SINWA FORMATION

The Sinwa Formation is considered to be the top of the Stuhini Group. The strata can be traced discontinuously throughout the map area (Souther, 1971), and serves as a local marker horizon between the Upper Triassic Stuhini Group strata and Lower to Middle Jurassic Laberge Group. Where exposed, the Sinwa Formation ranges in thickness from 5 to 20 m and unconformably overlies Stuhini Group clastic sedimentary rocks (Fig. 2). To the north in the Tagish Lake area, Mihalynuk (1995a, b) did not separate the different sedimentary rock sequences due to poor lateral continuity.

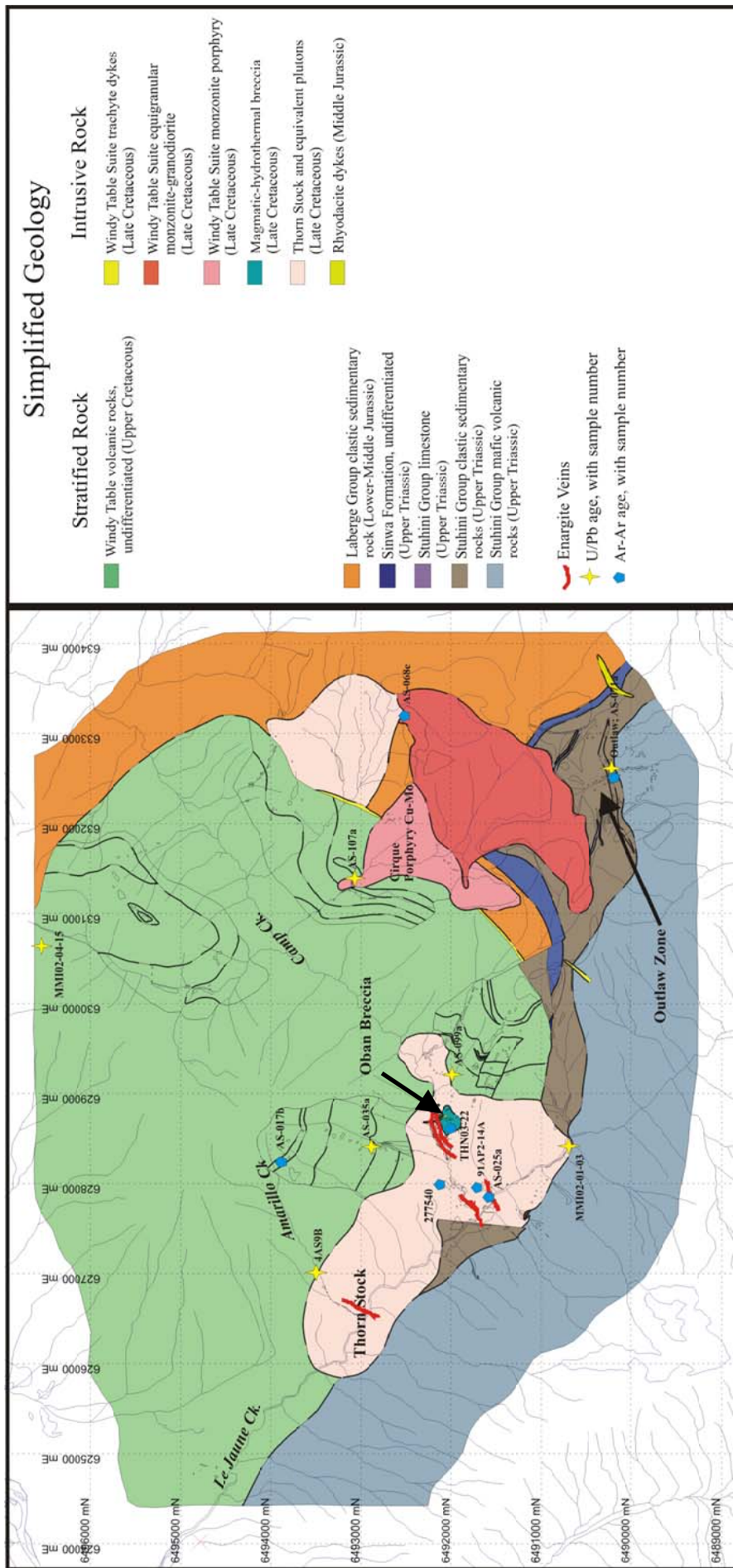


Figure 3. Simplified geology and geochronology sample locations at the Thorn property. Samples are outlined in Table 1 (see below). Map is modified from Baker (2003).

The Sinwa Formation has two main rock types, 1) limestone and 2) overlying clastic sedimentary rocks. Dolomitization, skarnification and recrystallization of limestone is common. In the study area, a boulder conglomerate containing volcanic and intrusive rocks may be correlative to the “Limestone Boulder Conglomerate (UTSI)” of Mihalyuk (1999), which separates Upper Triassic Stuhini Group strata from Pliensbachian argillites of the Laberge Group in the Kirtland and Moon Lake areas, north of the study area. Farther north in the Whitehorse area, sandstone and wacke are described as the clastic sedimentary rock associated with the boundary between Stuhini and Laberge Group strata (Wheeler, 1961; Hart and Radloff, 1990).

LABERGE GROUP

The Laberge Group extends from the Dease Lake area in the south to the Yukon in the north, well outside the NW BC volcanoplutonic belt on Figure 1. These strata are thought to be an overlap assemblage linking terranes by the Early Jurassic (Wheeler *et al.*, 1991; Mihalyuk, 1999).

The Laberge Group is the major of unit in the study area. Souther (1971) estimated the thickness of the Laberge Group to be 3100 m, although others estimated the thickness to be as much as 5000 m (*e.g.*, Bultman 1979). Typical rocks include boulder to cobble conglomerate (mafic volcanic clasts > intrusive clasts and intrusive clasts > mafic volcanic clasts), immature sandstones and siltstones, wackes, and argillites. Correlating individual sequences from Mt. Lester Jones to the Thorn property area is difficult due to quick lateral facies changes over short distances and lack of marker horizons.

Cretaceous (85-81 Ma) Volcanic and Sedimentary Rocks

Cretaceous subaerial volcanic and sedimentary rocks are rare but important strata throughout the study area. Plutonic equivalents of these strata are more common (see below). In the map area, these strata form three volcanic centres at Lisadele Lake, the Thorn property and the Metla property. Each are separated by some 10 to 20 km. Together, these volcanic and plutonic rocks are part of a northwesterly trending magmatic belt with associated hydrothermal alteration and sulphide minerals.

Historically, these strata were mapped as Tertiary Sloko Group volcanic rocks (*ca.* 55 Ma) by Souther (1971) in the Tulsequah map area. However, Mihalyuk (2003) reported a U/Pb age of 82.8 ± 0.6 Ma (MMI02-01-03, Table 1) from a rhyolite breccia on the Thorn property (Fig. 3), which suggests that the Sloko Group mapped by Souther (1971) includes significant Late Cretaceous volcanic rocks. Subsequent mapping and

U/Pb geochronology (summarized in Table 1) has confirmed the ages and extended the belt of Late Cretaceous volcanic rocks north and south of the Thorn property. These rocks are considered correlative to the Windy Table Suite volcanic rocks described by Mihalyuk (1999) in the Tagish Lake area.

The best-preserved section of these strata is located at the Thorn property. Here, approximately 1800 m of subaerial volcanic and related sedimentary rocks are preserved. The Thorn volcanic sequence is characterized by flat-lying strata, except around the margins, where the contact between older strata and Late Cretaceous volcanic rocks is steeply faulted causing local rotation and tilting of volcanic stratigraphy. This faulted margin is continuous along the eastern contact and forms a curvilinear trace across the geologic map (Fig. 3). In one location, the original stratigraphic contact between the volcanic rocks and older rocks is preserved (Fig. 4). Here, the 93 Ma quartz-feldspar-biotite porphyritic diorite of the Thorn stock (Mihalyuk, 2003) is overlain by boulder conglomerate composed of rounded clasts of porphyry diorite (see below). The section through the Late Cretaceous volcanic rocks and unit descriptions are outlined below.

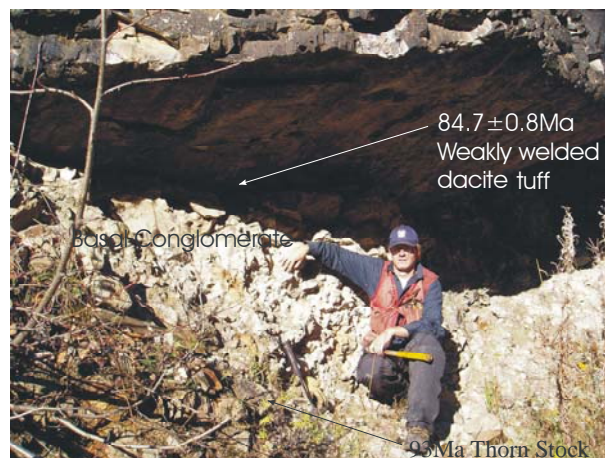


Figure 4. Unconformity at the base of Windy Table volcanic rocks: a 1 to 5 m thick basal conglomerate separates 93 Ma Thorn stock (base of photo) from 85 Ma subaerial volcanic rocks (top of photo). Note: Sample 4AS9B (Table 1) was collected from the weakly welded tuff above conglomerate in this photo.

THORN STRATIGRAPHIC SECTION THROUGH WINDY TABLE VOLCANIC ROCKS

The basal contact of the Windy Table volcanic rocks crops out for several tens of meters in Amarillo Creek at the Thorn property (Fig. 4). Here, the basal contact is a monomictic clast-supported, cobble to boulder conglomerate. Clasts are typically rounded and composed of quartz-feldspar-biotite porphyritic diorite to quartz diorite, likely of Thorn stock affinity. The .

TABLE 1. PRELIMINARY U/Pb AND ⁴⁰Ar/³⁹Ar GEOCHRONOLOGY OF MAGMATIC AND MINERALIZED ROCKS, PRELIMINARY RESULTS. * BESIDE SAMPLE NUMBERS INDICATE AGES FROM MIHALYNUK *ET AL.* (2003); ALL OTHER SAMPLES FROM THIS STUDY. ALL AGES ARE GIVEN WITH ERRORS AT 2 σ . 13 U/Pb SAMPLES AND 8 ⁴⁰Ar/³⁹Ar SAMPLES STILL IN PROGRESS.

Sample	Northing	Easting	Description	Interpreted Age (Ma)	Method (Mineral)
U/Pb					
<i>Thorn Area</i>					
AS-099a	6491930	629040	Rhyolite flow, fine grained, aphanitic	80.8 \pm 3.6/-4.9	U/Pb TIMS (Zircon)
AS-035a	6492888	628407	Trachyte flow, feldsparpheric, feldspar phenocrystic	81.1 \pm 1.5	U/Pb SHRIMP-RG (Zircon)
AS-107a	6493090	631320	Cirque monzonite, feldspar porphyritic	82.2 \pm 0.2	U/Pb TIMS (Zircon)
MMI02-04-15 *	6496260	630090	Sutlahine Rhyolite Breccia	82.8 \pm 0.6	U/Pb TIMS (Zircon)
4AS9B	6493530	627160	Weakly welded crystal tuff, feldsparpheric, <1% xenocrystic	84.7 \pm 0.8	U/Pb SHRIMP-RG (Zircon)
MMI02-01-03 *	6490890	628200	Thorn Stock; Bt-Hbld-Qtz-feldspar porphyritic diorite-qtz diorite	93.3 \pm 2.4	U/Pb TIMS (Zircon)
AS-071a	6490270	632543	Fine grained aphanitic rhyodacite dyke	168.1 \pm 0.7	U/Pb TIMS (Zircon)
<i>Mt Lester Jones Area</i>					
4AS11	6506538	612037	Bt-Hbld-feldspar porphyritic diorite	55.3 \pm 0.8	U/Pb SHRIMP-RG (Zircon)
MMI94-45-6 *	6510100	605100	Mt. Lester Jones Porphyry	83.8 \pm 0.2	U/Pb TIMS (Zircon)
MMI94-9-4 *	6513150	698800	Red Cap Porphyry	87.3 \pm 0.9	U/Pb TIMS (Zircon)
Ar-Ar (Cooling)					
<i>Thorn Area</i>					
AS-017b	6493800	628290	Trachyandesite sill, intruding Windy Table volcanic rocks	83.1 \pm 1.8	⁴⁰ Ar/ ³⁹ Ar (Muscovite)
AS-068e	6492585	633215	Equigranular monzonite bearing biotite and hornblende	90.7 \pm 3.6	⁴⁰ Ar/ ³⁹ Ar (Biotite)
Ar-Ar (Alteration)					
<i>Thorn Area</i>					
AS-025a	6491624	627740	In vein sericite from B-zone Qtz-enargite-tetrahedrite-pyrite vein	79.3 \pm 1.4	⁴⁰ Ar/ ³⁹ Ar (Sericite)
Outlaw	6490280	627650	Sericite adjacent to arsenopyrite from AS-071a	84.8 \pm 0.5	⁴⁰ Ar/ ³⁹ Ar (Biotite)
THN03-22	6491914	628769	In vein sericite from Oban Breccia-Thorn Property	87.7 \pm 0.6	⁴⁰ Ar/ ³⁹ Ar (Sericite)
277540	6491150	628070	Sericite from "unaltered" Thorn Stock	91.0 \pm 0.9	⁴⁰ Ar/ ³⁹ Ar (Sericite)
91AP2-14A *	6491640	627650	f.g. sericite/illite from Thorn Stock	91.0 \pm 1.0	⁴⁰ Ar/ ³⁹ Ar (Sericite)

Note: Abbreviations used above Sensitive High Resolution Ion Micro Probe Reverse Geometry (SHRIMP-RG), Thermal Ionization Mass Spectrometer (TIMS), Biotite (Bt), Hornblende (Hbld), Quartz (Qtz), fine-grained (f.g.)

conglomerate matrix is made up of coarse to fine sand-sized detritus, chiefly composed of coarse sand-sized diorite, rounded quartz, and subrounded feldspar, which has been replaced by sericite.

Above the basal conglomerate is an 80 m succession composed dominantly of dacitic to andesitic lapilli tuffs with lesser flows and volcanoclastic rocks. Individual beds do not extend for more than tens of metres along strike due to rapid lateral facies changes and lack of marker horizons. Tuffs are unwelded to weakly welded. In Amarillo Creek, a 15 to 80 cm lithic poor, weakly welded dacitic crystal tuff directly overlies the basal conglomerate. This tuff has a U/Pb SHRIMP-RG zircon age of 84.7 \pm 0.8 Ma (4AS9B, Table 1). This age marks the onset of Windy Table volcanism in the study area.

Stratigraphically above the tuff-dominated strata is a 120 m section of volcanoclastic-dominated strata with lesser tuffs. Individual beds are poorly sorted, can be difficult to distinguish, and are laterally discontinuous. Typically, clasts are volcanic rocks with lesser sedimentary rocks and intrusive rocks. Clasts are

subrounded to rounded, and range in size from boulder to fine sand.

A 360 m-section dominated by dacitic lapilli tuff overlies the volcanoclastic rocks. This section is similar to the lowermost sequence of tuffs. Approximately 15 m above the volcanoclastic sequence is a 5 m thick feldspar phenocrystic trachyte flow which returned an U-Pb zircon age of 81.1 \pm 1.5 Ma (AS-035a, Table 1).

Stratigraphically above the tuff and volcanoclastic rock dominated sequence is a 340 m thick section of flows, domes and intrusive rocks. At the headwaters of Amarillo Creek is a series of vertical dikes, which are inferred to be feeders to the extrusive lavas, as well as domes. Here, the domes and dikes are flow foliated. Foliation is generally flat lying, but is locally intensely folded (syn-magmatic) and steeply dipping in the feeder dikes. Overall, the lava-dominated section is characterized by fine-grained, dacitic feldspar phytic units at the base that upsection become coarser grained quartz-feldspar phenocrystic rhyolite flows. Minor tuffs and volcanoclastic rocks are intercalated with the lavas. A ⁴⁰Ar-³⁹Ar age on coarse muscovite of 83.1 \pm 1.8 Ma

(AS-017b, Table 1) was obtained from a trachyandesite sill intruding the strata about 215 m up from the base of this sequence.

Poorly outcropping volcanic and volcanoclastic strata compose another 900 m that extends to the current top of the volcanic sequence. Close to the top of the volcanic sequence, Mihalynuk (2003) reported a U-Pb (zircon) age of 82.8 ± 0.6 Ma (MMI02-04-15, Table 1) for a rhyolite breccia.

The available geochronology from the Windy Table volcanic rocks implies that some 1600 m of volcanic and volcanoclastic rocks may have been deposited within as much as 3 to 4 million years. However, it is also important to point out that the time range could be significantly less as the uncertainties on the ages overlap throughout the sequence suggesting that there could have been very rapid deposition of most of the volcanic sequence. Implicit in the thickness and similar aged volcanic facies is that the volcanic section at the Thorn is a remnant of a volcanic centre.

Intrusive Rocks

Three main periods of plutonism have been recognized in the study area. The oldest is represented by minor *ca.* 168 Ma intrusive rocks. The major period for the purposes of this study is represented by 92 to 81 Ma Late Cretaceous subvolcanic intrusive rocks. The youngest event consists of Early Tertiary magmatism related to the Sloko volcanism. The younger period of plutonism is rare in the study area and has only been recorded at one location north of Lisadele Lake (Fig. 1), but it is also reported near the Golden Bear mine (Brown and Hamilton, 2000).

PRE-LATE CRETACEOUS INTRUSIVE ROCKS

A 168.1 ± 0.7 Ma (AS-071a, Table 1) intrusion has been recognized in one location at the Thorn property. This intrusion is a 3 to 5 m wide, fine-grained, aphanitic rhyodacite dike intruding into Stuhini Group sedimentary rocks at the Outlaw prospect (Fig. 3). Previously, it has been informally suggested that these dikes may have been the source of the mineralizing fluids at the Outlaw. However, hydrothermal biotite from the same rock (Outlaw, Table 1) yield minimum ages of 84.8 ± 0.5 Ma (includes 84.3% of the ^{39}Ar with an inverse isochron age of 85.4 ± 1.3 Ma and initial $^{40}\text{Ar}/^{36}\text{Ar}$ of 279 ± 28). This suggests that the dikes and their margins simply focused younger hydrothermal fluids.

Jurassic plutons are common in the Coast batholith where they in part form the Fourth of July Plutonic Suite of Mihalynuk (1999). They are not known within the study area. The 168.1 ± 0.7 Ma age of intrusive rock at the Outlaw is, furthermore, not a common age for

Jurassic magmatism regionally. However, some cooling ages from Fourth of July Plutonic Suite are as young as 165 Ma (M. Mihalynuk, pers comm, 2004), which suggests the potential for plutonic rocks of similar age lying to the west of the study area.

LATE-CRETACEOUS INTRUSIVE ROCKS

Late Cretaceous subvolcanic plutons are widespread throughout the study area (Fig. 1). Known intrusive rocks of this age extend from as far north as Mt. Lester Jones to as far south as the Thorn property. Rocks of similar composition and texture were mapped and collected for geochronology between the Golden Bear mine and the Thorn property in an attempt to extend the volcanoplutonic belt. These southern rocks are as yet undated, and thus their precise relationship to the northern rocks is unknown.

The best understood portion of the belt is at the Thorn property where two pulses of magmatic activity are evident. The older of the two is represented by the quartz-feldspar-biotite porphyritic diorite and quartz diorite of the Thorn stock. This stock is unconformably overlain by *ca.* 85 to 82 Ma Windy Table volcanic rocks and intruded by similar-age Windy Table Plutonic Suite rocks.

93 Ma Intrusive Rocks

Plutonic rock of known 93 Ma age are regionally rare. Known examples of this are at the Thorn property (Mihalynuk, 2003), Jack Peak and Racine Lake (Mihalynuk, 1999). During the 2004 field season several small Thorn stock-like intrusive rocks were mapped and sampled between Golden Bear mine and Tulsequah mine. However, assigning plutonic rocks to particular periods of magmatic activity is difficult as similar lithologies are known to intrude as part of the Tertiary Sloko magmatic epoch (Mihalynuk, 1999). In the study area, only one age has been reported in this time period. Mihalynuk (2003) reports a U/Pb zircon age of 93.3 ± 2.4 Ma for the Thorn stock. The Thorn stock is the largest known example and covers a 3.5 by 1.5 km area.

The 93 Ma intrusions are best illustrated by the Thorn stock. The stock is a quartz-feldspar-biotite porphyritic diorite to quartz diorite. Marginal phases are fine-grained feldspar phyrlic and flow-banded. Hydrous phases are biotite and lesser hornblende. Common accessory minerals include magnetite and apatite. These rocks are pervasively chlorite and sericite altered.

Windy Table Suite

Windy Table plutonic rocks are common in the map area (Fig. 2). Three different compositional types of intrusions are mapped. The most common is a biotite-bearing, porphyritic monzonite that contains

conspicuous feldspar phenocrysts. These rocks have associated hydrothermal systems through the region. Examples include the 83.8 ± 0.2 Ma (MMI94-45-6, Table 1) Mt. Lester Jones porphyry (Mihalynuk, 2003), the 87.3 ± 0.9 Ma (MMI94-9-4) Red Cap porphyry (Mihalynuk, 2003) and the 82.2 ± 0.2 Ma (AS-107a, Table 1) Cirque monzonite (Simmons *et al.*, 2003). A second type of intrusion is a biotite-hornblende-bearing, medium-grained, equigranular, monzonite to granodiorite. None of this compositional type have yet been dated, however, in the Cirque at the Thorn property these intrusions intrude the Cirque monzonite, and are thus presumably of Late Cretaceous age. Other examples of this intrusive suite were mapped in the Bryar area and Lisadele Lake area (Fig. 1).

The least prevalent intrusive suite are fine-grained, aphanitic trachytic dikes, which crop out on the Thorn property. These rocks could represent subvolcanic equivalents or feeders to the trachytic flows in the Windy Table volcanic rocks.

55 MA POST-CRETACEOUS INTRUSIVE ROCKS

Souther (1971) mapped abundant early Tertiary Sloko plutonic rocks in the study. Between this study and Mihalynuk (2003), only one location is known where unequivocal Sloko plutonic rocks crop out. A feldspar-biotite porphyritic diorite was mapped in the Lisadele Lake area, where it intrudes into Laberge Group clastic sedimentary rocks. This rock returned a U/Pb zircon age of 55.3 ± 0.8 Ma (4AS11, Table 1). The petrologic similarity of this rock and the Thorn stock make it very difficult to unequivocally distinguish the two rock suites.

GEOCHEMICAL STUDIES - PRELIMINARY RESULTS

Geochemical studies of magmatic rocks along the belt have concentrated around the Thorn property where the geochronologic framework permits placing the compositional groups into distinct time packages. The goals of this study are to geochemically characterize the different rocks units, place constraints on the paleotectonic environment and note any changes in chemistry as the magmatic arc evolved through time. Major, trace and rare earth element data are available from 23 representative samples of all intrusive rocks and Late Cretaceous subaerial volcanic rocks in the Thorn property area. An additional 18 regional samples are in preparation or have not yet been analyzed. Preliminary interpretations are plotted in Figure 5. It is important to note that the rocks from the Thorn property were sampled in proximity to mineralized hydrothermal systems and thus have been altered to varying degrees, thus limiting the usefulness of the major elements to

characterize geochemical composition or tectonic environment in which these rocks were emplaced.

Middle Jurassic intrusive rocks are geochemically distinct from the Cretaceous intrusive and extrusive rocks. In general, the Jurassic intrusions have within plate affinity and tend to be more mafic and alkaline than younger intrusions (Fig. 5A,C-D). These intrusions are characterized by a relative enrichment compared to chondrite in light rare earth (LREE) and heavy rare earth elements (HREE), a shallow rare earth pattern decreasing toward the HREE and a sharp negative Eu anomaly (Fig. 5E). Unfractionated HREE patterns, such as those exhibited by Middle Jurassic intrusions, suggest that there was no garnet or hornblende in the residuum and likely represent a deep magma signature.

The 93 Ma intrusive rocks are not obviously geochemically distinct from other Late Cretaceous intrusive rocks. However, the 93 Ma rocks tend to have lower SiO₂ contents than other intrusive rocks. They also have a slight tholeiitic affinity compared to other intrusive rocks (Fig. 5B). The REE pattern exhibits unfractionated HREE and a minor negative Eu anomaly (Fig. 5F). The HREE pattern can be explained by either increased pressure at the melt generation site, leaving garnet as the stable phase in the residuum (*e.g.*, Kay and Abruzzi, 1996; Bissig *et al.*, 2003) or by an increased amount of water in the magma leading to hornblende fractionation and HREE depleted melts (*e.g.*, Haschke *et al.*, 2001; Bissig *et al.*, 2003). The small Eu depletion can be explained by oxidized conditions in the magma or a plagioclase-free residuum.

Windy Table Suite intrusive rocks exhibit much the same chemistry as 93 Ma intrusive rocks, with only minor chemical differences. For example, Windy Table intrusive rocks tend to have a compositional range from andesite to trachyte whereas the 93 Ma intrusive rocks are mainly dacite to andesite (Fig. 5A). The Windy Table intrusive rocks also have a slightly more calc-alkaline affinity (Fig. 5B). Most samples exhibit unfractionated HREE and a minor negative Eu anomaly, similar to 93 Ma intrusions (Fig. 5F). Two samples display an overall depletion of REE and an increased negative Eu anomaly. These samples are trachyte dikes, which tend to be more altered (sericite-silica-pyrite) which could explain the abnormal chemistry. Alternatively these dikes may also be *ca.* 55 Ma Sloko intrusive rocks.

Windy Table volcanic rocks have a wide array of compositions ranging from trachyte to andesite. On the Rb vs Y+Nb plot (Fig. 5D), three samples have a within plate affinity. These samples are lithic-bearing pyroclastic rocks, and the anomalous chemistry may reflect the influence on the bulk geochemical composition of lithic fragments. In general, the REE signature is similar to that of their intrusive equivalents, with the exception of a slightly wider spread in HREE concentration (Fig. 5E). The wider spread and abnormal

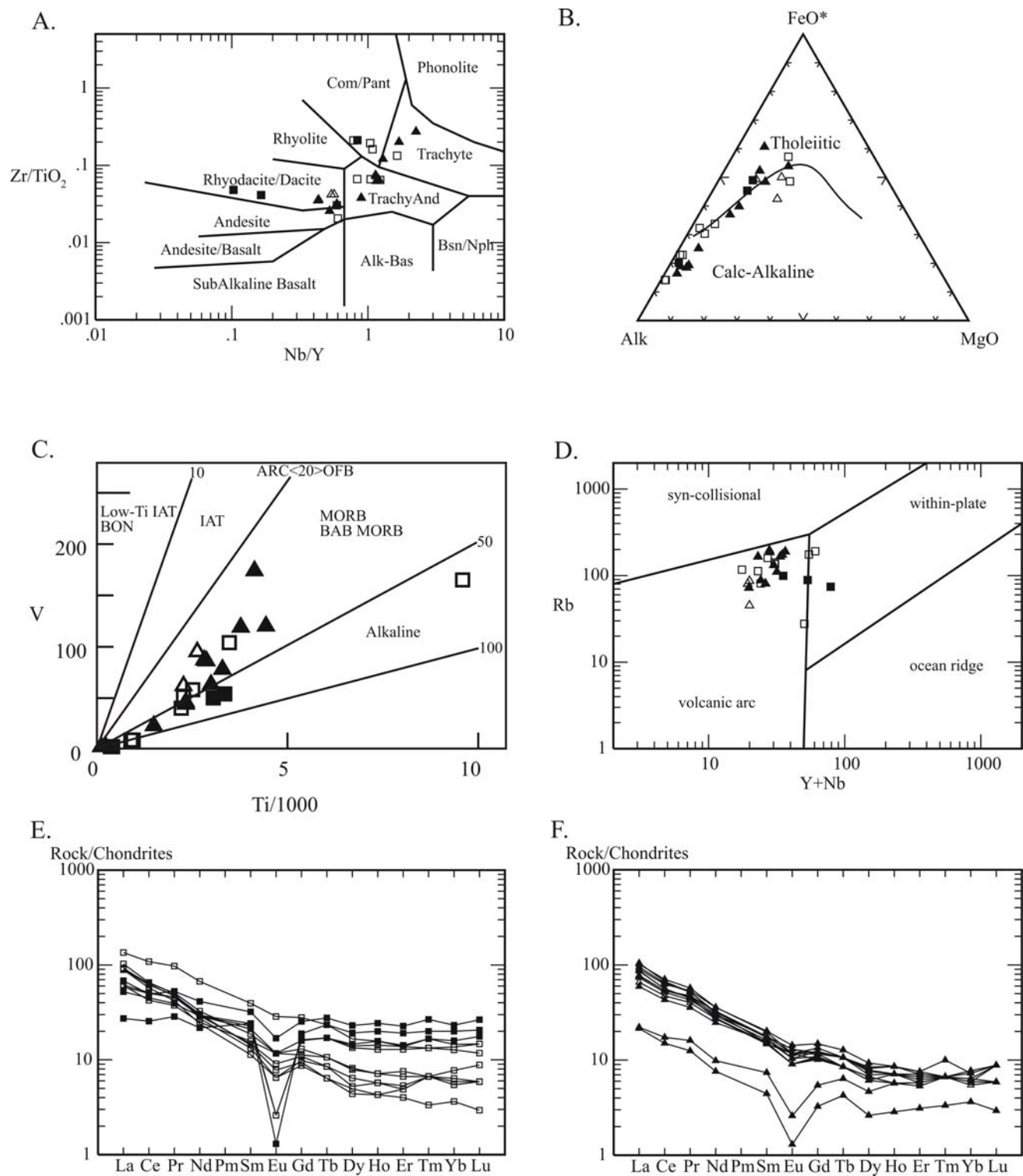


Figure 5. Geochemical discriminant and chondrite-normalized REE abundance diagrams for volcanic and subvolcanic intrusive rocks from the Thorn property and surrounding area. Closed squares represent Jurassic intrusive rocks, open squares represent Windy Table Suite felsic tuffaceous and flow rocks, closed triangles represent Windy Table Suite subvolcanic intrusive rocks and open triangles represent *ca.* 93 Ma Thorn stock and Thorn stock-like diorite-quartz diorite intrusions.

samples may be explained by the lithic fragment chemistry.

Magmatic rocks that fall within the Late Cretaceous time constraint generally have similar compositions. These similarities make it difficult to distinguish fundamental chemical characteristics between the ~93 Ma and ~83 Ma pulses of magmatism. More work is required on determining differences in REE and immobile element ratios between these rocks.

CHARACTERISTICS OF MAGMATIC-HYDROTHERMAL ALTERATION SPATIALLY AND TEMPORALLY ASSOCIATED WITH LATE CRETACEOUS MAGMATIC ROCKS

Magmatic-related hydrothermal alteration and sulfide-bearing rocks are common throughout the study area. Six styles of mineralization are associated with the Late Cretaceous volcanoplutonic belt: 1) quartz-pyrite-enargite-tetrahedrite veins, 2) breccia-hosted Ag-Pb-Zn-(Au-Cu)-bearing sulfides, 3) porphyry Cu-Mo, 4) quartz-arsenopyrite±sphalerite-galena veins and disseminations, 5) skarn and carbonate replacement and, 6) sedimentary rock-hosted or Carlin-like mineralization.

Quartz-pyrite-enargite veins are known only at the Thorn property. There, the veins are hosted in syn-mineralizing normal faults (Lewis, 2002) only within the 93 Ma Thorn stock. Sulphide minerals include pyrite, enargite, tetrahedrite/tennantite, with lesser sphalerite, galena, cassiterite and rare native gold and argentite. Veins are typically enveloped by a narrow 50 cm to 3 m zone of pyrophyllite-sericite-dickite alteration in a wider zone (5-100 m) of intense sericite-clay-pyrite (±dickite) alteration. These zones are flanked by weak clay-sericite-chlorite alteration grading out into chlorite with lesser sericite altered country rock. Pyrophyllite-dickite alteration and tin-bearing minerals (*e.g.*, cassiterite) suggest that the mineralizing system is hot and may have formed in the transition zone between deeper porphyry environment and the shallower epithermal environment.

The restriction of the veins to the Thorn stock suggests a genetic link between the veins and the host rocks. Support for this conclusion was provided by Mihalynuk (2003) who reported a $^{40}\text{Ar}/^{39}\text{Ar}$ age on sericite from intensely altered Thorn stock of 91.0 ± 1.0 Ma. However, attempts to confirm this age have resulted in conflicting data. As part of this study, a $^{40}\text{Ar}/^{39}\text{Ar}$ age on sericite (AS-025a, Table 1) enclosed in enargite from a different location on the Thorn property resulted in a minimum age of 79.3 ± 1.4 Ma (includes 84.4% of the ^{39}Ar with an inverse isochron age of 79.7 ± 2.3 Ma and initial $^{40}\text{Ar}/^{36}\text{Ar}$ of 292 ± 15). It is unclear at this time what the age discrepancy means.

Breccia-hosted Ag-Pb-Zn-(Au-Cu) mineralization occurs at the Metla and Thorn properties, and presumably at other unknown locations as several unmineralized breccia pipes were mapped in the Lisadele Lake area during the 2004 field season. The breccia-hosted prospects are characterized by clast-supported, rounded pebble to boulder breccia, where the ore minerals have replaced a fine-grained rock(?) matrix (Fig. 6). Sulphide minerals include pyrite, sphalerite and boulangerite with lesser chalcopyrite. At the Thorn property, sulphosalt is a dominant phase, whereas at the Metla there are only trace amounts of sulphosalt and chalcopyrite. At the Thorn, sericite occurs as narrow massive zones replacing the matrix of the breccia, this narrow sericite-dominated alteration is flanked by moderate sericite-clay-pyrite alteration grading to weak sericite-chlorite alteration. Sericite (THN03-22, Table 1) from the mineralized matrix, enclosed in pyrite-sphalerite-boulangerite mineralization from the Thorn property yields an age of 87.7 ± 0.6 Ma (includes 81.8% of the ^{39}Ar with an inverse isochron age of $87.6.7\pm 4.3$ Ma and initial $^{40}\text{Ar}/^{36}\text{Ar}$ of 297 ± 70), suggesting that it may be associated with a hydrothermal system produced by the 93 Ma suite of intrusions.



Figure 6. Pyrite-sulphosalt mineralization replacing matrix of magmatic hydrothermal breccia at the Thorn property.

Porphyry Cu-Mo deposits are the most widespread hydrothermal mineralizing type in the study area. Feldspar porphyritic monzonite is the most common host rock for porphyry Cu-Mo mineralization in the belt. Mineralization is characterized by thin (1 mm-8 cm) structurally controlled vein sets. Ore mineralization occurs as both disseminations in the host rock and in the vein sets. Vein mineralogy includes quartz-pyrite-chalcopyrite-molybdenite with lesser feldspar and rare sulphosalt. Where veining is most intense biotite-clay alteration dominates and is flanked by a broader zone of chlorite alteration. U/Pb geochronology (zircon) at the Thorn property on the Cirque monzonite gives an age maximum for porphyry Cu-Mo mineralization of 82.2 ± 0.2 Ma (AS-107a, Table 1).

Like the porphyry Cu-Mo mineralization, quartz-arsenopyrite veins and disseminations are also widespread. These veins were encountered from the Outlaw showing (Fig. 3) to the Red Cap showing, west of Mt. Lester Jones (Fig. 1). At the Red Cap, thin, massive vein swarms are hosted in shears along the contact between porphyritic dikes and altered Stuhini Group volcanic and sedimentary rocks. Typical vein mineralogy includes pyrite, arsenopyrite, galena, and sphalerite with lesser chalcopyrite and molybdenite in a quartz-carbonate matrix. During the 2004 field season previously unknown zones with this style of mineralization were mapped in the Jak, South King Salmon Lake and Bryar areas. Alteration is characterized by narrow zones, (tens of metres thick) of pervasive silica-sericite-clay (\pm biotite) alteration, which grades outwards into chlorite-clay alteration. At the Outlaw showing on the Thorn property, hydrothermal biotite (Outlaw, Table 1) adjacent to arsenopyrite was dated at 84.8 ± 0.5 Ma (includes 84.3% of the ^{39}Ar with an inverse isochron age of 85.4 ± 1.3 Ma and initial $^{40}\text{Ar}/^{36}\text{Ar}$ of 279 ± 28).

Skarn and carbonate replacement mineralization is common throughout the study area; however, limestone beds in the region are only thin (maximum of approximately 10 m) limiting the potential for skarn deposits. Examples can be found at the Bungee showing on the Thorn property, in the Bryar area and South King Salmon Lake area (Fig. 1). Discontinuous lenses, 2 to 8 m thick, of massive and semi-massive pyrrhotite-sphalerite with lesser galena and rare chalcopyrite characterize these occurrences. Typical skarn-related calc-silicate minerals including diopside and garnet increase in abundance towards the mineralized zone. The lack of precious metals and small size makes these less attractive exploration targets.

Oliver (1996) suggests that Golden Bear mineralization is similar to Carlin-type Au like those on the Carlin trend (*see* also Brown and Hamilton, 2000). There are no plutons in the immediate area of Golden Bear mine, however, a $^{40}\text{Ar}/^{39}\text{Ar}$ age was produced from hydrothermal sericite of 83.9 ± 1.2 Ma (Oliver, 1996) suggesting that the mineralizing fluids at Golden Bear may be derived from rocks of the Late Cretaceous volcanoplutonic belt.

DISCUSSION AND PRELIMINARY CONCLUSIONS

Although still in its infancy, preliminary results from this project give new insights into the nature, timing and distribution of magmatic rocks in the area south of the Taku river, northern Stikinia and their timing relationship to hydrothermal mineralization in the region. Mapping in the 2004 field season extended

the Late Cretaceous volcanoplutonic belt identified by Mihalynuk (2003) and Simmons (2003) north and south of its previously known limits. Furthermore, the Late Cretaceous belt may be divided into two distinct pulses of magmatic activity: a 94 to 87 Ma pulse of largely diorite porphyries and an 85 to 80 Ma pulse of sub-aerial volcanic rocks and co-magmatic subvolcanic intrusive rocks. It is not well understood which of these pulses of magmatism have more prospective hydrothermal systems associated with them. However, preliminary ages, as part of this study, from known magmatic-hydrothermal alteration along the belt suggests that the Late Cretaceous subvolcanic intrusions have associated hydrothermal systems spanning at least 91 to 79 Ma.

An important step in exploring for magmatic-hydrothermal deposits is to understand the timing and spatial relationships between hydrothermally altered rocks and the magmatic host and source rocks. At the Thorn property, $^{40}\text{Ar}/^{39}\text{Ar}$ ages on sericite from enargite veins suggest that hydrothermal alteration associated with these veins may be linked to younger Windy Table (85-81 Ma) magmatism. However, Mihalynuk (2003) suggests that sericite alteration associated with enargite veins is 91 Ma and may be associated with the older magmatic pulse. The discrepancy in ages is not understood at this time. Also at the Thorn property, sericite from breccia-hosted Ag-Pb-Zn-(Au-Cu) mineralization suggest that hydrothermal alteration may be linked to the 94 to 87 Ma magmatic pulse. At the Cirque showing on the Thorn property the timing of porphyry Cu-Mo mineralization is constrained to a minimum by the host *ca.* 82 Ma monzonite. A Pb isotope study is underway to help determine which magmatic pulse is most likely to be the source of fluids for mineralized veins.

Enargite veins have been a recent focus for exploration along the belt. Pyrophyllite alteration related to enargite veins at the Thorn property suggest that these veins formed in a hot and deep(?) environment, possibly at the porphyry-epithermal transitional depth beneath the leached cap. Fluid inclusion work is currently underway to constrain depth and temperature of ore mineral deposition in these veins. Historically, Late Cretaceous volcanic strata in the study area have been sporadically explored. Geochronology at the Thorn property suggest that Windy Table volcanic rocks overlap in time with alteration associated with Au-Ag-Cu-bearing enargite veins, leaving the possibility that the volcanic strata may host epithermal deposits topographically above the porphyry-epithermal transitional depths. Mapping during the 2004 field season identified similar volcanic stratigraphy north of the Thorn property indicating that more chronologically favourable strata may be found along the Late Cretaceous volcanoplutonic belt.

ACKNOWLEDGMENTS

Norm Graham of Discovery Helicopters provided excellent and timely helicopter service during the summer without whose help this project would not have progressed as planned. Tom Bond of Lakelse Air also provided excellent helicopter service. We thank Helen Smith for making life operate as normal while in the field. Jim Mortensen for valuable input geochronology and tectonics of magmatic rocks in the Cordillera. Mitch Mihalyuk has provided valuable information about the stratigraphy and geology of the northern Stikine Terrane, discussions about the timing of magmatic activity and hydrothermal alteration have been extremely valuable. Rimfire Minerals Corp. and Equity Engineering Ltd. provided logistical support for much of this project. We thank Dave Tupper of Solomon Resources Ltd. for allowing sampling on the Metla property. We also thank Shane Ebert who provided excellent insights about porphyry-epithermal mineralization and alteration in the field. Gayle McCreery, Brett McKay and Tim Sullivan provided outstanding company in the field. MDRU contribution P-180.

REFERENCES

- Baker, D.E.L. (2004): 2003 Geological, geochemical and diamond drilling report on the Thorn property; *British Columbia Ministry of Energy and Mines*, Assessment Report #27, 379 pages.
- Barker, F., Arth, J.G. and Stern, T.W. (1986): Evolution of the Coast batholith along the Skagway traverse, Alaska and British Columbia; *American Mineralogist*, Volume 71, pages 632-643.
- Bissig, T., Clark, A.H., Lee, J.K.W. and von Quadt, A. (2003): Petrogenetic and metallogenic responses to miocene slab flattening: new constraints from El Indio-Pascua Au-Ag-Cu belt, Chile/Argentina; *Mineralium Deposita*, Volume 38, pages 844-862.
- Brew, D.A. and Morrell, R.P. (1983): Intrusive rocks and plutonic belts of southeastern Alaska; *Geological Society of America*, Memoir 159, pages 171-193.
- Bultman, T.R. (1979): Geology and tectonic history of the Whitehorse Trough west of Atlin; unpublished PhD thesis, *Yale University*, 284 pages.
- Brown, D. and Hamilton, A. (2000): The Golden Bear mine: Carlin-type sediment-hosted, disseminated gold deposit in northwestern British Columbia, in *Geology and Ore Deposits 2000: The Great Basin and Beyond*, Cluer, J.K., Price, J.G., Struhsacker, E.M., Hardyman, R.F., and Morris, C.L., editors, *Geological Society of Nevada Symposium Proceeds*, May 15-18, 2000, pages 1002-1020.
- Hart, C.J.R., Pelletier, K.S., Hunt, J. and Fingland, M. (1989): Geological map of Carcross (105D/2) and part of Robinson (105D/7) map areas; *Indian and Northern Affairs Canada*, Open File Map 1989-1.
- Hart, C.J.R. and Radloff, J.K. (1990): Geology of the Whitehorse, Alligator Lake, Fenwick Creek, Carcross and part of the Robinson map areas (105D/11, 6, 3, 2 & 7), Yukon Territory; *Indian and Northern Affairs Canada*, Open File 1990-4, 113 pages and 4 map sheets.
- Haschke, M., Günther, A., Siebel, W., Scheuber, E. and Reutter, K.-J. (2001): Magma source variations of late Cretaceous-late Eocene magmatic rocks of the Chilean Precordillera (21.5-26°S): due to variable water fugacity or crustal thickening? poster on <http://sfb267.goeinf.fu-berlin.de/web/de/poster/posterb.asp>
- Kay, S.M. and Abbruzzi, J.M. (1996): Magmatic evidence for Neogene lithospheric evolution of the Central Andean "flat slab" between 30 and 32°S; *Tectonophysics*, Volume 259, pages 15-28.
- Kerr, F.A. (1948): Taku River map area, British Columbia; *Geological Survey of Canada*, Memoir 248.
- Lewis, P. (2002): Structural analysis of Au-Ag-Cu mineralization in the Camp Creek area, Thorn property; private report for Rimfire Minerals Corporation and First Au Strategies Corp., dated July 15, 2002. In H.J. Awmack (2003): 2002 Geological, Geochemical and Diamond Drilling Report on the Thorn Property, *B.C. Ministry of Energy and Mines*, Assessment Report #27, 120 pages.
- Mihalyuk, M.G., Meldrum, D., Sears, W.A. and Johannson, G.G. (1995a): Geology of the Stuhini Creek Area (104K/11); in *Geological Fieldwork 1994*, Grant, B. and Newell, J.M., editors, *B.C. Ministry of Energy Mines and Petroleum Resources*, Paper 1995-1, pages 321-342.
- Mihalyuk, M.G., Meldrum, D., Sears, W.A. and Johannson, G.G., Madu, B.E., Vance, S., Tipper, H.W. and Monger, J.W.H. (1995b): Geology and Lithochemistry of the Stuhini Creek Area (104K/11), *B.C. Ministry of Energy Mines and Petroleum Resources*, Open File 1995-5.
- Mihalyuk, M.G. (1999): Geology and Mineral Resources of the Tagish Lake Area, BC; *Ministry of Energy and Mines*, Bulletin 105.
- Mihalyuk, M.G., Mortensen, J., Friedman, R., Panteleyev, A. and Awmack, H.J. (2003): Cangold partnership: regional geologic setting and geochronology of high sulphidation mineralization at the Thorn property. British Columbia; *Ministry of Energy and Mines*, Geofile 2003-10.
- Oliver, J.L. (1996): Geology of Stikine assemblage rocks in the Bearskin (Muddy) and Tatsamenie Lake District, 104K/1 and 104K/8, northwestern British Columbia, Canada and characteristics of gold mineralization, Golden Bear mine: northwestern British Columbia; unpublished PhD thesis, *Queen's University*, 242 pages.
- Sawkins, F.J. (1990): Metal deposits in relation to plate tectonics, 2nd edn.: *Springer-Verlag*, Berlin, 461 pages.
- Sillitoe, R.H. (1972): Relation of metal provinces in western Americas to subduction of oceanic lithosphere; *Geological Society of America*, Bulletin, Volume 83, pages 813-818.
- Simmons, A., Tosdal, R., Baker, D. and Baknes, M. (2003): Geologic framework of the Thorn epithermal deposit, northwestern, BC; *British Columbia and Yukon Chamber of Mines*, poster abstract for the Mineral Exploration Roundup.

- Souther, J.G. (1971): Geology and mineral deposits of the Tulsequah map-area, British Columbia; *Geological Survey of Canada*, Memoir 362, 84 pages.
- Sutherland-Brown, A., Editor (1976): Porphyry deposits of the Canadian Cordillera; *Canadian Institute of Mining and Metallurgy*, Special Volume 15, 510 pages.
- Titley, S.R., Editor (1982): Advances in geology of the porphyry copper deposits, southwestern North America, Tucson, *University of Arizona Press*, 560 pages.
- Wheeler, J.O. (1961): Whitehorse map-area, Yukon Territory, (105D); *Geological Survey of Canada*, Memoir 312, 156 pages.
- Wheeler, J.O., Brookfield, A.J., Gabrielse, H., Monger, J.W.H., Tipper, H.W. and Woodsworth, G.J. (1991): Terrane map of the Canadian Cordillera; *Geological Survey of Canada*, Map 1713A, scale 1:2 000 000.

Workshops on Multielement and Multisite Regional Geochemical Survey (RGS) Anomalies Meriting Follow-Up Work in British Columbia

By C.P. Smyth

KEYWORDS: geochemistry, regional geochemical survey, RGS, Rocks to Riches, anomaly, target generation, MineMatch

INTRODUCTION

In 2003, the Rocks to Riches program funded a re-evaluation of British Columbia's Regional Geochemical Sampling (RGS) database for new exploration targets (Smyth, 2004a). This evaluation employed state-of-the-art data analysis techniques not previously applied in British Columbia. The results of the re-evaluation, which included assessment by the MineMatch[®] software system, were published on the Internet for easy public access and were also incorporated into the British Columbia Geological Survey's MapPlace website.

In 2004, the Rocks to Riches program funded the 'MineMatch Geochemistry Follow-Up Program' to assist the various exploration and prospecting communities in British Columbia to use the results of the RGS re-evaluation study to enhance their ability to find new mineral deposits in the province.

This was achieved by providing one-day 'target generation and follow-up' workshops free of charge in six centres throughout British Columbia, namely Smithers (16 attendees), Williams Lake (3), Cranbrook (1), Nelson (19), Kamloops (9) and Vancouver (23). These workshops taught participants how to use the the new RGS-based Internet resources to

pick the most promising areas of BC in which to conduct prospecting operations; and

use information on the www.rockstorichesbc.com website to assist with follow-up of the identified targets.

Each workshop used content drawn from the region in which it was being hosted, with an emphasis on identifying targets on ground unencumbered by existing claims, parkland or other restrictions. Heavy reliance was placed on using existing provincial Internet resources to assist with these considerations, as well as with integrating landform and other geological information into target characterization.

This paper clarifies the goals of the 2003 Rocks to Riches MineMatch Geochemistry Study, documents additional Internet resources developed for the 2004 project workshops, and summarizes the results of the six project workshops held in 2004.

PROJECT GOALS

Selecting areas in which to prospect is an activity undertaken at varying scales. At large (general) scales, it involves determining which broad regions are likely to be most rewarding; at small (area-specific) scales, it involves determining exactly where on the ground to expend costly human and mechanical effort on mapping, including sampling and data collection.

Although the project addressed the first of these in its publication of 27 deposit-type target distribution maps, the focus in the workshops was on the small scale — specifically on determining which individual drainages in British Columbia, based on their silt geochemistry, displayed evidence of economic mineralization **and might not have been investigated on the ground for this mineralization** — despite the long period of time over which the RGS data have been available and the free Internet-based mapping software available for their assessment.

This goal was achieved in two steps:

- 1) Selecting higher interest anomaly clusters from the MineMatch Geochemistry Study
- 2) Using the mapping capabilities of the MapPlace website (www.mapplace.ca) to establish whether the anomaly cluster may result from known mineralization.

The particular goal of the workshops was to make the results of the MineMatch Geochemistry study as accessible as possible to potential users not experienced in the Internet delivery of sophisticated mineral exploration aids.

WORKFLOW CONSIDERATIONS

Workflow issues are seldom considered explicitly in research-type activities such as anomaly identification and prioritization in mineral exploration. Where input datasets are large and complex, however, they can present significant barriers to successful completion of these tasks.

While the MineMatch Geochemistry study had automated the many potentially time-consuming steps in identifying anomaly clusters, the volume of data analyzed produced many targets for evaluation. Optimizing the workflow around deciding which of these may be of immediate interest to a prospector or exploration company, and documentation of the reasons for this interest, had not been addressed, and was therefore evaluated and optimized for these workshops.

In this regard, easy access to the primary analytical and lithological data on which anomaly clusters were based, as well as the need to print these data in a format easily reviewed by a human being, and easily filed, were considered important. The Filemaker Pro Version 7 database was identified as the most cost-effective means of providing for these needs on the Internet. All anomaly cluster sample data were imported into the system, and the necessary programs were written to provide the required functionality. Figure 1 illustrates the primary output from the resulting enhancement of the MineMatch Geochemistry Study, which is a single letter-sized printout showing all the analytical results available for an anomaly cluster sample, the primary rock type associated with the sample, the 99th percentile anomaly thresholds used for each analytical method, and the number of analyses used to determine this threshold. In the case of multiple-site anomaly clusters, the user can page between associated samples by clicking on the next/previous page icon in the left margin of the report. Reports and printouts from this system provided an important focus for the workshops.

Easy access to and printing of maps explaining possible sources of anomaly clusters, as well as their ownership

status, was an equally important component of the workshops. This was provided by the British Columbia Geological Survey's MapPlace website.

Finally, it was necessary to provide access to paper maps suitably scaled for the pencil-and-paper work that supplements most large map-evaluation projects. These A0-size 1:500 000-scale maps were prepared before each workshop, and made available in Adobe PDF format for download from the www.rockstorichesbc.com website after each workshop.

EXAMPLE ANOMALY CLUSTER

Ensuring that participants understood the relationships between anomaly clusters, component samples, sample analytical results, known mineral occurrences, mineral claim locations and streams and watersheds was an important introductory element to each workshop.

Figure 2 presents anomaly cluster 2507, which illustrates all these aspects of the MineMatch Geochemistry Study, namely

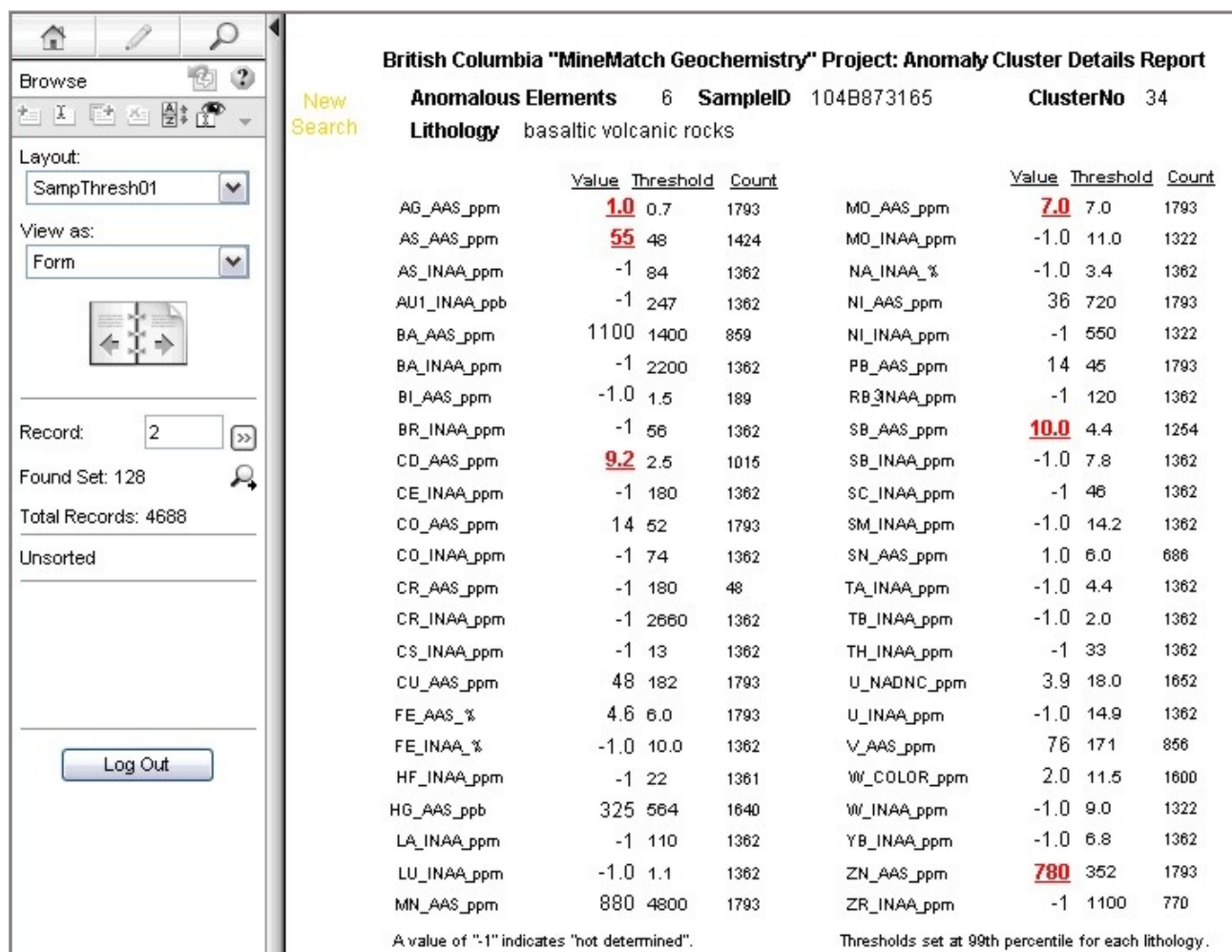


Figure 1. MineMatch Geochemistry Study anomaly cluster details report.

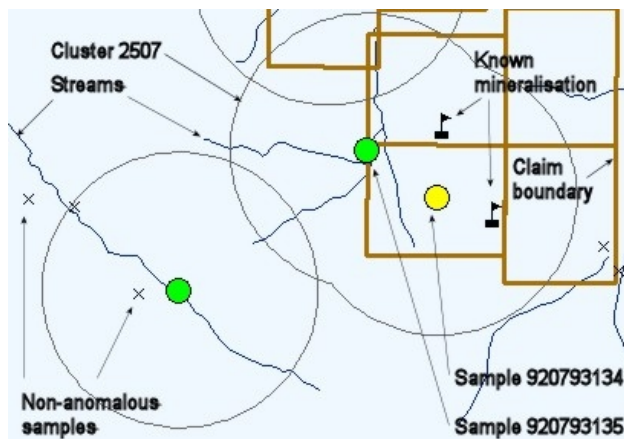


Figure 2. Relationships among anomaly clusters, component samples, known mineral occurrences, mineral claim locations and streams.

- 1) anomalous levels in economically interesting elements in two samples taken less than 2.5 km apart:
 Sample 920793134 – anomalous in Ag, Cu, Hg, Mo and W
 Sample 920793135 – anomalous in Ag, As and Pb
- 2) anomalous in one of the samples (920793134) probably explained by known mineralization within the catchment area of the sampled stream;
- 3) anomalous in the other sample (920793135) without a source in known mineralization — and which, unlike the former sample, is likely to arise from ground that is not subject to mineral claims. Note that the relatively subdued (but nevertheless real) levels of anomalism in this sample make it quite possible that it had not, with the data analysis tools readily available prior to the MineMatch Geochemistry Study, previously been identified as anomalous.

WORKSHOP STRUCTURE AND PRODUCTS

Workshops took place over one day, according to the following general structure:

- 9.00 am–10.30 am: Using the www.rockstorichesbc.com website to identify and prioritize drainages for follow-up work in the field
- 11.00 am–12.30 pm: Working toward establishing the ten best unstaked targets in the (workshop) region
- 1.30 pm–3.00 pm: Describing mineral deposits and deposit models: fieldwork and computer considerations
- 3.30 pm–5.00 pm: Evaluation of targets in areas of specific interest to attendees using the project and www.mapplace.ca websites, including those in already-staked ground

During the first part of the workshop, attendees were taken through the mapping and database querying tools available on the project website, advised on how to interpret the site's statistical reports and graphics, and shown how to investigate the contextual details of interesting anomaly clusters on the www.mapplace.ca website.

During the second session, the principles covered in the first session were applied to the workshop's focus area, starting with a precompiled list of anomaly clusters illustrating various aspects of anomaly assessment. Records were kept of anomaly clusters assessed, and conclusions regarding their level of interest to explorers. These records were posted on the project web site after the workshop. Table 1 illustrates the results of the Smithers workshop.

The third session examined the challenges inherent in describing mineral deposits, models and occurrences, and the advantages of using standard terminology for these purposes. With this background, which was fundamental to the development of the MineMatch system, attendees were advised on how to use the MineMatch reports available for each anomaly cluster as checklists of important geological criteria to look for when following up anomalies on the ground.

The final session was devoted to assessing project data from any areas of interest to attendees. This usually led to an active exchange of information between attendees, particularly between explorers and British Columbia Geological Survey staff, when the latter were present. On a number of occasions, it became apparent that an attendee had staked claims based on anomaly clusters observed on the project website prior to the workshop.

INTEGRATION WITH ADJOINING JURISDICTIONS

Since publication in January 2004 of the MineMatch Geochemistry Study, a similar study had been completed for the Yukon Territory (Smyth, 2004b). Arrangements were therefore made to plot anomaly clusters from southern Yukon on the same map as clusters from northern British Columbia for the Vancouver workshop, which focused on northwestern British Columbia because southwestern British Columbia had been covered during the Kamloops workshop. Although splitting and lumping of rock types into lithological units has been conducted according to different criteria north and south of the boundary, leading to occasional apparent geological discontinuities at the boundary, anomaly cluster groups are generally continuous across the border, a characteristic that assists in efficient prospecting on both sides of the boundary.

WORKSHOP EFFECT ON WEBSITE UTILIZATION

Usage logs of the www.rockstorichesbc.com website (Fig. 3) show a considerable increase immediately before, during and after the workshops, suggesting that they were successful in reigniting the interest initially shown in the site after its publication, which is also evident in the logs. It

TABLE 1. ANOMALY CLUSTER WORKSHEET FOR THE SMITHERS WORKSHOP.

Category	Cluster	Comments
Free	127	1 sample: Ag, Co, Cu, Fe, Mo, Pb, W
Free	212	1 sample: As, Co, Cu, Mo, Sb. Very close to 2 porphyry mineral occurrences in cluster
Free	2855	2 samples: Au, Cs, Cu, Fe, Mo
Free	2869	4 samples: Ag, As, Au, Br, Ce, Co, Cs, Cu, Fe, Mo, Sb, W. Probably from the Red Rose mineral occurrence, which may also explain cluster 2870
Free	2904	1 sample: Ag, Cd, Pb, Sb, Zn. In Babine Park
Free	2912	3 samples: Cd, Co, Cu, W, Zn. Source from known mineralization?
Free	2986	1 sample: Ag, Br, Ce, Cu, Hf, La, Mo, Sm, Ta, Tb, Th, U
Free	3008	3 samples, 1 of which sourced over "monzodiorite" with a sample population of only 6, yielding a poor quality 99th percentile. The other 2 samples are anomalous in: Bi, La, Mo, Na, U, W
Free	3088	1 sample: Ag, Br, Co, Cu, Fe, Hg, Mo, Ni, Sc, U, Zn. Good quality target
Free	3141	1 sample: Cu, Fe, Mo, W. Good quality target
Free	3157	2 samples: Cs, U, Tb, U, Yb
Free	3176	1 sample: Au, Ce, Co, Cr, Cs, Fe, Hf, La, Lu, Na, Ni, Rb, Sc, Sm, Ta, Tb, U, Yb, Zr. Exotic skarn?
Free	3198	1 sample: Ag, Cu, Mo, Pb, Sb, Zn. Claim over best (main) stream
Free	3222	1 sample: Ag, Cu, Hg, Lu, Sm, Tb, Yb. Good quality target
Free	3343	2 samples: Au, Cu, Mo, Sc. Low Cu, Mo, Au anomaly on free ground
Free	3370	2 samples: Bi, Cu, Fe, Mo, Th, U, W, Zn. Good quality target
Free	3387	2 samples: Cu, Mo, W. Good quality target
Held	26	2 samples: Ag, As, Cu, Mo, Ni, Sb, Zn
Held	205	5 samples: Ag, As, Au, Ba, Cu, Fe, Hg, Pb, Sb
Held	2888	1 sample: Ag, Pb, Sb
Held	2905	1 sample: Mo, W
Held	3058	3 samples: Ba, Cd, Hg, Mo, Ni, Pb, Zn

Anomaly Clusters probably not of interest

Poor	2939	Smithers - Invalid anomaly: Sample population of one
Poor	2946	Smithers - Invalid anomaly: Only 12 to 20 samples in populations
Poor	2977	Smithers - Invalid anomaly: No indication of sample population size
Poor	3035	Smithers - Invalid anomaly: Only 6 samples in the monzodiorite class of samples
Poor	3310	Smithers - Invalid anomaly: Only three samples in population
Poor	2399	Williams Lake - Probably unmapped ultramafics in sample area
Poor	2529	Williams Lake - Hg, Cr, Ni in greenschist(?)
Poor	2570	Williams Lake - Lu, Sm, Tb, Yb association in volcanics
Poor	2688	Williams Lake - Probably unmapped ultramafics in sample area
Poor	2701	Williams Lake - Typical REE enhanced without other elements of interest

is likely that much of this interest was from parties who did not feel qualified to exploit the website without the supplementary instruction in computer techniques provided by the workshops.

CONCLUSION

The Rocks to Riches Project funded six one-day workshops on selecting anomaly clusters for follow-up work from those reported in the 2003 MineMatch Geochemistry Study, which was also funded by the Rocks to Riches program. A primary goal of the workshops was to make the results of the 2003 study as accessible as possible to potential users not experienced in the Internet delivery of sophisticated mineral exploration aids. While workshop attendance was varied, participation by attendees was enthusias-

tic, positive feedback was received from all workshops, and utilization of the project website was increased substantially by the workshops.

Preparation for the workshops focused significant attention on the workflow surrounding anomaly prioritization and documentation. This resulted in upgrades to the project's website in respect of geochemical data querying and reporting, and in the provision of digital maps suitable for large-sheet plotting.

Lists of anomaly clusters on unclaimed ground with obvious economic potential were forthcoming from each workshop, and were posted to the project website. These lists are incomplete because of the relatively short duration of each workshop. Workshop attendees were provided with the skills to complete these lists in their own time.

Usage Statistics for rockstorichesbc.com

Summary Period: Last 12 Months

Generated 03-Dec-2004 07:46 Pacific Standard Time

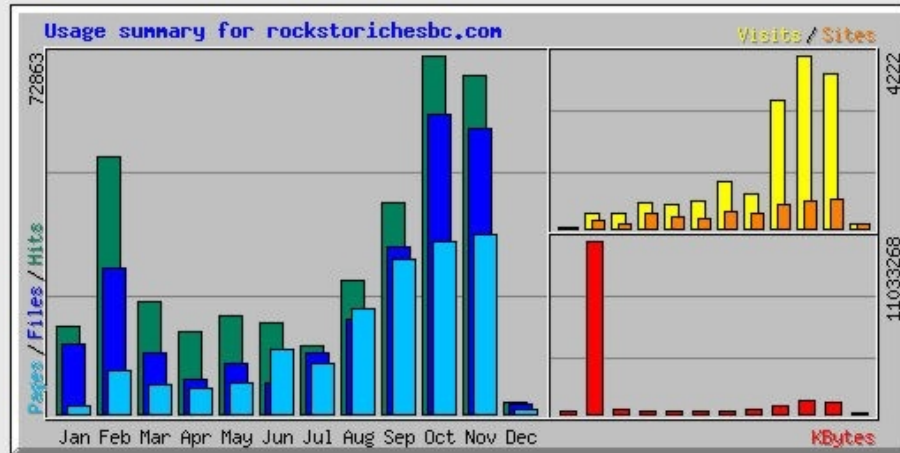


Figure 3. Usage logs of the www.rockstorichesbc.com website, showing a significant increase during the period of the project workshops.

A map was produced, and posted to the project website, which shows good continuity between groups of anomaly clusters in northwestern British Columbia and southern Yukon. This map is of value to those assessing trans-boundary mineralization trends.

ACKNOWLEDGMENTS

Project funding from the Government of British Columbia's 'Rocks to Riches' program is gratefully acknowledged.

REFERENCES

- Smyth, C. P. (2004) British Columbia regional geochemical cluster anomalies and best matches to mineral deposit types; in Geological Fieldwork 2004, *BC Ministry of Energy and Mines*, Paper 2004-1, pages 295–304.
- Smyth, C. P. (2004): Yukon mineral targets; www.yukonmineraltargets.com.